



HAL
open science

Plant-virus interactions : role of virus- and host-derived small non-coding RNAs during infection and disease

Nicolas Pitzalis

► To cite this version:

Nicolas Pitzalis. Plant-virus interactions : role of virus- and host-derived small non-coding RNAs during infection and disease. Virology. Université de Strasbourg, 2018. English. NNT : 2018STRAJ103 . tel-03920243

HAL Id: tel-03920243

<https://theses.hal.science/tel-03920243>

Submitted on 3 Jan 2023

HAL is a multi-disciplinary open access archive for the deposit and dissemination of scientific research documents, whether they are published or not. The documents may come from teaching and research institutions in France or abroad, or from public or private research centers.

L'archive ouverte pluridisciplinaire **HAL**, est destinée au dépôt et à la diffusion de documents scientifiques de niveau recherche, publiés ou non, émanant des établissements d'enseignement et de recherche français ou étrangers, des laboratoires publics ou privés.

UNIVERSITÉ DE STRASBOURG

**ÉCOLE DOCTORALE DES SCIENCES DE LA VIE ET DE LA SANTÉ
INSTITUT DE BIOLOGIE MOLÉCULAIRE DES PLANTES - CNRS UPR 2357**

THÈSE

présentée par :

Nicolas PITZALIS

Soutenue le : 9 Novembre 2018

pour obtenir le grade de : **Docteur de l'Université de Strasbourg**

Spécialité : Science de la Vie et de la Santé

Discipline : Science du Vivant Aspects Moléculaires et Cellulaires de la Biologie

**Plant-virus interactions: role of virus- and
host-derived small non-coding RNAs during
infection and disease**

THÈSE dirigée par :

Dr. HEINLEIN Manfred

Directeur de recherche, Université de Strasbourg, IBMP-CNRS

RAPPORTEURS EXTERNES :

Dr. GERMAN-RETANA Sylvie

Prof. Dr. KOGEL Karl-Heinz

Directeur de recherche, INRA - Bordeaux-Aquitaine – UMR 1332
Professeur, Directeur de recherche, Université Justus Liebig de
Giessen, Allemagne

EXAMINATEUR INTERNE :

Dr. BLEVINS Todd

Chargé de recherche, Université de Strasbourg, IBMP-CNRS

Acknowledgments

It has always been difficult for me to find the correct way and the right words to thank people who are dear to me and helped me during all these years. For me the ending of my thesis is not only representing the end of three years of work, but the end of eight years of work taken in account all the years at the University of Strasbourg.

Almost all the people I've met during my years of study have, in a way, helped and contributed to the accomplishment of my work that I don't see as an ending but as a fulfillment and mostly as a new beginning.

I will, of course, first start to thank the person who played one of the major roles during all these years of work, my half. You were able to support my terrible mood and stress at some moments, you calmed my doubts, listen to my numerous and countless complains... You made it possible for me, from time to time, to briefly step back from science, which really gave me a better look on my research or simply avoid exhausting myself too rapidly... There is not enough space to write how much I thank you, I hope you understand the sincerity of my words.

I want also to thank and at the same time apologize to my family to whom I have not given enough of my news and which I probably made feeling put aside sometimes... Thank you Mom, you, who aren't a biologist, who allowed me to learn my first exams. You kindly told me that you understood everything I was explaining although I know it was just to please me. Thank you, Dad, for all advises or for regularly asking me how I was doing, but also for asking me during my first year of PhD, if my internship was not finished yet. An innocent question that made me realize that the thesis is absolutely not an end state or something to be resting upon. Thanks to my brother, you have from time to time to straightened my ideas and reduced my stress with your precious presence.

It would be too long to thank you all one by one, my IBMP friends and colleagues (Caroline, Déborah, Florent and Pierre) for all the burgers, beers, advises and discussions we had in after-works or other distractions (sorry if I was not always present...). Arnaud, thanks for bringing me out for running (even though I was not laughing at all on our very first race) which had clarified my ideas and avoid the breakdown at some important moments. I want to thank the IBMP Newsletter team members (Hélène, Géraldine, Magalie, Lucie and Marlène) for all the great time we had, having a good coffee and croissants in the morning while discussing about all kind of gossip.

Even if the contacts are no longer regular, thanks to my university friends Gilles, Charles and Daniel. I will always remember our 3 bachelor years spent together (the laughs, TP/TD courses, the Subway with the famous "Chicken-Bacon-Ranch"!). A little thought also for Yannick for all the laughs and the Sushidos during the master degree. Also, many thanks to my "step-bro" Thomas, who always believed in me and taught me to trust myself.

Thanks to the Argentinians and proclaimed team members, Matias and the "Fat-i-gue" Gabriel, for the shared beers and discussions we had together. Congrats for your great and hard work at IBMP and for your really deserved publications. Eduardo Peña and his family, you made me smile at work under the beautiful sun of Argentina but also during the loneliness and cold Christmas period spent in Strasbourg.

As last but not least, I would like to thank my thesis advisor Dr. Manfred Heinlein for patience, scientific guidance, advise, support, immense knowledge and shared beers, which allowed me to graduate as a Doctor and especially to become a scientist. I would like to thank the committee members Dr. Sylvie German-Retana, Dr. Karl-Heinz Kogel and Dr. Todd Blevins for having accepted to evaluate my work through their precious knowledge. Also, I would like to thank, Damien Garcia and Michael Wassenegger for advising me during my mid-term, and César Llave and Livia Donaire for their kindness, great knowledge and for the help they provided during all this work.

Remerciements

Il a toujours été difficile pour moi de trouver la bonne manière et les mots justes pour remercier les personnes qui me sont chères et m'ayant aidé pendant toutes ces années. Pour moi, la fin de ma thèse ne représente pas seulement la fin de trois années de travail, mais la fin de huit années de travail, qui prennent également en compte tout mon cursus universitaire passé à Strasbourg.

Toutes les personnes que j'ai rencontrées et qui m'ont été proches pendant les années d'étude ont, d'une manière ou d'une autre, eu un rôle pour moi et contribuées à la réalisation de mon travail de thèse. Ce travail, je ne le vois pas comme une finalité mais un accomplissement et surtout un nouveau départ.

Je commencerai, bien évidemment, à remercier la personne qui a joué un rôle majeur durant toutes ces années de travail, ma moitié. Toi, qui as su supporter, à certains moments, mon humeur et mon terrible stress, calmer mes doutes, écouter ou déjouer mes nombreuses plaintes... Tu m'as permis, régulièrement, de prendre du recul sur la science, tu m'as donné la possibilité de voir mes recherches d'un autre œil ou éviter, simplement, de m'épuiser trop vite... C'est sûr, la place que je te dédis ici ne suffit pas et ne suffira d'ailleurs jamais pour décrire combien je te remercie et j'espère que tu comprends la sincérité de mes mots.

Je tiens également à remercier et en même temps m'excuser auprès de ma famille, à qui je n'ai certainement pas donné assez de nouvelles, et qui je pense, se sont sentis mis de côté à certains moments... Merci Maman, toi qui n'est pas biologiste, qui m'a permis de réviser mes premiers partiels, je me souviens quand j'essayais de t'expliquer mes cours et que tu disais gentiment que tu avais compris toutes mes explications, même si je sais que c'était juste pour me faire plaisir. Merci Papa pour les conseils, pour m'avoir régulièrement demandé comment j'allais, mais aussi pour m'avoir demandé au cours de ma première année de thèse, si mon stage était bientôt terminé, une phrase innocente qui m'a fait réaliser que la thèse n'est absolument pas un aboutissement ou ne représente pas des lauriers sur lesquels se reposer. Merci à toi aussi mon frangin, pour m'avoir de temps en temps remis à ma place et réduit mon stress avec ta précieuse compagnie.

Il serait trop long de les remercier un par un, mais merci à mes amis et collègues de l'IBMP (Caroline, Déborah, Florent et Pierre) pour tous les hamburgers, bières, conseils donnés et discussions que nous avons eu dans les after-work ou autres distractions (pardon d'ailleurs si je n'ai pas toujours été présent...). Merci Arnaud de m'avoir fait sortir pour aller courir (même si lors de notre toute première course je ne faisais pas le malin), ces courses ont toutes su m'éclaircir les idées et m'éviter de craquer aux moments importants. Merci aussi aux membres de l'équipe de la Newsletter (Hélène, Géraldine, Magalie, Lucie et Marlène) avec lesquels j'ai passé un bon moment en prenant un café et des croissants, tout en discutant de toutes sortes de commérages.

Même si les contacts ne sont plus réguliers, merci à mes amis universitaires Gilles, Charles et Daniel. Je me souviendrais toujours de nos 3 années de licence passées ensemble (les rires, les cours de TP/TD, le Subway avec le fameux « Chicken-Bacon-Ranch » !). Une petite pensée aussi pour Yannick, merci pour tous les rires pendant les cours et les Sushidos en master. Merci également à mon "Beauf" Thomas d'avoir toujours cru en moi et de m'avoir fait prendre confiance en moi.

Merci aux Argentins et proclamés membres de l'équipe, Matias et Gabriel alias « Fat-i-gue », pour les bières partagées, sympathique présence, toutes les discussions que nous avons eues ensemble et surtout félicitation pour votre dur travail à l'IBMP et publications vraiment méritées. Merci Eduardo Pena et sa famille, vous m'avez rendu le sourire au travail sous le beau soleil d'Argentine mais aussi, sous la difficile solitude et le froid de la période de Noël à Strasbourg.

Enfin, je tiens à remercier mon responsable de thèse, le Dr. Manfred Heinlein, pour sa patience, son orientation scientifique, ses conseils, son soutien, ses immenses connaissances et les quelques discussions partagées autour d'une bière qui m'ont permis de devenir docteur mais surtout un scientifique. Je tiens aussi à remercier les membres du comité, le Dr. Sylvie German-Retana, Dr. Karl-Heinz Kogel et Dr. Todd Blevins, pour avoir accepté d'évaluer mon travail grâce à vos connaissances précieuses. Je tiens également à remercier Damien Garcia et Michael Wassenegger pour m'avoir conseillé lors de ma mi-thèse ainsi que Cesar et Livia pour leur gentillesse, leur grande connaissance et leur aide durant tout ce travail.

Table of contents

Abbreviations	1
General introduction	6
Chapter I: Virus infection and mechanisms involved in disease	9
1. Introduction.....	9
1.1. Plasmodesmata	9
1.2. TMV and ORMV infection.....	11
1.3. TuMV infection.....	14
2. Publication: "The roles of membranes and associated cytoskeleton in plant virus replication and cell-to-cell movement" by Pitzalis and Heinlein 2017	21
Chapter II: RNA silencing and role of small RNAs	22
1. Introduction.....	22
2. RNA silencing pathways and their components.....	23
2.1. Role and function of DCL proteins	24
2.2. Role and function of AGO proteins.....	25
2.3. Role and function of RDR proteins	27
2.4. Role and function of HEN1 proteins	28
3. Roles and pathways of RNA silencing	29
3.1. miRNA biogenesis and function.....	30
3.2. phasiRNA biogenesis and function	31
3.3. Virus-derived siRNAs (vsiRNAs)	32
4. Draft manuscript: "Virus- and host-derived small RNAs coordinate infection in oilseed rape" by Pitzalis <i>et al.</i>	34
Chapter III: Plant-virus infection and disease symptoms	71
1. Introduction.....	71
1.1. The phenomenon of disease symptoms recovery	71
1.2. Role of VSR function in the formation of disease symptoms and recovery	74
1.3. A potential role of antiviral meristem resistance in recovery.....	75
1.4. The role of PTGS and TGS in recovery.....	76
1.5. Disease symptoms recovery in ORMV-infected Arabidopsis plants.....	78
2. My contributing role to the publication by Kørner <i>et al.</i> (2018).....	81
3. Conclusion	85
4. Publication: "Crosstalk between PTGS and TGS pathways in natural antiviral immunity and disease recovery" by Kørner <i>et al.</i> 2018.....	86
General conclusion	87
The role of virus-and host-derived small RNAs in plant-virus interactions	87

Processes that lead to viral symptom recovery and promote plant health.....	92
Materials and methods	94
I. Materials	94
1. Plant species	94
1.1. <i>Brassica napus</i>	94
1.2. <i>Arabidopsis thaliana</i>	94
1.2.1. T-DNA mutants.....	94
2. Viral strain and constructs	95
2.1. pCB-TuMV-GFP.....	95
2.2. ORMV virions	95
3. Antibodies.....	96
4. Primers	96
II. Methods	96
1. Plant culture	96
2. Inoculation of plants with virus	96
3. Measurement of specific RNA levels by reverse transcription followed by quantitative Polymerase Chain Reaction analysis (RT-qPCR)	97
3.1. Total RNA extraction and cDNA synthesis.....	97
3.2. cDNA quantification by RT-qPCR.....	98
4. 5'RACE (Rapid Analysis of cDNA Ends)	99
4.1. Total RNA extraction	100
4.2. Purification of mRNA from total RNA.....	100
4.3. Adapter ligation	100
4.4. Reverse transcription	101
4.5. cDNA fragment amplification by PCR (nested PCR)	101
5. DNA genome sequencing.....	102
5.1. DNA isolation	102
5.2. Sequencing and quality control.....	102
5.3. Alignment of DNA reads to the <i>Brassica napus</i> reference genome	102
5.4. SNP calling and cultivar-specific transcriptome construction	103
6. RNA sequencing.....	103
6.1. Total RNA isolation and quality control.....	103
6.2. mRNA sequencing and quality control	103
6.3. Alignment and annotation of mRNAseq reads	104
6.4. Differential expression analysis.....	104
7. sRNA sequencing	104

7.1. vsiRNA alignment	104
7.2. Identification of miRNAs	105
7.3. <i>De novo</i> miRNA and va-phasiRNA detection	105
7.4. Short read abundance and differential expression (DE) analysis.....	106
8. mRNA degradome sequencing.....	106
8.1. Sequencing of PAREseq libraries and quality control	107
8.2. Association of cleaved mRNA 5'ends with RISC-mediated mRNA cleavage.....	107
9. RNA analysis using the northern blotting technique.....	108
9.1. Total RNA extraction and size fractionation	108
9.2. RNA blotting.....	108
10. Protein analysis using the western blot technique.....	110
10.1. Total protein extraction and quantification	110
10.2. SDS-PAGE	111
10.3. Protein transfer and luminescent detection	111
References	113

Appendix

Appendix 1: Supplementary figures and tables of draft manuscript: "Virus- and host-derived small RNAs coordinate infection in oilseed rape" by Pitzalis *et al.*

Appendix 2: Supplementary figures and tables of publication: "Crosstalk between PTGS and TGS pathways in natural antiviral immunity and disease recovery" by Kørner *et al.* 2018

Résumé de thèse en français

Abbreviations

Viruses acronyms	Full name	Genus
BCMV	<i>Bean common mosaic virus</i>	Potyvirus
BCTV	<i>Beet curly top virus</i>	Curtovirus
BMV	<i>Brome mosaic virus</i>	Bromovirus
CalCuV	<i>Cabbage leaf curl virus</i>	Begomovirus
CaMV	<i>Cauliflower mosaic virus</i>	Caulimovirus
CMV	<i>Cucumber mosaic virus</i>	Cucumovirus
CymRDV	<i>Cymbidium ringspot virus</i>	Potexvirus
CymRSV	<i>Cymbidium ringspot tobusvirus</i>	Tombusvirus
LMV	<i>Lettuce mosaic virus</i>	Potyvirus
ORMV	<i>Oilseed rape mosaic virus</i>	Potyvirus
PepGMV	<i>Pepper golden mosaic virus</i>	Begomovirus
PVX	<i>Potato virus X</i>	Potexvirus
PVY	<i>Potato virus Y</i>	Potyvirus
SMV	<i>Soybean mosaic virus</i>	Potyvirus
TBRV	<i>Tomato black ring virus</i>	Nepovirus
TEV	<i>Tobacco etch virus</i>	Potyvirus
TMV	<i>Tobacco mosaic virus</i>	Tobamovirus
ToMV	<i>Tomato mosaic virus</i>	Tobamovirus
ToRSV	<i>Tomato ringSpot Virus</i>	Nepovirus
TRV	<i>Tobacco rattle virus</i>	Tobravirus
TSV	<i>Tobacco streak Virus</i>	Ilarvirus
TuMV	<i>Turnip mosaic virus</i>	Potyvirus
TuYV	<i>Turnip yellows virus</i>	Polerovirus
TVMV	<i>Tobacco vein mottling virus</i>	Potyvirus

Word abbreviations

(β -ME)	β -mercaptoethanol
ABA	Abscisic acid
ADF3	Actin depolymerization factor 3
AGO	ARGONAUTE
AtSuc:GFP	<i>Arabidopsis thaliana</i> sucrose symporter promoter driving expression of GFP
BAK1	BRASSINOSTEROID INSENSITIVE 1-ASSOCIATED KINASE 1
BG	β -(1.3)-Glucanase
BiFC	Biomolecular fluorescence complementation
BLOS2	Biogenesis of lysosome-related organelles complex 1 subunit 2
Ca ²⁺	Calcium
CalS	Callose synthase
casiRNA	<i>cis</i> -acting small interfering RNA

CB60G	Calmodulin-binding protein 60G
CDPK	Calcium-dependent protein kinase
CFDA	Carboxyfluorescein diacetate
ChIP	Chromatin immuno-precipitation
CI	Cylindrical inclusion protein
CIP	Calf intestinal phosphatase
ConTR01	Conditional TuMV resistance 01
COPI	Coat protein complex I
CP	Coat protein
Ct	Cycle threshold
DAMP	Damage-associated molecular pattern
DCL	Dicer-like
DE	Differential expression
DEAD-box	DExH-Box RNA helicase
DI	Defective interfering
DM	Mock-treated <i>B. napus</i> cv. Drakkar
dsRBD	dsRNA-binding domain
dsvRNA	double-stranded viral RNA
DT	Virus-treated <i>B. napus</i> cv. Drakkar
DTX47	DETOXIFICATION 47
DUB	Deubiquitinylation protein
DUF283	Domain of unknown function 283
eEF1A	Eukaryotic elongation factor 1A
EF2	Elongation factor 2
eIF	Eukaryotic initiation factor
eIFiso4E	Eukaryotic-Initiation factor isoform 4E
EIN5	ETHYLENE-INSENSITIVE 5
ER	Endoplasmic reticulum
ERES	ER exit site
ERF RAP 2	Ethylene-responsive transcription factor RELATED TO APETALA 2
ETI	Effector-triggered immunity
FC	Fold change
FLS2	FLAGELLIN SENSING 2
GFP	Green fluorescent protein
GO	Gene ontology
hc-siRNA	Heterochromatic small interfering RNA
HcPro	Helper component proteinase
HD-ZIPIII	Class-III homeodomain-leucine zipper
HEN1	HUA ENHANCER 1
HMW	High molecular weight RNA
HR	Hypersensitive resistance
hsRNA	Host-derived siRNA
JA	Jasmonic acid
L8z2	<i>A. thaliana</i> line 8z2

LCD	La-motif-containing domain
LMW	Low molecular weight
LRD	Leucine-rich domain
LRR	Leucine-rich repeat
MAMP	Microbe-associated molecular pattern
MAP	Microtubule-associated protein
MAPK	Mitogen-activated protein kinase
met-tRNA	Methionine-tRNA
miRNA	microRNA
MP	Movement protein
mRNAseq	mRNA sequencing
MT	Microtubule
MTA	Material transfer agreement
MTase	Methyltransferase domain
NAC60	NAC domain-containing protein 60
NB	Nucleotide binding
NB-LRR	Nucleotide-binding leucine-rich repeat
NGS	Next-generation sequencing
NIMIN-2	NIM1-INTERACTING 2
OAS	Origin of assembly
P3N-PIPO	Trans-frame N-terminus fused P3-PIPO
PABP	Poly(A)-binding protein
PAGE	Polyacrylamide gel electrophoresis
PAMP	Pathogen-associated molecular pattern
PARE	Parallel analysis of RNA ends
PAREseq	mRNA degradome profiling using PARE sequencing
PAZ	Piwi/Argonaute/Zwille
PD	Plasmodesmata
PDCB	PLASMODESMATA CALLOSE BINDING
PDLP	PLASMODESMATA-LOCATED PROTEIN
phasiRNA	Phased small interfering RNA
PIPO	Pretty interesting potyviral ORF
PM	Plasma membrane
POL IV	RNA polymerase VI
PP2A2	PHLOEM PROTEIN 2-LIKE A2
PPR	Pentatricopeptide repeat
pri-miRNA	Primary microRNA precursor
PRR	Pattern recognition receptor
PTGS	Post-transcriptional gene silencing
PTI	Pattern-triggered immunity
PVIP	VPg-interacting protein
QTL	Quantitative trait loci
RACE	Rapid amplification of cDNA ends
rasiRNA	Repeat-associated small interfering RNA

RdDM	RNA-directed DNA methylation
RDRP, RDR	RNA-dependent RNA polymerase
REn	Replication enhancer
retr01	Resistance 01
RIN	RNA integrity number
RIN4	RPM1-INTERACTING PROTEIN 4
RISC	RNA-induced silencing complex
RLK	Receptor-like kinase
RLP	Receptor-like protein
RNAi	RNA-interference
ROS	Reactive oxygen species
rpm	Reads per million
SA	Salicylic acid
SAM	Shoot apical meristem
SAR	Systemic acquired resistance
SCL	SCARECROW-LIKE
SDS	Sodium dodecyl sulphate
SEL	Size exclusion limit
SERK1	SOMATIC EMBRYOGENESIS RECEPTOR-LIKE KINASE 1
SGS3	SUPPRESSOR OF GENE SILENCING 3
siRNA	Small interfering RNA
SNARE	Soluble N-ethyl-maleimide-sensitive-factor attachment protein receptor
SNP	Single nucleotide polymorphism
SPL	SQUAMOSA PROMOTER-BINDING-LIKE
SR	Serine/arginine-rich
sRNA	Small RNA
sRNAseq	Small RNA sequencing
ssRNA	Single-stranded RNA
ST	Symptom Type
TAO1	TARGET OF AVR B OPERATION 1
TAP	Tobacco acid pyrophosphatase
tasiRNA	trans-acting small interfering RNA
TEMED	N,N,N',N'- tetramethyl-1,2-diaminométhane
TF	Transcription factor
TGS	Transcriptional gene silencing
TM	Mock-treated <i>B. napus</i> cv. Tanto
TOE2	TARGET OF EAT 2
TOM	TOBAMOVIRUS MULTIPLICATION
TrAP	Transcription activator protein
tRNA	Transfer RNA
TT	Virus-treated <i>B. napus</i> cv. Tanto
TuMV-GFP	GFP-tagged TuMV
UGPase	UDP-GLUCOSE PYROPHOSPHORYLASE
UTR	Untranslated region

VIGS	Virus-induced gene silencing
VPg	Genome-linked viral protein
VRC	Viral replication complex
vRNA	Viral RNA
vsiRNA	Virus-derived small interfering RNA
VSR	Viral suppressor of RNA silencing
XRN4	EXORIBONUCLEASE 4
Y2H	Yeast two-hybrid

General introduction

Virus infection in plants depends on the ability of viruses to replicate and spread their genomes from cell to cell and systemically through plasmodesmata (PD) and the connected phloem. Viruses encode only a limited set of proteins and depend on molecular mechanisms provided by their hosts for propagation. Numerous studies have illuminated cellular membrane- and cytoskeleton-associated mechanisms as well as specific host factors involved in virus replication and movement. However, our knowledge about gene regulatory processes that orchestrate virus infection remains limited. Viruses may employ mechanisms to manipulate host gene expression to ensure that defenses are minimized and resources required for viral replication are maximized, whereas the cell may counteract through opposite mechanisms that maximize defenses and minimize the resources for the virus. This battle between the virus and its host is best illustrated by a gene regulatory process known as post-transcriptional gene silencing (PTGS, also known as 'RNA silencing' or 'RNA interference' [RNAi]). During infection, PTGS functions as an important antiviral defense response that controls viral accumulation by targeting the viral RNA for cleavage or translational repression. Viruses, in turn, have evolved specific effector proteins (Viral Suppressor of RNA silencing, VSR) that interfere with the RNA silencing pathway at specific steps and thereby enhance their propagation. As the antiviral RNA silencing pathway shares components with other transcriptional and post-transcriptional RNA silencing pathways playing a role in the regulation of gene expression, viruses may apply their VSRs also for the modulation of host gene expression. In addition, while cellular alterations are most commonly orchestrated by virus-encoded proteins, viruses may manipulate their hosts also by using their virus genome-encoded small RNAs as RNA effectors. This strategy is best illustrated by DNA viruses belonging to the Herpesviridae family, which were found to encode between 1 and 14 miRNAs (Cox and Sullivan 2014). While some of these miRNAs engage in the regulation of viral gene expression during the viral replication cycle, other miRNAs act as mimics for endogenous cellular miRNAs and modulate the levels of host gene transcripts, thereby creating an environment more amenable to replication and/or latency (Gottwein et al. 2007; Kincaid et al. 2012). A similar strategy has also been evolved by certain plant pathogenic fungi. Similar to the DNA viruses in mammals, these fungi use small RNAs derived from their own genome to hijack the host RNA silencing pathway to target the expression of host defense genes and thereby enhance host susceptibility (Suffert et al. 2011; Weiberg et al. 2013). Based on these examples, it can be expected that also plant viruses have evolved such RNA effectors. Although most plant viruses are RNA viruses that replicate in the cytoplasm and, therefore, do not encode miRNAs (Aguado and tenOever 2018),

the virus-derived small interfering RNAs (vsiRNAs) that are produced during antiviral silencing may have the potential to target host genes. In addition, given the sheer amount of small RNAs produced by RNA silencing pathways in plants, it may also be conceivable that plants themselves encode small RNAs with homology to viruses that infect them and that are part of the arms arsenal available to plants to control their viruses. Certain reported cases in *Arabidopsis* literature, illustrate that vsiRNAs and VSRs have the potential to interfere with host processes required for normal host cellular function and development (Kasschau et al. 2003; Qi et al. 2009; Jay et al. 2011; Hu et al. 2011; Avina-Padilla et al. 2015). Therefore, it appears likely that such mechanisms may be involved in the triggering of virus-induced diseases in cultivated plants, which cause losses worth of 20-60 billion US\$ worth in yield annually (Randles and Ogle 1997; Sastry and Zitter 2014).

This thesis project was aimed to address the role of host- and virus-encoded small RNAs in plant:virus interactions during virus spread in infected tissues and in determining host disease. The thesis is organized in three different chapters:

Chapter I introduces the viruses *Oilseed rape mosaic virus* (ORMV) and *Turnip mosaic virus* (TuMV) that were used as pathogens in the present thesis, describes cellular mechanisms involved their cell-to-cell movement and presents a review article (Pitzalis and Heinlein 2017) describing viral movement mechanisms and the potential role of endoplasmic reticulum:plasma membrane (ER:PM) contact sites and associated proteins during infection.

Chapter II describes the results of a project applying Next Generation Sequencing (NGS) approaches to the analysis of virus infection and which led to important new insights into the functions of host- and virus derived-small RNAs in regulating their specific RNA targets during the spread of infection in leaves. This work was applied to local sites of infection caused by an economically important virus (TuMV) within the leaves of rapeseed (*Brassica napus*, 'Canola'), an economically important oilseed crop species. Thus, the obtained results suggest important new gene targets for crop breeding.

Finally, work described in **Chapter III** revealed the genetic and functional basis of disease symptoms and symptoms recovery observed in *Arabidopsis* plants infected with ORMV. Symptoms recovery relates to the ability of plants to recover from an established viral disease. Understanding this phenomenon is a key to important mechanisms that support plant health and the survival of plants in natural environments full of viruses. The results of this study were published in the journal *Nature Plants* (Kørner et al. 2018) and led to the important discovery that recovery does not require the silencing inhibition of the virus but is associated with the achievement of a tolerant state in which the virus and the host can coexist without disease. The work led to the identification of RNA silencing

pathway genes and of a mechanism by which plants use these RNA silencing pathway genes for the robust production of secondary small interfering RNAs (siRNAs) as well as intercellular communication and systemic regulation to use these siRNAs to downregulate the virus-encoded VSR in physiological sink tissues and thereby achieve the tolerant state in newly emerging leaves (Kørner et al. 2018).

Together, the results described in these three chapters of the thesis provide novel insights into the regulatory mechanisms involved in the interaction of viruses with their hosts and which have the potential to indicate novel strategies for crop protection.

Chapter I: Virus infection and mechanisms involved in disease

1. Introduction

Viruses use different mechanisms for plant-to-plant transmission (Hosford 1967; Hull 2009) and for their propagation within the infected plants (Verchot-Lubicz et al. 2010; Niehl and Heinlein 2011; Agbeci et al. 2013; Laliberte and Zheng 2014; Liou et al. 2015; Schoelz et al. 2016; Pitzalis and Heinlein 2017). As plants are sessile, viruses usually depend on fungi, nematodes, protists, or insects as vectors for transmission. Moreover, several viruses, for example the tobamoviruses (e.g. *Tobacco mosaic virus*, TMV), are mechanically transmitted by wind, water, soil, seeds, as well as by humans through virus-infected plant handling and processing (Hull 2009).

Work described in this thesis involved experimentation with TMV and ORMV as well as with TuMV, a potyvirus. Whereas TMV and ORMV are mechanically transmitted, TuMV is transmitted by several aphid species. Once a virus has been transmitted and entered a host cell, it is uncoated and translated to produce proteins required for replication, cell-to-cell movement, viral counter-defense (e.g. a Viral Suppressor of RNA silencing, VSR), virion assembly and transmission.

1.1. Plasmodesmata

Viruses cause systemic plant infection by cell to cell movement through PD and long-distance movement via the phloem (Deom et al. 1987; Wolf et al. 1989; Heinlein 2002; Lucas et al. 2006; Guenoune-Gelbart et al. 2008; Benitez-Alfonso et al. 2010; Sager and Lee 2014; Heinlein 2015). The PD are symplastic channels in the cell walls through which adjacent plant cells communicate. They are about 50 nm in diameter and provide a direct passageway for the intercellular transport of diffusible factors (e.g. metabolites, certain hormones, ions), and macromolecules (Lucas and Wolf 1993; Kragler et al. 1998; Cantrill et al. 1999; Heinlein 2002; Heinlein and Epel 2004; Kragler 2013). The PD provide both cytoplasmic as well as membrane continuity between adjacent cells. The plasma membrane (PM) delimits the PD channel against the surrounding cell wall and a thin tubule of the endoplasmic reticulum (ER) (the “desmotubule”) extends through the center of the channel (Ding et al. 1992)(see Figure 1). The cytoplasmic space (also referred as the “cytoplasmic sleeve”) between the PM and the desmotubule is thought to represent the major pathway for intercellular molecular trafficking. The size of this space determines the size exclusion limit (SEL) of PD, thus the maximal size of molecules that can be transported through this channel. The PD SEL is under tight

control and dynamically regulated to control PD permeability. Thus, in allowing multicellularity, the PD also act as important gatekeepers permitting or restricting the cell-to-cell trafficking of informational macromolecules in response to intrinsic and extrinsic signals, thereby playing a crucial role during plant development and immunity against pathogen attack (Lee and Lu 2011; Lee 2014; Sager and Lee 2014; Tilsner et al. 2016; Brunkard and Zambryski 2017; Cheval and Faulkner 2018; Sager and Lee 2018).

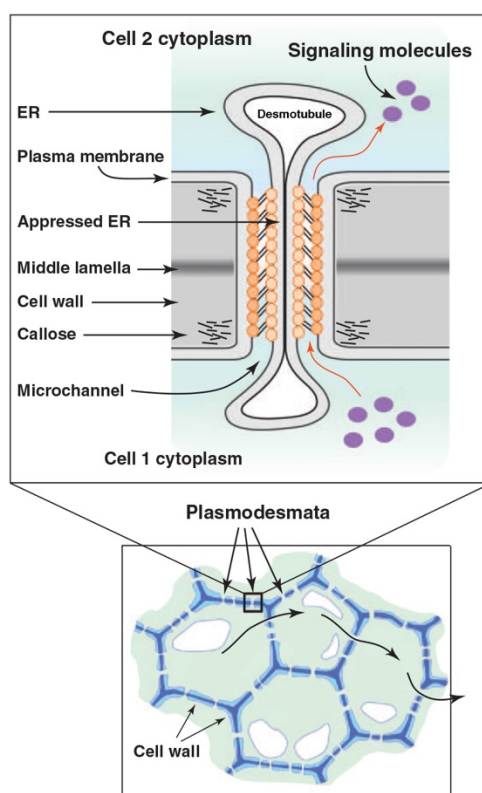


Figure 1: Schematic illustration of plasmodesmata (PD)

Ultrastructure and cell-to-cell trafficking of diffusible signalling molecules (modified from Lee et al. 2011). The SEL of PD is regulated primarily by the degree of callose deposition in the cell wall near the PD neck regions. In addition, the SEL may also be regulated by proteins that tether the ER to the plasma membrane (orange-yellow spheres and short rods) and may regulate the size of the cytoplasmic sleeve between these membranes.

The mechanism regulating PD SEL is not clearly resolved today, but appears to involve alterations in Calcium (Ca^{2+}) levels, the redox state within the cell, and phytohormones. The major mechanism by which the SEL is increased or decreased involves the deposition and degradation of callose in the cell walls around the neck regions of PD (Olesen and Robards 1990; Iglesias and Meins 2000; Bucher et al. 2001; Radford and White 2001). The deposition of callose by callose-synthase (CalS) reduces PD SEL by moving the PM closer to the desmotubule (Olesen and Robards 1990; Simpson et al. 2009;

Gui et al. 2014; Grison et al. 2015), whereas the degradation of callose deposits by β -(1.3)-Glucanase (BGs) increases the PD SEL by increasing the size of the cytoplasmic sleeve (Iglesias and Meins 2000; Bucher et al. 2001; Radford and White 2001; Levy et al. 2007). Upstream to callose synthesis, Ca^{2+} , has been found to regulate intercellular communication by closure of PD in staminal hairs of *Setcreasea purpurea* (Tucker 1990). During PD closure, Ca^{2+} may function as a putative regulator of CalS (Andrawis et al. 1993). Callose deposition at PD is also induced by the accumulation of reactive oxygen species (ROS), which are known to take part in regulating development and pathogen responses (Bolwell et al. 2002; Pitzschke et al. 2006; Torres 2010). ROS accumulation increases callose deposition at PD (Benitez-Alfonso and Jackson 2009; Benitez-Alfonso et al. 2010) and influences the abundance of Ca^{2+} (Bolwell et al. 2002; Foreman et al. 2003). It seems that a ROS- Ca^{2+} activation system is able to trigger callose deposition at PD but the underlying mechanism is still unknown (Benitez-Alfonso et al. 2011; De Storme and Geelen 2014; Tilsner et al. 2016). PD are associated with numerous proteins implicated in regulating PD permeability such as different receptor kinases involved in the sensing of pathogens and developmental signals, the PD-located Protein (PDL) family of proteins, and callose-binding proteins (PDCBs). Moreover, the desmotubule may be associated with Ca^{2+} -sensitive proteins that tether the desmotubule to the PM and control the size of the cytoplasmic sleeve by varying tether length in response to Ca^{2+} (Tilsner et al. 2016; Sager and Lee 2018).

1.2. TMV and ORMV infection

ORMV, also known as *Youcai mosaic virus* or *Chinese rape mosaic virus* (Aguilar et al. 1996), is an *Arabidopsis*-infecting tobamovirus. Compared to TMV, the 3' Untranslated Region (UTR) of ORMV is longer than in TMV and differences exist between the viruses in the overlap of movement protein (MP) and coat protein (CP) open reading frames (ORFs). *Tobamoviruses* have been classified into different subgroups according to the sequence location of their origin of virion assembly (OAS) (Fukuda et al. 1981; Gibbs 1986). The OAS is the viral RNA region used to target and initiate particle assembly by forming aggregates of CP in the form of discs leading to the formation of virions. ORMV and TMV differ in the host range in which they cause disease. Whereas ORMV efficiently infects and causes symptoms in *Cruciferae* plants such as *Arabidopsis*, TMV and the highly homologous *Tomato mosaic virus* (ToMV) efficiently infect and cause symptoms in *Solanacea* plants such as tobacco, tomato and pepper (Melcher 2003; Cai et al. 2009). TMV and ORMV have a positive-sense ssRNA genome of about 6300 nt in length. The viral RNA is capped at the 5' end and forms a tRNA-like structure at the

3' end (see Figure 2). The TMV and ORMV genomes contain three major ORFs. The first ORF encodes two subunits of the replicase (126k/183k for TMV; 125k/182k for ORMV), whereby the larger subunit is produced by translational read-through of an amber-stop codon. The shorter protein contains 5' methyltransferase and helicase domains, whereas the longer protein in addition contains an RNA-dependent RNA polymerase (RDR) domain (Beier et al. 1984).

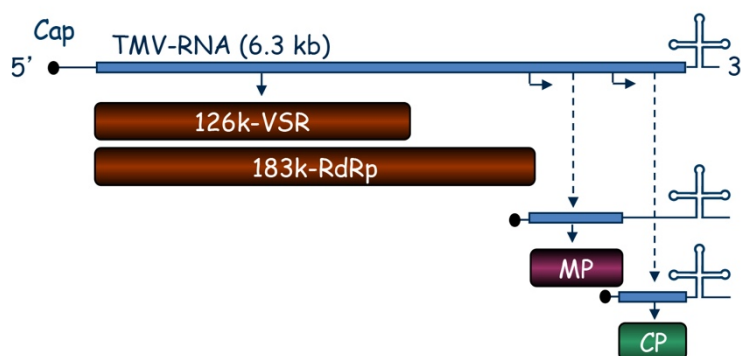


Figure 2: The RNA genome of TMV and encoded proteins

The RNA genome of TMV is capped at its 5' end and forms a tRNA-like structure at the 3' end. The RNA encodes four proteins, the large 183 kDa (183k-RdRp) and small 126 kDa (126k-VSR) subunits of the replicase, the 30 kDa movement protein (MP), and the 17.5 kDa coat protein (CP). The large 183 kDa replicase subunit is produced by read-through of an amber stop codon that terminates the translation of the short subunit. The two replicase subunits interact *in vivo*. Whereas the large subunit contains an RNA-dependent RNA polymerase domain and is sufficient for replication of viral RNA, the small subunit has Viral Suppressor of RNA silencing (VSR) activity and increases viral replication efficiency.

The small replicase subunit has VSR activity and suppresses antiviral RNA silencing by sequestration of small RNA duplexes, thereby interfering with small RNA loading into the RNA-induced silencing complex (RISC) (Kubota et al. 2003; Ding et al. 2004; Csorba et al. 2007; Vogler et al. 2007). The replicase subunits are translated from the viral RNA that enters the cell whereas the MP and CP encoded by the two remaining ORFs are translated during viral replication from sub-genomic RNAs. The 30 kDa MP is required for the cell-to-cell spread of the virus and was the first protein known to facilitate virus movement (Deom et al. 1987; Holt and Beachy 1991). Studies on this prototype MP revealed that this protein targets PD and triggers an increase in the PD SEL (Wolf et al. 1989). This activity has been correlated with a reduction in callose-deposition in the PD neck regions (Ueki et al. 2010) and may involve a direct or indirect interaction of MP with a callose-degrading BG (Zavaliev et al. 2013). The MP interacts with ER membranes and microtubules (MTs) (Heinlein et al. 1995; Heinlein et al. 1998; Reichel and Beachy 1998; Ashby et al. 2006; Ferralli et al. 2006; Fujiki et al. 2006; Peiro et al. 2014) and plays fundamental roles in the anchoring of viral replication complexes (VRCs) at distinct, MT-associated, cortical ER sites (Boyko et al. 2000a,b; Niehl et al. 2013b; Peña

and Heinlein 2013; Heinlein 2015). According to current models, which are also described in the attached review by Pitzalis and Heinlein (2017), infection starts when the mechanically transmitted virion is uncoated and the free viral RNA (vRNA) binds to the ER via its 5'CAP (Christensen et al. 2009). Subsequently, the replicase, which is translated from the vRNA, binds to the 5'UTR for replication (Kawamura-Nagaya et al. 2014). The MP, which then also becomes translated, anchors the ER-associated VRCs to MT. The MT-associated ER sites (also called "cMERs") are proposed to be equivalent to cortical sites of MT-associated, stable ER proposed to function as hubs for membrane trafficking and exchange/delivery of membrane cargo (Niehl et al. 2013b; Peña and Heinlein 2013; Heinlein 2015), through which the VRCs may recruit membranes and host factors. For example, the host proteins TOBAMOVIRUS MULTIPLICATION (TOM) 1, 2a and 3 are involved in the formation of VRCs (Ishibashi et al. 2010). Detachment of the VRCs allows their trafficking along the ER, which is continuous through PD (Ding et al. 1992) and provides a direct route for cell-to-cell movement. MP-containing VRC particle movements along the ER occur in a stop-and-go fashion and are guided by MT (Boyko et al. 2007; Niehl et al. 2013b; Peña and Heinlein 2013; Niehl et al. 2014; Heinlein 2015). The ER membrane is tightly associated with actin filaments and numerous studies demonstrated the role of myosin motor proteins in ER motility and the transport of organelle and membrane cargo along the ER-actin network (Boevink et al. 1998; Avisar et al. 2008; Peremyslov et al. 2008; Prokhnevsky et al. 2008; Sparkes et al. 2008; Sparkes et al. 2009; Ueda et al. 2010; Griffing et al. 2017). Consistently, it was shown that the intra-and intercellular movement of the MP-containing particles along the ER as well as the intercellular spread of TMV infection depend on actin and specific class VIII and class XI myosins (Wright et al. 2007; Sambade et al. 2008; Harries et al. 2009; Hofmann et al. 2009; Amari et al. 2014). Thus, VRC movement occurs along the ER while MTs initially anchor VRCs at specific ER sites and guide their movements along the ER-actin network (Niehl et al. 2013b; Peña and Heinlein 2013; Heinlein 2015; Pitzalis and Heinlein 2017). However, not all of the early VRCs are mobile. Instead most of them remain stationary and grow over time to become viral factories.

During these later stages of infection also the 17.5 kDa CP is produced and encapsidates replicated vRNA. The rod-shaped TMV particle contains 2130 CP subunits (Dunigan et al. 1988) and provides stable protection of the viral genome until the virus is mechanically transmitted to a new host. The CP is dispensable for viral cell-to-cell movement but plays a yet unknown role in the long distance spread of infection via the vascular phloem (Saito et al. 1990; Holt and Beachy 1991; Hilf and Dawson 1993).

The MP of ORMV associates with MT-associated ER sites like the MP of TMV and is proposed to support ORMV movement by mechanisms similar to the model described for TMV above. However, unlike the MP of TMV, the MP of ORMV is expressed at a lower level and does not accumulate in viral factories and along MTs to a level seen with the MP of TMV (Niehl et al. 2014). The observation that the MP of TMV accumulates in viral factories and along MT before it is degraded during late stages of infection was a motivation for studies showing that the MP is a MT-associated protein (MAP) able to bind directly to the MT surface (Ashby et al. 2006) and for addressing the mechanism of MP turnover. During infection, the MP becomes polyubiquitylated and degraded by the 26S proteasome (Reichel and Beachy 2000). Interestingly, the MP fraction that accumulates along MTs during late infection is not ubiquitylated (Ashby et al. 2006). Consistently, it was shown that the degradation of MP depends on CELL DIVISION CYCLE 48 (CDC48), a triple A (AAA) ATPase (these ATPases are machines that use ATP hydrolysis to exert force on macromolecules for unfolding and translocation) that interacts with MP and extracts the protein from the ER (Niehl et al. 2012). CDC48 substrates are de-ubiquitylated before extraction from the ER and become re-ubiquitylated before degradation by the proteasome (Ernst et al. 2011; Tsai and Weissman 2011). This suggests the hypothesis, that ubiquitylated MP is de-ubiquitylated and then extracted from MT-associated ER-localized virus factories by CDC48. Once present in high amounts in the cytoplasm, the MP aligns along MT according to its intrinsic MAP activity before it is re-ubiquitylated and degraded by the proteasome (Niehl et al. 2012; Niehl et al. 2013a). More recent studies indicate that the MP is also a target of deubiquitylation (DUB) enzymes (Niehl et al. unpublished), which is consistent with this model.

1.3. TuMV infection

TuMV belongs to the Potyvirus family, the second largest plant virus family after *Geminiviridae* (Ivanov et al. 2014), and is among the most damaging plant viruses worldwide (Tomlinson 1987; Nguyen et al. 2013; Yasaka et al. 2015). Potyviruses give rise to different types of symptoms such as yellow mosaic patterning, leaf tip necrosis, or the formation of black necrotic ring spots, and can cause growth inhibition and strong seed losses (Tomlinson et al. 1970 ; Hull 2014; Kenyon et al. 2014). TuMV infects a wide range of 318 species in 156 genera of 43 families. Among the hosts are wild and cultivated *Brassica* species, in which it causes different types of symptoms, seed losses, and even plant death (Tomlinson et al. 1970; Walsh and Tomlinson 1985; Tomlinson 1987; Edwardson and Christie 1991; Moreno and Fereres 2012).

The filamentous viral particles of potyviruses contain a positive-sense, single-stranded (ss)RNA genome of 10 kb. Following transmission and entry of the filamentous virions into the host cell by the stylet of aphids, the vRNA is uncoated and translated into a single polyprotein (Carrington et al. 1989; Nicolas and Laliberté 1992), which is then processed into eleven proteins by virus-encoded proteolytic cleavage. The vRNA carries a genome-linked viral protein (VPg) at its 5' end and is 3' poly-adenylated. Processing of the virus-encoded polyprotein leads to the production of the Protease P1, the Helper Component Proteinase (HcPro), the Protease P3, the two 6 kDa proteins 6K1 and 6K2, a cylindrical inclusion CI protein, the VPg, the cysteine protease NIa-Pro, the nuclear inclusion b (NIb; RDR), the CP, and the P3-“Pretty Interesting Potyviral ORF” Protein (P3-PIPO), which is produced as a trans-frame fusion to the amino terminus of P3 (P3N-PIPO) (Vijayapalani et al. 2012). Seven of the nine polyprotein cleavages are processed by NIa-Pro, whereas the two remaining cleavages occur by cis-cleavage by the P1 and HcPro proteases at their own C-terminal end (Carrington et al. 1989; Verchot et al. 1992). The vRNA is used for both translation and replication but the exact process of replication in potyviruses is still unclear. P3, VPg, NIa-Pro, NIb, 6K2, Hc-Pro, vRNA and double-stranded viral RNA (dsvRNA) are present in VRCs (Schaad et al. 1997; Li et al. 1997; Haldeman-Cahill et al. 1998; Fellers et al. 1998; Thivierge et al. 2008; Cui et al. 2010; Wei et al. 2010a; Ala-Poikela et al. 2011). Translation and replication are closely linked and occur in association with the ER membrane (Martin et al. 1995; Schaad et al. 1997). During infection the ER produces organelle-like vesicles that function as compartments for potyviral replication (Wei et al. 2010a). Each vesicle originates from a single translated genome into which viral proteins are also translated (Cotton et al. 2009). The replication protein 6K2 is found also in larger, perinuclear compartments derived from the ER (Schaad et al. 1997). These structures are functionally linked to the production of 6K2 vesicles and their trafficking to the cortical ER via transvacuolar strands (Grangeon et al. 2012). The 6K2 protein was shown to colocalize with the ER exit site (ERES) proteins Sar1, Sec23, and Sec24. Disruption of the two major coating machineries involved in ER-Golgi trafficking, the coat protein complex I (COPI) and COPII, led to reduced accumulation of 6K2 at ERES, smaller sizes of infection foci on leaves, and reduced TEV-GFP fluorescence, thus supporting the importance of ER-Golgi trafficking for efficient infection (Wei and Wang 2008). After accumulation at ERES and transport via the COPI/II Golgi early secretory pathway, the VRC-containing vesicles are transported along actin microfilaments to chloroplasts using a myosin XI-K and XI-2-dependent mechanism (Wei et al. 2010a; Agbeci et al. 2013). The presence of these vesicles at chloroplasts is indicated by the observation of 6K2 protein aggregates and the formation of membrane

invaginations at the chloroplast envelope (Cotton et al. 2009; Wei et al. 2010a). Experiments involving the down-regulation of Syp71, a component of the Soluble N-ethyl-maleimide-sensitive-factor Attachment protein REceptor (SNARE) complex involved in vesicle-membrane fusion, indicated that the fusion of the VRC-containing vesicles with the chloroplast membrane is essential for successful viral infection (Wei et al. 2013). Thus, potyvirus replication occurs within chloroplasts as well as on the ER. While the formation of the ER-derived vesicles and their trafficking to chloroplast is not absolutely essential for virus replication, the formation and trafficking of the vesicles is nevertheless necessary for virus cell-to-cell movement. Yeast two-hybrid and co-immunoprecipitation experiments coupled to deletion mapping and site-specific mutagenesis indicated that the formation of the mobile ER-derived vesicles require the N-terminal soluble domain of 6K2, which interacts with Sec24a, a COPII coatomer component. Mutations in the 6K2 N-terminus that interfere with vesicle formation still allowed virus replication but abolished virus cell-to-cell movement. Moreover, TuMV systemic movement was delayed in an Arabidopsis mutant defective in Sec24a (Jiang et al. 2015). Thus, the motile ER-derived 6K2 vesicles contribute to the distribution and propagation of viral replication centers in the infected cell and are essential for transporting the infectious viral RNA into the neighboring cells (see Figure 3). Consistent with their role in virus movement, the 6K2 vesicles are also transported to PD and can move cell-to-cell (Grangeon et al. 2013). However, the mechanism of movement through the PD is still unclear. Unlike most other viruses, potyviruses do not encode a designed MP. Instead many viral proteins have been reported to have MP-related functions. HcPro and the CP can increase the SEL of PD (Rojas et al. 1997). In addition, CP and the cylindrical inclusion (CI) protein are required for virus intercellular movement (Dolja et al. 1994; Dolja et al. 1995; Carrington and Whitham 1998). CI was shown to associate with PD and to produce conspicuous conical structures that extend through PD (Rodriguez-Cerezo et al. 1997; Roberts et al. 1998). CI targets PD through interaction with P3N-PIPO (Wei et al. 2010b), which itself is targeted to the PM through an interaction with the host protein PCaP1 (Vijayapalani et al. 2012). However, how the 6K2-associated vesicles that contain the viral RNA interact with these potyvirus-induced movement structures for movement through PD is still not known. Nevertheless, a recent study demonstrated that the intercellular movement of 6K2 vesicles depends on the interaction of 6K2 with CI. Thus, CI structures at PD may act as a docking point for 6K2 vesicles destined for intercellular transport (Movahed et al. 2017).

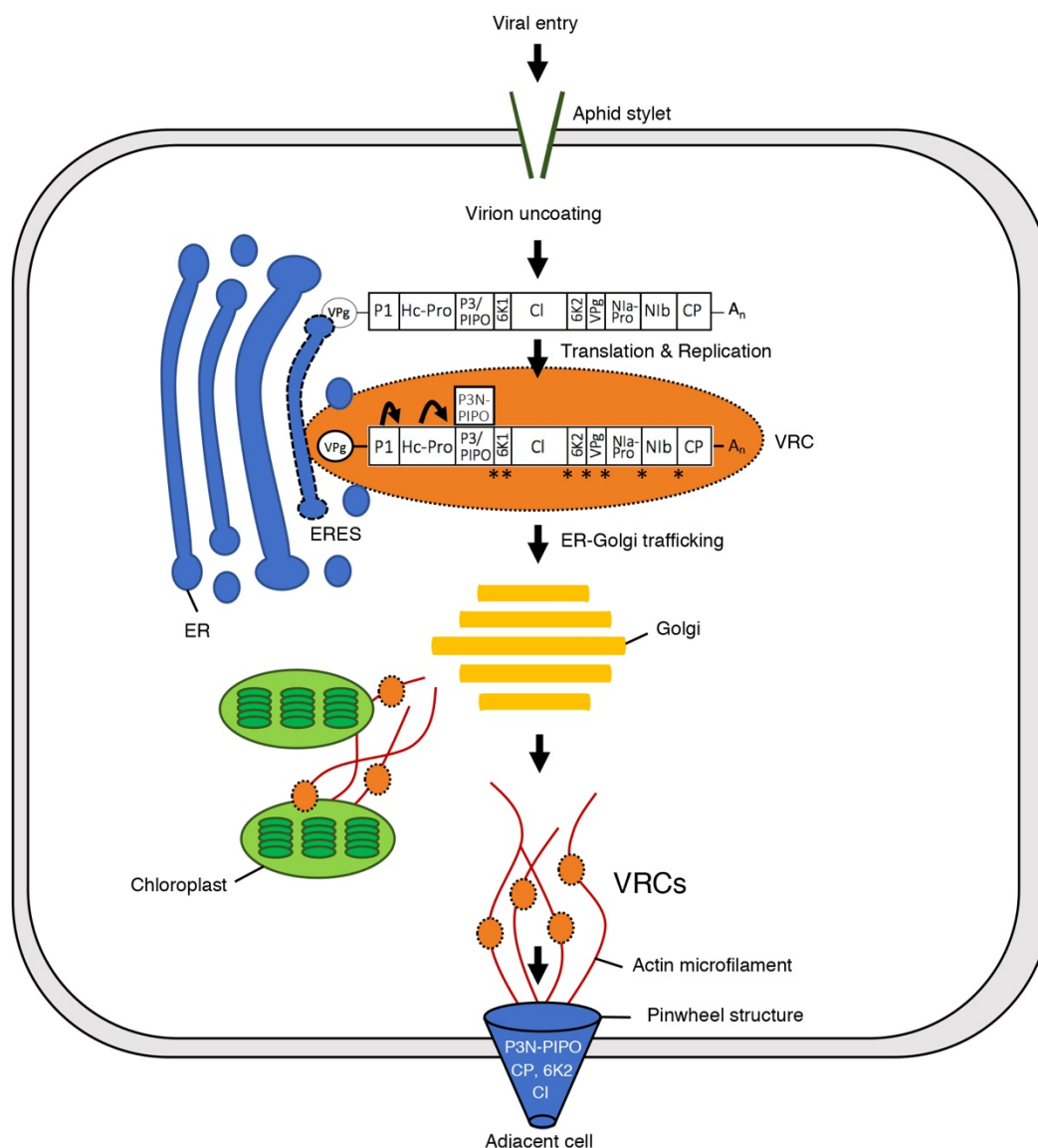


Figure 3: Potyvirus infection

The filamentous particle is uncoated, and the viral RNA is translated and replicated. Viral replication and production of viral replication complexes (VRCs) take place close to the ER at ER-exit sites (ERES). VRC-containing vesicles move along actin microfilaments to chloroplasts and also to pinwheel structures formed at PD for cell-to-cell movement.

Although viruses are generally believed to move their genomes over long-distances into other leaves via the phloem, GFP-tagged 6K2 vesicles were observed in xylem vessels as well as in phloem sieve elements of infected plants (Wan et al. 2015). The authors suggest that the 6K2 vesicles may enter into immature xylem vessels and replicate in the cytoplasm and then move upward in the plant before programmed cell death occurs and the xylem becomes a hollow vessel. It would be interesting to see by which mechanism the vesicles can enter and exit the xylem. It has been observed that membrane-impermeant fluorophores such as carboxyfluorescein-diacetate (CFDA) and also much larger Texas Red-labeled dextran (10 kD) molecules unload from xylem via the xylem

vessel-xylem parenchyma pit membranes, potentially by endocytosis (Botha et al. 2008). Such pathway may also be used by TuMV, since 6K2 was observed in xylem parenchyma cells. Several other cases where virus particles or components were found in xylem have been reported previously (Andrianifahanana et al. 1997; Opalka et al. 1998; French and Elder 1999; Ding et al. 2001; Verchot et al. 2001; Moreno et al. 2004; Betti et al. 2012; Manabayeva et al. 2013). Thus, several systems are available that may ultimately challenge the stronghold model that systemic virus movement occurs strictly via the phloem.

The attached review article by Pitzalis and Heinlein (2017) provides an overview about the major pathways used by plant viruses for their cell-to-cell movement. As described in detail above, TMV exemplifies a pathway that targets PD and spreads into adjacent cells by movement of mobile VRCs along the ER-actin network. Since this network is continuous through PD into adjacent cells, this type of movement may not require a specific docking mechanism at PD but certainly depends on a MP or other proteins with MP-related functions able to modify the gating function of PD in order to allow VRC movement through the channel. This pathway of virus movement is in contrast to the pathway used by viruses that move cell-to-cell in the form of whole virion particles. To allow whole virion movement, some of these viruses were shown to cause strong structural alterations in PD structure by replacing the centrally located desmotubule by a tubule-like structure assembled by viral MP. Tubule assembly by these “tubule-forming” viruses and their intercellular movement depend on members of the PDLF family that act as docking point for tubule-forming MPs at PD (Amari et al. 2011). To allow virion movement through the tubule, the tubule-guided movement mechanism usually depends on an interaction between MP and CP. The tubule-guided movement mechanism also depends on the secretory pathway which is required for targeting PDLF to PD. As described above, potyviruses use a special mechanism for movement that neither fits to the tubule-guided mechanism, nor to the non-tubule-guided mechanism used by TMV.

The review article by Pitzalis and Heinlein (2017) continues to further discuss the roles of the ER-Golgi secretory pathway in virus infection and then focusses on the roles of myosin motor proteins, particularly on class VIII myosins. These plant-specific motor proteins were shown to be essential for efficient TMV movement and function in the targeting of the MP to PD (Amari et al. 2014). Myosin VIII proteins also have been localized to PD (Reichelt et al. 1999; Baluska et al. 2001; Golomb et al. 2008; Haraguchi et al. 2014). The potential function of myosin VIII is discussed together with the potential roles of the synaptotagmin SYT1/SYTA. This protein is a target of MP (Lewis and

Lazarowitz 2010; Uchiyama et al. 2014; Levy et al. 2015) and is supposed to act as a tether protein that links the ER to the PM at ER-PM contact sites. Both class VIII myosin and SYT1/SYTA are discussed as potential components of ER-PM contact sites within PD and at the cortical ER sites at which viruses like TMV set up their replication complexes. The PD is proposed to contain ER-PM contact sites because of the very close apposition of ER and PM along the length of the PD channel (Tilsner et al. 2016). Although the SEL of PD is regulated by deposition and removal of callose in the PD neck regions, the SEL may also be regulated by myosin VIII and synaptotagmin as ER-embedded proteins that may tether the ER to the PM and determine the size of the cytoplasmic sleeve by regulating their tether length. Hypothetical models are presented to explain how MP could modify the PD SEL through interaction with these tether proteins. The two mechanisms are not mutually exclusive and may instead complement each other in regulating PD. Whereas tether contraction may allow rapid and short-term PD regulation to control trafficking of individual molecules (e.g. virus) between individual cells or groups of cells, the enzymatic changes in callose levels in the cell walls surrounding the PD may allow the plant to change PD conductivity over the longer term and thus to respond more persistently to developmental or environmental cues. The observation that the MP of TMV increases the SEL of PD only transiently during infection (Oparka et al. 1997) and also the reported molecular interaction of MP with SYT1 (Lewis and Lazarowitz 2010; Uchiyama et al. 2014; Levy et al. 2015; Ishikawa et al. 2018; Yuan et al. 2018) support the model that MP alters PD SEL through manipulating SYT1 tether length in PD. The regulation of PD SEL by membrane tethering proteins is in agreement with the ability of PD to regulate their SEL in response to Ca^{2+} (Tucker and Boss 1996) as Ca^{2+} concentration influences tether length as shown for mammalian Syt-1 (Fernandez-Busnadiego et al. 2015). Thus, MP may change the SEL of PD through direct interactions with the tether proteins or rather indirectly by causing changes in the local concentration of Ca^{2+} within the channel.

The article then continues to discuss the possibility that ER-PM contact sites may represent the primary target of viral MP. This idea comes from the fact that ER-PM contact sites are associated with ER-actin and MT, thus cellular components that also coincide at the cortical MT-associated ER sites at which TMV forms mobile VRCs with the help of MP. It is proposed that the MP may target (i) SYT1 localized at MT-associated ER sites to establish mobile VRCs and (ii) SYT1 localized at PD to modify SYT1 tether length to allow the mobile VRCs to move through PD. However, this model is highly speculative and must be addressed by further experimentation before conclusions can be

drawn. Nevertheless, a recent publication supports this model by showing that SYTA binds to the N-terminal region of MP and stabilizes the interaction of MP with PD (Yuan et al. 2018).

PITZALIS AND HEINLEIN 2017. THE ROLES OF MEMBRANES AND ASSOCIATED CYTOSKELETON IN PLANT VIRUS REPLICATION AND CELL-TO-CELL MOVEMENT. J EXP BOT 69, 117-132.

Chapter II: RNA silencing and role of small RNAs

1. Introduction

Virulence comes from the Latin “*virulentus*” and associates “*vīrus*” (poisonous liquid) and “*ulentus*” (full of). It defines the capacity of a pathogen to accumulate in the host. To do so, the host must provide the cellular mechanisms and the host factors the pathogen requires for propagation. The lack of any such factors reduces the ability of the pathogen to be virulent and is at the basis of host recessive resistance. In addition, the pathogen must have evolved the capacity to efficiently interact with these host mechanisms and host factors. Moreover, to propagate efficiently, the pathogen should be able to overcome the host defense mechanisms. To protect themselves against invading pathogens, hosts have evolved the ability to recognize conserved molecules associated with the presence of pathogens (e.g. with pathogen-recognition receptors) and to raise different defense layers such as Pattern-Triggered Immunity (PTI) and the expression of defense-related genes, or RNA silencing. To break these barriers, pathogens have evolved effector proteins that interfere with these defense pathways by various mechanisms. In some hosts this has led to the evolution of resistance genes triggering Effector Triggered Immunity (ETI), which finally often initiate a hypersensitive response upon recognition of the pathogen effector, or of its activity, leading to the death of the infected cell. In these hosts, the pathogen has lost its virulence and is “avirulent”, and the gene of the pathogen that encodes the effector, which is recognized by the protein encoded by the host resistance gene, is referred to as the “avirulence gene” (“Gene-for-gene” resistance).

In comparison to bacteria and fungi, viruses encode only a limited number of proteins (see Chapter I). Most of them associate with host mechanisms for replication as well as for intercellular and systemic spread of their infectious genomes, whereas other specific proteins act as effectors to suppress host defense. Only since recently, it is known that plant viruses can trigger PTI (Kørner et al. 2013; Niehl et al. 2016; Nicaise and Candresse 2017) and only few effectors of some viruses able to suppress PTI have been identified so far (Gouveia et al. 2017; Nicaise and Candresse 2017; Kong et al. 2018).

However, the major defense response controlling the accumulation of viruses in infected plant cells is RNA silencing, which relies on the production of small 21-24 nt long siRNAs and microRNAs (miRNAs) that associate with an ARGONAUTE (AGO) protein-containing RNA-induced Silencing Complex (RISC) to target viral and host RNAs for cleavage or translational repression in a target sequence-specific manner (Bologna and Voinnet 2014). Viruses encode effector proteins that

suppress RNA silencing (VSR) (Csorba et al. 2015) and Arabidopsis mutants affected in DICER-Like (DCL) and other RNA silencing pathway genes showed enhanced susceptibility (Mourrain et al. 2000; Morel et al. 2002; Bouché et al. 2006; Deleris et al. 2006), thus indicating the importance of RNA silencing in antiviral defense and plant-virus co-evolution (Pumplin and Voinnet 2013). However, the role of RNA silencing in plant:virus interactions may be more complex as it targets both the virus and its host. For example, it is conceivable that similar to certain mammalian DNA viruses (Herpesviridae) (Hook et al. 2014) and plant-pathogenic fungi (Weiberg et al. 2013), also plant viruses may have evolved the ability to hijack the host RNA silencing pathway with their own small RNAs in order to modulate host gene expression.

To further explore the function of small RNAs (sRNAs) during plant:virus interactions, we have used next-generation RNA profiling technologies and specific gene analysis to address the function of sRNAs accumulating during early TuMV infection in leaves of oilseed rape (*Brassica napus*). As described in the attached draft manuscript by Pitzalis et al., this work led to the identification of a whole network of host- and virus-derived sRNAs correlated with specific host mRNA and viral RNA cleavage events during infection. The observations indicate that viruses and their hosts exchange multiple sRNA signals for mutual control and regulation.

The attached draft manuscript (Pitzalis et al.) and also Chapter III mention numerous components of different RNA silencing pathways, which are briefly explained in the following paragraphs.

2. RNA silencing pathways and their components

RNA silencing relies on pathways that involve the production of 21-24 nt long sRNAs from double-stranded sRNA precursor molecules by DICER enzymes [DICER-Like (DCL), in plants]. Upon cleavage of dsRNA into 21-24 nt sRNA duplexes, one strand of a given duplex associates with an AGO family protein within RISC and guides this complex for sequence-specific, AGO-mediated, slicing or translational repression of the corresponding target transcript (Hammond et al. 2000; Zamore et al. 2000). The endogenous dsRNA molecules that function as substrates for DCL enzymes can originate from transcripts of dedicated miRNA (MIR) genes able to fold into hairpin structures, or can represent long dsRNA molecules produced by transcription of inverted repeat loci, the alignment of overlapping transcripts produced from opposite strands of DNA, or the activity of viral or endogenous RDR that convert single stranded (ss) RNA molecules into dsRNA molecules. Unlike the miRNAs that are encoded by MIR genes, the sRNAs that are derived from DCL processing of long

dsRNA precursors are referred to as siRNAs. The RISC-mediated cleavage of viral RNA or of mRNA transcripts of transgenes can be amplified by RDR enzymes by conversion of the RNA cleavage fragments into new dsRNA, thereby providing new dsRNA template for the production of “secondary sRNAs” that again target the same transcript or viral RNA. This process involves “transitivity”, which describes the fact that the secondary siRNAs involved in secondary silencing are different from the siRNA that caused the initial cleavage event and map to the target transcript to sites adjacent to the original siRNA (Dalmay et al. 2000; Himber et al. 2003). An interesting and important feature of siRNAs and of some miRNAs is their intercellular and systemic mobility through PD (Vatén et al. 2011) and phloem by which they coordinate abiotic and biotic stress responses across the plants (Buhtz et al. 2008; Molnar et al. 2010; Brosnan and Voinnet 2011; Melnyk et al. 2011; Zhang et al. 2014; Borges and Martienssen 2015; Lewsey et al. 2016). The systemic mobility of siRNAs and the systemic silencing of their targets is supported by the increased level of target-specific siRNAs produced by RDR-dependent secondary siRNA production (Himber et al. 2003). The *A. thaliana* genome encodes four DCLs (DCL1 to DCL4), ten AGOs (AGO1 to AGO10) and six RDRs (RDR1 to RDR6) (Vazquez 2006) that function in different RNA silencing pathways.

2.1. Role and function of DCL proteins

DICER proteins are ribonucleases that belong to the RNase III (also called RNase C) family. Initially found in *Escherichia coli* (Chen et al. 1990), they were later found to be present and conserved also among flies, plants, fungi and mammals (Bernstein et al. 2001). The DCL proteins in Arabidopsis were originally identified as SIN1/SUS1/CAF and were then re-named because of their similarity to DICER proteins in *Drosophila* and *Coenorhabditis* (Schauer et al. 2002). For example, the *A. thaliana* DCL1 was shown to share with DICER1 proteins of *S. pombe*, *C. elegans*, *D. melanogaster*, *Mouse* or *Human* species the DExD/H-Box RNA helicase (DEAD-box) and helicase-C domains both used for unwinding secondary RNA structures (Tanner and Linder 2001), a Domain of Unknown Function 283 (DUF283), which may help for targeting helper proteins (Qin et al. 2010), a PIWI/ARGONAUTE/ZWILLE (PAZ) domain used as a binding module able to recognize the 3' end of sRNAs (Song et al. 2003), two catalytic RNase III domains, and one or two dsRNA-binding domain (dsRBD) important for sRNA binding and miRNA accumulation (Schauer et al. 2002; Margis et al. 2006; Chapman and Carrington 2007; Bologna and Voinnet 2014) (see DCLs, Figure 4).

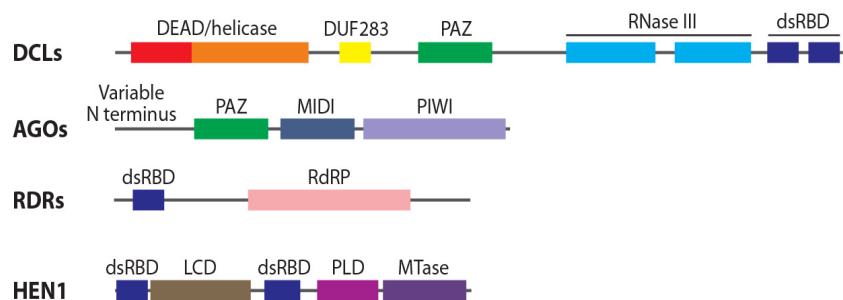


Figure 4: Conserved domain organization of RNA silencing pathway proteins (modified from Bologna and Voinnet 2014).

Whereas DCL1 is predominantly involved in the processing of 21-24 nt miRNAs from miRNA precursors transcribed from MIR genes (Reinhart et al. 2002), DCL2 and DCL4 target long dsRNA molecules and produce 22 and 21 nt long siRNAs, respectively. They play a major role in antiviral silencing in *Arabidopsis* (Akbergenov et al. 2006; Blevins et al. 2006; Deleris et al. 2006) by cleaving viral dsRNA, which is produced by the viral RDR (replicase) during viral replication, into viral siRNAs (vsiRNAs). DCL1 and DCL4 [and an additional DCL5 in rice (previously called DCL3b)] are involved together in the biogenesis of 21-24 nt trans-acting small interfering RNAs (tasiRNAs) and phased small interfering RNAs (phasiRNAs), derived from long dsRNAs produced by RDR6 and/or RDR1 from transcripts encoded by TAS and PHAS loci (Peragine et al. 2004; Vazquez et al. 2004; Song et al. 2012). DCL2 functions as a surrogate for DCL4 function in producing vsiRNAs (Gascioli et al. 2005) and was shown also to stimulate transitive secondary siRNA production together with RDR6 (Parent et al. 2015). DCL3 has a central function in transcriptional gene silencing (TGS) by processing 24 nt long siRNAs from dsRNA molecules generated by RDR2 from RNAs transcribed by RNA polymerase VI (POL IV) from intergenic or repetitive regions, transposons, and other loci undergoing RNA-dependent DNA methylation (RdDM) (Xie et al. 2004; Henderson et al. 2006; Pontes et al. 2006; Matzke et al. 2009; Blevins et al. 2015).

2.2. Role and function of AGO proteins

The AGO proteins are highly conserved among organisms (Carmell et al. 2002) and represent the main RNA silencing effectors by acting as the “slicers” of the RISC complex (Fang and Qi 2016). AGOs are RNase H-like enzymes containing a variable N-terminal domain and a conserved RNA-binding PAZ (for PIWI, AGO, and Zwiille), MID (middle) domain able to recognize the 5' nucleotide of sRNAs, and PIWI domains able to correctly position the RNAs relative to their target and to perform double

stranded-RNA-guided hydrolysis of ssRNA (Song et al. 2004; Wang et al. 2009; Wei et al. 2012) (see AGOs, Figure 4). The number of AGO proteins ranges from 1 AGO in *S. pombe* to 27 AGOs in *C. elegans*. The different AGO proteins share similarities but not all share slicing activity functions. For example, most miRNAs and their associated AGOs in animals function in translational repression rather than cleavage because of limited complementarity with the target RNA in the sRNA seed region (nucleotide 2 to 7) (Lewis et al. 2003; Lewis et al. 2005; Bhattacharyya et al. 2006; Mallory and Vaucheret 2010). The functions of the 10 AGO proteins in *Arabidopsis* have been reviewed in detail (Bologna and Voinnet 2014; Zhang et al. 2015). Although translational repression is also observed in plants and involves miRNA- and siRNA-guided AGO1 and AGO10 (Brodersen et al. 2008), slicing appears to be the dominant activity of AGO proteins in plants (Song et al. 2004) and has been experimentally demonstrated for *Arabidopsis* AGO1, AGO2, AGO7, and AGO10 (mediating PTGS) and AGO4 (mediating TGS) (Zhu et al. 2011; Carbonell et al. 2012; Manavella et al. 2012). miRNAs are loaded into AGO1, AGO2, AGO7 and AGO10 to guide mRNA target cleavage during stress responses, plant development, and antibacterial immunity (Baumberger and Baulcombe 2005; Montgomery et al. 2008). AGO1 also acts as an effector for tasiRNA production and function (see paragraph 3.2), and also mediates antiviral silencing upon loading with 21 and 22 nt vsiRNAs produced by DCL4 and DCL2, respectively (Pumplin and Voinnet 2013). AGO1 is associated with endomembranes and its homeostasis is controlled by miR168-AGO1 dependent slicing and miR168-AGO10-dependent translational repression of its mRNA. Moreover, the P0 VSR of polioviruses targets AGO1 for ubiquitinylation and subsequent degradation by autophagy (Derrien et al. 2012). AGO10, the closest AGO1 homolog in *Arabidopsis* specifically binds miRNA members of the MIR165/166 family to regulate shoot apical meristem development (Zhu et al. 2011). Current models suggest that AGO10 may compete with AGO1 for miR165/166 to protect the target RNAs (encoding class-III HomeoDomain-leucine ZIPper [HD-ZIPIII] transcription factors) for expression in the meristems (Zhang and Zhang 2012; Bologna and Voinnet 2014). AGO10 also associates with miR168 to mediate the translational repression of AGO1 mRNA (Mallory et al. 2009) and was shown to act in antiviral defense against TuMV in inflorescence tissues (Garcia-Ruiz et al. 2015). AGO2 displays additive and overlapping functions with AGO1. Like AGO1, also AGO2 functions in antiviral defense and loads vsiRNAs to trigger cleavage of the vRNA (Takeda et al. 2008; Mallory and Vaucheret 2010; Bologna and Voinnet 2014). Similar to regulation of AGO1 by miR168, AGO2 is regulated by miR403 in an AGO1-dependent manner (Allen et al. 2005). Thus, AGO2 can act as a

surrogate AGO to AGO1, when AGO1 itself is not available, for example when targeted by poliovirus P0.

AGO7 is almost exclusively associated with miR390 to initiate the biogenesis of tasiRNAs from the TAS3 gene (Montgomery et al. 2008) but also plays a role in antiviral defense in leaves (Garcia-Ruiz et al. 2015).

AGO4, AGO6 and AGO9 were shown to bind DCL3-dependent 24 nt heterochromatic small interfering RNAs (hcRNAs) and to act in RdDM (Zheng et al. 2007; Gao et al. 2010; Havecker et al. 2010; Blevins et al. 2015). Whereas AGO6 and AGO9 load hcRNAs derived from transposable elements (Olmedo-Monfil et al. 2010; McCue et al. 2015), AGO9 incorporates hcRNAs to control female gamete formation (Olmedo-Monfil et al. 2010). AGO5 was shown to associate with phasiRNAs, may induce megagametogenesis (Mi et al. 2008; Tucker et al. 2012; Komiya et al. 2014; Zhang et al. 2015) and to trigger antiviral defense against systemic PVX infection in Arabidopsis (Brosseau and Moffett 2015). The exact function(s) of AGO3 and AGO8 have not yet been determined.

AGO proteins generally act as platforms to bind proteins containing Gly-Trp (GW) dipeptides. These “GW proteins” often act as essential cofactors in various RNA silencing reactions (El-Shami et al. 2007; Till et al. 2007; Poulsen et al. 2013).

2.3. Role and function of RDR proteins

RDR proteins are RNA-dependent RNA polymerases that produce dsRNAs from single-stranded RNA templates. They are found in RNA viruses, plants, fungi, protists and *C. elegans* but are absent in *Drosophila* and mammals. They are characterized by the presence of a catalytic psi- β -barrel DxDGD (DFDGD in Arabidopsis) motif at the C-terminus, which is highly conserved among the identified eukaryotic and viral RDRs (Makeyev and Bamford 2002; Wassenegger and Krczal 2006) (see RDRs, Figure 4). As already mentioned, these proteins have a key role in producing long dsRNA substrates for the sequential processing of secondary siRNAs by DCL2 and DCL4. By linkage with specific siRNA-processing DCLs, the different RDRs are functionally diversified into different RNA silencing pathways. Loss of RDR1, RDR2, or RDR6 results in enhanced susceptibility to RNA and DNA viruses, thus confirming their important role in antiviral defense (Pumplin and Voinnet 2013). One of the major roles of RDR1 and RDR6 is to produce dsRNA to amplify vsiRNAs production by DCL2 and DCL4 for antiviral silencing (Donaire et al. 2008; Wang et al. 2010). RDR6 is the most studied RDR. In addition to its major role in antiviral defense (Himber et al. 2003; Schwach 2005; Vazquez 2006),

RDR6 is also the major RDR involved in the production of tasi- and phasiRNAs (Vazquez 2006) and has important functions during plant development, for example in the regulation of self-incompatibility (Tantikanjana et al. 2009), juvenile-to-adult phase change (Peragine et al. 2004), or leaf and pistil development (Peragine et al. 2004; Willmann et al. 2011).

RDR2 has a prominent role in TGS by conversion of capped or non-capped ssRNAs transcribed by POLIV from heterochromatic regions into dsRNAs for sequential processing by DCL3 into 24 nt long hcRNAs and loading into AGO4-RISC. RDR2 plays a central role in RNA-mediated DNA methylation, histone modification, and telomeric heterochromatic formation and its maintenance (Vrbsky et al. 2010; Blevins et al. 2015). RDR2 has also been shown to be involved in nucleolar dominance (silencing of one parental set of ribosomal RNA genes) (Autran et al. 2011). RDR2 and RDR6 are both involved in female gamete formation with the presence of multiple abnormalities in female gametophytes in *rdr2* and *rdr6* mutants (Olmedo-Monfil et al. 2010) as well as in transgene silencing. The exact functions of RDR3 and RDR5 have not been shown until now and remain to be demonstrated.

2.4. Role and function of HEN1 proteins

HUA ENHANCER 1 (HEN1) is a RNA methyltransferase (fully named S-adenosyl-L-methionine-dependent RNA methyltransferase) that ligates a methyl group (CH₃) onto the 2'-OH of each strand of all DCL-derived products (Li et al. 2005; Yu et al. 2005; Yang et al. 2006). HEN1-mediated methylation causes the stabilization of sRNAs by preventing their uridylation degradation signaling (Yu et al. 2005; Kim et al. 2010). HEN1 has five domains. Four of them directly interact with sRNA substrates, namely the two dsRNA binding domains (dsRBD1 located at the N-terminus and dsRBD2 located in the center), the La-motif-containing domain (LCD), which specifically recognizes the 3'-OH group (Bologna and Voinnet 2014), and the methyltransferase domain (MTase) (Yu et al. 2005). The fifth domain is the PPlase-like domain (PLD), which does not interact with sRNA substrates (Huang et al. 2009). This domain has been proposed to function as a protein-protein interaction domain (Ying et al. 2009; Vasudevan et al. 2015) (see HEN1, Figure 4). It has been speculated that the methylation mechanism is initiated by the targeting of the 18-24 nt siRNA duplex by dsRBD1 and dsRBD2, which places one of the terminal ends of the duplex close to the MTase domain and the other end close to the LCD domain for protection (Ying et al. 2009). The MTase then methylates the 3' terminus in a Mg²⁺-dependent mechanism.

3. Roles and pathways of RNA silencing

DCL proteins that process miRNAs and siRNAs from RNA precursor molecules and AGO-RISC complexes that use these miRNAs and siRNAs for RNA cleavage or translational repression constitute the core components of many known RNA silencing pathways. The different pathways are distinguished by the specific types and origins of sRNA, their specific processing by specific DCL proteins, their specific association with specific AGO proteins, and their specific role. Generally, RNA silencing pathways act at either the transcriptional or post-transcriptional levels. TGS acts in the nucleus and uses DCL3-dependent 24 nt siRNAs referred to as repeat-associated siRNAs (rasiRNAs) or heterochromatic siRNA (hcrRNAs). The hcrRNAs are processed from dsRNA precursors generated by RDR2 from RNA POL IV transcripts of heterochromatic regions and associate with AGO4 to guide RNA-dependent DNA methylation (RdDM) and histone modification leading to the epigenetic modification of transposons and endogenous repeat loci (Matzke et al. 2009) (Figure 5a). PTGS pathways, in contrast, use either miRNAs derived from MIR genes or siRNAs processed from different long dsRNA precursors (e.g. viral dsRNA, extended hairpin mRNAs encoded by inverted repeat loci, dsRNAs produced by RDR using viral RNA or single-stranded RNAs derived from TAS or PHAS loci as template) to regulate the abundance of mRNAs (or viral RNAs) and proteins by mRNA cleavage or translational repression.

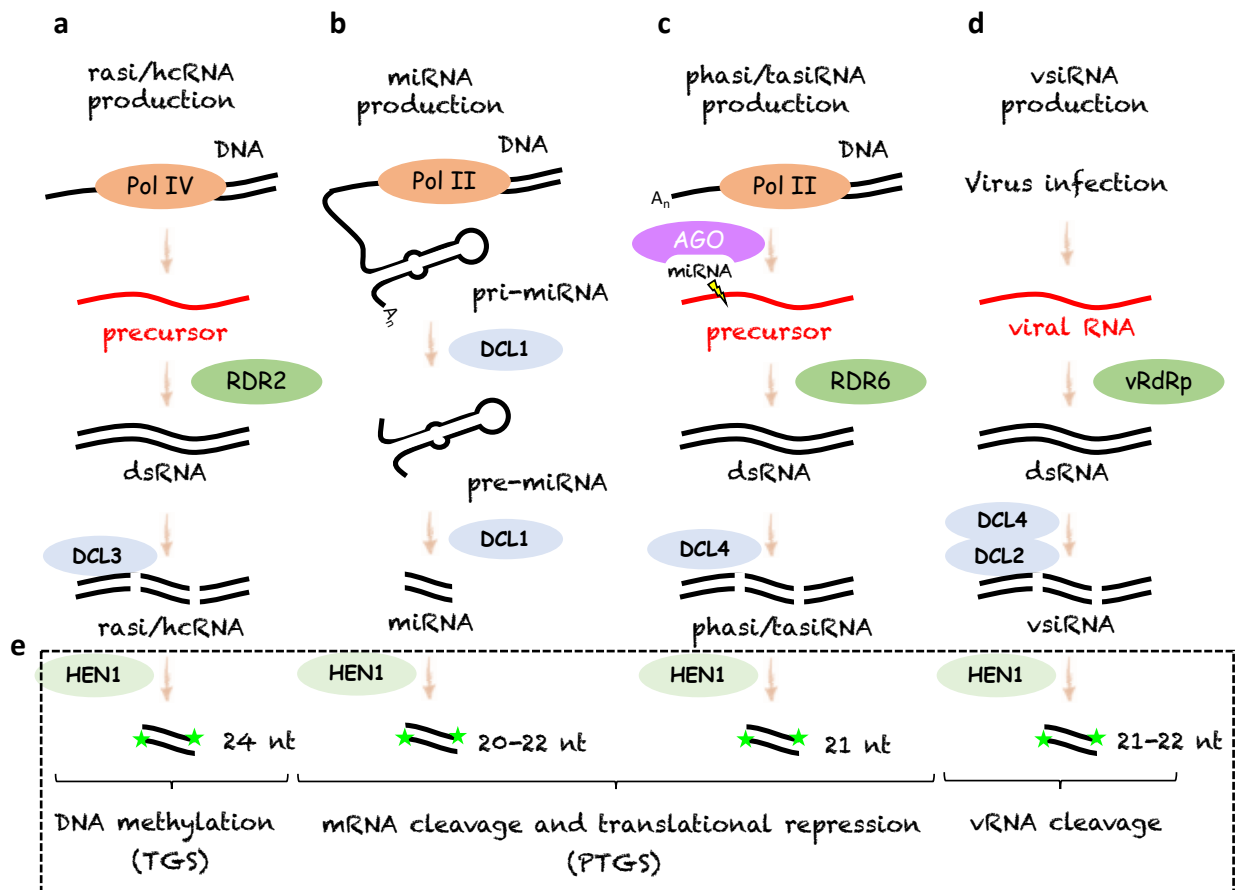


Figure 5: Biogenesis of sRNAs and RNA silencing pathways

a. PolIV transcripts derived from transposable elements and repeats are converted to dsRNA by RDR2 and then cleaved by DCL3 into rasi/hcRNAs. **b.** After transcription of pri-miRNA from a MIR gene by RNA polymerase II (Pol II) the double-stranded foldback structure is cleaved by DCL1 into a 20-22 nt long miRNA duplex. **c.** PhasiRNAs (which include tasiRNAs) are transcribed from coding genes or non-coding genes (e.g. TAS genes in Arabidopsis) by Pol II and converted into dsRNA by the RDR6 protein. The dsRNA is then processed by DCL4 into phased 21 nt siRNAs. **d.** Viral RNA replication by the viral RNA dependent RNA polymerase (vRdRp) leads to the formation of double-stranded RNA (dsRNA) which is cleaved by DCL2 and DCL4 into 21-22 nt long siRNA duplexes. **e.** rasi/hcRNA, miRNA, phasi/tasiRNA, and vsiRNA are methylated by HEN1 and loaded into the AGO-RISC complex for DNA methylation and chromatin formation/maintenance (TGS) or direct cleavage or translational repression of target RNA (PTGS).

3.1. miRNA biogenesis and function

miRNAs are 20-22 nt long sRNAs derived from non-coding MIR genes (Figure 5b). Transcription of the MIR gene by RNA polymerase II (Pol II) leads to production of capped, single-stranded and polyadenylated primary miRNA (pri-miRNA) that folds into a hairpin-like structure. Initial cleavage by DCL1 leads to a shorter stem-loop structure called precursor miRNA (pre-miRNA), which is again cleaved by DCL1 to produce the mature miRNA duplex (Reinhart et al. 2002; Kurihara and Watanabe 2004; Qi et al. 2005; Park et al. 2005). Following methylation by HEN1 at both 3'-ends the duplex is exported from the nucleus into the cytoplasm dependent on an exportin-5 homolog called HASTY. In the cytoplasm, one strand of the duplex is loaded into a RISC complex containing either AGO1,

AGO2, AGO7 or AGO10 to guide the complex to its mRNA target for sequence-specific cleavage. Published miRNA sequences and associated annotations are deposited in the miRbase database (<http://www.mirbase.org>; Kozomara and Griffiths-Jones 2014).

3.2. phasiRNA biogenesis and function

phasiRNAs are generated from a long dsRNA precursor at intervals of 21-26 nt (Figure 5c). As exemplified by the category of *Arabidopsis* *trans*-acting siRNAs (tasiRNAs), phasiRNAs are derived from an mRNA converted to dsRNA by RDR6 and processed by DCL4 (Vazquez et al. 2004). The origin of referring to some phasiRNAs as tasiRNAs stems from their ability to act like miRNAs in homology-dependent manner, directing AGO1-dependent cleavage of mRNAs from genes other than that of their source mRNA (Fei et al. 2013). The term phased indicates that the phasiRNAs are produced in a head-to-tail arrangement, starting precisely at a specific nucleotide. This specific nucleotide is usually determined by cleavage of the transcript by a 22 nt-long miRNA or siRNA (e.g. tasiR2140; Chen et al. 2007), which is followed by dsRNA formation and DCL4 cleavage. Due to the phasing of the siRNAs, the phasiRNA-producing PHAS loci can be identified with the help of computational algorithms. Such algorithms can be used in genome-wide scanning and allow identifying PHAS loci according to a p-value or phasing score as a threshold or cutoff. In *Arabidopsis*, this approach led to the original identification of tasiRNAs as well as to the identification of new phasiRNA-producing loci. Importantly, many of these these phasiRNA-producing loci actually represent coding genes [many of which encode Nucleotide-Binding, Leucine-Rich Repeat (NB-LRR) proteins, PENTATRICOPEPTIDE REPEAT (PPR) proteins, or MYB transcription factors (Howell et al. 2007; Zhai et al. 2011; Xia et al. 2012; Zhu et al. 2012)], thus showing that phased, secondary siRNAs can be generated from protein-coding transcript and not only from non-coding genes, such as TAS genes. It is important to note that phasiRNAs are defined just as being phased whereas tasiRNAs are defined as being phased and shown to be *trans*-acting (Zhai et al. 2011). Although phasiRNAs were shown to act in *trans* (tasi-RNAs), they may also act in *cis* (called casiRNAs) and be part of a self-regulatory network (Zhai et al. 2011), in which phased siRNAs target homologous regions in both the transcript of origin and in transcripts of homologous genes, enabling the plant to maintain the homeostasis of transcripts encoded by the whole gene family. Such autoregulatory network plays an important role in controlling the expression of hundreds of homologous of NB-LRR genes present in *Medicago* (Young et al. 2011; Zhai et al. 2011) or potato (Wang et al. 2011; Xu et al. 2011a; Zhai et al. 2011; Lozano et al. 2012; Shivaprasad et al. 2012).

Interestingly, certain coding genes in *Arabidopsis* were shown to produce phasiRNAs only upon viral infection and to play a role in defense against infection by *Cucumber mosaic virus* (CMV) and TuMV (Cao et al. 2014a). These virus-activated siRNAs (vasiRNAs) were processed from dsRNA generated by RDR1 rather than RDR6 and associated with AGO2 for target cleavage.

3.3. Virus-derived siRNAs (vsiRNAs)

Replication of RNA viruses leads to the production of viral dsRNA as a replication intermediate. This dsRNA is recognized by the host and triggers RNA silencing as an antiviral defense response in which the viral dsRNA is processed by DCL4 and DCL2 into 21-22 nt long vsiRNAs (Blevins et al. 2006; Deleris et al. 2006). Although the cleavage of the viral replication intermediate already interferes with efficient viral replication, vsiRNAs are methylated by HEN1 and incorporated into AGO1, AGO2, and AGO10 (Pumplin and Voinnet 2013; Garcia-Ruiz et al. 2015) for further RISC-mediated cleavage of viral RNA (Voinnet 2005; Pantaleo et al. 2007). RDR6, but also RDR1 and RDR2 support antiviral RNA silencing through the production of secondary vsiRNAs (Donaire et al. 2008; Vaistij and Jones 2009). To counter-act antiviral RNA silencing, viruses evolved specialized proteins known as suppressor of RNA silencing (VSR). The VSRs of different viruses have evolved independently and inhibit distinct steps of the silencing pathway (Table 1; Csorba et al. 2015).

Table 1: Examples of identified VSRs and their activity

Viruses	VSR function	Inhibited RNA silencing pathway step
P14 (PoLV), NS3 (RSV)	dsRNA binding	Inhibition of vRNA cleavage and vsiRNA production
CaMV leader	Decoy RNA	
P38 (TCV), P1 (RYMV)	Blocking DCL activity	
CaMV P6	Inhibition of DCL co-factor	
P19 (TBSV), Hc-Pro (TuMV), 126k (TMV)	Sequestration of ds-siRNA duplex	Inhibition of vsiRNA activity
RNase 3 (SPVD)	Direct ds-siRNA cleavage	
Hc-Pro (TuMV)	HEN1 ds-siRNA binding	
P6 RYSV), Hc-Pro (TuMV)	RDR6 inhibition	Inhibition of secondary siRNAs processivity
P2 (RSV), VPg (PVA)	RDR6 co-factor inactivation	
P25 (PVX), P0 (BWYV)	AGO degradation	Inactivation of RISC complex activity (vRNA or host mRNA PTGS and TGS inhibition)
P38 (TCV), P1 (SPMMV)	AGO inactivation	

The VSRs of several viruses, including the tombusvirus P19, the potyvirus HcPro, and the tobamoviral p122/p125/p126 proteins sequester siRNA duplexes after DCL processing and inhibit their HEN1 methylation of siRNAs and their incorporation into RISC. Some VSRs act earlier in the pathway, such as the sobemovirus P1 or the carmovirus P38 that inhibit the processing of siRNAs by DCL4, or act downstream in the pathway, such as the polerovirus P0 that targets AGO1 for degradation.

Several plant pathogenic fungi were shown to hijack the host RNA silencing pathway with their own siRNAs to manipulate the expression of defense-related genes, in a process referred to “cross-kingdom RNAi” (Weiberg et al. 2015). Given that viruses replicate within cells, it seems likely that they have evolved similar strategies to target host genes with their own vsiRNAs. Indeed, the cloning of host-derived sequences into the replicating virus genome is used as a strategy to silence plant genes in a process call virus-induced gene silencing (VIGS). There is indeed evidence that natural viruses encode vsiRNAs that can act *in trans*. Early studies demonstrated that vsiRNAs of *Cymbidium ringspot virus* (CymRDV) target subviral satellite RNA (Pantaleo and Burgyan 2008). Moreover, vsiRNAs produced by TMV-Cg were shown to cleave two *Arabidopsis* mRNA targets (Qi et al. 2009) and vsiRNAs from the Y-satellite of *Cucumber mosaic virus* (CMV) cleaved a *Nicotiana benthamiana* chlorophyll synthesis gene (Shimura et al. 2011; Smith et al. 2011). More recent approaches utilizing genome-wide studies to correlate vsiRNAs and host RNA degradome data using CleaveLand software (Addo-Quaye et al. 2009) revealed numerous potential mRNAs that are targeted by viruses in *Vitis vinifera* (Miozzi et al. 2013). However, while improved degradome analysis software became available (e.g. PAREsnip, Folkes et al. 2012; sPARTA, Kakrana et al. 2014) and an increasing number of studies aim to identify novel miRNAs and their targets in various species (e.g. Baksa et al. 2015; Cao et al. 2014b; Wang et al. 2016), the further analysis of the sRNA network utilized by both viruses and their hosts to control viral accumulation and gene expression in the infected cell is lagging behind. Knowing more about this network will greatly increase our understanding of plant:virus interactions.

4. Draft manuscript: “Virus- and host-derived small RNAs coordinate infection in oilseed rape” by Pitzalis *et al.*

Nicolas Pitzalis¹, Khalid Amari¹, Stéphanie Graindorge¹, David Pflieger¹, Livia Donaire^{2#}, Christina Querfurth³, Michael Wassenegger³, César Llave², and Manfred Heinlein^{1,*}

¹Université de Strasbourg, CNRS, IBMP UPR2357, F-67000 Strasbourg, France

²Department of Environmental Biology, Centro de Investigaciones Biológicas, Consejo Superior de Investigaciones Científicas (CIB-CSIC), Madrid, Spain

³AlPlanta – Institute for Plant Research, Neustadt, Germany

#Current address: Centro de Edafología y Biología Aplicada del Segura (CEBAS)-CSIC, Murcia, Spain

*To whom correspondence should be addressed:

manfred.heinlein@ibmp-cnrs.unistra.fr

Introduction

Viruses are among the parasites that induce the most severe damages on cultivated plants, estimated to cause up to US \$30 billion worth of damage worldwide to agriculture and forestry industries (Randles and Ogle 1997; Sastry and Zitter 2014). In view of the major economic problem caused by viruses, breeders usually rely on the development of resistant cultivars. However, this strategy often turns out not to be durable since virus evolution favors the emergence of adapted virus populations able to overcome such resistance (Garcia-Arenal and McDonald 2003). Although the incidence of plant virus diseases can be controlled to some extent by controlling the viral insect vectors, the repeated application of insecticides poses a threat to our environment. The development and application of innovative and sustainable approaches for protecting cultivated plants against their pathogenic viruses depends on the identification of gene targets that are part of the fundamental molecular mechanisms that determine virus: host compatibility and disease. Viruses utilize host mechanisms to support their replication and movement and, at the same time, trigger host defense responses. Numerous previous studies have demonstrated that viral infection in susceptible hosts is associated with the altered expression of genes and the activation of defense responses such as Pattern-Triggered-Immunity (PTI) (Kørner et al. 2013) and RNA silencing (Ding and Voinnet 2007). Both defense responses are triggered by the recognition of double-stranded RNA (dsRNA) produced during viral replication. However, whereas PTI involves BAK1 (Kørner et al. 2013) and the recognition of dsRNAs by an unknown pathogen-recognition receptor together with SOMATIC EMBRYOGENESIS RECEPTOR-LIKE KINASE 1 (SERK1) as a potential co-receptor (Niehl et al. 2016), RNA silencing relies on the recognition of dsRNA by DICER-LIKE (DCL) proteins. Moreover, PTI involves the activation of transcriptional signaling cascades and confers broad-spectrum pathogen resistance (Dodds and Rathjen 2010; Jones and Dangl 2006; Spoel and Dong 2012), whereas RNA silencing relies on the production of small 21-24 nt long small interfering RNAs (siRNAs) and microRNAs (miRNAs) that associate with an ARGONAUTE (AGO) protein-containing RNA-induced silencing complex (RISC) to target viral and host RNAs for cleavage or translational repression in a target sequence-specific manner (Bologna and Voinnet 2014). RNA silencing plays a central role in plant-virus interactions as it targets both the virus and its host. Viruses encode effector proteins that suppress RNA silencing (VSR) (Csorba et al. 2015) and Arabidopsis mutants affected in DCL and other RNA silencing pathway genes showed enhanced susceptibility (Bouché et al. 2006; Deleris et al. 2006; Morel et al. 2002; Mourrain et al. 2000), thus indicating the importance of RNA silencing in antiviral defense and plant-virus co-evolution (Pumplin and Voinnet 2013). However, the role of

RNA silencing in plant:virus interactions may be more complex. For example, it is conceivable that similar to certain mammalian DNA viruses (Herpesviridae) (Hook et al. 2014) and plant-pathogenic fungi (Weiberg et al. 2013), also plant viruses may have evolved the ability to hijack the host RNA silencing pathway with their own small RNAs in order to modulate host gene expression.

To further explore the function of sRNAs during plant:virus interactions, we here used next-generation RNA profiling technologies and specific gene analysis to address the function of sRNAs accumulating during early *Turnip mosaic virus* (TuMV) infection in leaves of oilseed rape (*Brassica napus*). sRNA:RNA target pairs correlated with specific host mRNA and viral RNA cleavage events during infection were identified. Moreover, our analysis revealed the targeting of specific host genes by virus-encoded siRNAs. The results also suggest the existence of specific host genes that function as virus-induced hubs for secondary siRNA synthesis and the regulation of downstream secondary gene target networks. We also show that the virus itself is targeted for RISC-mediated cleavage by sRNAs encoded by the host. This finding indicates that the network of sRNA-mediated interactions between the virus and its host includes the activity of plant-encoded sRNAs with homology to viral genomes and that are part of the arms arsenal available to plants to control their viruses. Collectively, the observations indicate that viruses and their hosts cells form tightly organized niches in which both sides exchange multiple sRNA signals for mutual control and regulation. *B. napus* is a global economically important crop grown for its oil-rich seeds and vulnerable to a number of widespread viruses including TuMV. By focusing the analysis on dissected local sites of infection in leaves, we identified regulatory hubs and sRNA target genes that control plant-virus interactions during the onset of virus infection before disease symptoms arise. The identified genes and mechanisms are potential targets for crop breeding aiming to interfere with the onset of infection already during early stages.

Results

The rapeseed cultivars Drakkar and Tanto differ in susceptibility to TuMV-GFP

The analysis involved two different commercial *B. napus* cultivars, Tanto and Drakkar, which showed strong differences in their susceptibility for GFP-tagged TuMV (TuMV-GFP) (Fig. 1). Both cultivars develop green fluorescent infection foci visible under UV light in the inoculated leaves. However, although the foci in the two cultivars develop and further grow similarly in size, the foci in Drakkar leaves are homogeneously green fluorescent (Fig. 1a), whereas the foci in the Tanto leaves occur as

fluorescent halos (Fig. 1b). This halo-like phenotype of infection sites were previously reported for GFP-tagged viruses with compromised VSR activity (Garcia-Ruiz et al. 2015; Kubota et al. 2003; Vogler et al. 2007) indicating that the virus is silenced or otherwise inhibited shortly after infection of new cells. Consistent with a stronger antiviral response in Tanto, infection foci in Tanto leaves contain slightly less viral RNA as compared to the foci in Drakkar leaves (Fig. 1e). The difference between the two cultivars in TuMV susceptibility is also expressed at the level of systemic infection. Whereas Drakkar plants show extensive green fluorescent areas in the local and systemic tissues two to three weeks after inoculation (Fig. 1c), the upper leaves in Tanto plants show only few dispersed fluorescent spots (Fig. 1d).

Profiling of TuMV-GFP induced gene expression within local infection foci in Drakkar and Tanto leaves

Local green fluorescent infection foci in leaves and similar leaf samples of mock-treated plants were excised for transcriptome profiling using RNAseq. The analysis was performed for three independent replicate infection experiments, thus involving three independent RNA samples each for mock-treated Drakkar (DM), mock-treated Tanto (TM), virus-treated Drakkar (DT), and virus-treated Tanto (TT). To determine the profiles of sRNAs and their activity in mRNA target cleavage, exactly the same 12 RNA samples were also used for sRNA and mRNA degradome profiling (sRNAseq and PAREseq). The RNAseq analysis of the 12 samples gave 35 to 72 million clean paired reads per sample (Table S1). To allow appropriate mapping of the reads the Drakkar and Tanto DNA genomes were re-sequenced with 15 x coverage (Table S2) and reconstructed by alignment of the respective genomic sequencing data to the Darmor-bzh reference genome (Chalhoub et al. 2014) and by inferring the cultivar-specific high confidence single nucleotide polymorphisms (SNPs) (about 1.5 SNPs per kilobase; Table S2; Fig. S1) into the reference sequence. Using the reconstructed Drakkar- and Tanto-specific DNA genome data, around 80 % of the quality-filtered mRNAseq reads could be mapped with a maximum of one mismatch (Table S1).

Differential mRNA expression analysis revealed numerous transcripts that are significantly either up or down-regulated in virus-infected cells as compared to cells of mock-treated samples in both cultivars or in a cultivar-specific manner (Fig. 1f). The 24 genes that were most strongly regulated at transcript levels in both cultivars (fold change $[\log_2] \geq +4/-4$; $p < 0.05$; Fig. S2) may provide an important signature profile for early virus infection in rapeseed. These include a transcript predicted to encode CALMODULIN-BINDING PROTEIN 60G (CB60G), a master immune regulator that

promotes the expression of key genes involved in salicylic acid (SA) biosynthesis and in regulating pathogen-associated molecular pattern (PAMP)-triggered immunity (PTI), effector-triggered immunity (ETI) and systemic acquired resistance (SAR) (Sun et al. 2015). Genes that are expressed in a cultivar-specific manner or which show stronger regulation in one cultivar than in the other are candidates involved in determining the difference in virus susceptibility between the two cultivars (Table S3 – S7). Consistent with resistance, transcripts highly abundant specifically in Tanto encode proteins playing a role in defense, such as DETOXIFICATION 47 (DTX47)/EDS5, 4-SUBSTITUTED BENZOATES-GLUTAMATE LIGASE GH3.12, and NIM1-INTERACTING 2 (NIMIN-2), all of which play a role in the regulation of SA synthesis or the activation of genes downstream in the SAR pathway (Carviel et al. 2014; Hermann et al. 2013; Jagadeeswaran et al. 2007; Nawrath et al. 2002; Nobuta et al. 2007; Zwicker et al. 2007), whereby DTX47 was shown to be directly involved in the defense against viruses (Ishihara et al. 2008). Another highly induced gene encodes TARGET OF AVR B OPERATION1 (TAO1), a TIR-NB-LRR receptor-like protein previously known to also contribute to disease resistance induced by the *Pseudomonas syringae* effector AvrB (Eitas et al. 2008). Efficient progression of virus infection in Drakkar correlates with high levels of transcripts involved in membrane transport, the suppression of plant defense responses, and, potentially, in the regulation of plasmodesmata (PD)-mediated intercellular transport. For example, we found a strong induction of expression of the coatamer alpha-2 subunit of the COPI coatamer complex (Ahn et al. 2015), which is consistent with the role COPI vesicles in the replication of TuMV and other potyviruses (Wei and Wang 2008). The strongly induced NAC domain-containing protein 60 (NAC60) is a transcription factor activated at the ER that attenuates the sensitivity to abscisic acid (ABA). ABA has been shown to inhibit virus infection and is implicated to play a role in antiviral silencing and callose deposition at PD (Alazem and Lin 2017). NAC60 also reduces expression of ABI4 gene, which has been implicated in viral resistance (Alazem et al. 2014). The induction of transcripts encoding the leucine-rich repeat (LRR) receptor-like serine/threonine-protein kinase RPK2 is of particular interest as this protein forms heteromeric complexes with BAM1 which was recently shown to localize to PD, to promote the spread of the RNA silencing signal, and is targeted by a viral protein to inhibit antiviral RNA-silencing signaling (Rosas-Diaz et al. 2018). Thus, RPK2 may be induced during TuMV infection to regulate BAM1 and thereby control antiviral RNA silencing signaling through PD. A gene that is induced in Drakkar as well as in Tanto encodes a protein homologous to Arabidopsis PATELLIN-6 (PATL6), which was shown to be involved in resistance against *Alfalfa mosaic virus*, to interact with the viral movement protein (MP) and to prevent the targeting of MP to PD (Peiro et al. 2014). Other

induced transcripts encode TOPLESS-RELATED PROTEIN 2 (TPR2) and CYTOKININ DEHYDROGENASE 3 (CKX3), both of which are involved in the suppression of defense responses. TPR2 is a transcriptional corepressor and negative regulator of jasmonate responses (Pauwels et al. 2010), whereas CKX3 is a cytokinin-degrading enzyme that may control cytokinin levels implicated to determine the amplitude of immune responses and the outcome of plant-pathogen interactions (Argueso et al. 2012; Choi et al. 2010). Consistent with efficient systemic movement of the virus, TuMV-infection in Drakkar downregulates a transcript for PHLOEM PROTEIN 2-LIKE A2 (PP2A2) that together with PP2A1 can form high-molecular mass polymers to block phloem sieve plate pores (Fu et al. 2014).

The virus-induced differential expression profiles of several genes were validated by RT-qPCR using RNA samples of mock- and virus-treated Drakkar and Tanto plants of five independent biological experiments. The results generally confirmed the virus-induced changes in gene expression (Fig. S2) indicated by RNAseq data.

mRNA cleavage by miRNAs

The replicative sRNAseq datasets provided 27-52 Mio clean and quality-filtered (18-30 nt) reads per sample (Table S1). The sRNA size profiles within the libraries showed the expected changes in distribution of sizes upon RNA virus infection (Fig. S3). Mock-treated Drakkar and Tanto plants showed typical and very similar sRNA size profiles of predominantly 21nt – 24 nt long sRNAs, with likely DCL3-derived 24 nt sRNAs representing the major species. In contrast, the sRNA profiles in the virus-treated plants were dominated by virus-derived 21 nt and 22 nt siRNAs (84% and 74% of the 21 nt sRNAs are virus-derived in infected Drakkar and Tanto plants, respectively), which is consistent with the presence of the virus and the processing of viral dsRNA by DCL4 and DCL2, respectively. Moreover, host-derived sRNAs showed a strong increase in the number of 21 nt sRNAs, whereas the number of sRNAs belonging to other size classes, except the 22 nt size class, was strongly reduced. These alterations in the pattern of host sRNAs may represent an accumulation of miRNAs in virus-infected tissues, as previously observed (Hu et al. 2011; Tagami et al. 2007; Vogler et al. 2007). The virus-derived siRNAs aligned to the TuMV genome along its entire length, on both plus (+) and minus (-) strands. (Fig. S4)". The virus-genome aligned siRNA profiles of peaks and valleys are almost identical between Drakkar and Tanto, thus demonstrating that the cultivar-specific differences in the susceptibility for the virus cannot be explained by obvious differences in vsRNA processing or accumulation.

Host-derived miRNAs were identified by mapping the sRNA reads to *Brassicaceae* mature miRNA family sequences deposited in miRBase (Kozomara and Griffiths-Jones 2014) and by analyzing them for miRNA prediction with ShortStack (Axtell 2013; Shahid and Axtell 2014). ShortStack annotates miRNAs on the basis of specific criteria, including a requirement of the corresponding star sequence present in the sRNA data and its mapping near the candidate miRNA sequence within the same gene. Our list of known and predicted miRNAs was complemented by *B. napus* miRNAs reported in publications and contained 1047 miRNAs to which our sRNAs were aligned (Table S8). Around 8 million sRNA reads per condition could be mapped to 652 expressed miRNA species and, of these, 53 miRNAs and 47 miRNAs were present only in either Drakkar and Tanto, respectively.

To identify mRNAs targeted for cleavage by miRNAs and other sRNAs expressed in the mock- and virus-treated plants the replicate DM, DT, TM and TT samples were also used for the sequencing of the mRNA degradome by PAREseq. The PAREseq reads consist of 20 nt signatures derived from mono-phosphorylated, non-capped 5' ends of the 3' fragments of mRNAs following cleavage by RISC, Dicer, or other degradation processes. By applying the combination of PAREseq, mRNAseq, and sRNAseq reads for degradome analysis with PAREsnip software (Folkes et al. 2012), we identified sRNA:mRNA pairs that are functional in sRNA-mediated RNA cleavage events. Our degradome and sRNA data sets derived from leaf samples of twelve independent replicate biological experiments with non-infected mock and TuMV-infected Drakkar and Tanto plants were consistent with the activity of numerous *B. napus* miRNAs involved in the RISC-mediated cleavage of mRNA targets known already in Arabidopsis and other species. The analysis agreed the activity of previously known *B. napus* members (annotated in miRbase) of miRNA families targeting the mRNA transcripts for SQUAMOSA PROMOTER-BINDING-LIKE (SPL) proteins (bna-miR156), Auxin response factors (ARFs) (bna-miR160), SCARECROW-LIKE (SCL) proteins (bna-miR171), Ethylene-responsive transcription factor (ERF) RELATED TO APETALA 2 (RAP2), TARGET OF EAT 2 (TOE2), and APETALA 2 (bna-miR172), Auxin signaling F-box (TIR1/AFB2/AFB3) proteins (bna-miR393), CHLOROPLASTIC SUPEROXIDE DISMUTASE (bna-miR398), and ARGONAUTE 2 (bna-miR403) (Table S9). Several members of these mRNA target families are also presumably targeted by previously unknown *B. napus* miRNAs identified by ShortStack (Table S10) or by miRNAs sequences present in miRbase but previous described only in other species (Table S11). Our degradome data also indicate the cleavage of several predicted targets by sRNAs that we annotated as "miRNA-related sRNAs" since they carry small mismatches to miRNA sequences in other species (Table S12). Some of these sequences were identified by ShortStack as genuine *B. napus* miRNAs (Table S13). Our replicate degradome data also

indicate that certain known miRNAs likely cause the cleavage of mRNA transcripts that were previously unknown as specific targets (Table S14). For example, a miRNA homologous to the *B. rapa* bra-miR1885b targets transcripts of BIOGENESIS OF LYSOSOME-RELATED ORGANELLES COMPLEX 1 SUBUNIT 2 (BLOS2), and the mRNA of the cytochrome c oxidase assembly protein COX19 is indicated as a target of the *B. napus* miRNA bna-miRC23a-3.

The cleavage breakpoints indicated by several miRNA:mRNA target pairs were confirmed RLM-5'RACE assays with independent, newly created, biological samples (Figs. S5-S9). For example, the targeting of ARF10 mRNA by bna-miR160c produced a highly defined degradome signature along the transcript in mock as well as infected Drakkar and Tanto samples, and the respective cleavage site could be clearly mapped also by 5'RACE (Fig.S5). Other examples of miRNA:mRNA target pairs confirmed by 5'RACE are bna-miR1885:TAO1 (Fig. S6), bna-miR403:AGO2 (Fig. S7), bna-mi1885b:BLOS2 (Fig. S8), or bna-miR172:APETALA2 (Fig. S9).

miRNA and mRNA target levels are not always correlated

Infection by TuMV-GFP leads to varying changes in the levels of the specific miRNAs and these changes are conspicuously similar between infection foci in Drakkar and Tanto. However, the virus-induced changes in the levels of the miRNAs does not always correspond to the expected reduction in the steady state level of the respective target mRNA. The complete data describing identified miRNA:mRNA target pairs and the respective miRNA and mRNA target expression levels in the two cultivars are summarized in Table S15 and an overview over miRNA and mRNA target expression levels is provided in Table S16. Several miRNA:mRNA target pairs follow the expected rule that an increase, or decrease, in the level of a specific miRNA should lead to a decrease, or increase, in level of the corresponding mRNA target, respectively. Amongst the targets showing cleavage in at least three of the twelve total samples, the miRNAs of the miRNA:mRNA target pairs miR403:AGO2, miR172:ERF RAP2-7, miR160c:ARF16, miR393:ASB2/3, miR156:SPL11, and miR172:APETALA2, are down-regulated upon infection and lead to a corresponding increase in the amount of the corresponding mRNA (Table S15). Conversely, the levels of miRNAs of other miRNA:mRNA target pairs, such as miR171:SCL, are increased and show a corresponding decrease of the corresponding mRNA. On the other hand, several other target pairs did not show these expected results. For example, the mRNAs of the target pairs miR1885b:BLOS2 or miR398:Superoxide dismutase 2 [Cu-Zn] (CSD2) accumulated upon infection, although their corresponding miRNAs increased. Similarly, several miRNA:mRNA target pairs correlated with lower levels of both the miRNAs and mRNAs.

Some miRNA:mRNA target pairs showed the expected results in mRNA levels in only one of the two cultivars but not in the other. These findings demonstrate that miRNA levels do not necessarily correspond to miRNA activity in mRNA target cleavage. Moreover, RISC-mediated cleavage is only one of several mechanisms by which cellular mRNA levels are regulated.

TuMV uses vsiRNAs to target host genes

The sRNA data analysis revealed that TuMV-infected cells produce about 300000 unique siRNA sequences derived from the positive and negative strands of the virus. The replicative PAREsnip data indicated the presence of 205 sRNA:mRNA target pairs (that involve 87 virus-derived siRNAs (vsiRNAs) that occur exclusively in the infected tissues and show 100% sequence homology to the virus and no significant sequence homology to the host (Table S17). As is shown in Fig. 2, the vsiRNA with the potential to interact with host mRNA cleavage are derived from both the minus and plus strands of the virus and map at various positions along the viral genome. Eight of the vsiRNAs stand out as they are repetitively associated with cleavage events in 17 different transcripts and were detected in at least two of the six independent degradomes of infected plants studied by PAREseq/PAREsnip (Table S18, vsiRNA:mRNA target pairs highlighted in Figure 2). Among the 17 different vsiRNA:mRNA target pairs, we found one unique vsiRNA (AAGAATCTGATGATGCTGT) capable of interacting with transcripts of eight genes encoding the ethylene response factors (ERFs) RAP2-7, TOE2, and APETALA2 (Table S18, Fig. 2G). Given that the ERFs targeted by the vsiRNA AAGAATCTGATGATGCTGT are also regulated by miR172, we wondered whether the vsiRNA could mimic the function of miR172. As is shown in Fig. 2b, and more in detail in Fig. S10, this vsiRNA indeed shows high homology to bna-miR172 and would cleaves exactly the same position within target sequence. Since the host downregulates miR172 levels upon infection (Fig. S10, d), the vsiRNA may complement this reduced amount of miR172 in order to control the expression of these ERFs. The PAREseq/PAREsnip data for host mRNA targets of vsiRNA (Table S18) provide evidence for specific roles of vsiRNA targeting mRNAs particularly in Drakkar, such as mRNAs encoding the pseudokinase ZED1, the cysteine-protease aleurain, and the serine/arginine-rich (SR) splicing factor RS31A. The pseudokinase ZED1 is an important mediator of effector-triggered immunity (Lewis et al. 2013; Seto et al. 2017), whereas the cysteine-protease aleurain plays an important role in hypersensitive responses and programmed cell death (Lu et al. 2015). SR proteins are essential factors in regulating pre-mRNA constitutive and alternative splicing (Jeong 2017). They also act in RNA surveillance and promote RNA degradation through the nonsense-mediated RNA decay

pathway (Zhang and Krainer 2004). In plants, SR proteins play numerous roles in stress tolerance (Duque 2011), and were shown to be involved in the splicing of RNA encoding plant immune receptors (Xu et al. 2011b). Nevertheless, the identified vsiRNA:mRNA target pairs are correlated with rather moderate yet significant downregulation of some of the target genes, thus indicating that the virus may use specific vsiRNAs to prevent a strong induction of these defense-related genes in infected cells.

TuMV infection triggers the widespread targeting of mRNAs through activation of secondary siRNA production from PHAS loci.

In addition to AGO1, also other AGO proteins, particularly AGO2, play important roles in antiviral defense (Carbonell and Carrington 2015; Garcia-Ruiz et al. 2015). The expression of AGO2 is controlled by AGO1 through miR403 (Harvey et al. 2011). Consistently, our PARE analysis predicted cleavage of AGO2 mRNAs (BnaCnng68320D and BnaA05g14760D) by miR403 (Fig. S7) in both mock-treated and TuMV-infected *B. napus* samples BnaC06g41790D). Nevertheless, infection triggered the downregulation of miR403 and upregulation of AGO2 mRNA levels. Interestingly, infection also caused a strong production of secondary, phased siRNAs (phasiRNAs) from AGO2 mRNA in both Drakkar and Tanto plants (Fig. 3a). The TuMV-associated activation of phased siRNA production from coding genes has been described in Arabidopsis (Cao et al. 2014) and may as well occur in *B. napus*. To identify other coding genes that produce virus-associated phasiRNAs (va-phasiRNAs) upon TuMV infection, we mapped the virus-induced siRNAs found in our sRNA data to the Drakkar and Tanto coding genes and filtering these genes by applying thresholds for the number of siRNAs mapped to the coding regions of genes (>100 reads), the gene-specific PHAS score calculated by Shortstack (>30), and for the ratio in the number of specific va-phasiRNAs found in infected tissues versus mock-treated tissues (rpm infected / rpm mock >2). Using this approach, we identified 128 coding genes that act as PHAS loci and produce va-phasiRNAs in Drakkar (Table S19) and 253 coding genes that that act as PHAS loci and produce va-phasiRNAs in Tanto (Table S20), and of which 98 coding genes produce va-phasiRNAs in both cultivars (Table S21). As has been shown in detail for tasiRNAs in Arabidopsis, phasiRNAs are produced by conversion of the gene transcript into dsRNA followed by phased cleavage into phasiRNA duplexes (Fei et al. 2013). The production of phasiRNAs from coding genes can have varying effects, from controlling the homeostasis of the specific mRNA and encoded protein to the suppression of the specific gene and other homologous members of the same gene families (Fei et al. 2013). As known by the prototype example of trans-acting siRNAs

(tasiRNAs (Vazquez et al. 2004)) and by several new examples involving coding genes such as NB-LRR, PPR and MYB genes, phasiRNAs may also act *in trans* by directing AGO-dependent slicing of mRNAs of genes other than that of their source mRNA (Fei et al. 2013). To determine whether the va-phasiRNAs found in our analysis are functional and cause the cleavage of secondary mRNA targets *in trans*, we used them as query in our PAREsnip analysis of our sequenced degradome libraries prepared from mock-treated and virus-infected tissues. We could not find any of the AGO2 mRNA-derived va-phasiRNAs in our PARE analysis, thus indicating that the AGO2 va-phasiRNAs do not act in RISC-mediated slicer activity. va-phasiRNAs produced by several other genes [for example BnaC02g40260D encoding Elongation factor 2 (EF2) (Fig. 3b) or BnaA05g28710D encoding CDC48E (Fig. 3c)] were similarly absent in our PAREsnip database and may similarly be inactive in guiding RISC-mediated target RNA cleavage. However, among other va-PHAS genes, we found members of three small gene families particularly involved in the production of va-phasiRNAs and engaged in secondary mRNA target cleavage. These three gene families are predicted to encode Chlorophyll a-b binding protein 1 (BnaA04g20150D, BnaAnng22920D, BnaC03g59520D, BnaA07g07560D, BnaA03g15830D, BnaC03g18980D, BnaA09g26570D, BnaA08g17660D, BnaC05g22880D, BnaC04g10770D, BnaC04g10780D), NBR1 homolog (NBR1, BnaA01g14050D, BnaA03g46880D, BnaC07g39070D, BnaC01g16550D, BnaC08g11760D), and a protein with homology to yeast ART1/TAR1 (Transcript Antisense to Ribosomal RNA) (Galopier and Hermann-Le Denmat 2011) (BnaAnng22160D, BnaA09g04420D, BnaC08g46150D, BnaAnng21760D). These three gene families alone were found to produce 415 different unique va-phasiRNAs induced upon infection (Tables S22-S24) and associated with 969 unique va-phasiRNA:RNA target pairs targeting 413 different genes upon infection. Whereas va-phasiRNAs derived from both dsRNA strands of genes for Chlorophyll a-b binding protein 1 were found to target their own transcript or other highly homologous transcripts of the same gene family (Table S25), va-phasiRNAs derived from NBR1 and TAR1 genes also target the mRNAs of other genes (Table S26 and Table 27). A predominant group of target genes for NBR1 va-phasiRNAs that was redundantly identified in several PARE analysis replicates encodes ACTIN DEPOLYMERIZATION FACTOR 3 (ADF3) (Table S26). ADF3 was recently shown to play an important role in plant defense against aphids (Mondal et al. 2018). It is interesting that the trans-acting NBR1-derived va-phasiRNAs with secondary gene targets map exactly to the peaks of va-phasiRNA production along the NBR1 transcript (Fig. 4). This suggests that the efficient cleavage of va-phasiRNA targets is already programmed at the level of the va-phasiRNA-producing

gene or that the va-phasiRNAs associated with target cleavage are stabilized by association with their effector complexes.

Taken together, these observations demonstrate that virus infection in rapeseed triggers the production of secondary siRNAs from numerous coding genes. Some of these genes, like those encoding AGO2, EF2, or CDC48E produce secondary siRNAs that do not participate in guiding RISC and, therefore, may represent end-products of an RDR-dependent mRNA degradation pathway to maintain mRNA homeostasis upon infection. Other genes like those encoding Chlorophyll a-b binding protein 1, NBR1, and TAR1, produce trans-acting siRNAs with the predicted potential to target mRNAs of homologous genes within the same gene family or mRNAs of other genes.

Targeting of viral RNA by virus- and host-derived sRNAs

Although antiviral defense relies to some extent on the degradation of viral dsRNA by DCL enzymes, virus-derived siRNAs were found in association with AGO proteins (Garcia-Ruiz et al. 2015; Pantaleo et al. 2007; Zhang et al. 2006), thus suggesting a role of RISC-mediated viral RNA cleavage. Given that the viral genomic RNA of TuMV is polyadenylated in infected cells and degradome analysis by PARE relies on the analysis of polyadenylated RNA fragments, we wondered whether we can find virus-specific degradome signatures of the viral (+) and (-) strands in our degradome data from infected samples. PAREsnip analysis revealed 56 unique vsiRNAs derived from the negative strand of the virus present in unique vsiRNA:vRNA target pairs, thus suggesting that viral genomic RNA is indeed cleaved by vsiRNA-programmed RISC. We found 36 unique vsiRNA:vRNA target pairs in Drakkar (Table S28) and 58 unique vsiRNA:vRNA target pairs in Tanto (Table 29). Of these, 26 unique vsiRNAs:vRNA target pairs were commonly found in both Drakkar and Tanto, whereas four and 26 of the unique pairs were Drakkar- and Tanto-specific, respectively. Although most of the cultivar-specific pairs rank relatively low with respect to the number of their specific vRNA cleavage fragments, the vsiRNA CAGTGCTGCTGCTTTCATCTG was associated with vRNA cleavage events at relatively high frequencies specifically in Tanto.

Interestingly, in addition these vsiRNA derived from the virus, we identified 87 unique virus-targeting sRNAs that were derived from the host (hsRNAs, host-derived siRNAs). We found 45 unique hsRNA:vRNA target pairs in Drakkar (Table S30) and 64 unique hsRNA:vRNA target pairs in Tanto (Table S31). 23 of the unique hsRNA:vRNA target pairs occurred in both cultivars and 22 and 41 of them were Drakkar- and Tanto-specific, respectively. The most frequent RISC-mediated vRNA cleavage events potentially involving vsiRNAs and hsRNAs were detected in the 3' region of the viral

RNA (Fig. 5), which may be caused by a limitation in the length of cDNAs synthesized for PAREseq analysis. vsiRNA:vRNA and hsRNA:vRNA pairs found in both cultivars and associated with cleavage events found at the same positions of the vRNA in both cultivars provide mutual support for the significance of these viral sites of RISC-mediated cleavage. Cultivar-specific sites of vRNA cleavage may be related to the difference in viral susceptibility between Drakkar and Tanto. Interestingly, several of the hsRNA-mediated cleavage events were found to involve trans-acting va-phasRNAs derived from NBR1 and TAR1 genes (Table S30 and Table S31). However, the large majority of the cleavage events were associated with unique hsRNAs derived from genes annotated as disease resistance genes TAO1 and RPP5, both encoding TIR-NB-LRR receptor-like proteins. These and several other genes associated with hsRNA-mediated antiviral vRNA cleavage produce numerous secondary siRNAs in both mock-treated as well as TuMV-infected plants (Figure S11). Thus, these genes produce antiviral siRNAs already before infection.

Discussion

sRNAs have emerged as key players of RNA silencing in the regulation of various biological processes, including plant growth and development, host immunity and pathogen virulence. As viruses replicate within plant cells viruses become an integrated part of this sRNA-mediated regulatory network. The plant host silencing machinery is known to process the double-stranded viral replication intermediates into primary and secondary vsiRNAs to use them as guides for cleavage of vRNA by AGO-RISC and that viruses suppress this antiviral host activity with their VSRs. However, although sRNAs and protein effectors in fungi, oomycetes, and bacteria have been shown to function in promoting pathogen virulence (Weiberg et al. 2014), much less is known about the potential of viruses to use their vsiRNAs and VSRs to target the expression of host genes. While the general impact of viral infection on host transcriptomes, the profiles of sRNAs, the methylation of sRNAs, and activities of specific miRNAs and few virus- or viroid-derived siRNAs have been described (e.g. Hu et al. 2011; Huang et al. 2016; Niu et al. 2015; Ruiz-Ferrer and Voinnet 2009; Varallyay et al. 2010; Whitham et al. 2006), a deep understanding of host and viral sRNA activities in mutual regulation within the viral niche of infected leaf cells engaged in local viral replication and spread has not yet been achieved. The current study has applied a combination of different replicate RNA profiling approaches to the analysis of distinct local sites of early TuMV infection in rapeseed leaves. By using rapeseed cultivars strongly differing in susceptibility to this economically important virus (Edwardson and Christie 1991; Shattuck 1992) the data distinguish general mechanisms involved in

virus infection from those that may correspond to resistance. Transcriptional RNAseq profiling revealed the regulation of virus-responsive genes whereas the combination of sRNAseq with PAREseq profiles allowed us to correlate the occurrence of cleaved mRNA 5'ends with corresponding sRNA:mRNA target pairs and thereby identify the virus-induced activity of sRNAs, including previously unknown miRNAs and siRNAs, in RISC-mediated RNA target cleavage. Collectively, the results draw a novel picture of interactions between a virus and its host (Fig. 6) in which the mutual regulation of host mRNAs and the viral RNA genome by host and virus-derived small RNAs plays a central role.

First of all, the results establish the novel finding that the host apparently uses endogenous siRNAs to target the virus, whereas the virus, in turn, uses vsRNAs to target the host. The host-derived siRNAs that target the virus are derived from genes that convert all or part of their mRNA transcripts into secondary siRNAs. Such production of phased secondary siRNAs (phasiRNAs) has emerged as a regulatory mechanism for coding genes, particularly of nucleotide-binding, leucine-rich repeat (NB-LRR) disease resistance genes (Fei et al. 2013). Consistently, we found that siRNAs that target the virus are predominantly derived from resistance genes TAO1 and RPP5. This finding indicates that by conversion of their transcripts to siRNAs, resistance genes have the capacity to provide RNA-based immunity in addition to protein-based immunity. Interestingly, TAO1 and RPP5 produce phasiRNAs also in the absence of the virus suggesting that antiviral siRNA production from these genes serves to provide basal antiviral immunity already in naïve plants. Additional siRNAs targeting the virus derive from genes that produce siRNAs only upon infection, such as the Chorophyll a, b-binding protein 1 and NBR1 genes, or produce additional siRNAs upon infection such as the TAR1 genes. As previously noted in Arabidopsis and other viral host systems (Cao et al. 2014; Zheng et al. 2015), we found that virus infection indeed promotes a dramatic induction of phased secondary siRNA (va-phasiRNA) production from coding genes. According to our results, the va-phasiRNAs induced by TuMV infection in rapeseed greatly differ in their activity as guides for RISC in a manner dependent on the gene of origin. Some genes produce va-phasiRNAs not participating in RISC-mediated mRNA target cleavage (e.g. AGO2 genes), whereas other genes produce phasiRNAs that do participate in RISC-mediated mRNA target cleavage and target the gene of origin as well as homologous genes in the same gene family (e.g. Chorophyll-a,b-binding protein 1 genes). Yet other genes produce va-phasiRNAs that target other genes (e.g. NBR1 and TAR genes). The induction of va-phasiRNAs likely serves to dampen the effects of infection on transcript homeostasis. This might be particularly true for va-phasiRNAs that do not participate in RISC-mediated target cleavage, or

target only the gene of origin or genes within the same family. On the other hand, the loci that produce trans-acting va-phasiRNAs may be induced by the virus to modify the expression of secondary mRNA targets. This is supported, for example, by the virus-induced targeting of genes for ACTIN-DEPOLYMERIZING FACTOR 3 by NBR1-derived va-phasiRNAs, which may represent a virus-induced mechanism to lower defense against aphids that the virus needs for plant-to-plant transmission. These and other genes targeted by virus-induced and predominantly NBR1-derived va-phasiRNAs identify NBR1 genes as virus-inducible hubs for secondary trans-acting siRNA production and for the virus-induced manipulation of secondary mRNA targets. As NBR1-derived va-phasiRNAs also target the virus, the evolution of NBR1 genes as virus-inducible hubs for secondary trans-acting siRNA production may have occurred on the basis of the precondition that the va-phasiRNAs derived from the same hub will, in turn, also control the virus. It is intriguing that the *B. napus* NBR1 genes are highly homologous to the selective autophagy receptor protein AT4G24690/NBR1 gene in Arabidopsis (81-84% identity), which has been implicated in antiviral defenses involving the degradation of viral proteins and particles by autophagy (Hafren et al. 2017; Hafren and Hofius 2017). This protein was in particular shown to suppress TuMV infection in Arabidopsis by targeting the VSR of the virus (HcPro) (Hafren et al. 2018). Thus, by conversion of NBR1 mRNA into secondary siRNAs the virus gains widespread control over host gene expression and also suppresses NBR1 mRNA levels to control the antiviral functions of the NBR1 protein (Fig. 7).

Among the host mRNAs targeted by virus-derived siRNAs (vsRNAs), we identified 17 unique transcripts representing the most significant targets in both Drakkar and Tanto. Interestingly, all these transcripts encode ethylene responsive factors (ERFs) and are targeted by a specific unique vsiRNA. The targeted ERFs all contain a repression domain and therefore can act to actively inhibit transcription (Licausi et al. 2013). The vsiRNA mediates the cleavage of these transcripts at exactly the site usually cleaved by miR172. Since this miRNA is downregulated upon infection, this vsiRNA may mimic miR172 to maintain efficient control over the expression of ERFs, which regulate plant responses to biotic and abiotic stresses (Licausi et al. 2013; Muller and Munne-Bosch 2015). It is interesting that this vsiRNA is only 19 nucleotides (nt) in length. This particular length may have been selected to evade capturing by the TuMV VSR (HcPro), which specifically binds 21 and 22 nt sRNAs (Del Toro et al. 2017; Valli et al. 2018). Thus, unlike the 21 nt long miR172, which is prone to capturing by HcPro, the vsiRNA may remain active even at high VSR levels (Fig. 8). The observation that the mRNAs for ERFs and other host mRNA targets of vsiRNAs are only moderately

downregulated during infection suggests that the vsRNA-mediated interaction of the virus with these genes may have evolved to interfere with a strong induction of these defense-related genes in infected cells.

The sRNA-mediated mechanisms described here were identified in two different rapeseed cultivars, which confirms the significance of the observations. Although these cultivars differ strongly in their susceptibility towards TuMV, the sRNA-mediated mechanisms seem rather be unrelated to these differences. Although we found cultivar specific cleavage sites in the vRNA, infection in these cultivars generally cause rather similar changes in the levels of host sRNAs and their mRNA targets. The specific susceptibility of the cultivars for TuMV infection is rather correlated with strong differences in the virus-induced mRNA levels of other genes. Resistance in Tanto is correlated with the cultivar-specific or pronounced expression of several important defense-related genes, (e.g. DTX47/EDS5, GH3.12, NIMIN-2, TAO1), whereas promoted infection in Drakkar correlates with the cultivar-specific or pronounced expression of genes involved in virus replication and movement (e.g. a COP-I subunit), the down-regulation of genes with potential to inhibit systemic movement (e.g. PPA2), or the attenuation of plant defenses (e.g. NAC60, RPK2, TPR2, CKX3). These genes, and also the NBR1 and TAR1 genes that spawn virus-induced secondary siRNAs for widespread virus-induced gene regulation, may represent important targets for plant engineering.

Materials and Methods

Plant materials, plant growth conditions, virus inoculation, and RNA extraction

Brassica napus cv. Drakkar and *Brassica napus* cv. Tanto plants grown for 4-5 weeks in a growth chamber at 24 °C with a 16h photoperiod were mechanically inoculated with freshly prepared crude extract (sap) of donor *B. napus* cv Drakkar plants systemically infected with TuMV-GFP. The donor plants were mechanically inoculated with sap from systemically infected *Nicotiana benthamiana* plants. Sap was always created by grinding infected leaves in 75 mM potassium phosphate buffer pH 7.5 in a cooled mortar. To create the original *N. benthamiana* donor plants, five weeks old *N. benthamiana* plants grown at 25°C with a 16h photoperiod were inoculated by agroinfiltration of two leaves per plant with *A. tumefaciens* strain GV3101 containing the binary plasmid pCB-TuMV-GFP (Dunoyer et al. 2004; Lellis et al. 2002). The agrobacteria were grown over night and pressure-injected at an OD_{600nm} of 0.5 using a syringe without needle. The TuMV (UK1) construct present in plasmid pCB-TuMV-GFP (GenBank: EF028235.1) has been verified by sequencing before use.

Inoculated leaves were monitored with a handheld UV lamp (UVP Blak-Ray B-100) to reveal GFP fluorescent infection sites. TuMV-GFP infection sites in the inoculated leaves of *B. napus* cv Drakkar and *B. napus* cv Tanto plants were carefully isolated at 12 dpi with a 0.5 cm micropunch and immediately frozen in liquid nitrogen. Leaf disks of mock treated *B. napus* cv Drakkar (sample DM) and mock-treated *B. napus* cv Tanto plants (sample TM) as well as infection sites on virus-treated *B. napus* cv Drakkar (sample DT) and infection sites on virus-treated *B. napus* cv Tanto plants (sample TT) were dissected from three independent inoculation experiments. Thus, three samples each of DM, DT, TM, and TT, were created.

Total RNA of each sample was extracted from ca 200 dissected leaf-disks / infection foci. Two grams (2 g) of these were ground in liquid nitrogen and RNA was purified using the RNeasy Mini Kit (Qiagen). The quality of each RNA sample was verified by gel electrophoresis and BioAnalyzer (Agilent technologies) techniques. The relative number of viral genomes in the samples was determined by RT-qPCR amplifying the TuMV CP cistron using oligonucleotide TGTTCCGGCTTGGATGGAA as forward primer and oligonucleotide TTAACGTCCTCGGTCGTATGC as reverse primer within 30 ng total RNA. sRNAseq and mRNAseq sequencing libraries were constructed and sequenced (Illumina HiSeq2000) by aScidea Computational Biology Solutions (<http://www.ascidea.com/>). mRNA and sRNA reads were created by (2x100bp) paired-end sequencing and (1x50bp) sequencing, respectively.

Degradome sequencing

Degradome libraries were constructed from each RNA sample essentially as described previously (German et al. 2009). Briefly, mRNA was purified from 75-150 µg of total RNA using the Dynabeads mRNA direct purification kit (Ambion). 1 µg of the isolated mRNA was ligated to a 5' RNA adapter, purified using Dynabeads and used for the cDNA synthesis, PCR amplification and MmeI digestion. The 20 nt DNA fragments resulting from MmeI digestion were purified by polyacrylamide gel electrophoresis (PAGE) and 3' ligated to a dsDNA adapter. The ligation products were further purified by PAGE and amplified by PCR using indexed Illumina primers (Illumina primers RPI1 to RPI4) to allow multiplexing during sequencing. The final libraries consisting of amplicons of approximately 125 bp were again purified by PAGE. The suitability of our libraries for high-throughput sequencing was tested by cloning them into TOPO vector and low-scale sequencing of individual clones. After quantification using Nanodrop, the degradome libraries were sequenced (1x 50 bp) on an Illumina HiSeq2000 platform by aScidea.

Whole genome re-sequencing

DNA isolated from 1.9 g fast-frozen leaf tissue of *B. napus* cv Drakkar and *B. napus* cv Tanto plants was used for creation of 800 bp insert PCR-free libraries and subsequent paired-end sequencing (2*150 bp) on an Illumina HiSeq 4000 platform (BGI Tech Solutions, Hongkong). The 123 Mio clean reads obtained for each cultivar were mapped to the *B.napus* “Darmor-bzh” reference genome sequence (Genoscope v4.1; (Chalhoub et al. 2014)) with the Burrows-Wheeler Aligner **BWA-MEM** algorithm ((Li and Durbin 2009); RRID:SCR_010910) version **v0.7.15-r1142**, using default parameters. Duplicated reads were marked with **Picard-tools** (RRID:SCR_006525; <http://broadinstitute.github.io/picard/>) version **v1.140** and SNPs calling was performed with GATK **HaplotypeCaller** ((McKenna et al. 2010), RRID:SCR_001876) version **v3.3-0**. Only high-quality homozygous SNPs were kept using the filters: QD < 2.0 || FS > 60.0 || MQ < 40.0 || MQRankSum < -12.5 || ReadPosRankSum < -8.0 || DP < 4. Representative genomes for Drakkar and Tanto cultivars were constructed by inferring these cultivar-specific high confidence SNPs into the reference sequence with GATK **FastaAlternateReferenceMaker** (RRID:SCR_001876; https://software.broadinstitute.org/gatk/documentation/tooldocs/3.8-0/org_broadinstitute_gatk_tools_walkers_fasta_FastaAlternateReferenceMaker.php). The reconstructed Drakkar and Tanto genomes were used for the rest of the analysis.

Bioinformatic analysis of mRNA, sRNA, and degradome profiles

mRNAseq raw reads libraries were quality checked with **FastQC** (RRID:SCR_014583) version **v0.11.2** and cleaned with **cutadapt** (RRID:SCR_011841) version **v1.8.1** for adapter removal, N removal and quality filtering. Reads longer than 60 bp and with a Phred score greater than 30 were kept. The clean RNAseq reads from the Tanto and Drakkar samples were then aligned to the reconstructed Tanto and Drakkar genomes, respectively, using **Tophat2** ((Kim et al. 2013), <https://ccb.jhu.edu/software/tophat/index.shtml>) version **v2.0.13**, allowing one mismatch and applying **Bowtie2** ((Langmead and Salzberg 2012), <http://bowtie-bio.sourceforge.net/bowtie2/index.shtml>) as its read-alignment engine. Genes were re-annotated with **blastx** against the *Arabidopsis thaliana* genome (with default parameters) and the Arabidopsis gene identifiers were used to receive the gene ontology (GO) annotations from the protein knowledgebase (UniProtKB). For differential expression analysis the mapped reads were counted using the **SAMtools** (Li et al. 2009) (RRID:SCR_002105) **idxstats tool** version **v1.1**, and analyzed using **Bioconductor - DESeq2** (Love et al. 2014)(RRID:SCR_015687) version **v1.10.0**. The results were

filtered for expressed transcripts with at least 150 mean reads and showing statistically significant changes (p -value < 0.05) in expression between conditions.

sRNAseq raw read libraries were quality checked and reads were filtered like the mRNAseq read libraries. Clean reads that were 18 nt to 30 nt in length and that had a Phred score higher than 30 were kept and then annotated by mapping them with no mismatches to TuMV-GFP and to miRNAs of *Brassicaceae* (*B. napus*, *B. oleracea*, *B. rapa*, *A. thaliana*, *A. lyrata*) compiled from miRbase (Kozomara and Griffiths-Jones 2014) using **Bowtie2** (Langmead and Salzberg 2012) version **v2.2.9** and applying the option “-t -N 0 --end-to-end --very-sensitive --score-min C,0,0” with no mismatch for virus -derived sRNAs. The set of miRNAs derived from miRbase was complemented by miRNAs described in recent publications (Jiang et al. 2014; Lukasik et al. 2013; Xu et al. 2012) and by miRNAs derived from miRNA genes predicted by **ShortStack** (Axtell, 2013)(RRID:SCR_010834). We used ShortStack version **v3.4**. in *de novo* mode and the list of predicted miRNAs was filtered to keep only clusters with: Dicer call 21, 22, 24nt, and MIRNAs step Y_N15. The total list of known miRNAs contained 1047 miRNAs, against which the sRNA reads were aligned. sRNA reads that were strongly induced by infection and could be mapped to both strands of *B. napus* coding genes but not to the viral genome likely represent a specific class of RDR1-dependent siRNAs identified in Arabidopsis and known as vasiRNAs (virus-associated siRNAs, (Cao et al. 2014)). Although the virus-induced *B. napus* siRNAs show phasing along the transcript of origin like vasiRNAs, we do not know the specific RDR by which these siRNAs are produced. Therefore, we refer to these siRNAs as “va-phasiRNAs” rather than to vasiRNAs. We focused our analysis on va-phasiRNAs that were 21 nt in length and represented by at least 100 reads in the samples from infected tissues. Moreover, va-phasiRNA-producing genes had a PHAS Score higher than 30 (determined by **ShortStack**). The virus-induced and phased production of the va-phasiRNAs was verified by visualization of the gene-specific siRNA pattern with the Integrated Genome Viewer tool IGV 2.3 (Thorvaldsdottir et al. 2013).

Similar as for mRNAseq and siRNAseq reads, also the sequenced degradome read libraries were cleaned with **cutadapt** (RRID:SCR_011841) version **v1.8.1** for adapter removal, N removal and quality filtering. Clean libraries were then analysed with **PAREsnip** (Folkes et al. 2012) implemented in the UEA sRNA Workbench (<http://srna-workbench.cmp.uea.ac.uk/>; (Stocks et al. 2018) version v4.2.1 alphaD, with min read abundance set to 100 and default parameters, and using the sRNAseq and mRNAseq data as inputs to predict sRNA:mRNA pairs associated with identified monophosphorylated mRNA 5'ends and consistent with sRNA-mediated RNA target cleavage. Specific cleavage events were normalized and compared between samples in reads per million (rpm;

number of specific cleavage events multiplied by 10^6 and divided by the total number of cleavage events in the degradome library). The sums of normalized cleavage events occurring in the three replicates per condition (specific cultivar/specific treatment) were used to compare specific cleavage events between conditions. The gene or viral origins of the sRNAs associated with specific mRNA or viral RNA cleavage events were identified by extracting the sRNA associated with a specific cleavage event from PAREsnip and by aligning its sequence to the cultivar/viral transcriptome without mismatch, using **Bowtie 2**. A role of a given sRNA (e.g. miRNA, vasiRNA, vsRNA) in specific RNA target cleavage was determined by searching the sRNA:RNA target pair outputs of PAREsnip with the specific sRNA query sequence(s).

Quantitative RT-PCR

Total RNA was isolated from ca 150 leaf disk samples of infection sites or of mock-treated, non-infected control tissues each pooled from ten plants, respectively. After grinding, 0.1 g fine powder was homogenized and extracted with Trizol reagent (Invitrogen, USA) following the manufacturer's instructions. RNA quantities were determined by spectrophotometric analysis using Nanodrop equipment (Thermo Scientific, USA). 1-2 μg of the RNA preparations were reverse-transcribed using an oligo dT primer and SuperScript IV reverse transcriptase (200 U/ μl) (Invitrogen). The abundance of specific transcript was measured by probing the cDNA by quantitative real-time PCR using a SYBR-green master mix (Roche) and allele-specific primers (Table S32) in a Lightcycler 480 (Roche). Because the mRNAseq data refer to changes in the expression of specific A- or-C-genome-specific alleles, the analysis was performed with genes for which allele-specific, intron-spanning primer sets showing no homology to any other paralogs or homologous sequences could be designed. The specific transcript levels were measured in five independent biological replicate samples for each cultivar and respective mock-treated and virus-infected conditions. Each RNA sample was analyzed by three technical replicates and specific RNA levels were normalized against the levels of transcripts produced by two known housekeeping genes (Bra011516 encoding a TIP41-like protein and BnaA08g11790D ('BnaUP1'; unknown function) (Wang et al. 2014; Zhang et al. 2014)). Significant differences in mRNA abundance between samples of the mock- and virus-treated conditions were determined by an F-test (test for homoscedasticity) followed by a t-test. The statistical significance levels in figures are shown with asterisks: $p < 0.05 = *$; $p < 0.01 = **$; $p < 0.001 = ***$.

5' RACE

mRNA 5' ends were analyzed by 5' RACE as described previously (Llave et al. 2011; Llave et al. 2002). poly(A)⁺ mRNA was purified from 1-5 µg total RNA using a magnetic isolation module (NEBNext[®], BioLabs) and ligated to the GeneRacer RNA oligo 5' RACE adapter (Invitrogen) using T4 RNA ligase (New England BioLabs). The ligation product was purified using Illustra Microspin S-300 Sephacryl columns (GE Healthcare) and reverse transcribed into cDNA using an oligo(dT)₂₀ primer and SuperScript IV reverse transcriptase (200 U/µl, Invitrogen). Each cDNA was then used for PCR amplification using the GeneRacer 5' RACE outer primer mapping to a sequence within the 5' adapter and two nested, gene specific primers (Table S33). The PCR products were purified with a PCR clean-up kit (Macherey-Nagel) and sequenced with an ABI3130xl sequencer (Applied Life Technologies).

Acknowledgements

This work has been subject to the trinational PLANT-KBBE 2012 project GAMAVIR. We acknowledge funding from the French Agence National de la Recherche (grant ANR-13-KBBE-0005-01), the Swiss National Science Foundation (SNF, grant 31003A_140694), and the Région Alsace (PhD fellowship for NP) to MH, from the Spanish Ministerio de Economía y Competitividad (MINECO, grant ???) to CL, and the Deutsche Forschungsgemeinschaft (DFG, PCIN-2013-064) to MW.

References

- Ahn, H.K., Kang, Y.W., Lim, H.M., Hwang, I., Pai, H.S., 2015. Physiological functions of the COPI complex in higher plants. *Mol Cells* 38, 866-875.
- Alazem, M., Lin, K.Y., Lin, N.S., 2014. The abscisic acid pathway has multifaceted effects on the accumulation of *Bamboo mosaic virus*. *Mol Plant Microbe Interact* 27, 177-189.
- Alazem, M., Lin, N.S., 2017. Antiviral roles of abscisic acid in plants. *Front Plant Sci* 8, 1760.
- Argueso, C.T., Ferreira, F.J., Epple, P., To, J.P., Hutchison, C.E., Schaller, G.E., Dangl, J.L., Kieber, J.J., 2012. Two-component elements mediate interactions between cytokinin and salicylic acid in plant immunity. *PLoS Genet* 8, e1002448.
- Axtell, M.J., 2013. ShortStack: comprehensive annotation and quantification of small RNA genes. *RNA* 19, 740-751.
- Bologna, N.G., Voinnet, O., 2014. The diversity, biogenesis, and activities of endogenous silencing small RNAs in Arabidopsis. *Annu Rev Plant Biol* 65, 473-503.

- Bouché, N., Laressergues, D., Gascioli, V., Vaucheret, H., 2006. An antagonistic function for Arabidopsis DCL2 in development and a new function for DCL4 in generating viral siRNAs. *EMBO J* 25, 3347-3356.
- Cao, M., Du, P., Wang, X., Yu, Y.Q., Qiu, Y.H., Li, W., Gal-On, A., Zhou, C., Li, Y., Ding, S.W., 2014. Virus infection triggers widespread silencing of host genes by a distinct class of endogenous siRNAs in Arabidopsis. *Proc Natl Acad Sci U S A* 111, 14613-14618.
- Carbonell, A., Carrington, J.C., 2015. Antiviral roles of plant ARGONAUTES. *Curr Opin Plant Biol* 27, 111-117.
- Carviel, J.L., Wilson, D.C., Isaacs, M., Carella, P., Catana, V., Golding, B., Weretilnyk, E.A., Cameron, R.K., 2014. Investigation of intercellular salicylic acid accumulation during compatible and incompatible Arabidopsis-*Pseudomonas syringae* interactions using a fast neutron-generated mutant allele of EDS5 identified by genetic mapping and whole-genome sequencing. *PLoS One* 9, e88608.
- Chalhoub, B., Denoeud, F., Liu, S., Parkin, I.A., Tang, H., Wang, X., Chiquet, J., Belcram, H., Tong, C., Samans, B., Correa, M., Da Silva, C., Just, J., Falentin, C., Koh, C.S., Le Clainche, I., Bernard, M., Bento, P., Noel, B., Labadie, K., Alberti, A., Charles, M., Arnaud, D., Guo, H., Daviaud, C., Alamery, S., Jabbari, K., Zhao, M., Edger, P.P., Chelaifa, H., Tack, D., Lassalle, G., Mestiri, I., Schnell, N., Le Paslier, M.C., Fan, G., Renault, V., Bayer, P.E., Golicz, A.A., Manoli, S., Lee, T.H., Thi, V.H., Chalabi, S., Hu, Q., Fan, C., Tollenaere, R., Lu, Y., Battail, C., Shen, J., Sidebottom, C.H., Wang, X., Canaguier, A., Chauveau, A., Berard, A., Deniot, G., Guan, M., Liu, Z., Sun, F., Lim, Y.P., Lyons, E., Town, C.D., Bancroft, I., Wang, X., Meng, J., Ma, J., Pires, J.C., King, G.J., Brunel, D., Delourme, R., Renard, M., Aury, J.M., Adams, K.L., Batley, J., Snowdon, R.J., Tost, J., Edwards, D., Zhou, Y., Hua, W., Sharpe, A.G., Paterson, A.H., Guan, C., Wincker, P., 2014. Plant genetics. Early allopolyploid evolution in the post-Neolithic *Brassica napus* oilseed genome. *Science* 345, 950-953.
- Choi, J., Huh, S.U., Kojima, M., Sakakibara, H., Paek, K.H., Hwang, I., 2010. The cytokinin-activated transcription factor ARR2 promotes plant immunity via TGA3/NPR1-dependent salicylic acid signaling in Arabidopsis. *Dev Cell* 19, 284-295.
- Csorba, T., Kontra, L., Burgyan, J., 2015. Viral silencing suppressors: Tools forged to fine-tune host-pathogen coexistence. *Virology* 479-480C, 85-103.
- Del Toro, F.J., Donaire, L., Aguilar, E., Chung, B.N., Tenllado, F., Canto, T., 2017. Potato virus Y Hcpro suppression of antiviral silencing in *Nicotiana benthamiana* plants correlates with its ability to bind *in vivo* to 21- and 22-nucleotide smallRNAs of viral sequence. *J Virol* 91, e00367-17.
- Deleris, A., Gallego-Bartolome, J., Bao, J., Kasschau, K.D., Carrington, J.C., Voinnet, O., 2006. Hierarchical action and inhibition of plant Dicer-like proteins in antiviral defense. *Science* 313, 68-71.
- Ding, S.W., Voinnet, O., 2007. Antiviral immunity directed by small RNAs. *Cell* 130, 413-426.

- Dodds, P.N., Rathjen, J.P., 2010. Plant immunity: towards an integrated view of plant-pathogen interactions. *Nat Rev Genet* 11, 539-548.
- Dunoyer, P., Thomas, C., Harrison, S., Revers, F., Maule, A., 2004. A cysteine-rich plant protein potentiates Potyvirus movement through an interaction with the virus genome-linked protein VPg. *J Virol* 78, 2301-2309.
- Duque, P., 2011. A role for SR proteins in plant stress responses. *Plant Signal Behav* 6, 49-54.
- Edwardson, J.R., Christie, R.G., 1991. *The Potyvirus Group*. Univ. of Florida Press.
- Eitas, T.K., Nimchuk, Z.L., Dangl, J.L., 2008. Arabidopsis TAO1 is a TIR-NB-LRR protein that contributes to disease resistance induced by the *Pseudomonas syringae* effector AvrB. *Proc Natl Acad Sci U S A* 105, 6475-6480.
- Fei, Q., Xia, R., Meyers, B.C., 2013. Phased, secondary, small interfering RNAs in posttranscriptional regulatory networks. *Plant Cell* 25, 2400-2415.
- Folkes, L., Moxon, S., Woolfenden, H.C., Stocks, M.B., Szittyá, G., Dalmay, T., Moulton, V., 2012. PAREsnip: a tool for rapid genome-wide discovery of small RNA/target interactions evidenced through degradome sequencing. *Nucleic Acids Res* 40, e103.
- Fu, M., Xu, M., Zhou, T., Wang, D., Tian, S., Han, L., Dong, H., Zhang, C., 2014. Transgenic expression of a functional fragment of harpin protein Hpa1 in wheat induces the phloem-based defence against English grain aphid. *J Exp Bot* 65, 1439-1453.
- Galopier, A., Hermann-Le Denmat, S., 2011. Mitochondria of the yeasts *Saccharomyces cerevisiae* and *Kluyveromyces lactis* contain nuclear rDNA-encoded proteins. *PLoS One* 6, e16325.
- Garcia-Arenal, F., McDonald, B.A., 2003. An analysis of the durability of resistance to plant viruses. *Phytopathology* 93, 941-952.
- Garcia-Ruiz, H., Carbonell, A., Hoyer, J.S., Fahlgren, N., Gilbert, K.B., Takeda, A., Giampetruzzi, A., Garcia Ruiz, M.T., McGinn, M.G., Lowery, N., Martinez Baladejo, M.T., Carrington, J.C., 2015. Roles and programming of Arabidopsis ARGONAUTE proteins during *Turnip mosaic virus* infection. *PLoS Pathog* 11, e1004755.
- German, M.A., Luo, S., Schroth, G., Meyers, B.C., Green, P.J., 2009. Construction of Parallel Analysis of RNA Ends (PARE) libraries for the study of cleaved miRNA targets and the RNA degradome. *Nat Protoc* 4, 356-362.
- Hafren, A., Hofius, D., 2017. NBR1-mediated antiviral xenophagy in plant immunity. *Autophagy* 13, 2000-2001.
- Hafren, A., Macia, J.L., Love, A.J., Milner, J.J., Drucker, M., Hofius, D., 2017. Selective autophagy limits *Cauliflower mosaic virus* infection by NBR1-mediated targeting of viral capsid protein and particles. *Proc Natl Acad Sci U S A* 114, E2026-E2035.

- Hafren, A., Ustun, S., Hochmuth, A., Svenning, S., Johansen, T., Hofius, D., 2018. *Turnip mosaic virus* counteracts selective autophagy of the viral silencing suppressor HCpro. *Plant Physiol* 176, 649-662.
- Harvey, J.J., Lewsey, M.G., Patel, K., Westwood, J., Heimstadt, S., Carr, J.P., Baulcombe, D.C., 2011. An antiviral defense role of AGO2 in plants. *PLoS One* 6, e14639.
- Hermann, M., Maier, F., Masroor, A., Hirth, S., Pfitzner, A.J., Pfitzner, U.M., 2013. The Arabidopsis NIMIN proteins affect NPR1 differentially. *Front Plant Sci* 4, 88.
- Hook, L., Hancock, M., Landais, I., Grabski, R., Britt, W., Nelson, J.A., 2014. Cytomegalovirus microRNAs. *Curr Opin Virol* 7, 40-46.
- Hu, Q., Hollunder, J., Niehl, A., Korner, C.J., Gereige, D., Windels, D., Arnold, A., Kuiper, M., Vazquez, F., Pooggin, M., Heinlein, M., 2011. Specific impact of tobamovirus infection on the Arabidopsis small RNA profile. *PLoS One* 6, e19549.
- Huang, J., Yang, M., Lu, L., Zhang, X., 2016. Diverse functions of small RNAs in different plant-pathogen communications. *Front Microbiol* 7, 1552.
- Ishihara, T., Sekine, K.T., Hase, S., Kanayama, Y., Seo, S., Ohashi, Y., Kusano, T., Shibata, D., Shah, J., Takahashi, H., 2008. Overexpression of the *Arabidopsis thaliana* EDS5 gene enhances resistance to viruses. *Plant Biol (Stuttg)* 10, 451-461.
- Jagadeeswaran, G., Raina, S., Acharya, B.R., Maqbool, S.B., Mosher, S.L., Appel, H.M., Schultz, J.C., Klessig, D.F., Raina, R., 2007. Arabidopsis GH3-LIKE DEFENSE GENE 1 is required for accumulation of salicylic acid, activation of defense responses and resistance to *Pseudomonas syringae*. *Plant J* 51, 234-246.
- Jeong, S., 2017. SR proteins: binders, regulators, and connectors of RNA. *Mol Cells* 40, 1-9.
- Jiang, J., Lv, M., Liang, Y., Ma, Z., Cao, J., 2014. Identification of novel and conserved miRNAs involved in pollen development in *Brassica campestris* ssp. *chinensis* by high-throughput sequencing and degradome analysis. *BMC Genomics* 15, 146.
- Jones, J.D., Dangl, J.L., 2006. The plant immune system. *Nature* 444, 323-329.
- Kim, D., Pertea, G., Trapnell, C., Pimentel, H., Kelley, R., Salzberg, S.L., 2013. TopHat2: accurate alignment of transcriptomes in the presence of insertions, deletions and gene fusions. *Genome Biol* 14, R36.
- Kørner, C.J., Klauser, D., Niehl, A., Dominguez-Ferreras, A., Chinchilla, D., Boller, T., Heinlein, M., Hann, D.R., 2013. The immunity regulator BAK1 contributes to resistance against diverse RNA viruses. *Mol Plant Microbe Interact* 26, 1271-1280.
- Kozomara, A., Griffiths-Jones, S., 2014. miRBase: annotating high confidence microRNAs using deep sequencing data. *Nucleic Acids Res* 42, D68-73.

- Kubota, K., Tsuda, S., Tamai, A., Meshi, T., 2003. *Tomato mosaic virus* replication protein suppresses virus-targeted posttranscriptional gene silencing. *J Virol* 77, 11016-11026.
- Langmead, B., Salzberg, S.L., 2012. Fast gapped-read alignment with Bowtie 2. *Nat Methods* 9, 357-359.
- Lellis, A.D., Kasschau, K.D., Whitham, S.A., Carrington, J.C., 2002. Loss-of-susceptibility mutants of *Arabidopsis thaliana* reveal an essential role for eIF(iso)4E during potyvirus infection. *Curr Biol* 12, 1046-1051.
- Lewis, J.D., Lee, A.H., Hassan, J.A., Wan, J., Hurley, B., Jhingree, J.R., Wang, P.W., Lo, T., Youn, J.Y., Guttman, D.S., Desveaux, D., 2013. The *Arabidopsis* ZED1 pseudokinase is required for ZAR1-mediated immunity induced by the *Pseudomonas syringae* type III effector HopZ1a. *Proc Natl Acad Sci U S A* 110, 18722-18727.
- Li, H., Durbin, R., 2009. Fast and accurate short read alignment with Burrows-Wheeler transform. *Bioinformatics* 25, 1754-1760.
- Li, H., Handsaker, B., Wysoker, A., Fennell, T., Ruan, J., Homer, N., Marth, G., Abecasis, G., Durbin, R., Genome Project Data Processing, S., 2009. The Sequence Alignment/Map format and SAMtools. *Bioinformatics* 25, 2078-2079.
- Licausi, F., Ohme-Takagi, M., Perata, P., 2013. APETALA2/Ethylene Responsive Factor (AP2/ERF) transcription factors: mediators of stress responses and developmental programs. *New Phytol* 199, 639-649.
- Llave, C., Franco-Zorrilla, J.M., Solano, R., Barajas, D., 2011. Target validation of plant microRNAs. *Methods Mol Biol* 732, 187-208.
- Llave, C., Xie, Z., Kasschau, K.D., Carrington, J.C., 2002. Cleavage of Scarecrow-like mRNA targets directed by a class of *Arabidopsis* miRNA. *Science* 297, 2053-2056.
- Love, M.I., Huber, W., Anders, S., 2014. Moderated estimation of fold change and dispersion for RNA-seq data with DESeq2. *Genome Biol* 15, 550.
- Lu, H., Chandrasekar, B., Oeljeklaus, J., Misas-Villamil, J.C., Wang, Z., Shindo, T., Bogyo, M., Kaiser, M., van der Hoorn, R.A., 2015. Subfamily-specific fluorescent probes for cysteine proteases display dynamic protease activities during seed germination. *Plant Physiol* 168, 1462-1475.
- Lukasik, A., Pietrykowska, H., Paczek, L., Szweykowska-Kulinska, Z., Zielenkiewicz, P., 2013. High-throughput sequencing identification of novel and conserved miRNAs in the *Brassica oleracea* leaves. *BMC Genomics* 14, 801.
- McKenna, A., Hanna, M., Banks, E., Sivachenko, A., Cibulskis, K., Kernytsky, A., Garimella, K., Altshuler, D., Gabriel, S., Daly, M., DePristo, M.A., 2010. The Genome Analysis Toolkit: a MapReduce framework for analyzing next-generation DNA sequencing data. *Genome Res* 20, 1297-1303.

- Mondal, H.A., Louis, J., Archer, L., Patel, M., Nalam, V.J., Sarowar, S., Sivapalan, V., Root, D.D., Shah, J., 2018. Arabidopsis ACTIN-DEPOLYMERIZING FACTOR3 Is required for controlling aphid feeding from the phloem. *Plant Physiol* 176, 879-890.
- Morel, J.B., Godon, C., Mourrain, P., Beclin, C., Boutet, S., Feuerbach, F., Proux, F., Vaucheret, H., 2002. Fertile hypomorphic ARGONAUTE (*ago1*) mutants impaired in post-transcriptional gene silencing and virus resistance. *Plant Cell* 14, 629-639.
- Mourrain, P., Beclin, C., Elmayan, T., Feuerbach, F., Godon, C., Morel, J.B., Jouette, D., Lacombe, A.M., Nikic, S., Picault, N., Remoue, K., Sanial, M., Vo, T.A., Vaucheret, H., 2000. Arabidopsis SGS2 and SGS3 genes are required for posttranscriptional gene silencing and natural virus resistance. *Cell* 101, 533-542.
- Muller, M., Munne-Bosch, S., 2015. Ethylene response factors: a key regulatory hub in hormone and stress signaling. *Plant Physiol* 169, 32-41.
- Nawrath, C., Heck, S., Parinthawong, N., Metraux, J.P., 2002. EDS5, an essential component of salicylic acid-dependent signaling for disease resistance in Arabidopsis, is a member of the MATE transporter family. *Plant Cell* 14, 275-286.
- Niehl, A., Wyrsh, I., Boller, T., Heinlein, M., 2016. Double-stranded RNAs induce a pattern-triggered immune signaling pathway in plants. *New Phytol* 211, 1008-1019.
- Niu, D., Wang, Z., Wang, S., Qiao, L., Zhao, H., 2015. Profiling of small RNAs involved in plant-pathogen interactions. *Methods Mol Biol* 1287, 61-79.
- Nobuta, K., Okrent, R.A., Stoutemyer, M., Rodibaugh, N., Kempema, L., Wildermuth, M.C., Innes, R.W., 2007. The GH3 acyl adenylase family member PBS3 regulates salicylic acid-dependent defense responses in Arabidopsis. *Plant Physiol* 144, 1144-1156.
- Pantaleo, V., Szittyá, G., Burgyan, J., 2007. Molecular bases of viral RNA targeting by viral small interfering RNA-programmed RISC. *J Virol* 81, 3797-3806.
- Pauwels, L., Barbero, G.F., Geerinck, J., Tilleman, S., Grunewald, W., Perez, A.C., Chico, J.M., Bossche, R.V., Sewell, J., Gil, E., Garcia-Casado, G., Witters, E., Inze, D., Long, J.A., De Jaeger, G., Solano, R., Goossens, A., 2010. NINJA connects the co-repressor TOPLESS to jasmonate signalling. *Nature* 464, 788-791.
- Peiro, A., Izquierdo-Garcia, A.C., Sanchez-Navarro, J.A., Pallas, V., Mulet, J.M., Aparicio, F., 2014. Patellins 3 and 6, two members of the Plant Patellin family, interact with the movement protein of *Alfalfa mosaic virus* and interfere with viral movement. *Mol Plant Pathol* 15, 881-891.
- Pumplin, N., Voinnet, O., 2013. RNA silencing suppression by plant pathogens: defence, counter-defence and counter-counter-defence. *Nat Rev Microbiol* 11, 745-760.
- Randles, J., Ogle, H., 1997. Viruses and viroids as agents of plant disease., in: Brown, J.F., Ogle, H.J. (Eds.), *Plant pathogens and plant diseases*. Rockvale Publication, Australia, pp. 104-126.

- Rosas-Diaz, T., Zhang, D., Fan, P., Wang, L., Ding, X., Jiang, Y., Jimenez-Gongora, T., Medina-Puche, L., Zhao, X., Feng, Z., Zhang, G., Liu, X., Bejarano, E.R., Tan, L., Zhang, H., Zhu, J.K., Xing, W., Faulkner, C., Nagawa, S., Lozano-Duran, R., 2018. A virus-targeted plant receptor-like kinase promotes cell-to-cell spread of RNAi. *Proc Natl Acad Sci U S A* 115, 1388-1393.
- Ruiz-Ferrer, V., Voinnet, O., 2009. Roles of plant small RNAs in biotic stress responses. *Annu Rev Plant Biol* 60.
- Sastry, S.K., Zitter, T., 2014. Management of virus and viroid diseases of crops in the tropics, *Plant virus and viroid diseases in the tropics*. Springer, Dordrecht, pp. 149-480.
- Seto, D., Koulana, N., Lo, T., Menna, A., Guttman, D.S., Desveaux, D., 2017. Expanded type III effector recognition by the ZAR1 NLR protein using ZED1-related kinases. *Nature Plants* 3, 17027.
- Shahid, S., Axtell, M.J., 2014. Identification and annotation of small RNA genes using ShortStack. *Methods* 67, 20-27.
- Shattuck, V.I., 1992. The biology, epidemiology and control of *Turnip mosaic virus*. *Plant Breed. Rev.* 14, 199-238.
- Spoel, S.H., Dong, X., 2012. How do plants achieve immunity? Defence without specialized immune cells. *Nat Rev Immunol* 12, 89-100.
- Stocks, M.B., Mohorianu, I., Beckers, M., Paicu, C., Moxon, S., Thody, J., Dalmay, T., Moulton, V., 2018. The UEA sRNA Workbench (version 4.4): a comprehensive suite of tools for analyzing miRNAs and sRNAs. *Bioinformatics*, in press. doi: 10.1093/bioinformatics/bty338.
- Sun, T., Zhang, Y., Li, Y., Zhang, Q., Ding, Y., Zhang, Y., 2015. ChIP-seq reveals broad roles of SARD1 and CBP60g in regulating plant immunity. *Nat Commun* 6, 10159.
- Tagami, Y., Inaba, N., Kutsuna, N., Kurihara, Y., Watanabe, Y., 2007. Specific enrichment of miRNAs in *Arabidopsis thaliana* infected with *Tobacco mosaic virus*. *DNA Res* 14, 227-233.
- Thorvaldsdottir, H., Robinson, J.T., Mesirov, J.P., 2013. Integrative Genomics Viewer (IGV): high-performance genomics data visualization and exploration. *Brief Bioinform* 14, 178-192.
- Valli, A.A., Gallo, A., Rodamilans, B., Lopez-Moya, J.J., Garcia, J.A., 2018. The HCPPro from the Potyviridae family: an enviable multitasking Helper Component that every virus would like to have. *Molecular Plant Pathology* 19, 744-763.
- Varallyay, E., Valoczi, A., Agyi, A., Burgyan, J., Havelde, Z., 2010. Plant virus-mediated induction of miR168 is associated with repression of ARGONAUTE1 accumulation. *EMBO Journal* 29, 3507-3519.
- Vazquez, F., Vaucheret, H., Rajagopalan, R., Lepers, C., Gascioli, V., Mallory, A.C., Hilbert, J.L., Bartel, D.P., Creté, P., 2004. Endogenous trans-acting siRNAs regulate the accumulation of *Arabidopsis* mRNAs. *Mol Cell* 16, 69-79.

- Vogler, H., Akbergenov, R., Shivaprasad, P.V., Dang, V., Fasler, M., Kwon, M.O., Zhanybekova, S., Hohn, T., Heinlein, M., 2007. Modification of small RNAs associated with suppression of RNA silencing by tobamovirus replicase protein. *J Virol* 81, 10379-10388.
- Wang, Z., Chen, Y., Fang, H., Shi, H., Chen, K., Zhang, Z., Tan, X., 2014. Selection of reference genes for quantitative reverse-transcription polymerase chain reaction normalization in *Brassica napus* under various stress conditions. *Mol Genet Genomics* 289, 1023-1035.
- Wei, T., Wang, A., 2008. Biogenesis of cytoplasmic membranous vesicles for plant potyvirus replication occurs at endoplasmic reticulum exit sites in a COPI- and COPII-dependent manner. *J Virol* 82, 12252-12264.
- Weiberg, A., Wang, M., Bellinger, M., Jin, H., 2014. Small RNAs: a new paradigm in plant-microbe interactions. *Annu Rev Phytopathol* 52, 495-516.
- Weiberg, A., Wang, M., Lin, F.M., Zhao, H., Zhang, Z., Kaloshian, I., Huang, H.D., Jin, H., 2013. Fungal small RNAs suppress plant immunity by hijacking host RNA interference pathways. *Science* 342, 118-123.
- Whitham, S.A., Yang, C., Goodin, M.M., 2006. Global impact: elucidating plant responses to viral infection. *Mol Plant Microbe Interact* 19, 1207-1215.
- Xu, M.Y., Dong, Y., Zhang, Q.X., Zhang, L., Luo, Y.Z., Sun, J., Fan, Y.L., Wang, L., 2012. Identification of miRNAs and their targets from *Brassica napus* by high-throughput sequencing and degradome analysis. *BMC Genomics* 13, 421.
- Xu, S., Zhang, Z., Jing, B., Gannon, P., Ding, J., Xu, F., Li, X., Zhang, Y., 2011. Transportin-SR is required for proper splicing of resistance genes and plant immunity. *PLoS Genet* 7, e1002159.
- Zhang, H., Liu, W.Z., Zhang, Y., Deng, M., Niu, F., Yang, B., Wang, X., Wang, B., Liang, W., Deyholos, M.K., Jiang, Y.Q., 2014. Identification, expression and interaction analyses of calcium-dependent protein kinase (CPK) genes in canola (*Brassica napus* L.). *BMC Genomics* 15, 211.
- Zhang, X., Yuan, Y.R., Pei, Y., Lin, S.S., Tuschl, T., Patel, D.J., Chua, N.H., 2006. *Cucumber mosaic virus*-encoded 2b suppressor inhibits Arabidopsis Argonaute1 cleavage activity to counter plant defense. *Genes Dev* 20, 3255-3268.
- Zhang, Z., Krainer, A.R., 2004. Involvement of SR proteins in mRNA surveillance. *Mol Cell* 16, 597-607.
- Zheng, Y., Wang, Y., Wu, J., Ding, B., Fei, Z., 2015. A dynamic evolutionary and functional landscape of plant phased small interfering RNAs. *BMC Biol* 13, 32.
- Zwicker, S., Mast, S., Stos, V., Pfitzner, A.J., Pfitzner, U.M., 2007. Tobacco NIMIN2 proteins control PR gene induction through transient repression early in systemic acquired resistance. *Mol Plant Pathol* 8, 385-400.

Figures:

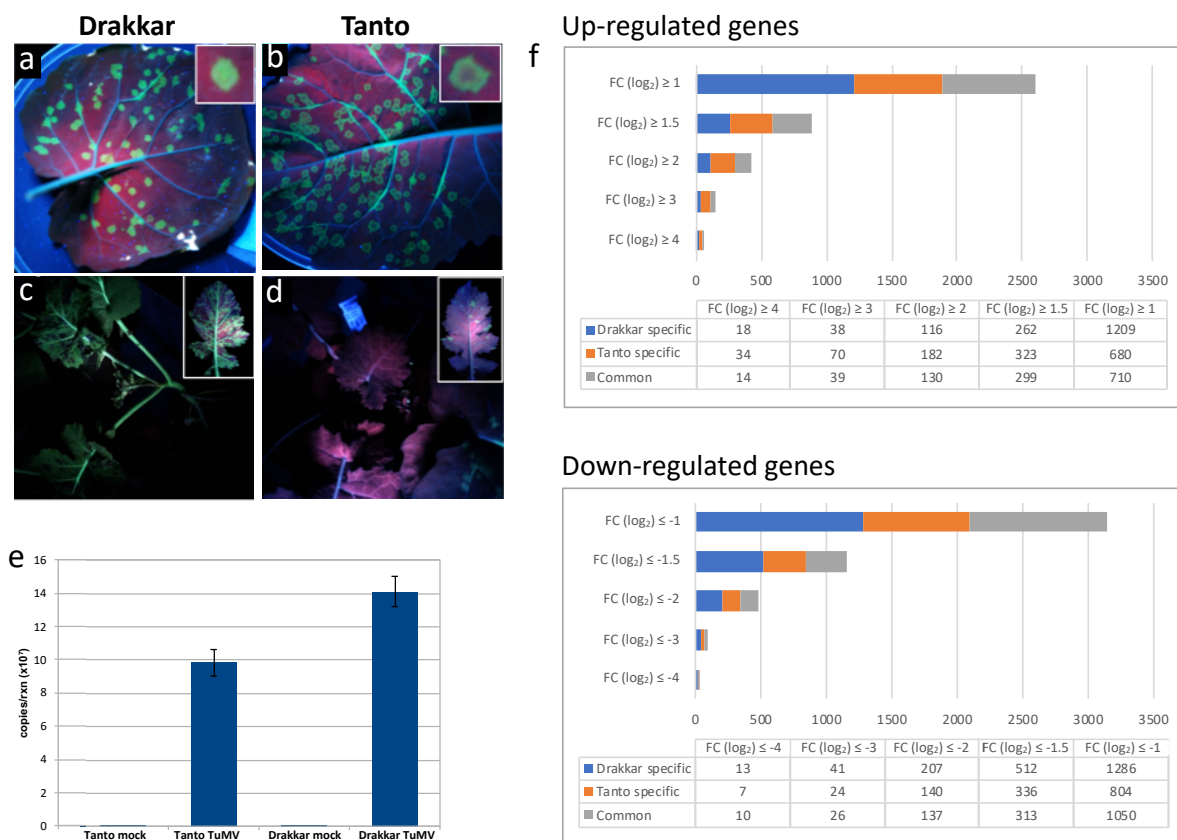


Fig. 1. TuMV-GFP infection in *B. napus*. **a-d**, local (6 dpi; **a, b**) and systemic (14 dpi; **c, d**) TuMV-GFP infection in Drakkar (**a, c**) and Tanto (**b, d**). Local infection foci in leaves have a disk-shaped appearance in Drakkar (**a**) and halo-shaped appearance in Tanto (**b**). TuMV exhibits efficient systemic spread in Drakkar (**c**) but not in Tanto (**d**). **e**, number of TuMV-GFP genome copies within expanded local infection foci at 12 dpi determined by RT-qPCR. Genome copies present in 30 ng total RNA were calculated using a RT-qPCR standard curve obtained for samples with known concentrations of *in vitro*-transcribed TuMV RNA. **f**, number of up- and down-regulated genes within infection foci of infected Drakkar and Tanto plants. The number of differentially expressed genes differs according to the applied fold change (FC) threshold (log₂ values). Considered mRNAs were represented by at least 150 mean reads (treatment and control) in each replicate experiment and showing statistically significant changes (p-value < 0.05) in expression between control and treatment conditions.

encoded by the viral RNA are indicated on top of the figure. The vsiRNA profiles as well as the profiles of vsiRNAs associated with host mRNA cleavage (grey and black dots with lines indicating the position along the viral RNA) are almost identical between Drakkar and Tanto. The vsiRNA:mRNA target pairs of most significant vsiRNAs (black dots) are shown and indicated by capital letters. The vsiRNA labelled with G mimics miR172 and was found associated with cleavage of different mRNAs encoding ethylene-responsive factors (G^{1-4}). **b**, the vsiRNA labeled with 'G' in figure **a** is similar in sequence to bna-miR172a and bna-miR172b and is associated with cleavage at exactly the same site of target mRNA.

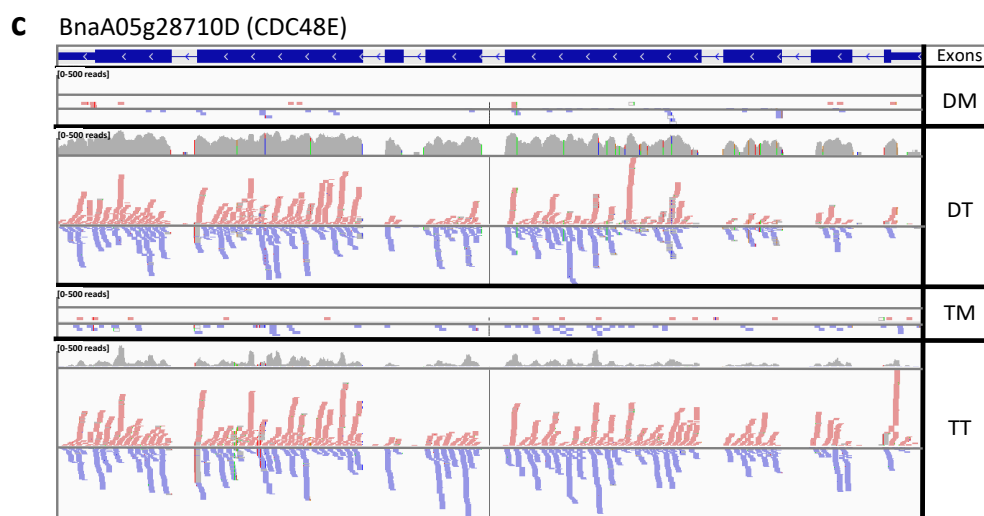
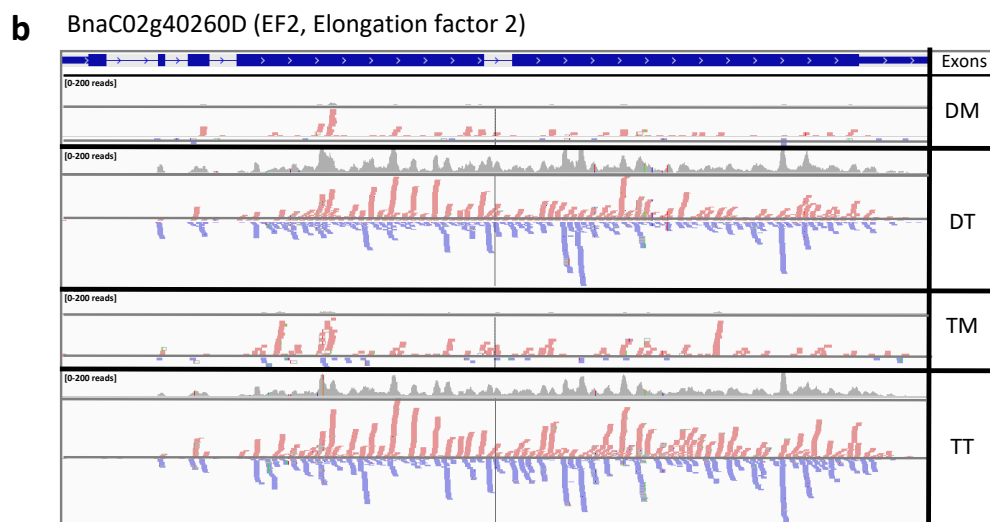
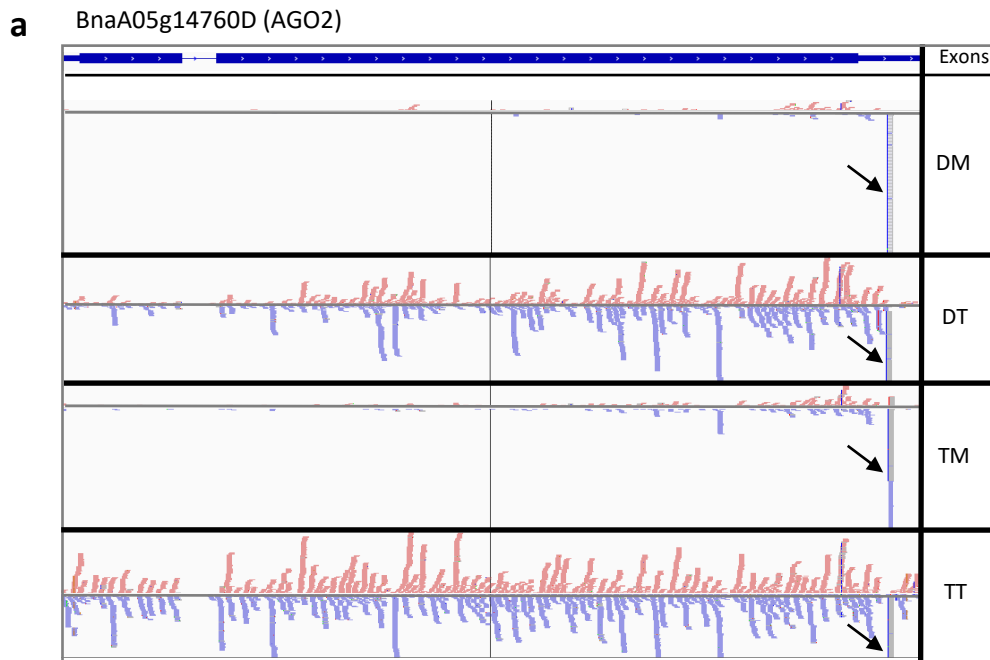


Fig. 3. Virus infection triggers the production of secondary va-phasiRNA from coding genes. a-c, Examples of va-phasiRNA-producing genes. The va-phasiRNAs of these genes were not associated with RISC-mediated RNA cleavage. For each example, the exon-intron structure of the mRNA and the alignment to the length of the mRNA of unique sRNAs sequenced in DM, DT, TM, and TT samples is shown. Unique sRNA reads derived from the positive and negative strand of the dsRNA are shown in red and blue, respectively. **b and **c** show the amount of aligned sRNA reads (in grey). Arrows in **a**, position of miR403.**

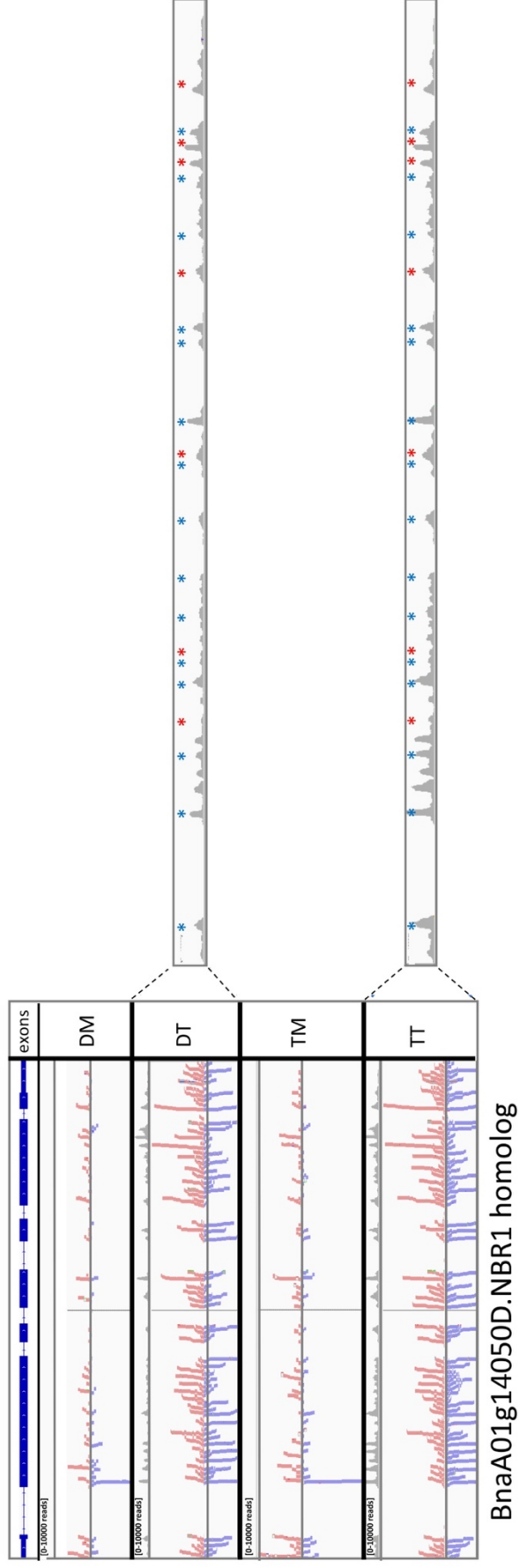


Fig. 4. NBR1-derived trans-acting va-phasiRNAs. NBR1-derived va-phasiRNAs associated with mRNA-target cleavage are derived from peaks of va-phasiRNA production. va-phasiRNAs derived from the positive and negative strand of NBR1 dsRNA are shown in red and blue, respectively.

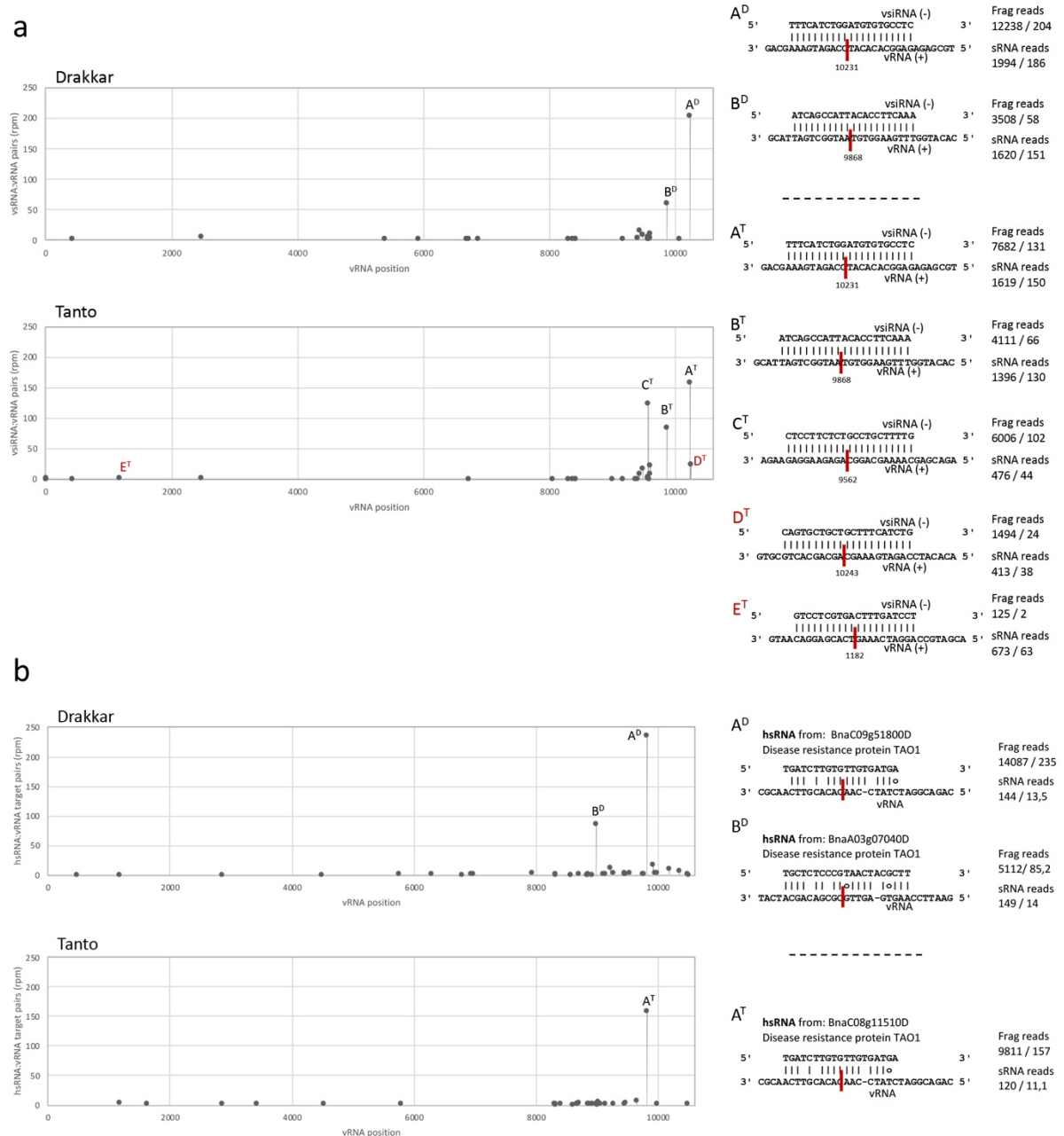


Fig. 5. RISC-mediated cleavage of viral RNA by virus and host siRNAs. a, vRNA cleavage by vsiRNAs; b, vRNA cleavage by host-derived siRNAs (hsRNAs). The distribution of vsiRNA:vRNA target pairs (rpm) and hsRNA:vRNA target pairs (rpm) along the vRNA is shown. The pattern of vRNA cleavage by vsiRNAs and hsRNAs is very similar between Drakkar and Tanto. vsiRNA:vRNA target pairs D^T and E^T were found in Tanto but not in Drakkar. Target pair alignments are shown together with the numbers for specific PARE signature fragment reads (Frag reads: total reads / rpm) and respective vsiRNA and hsRNA reads (sRNA reads: total reads / rpm).

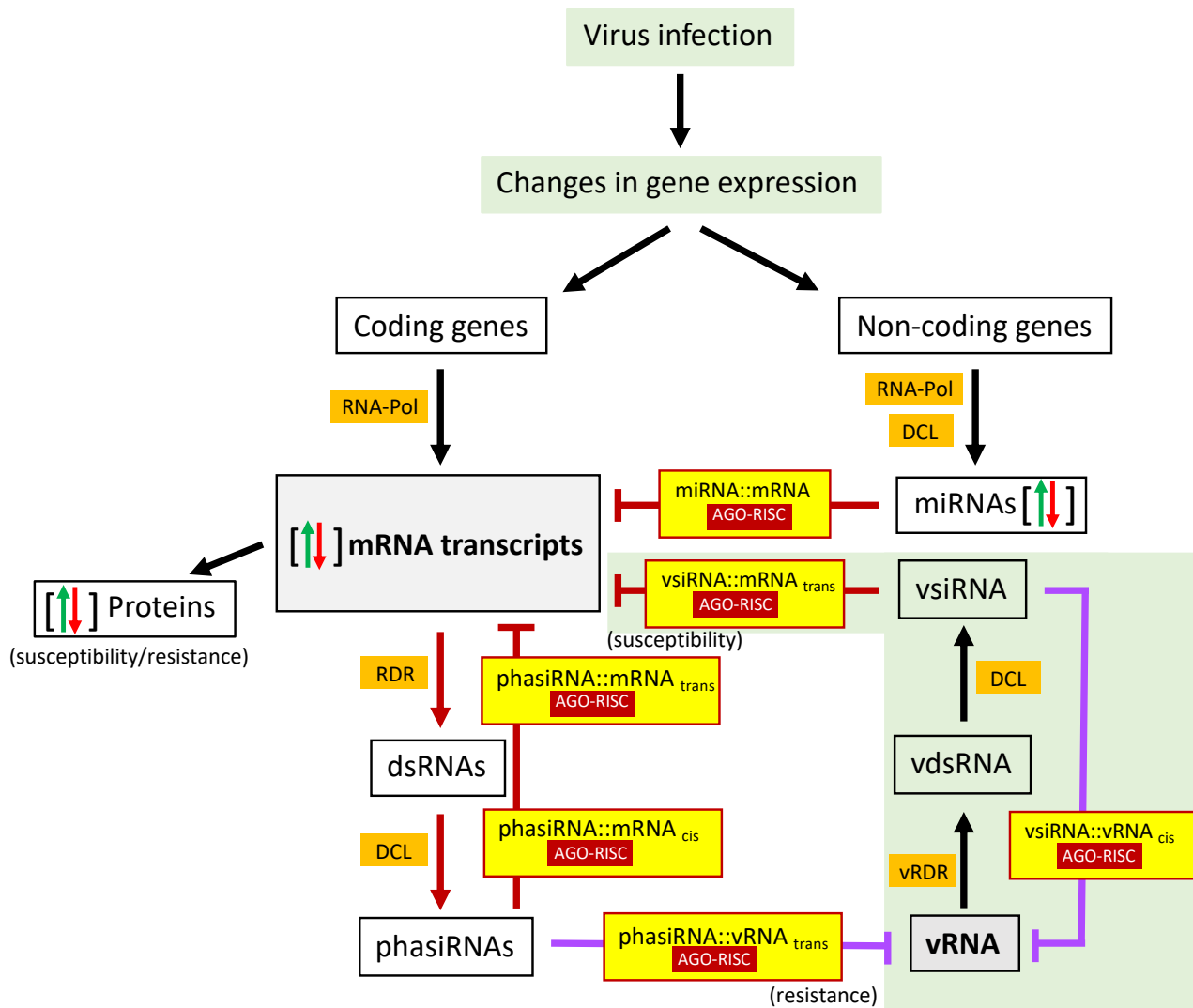


Fig. 6. Model of multiple virus:host interactions involving sRNAs. Virus infection causes changes in expression of coding and non-coding genes. Resulting changes in the levels of mRNA transcripts can lead to changes in the levels of encoded proteins that may play an important role in the determination of host susceptibility and resistance. Changes in the expression of non-coding genes leads to changes in the levels of miRNAs, which, in turn, control the levels of their mRNA targets by miRNA guided, RISC-mediated mRNA cleavage. Virus infection also triggers the ability of some genes to convert their mRNA transcripts via the formation of dsRNA into va-phasiRNAs. For some genes, va-phasiRNAs are the end product of a virus-induced pathway to control the transcript level (e.g. AGO2), whereas for other genes va-phasiRNAs engage RISC-mediated cleavage of either the transcript of origin, the transcript of origin as well as the transcripts of homologous genes in the same family, or of transcripts of other genes. The induction of va-phasiRNAs thus allows the virus to induce widespread regulation of secondary gene targets. The replicating virus, in turn, is primarily

controlled by DCL-mediated cleavage. However, DCL cleavage, again in turn, allows the virus to use its own vsiRNAs for RISC-mediated cleavage of host mRNA transcripts. The virus-induced RISC-mediated cleavage of host transcripts by va-phasiRNAs and vsiRNAs is, once again in turn, balanced by the ability of the host to also use vsiRNAs and va-phasiRNAs to target the viral RNA.

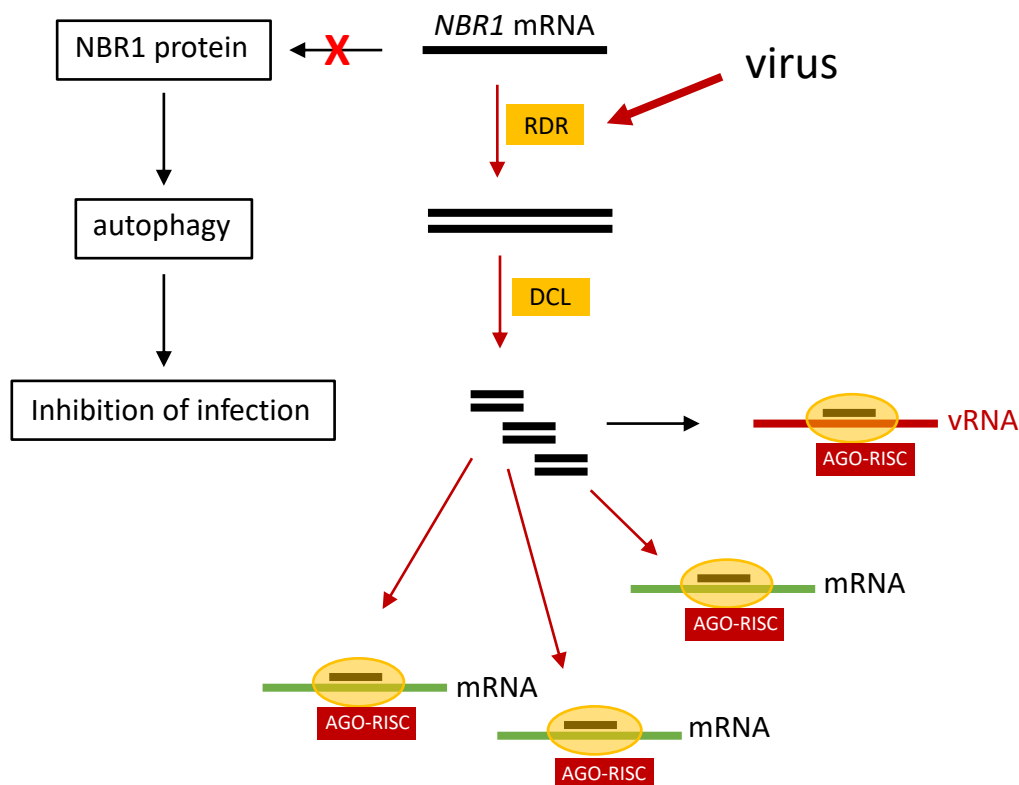


Fig. 7. NBR1 is a regulatory hub for plant:virus interactions. The NBR1 protein controls virus infection by targeting viral effector proteins (e.g. the VSR of TuMV) and viral particles for degradation by autophagy. The virus, in turn, triggers conversion of NBR1 mRNA into transacting va-phasiRNAs to induce widespread control over NBR1 and other gene targets. However, NBR1 va-phasi-RNAs also target the virus. Thus, the evolution of NBR1 as a virus-inducible hub for transacting siRNA production may be counterbalanced by an ability of the host to use the same locus to target the virus.

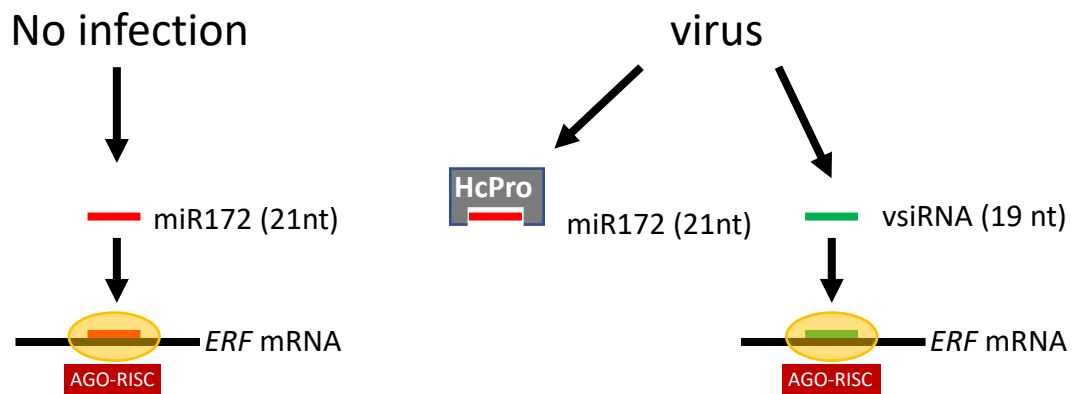


Fig. 8. A vsiRNA mimics and complements bna-miR172. In the absence of infection, the 21 nt long bna-miR172 controls the levels of mRNAs for ethylene-responsive transcription factor (ERF). During infection, bna-miR172 is trapped and inactivated by the VSR of the virus (HcPro). To keep ERF expression low, TuMV encodes a vsiRNA that mimics miR172. Because this vsiRNA is only 19 nt in length it escapes sequestration by HcPro and therefore remains active in the presence of the VSR.

Supplementary Figures and Tables are shown in APPENDIX 1.

Chapter III: Plant-virus infection and disease symptoms

1. Introduction

Viral accumulation as well as the viral recruitment of host factors and membranes, and the interference of viral proteins with normal host cell processes can lead to various effects on plant growth and physiology. However, while certain plant:virus combinations lead to disease, other plant:virus interactions remain free of symptoms and undergo tolerance, a state in which the plant and the virus can coexist (Roossinck and Bazán 2017). Diseases caused by viruses and other pathogens in cultivated crop plants and associated losses in yield represent a global threat for food security (Calil and Fontes 2017). Thus, studies to achieve an understanding of the mechanisms that determine disease versus tolerance are of utmost importance.

A key to the mechanisms determining disease versus tolerance is provided by the phenomenon of “disease symptoms recovery”. This phenomenon describes the occurrence of healthy, “recovered” leaves on a diseased plant. Although symptoms recovery was generally believed to be caused by a strong host response able to overcome the pathogen, our team could show that *Arabidopsis* plants infected with ORMV undergo recovery without interfering with viral propagation. Therefore, this work showed that symptoms recovery can occur through an achievement of a tolerant state in which the virus and its host can coexist without disease (Kørner et al. 2018). The aim of this chapter is to draw the historical context of recovery, its correlation with RNA silencing, and the recent findings about this phenomenon. This chapter is followed by a description of my authorship contribution to the attached publication of Kørner et al. (2018).

1.1. The phenomenon of disease symptoms recovery

The phenomenon of symptoms recovery was described already 90 years ago for a *Tobacco ringspot virus* (*Nepovirus* genus) infection in tobacco plants (Wingard 1928) (Figure 6). Recovery in these plants occurred after 23 days of ringspot virus infection. The recovered leaves were reported immune to a second infection by the same virus. However, 90 years ago the underlying mechanism was a total mystery.

JOURNAL OF AGRICULTURAL RESEARCH

VOL. 37

WASHINGTON, D. C., AUGUST 1, 1928

No. 3

HOSTS AND SYMPTOMS OF RING SPOT, A VIRUS DISEASE OF PLANTS¹

By S. A. WINGARD²*Associate Plant Pathologist, Virginia Agricultural Experiment Station*

INTRODUCTION

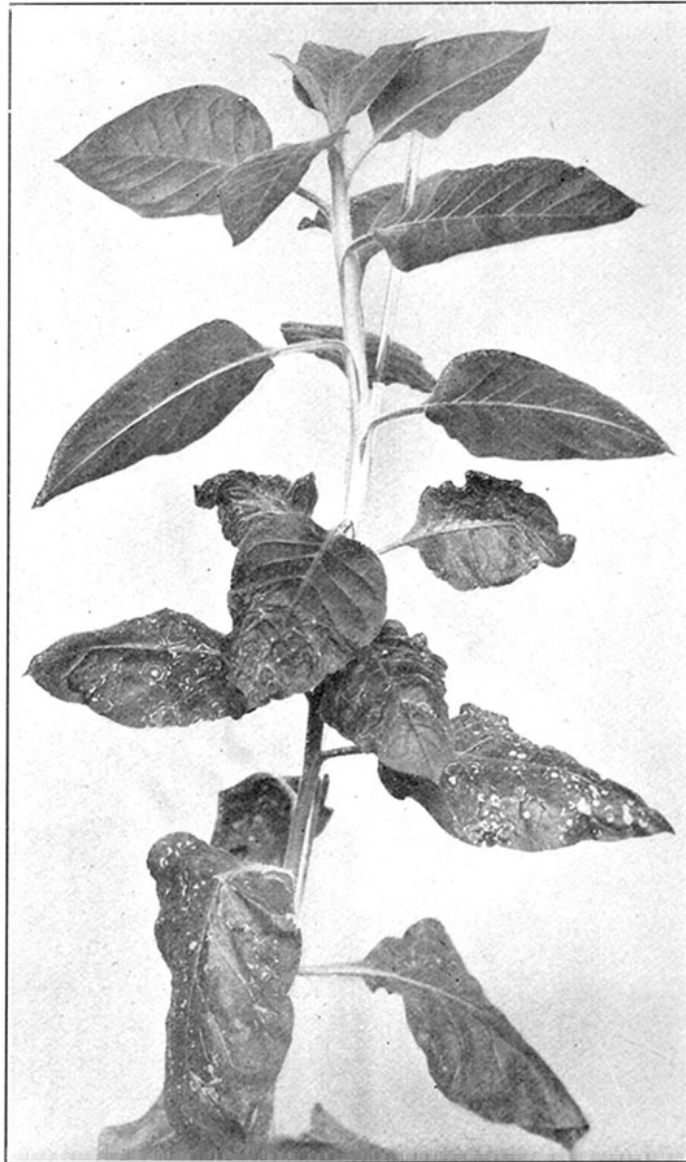


Figure 6: Recovery: occurrence of healthy leaves on symptomatic plants.

Symptoms recovery in tobacco plants infected with *Tobacco ringspot virus*. Recovered leaves are immune to a second infection with the same type of virus. Crude extract preparation of these leaves is infectious to other plants (From Baulcombe 2004).

Research on recovery only started more than 60 years later, when it was found that infection of tobacco plants that were transgenic for either the *Tobacco etch virus* (TEV) CP or the *Potatovirus Y* (PVY) CP with TEV or PVY, respectively, first led to disease and then to recovery (Lindbo et al. 1993; Smith 1994). Similar to the original observations by Wingard, 1928, both transgenic plants showed immunity to a secondary infection.

Interestingly, resistance was only against the same virus used in the initial infection but not against the other virus. Thus, the recovered leaves of the plants infected with TEV showed resistance against secondary infection by TEV but were susceptible to PVY infection. Similarly, the recovered leaves of PVY-infected plants were susceptible for TEV or *Tobacco vein mottling virus* (TVMV) but resistant against secondary infection by PVY. These findings indicated that the resistance occurring in recovered leaves is virus-specific (Lindbo et al. 1993; Smith 1994). Interestingly, transgenic plants expressing a non-translatable PVY CP ORF also showed symptoms recovery upon infection with the cognate virus. This was the strong sign indicating that the mechanism behind symptoms recovery was sequence-specific and RNA-based (Smith 1994). Although today one may immediately consider RNA silencing as the responsible mechanism, the TGS and PTGS pathways and the role of small RNAs in these pathways were not yet known at this time. However, three publications established that recovery during infection by *Cauliflower mosaic virus* (CaMV) in *Brassica oleracea gongylodes*, by *Tomato black ring virus* (TBRV, *Nepovirus*) in *Nicotiana clevelandii*, and by *Tobacco rattle virus* (TRV) in *N. benthamiana* plants was correlated with reduced vRNA levels in recovered leaves as compared to symptomatic tissues, which suggesting that recovery may be related to transgene-induced gene silencing and cross-protection (Covey et al. 1997; Ratcliff et al. 1997; Ratcliff et al. 1999).

It was then soon realized that the occurrence of symptoms recovery depends on specific plant-virus combinations and is influenced by environmental factors such as daylength and temperature (Ghoshal and Sanfaçon 2014). Moreover, a reduction in vRNA levels during symptoms recovery was not always observed. This was reported, for example, in recovered tissues developed in tobacco plants infected with *Tobacco streak virus* (TSV) (Xin and Ding 2003) or in recovered tissues of *N. benthamiana* plants infected with *Tomato ringspot virus* (ToRSV) (Jovel et al. 2007). These findings suggested that symptoms recovery may not necessarily correlate with reduced viral replication or the degradation of vRNA.

1.2. Role of VSR function in the formation of disease symptoms and recovery

Understanding recovery also depends on an understanding of mechanisms that cause disease in the first place. Here, the VSRs play a specific role, because the mechanisms through which they act to suppress antiviral silencing (e.g. sequestration of small RNAs or degradation of AGO protein) are prone to also affect RNA silencing-based pathways involved in controlling host gene expression. The involvement of VSR activity in pathogenicity and symptom severity has been highlighted in several studies (e.g. Voinnet et al. 1999; Moissiard and Voinnet 2004; Voinnet 2005; Csorba et al. 2015). For example, Arabidopsis leaves constitutively expressing VSRs such as the pecluviral P15, the potyviral Hc-Pro, or the closteroviral P21 show disease symptoms with similarity to disease symptoms produced during viral infection, and the severity of the disease symptoms induced by expression of a specific VSR correlated with the efficiency by which the respective VSR controls antiviral RNA silencing (Voinnet 2005). Consistent with the role of VSR activity in disease symptom development, ectopic over-expression of Hc-Pro (PVY) or P25 (PVX) was shown to prevent recovery usually seen in tobacco plants infected with nepoviruses (Santovito et al. 2014; Siddiqui et al. 2008). In addition, the VSR of *Cucumber mosaic virus* (CMV), the 2b protein, is fundamental for disease symptom formation in *N. tabacum* or *A. thaliana* (Col-0), as a corresponding virus with compromised VSR activity (CMV Δ 2b) did not trigger symptoms (Lewsey et al. 2009). Consistently, infection also with other viruses carrying mutations in their VSRs often resulted in recovery phenotypes (Hormuzdi and Bisaro 1995; Chu et al. 2000; Szittyta et al. 2002; Omarov et al. 2006; Raja et al. 2008; Wu et al. 2010). This indicates that symptoms are induced by VSR activity and that a lack of VSR activity can allow recovery. However, this conclusion does not hold for all viruses, or virus strains. For example, for the subgroup IA strain Fny-CMV, both the wildtype and the VSR-deficient Fny-CMV Δ 2b induced symptoms in *Chenopodium* species, *N. occidentalis* and five different *A. thaliana* ecotypes; Fny-CMV Δ 2b allowed recovery only in the Arabidopsis C24 ecotype (Lewsey et al. 2009). Nevertheless, symptoms recovery is often permitted by viruses that express only weak VSRs and are not able to suppress the RNA silencing pathway efficiently (Martin-Hernandez and Baulcombe 2008; Ghoshal and Sanfaçon 2015). Thus, collectively, these findings indicated that disease symptoms are likely provoked by a strong VSR and that symptoms recovery may occur if the VSR is weak or weakened by mutation. However, as already mentioned, although a weak or

weakened VSR should be correlated with vRNA degradation, lower vRNA levels were not always observed. Translational repression rather than RNA degradation was proposed for recovery of *N. benthamiana* plants infected by *Tobacco ringspot virus* (ToRSV) (Jovel et al. 2007) since a temperature-dependent enhancement of recovery was correlated with a requirement for AGO1 and reduced translation of viral proteins despite the presence of enhanced levels of viral RNA and siRNAs (Ghoshal and Sanfaçon 2014). Thus, recovery may involve a mechanism that weakens VSR activity without necessarily causing an effect on vRNA.

1.3. A potential role of antiviral meristem resistance in recovery

Since leaves emerge from the shoot apical meristem (SAM), the mechanism leading to the emergence of a healthy leaf rather than a diseased leaf on a systemically infected and diseased plant must be localized to the SAM. Interestingly, some viruses are unable to infect the meristem. The underlying mechanism of meristem resistance in these cases may be related to the mechanism of recovery in cases allowing virus entry. The failure of *Potato virus X* (PVX) to infect the *N. benthamiana* meristem was correlated with RDR6 activity, as shown with silenced RDR6 RNAi plants (Schwach et al. 2005). Since RDR6 is required for secondary siRNA production and the amplification of antiviral RNA silencing (Himber et al. 2003; Vazquez 2006), it was proposed that meristem resistance against the virus is due to secondary virus-derived siRNAs that spread systemically and immunize the meristem ahead of the virus (Schwach et al. 2005). An RDR polymerase activity was also invoked to explain the resistance of the tobacco apical meristem against invasion by CMV (Mochizuki and Ohki 2004). Interestingly, using immunohistochemical staining and *in situ* hybridization, it was shown that CMV was not excluded from the SAM. Rather, this virus was initially present at 7 days post-inoculation (dpi) and only later cleared (at 14 dpi). Consistent with this clearance, CMV-derived siRNAs were present in the SAM up to 24 dpi. Based on these observations, the authors concluded that the SAM in tobacco can clear viral infection by RNA silencing.

This case is one example showing that infected plants can undergo symptom recovery initiated in the SAM even if the infecting virus initially entered the SAM (Ghoshal and Sanfaçon 2015). In these cases, symptoms recovery may be due to a weak VSR or recovery from VSR activity (as described further above) rather than by recovery from the virus. For example, TRV

expresses a weak VSR called 16K. This virus is able to infect and systemically spread into the SAM of *N. benthamiana* plants whereas a mutant TRV with a inactivated VSR (TRV:stop) fails to reach the SAM (Martin-Hernandez and Baulcombe 2008). Interestingly, neither wild type TRV nor TRV:stop trigger symptoms or recovery. Based on these observations, it was proposed that viruses expressing only a weak VSRs are nevertheless able to enter the meristem and induce the accumulation of vRNA similar to viruses with a strong VSR. However, as compared to viruses with a strong VSR, viruses like TRV accumulate only transiently and to a lower level, which consequently will trigger weaker antiviral silencing responses and less damage, thus allowing recovery (Martin-Hernandez and Baulcombe 2008; Ghoshal and Sanfaçon 2015).

1.4. The role of PTGS and TGS in recovery

A decrease in vRNA concentration in recovered tissues (which is not seen in all cases of recovery) and the described role of RDR6, secondary siRNAs, and VSRs in recovery indicates that recovery can involve the degradation of the viral genome by antiviral PTGS. Antiviral RNA silencing acts through DCL and AGO-RISC mediated cleavage (Szittyá et al. 2002). A role of RISC-mediated cleavage of viral RNA in symptoms recovery has been indicated by the analysis of infection of *N. benthamiana* plants with *Cymbidium ringspot tombusvirus* (CymRSV). A VSR-defective CymRSV mutant (CymRSV19stop), which is unable to express the VSR p19, was shown to allow symptoms recovery. The recovered leaves showed an accumulation of 21- to 25-nt long vsiRNAs indicating a role of vsiRNAs in recovery. Moreover, evidence was presented indicating that these vsiRNAs are used as guides for the cleavage of co-replicating defective interfering (DI) RNAs *in trans* thus suggesting their incorporation into RISC (Szittyá et al. 2002). Pantaleo et al. (2007), used the expression of a sensor construct consisting of a GFP-encoding RNA fused to viral RNA in recovered leaves of an CymRSV19stop-infected plant to demonstrate that the virus-derived siRNAs target the sensor construct by RISC-mediated RNA cleavage. Using size fractionation, vsiRNAs and miRNAs were found to be bound by the same protein complex consistent with the size of the RISC complex. Based on these observations, the authors concluded that PTGS employing RISC-mediated cleavage of vRNA was responsible for symptoms recovery in leaves. The correlation of vRNA cleavage with

recovered tissues was corroborated with other plant-virus systems (Omarov et al. 2007; Scholthof et al. 2011).

In some cases, symptom recovery in plants infected with RNA viruses has been associated with RISC-mediated translational repression rather with cleavage of the vRNA. For example, recovery in *N. benthamiana* plant infected with *Tomato ringspot virus* (ToRSV) involved the translational inhibition of ToRSV-encoded CP and MP genes (Ghoshal and Sanfaçon 2014). Consistent with a role of AGO1 in antiviral RISC (Carbonell and Carrington 2015; Garcia-Ruiz et al. 2015; Morel et al. 2002), symptom recovery was blocked in *N. benthamiana* in which AGO1 was silenced by RNAi.

There is experimental evidence indicating that plant recovery from symptoms of infection by DNA viruses is caused by viral silencing involving components of the TGS pathway. Direct evidence of a role of TGS in recovery came from observations with a VSR-deficient *Beet curly top virus* (BCTV L2⁻) in Arabidopsis (Raja et al. 2008). Using BCTV infection and chromatin immunoprecipitation (ChIP), the authors showed that Arabidopsis plants impaired in DNA methylation, exhibited reduced viral methylation and increased susceptibility to the virus. In contrast, BCTV L2⁻ infection led to the development of recovered leaves and these leaves contained hypermethylated viral DNA. Furthermore, symptom recovery was blocked in plants mutant for AGO4, a central component of the RdDM pathway (Zheng et al. 2007; Havecker et al. 2010; Gao et al. 2010; Blevins et al. 2015). Using the same ChIP procedure, the authors demonstrated that viral DNA methylation was abolished in these plants. These observations demonstrated the role of TGS in viral DNA methylation, which reduced the virulence of the virus and resulted in recovery of infected plants from disease symptoms.

Other studies revealed that antiviral defense and symptoms recovery in plants infected with DNA viruses also involves PTGS in addition to TGS (Rodriguez-Negrete et al. 2009; Pooggin 2013). Initial findings showed that infection of Arabidopsis with the geminivirus *Cabbage leaf curl virus* (CaLCuV) triggered symptoms recovery and that 21-, 22-, and 24-nt long siRNAs accumulated in these symptom-free leaves (Blevins et al. 2006). The 21- nt and 22-nt long siRNAs and the 24 -nt long siRNAs represent central components of PTGS and TGS pathways, respectively. Moreover, recovery was inhibited in the PTGS mutants *dcl4*, *rdr6*, *sgs3* and *hen1* (Muangsan et al. 2004; Blevins et al. 2006). Small RNAs of the 21nt and 22nt sizes classes as well as of the 24 nt size category were also present in the recovered leaves of pepper plants

infected with the geminivirus *Pepper golden mosaic virus* (PepGMV) (Rodriguez-Negrete et al. 2009). Many of these siRNAs were derived from the virus and could be mapped all along the viral genome. It is interesting that the 21-22 nt vsRNAs mapped to the coding genes of the virus, whereas the 24 nt siRNAs were derived from a strongly methylated viral intergenic region. The methylation level of this intergenic region was lower in the symptomatic leaves as compared to recovered leaves, which suggested a role of viral DNA methylation in recovery. Using bisulfite sequencing for the profiling of BCTV L2⁻ DNA methylation in systemically infected *Arabidopsis* wildtype plants and mutants affected in RdDM such as *drb3*, *dcl3*, and *ago4* demonstrated that these mutants failed to show symptom recovery and also were impaired in inducing strong cytosine methylation of the viral DNA genome (Raja et al. 2014). Consistent with a role of DCL3 and AGO4 in RdDM (Raja et al. 2008; Blevins et al. 2011), CoIP and biomolecular fluorescence complementation (BiFC) experiments demonstrated a direct interaction of DRB3 with DCL3 and AGO4 (Raja et al. 2014).

1.5. Disease symptoms recovery in ORMV-infected *Arabidopsis* plants

Although the role of PTGS in symptoms recovery in plants infected with RNA viruses and the role of both PTGS and TGS in symptoms recovery in plants infected with DNA viruses has been established, the full network of RNA-silencing based interactions between viruses and their plant hosts remains unclear. The publication of Kørner et al. (2018) to which I have contributed and which is attached herein, describes the interaction between *Arabidopsis* plants and the tobamovirus ORMV and provides deep insights into the mechanisms and genetic requirements involved in disease symptom formation and symptoms recovery.

ORMV belongs to the same virus family as the well-known TMV, but unlike TMV, ORMV produces strong disease symptoms in *Arabidopsis*. Importantly, we found that ORMV first induces symptoms and later allows symptoms recovery (Kørner et al. 2018; Fig. 1a-b; Fig. S1), which opened the way for genetic analysis of this phenomenon. Infected plants show severe disease symptoms at 14 dpi and start to develop recovered leaves at 23-25 dpi. As shown in Fig.1b of Kørner et al. (2018), the leaves of the infected plants were categorized at 28 dpi according to their symptom types to facilitate their analysis. The oldest leaves at the bottom of the plant were already present before inoculation and remained non-symptomatic but showed signs of necrosis presumably due to age (symptom type 1, ST1). Leaves that were still

young and physiological sinks at the time of inoculation were symptomatic. The lower, older leaves in this category showed different degrees of curling (symptom type 2, ST2), whereas the younger, more upper leaves showed stronger symptoms with strongly serrated margins (symptom type 3, ST3). Interestingly, several of the ST3 leaves showed a transition between leaf areas with symptoms restricted the tip and symptom-free areas at the leaf base. This transition occurred along a very distinct line at which a decision between disease and recovery apparently was made. Finally, the youngest leaves at the top of the plant were fully recovered and completely free of disease symptoms (symptom type 4, ST4). The transition between the diseased and healthy areas in ST3 “transition leaves” and the observation that symptoms in these leaves were limited to the leaf base suggested that the transition to recovery occurred along the border between source and sink tissues. This hypothesis was corroborated by infection of AtSUC:GFP plants as a source/sink marker (Imlau, 1999), which demonstrated that recovery indeed occurs in sink leaves and that leaves showing both diseases and recovered areas undergo the sink-to-source transition (Supplementary Fig. 14). To determine whether symptom recovery was correlated with a decrease in the level of viral RNA, the different symptom types were probed by *in situ* hybridization (Kørner et al. 2018; Fig. 1c) and northern blotting (Kørner et al. 2018; Fig. 1d) using probes against the virus. Interestingly, the results showed that the recovered leaves contained viral RNA to the same level as the symptomatic leaves. The northern blot analysis also demonstrated that the RNA was full-length and, furthermore, that both strands of the viral RNA were present, thus indicating that the virus was actively replicating in recovered leaves as well as in symptomatic leaves.

I already mentioned evidence indicating a role of the VSR in the formation of disease symptoms and that recovery may occur in the presence of a weak or weakened VSR (see paragraph 1.2). To determine whether disease symptoms and disease recovery in ORMV-infected *Arabidopsis* plants correlate with VSR activity, we infected plants of *Arabidopsis* line 8z2, which expresses a continuously silenced, double 35S promoter-driven GFP transgene (Glazov et al. 2003). Using this approach we could show that ORMV infection restores GFP expression from this gene (Kørner et al. 2018; Fig. 1 e-g), thus indicating that the VSR activity, which is known to reside in the small replicase subunit [125k protein of ORMV (Hu et al. 2011; Malpica-López et al. 2018); 126k protein of TMV (Vogler et al. 2007); 122k protein of crTMV (Csorba et al. 2007)], suppresses PTGS activity. Importantly, green fluorescence coincided

with symptomatic tissues but was absent in recovered tissues demonstrating that VSR activity is active in the symptomatic leaves and suppressed in the recovered leaves. RT-qPCR measurements were used to confirm that GFP mRNA levels were high in symptomatic leaves and low in the recovered leaves (Kørner et al. 2018; Fig. S2a). The correlation between symptom phenotypes and VSR activity was investigated by specific detection of viral and endogenous sRNAs. As shown previously (Hu et al. 2011), miR398 accumulated in ORMV-infected tissues. However, accumulation of this miRNA was restricted to symptomatic tissues with VSR activity, whereas recovered tissues with low or absent VSR activity also showed low levels of this miRNA. Also, ORMV-derived siRNAs accumulated to higher levels in symptomatic tissue and showed lower levels in recovered tissues (Kørner et al. 2018; Fig. S2). These findings are consistent with previous described correlations between tobamoviral VSR activity and specific sRNA accumulation (Blevins et al. 2006; Csorba et al. 2007; Hu et al. 2011). The correlation between symptoms and VSR activity were further demonstrated by infecting the *A. thaliana* suc:sul line (Himber et al. 2003), whose vein-centered chlorosis phenotype disappeared in the symptomatic leaves thus indicating the presence of VSR activity (ST2-ST3), but was distinctly visible along the veins in the recovered ST4 leaves, thus indicating the absence of VSR activity (Kørner et al. 2018; Fig. S3).

The analysis to this point demonstrated that recovery from symptoms in ORMV-infected plants occurs in sink tissues and is associated with the loss or strong reduction in VSR activity. However, given that the recovered leaves contained normal levels of replicating viral RNA, recovery was not caused by antiviral RNA silencing, but rather due to the silencing of VSR activity. Western blot assays using antibodies against the 125k-VSR protein demonstrated that the VSR was present in recovered leaves (Kørner et al. 2018; Fig. S13). Thus, recovery could not be correlated with translational repression of VSR expression. Rather, recovery was indeed due to the inhibition of the functional activity of the expressed protein. Based on the finding that symptoms recovery is restricted to sink tissues, we proposed that the suppression of VSR activity occurs in sink tissues.

The pathway leading to VSR inactivation in sink tissues was finally highlighted by genetic analysis using a library of known mutants affected in PTGS and TGS pathways (Kørner et al. 2018; Table 1, Table 2, Table S1, Table S2).

Infection of these mutants with ORMV was used to identify mutants showing impaired or enhanced symptoms recovery. In essence, the results of this analysis demonstrated that the

occurrence of symptoms recovery depends on the DCL4/RDR6/SGS3 pathway, which produces primary and secondary endogenous and viral siRNAs (Bologna and Voinnet, 2014). Moreover, mutants accumulating higher levels of secondary vsRNAs (*dcl3-1* and *xrn4/ein5*) recovered earlier, thus indicating that recovery is the more likely the more vsRNAs are produced. The analysis also showed that recovery in our system is independent of TGS pathway components, except for Pol IV and RDR2. Interestingly, these two proteins have been implicated to play a role in the spread or reception of systemic silencing signals (Dunoyer et al. 2007; Brosnan et al. 2007; Smith et al. 2007; Eamens et al. 2008). Based on our findings, we proposed that the mechanism that leads to VSR inactivation and symptoms recovery involves the trafficking of mobile vsRNAs from source to sink and that the vsRNAs that accumulate in sink tissues saturate the VSR so that its ability to sequester and interfere with the activity of other sRNAs, such as the GFP-mRNA derived siRNAs in the z82 line or miRNAs involved in the regulation of plant development, is suppressed (Kørner et al. 2018; Fig. 3). Because the virus remains mostly unaffected by these mechanisms leading to symptoms recovery and continues to propagate, our study clearly demonstrated that plants can use sRNAs and intercellular communication to overcome an established disease and achieve a tolerant state in which both virus and host can coexist.

2. My contributing role to the publication by Kørner et al. (2018)

In the context of this work, I conducted experiments of ORMV infection in several *A. thaliana* PTGS and TGS mutants, analyzed the symptom phenotypes and performed molecular characterization by northern and western blot analysis (Figure 1d; Figure S12, and Figure S13), which aimed to answer several main questions in the understanding of the recovery phenomenon (see APPENDIX 2 for Supplementary Figures and Tables of Kørner et al. 2018).

Figure 1d shows a northern blot analysis of recovered leaves (except second lane from the left, symptomatic leaves) of wildtype plants and of single (*dcl3*, *ein5*, *rdr2*, *rdr6*) as well as of double mutants (*ein5 rdr6*, *dcl2 dcl4*) in which I have used radiolabeled probes to detect positive-sense (+) and negative sense (-) viral RNA. The result demonstrates that recovered leaves contain full-length genomic and subgenomic viral RNAs. The detection of negative sense viral RNA showed that the virus was actively replicating in recovered tissues. Moreover,

levels of viral RNAs appeared almost unchanged in the RNA silencing pathway mutants. However, the same mutants were shown to affect recovery in other experiments. Thus, recovery was found to occur independently from effects on viral RNA or viral replication.

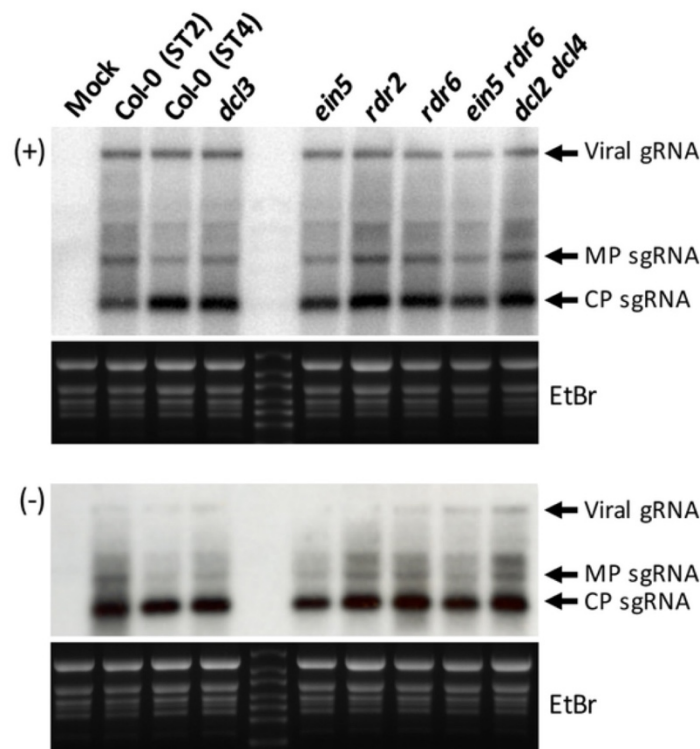


Figure 1d. Two independent northern blots showing viral plus (+) and minus (-)-sense genomic and sub-genomic viral RNAs in RNA extracts of non-recovered ST2 and recovered ST4 leaves of WT Col-0 plants and in recovered ST4 leaves of different silencing pathway mutants. The viral RNA pattern is identical to the viral RNA patterns reported in previous publications. The blot combines independent samples (each sample representing 20 infected plants, that is, recovery experiments) from WT plants (Col-0) and mutants undergoing recovery (*dcl3*, *ein5* and *ein5 rdr6*) or not undergoing recovery (*rdr2*, *rdr6* and *dcl2 dcl4*) in upper leaves, and demonstrates that upper leaves contain full-length plus and minus-sense viral RNA irrespective of recovery.

Figure S12 shows a small RNA northern blot in which I confirmed the expected effects of specific RNA pathway mutations on the synthesis and accumulation of specific sRNAs. The same small RNA blot was probed several times with different radiolabeled oligonucleotide probes to detect different sRNA species in the same samples. Probing siRNAs derived from the 5S repeat (*ra-si1003*) reports on the functionality of the TGS pathway, whereas probing tasiRNA255, miRNA160, and ORMV vsRNA, reports on the functionality of PTGS pathways involved in tasiRNA, miRNA, and vsRNA synthesis. As expected and previously shown (Blevins et al. 2006; Blevins et al. 2015), *dcl3* and *rdr2* mutants are defective in the production of 24 nt

siRNAs and repeat-associated siRNAs associated with TGS but do not affect any of the sRNA species associated with PTGS. In contrast the other mutants tested do not affect 24 nt species involved in TGS but specific classes of 21-22 nt sRNA involved in PTGS. Thus, *rdr6*, *ein5-rdr6*, as well as *dcl2-dcl4* were defective in the production of 21nt trans-acting siRNAs, as expected. Moreover, *dcl2-dcl4* affected the production of vsiRNAs. As expected, mutant *ein5* showed a strong increase in the level of vsiRNAs as expected. *ein5* plants are defective in exonuclease 4 (XRN4) activity (Olmedo et al. 2006; Potuschak et al. 2006; De Vleeschauwer et al. 2014) involved in RNA decay and thus provide increased levels of RNA template for secondary vsiRNA production. These increase levels of secondary vsiRNAs are consistent with enhanced recovery in the *ein5* plants (Kørner et al. 2018, Fig S8).

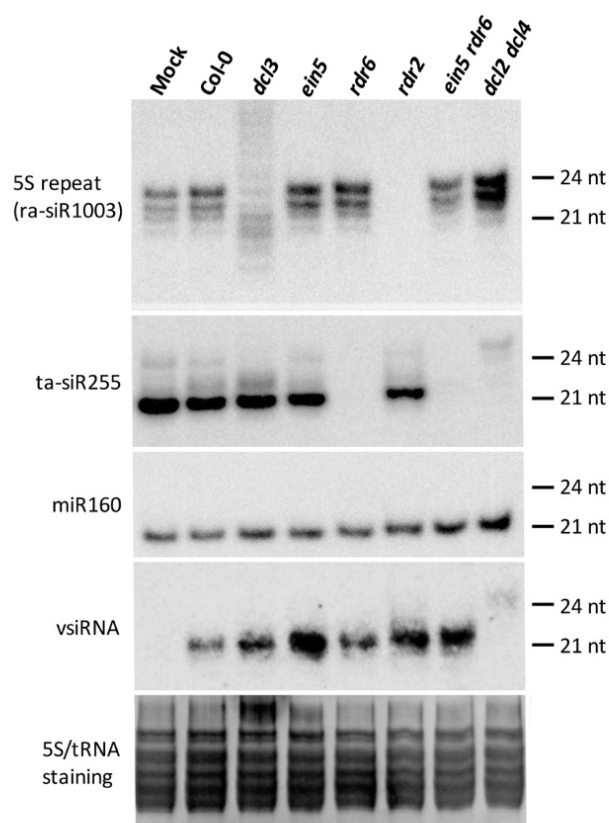


Figure S12: sRNA analysis of infected Col-0 wild type plants and silencing pathway mutants.

sRNA species in recovered ST4 (Col-0, *dcl3*, *ein5*) and corresponding non-recovered leaves of mutants (*rdr6*, *rdr2*, *ein5 rdr6*, *dcl2 dcl4*), in which recovery is absent, were analyzed. The analysis was performed with the same RNA samples also used for viral RNA analysis (Fig. 1d). The mutants affected the accumulation of specific sRNA species as expected. None of the mutants affected the accumulation of miR160. The accumulation of 5S rDNA repeat-derived ra-siR1003 was affected in *dcl3* and *rdr2* mutants but not in *rdr6* mutants, whereas the production of tasiR255 was affected in *rdr6*, *ein5 rdr6*, and *dcl2 dcl4* mutants but not in *rdr2* or *dcl3* mutants. As is also expected, production of vsiRNAs was abolished in *dcl2 dcl4*, as is consistent with the lack of recovery in this double mutant. Relative to Col-0 wild type, the vsiRNA levels were higher in mutants showing enhanced recovery (*ein5*, *dcl3*) and reduced in *rdr6*, which interferes with the formation of secondary siRNAs and does not support recovery.

Figure S13 represents a western blot analysis to detect the 125k-VSR in samples taken from recovered leaves of wild type and mutant plants infected with ORMV. The results show that the VSR is expressed in infected tissues irrespective of recovery, thus demonstrating that the absence of VSR activity in recovered leaves cannot be ascribed to translational suppression of the protein.

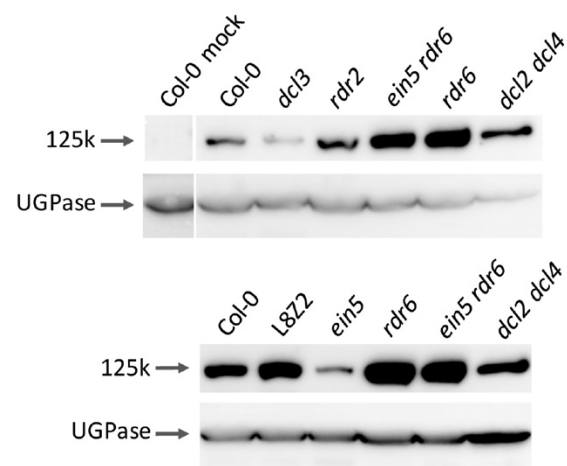


Figure S13: VSR expression in recovered leaves of infected Col-0 wild type plants and silencing pathway mutants.

The 125k-VSR is expressed in infected tissues irrespective of recovery. The amount of the VSR in recovered leaves is lower in mutants undergoing early recovery (*ein5*, *dcl3*) and higher in the upper leaves of *rdr6* mutants in which recovery is inhibited. L822 plants, which contain a continuously active silencing system, produce relatively high levels of the VSR whereas *dcl2 dcl4* plants, in which siRNA synthesis is inhibited, contain relatively low levels of the VSR. UGPase, UDP-glucose pyrophosphorylase.

In addition to these northern blots and western blots, I also performed experiments demonstrating the inhibition of symptoms recovery in transgenic plants expressing the VSR from a closterovirus (P21) or the VSR from a tombusvirus (P19) (Kørner et al. 2018; Fig. S4).

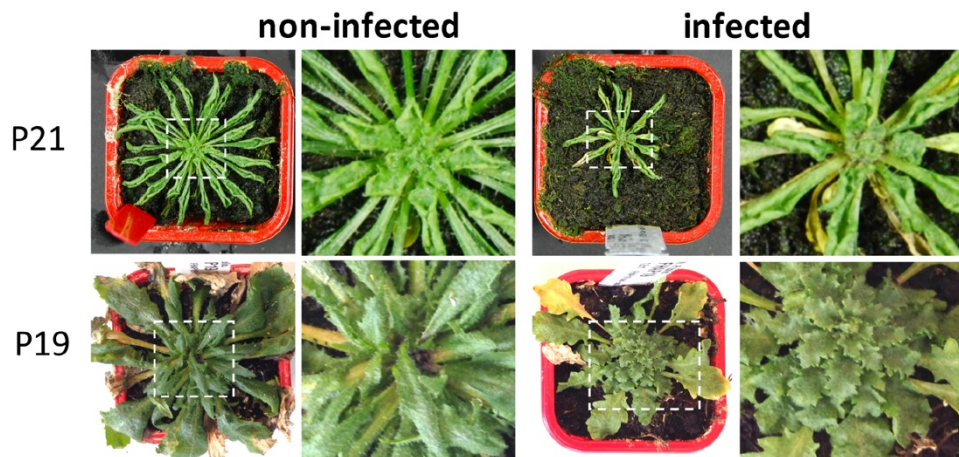


Figure S4: Suppression of recovery in VSR-expressing transgenic plants.

Mock- and ORMV-infected plants expressing either closterovirus P21-VSR or the tombusvirus P19-VSR. Plant areas within the dashed rectangles are shown enlarged. Neither P21 nor P19 plants allow disease recovery.

3. Conclusion

In this paper, the phenomenon of symptoms recovery in *Arabidopsis* was studied. This led to the identification of RNA silencing pathway genes that are involved and also unraveled the importance of an interesting interplay between a virus-encoded VSR and small RNAs in the determination of health versus disease.

The results demonstrate that symptoms recovery can occur in leaves undergoing normal virus replication and accumulation. Thus, plants have the capacity to achieve a state of tolerance and recover from an established disease despite the presence of an ongoing virus replication. Moreover, recovery can occur simply through inhibition of VSR activity. This may imply that plants could be protected against disease through strategies aiming at the inhibition of the VSR. Based on our observations and genetic requirements for recovery, we propose that the VSR is inhibited by mobile vsiRNAs that accumulate by systemic transport from source to sink. The sharp border between recovered and non-recovered tissues occurs along the sink-to-source transition suggests that the symptom-free sink-tissues will undergo disease as soon as these tissues mature and undergo the transition from sink to source. This may imply that the tolerance of plants for viruses could be supported by strengthening vsiRNA production (as shown in *dcl3* and *ein5/xrn4* mutants for ORMV) and by choosing growth conditions that support sink strength and a prolongation of juvenile growth.

KØRNER ET AL. 2018. CROSSTALK BETWEEN PTGS AND TGS PATHWAYS IN NATURAL ANTIVIRAL IMMUNITY AND DISEASE. NATURE PLANTS 4, 157-164.

General conclusion

The major goal of this thesis was to gain new insights into plant-virus interactions by elucidating the role of virus- and host-derived small RNAs in the regulation of gene expression during the local spread of virus infection in leaves and also in mechanisms determining plant disease and recovery. As part of my thesis I also contributed to a review article discussing current models of virus movement through PD (Pitzalis and Heinlein 2017).

The role of virus-and host-derived small RNAs in plant-virus interactions

The cellular events involved in local viral replication and cell-to-cell-movement have been intensely studied in recent years. However, we still know very little about plant:virus interactions playing a role in orchestrating these processes at the level of gene expression. Thus, as described in Chapter II of this thesis, different deep sequencing approaches (RNAseq, sRNAseq, PAREseq) were used to investigate the virus-induced changes in the host transcriptome and the regulation of genes and of the virus by virus- and host-encoded sRNAs. Using bioinformatic analysis of the sequencing data, the focus was laid on the identification of host-or virus-derived sRNAs that target host mRNA transcripts or viral RNA by RISC-mediated cleavage. The work was applied to TuMV infection in rapeseed (*B. napus*), which represents an economically important crop-pathosystem. To gain information related to the process of ongoing virus replication and spread, we used a GFP-tagged version of the virus, which allowed us to isolate RNA samples from local sites of spreading infection in the inoculated leaves. Reliable data and conclusions were achieved through the analysis of samples from three independent biological experiments. Moreover, the use of samples from two different cultivars allowed us to interpret the results in relation to the cultivar-specific susceptibility for the virus. Importantly, the different NGS approaches (RNAseq, sRNAseq, PAREseq) were always applied to the same individual RNA samples, so that the different levels of analysis and respective results for a given sample could be combined, mutually correlated and interpreted.

Genome-wide mRNAseq analysis revealed numerous genes showing differences in the accumulation of their transcripts between mock-treated and virus-treated samples. Among these, numerous virus-induced genes were significantly up or down-regulated either in both

cultivars or in a cultivar-specific manner. Some of the differentially expressed transcripts are predicted to encode proteins that are known to play important roles in pathogen defense. One example is CALMODULIN-BINDING PROTEIN 60G (CB60G), which is induced in both cultivars and known to act as a master immune regulator that promotes the expression of key genes involved in salicylic acid (SA) biosynthesis and in regulating PAMP-PTI, ETI and systemic acquired resistance (SAR) (Sun et al. 2015). Viral susceptibility in the cultivar Drakkar correlated, for example, with a strong induction of expression of the coatomer alpha-2 subunit of the COPI coatomer complex (Ahn et al. 2015), which may play a role in the formation of vesicles involved in TuMV replication and movement (Wei and Wang 2008) (see Chapter I). On the other hand, the more resistant phenotype of the cultivar Tanto was correlated, for example, with the specific induction of transcripts encoding TARGET OF AVRB OPERATION1 (TAO1), a TIR-NB-LRR receptor-like protein (Eitas et al. 2008). The general validity of our mRNAseq data was confirmed by testing the expression of several genes by RT-qPCR analysis, in which both the original RNA that was analyzed by NGS-mRNAseq as well as novel RNA samples from four new and independent infection experiments were used. This part of the work provided lists of genes with induced or suppressed transcript levels in local TuMV-GFP infection sites formed in two different cultivars differing in virus susceptibility, and these lists are ranked according to the strength of the observed changes.

To reveal mRNAs that might be targeted by virus-induced host-or-virus-derived sRNA, the sRNA reads were first counted and aligned to both the viral genome and the Tanto and Drakkar transcriptomes and annotated. As has been noted by previous studies (e.g. Hu et al. 2011; Tagami et al. 2007; Vogler et al. 2007), virus infection triggered drastic changes in the sRNA length profile. Whereas the sRNAs from Tanto and Drakkar mock samples showed identical and typical profiles of predominantly 21 nt - 24 nt long sRNAs, the profiles were greatly dominated by virus-derived 21 nt and 22 nt siRNAs upon infection (vsiRNAs). These profiles as well as the profiles of vsiRNAs aligned to the TuMV genome were almost identical between both *B. napus* cultivars, indicating that the differences in susceptibility for the virus cannot be explained by obvious differences in sRNA processing. By mapping the host-derived sRNAs to *Brassicaceae* miRNAs in the miRbase database (Kozomara and Griffiths-Jones 2014), several of the reads could be annotated to known miRNAs. Moreover, by using Shortstack software (Axtell 2013), numerous previously unknown miRNAs were identified.

The sRNA and mRNA data were finally combined with the results of PAREseq analysis to reveal sRNAs that align to cleaved mRNA 5' ends and satisfy the conditions of RISC pairing using PAREsnip software (Folkes et al. 2012). The analysis revealed already known miRNAs:mRNA target pairs, such as miRNAs targeting the mRNAs for specific Squamosa promoter-binding-like (SPL) proteins, Auxin response factors (ARFs), Scarecrow-like (SCL) proteins, Ethylene-responsive transcription factors (RAP2-7, AP2), Auxin signaling F-box proteins (AFB2, AFB3), and Superoxide dismutase proteins (Llave et al. 2002 ; Rhoades et al. 2002 ; Allen et al. 2005 ; Wang et al. 2005a ; Wang et al. 2005b ; Kim et al. 2006; Gandikota et al. 2007; Vidal et al. 2010; Si-Ammour et al. 2011; Yu et al. 2012; Lu et al. 2013; Ma et al. 2014; Jung et al. 2014; Xu et al. 2016) and thereby confirmed the accuracy of PARE analysis. In addition, the analysis led to the identification of new miRNA:mRNA target pair candidates, such as miR1885b:BLOS2 or miRC23a:COX19. The cleavage activity of some of the known and predicted miRNA:mRNA target pairs was confirmed by gene-specific 5' RACE assays using repetitive, newly created biological samples.

One of the important aims was to determine whether the infecting virus may use vsiRNAs processed from its genome as RNA effectors for the RISC-mediated targeting of host genes. The analysis indeed revealed the presence of vsiRNAs in predicted vsiRNA:mRNA target pairs which appeared only after infection. A predominant vsiRNA was found in predicted vsiRNA:mRNA target pairs involving transcripts of ERF genes that are also targeted by miR172. This specific vsiRNA was found similar in sequence to miR172 and to engage in predicted cleavage of exactly the same site in the target mRNA. This suggests that viruses may encode vsiRNAs evolved to mimic the activity of host miRNAs and, thereby, to control the specific miRNA target genes during infection.

The mapping of sRNAs to the two cultivar transcriptomes and the analysis of the alignment with the ShortStack program (Axtell 2013) led to the identification of numerous *PHAS* loci that produce phased, secondary, small interfering RNAs (phasiRNAs). PhasiRNAs are produced by conversion of a transcript into dsRNA by RDR6 or RDR1 and subsequently processing of the dsRNA into phased siRNAs by DCL4 (Fei et al. 2013). The production of phasiRNAs is thought to represent a mechanism to down-regulate the specific transcript from which they are derived as well as to produce siRNAs able to target homologous sequences *in trans* (Fei et al. 2013). Thus, unlike the non-coding TAS genes in *Arabidopsis*, which were among the first loci known to produce phased tasiRNAs (Vazquez et al. 2004), *PHAS* loci refer to coding genes,

many of which are NB-LRR family genes involved in pathogen defense, as well as genes of the PPR and MYB families, as shown in *Arabidopsis*, *Medicago*, and peach (Fei et al. 2013; Zhai et al. 2011). The analysis of *PHAS* loci in mock-treated and TuMV-infected *B. napus* plants revealed that certain *PHAS* loci produce phasiRNAs only after infection. The production of virus-associated secondary siRNAs (vasiRNAs) from coding genes upon virus infection has been previously noted in *Arabidopsis* and found to require RDR1 for vasiRNA synthesis and AGO2 for mRNA target cleavage (Cao et al. 2014a). Thus, the vaPHAS loci identified in our analysis may represent vasiRNA-producing loci. However, because the pathway for the synthesis of the phasiRNAs in *B. napus* is not clarified, it is preferable to distinguish them as va-phasiRNAs. Our study indicates that virus infection in rapeseed stimulates the production of phasiRNAs at numerous defense-related coding genes (e.g. TAO1, AGO2, NBR1 homolog). Among these genes we found family members of three small gene families (encoding Chlorophyll a-b binding protein 1, NBR1 homolog, and TAR1) that produce va-phasiRNAs associated with cleavage of their own transcript or of transcripts of homologous genes in the same gene family. This suggests that the process of va-phasiRNA production may represent a mechanism to dampen the effects of infection on transcript homeostasis. Interestingly, members of the NBR1 and TAR1 family also produce va-phasiRNAs with potential to target mRNA transcripts of other genes. The data suggest that particularly NBR1 may represent a virus-induced hub for siRNA synthesis and the virus-induced targeting of a whole network of other genes.

The results of PAREsnip analysis indicate that also the viral genome can be cleaved by virus- and host-derived siRNAs (siRNAs, hsRNA). The large majority of the cleavage events were associated with unique hsRNAs derived from genes annotated as disease resistance genes TAO1 and RPP5, both encoding TIR-NB-LRR receptor-like proteins. The cleavage of the vRNA though vasiRNAs or hsRNAs may contribute to cultivar-specific susceptibility for the virus, as some cleavage sites are predicted in a cultivar-specific manner. Interestingly, some of the predicted hsRNA:vRNA target pairs include trans-acting va-phasiRNAs derived from NBR1 and TAR1 genes, which may support the hypothesis that the evolution of NBR1 genes as virus-inducible hubs for secondary tasiRNA production may have occurred on the precondition that the va-phasiRNAs derived from the same hub will, in turn, also control the virus. It is intriguing also that the *B. napus* NBR1 genes are highly homologous to the selective autophagy receptor

protein AT4G24690/NBR1 gene in Arabidopsis (81-84% identity), which has been implicated in antiviral defenses involving the degradation of viral proteins and particles by autophagy (Hafren et al. 2017; Hafren and Hofius 2017). This protein was shown to suppress TuMV infection in Arabidopsis by targeting the VSR of the virus (HcPro) (Hafren et al. 2018). Thus, by inducing the conversion of NBR1 mRNA into secondary siRNAs the virus may have gained the possibility to achieve widespread control over host gene expression and at the same time also to suppresses NBR1 mRNA levels and thereby control the antiviral functions of the NBR1 protein.

In conclusion, this study involved NGS analysis and *in vivo* experiments performed in *B. napus*, the most widely produced oilseed crop in the European Union. The results highlight differential expressed genes and virus- or host-derived sRNAs correlated with cleaved mRNA 5' ends indicating their role in RISC-mediated cleavage. Collectively, the data suggest that *B. napus* uses endogenous siRNAs derived from resistance genes to target the virus, whereas the virus, in turn, uses its own vsiRNAs to target the host. Moreover, by inducing the production of secondary siRNAs from coding genes, the virus appears to gain the possibility to target other genes. The virus-responsive genes and particularly the genes predicted as targets of vsiRNAs or va-phasiRNAs may play an important role during virus infection in *B. napus* and could represent important new candidate loci for crop improvement. However, it is important to note that the identified sRNA:RNA target pairs are predicted and that additional experiments are needed to prove that these target pairs are indeed functional in RISC-mediated RNA cleavage. One approach to gain supporting evidence could be by using AGO- immunoprecipitation for determining whether specific sRNAs in question are indeed present in AGO-RISC complexes. RISC-mediated cleavage of an mRNA target is usually confirmed by expression of a reporter construct in which the sRNA target sequence (and in a control construct, a mutant target sequence) is fused to a reporter, for example a transcript for GFP, and by comparing reporter expression (which is reduced by reporter RNA cleavage) between infected and control tissues. However, this approach may require the production of transgenic plants, since *B. napus* is not suitable for transient expression assays based on agroinfiltration. Given that the DNA genomes of Drakkar and Tanto were sequenced as part of this project, it may be possible to identify cultivar-specific SNPs that map to cultivar-specific sRNA:mRNA target pairs and use these SNPs in genetic crosses to correlate the SNPs and

specific mRNA cleavage by gene-specific 5'RACE experiments. The role of genes during virus infection should be tested using gene-specific mutants. However, given that *B. napus* is an allotetraploid species with an highly amplified genome (Chalhoub et al. 2014), it is almost impossible to create recessive mutants in which a given function is no longer expressed. The functional analysis of genes rather depends on dominant approaches such as VIGS, RNAi or CRISPR/CAS9, all of which have the potential to affect the expression of all members of a given gene family.

Nevertheless, the findings obtained in this study have revealed a complex network of potential sRNA-mediated interactions between *B. napus* and invading virus and led to the identification of important new gene targets for crop improvement.

Processes that lead to viral symptom recovery and promote plant health

Viruses are obligate intracellular parasites, and most studies of viruses have focused on describing their association with diseases. However, viral infection does not always trigger diseases. Although virus diversity surveys demonstrated that viruses were present in thousands of plants, no disease symptoms were seen that could be correlated with the presence of virus, even if the plants contained viruses related to important crop pathogens (Roossinck 2012; Roossinck and Bazán 2017; Roossinck and García-Arenal 2015). Thus, most plants in the wild appear to be tolerant to viruses and pathology from virus infection can be seen as an exception, rather than the rule. Given that viruses produce diseases and important yield losses in crops, it is very important to gain an understanding of the processes by which plants can promote their health in the presence of viruses. To gain such insight, the phenomenon of “symptoms recovery”, thus the ability of plants to recover from disease, was studied. Using ORMV infection in *Arabidopsis* as a model, it was found that recovery occurred in the presence of replicating virus thus indicating that recovered leaves had gained a state of tolerance. By further analysis we showed that disease symptoms correlated with VSR activity and that the plant achieved tolerance through the ability to gain control over this activity. By screening *Arabidopsis* mutants affected in various defense- and hormone-related pathways the underlying mechanism was found to involve post-transcriptional RNA silencing pathway genes that are required for the synthesis of primary and secondary siRNAs as well as transcriptional silencing pathway genes previously implied in systemic RNA silencing

signaling. Moreover, mutants that support enhanced siRNA production also showed enhanced recovery. Together with the additional finding that recovery was restricted to sink tissues, this led us to the model that recovery occurs upon transport of virus-derived siRNAs (vsiRNAs) from source to sink and that the vsiRNAs that accumulate in sink tissues finally cause saturation and inhibition of the VSR activity responsible for disease.

Overall, this study demonstrates that plants can use RNA silencing coupled to intercellular communication and systemic regulation to (gain) control (over) VSR activity in the distant, young tissues and thereby control (overcome an established) disease. This conclusion implies that plant health can be promoted by sink strength and by controlling the activity of genes that act against efficient vsiRNA production (e.g. EIN5/XRN4). The results are consistent with previous reports indicating the importance of RNA silencing and of a “weak” VSR in recovery. However, unlike in these previous reports, our findings argue against a requirement of viral inhibition or clearance as a precondition for recovery; we rather show that the virus itself is not affected during this process. Thus, recovery does not depend on the “killing of the pathogen” but rather on the ability of the infected plants to properly “deal” with the virus. This ability of plants to remain healthy despite the ubiquitous presence of viruses in the environment should indeed be expected as a result of virus-host co-evolution. To support propagation, a virus should not kill its host but rather promote its fitness. The occurrence of serious viral diseases in cultivated plants may be the result of extensive crop breeding that may have led to the loss of important mechanisms evolved during co-evolution.

Materials and methods

I. Materials

1. Plant species

1.1. *Brassica napus*

In this work, two different *B. napus* cultivars were used. Both cultivars are spring rapeseed varieties stemming from french breeding programs and developed by the company SERASEM (France). The cultivar 'Drakkar' is a 'double low' cultivar (low for toxic glucosinolates and erucic acid) approved for research in France in 1986. It has been used as an experimental host for genetic transformation (for example, Han et al. 2001) and the profiling of phloem sap contents (Buhtz et al. 2008; Hanhart et al. 2017). Seeds for this cultivar were provided by Michael Wassenegger (RLP AgroScience GmbH, AIPLanta - Institute for Plant Research, Neustadt an der Weinstrasse, Germany). The cultivar 'Tanto' has been approved in 1990 for research and used by INRA for the development of a *B. napus* Tilling platform using a collection of collection of 8500 EMS mutant lines. Seeds of this cultivar were provided by the company ANOVA⁺ (Evry, France).

1.2. *Arabidopsis thaliana*

1.2.1. T-DNA mutants

T-DNA mutants mentioned in the publication by Kørner et al. (2018) were provided by Franck Vazquez (University of Basel, Switzerland). Tables 2 provide all recovery T-DNA mutants used for my contribution in Kørner et al. (2018).

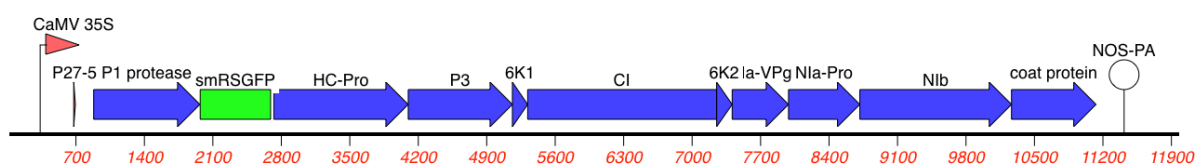
Tables 2: T-DNA mutants

Locus in Arabidopsis	T-DNA lines	Background	Annotations
AT3G43920	dcl3-1	Col 0	Dicer-Like 3
AT1G54490	ein5-1	Col 0	Ethylene Insensitive 5
AT4G11130	rdr2-2	Col 0	RNA-Dependent RNA Polymerase 2
AT3G49500	rdr6-15	Col 0	RNA-Dependent RNA Polymerase 6
	double mutant ein5-Rdr6	Col 0	-
	double mutant dcl2-4	Col 0	-
	P19 expressing lines	Col 0	-
	P21 expressing lines	Col 0	-
	Line 8z2	Col 0	-

2. Viral strain and constructs

2.1. pCB-TuMV-GFP

The binary plasmid pCB-TuMV-GFP (Lellis et al. 2002; Dunoyer et al. 2004; GenBank: EF028235.1) encodes the UK1 strain of TuMV modified by a Green Fluorescent Protein (GFP) cistron cloned between the P1 and HCpro sequences of the polyprotein (Fig. X). The binary plasmid is based on a pGREEN II backbone providing resistance to kanamycin and gives rise to infectious RNA upon transcription from an upstream 35S promoter in plant cells. The TuMV-GFP coding sequence was verified by DNA sequencing before use.



2.2. ORMV virions

ORMV virions were purified from systemically infected *Nicotiana benthamiana* leaves that were mechanically inoculated with infectious RNA produced by *in vitro* transcription of viral RNA from the pBTI ORMV IC clone (provided by Greg Pogue (Large Scale Biosciences, Vacaville) and were used for inoculation of *N. benthamiana* and *A. thaliana* plants as

described in previous publications of the team (Hu et al. 2011; Kørner et al. 2013; Niehl et al. 2014).

3. Antibodies

Antibody	Name	Detection	Origin	Host / Clonality	Use
Primary antibody	UGPase	Anti-UDP glucose pyrophosphorylase	Agrisera (Vännäs, Sweden)	Rabbit / Polyclonal	1:5000 TBS-T 0.5% milk
	125k	125k ORMV replicase	Malpica-Lopez et al., 2018	Rabbit / Polyclonal	1:3500 TBS-T 5% milk
Secondary antibody	GAR	Goat Anti Rabbit antibody conjugated to HoRseradish Peroxidase (HRP)	Invitrogen	Goat / Polyclonal	1:10000 TBS-T 5% milk

4. Primers

Tables 3: Primers for nested PCR during 5'RACE

	Name	Nucleic acid sequences (5' - 3')	Gene annotations
5' RACE adapter	5'RACE Adapter	GCUGAUGGCGAUGAAUGAACACUGCGUUUGCUGGCUUUGAUGAAA	-
5' RACE adapter primers	5'RACE outer primer	GCTGATGGCGATGAATGAACACTG	-
	5'RACE inner primer	CGCGGATCCGAACACTGCGTTTGCTGGCTTTGATG	
Gene-specific primers	BnaA07g13830D-1	TTTCTCCTCTTCTCCGC	Auxin response factor 10
	BnaA07g13830D-2	CTTCTCCTCCTTCTCCGCCTC	
	BnaAnng18540D-1	GGGAGAAGCGAAGACAGT	Scarecrow-like protein 6
	BnaAnng18540D-2	GTCGGGAGAAGCGAAGACAGTG	
	BnaCnng68320D-1	CACCATAAGTAGTCTCCGCTC	Protein argonaute 2
	BnaA05g14760D-1	CCATTACATAATGCAGTCTGCTCC	Protein argonaute 2
	BnaA09g14980D-1	GACCAACCTCTCCCTG	Disease resistance protein TAO1 (ECO:0000305)
	BnaA09g14980D-2	CACACAGGTTTCATCAAAGG	
	BnaCnng44780D-1	GTTTGGTTCAGACACAATGAAACG	Biogenesis of lysosome-related organelles complex 1 subunit 2
	BnaCnng44780D-2	CGATGTTGATGATGACGACACTCAG	
BnaA01g34730D-1	CATGAGAGAAGGTTGGAAGC	Floral homeotic protein APETALA 2	

II. Methods

1. Plant culture

Seeds were sown on soil. 5 to 7 days after germination, *B. napus* seedlings were transplanted into 13 cm pots; Arabidopsis seedlings were transplanted at 15 days after germination into 7 cm pots. Before using them for experiments (i.e. infection with virus), the plants were further grown for 4-5 weeks in a growth chamber with a 16h photoperiod at 24°C and 70% humidity.

2. Inoculation of plants with virus

Four weeks old *Brassica napus* plants were mechanically inoculated with TuMV using crude extract (sap) of previously infected plants and rubbing 2 leaves per plant with a gloved finger covered with sap in the presence of an abrasive (Celite®545). The sap was created from leaves that were previously harvested (at 20 days post inoculation, dpi) from systemically infected

B. napus cv Drakkar plants and by grinding them in 10 mM K₂HPO₄ buffer pH 7.5 (using 3 ml buffer per gram leaf material). These TuMV donor plants were initially mechanically inoculated with sap from systemically infected *Nicotiana benthamiana* plants. To create the original *N. benthamiana* donor plants, five weeks old *N. benthamiana* plants grown at 25°C with a 16h photoperiod were inoculated by agroinfiltration of two leaves per plant with *A. tumefaciens* strain GV3101 transformed with plasmid pCB-TuMV-GFP as described in Dunoyer et al. (2004) paragraph “Virus and plant material” in Materials and Methods. For agroinfiltration, the agrobacteria were grown over night and pressure-injected into leaves at an OD_{600nm} of 0.5 using a syringe without needle.

Three weeks old *Arabidopsis* plants were inoculated with ORMV by rubbing three leaves (pre-powdered with Celite®545) with a cotton tip in the presence of 150 ng purified ORMV virions per leaf (Kørner et al. 2018).

3. Measurement of specific RNA levels by reverse transcription followed by quantitative Polymerase Chain Reaction analysis (RT-qPCR)

3.1. Total RNA extraction and cDNA synthesis

TuMV-GFP infection sites developed in the inoculated leaves of *B. napus* plants were revealed by monitoring GFP fluorescence with a handheld UV lamp (UVP Blak-Ray B-100). At 12 dpi, fluorescent foci were carefully isolated by cutting leaf discs with a 0.5 cm micropunch and immediately frozen in liquid nitrogen. Leaf discs were also harvested from control plants treated with buffer without virus.

Total RNA was isolated from ca 150 leaf disk samples of infection sites or of mock (buffer)-treated, non-infected control tissues, each pooled from ten plants, respectively. After grinding in N₂, 0.1 g fine powder was homogenized and extracted with 1.4 ml Trizol reagent (Invitrogen, USA) until defrosting. After addition of chloroform to 20% (volume to volume) (300 µl), the sample was strongly vortexed for 40 sec. Following centrifugation at 9000 g for 15 min, the upper aqueous phase was transferred to a new tube and after mixing with an equal volume of cold pure isopropanol stored for 30 min at -20°C. After centrifugation at 10150 g (4°C) the lower aqueous phase was kept and supplemented with 1.4 ml cold 70% ethanol. This was followed by centrifugation at 9000 g for 5 min, after which the supernatant

was discarded and the pellet dried for 15-20 min at room temperature. Finally, the RNA in the pellet was resolubilized in 50 μ l RNase-free water heated to 60°C. The concentration of the isolated RNA was quantified by spectrophotometric measurement at 260 nm absorbance using Nanodrop equipment (Thermo Scientific, USA) (Purity: $A_{260}/A_{280} > 1.8$, $A_{260}/A_{230} > 2.0$) and stored at -20°C. For cDNA synthesis, the quality of the RNA sample was verified by an 1% agarose gel electrophoresis in 1x TBE [(90 mM Tris-base, 90 mM Boric acid, 2 mM EDTA (Ethylene Diamine Tetraacetic Acid, pH 8.3)] at constant voltage (100 V). 1-2 μ g of the RNA was reverse-transcribed in the presence of an oligo(dT)₂₀ primer and the SuperScript IV reverse transcriptase (200 U/ μ l) following the manufacturer's instructions (Invitrogen).

3.2. cDNA quantification by RT-qPCR

PCR is an *in vitro* polymerase chain reaction technique that allows the exponential amplification of a DNA sequence by a thermostable DNA polymerase. It requires a pair of oligonucleotide primers hybridizing to flanking regions of the sequence selected for amplification, a complementary DNA strand as template and deoxynucleotide triphosphates (dGTPs, dCTPs, dATPs and dTTPs) for primer extension DNA synthesis. The abundance of specific transcript was measured by probing 1 μ l cDNA by quantitative real-time PCR using 5 μ l SYBR-green master mix (Roche) and 2 μ l of 2.5 μ M allele-specific oligonucleotide primers (12.5 μ l forward and reverse primer in 475 μ l water; see Table 3 for a list of primers used) in a Lightcycler 480 (Roche). The PCR program used for cDNA amplification and measurement is shown in table 4.

Table 4: qRT-PCR amplification conditions

Steps	Temp (°C)	Time	Cycles
Initiale denaturation	95	5 min	1
Denaturation	95	10 s	
Hybridization	60	15 s	45
Elongation	72	15 s	
	95	5 s	
Final cycle	55	1 min	1
	95	Continuous	
Cooling	40	30 s	1

The specific transcript levels were measured by applying three technical replicates for each sample. To compare different samples, the measured transcript level quantified as cycle threshold (Ct) values was normalized against the Ct values for RNA transcripts of two known “housekeeping” genes [TIP41-like protein; BnaA08g11790D (Zhang et al. 2014; Wang et al. 2014)]. The RT-qPCR analysis was performed the same way for each sample (e.g. virus- versus buffer-treated, one *B. napus* cultivar versus another). Assuming a Normal distribution of the data, a statistical Fisher’s F-test was performed to determine variance equality (homoscedastic or heteroscedastic variance), which was needed for a subsequent student’s T-test to calculate the probability of difference between populations and, thus, to determine whether mRNA abundances between control and treated samples were significantly different ($p < 0.05 = *$; $p < 0.01 = **$; $p < 0.001 = ***$).

4. 5’RACE (Rapid Analysis of cDNA Ends)

Non-capped mRNA 5’ends that occur upon RISC-mediated RNA cleavage were analyzed by 5’RACE as described previously (Llave et al. 2002; Llave et al. 2011). RLM (RNA Ligase-Mediated)-RACE kits are usually optimized for the cloning of cDNA of capped full-length mRNA molecules. In this procedure, the RNA is treated with calf intestinal phosphatase (CIP) to avoid the cloning of non-capped molecules carrying a 5’ monophosphate (degraded mRNA, rRNA, tRNA and DNA) and with tobacco acid pyrophosphatase (TAP) to remove the cap structure on the full-length mRNA. Since we aimed to apply 5’RACE for the cloning and identification of mRNA molecules that are non-capped and 5’ monophosphorylated due to RISC-mediated cleavage, these two enzymatic steps were avoided. Instead, poly-adenylated RNA was used to ligate the 5’RACE RNA adapter to available mono-phosphorylated 5’ RNA ends. As shown in figure 7, the ligation product was then reverse transcribed into cDNA using an oligo dT primer. The cDNA was then amplified with nested RACE adapter-specific and gene-specific primers to create gene-specific cDNA fragments that were further analyzed by electrophoresis through a 1% agarose gel in 1x TBE [(90 mM Tris-base, 90 mM Boric acid, 2 mM EDTA (Ethylene Diamine Tetraacetic Acid) pH 8.3] at constant voltage (100 V) and sequenced the IBMP platform with gene-specific primers and the ABI3130xl sequencer (Applied Life Technologies).

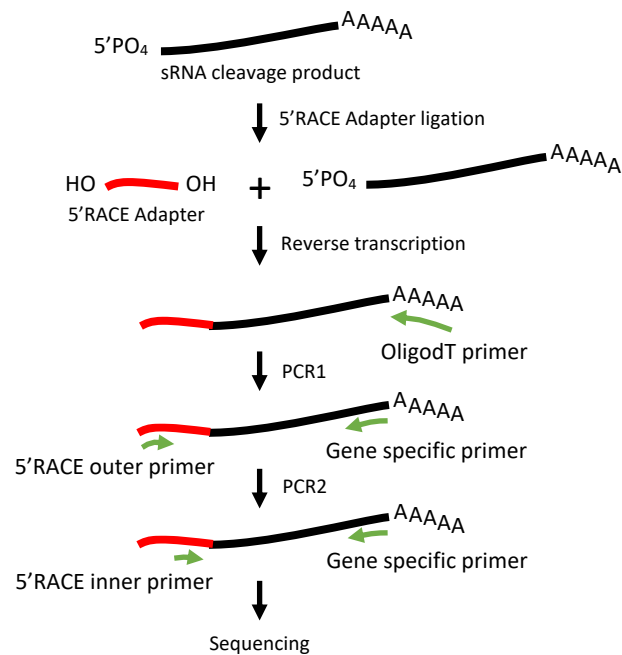


Figure 7: 5'RACE analysis of mRNA molecules with monophosphorylated, non-capped 5' ends.

4.1. Total RNA extraction

Total RNA was extracted as described under paragraph 3.1

4.2. Purification of mRNA from total RNA

Polyadenylated mRNA was purified from 1-5 μ g total RNA by binding to oligo d(T)₂₅-coupled paramagnetic beads and separation with a magnetic isolation module [NEBNext[®] Poly(A) RNA Magnetic Isolation Module (E7490L), BioLabs] according to the manufacturer's instructions. Each purified mRNA sample was quantified and the quality was measured according to the RNA Integrity Number (RIN) and 18S/28S ribosomal ratio using the Agilent RNA 6000 Pico Chip kit and by running the electrophoretic assays with the 2100 Bioanalyzer system (Agilent Technologies).

4.3. Adapter ligation

Ligation of the GeneRacer RNA oligo 5'RACE adapter (Invitrogen; see Table 2) to mRNA molecules carrying a monophosphate at the 5' end was performed as described in Llave et al. 2011 and following the manufacturer's instructions of T4 RNA ligase (New England BioLabs).

In a sterile Eppendorf tube were mixed 2 ng of RNA oligonucleotide adapter and 1 ng Poly(A) purified RNA, incubated for 5 min at 65°C to relax secondary structures. After incubation, the mixture was supplemented with 1 µl 10X ligation buffer, 1 µl RNaseOUT (40 U/µl), 1 µl T4 RNA ligase, 1 µl ATP (10 mM) and filled up with sterilized milliQ water to 10 µl final volume. After incubation at 37°C for 1h, the ligation products were separated from non-incorporated adapter molecules using an Illustra Microspin S-300 Sephacryl size filtration column (GE Healthcare) and centrifugation for 1 min at 735 g.

4.4. Reverse transcription

Eight µl of the RACE adapter-ligated RNA were used for cDNA synthesis as described in paragraph 3.1 with the exception that the reaction with SuperScript IV reverse transcriptase was done for 20 min at 60°C.

4.5. cDNA fragment amplification by PCR (nested PCR)

Sample preparation and conditions used for 5'RACE nested PCR amplification are detailed in table 5 and represent the same conditions used in Llave et al. 2011 and follows the manufacturer's instructions of the GoTaq® G2 Hot Start Polymerase (Promega). The sample preparation has been performed on ice and directly placed in 94°C pre-heated PCR block for amplification. Nested PCR requires two independent amplifications starting first with a gene-specific outer primer amplification followed by a second gene-specific inner primer amplification as shown in figure 7.

Table 5: Sample preparation and nested PCR conditions for 5'RACE.

Nested PCR amplification		Volumes	Steps			
Colorless GoTaq®Flexi Buffer PCR buffer (5x)	10 µl		Initiale denaturation	94	5 min	1
MgCl ₂ (25 mM)	3 µl		Denaturation	94	30 s	5
dNTP mix (10 mM each)	1 µl		Hybridization	70	1 min	
GSP (10 mM)	1 µl		Denaturation	94	30 s	5
5'RACE Outer Primer (10 mM)	1 µl		Hybridization	65	1 min	
5'END cDNA	1 - 2 µl		Denaturation	94	30 s	20-25
Taq DNA polymerase (5 U/ml)	0.5 µl		Hybridization	60	30 s	
Final volume	50 µl		Elongation	72	1 min	
			Final elongation	72	10 min	1

5. DNA genome sequencing

The genomes of the *B. napus* cultivars Drakkar and Tanto were analyzed by paired-end (2x 100 bp) sequencing and the reads were aligned to the published transcriptome of *B. napus* cultivar “Darmor-bzh” (Chalhoub et al. 2014; Genoscope v4.1, <http://www.genoscope.cns.fr/brassicapapus/>). Identified SNPs were inferred into the Darmor transcriptome to create the cultivar-specific transcriptomes that were used for the cultivar specific mapping of the mRNAseq, sRNAseq, and PAREseq reads.

5.1. DNA isolation

DNA was isolated by aScidea Computational Biology Solutions (<http://www.ascidea.com/>) from 1.9 g fast-frozen leaf tissue of *B. napus* cv Drakkar and *B. napus* cv Tanto plants.

5.2. Sequencing and quality control

The sequencing was performed with 800 bp insert PCR-free libraries and subsequent paired-end sequencing (2*100 bp) on an Illumina HiSeq 4000 platform (BGI Tech Solutions, Hongkong). Raw libraries were quality checked with FastQC (RRID:SCR_014583) version v0.11.2 and cleaned with cutadapt (RRID:SCR_011841) version v1.8.1 to remove adapters, ambiguous bases, and low-quality reads. Reads longer than 60 bp and with a Phred score greater than 30 were kept. The Phred quality scores reflect the nucleotide error probabilities. A Phred score of 30 reflects a base call accuracy of 99.9%.

5.3. Alignment of DNA reads to the *Brassica napus* reference genome

The 123 Mio clean reads obtained for each cultivar were mapped to the genome of European winter oilseed *B. napus* Darmor-bzh using the Burrows-Wheeler Aligner (Li and Durbin 2009; RRID:SCR_010910) version v0.7.15-r1142. The BWA-MEM algorithm was used with default parameters. Duplicated reads were marked and removed with Picard-tools (RRID:SCR_006525; <http://broadinstitute.github.io/picard/>) version v1.140 (Illumina sequencing involves several PCR amplification steps that may produce duplicated reads. If there is a wrongly sequenced nucleotide in these reads, the error is multiplied. Picard-tools identify and remove these reads derived from PCR duplicates to increase sequencing quality and to increase the reliability of the given sequence data and SNP calling).

5.4. SNP calling and cultivar-specific transcriptome construction

SNPs present in the DNA of Drakkar and Tanto in comparison to the DNA of Darmor-bzh were identified using GATK HaplotypeCaller (McKenna et al. 2010), RRID:SCR_001876) version v3.3-0. Only high-quality homozygous SNPs were kept using the following filters: QD < 2.0 || FS > 60.0 || MQ < 40.0 || MQRankSum < -12.5 || ReadPosRankSum < -8.0 || DP < 4.

Representative transcriptome genomes of Drakkar and Tanto cultivars were constructed by inferring each cultivar-specific high confidence SNPs into the Darmor-bzh reference genome using GATK FastaAlternateReferenceMaker (RRID:SCR_001876) https://software.broadinstitute.org/gatk/documentation/tooldocs/3.8-0/org_broadinstitute_gatk_tools_walkers_fasta_FastaAlternateReferenceMaker.php).

6. RNA sequencing

6.1. Total RNA isolation and quality control

For deep sequencing profiling of RNA, total RNA of each sample was extracted as described in paragraph 3.1, except that ca. 200 dissected leaf-disks were harvested at 12 dpi. Two grams (2 g) of these leaf disks were ground in liquid nitrogen and RNA was purified using the RNAeasy Mini Kit (Qiagen). The quality of each RNA sample was verified by gel electrophoresis and BioAnalyzer (Agilent technologies) techniques as described (paragraph 4.2). Each individual total RNA sample was divided into three aliquots, each used for further analysis by mRNAseq (transcriptome profiling), sRNAseq (small RNA profiling), and PAREseq (mRNA degradome profiling using Parallel Analysis of RNA ends (PARE)).

6.2. mRNA sequencing and quality control

The total RNA preparations were used for mRNA isolation, the construction of mRNAseq paired-end libraries (2*100bp) and Illumina HiSeq2000 sequencing by the company “aScidea Computational Biology Solutions” (<http://www.ascidea.com/>; Barcelona, Spain). The mRNAseq raw reads libraries were quality-checked with FastQC (RRID:SCR_014583) version v0.11.2 and cleaned with cutadapt (RRID:SCR_011841) version v1.8.1 for adapter removal,

“N” base removal, and quality filtering. Reads longer than 60 bp and with a Phred score greater than 30 were kept.

6.3. Alignment and annotation of mRNAseq reads

Tanto and Drakkar clean mRNAseq reads were aligned to the reconstructed Tanto and Drakkar transcriptome, respectively, using Tophat2 (Kim et al. 2013, <https://ccb.jhu.edu/software/tophat/index.shtml>) version v2.0.13. The Bowtie2 aligner was chosen allowing one mismatch (Langmead and Salzberg 2012, <http://bowtie-bio.sourceforge.net/bowtie2/index.shtml>). Genes were annotated using blastx on the *Arabidopsis thaliana* genome with default parameters. The *Arabidopsis* TAIR10 gene identifiers were used to retrieve the gene ontology (GO) annotations from the UniProtKB database.

6.4. Differential expression analysis

After mapping to the transcriptome the unique mapped RNAseq reads were counted using the SAMtools (Li et al. 2009, RRID:SCR_002105) idxstats tool version v1.1. The counts of mapped reads were then used for differential expression analysis with DESeq2 (Love et al. 2014), RRID:SCR_015687) version v1.10.0.

7. sRNA sequencing

sRNAseq paired-end libraries (1*50 bp) were constructed and sequenced on an Illumina HiSeq2000 sequencer by aScidea Computational Biology Solutions (<http://www.ascidea.com/>, Barcelona, Spain). The sRNAseq raw read libraries were quality checked and remaining reads were filtered like the mRNAseq read libraries. Clean reads that were 18 nt to 30 nt in length and that had a Phred score higher than 30 were kept.

7.1. vsiRNA alignment

Virus-derived siRNAs were identified by mapping the clean sRNAseq reads to the TuMV-GFP genome (described in paragraph 2.1 pCB-TuMV-GFP) with Bowtie2 (Langmead and Salzberg

2012) version v2.2.9 using the following options "-t -N 0 --end-to-end --very-sensitive --score-min C,0,0" with no mismatch for virus-derived sRNAs. These reads have been re-mapped to the cultivar-specific transcriptomes to verify the absence of homology in the plants.

7.2. Identification of miRNAs

Reads were mapped to miRNAs of *B. napus*, *B. oleracea*, *B. rapa*, *A. thaliana* and *A. lyrata* annotated in miRbase21 as well as to new Brassica miRNAs described in three publications (Xu et al. 2012; Lukasik et al. 2013; Jiang et al. 2014).

7.3. *De novo* miRNA and va-phasiRNA detection

To identify *B. napus* miRNAs that are still unknown, we analyzed the reads with ShortStack (Axtell 2013) (v3.4, RRID:SCR_010834) in *de novo* mode. ShortStack annotates miRNAs on the basis of specific criteria, including a requirement of the corresponding star sequence present in the sRNA data and its mapping near the candidate miRNA sequence within the same gene. The list of predicted miRNAs was filtered to keep only candidates (clusters) with: DicerCall 21, 22, 24nt, and MIRNAs step Y_N15. The DicerCall reflects the predominant RNA size observed in the locus (not necessarily the majority). The N15 step is the last step in the analysis. By choosing the option Y-N15, only the sRNA reads that have passed all selective steps of miRNA identification, including the sequencing of the exact miRNA star sequences, are selected and identified as miRNAs.

We focused our analysis of sequenced sRNAs also on the identification of siRNAs that are particularly induced upon virus infection. Similar to virus-associated, RDR1-dependent siRNAs (vasiRNAs) reported for Arabidopsis (Cao et al. 2014a), we found siRNAs that derive from coding genes that convert their transcripts into dsRNA followed by phased DCL-mediated cleavage and which we named "virus-associated phased siRNAs (va-phasiRNAs)". The unique va-phasiRNAs in our database were predominantly 21 nt in length, represented by at least 100 reads in the samples from virus-infected tissues, and exceeded their normalized abundance in virus-treated tissues over their abundance in non-infected control tissues (mock) by at least a factor of 2 ($\text{rpm infected} / \text{rpm mock} > 2$) (read per million (rpm); number of reads are multiplied by 10^6 and divided by the total number of cleavage events in the

corresponding sequenced library). Moreover, the corresponding va-phasiRNA-producing genes showed a PhaseScore (the quality of the phasing register) higher than 30 (determined by Shortstack). The virus-induced and phased production of the va-phasiRNAs was verified by visualization of the gene-specific siRNA pattern with the Integrated Genome Viewer tool IGV 2.3 (Thorvaldsdóttir et al. 2013).

7.4. Short read abundance and differential expression (DE) analysis

The abundance of our known and predicted miRNAs and va-phasiRNAs was estimated after mapping using idxstats command of SAMtools v1.1 (Li et al. 2009) (RRID:SCR_002105). The differential expression analysis for miRNAs was performed with DESeq2 (Love et al. 2014), RRID:SCR_015687) version v1.10.0.

8. mRNA degradome sequencing

The construction of PARE libraries was performed according to the protocol of German et al. (2009) with modifications, which concerned particularly the purification of each intermediate reaction product during the procedure. This part of the work was done by Khalid Amari (former Post-doc) in collaboration with Livia Donaire and César Llave in the CIB-CSIC Institute, Madrid (Spain). Similar to 5'RACE, the construction of PARE libraries involves mRNA purification (affinity binding to oligo dT-coated beads), 5'RNA adapter ligation, reverse transcription, an additional Mmel enzyme treatment causing cleavage of the cDNAs at a position 20 bp downstream of the original 5' end of the mRNA, subsequent 3'RNA adapter ligation to the new cDNA3' ends, PCR amplification, and high-throughput sequencing.

Thus, the procedure started by ligating 1 ug of purified mRNA to a 5' RNA adapter. After a new purification step of mRNA again using oligo dT-coupled Dynabeads, cDNA synthesis, short PCR amplification and Mmel digestion were performed as described (German et al. 2009). Digested fragments of \approx 20 nt were then purified by PAGE, and 3' ligated to a dsDNA adapter. The ligation products were further purified by PAGE and amplified using Illumina primers. The final amplicons of approximately 125 bp were again purified by PAGE. To allow sample multiplexing in the sequencing reaction, different indexed primers were used in the amplification step (Illumina primers RPI1 to RPI4). The amplicon structure was then checked

by cloning into TOPO vector and low-scale sequencing of individual clones. All clones analyzed contained inserts according to the predicted structure when libraries prepared from Drakkar were tested.

8.1. Sequencing of PAREseq libraries and quality control

The PAREseq libraries were sequenced (1x 50 bp) on an Illumina HiSeq2000 platform by aScidea Computational Biology Solutions (<http://www.ascidea.com/>). The sequenced PAREseq read libraries were cleaned with cutadapt (RRID:SCR_011841) version v1.8.1 for adapter removal, removal of reads with “N” bases, and quality filtering.

8.2. Association of cleaved mRNA 5' ends with RISC-mediated mRNA cleavage

To determine whether the cleaved 5' mRNA ends identified by PAREseq analysis could be caused by RISC-mediated RNA cleavage, the sample-specific PAREseq library was aligned to the cultivar-specific transcriptome and correlated with sRNAs (determined by sRNAseq) from the same original total RNA sample with PAREsnip software (Folkes et al. 2012) implemented in the UEA sRNA Workbench version v4.2.1a (Stocks et al. 2018). The default parameters were used except for the “min read abundance” option set to 100. The analysis with this software allows the identification of potential mRNA:sRNA target pairs involved in sRNA-mediated RNA cleavage. Since the RNA genome of TuMV is polyadenylated, the PARE analysis included the analysis of 5' ends of viral RNA.

To compare predicted cleavage events between samples, the specific PAREseq reads associated with RISC-mediated mRNA cleavage events were normalized as reads per million. The sums of normalized cleavage events that occurred in the three biological replicates per condition (specific *B. napus* cultivar/specific treatment) were used to compare the occurrence and abundance of specific cleavage events between conditions. The gene or viral origins of sRNAs associated with specific mRNA or vRNA cleavage were identified by extracting the sRNA associated with a specific cleavage event from the PAREsnip analysis and by aligning its sequence to the transcriptome or viral genome without mismatch.

9. RNA analysis using the northern blotting technique

9.1. Total RNA extraction and size fractionation

RNA extraction from *Arabidopsis* plants was performed essentially as described under paragraph 3.1 for RNA from *B. napus* leaves. Here, total RNA was extracted by homogenizing 0.7 g *Arabidopsis* leaf material derived from the pools of several ORMV-infected (35 dpi) or non-infected *Arabidopsis* leaves, into fine powder in liquid N₂. In contrast to the protocol described in paragraph 3.1, the volumes of chemicals were adapted to the weight of *Arabidopsis* grinded tissues. Thus, 10 ml of TRI REAGENT® (MRC) were added to the crude extract and supplemented with 2 ml Chloroform in the suspension followed by strong vortexing to create a homogenous mixture. After centrifugation and precipitation, the pellet was washed with 10 ml of 70% EtOH and after discarding of the supernatant, the pellet was dried for 15-20 min at room temperature and finally resuspended in 150 µL RNase-free water heated to 60°C. The RNA in the resuspended pellet was quantified with a NanoDrop microvolume spectrophotometer at 260 nm absorbance.

To separate high molecular weight (HMW) RNA (e.g. mRNA) from low molecular weight (LMW) RNA (e.g. small RNAs), the isolated total RNA was size-fractionated with the RNeasy Mini Kit® (QIAGEN) by applying the RNA cleanup protocol with some modifications, as described by Blevins (2017). For instance, the RTL buffer was supplemented with 10 µl β-mercaptoethanol (β-ME) per ml and the sample was adjusted to 90 µg total RNA. Moreover, all the flow-through was kept for collecting the LMW RNA.

Eluted HMW and LMW RNA fractions were precipitated by addition of an equal volume of isopropanol, overnight incubation at -20°C and centrifugation at 14 000 g in the cold (4°C). The precipitated RNA was resuspended in RNase-free water and the concentration was determined with a NanoDrop microvolume spectrophotometer at 260 nm.

9.2. RNA blotting

The procedure of Northern blotting for the detection of specific HMW and LMW RNA molecules is mentioned in Kørner et al. (2018) and followed exactly the steps described in J. Sambrook, D. William Russell CSHL Press, 2006 (Volume 1, Chapter 7, Protocol 6 and 7) for

HMW RNA and the procedures described by Akbergenov et al. (2006) and Blevins (2017) for LMW RNA.

For the specific probing of HMW RNA, 8 µg of HMW RNA were used for electrophoresis through the formaldehyde agarose gel. The RNA was then transferred and fixed onto nitrocellulose membrane as described in J. Sambrook, D. William Russell CSHL Press, 2006 (Volume 1, Chapter 7, Protocol 6 and 7). The RNA was crosslinked to the membrane by UV irradiation (1400 x 100 µJ/cm²). For detection of abundant, HMW, positive sense, genomic viral RNA, the RNA on the blot was probed by hybridization with a sequence-specific mix of oligonucleotide probes (with sequences complementary to the viral RNA) that were end-labelled with γ[³²P]-dATP. The probes were prepared in 20 µl reactions containing 1 µl T4 Polynucleotide-Kinase (Thermo Scientific), 0.3 µl 100 µM oligo-nucleotides, 2 µl 10X PNK buffer A, 4.5 µl γ[³²P]-dATP (~ 50 µCi) and 12 µl H₂O that were incubated for 30 min at 37°C. For detection of rare molecules such as negative strand viral RNA, a 200 bp long RNA probe generated by T7 promoter-driven *in vitro* transcription in the presence of α[³²P]-dUTP was used. The short oligonucleotide probes were purified through illustra MicroSpin G-25 Columns (GE Healthcare Life Sciences) and centrifugation at 735g for 1 min, whereas the longer probe was cleaned by phenol/chloroform extraction and 100% ethanol precipitation. The probes were applied to a nitrocellulose membrane (N+, Amersham) previously pre-hybridized for 4 hours in 10 ml PerfectHyb™ Plus buffer (Sigma). The specific probes were then added and the membrane followed by incubation in this solution overnight at 37°C for detection of abundant viral positive RNA strand and 70°C for detection of the less abundant negative strand. The membranes probed with oligonucleotide or *in vitro* transcript probes were washed in 2x SSC (300mM NaCl, 30mM Na-Citrate, pH 7) containing 2% SDS (Sodium Dodecyl Sulphate) at 50°C for 5 min or 10 min at 60°C, respectively. To visualize the hybridized probes on the membrane, the membranes were exposed to a storage phosphor screen (for 1h to visualize the viral genomic RNA; for one week to visualize the viral negative strand RNA). The storage phosphor screen was then imaged with a Typhoon FLA-7000 laser scanner (GE Healthcare).

For probing of LMW RNA, 5 µg of the LMW RNAs were separated by electrophoresis through a 16 % polyacrylamide urea gel [12.0 ml 30% acrylamide bisacrylamide (19:1), 18 ml urea solution (11.1 g urea, 6.0 ml 5x TBE (54 g Tris-base, 27.5 g boric acid, 20 ml 0.5 M EDTA pH 8.0

in 1 L milliQ water)) supplemented with 30 μ l of TEMED (N,N,N',N'-TetraMethyl-1,2-Diaminométhane), 300 μ l APS (ammonium persulfate) (10%)]. The polyacrylamide gel was pre-run in 1x TBE for 20 min at 15W before loading of the sample and the wells were washed using a syringe to remove any excess of urea. The samples were dried for 40 min at room temperature by sublimation in a SpeedVac Concentrator (Thermo Scientific) and resuspended in 8 μ l RNA loading buffer (95% formamide, 0.025% bromophenol blue, 0.025% xylene cyanol FF, 5 mM EDTA, 0.025% SDS, pH 8.5). Before loading, the samples were heated to 95°C for 3 min and cooled on ice. The electrophoresis was run for 1h30 at 15W in 1X TBE. After electrophoresis, the RNA in the gel was stained for 8 min in Ethidium bromide (EtBr) solution (400 ml 1X TBE, 20 μ l EtBr (from a 10 mg/ml stock) photographed (GelDoc 2000, Bio-Rad), and washed for 20 min in 1X TBE.

Next, the gel was blotted overnight onto a Hybond N+ membrane (GE Healthcare, UK) by capillarity blotting in 0.5X TBE buffer followed by crosslinking the RNA to the membrane by UV (140 mJ/cm²). Oligonucleotide probes were prepared and purified as described for HMW probes. The membrane was pre-hybridized for 4 hours in 10 ml Perfect-Hyb buffer (Sigma, USA) at 40°C, followed by the overnight hybridization in the same buffer with the specific probes at 37 °C. Blots were washed three to five times in 0.5% SDS; 2x SSC at 37 °C. For detection of different sRNAs in the same RNA extract, the blots were stripped by three consecutive washes with boiling 0.5% SDS each for 20 min before re-probing. The membrane was exposed two- to seven-days to a storage phosphor screen, which was then imaged with a Typhoon FLA-7000 laser scanner (GE Healthcare).

10. Protein analysis using the western blot technique

10.1. Total protein extraction and quantification

As described in Kørner et al. (2018), 0.1g Arabidopsis leaf tissues were homogenized to fine powder in liquid N₂. After addition of 400-600 μ l extraction buffer (10% glycerol, 5% β -ME, 75 mM Tris-HCl pH 6.8) and homogenization with the help of a Silimat® shaking machine, the sample was heated at 95°C with 2% SDS for 5 min and centrifuged at 14 000 g for 10 min. The aqueous phase was extracted, boiled 10 min at 95°C for their denaturation and quantified using the Bradford protein assay (Bio-Rad). The protein extract was then mixed to 1x with

Laemmli buffer (62,5 mM Tris-HCl pH 6.8, 3% SDS, 10% glycerol, 0.1% bromophenol blue, 5% β -ME), boiled again 5 min at 95°C before loading into a polyacrylamide gel.

10.2. SDS-PAGE

Proteins were separated by PAGE under denaturing conditions in the presence of SDS using Bio-Rad electrophoresis equipment. The acrylamide gel was polymerized in the presence of APS as a radical initiator and TEMED as catalyst. The acrylamide/bisacrylamide percentage in the separation gel was chosen according to the size of the proteins to be analyzed (generally between 8 % and 15%).

Protein samples were heated in Laemmli buffer for 10 min at 95 °C, mixed and cleared by centrifugation at 14,000 g for 10 min. Between 5 and 25 μ L (\approx 20 μ g) of protein solution were loaded per well. Protein size markers (PageRuler™ 10-170 kDa, Thermo Scientific, 7 μ L) were loaded in parallel. The electrophoresis was performed in 1x Tris-Glycine-SDS buffer (25 mM Tris-base, pH 8.3, 192 mM Glycine) at constant voltage (90 V).

10.3. Protein transfer and luminescent detection

The protein gel was rinsed in transfer buffer (25 mM Tris-base, pH 8.3; glycine 250 mM) to partially remove the remaining SDS. Immobilon-P (Millipore) membrane was cut to the size of the gel, activated in 96% ethanol for 15 sec and briefly rinsed in transfer buffer. The gel and the membrane were placed in a transfer system (Mini Trans-Blot Cell, Bio-Rad) between Whatmann papers and sponges. The transfer was carried out at 90V for 130 min. The membrane was then rinsed for 10 min in TBS-T buffer (1x TBS and 0.1% Tween20®) and pre-incubated in TBS-T / 5% milk powder for 60 min at room temperature to saturate the unspecific sites. After addition of primary antibodies and further incubation at 10 rpm shaking on a Duomax 1030 (Heidolph) apparatus overnight at 4 °C (for dilutions see Material paragraph 4), the membrane was washed 3 times in TBS-T / 5% milk buffer for 10 min. The membrane was then incubated for 1h in the same buffer and in the presence of horseradish peroxidase-coupled secondary antibodies (see Material paragraph 4) at room temperature and again washed for 3 times in TBS-T buffer for 10 min. The location of the antibody-labeled proteins on the membrane was revealed by chemiluminescent detection using "Lumi-Light^{PLUS}

Western Blotting Substrate" (Roche Diagnostics) according to the manufacturer's recommendations (volume to volume black and white solution, 1 min contact with the membrane) and documented by imaging with a FUSION FX western blot and chemiluminescence imaging system (Vilber Lourmat, France). The membrane was stained with Coomassie blue (50% ethanol, 10% acetic acid, 0.25% Coomassie R250 blue) to visualize the amount of transferred protein.

References

- Addo-Quaye, C., Miller, W., Axtell, M.J., 2009. CleaveLand: a pipeline for using degradome data to find cleaved small RNA targets. *Bioinformatics* 25, 130–131.
- Agbeci, M., Grangeon, R., Nelson, R.S., Zheng, H., Laliberte, J.F., 2013. Contribution of host intracellular transport machineries to intercellular movement of *Turnip mosaic virus*. *PLoS Pathog* 9, e1003683.
- Aguado, L. C., tenOever, B., 2018. RNA virus building blocks—miRNAs not included. *PLoS Pathog*, 14, e1006963.
- Aguilar, I., Sanchez, F., Martin, A., Martinez-Herrera, D., Ponz, F., 1996. Nucleotide sequence of chinese rape mosaic virus (*Oilseed rape mosaic virus*), a crucifer tobamovirus infecting *Arabidopsis thaliana*. *Plant Mol. Biol.* 30, 191–97.
- Ahn, H.K., Kang, Y.W., Lim, H.M., Hwang, I., Pai, H.S., 2015. Physiological functions of the COPI complex in higher plants. *Mol Cells* 38, 866–875.
- Akbergenov, R., Si-Ammour, A., Blevins, T., Amin, I., Kutter, C., Vanderschuren, H., Zhang, P., Gruissem, W., Meins, F., Hohn, T., Pooggin, M.M., 2006. Molecular characterization of geminivirus-derived small RNAs in different plant species. *Nucleic Acids Res* 34, 462–471.
- Ala-Poikela, M., Goytia, E., Haikonen, T., Rajamaki, M.L., Valkonen, J.P.T., 2011. Helper component proteinase of the genus potyvirus is an interaction partner of translation initiation factors eIF(Iso)4E and eIF4E and contains a 4E binding motif. *J Virol* 85, 6784–94.
- Alazem, M., Lin, K.Y., Lin, N.S., 2014. The abscisic acid pathway has multifaceted effects on the accumulation of *Bamboo mosaic virus*. *Mol Plant Microbe Interact* 27, 177–189.
- Alazem, M., Lin, N.S., 2017. Antiviral roles of abscisic acid in plants. *Front Plant Sci* 8, 1760.
- Allen, E., Xie, Z., Gustafson, A.M., Carrington, J.C., 2005. microRNA-directed phasing during trans-acting siRNA biogenesis in plants. *Cell* 121, 207–221.
- Amari, K., Di Donato, M., Dolja, V.V., Heinlein, M., 2014. Myosins VIII and XI play distinct roles in reproduction and transport of *Tobacco mosaic virus*. *PLoS Pathog* 10, e1004448.
- Amari, K., Lerich, A., Schmitt-Keichinger, C., Dolja, V.V., Ritzenthaler, C., 2011. Tubule-guided cell-to-cell movement of a plant virus requires class XI myosin motors. *PLoS Pathogens* 7 (10), e1002327.
- Andrawis, A., Solomon, M., Delmer, D.P., 1993. Cotton fiber annexins: a potential role in the regulation of callose synthase. *Plant J* 3, 763–72.
- Andrianifahanana, M., Lovins, K., Dute, R., Sikora, E., Murphy, J.F., 1997. Pathway for phloem-dependent movement of *Pepper mottle potyvirus* in the stem of *Capsicum annuum*. *Phytopathol* 87, 892–98.
- Argueso, C.T., Ferreira, F.J., Epple, P., To, J.P., Hutchison, C.E., Schaller, G.E., Dangl, J.L., Kieber, J.J., 2012. Two-component elements mediate interactions between cytokinin and salicylic acid in plant immunity. *PLoS Genet* 8, e1002448.

- Ashby, J., Boutant, E., Seemanpillai, M., Groner, A., Sambade, A., Ritzenthaler, C., Heinlein, M., 2006. *Tobacco mosaic virus* movement protein functions as a structural microtubule-associated protein. *J Virol* 80, 8329–44.
- Autran, D., Baroux, C., Raissig, M.T., Lenormand, T., Wittig, M., Grob, S., Steimer, A., Barann, M., Klostermeier, U.C., Leblanc, O., Vielle-Calzada, J.P., Rosenstiel, P., Grimanelli, D., Grossniklaus, U., 2011. Maternal epigenetic pathways control parental contributions to Arabidopsis early embryogenesis. *Cell* 145, 707–719.
- Avina-Padilla, K., Martinez de la Vega, O., Rivera-Bustamante, R., Martinez-Soriano, J.P., Owens, R.A., Hammond, R.W., Vielle-Calzada, J.P., 2015. *In silico* prediction and validation of potential gene targets for pospiviroid-derived small RNAs during tomato infection. *Gene* 564, 197–205.
- Avisar, D., Prokhnevsky, A.I., Makarova, K.S., Koonin, E.V., Dolja, V.V., 2008. Myosin XI-K is required for rapid trafficking of golgi stacks, peroxisomes, and mitochondria in leaf cells of *Nicotiana benthamiana*. *Plant Physiol* 146, 1098–1108.
- Axtell, M.J., 2013. ShortStack: comprehensive annotation and quantification of small RNA genes. *RNA* 19, 740–751.
- Baksa, I., Nagy, T., Barta, E., Havelda, Z., Várallyay, É., Silhavy, D., József, B., Szittyá, G., 2015. Identification of *Nicotiana benthamiana* microRNAs and their targets using high throughput sequencing and degradome analysis. *BMC Genomics* 16, 1025.
- Baluska, F., Cvrcková, F., Kendrick-Jones J., Volkmann, D., 2001. Sink plasmodesmata as gateways for phloem unloading. Myosin VIII and calreticulin as molecular determinants of sink strength? *Plant Physiol* 126, 39–46.
- Baulcombe, D.C., 2004. RNA Silencing in plants. *Nature* 431, 356–63.
- Baumberger, N., Baulcombe, D.C., 2005. Arabidopsis ARGONAUTE 1 is an RNA Slicer that selectively recruits microRNAs and short interfering RNAs. *Proc Natl Acad Sci U S A* 102, 11928–11933.
- Beier, H., Barciszewska, M., Krupp, G., Mitnacht, R., Gross, H.J., 1984. UAG readthrough during TMV RNA translation: isolation and sequence of two tRNAs with suppressor activity from tobacco plants. *EMBO* 3, 351–56.
- Benitez-Alfonso, Y., Faulkner, C., Ritzenthaler, C., Maule, A.J., 2010. Plasmodesmata: gateways to local and systemic virus infection. *Mol Plant Microbe Interact* 23, 1403–12.
- Benitez-Alfonso, Y., Jackson, D., 2009. Redox homeostasis regulates plasmodesmal communication in Arabidopsis meristems. *Plant Signal Behav* 4, 655–59.
- Benitez-Alfonso, Y., Jackson, D., Maule, A., 2011. Redox regulation of intercellular transport. *Protoplasma* 248, 131–40.
- Bernstein, E., Caudy, A.A., Hammond, S.M., Hannon, G.J., 2001. Role for a bidentate ribonuclease in the initiation step of RNA interference. *Nature* 409, 363–366.
- Betti, C., Lico, C., Maffi, D., D’Angeli, S., Altamura, M.M., Benvenuto, E., Faoro, F., Baschieri, S., 2012. *Potato virus X* movement in *Nicotiana benthamiana*: new details revealed by chimeric coat protein variants. *Mol Plant Pathol* 13, 198–203.

- Bhattacharyya, S.N., Habermacher, R., Martine, U., Closs, E.I., Filipowicz, W., 2006. Relief of microRNA-mediated translational repression in human cells subjected to stress. *Cell* 125, 1111–1124.
- Blevins, T., Podicheti, R., Mishra, V., Marasco, M., Wang, J., Rusch, D., Tang, H., Pikaard, C.S., 2015. Identification of Pol IV and RDR2-dependent precursors of 24 nt siRNAs guiding *de novo* DNA methylation in Arabidopsis. *eLife* 4, 1-22.
- Blevins, T., Rajeswaran R., Shivaprasad, P.V., Beknazariants, D., Si-Ammour A., Park, H.S., Vazquez F., Robertson, D., Meins F., Hohn T., Pooggin, M.M., 2006. Four plant dicers mediate viral small RNA biogenesis and DNA virus induced silencing. *Nucleic Acids Res* 34, 6233-6246.
- Blevins, T., Rajeswaran, R., Aregger, M., Borah, B.K., Schepetilnikov, M., Baerlocher, L., Farinelli L., Meins F., Hohn T., and Pooggin M.M., 2011. Massive production of small RNAs from a non-coding region of *Cauliflower mosaic virus* in plant defense and viral counter-defense. *N.A.R* 39, 5003–14.
- Boevink, P., Oparka, K., Cruz, S.S., Martin, B., Betteridge, A., Hawes, C., 1998. Stacks on tracks: the plant golgi apparatus traffics on an actin/ER network. *Plant J* 15, 441–47.
- Bologna, N.G., Voinnet, O., 2014. The diversity, biogenesis, and activities of endogenous silencing small RNAs in Arabidopsis. *Annu Rev Plant Biol* 65, 473-503.
- Bolwell, G., Bindschedler, P.L.V., Blee, K.A., Butt, V.S., Davies, D.S., Gardner, S.L., Gerrish, C., Minibayeva, F., 2002. The apoplastic oxidative burst in response to biotic stress in plants: a three-component system. *J Exp Bot* 53, 1367–76.
- Borges, F., Martienssen, R.A., 2015. The expanding world of small RNAs in plants. *Nat Rev Mol Cell Biol* 16, 727–741.
- Botha, C.E.J., Aoki, N., Scofield, G.N., Liu, L., Furbank, R.T., White, R.G., 2008. A xylem sap retrieval pathway in Rice leaf blades: evidence of a role for endocytosis? *J Exp Bot* 59, 2945–54.
- Bouché, N., Laressergues, D., Gascioli, V., Vaucheret, H., 2006. An antagonistic function for Arabidopsis DCL2 in development and a new function for DCL4 in generating viral siRNAs. *EMBO J* 25, 3347-3356.
- Boyko, A., Kathiria, P., Zemp, F.J., Yao, Y., Pogribny, I., Kovalchuk, I., 2007. Transgenerational changes in the genome stability and methylation in pathogen-infected plants: virus-induced plant genome instability. *Nucleic Acids Res* 35, 1714–25.
- Boyko, V., Ferralli, J., Ashby, J., Schellenbaum, P., Heinlein M., 2000a. Function of microtubules in intercellular transport of plant virus RNA. *Nat Cell Biol* 2, 826–32.
- Boyko, V., Ferralli, J., Heinlein, M., 2000b. Cell-to-cell movement of TMV RNA is temperature-dependent and corresponds to the association of movement protein with microtubules. *Plant J* 22, 315-325.
- Brodersen, P., Sakvarelidze-Achard, L., Bruun-Rasmussen, M., Dunoyer, P., Yamamoto, Y.Y., Sieburth, L., Voinnet, O., 2008. Widespread translational inhibition by plant miRNAs and siRNAs. *Science* 320, 1185–1190.
- Brosnan, C.A., Mitter, N., Christie, M., Smith, N.A., Waterhouse, P. M., Carroll, B. J., 2007. Nuclear gene silencing directs reception of long-distance mRNA silencing in Arabidopsis. *Proc Natl Acad Sci U S A* 104, 14741–46.

- Brosnan, C.A., Voinnet, O., 2011. Cell-to-cell and long-distance siRNA movement in plants: mechanisms and biological implications. *Curr Opin Plant Biol* 14, 580–587.
- Brosseau, C., Moffett, P., 2015. Functional and genetic analysis identify a role for Arabidopsis ARGONAUTE 5 in antiviral RNA silencing. *Plant Cell* 27, 1742–1754.
- Brunkard, J.O., Zambryski, P.C., 2017. Plasmodesmata enable multicellularity: new insights into their evolution, biogenesis, and functions in development and immunity. *Curr Opin Plant Biol* 35, 76–83.
- Bucher, G.L., Tarina, C., Heinlein, M., Serio, F.D., Meins, F., Iglesias, V.A., 2001. Local expression of enzymatically active class I β -1, 3-Glucanase enhances symptoms of TMV infection in tobacco. *Plant J* 28, 361–69.
- Buhtz, A., Springer, F., Chappell, L., Baulcombe, D.C., Kehr, J., 2008. Identification and characterization of small RNAs from the phloem of *Brassica napus*. *Plant J* 53, 739–49.
- Cai, L., Chen, K., Zhang, X., Yan, L., Hou, M., Xu, Z., 2009. Biological and molecular characterization of a crucifer tobamovirus infecting oilseed rape. *Bio Gen* 47, 451–61.
- Calil, L.P., Fontes, E.P.B., 2017. Plant immunity against viruses: antiviral immune receptors in focus. *Anna Bot* 119, 711–23.
- Cantrill, L.C., Overall, R.L., Goodwin, P.B., 1999. Cell-to-cell communication via plant endomembranes. *Cell Biol* 23, 653–61.
- Cao, M., Du, P., Wang, X., Yu, Y.Q., Qiu, Y.H., Li, W., Gal-On, A., Zhou, C., Li, Y., Ding, S.W., 2014a. Virus infection triggers widespread silencing of host genes by a distinct class of endogenous siRNAs in Arabidopsis. *Proc Natl Acad Sci U S A* 111, 14613–14618.
- Cao, X., Wu, Z., Jiang, F., Zhou, R., Yang, Z., 2014b. Identification of chilling stress-responsive tomato microRNAs and their target genes by high-throughput sequencing and degradome analysis. *BMC Genomics* 15, 1–16.
- Carbonell, A., Carrington, J.C., 2015. Antiviral roles of plant ARGONAUTES. *Curr Opin Plant Biol* 27, 111–17.
- Carbonell, A., Fahlgren, N., Garcia-Ruiz, H., Gilbert, K.B., Montgomery, T.A., Nguyen, T., Cuperus, J.T., Carrington, J.C., 2012. Functional analysis of three Arabidopsis ARGONAUTES using slicer-defective mutants. *Plant Cell* 24, 3613–3629.
- Carmell, M.A., Xuan, Z., Zhang, M.Q., Hannon, G.J., 2002. The Argonaute family: tentacles that reach into RNAi, developmental control, stem cell maintenance, and tumorigenesis. *Gen Dev* 16, 2733–2742.
- Carrington, J.C., Freed, D.D., Sanders, T.C., 1989. Autocatalytic processing of the potyvirus Helper component proteinase in *Escherichia coli* and *in vitro*. *J Virol* 63, 4459–63.
- Carrington, J.C., Whitham, S.A., 1998. Viral invasion and host defense: strategies and counter-strategies. *Curr Opin Plant Biol* 1, 336–41.
- Carviel, J.L., Wilson, D.C., Isaacs, M., Carella, P., Catana, V., Golding, B., Weretilnyk, E.A., Cameron, R.K., 2014. Investigation of intercellular salicylic acid accumulation during compatible and incompatible Arabidopsis-*Pseudomonas syringae* interactions using a fast neutron-generated mutant allele of EDS5 identified by genetic mapping and whole-genome sequencing. *PLoS One* 9, e88608.

- Chalhoub, B., Denoeud, F., Liu, S., Parkin, I.A., Tang, H., Wang, X., Chiquet, J., Belcram, H., Tong, C., Samans, B., Correa, M., Da Silva, C., Just, J., Falentin, C., Koh, C.S., Le Clainche, I., Bernard, M., Bento, P., Noel, B., Labadie, K., Alberti, A., Charles, M., Arnaud, D., Guo, H., Daviaud, C., Alamery, S., Jabbari, K., Zhao, M., Edger, P.P., Chelaifa, H., Tack, D., Lassalle, G., Mestiri, I., Schnel, N., Le Paslier, M.C., Fan, G., Renault, V., Bayer, P.E., Golicz, A.A., Manoli, S., Lee, T.H., Thi, V.H., Chalabi, S., Hu, Q., Fan, C., Tollenaere, R., Lu, Y., Battail, C., Shen, J., Sidebottom, C.H., Wang, X., Canaguier, A., Chauveau, A., Berard, A., Deniot, G., Guan, M., Liu, Z., Sun, F., Lim, Y.P., Lyons, E., Town, C.D., Bancroft, I., Wang, X., Meng, J., Ma, J., Pires, J.C., King, G.J., Brunel, D., Delourme, R., Renard, M., Aury, J.M., Adams, K.L., Batley, J., Snowdon, R.J., Tost, J., Edwards, D., Zhou, Y., Hua, W., Sharpe, A.G., Paterson, A.H., Guan, C., Wincker, P., 2014. Plant genetics. Early allopolyploid evolution in the post-neolithic *Brassica napus* oilseed genome. *Science* 345, 950-953.
- Chapman, E.J., Carrington, J.C., 2007. Specialization and evolution of endogenous small RNA pathways. *Nat Rev Genet* 8, 884–896.
- Chen, H.M., Li, Y.H., Wu, S.H., 2007. Bioinformatic prediction and experimental validation of a microRNA-directed tandem trans-acting siRNA cascade in Arabidopsis. *Proc Natl Acad Sci U S A* 104, 3318–3323.
- Chen, S.M., Takiff, H.E., Barber, A.M., Dubois, G.C., Bardwell, J.C.A., Cout, D.L., 1990. Expression and characterization of RNase III and Era proteins. *J Bio Chem* 265, 2888.
- Cheng Y., Lazarowitz, S.G., Citovskya, V., 2018. The plasmodesmal localization signal of TMV MP is recognized by plant synaptotagmin SYTA. *MBIO* 9, 1–8.
- Cheval, C., Faulkner, C., 2018. Plasmodesmal regulation during plant–pathogen interactions. *New Phytol* 217, 62–67.
- Choi, J., Huh, S.U., Kojima, M., Sakakibara, H., Paek, K.H., Hwang, I., 2010. The cytokinin-activated transcription factor ARR2 promotes plant immunity via TGA3/NPR1-dependent salicylic acid signaling in Arabidopsis. *Dev Cell* 19, 284-295.
- Christensen, N., Tilsner, J., Bell, K., Hammann, P., Parton, R., Lacomme, C., Oparka, K., 2009. The 5' cap of *Tobacco mosaic virus* (TMV) is required for virion attachment to the actin/endoplasmic reticulum network during early infection. *Traffic* 10, 536–51.
- Chu, M., Desvoyes, B., Turina, M., Noad, R., Scholthof, H.B., 2000. Genetic dissection of *Tomato bushy stunt virus* P19-protein-mediated host-dependent symptom induction and systemic invasion. *Virology* 266, 79–87.
- Cotton, S., Grangeon, R., Thivierge, K., Mathieu, I., Ide, C., Wei, T., Wang, A., Laliberte, J.F., 2009. *Turnip mosaic virus* RNA replication complex vesicles are mobile, align with microfilaments, and are each derived from a single viral genome. *J Virol* 83, 10460–71.
- Covey, S.N., Al-Kaff, N.S., Langara, A., Turner, D.S., 1997. Plants combat infection by gene silencing. *Nature* 385, 781–82.
- Cox, J. E., Sullivan, C.S., 2014. Balance and stealth: the role of noncoding RNAs in the regulation of virus gene expression. *Annu Rev Virol* 1, 89–109.
- Csorba, T., Bovi, A., Dalmay, T., Burgyan, J., 2007. The p122 subunit of *Tobacco mosaic virus* replicase is a potent silencing suppressor and compromises both small interfering RNA- and microRNA-mediated pathways. *J Virol* 81, 11768–80.

- Csorba, T., Kontra, L., Burgyan, J., 2015. Viral silencing suppressors: tools forged to fine-tune host-pathogen coexistence. *Virology* 479–480, 85–103.
- Cui, X., Wei, T., Chowda-Reddy, R.V., Sun, G., Wang, A., 2010. The Tobacco etch virus P3 protein forms mobile inclusions via the early secretory pathway and traffics along actin microfilaments. *Virology* 397, 56–63.
- Dalmay, T., Hamilton, A., Rudd, S., Angell, S., Baulcombe, D.C., 2000. An RNA-dependent RNA polymerase gene in Arabidopsis is required for posttranscriptional gene silencing mediated by a transgene but not by a virus. *Cell* 101, 543–553.
- De Storme, N., Geelen, D., 2014. Callose homeostasis at plasmodesmata: molecular regulators and developmental relevance. *Front Plant Sci* 5, 1–24.
- De Vleeschauwer, D., Xu, J., Höfte, M., 2014. Making sense of hormone-mediated defense networking: from Rice to Arabidopsis. *Front Plant Sci* 5, 1–15.
- Del Toro, F.J., Donaire, L., Aguilar, E., Chung, B.N., Tenllado, F., Canto, T., 2017. *Potato virus Y* Hcpro suppression of antiviral silencing in *Nicotiana benthamiana* plants correlates with its ability to bind *in vivo* to 21- and 22-nucleotide smallRNAs of viral sequence. *J Virol* 91, e00367-17.
- Deleris, A., Gallego-Bartolome, J., Bao, J., Kasschau, K.D., Carrington, J.C., Voinnet, O., 2006. Hierarchical action and inhibition of plant Dicer-like proteins in antiviral defense. *Science* 313, 68-71.
- Deom, C.M., Oliver, M.J., Beachy, R.N., 1987. The 30-kilodalton gene product of *Tobacco mosaic virus* potentiates virus movement. *Science* 237, 389–93.
- Derrien, B., Baumberger, N., Schepetilnikov, M., Viotti, C., De Cillia, J., Ziegler-Graff, V., Isonoc, E., Schumacher, K., Genschik, P., 2012. Degradation of the antiviral component ARGONAUTE 1 by the autophagy pathway. *Proc Natl Acad Sci U S A* 109, 15942–15946.
- Ding, B., Turgeon, R., Parthasarathy, M.V., 1992. Substructure of freeze-substituted plasmodesmata. *Protoplasma* 169, 28–41.
- Ding, S.W., Voinnet, O., 2007. Antiviral immunity directed by small RNAs. *Cell* 130, 413-426.
- Ding, X.S., Boydston, C.M., Nelson, R.S., 2001. Presence of *Brome mosaic virus* in Barley guttation fluid and its association with localized cell death response. *Phytopatho* 91, 440–48.
- Ding, X.S., Liu, J., Cheng, N.H., Folimonov, A., Hou, Y.M., Bao, Y., Katagi, C., Carter, C., Nelson, R., 2004. The *Tobacco mosaic virus* 126-kDa protein associated with virus replication and movement suppresses RNA silencing. *Mol Plant Microbe Interact* 17, 583–92.
- Dodds, P.N., Rathjen, J.P., 2010. Plant immunity: towards an integrated view of plant-pathogen interactions. *Nat Rev Genet* 11, 539-548.
- Dolja, V.V., Haldeman, R., Montgomery, A.E., Vandenbosch, K.A., Carrington, J.C., 1995. Capsid protein determinants involved in cell-to-cell and long distance movement of *Tobacco etch potyvirus*. *Virology* 206, 1007–16.
- Dolja, V.V., Haldeman, R., Robertson, N.L., Dougherty, W.G., Carrington, J.C., 1994. Distinct functions of capsid protein in assembly and movement of *Tobacco etch virus*. *EMBO* 13, 1482–91.

- Donaire, L., Barajas, D., Martinez-Garcia, B., Martinez-Priego, L., Pagan, I., Llave, C., 2008. Structural and genetic requirements for the biogenesis of *Tobacco rattle virus*-derived small interfering RNAs. *J Virol* 82, 5167–5177.
- Dunigan, D.D., Dietzgen, R.G., Schoelz, J.E., Zaitlin, M., 1988. *Tobacco mosaic virus* particles contain ubiquitinated coat protein subunits 312, 310–12.
- Dunoyer, P., Himber C., Ruiz-Ferrer, V., Alioua, A., Voinnet, O., 2007. Intra- and intercellular RNA interference in *Arabidopsis thaliana* requires components of the microRNA and heterochromatic silencing pathways. *Nature Gen* 39, 848–56.
- Dunoyer, P., Thomas, C., Harrison, S., Revers, F., Maule, A., 2004. A cysteine-rich plant protein potentiates Potyvirus movement through an interaction with the virus genome-linked protein VPg. *J Virol* 78, 2301-2309.
- Duque, P., 2011. A role for SR proteins in plant stress responses. *Plant Signal Behav* 6, 49-54.
- Eamens, A., Vaistij, F.E, Jones, L., 2008. NRPD1a and NRPD1b are required to maintain post-transcriptional RNA silencing and RNA-directed DNA methylation in *Arabidopsis*. *Plant J.* 55, 596–606.
- Edwardson, J.R., Christie, R.G., 1991. The potyvirus group. *Florida Agri Exp Stat Mono.* Vol. 16.
- Eitas, T.K., Nimchuk, Z.L., Dangl, J.L., 2008. *Arabidopsis* TAO1 is a TIR-NB-LRR protein that contributes to disease resistance induced by the *Pseudomonas syringae* effector AvrB. *Proc Natl Acad Sci U S A* 105, 6475-6480.
- El-Shami, M., Pontier, D., Lahmy, S., Braun, L., Picart, C., Vega, D., Hakimi, M.A., Jacobsen, S.E., Cooke, R., Lagrange, T., 2007. Reiterated WG/GW motifs form functionally and evolutionarily conserved ARGONAUTE-binding platforms in RNAi-related components. *Gen Dev*, 21, 2539–2544.
- Ernst, R., Claessen, J.H., Mueller, B., Sanyal, S., Spooner, E., Van Der Veen, A.G., Kirak, O., Schlieker, C.D., Weihofen, W.A., Ploegh, H.L., 2011. Enzymatic blockade of the ubiquitin-proteasome pathway. *PLoS Biol* 8, e1000605.
- Fang, X., Qi, Y., 2016. RNAi in plants: an argonaute-centered view. *Plant Cell* 28, 272–285.
- Fei, Q., Xia, R., Meyers, B.C., 2013. Phased, secondary, small interfering RNAs in posttranscriptional regulatory networks. *Plant Cell* 25, 2400-2415.
- Fellers, J., Wan, J., Hong, Y., Collins, G.B., Hunt, A.G., 1998. In vitro interactions between a potyvirus-encoded, genome-linked protein and RNA-dependent RNA polymerase. *J Gen Virol* 79, 2043–49.
- Fernandez-Busnadiego, R., Saheki, Y., De Camilli, P., 2015. Three-dimensional architecture of extended synaptotagmin-mediated endoplasmic reticulum-plasma membrane contact sites. *Proc Natl Acad Sci U S A* 112, E2004-13.
- Ferralli, J., Ashby, J., Fasler, M., Boyko, V., Heinlein, M., 2006. Disruption of microtubule organization and centrosome function by expression of *Tobacco mosaic virus* movement protein. *J Virol* 80, 5807–21.
- Folkes, L., Moxon, S., Woolfenden, H.C., Stocks, M.B., Szitty, G., Dalmay, T., Moulton, V., 2012. PAREsnip: a tool for rapid genome-wide discovery of small RNA/target interactions evidenced through degradome sequencing. *Nucleic Acids Res* 40, e103.

- Foreman, J., Demidchik, V., Bothwell, J.H., Mylona, P., Miedema, H., Torres, M.A., Linstead, P., Costa, S., Brownlee, C., Jones, J.D., Davies, J.M., Dolan, L., 2003. Reactive oxygen species produced by NADPH oxidase regulate plant cell growth. *Nature* 422, 442–46.
- French, C.J., Elder, M., 1999. Virus particles in guttate and xylem of infected Cucumber (*Cucumis sativus* L.). *Ann Appl Biol* 134, 81–87.
- Fu, M., Xu, M., Zhou, T., Wang, D., Tian, S., Han, L., Dong, H., Zhang, C., 2014. Transgenic expression of a functional fragment of harpin protein Hpa1 in wheat induces the phloem-based defence against English grain aphid. *J Exp Bot* 65, 1439–1453.
- Fujiki, M., Kawakami, S., Kim, R.W., Beachy, R.N., 2006. Domains of *Tobacco mosaic virus* movement protein essential for its membrane association. *J Gen Virol* 87, 2699–2707.
- Fukuda, M., Meshi, T., Okada, Y., Otsuki, Y., Takene, I., 1981. Correlation between particle multiplicity and location on virion RNA of the assembly initiation site for viruses of the *Tobacco mosaic virus* Group 78, 4231–35.
- Galopier, A., Hermann-Le Denmat, S., 2011. Mitochondria of the yeasts *Saccharomyces cerevisiae* and *Kluyveromyces lactis* contain nuclear rDNA-encoded proteins. *PLoS One* 6, e16325.
- Gao, Z., Liu, H.L., Daxinger, L., Pontes, O., He, X., Qian, W., Lin, H., Xie, M., Lorkovic, Z.J., Zhang, S., Miki, D., Zhan, X., Pontier, D., Lagrange, T., Jin, H., Matzke, A.J.M., Matzke, M., Pikaard, C.S., Zhu J.K., 2010. An RNA polymerase II-and AGO4-associated protein acts in RNA-directed DNA methylation. *Nature* 465, 106–9.
- Garcia-Arenal, F., McDonald, B.A., 2003. An analysis of the durability of resistance to plant viruses. *Phytopathology* 93, 941–952.
- Garcia-Ruiz, H., Carbonell, A., Hoyer, J.S., Fahlgren, N., Gilbert, K.B., Takeda, A., Giampetruzzi, A., Garcia Ruiz, M.T., McGinn, M.G., Lowery, N., Martinez Baladejo, M.T., Carrington, J.C., 2015. Roles and programming of Arabidopsis ARGONAUTE proteins during *Turnip mosaic virus* infection. *PLoS Pathog* 11, e1004755.
- Gascioli, V., Mallory, A.C., Bartel, D.P., Vaucheret, H., 2005. Partially redundant functions of Arabidopsis DICER-like enzymes and a role for DCL4 in producing trans-acting siRNAs. *Curr Biol* 15, 1494–1500.
- German, M.A., Luo, S., Schroth, G., Meyers, B.C., Green, P.J., 2009. Construction of Parallel Analysis of RNA Ends (PARE) libraries for the study of cleaved miRNA targets and the RNA degradome. *Nat Protoc* 4, 356–362.
- Ghoshal, B., Sanfacon, H., 2014. Temperature-dependent symptom recovery in *Nicotiana benthamiana* plants infected with *Tomato ringspot virus* is associated with reduced translation of viral RNA2 and requires ARGONAUTE 1." *Virology* 456, 188–97.
- Ghoshal, B., Sanfacon, H., 2015. Symptom recovery in virus-infected plants: revisiting the role of RNA silencing mechanisms. *Virology* 479, 167–79.
- Gibbs, A., 1986. Tobamovirus classification. *Plant Viruses, The Rod-Shaped Plant Viruses* 2, 167–80.
- Glazov, E., Phillips, K., Budziszewski, G.J., Meins, F., Levin, J.Z., 2003. A gene encoding an RNase D exonuclease-like protein is required for post-transcriptional silencing in Arabidopsis. *Plant J.* 35, 342–49.

- Golomb, L., Abu-Abied, M., Belausov, E., Sadot, E., 2008. Different subcellular localizations and functions of Arabidopsis myosin VIII. *BMC Plant Biol* 8, 3.
- Gottwein, E., Mukherjee, N., Sachse, C., Frenzel, C., Majoros, W.H., Chi, J.T., Braich, R., Manoharan, M., Soutschek, J., Ohler, U., Cullen, B.R., 2007. A viral microRNA functions as an orthologue of cellular miR-155. *Nature* 450, 1096–1099.
- Gouveia, B.C., Calil, L.P., Machado, J.P.B., Santos, A.A, Fontes, E.P.B., 2017. Immune receptors and co-receptors in antiviral innate immunity in plants. *Front Microbiol* 7, 1–14.
- Grangeon, R., Agbeci, M., Chen, J., Grondin, G., Zheng, H., Laliberte, J.F., 2012. Impact on the endoplasmic reticulum and golgi apparatus of *Turnip mosaic virus* infection. *J Virol* 86, 9255–65.
- Grangeon, R., Jiang, J., Wan, J., Agbeci, M., Zheng, H., Laliberte, J.F., 2013. 6K2-induced vesicles can move cell to cell during *Turnip mosaic virus* infection. *Front Microbiol* 4, 351.
- Griffing, L.R., Lin, C., Perico, C., White, R.R., Sparkes, I., 2017. Plant ER geometry and dynamics: biophysical and cytoskeletal control during growth and biotic response. *Protoplasma* 254, 43–56.
- Griffiths-Jones, S., 2004. The microRNA registry. *Nucleic Acids Res* 32, 109–111.
- Griffiths-Jones, S., Grocock, R.J., Dongen, S.V., Bateman, A., Enright, A.J., 2006. miRBase: microRNA sequences, targets and gene nomenclature. *Curr Prot Bioinformatics* 34, 1291–12910.
- Griffiths-Jones, S., Saini, H.K., Van Dongen, S., Enright, A.J., 2008. miRBase: Tools for microRNA genomics. *Nucleic Acids Res* 36, 154–158.
- Grisson, M.S., Brocard, L., Fouillen, L., Nicolas, W., Wewer, V., Dörmann, P., Nacir, H., Benitez-Alfonso, Y., Claverol, S., Germain, V., Boutté, Y., Mongrand, S., Bayer, E.M., 2015. Specific membrane lipid composition is important for plasmodesmata function in Arabidopsis. *Plant Cell* 27, 1228–50.
- Guenoune-Gelbart, D., Elbaum, M., Sagi, G., Levy, A., Epel, B.L., 2008. *Tobacco mosaic virus* (TMV) replicase and movement protein function synergistically in facilitating TMV spread by lateral diffusion in the plasmodesmal desmotubule of *Nicotiana benthamiana*. *Mol Plant Microbe Interact* 21, 335–45.
- Gui, J., Liu, C., Shen, J., Li, L., 2014. Grain setting defect1, encoding a remorin protein, affects the grain setting in Rice through regulating plasmodesmatal conductance. *Plant Physiol* 166, 1463–78.
- Hafren, A., Hofius, D., 2017. NBR1-mediated antiviral xenophagy in plant immunity. *Autophagy* 13, 2000–2001.
- Hafren, A., Macia, J.L., Love, A.J., Milner, J.J., Drucker, M., Hofius, D., 2017. Selective autophagy limits *Cauliflower mosaic virus* infection by NBR1-mediated targeting of viral capsid protein and particles. *Proc Natl Acad Sci U S A* 114, E2026–E2035.
- Hafren, A., Ustun, S., Hochmuth, A., Svenning, S., Johansen, T., Hofius, D., 2018. *Turnip mosaic virus* counteracts selective autophagy of the viral silencing suppressor HCpro. *Plant Physiol* 176, 649–662.
- Haldeman-Cahill, R., Daros, J.A., Carrington, J.C., 1998. Secondary structures in the capsid protein coding sequence and 3' nontranslated region involved in amplification of the *Tobacco etch virus* genome. *J Virol* 72, 4072–9.
- Hammond, S.M., Bernstein, E., Beach, D., Hannon, G.J., 2000. An RNA-directed nuclease mediates post-transcriptional gene silencing in *Drosophila* cells. *Nature* 404, 293–296.

- Hanhart, P., Thieß, M., Amari, K., Bajdzienko, K., Giavalisco, P., Heinlein, M., Kehr, J., 2017. Bioinformatic and expression analysis of the *Brassica napus* L. cyclophilins. *Sci Rep* 7, 1514
- Han, J., Lühs, W., Sonntag, K., Zähringer, U., Borchardt, D.S., Wolter, F.P., Heinz, E., Frentzen, M., 2001. Functional characterization of beta-ketoacyl-CoA synthase genes from *Brassica napus* L. *Plant Mol Biol* 46, 229-39.
- Haraguchi, T., Tominaga, M., Matsumoto, R., Sato, K., Nakano, A., Yamamoto, K., Ito, K., 2014. Molecular characterization and subcellular localization of Arabidopsis class VIII myosin, ATM1. *J Biol Chem* 289, 12343–55.
- Harries, P.A., Park, J.W., Sasaki, N., Ballard, K.D., Maule, A.J., Nelson, R.S., 2009. Differing requirements for actin and myosin by plant viruses for sustained intercellular movement. *Proc Natl Acad Sci U S A* 106, 17594–99.
- Harvey, J.J., Lewsey, M.G., Patel, K., Westwood, J., Heimstadt, S., Carr, J.P., Baulcombe, D.C., 2011. An antiviral defense role of AGO2 in plants. *PLoS One* 6, e14639.
- Havecker, E.R., Wallbridge, L.M., Hardcastle, T.J., Bush, M.S., Kelly, K.A., Dunn, R.M., Schwach, F., Doonan, J.H., Baulcombe, D.C., 2010. The Arabidopsis RNA-directed DNA methylation argonautes functionally diverge based on their expression and interaction with target loci. *Plant Cell* 22, 321–34.
- Heinlein, M., 2002. Plasmodesmata: dynamic regulation and role in macromolecular cell-to-cell signaling. *Curr Opin Plant Biol* 5, 543–52.
- Heinlein, M., 2015a. Plant virus replication and movement. *Virology* 479, 657–71.
- Heinlein, M., Epel, B.L., 2004. Macromolecular transport and signaling through plasmodesmata. *Rev Cyto* 235, 93–164.
- Heinlein, M., Epel, B.L., Padgett, H.S., Beachy, R.N., 1995. Interaction of tobamovirus movement proteins with the plant cytoskeleton. *Science* 270, 1983–85.
- Heinlein, M., Wood, M.R., Thiel, T., Beachy, R.N., 1998. Targeting and modification of prokaryotic cell-cell junctions by *Tobacco mosaic virus* cell-to-cell movement protein. *Plant J* 14, 345–51.
- Henderson, I.R., Zhang, X., Lu, C., Johnson, L., Meyers, B.C., Green, P.J., Jacobsen, S.E. 2006. Dissecting *Arabidopsis thaliana* DICER function in small RNA processing, gene silencing and DNA methylation patterning. *Nature Gen* 38, 721–725.
- Hermann, M., Maier, F., Masroor, A., Hirth, S., Pfitzner, A.J., Pfitzner, U.M., 2013. The Arabidopsis NIMIN proteins affect NPR1 differentially. *Front Plant Sci* 4, 88.
- Hilf, M.E., Dawson, W.O., 1993. The tobamovirus capsid protein functions as a host-specific determinant of long-distance movement. *Virology* 193, 106-114.
- Himber, C., Dunoyer, P., Moissiard, G., Ritzenthaler, C., Voinnet, O., 2003. Transitivity-dependent and -independent cell-to-cell movement of RNA Silencing." *EMBO* 22, 4523–33.
- Hofmann, C., Niehl, A., Sambade, A., Steinmetz, A., Heinlein, M., 2009. Inhibition of TMV movement by expression of an actin-binding protein. *Plant Physiol* 149, 1810–23.

- Holt, C.A., Beachy, R.N., 1991. *In vivo* complementation of infectious transcripts *Tobacco mosaic virus* cDNAs in transgenic from mutant plants. *Virology* 181, 109–17.
- Hook, L., Hancock, M., Landais, I., Grabski, R., Britt, W., Nelson, J.A., 2014. Cytomegalovirus microRNAs. *Curr Opin Virol* 7, 40-46.
- Hormuzdi, S.G., Bisaro, D.M., 1995. Genetic analysis of *Beet curly top virus*: examination of the roles of L2 and L3 genes in viral pathogenesis. *Virology* 206, 1044–54.
- Hosford, R.M., 1967. Transmission of plant viruses by Dodder 33, 387–406.
- Howell, M.D., Fahlgren, N., Chapman, E.J., Cumbie, J.S., Sullivan, C.M., Givan, S.A., Kasschau, K.D., Carrington, J.C., 2007. Genome-wide analysis of the RNA-DEPENDENT RNA POLYMERASE6/DICER-LIKE4 pathway in *Arabidopsis* reveals dependency on miRNA- and tasiRNA-directed targeting. *Plant Cell* 19, 926–942.
- Hu, Q., Hollunder, J., Niehl, A., Kørner, C.J., Gereige, D., Windels, D., Arnold, A., Kuiper, M., Vazquez, F., Pooggin, M.M., Heinlein, M., 2011. Specific impact of tobamovirus infection on the *Arabidopsis* small RNA profile. *PLoS One* 6, e19549.
- Huang, J., Yang, M., Lu, L., Zhang, X., 2016. Diverse functions of small RNAs in different plant-pathogen communications. *Front Microbiol* 7, 1552.
- Hull, R., 2009. *Comparative Plant Virology*. Elsevier 31, 70-76.
- Hull, R., 2014. Symptoms and Host Range. *Plant Virol* 5, 145-198.
- Iglesias, V.A., Meins, F., 2000. Movement of plant viruses is delayed in a β -1,3-Glucanase-deficient mutant showing a reduced plasmodesmatal size exclusion limit and enhanced callose deposition. *Plant J* 21, 157–66.
- Imlau, A., 1999. Cell-to-cell and long-distance trafficking of the green fluorescent protein in the phloem and symplastic unloading of the protein into sink tissues. *Plant Cell* 11, 309–22.
- Ishibashi, K., Nishikiori, M., Ishikawa, M., 2010. Interactions between tobamovirus replication proteins and cellular factors: their impacts on virus multiplication. *Mol Plant Microbe Interact* 23, 1413–19.
- Ishihara, T., Sekine, K.T., Hase, S., Kanayama, Y., Seo, S., Ohashi, Y., Kusano, T., Shibata, D., Shah, J., Takahashi, H., 2008. Overexpression of the *Arabidopsis thaliana* EDS5 gene enhances resistance to viruses. *Plant Biol* 10, 451-461.
- Ishikawa, K., Tamura, K., Ueda, H., Ito, Y., Nakano, A., Hara-Nishimura, I., Shimada T., 2018. Synaptotagmin-associated endoplasmic reticulum–plasma membrane contact sites are localized to immobile ER tubules. pp.00498.2018.
- Ivanov, K.I., Eskelin, K., Löhmus, A., Mäkinen, K., 2014. Molecular and cellular mechanisms underlying potyvirus infection. *J Gen Virol* 95, 1415–29.
- Jagadeeswaran, G., Raina, S., Acharya, B.R., Maqbool, S.B., Mosher, S.L., Appel, H.M., Schultz, J.C., Klessig, D.F., Raina, R., 2007. *Arabidopsis* GH3-LIKE DEFENSE GENE 1 is required for accumulation of salicylic acid, activation of defense responses and resistance to *Pseudomonas syringae*. *Plant J* 51, 234-246.

- Jay, F., Wang, Y., Yu, A., Taconnat, L., Pelletier, S., Colot, V., Renou, J.P., Voinnet, O., 2011. Misregulation of AUXIN RESPONSE FACTOR 8 underlies the developmental abnormalities caused by three distinct viral silencing suppressors in Arabidopsis. *PLoS Pathog* 7, e1002035.
- Jeong, S., 2017. SR proteins: binders, regulators, and connectors of RNA. *Mol Cells* 40, 1-9.
- Jiang, J., Lv, M., Liang, Y., Ma, Z., Cao, J., 2014. Identification of novel and conserved miRNAs involved in pollen development in *Brassica campestris ssp. chinensis* by high-throughput sequencing and degradome analysis. *BMC Genomics* 15, 146.
- Jiang, J., Patarroyo, C., Cabanillas, D.G., Zheng, H., Laliberte, J.F., 2015. The vesicle-forming 6K2 protein of *Turnip mosaic virus* interacts with the COPII coatome Sec24a for viral systemic infection. *J Virol* 89, 6695–6710.
- Jones, J.D., Dangl, J.L., 2006. The plant immune system. *Nature* 444, 323-329.
- Jovel, J., Walker, M., Sanfacon, H., 2007. Recovery of *Nicotiana benthamiana* plants from a necrotic response induced by a Nepovirus is associated with RNA silencing but not with reduced virus titer. *J Virol* 81, 12285–97.
- Kakrana, A., Hammond, R., Patel, P., Nakano, M., Meyers, B.C., 2014. sPARTA: a parallelized pipeline for integrated analysis of plant miRNA and cleaved mRNA data sets, including new miRNA target-identification software. *Nucleic Acids Res* 42, e139.
- Kasschau, K.D., Xie, Z., Allen, E., Llave, C., Chapman, E.J., Krizan, K.A., Carrington, J.C., 2003. P1/Hc-Pro, a viral suppressor of RNA silencing, interferes with Arabidopsis development and miRNA function. *Dev Cell* 4, 205–217.
- Kawamura-Nagaya, K., Ishibashi, K., Huang, Y.P., Miyashita, S., Ishikawa, M., 2014. Replication protein of *Tobacco mosaic virus* cotranslationally binds the 5' untranslated region of genomic RNA to enable viral replication. *Proc Natl Acad Sci U S A* 111, E1620-E1628.
- Kenyon, L., Kumar, S., Tsai, W.S., Hughes, J.A., 2014. Virus diseases of Peppers (*Capsicum spp.*) and their control. *Adv Virus Res.* 90, 297-354.
- Kim, D., Pertea, G., Trapnell, C., Pimentel, H., Kelley, R., Salzberg, S.L., 2013. TopHat2: accurate alignment of transcriptomes in the presence of insertions, deletions and gene fusions. *Genome Biol* 14, R36.
- Kim, Y.K., Heo, I., Kim, V.N., 2010. Modifications of small RNAs and their associated proteins. *Cell* 143, 703–709.
- Kincaid, R.P., Burke, J.M., Sullivan, C.S., 2012. RNA virus microRNA that mimics a B-cell oncomiR. *Proc Natl Acad Sci U S A* 109, 3077–3082.
- Komiya, R., Ohyanagi, H., Niihama, M., Watanabe, T., Nakano, M., Kurata, N., Nonomura, K.I., 2014. Rice germline-specific Argonaute MEL1 protein binds to phasiRNAs generated from more than 700 lincRNAs. *Plant J* 78, 385–397.
- Kong, J., Wei, M., Li, G., Lei, R., Qiu, Y., Wang, C., Li, Z.H., Zhu, S., 2018. The *Cucumber mosaic virus* movement protein suppresses PAMP-triggered immune responses in Arabidopsis and tobacco. *Bio and Bioph Res Com* 498, 395–401.

- Kørner, C.J., Klauser, D., Niehl, A., Dominguez-Ferreras, A., Chinchilla, D., Boller, T., Heinlein, M., Hann, D.R., 2013. The immunity regulator BAK1 contributes to resistance against diverse RNA viruses. *Mol Plant Microbe Interact* 26, 1271–80.
- Kørner, C.J., Pitzalis, N., Peña E.J., Erhardt, M., Vazquez, F., Heinlein, M., 2018. Crosstalk between PTGS and TGS pathways in natural antiviral immunity and disease recovery. *Nature Plants* 4, 157–64.
- Kozomara, A., Griffiths-Jones, S., 2011. miRBase: integrating microRNA annotation and deep-sequencing data. *Nucleic Acids Res* 39, 152–157.
- Kozomara, A., Griffiths-Jones, S., 2014. miRBase: annotating high confidence microRNAs using deep sequencing data. *Nucleic Acids Res* 42, D68–73.
- Kragler, F., 2013. Plasmodesmata: intercellular tunnels facilitating transport of macromolecules in plants. *Cell Tissue Res* 352, 49–58.
- Kragler, F., Lucas, W.J., Monzer, J., 1998. Plasmodesmata: dynamics, domains and patterning. *Ann Bot* 81, 1–10.
- Kubota, K., Tsuda, S., Tamai, A., Meshi, T., 2003. *Tomato mosaic virus* replication protein suppresses virus-targeted posttranscriptional gene silencing. *J Virol* 77, 11016–26.
- Kurihara, Y., Watanabe, Y., 2004. From the cover: Arabidopsis micro-RNA biogenesis through Dicer-like 1 protein functions. *Proc Natl Acad Sci U S A* 101, 12753–12758.
- Laliberte, J.F., Zheng, H., 2014. Viral manipulation of plant host membranes. *Annu Rev Virol* 1, 237–59.
- Langmead, B., Salzberg, S.L., 2012. Fast gapped-read alignment with Bowtie 2. *Nat Methods* 9, 357–359.
- Lee, J.Y., 2014. New and old roles of plasmodesmata in immunity and parallels to tunneling nanotubes. *Plant Sci* 221, 13–20.
- Lee, J.Y., Lu, H., 2011. Plasmodesmata: the battleground against intruders. *Plant Sci* 16, 201–10.
- Lellis, A.D., Kasschau, K.D., Whitham, S.A., Carrington, J.C., 2002. Loss-of-susceptibility mutants of *Arabidopsis thaliana* reveal an essential role for eIF(iso)4E during potyvirus infection. *Curr Biol* 12, 1046–1051.
- Levy, A., Erlanger, M., Rosenthal, M., Epel, B.L., 2007. A plasmodesmata-associated β -1,3-Glucanase in Arabidopsis. *Plant J* 49, 669–82.
- Levy, A., Zheng, J.Y., Lazarowitz, S.G., 2015. Synaptotagmin SYTA forms ER-plasma membrane junctions that are recruited to plasmodesmata for plant virus movement. *Curr Biol* 25, 2018–25.
- Lewis, B.P., Burge, C.B., Bartel, D.P., 2005. Conserved seed pairing, often flanked by adenosines, indicates that thousands of human genes are microRNA targets. *Cell* 120, 15–20.
- Lewis, B.P., Shih, I.H., Jones-Rhoades, M.W., Bartel, D.P., Burge, C.B., 2003. Prediction of mammalian microRNA targets. *Cell* 115, 787–798.
- Lewis, J.D., Lazarowitz, S.G., 2010. Arabidopsis synaptotagmin SYTA regulates endocytosis and virus movement protein cell-to-cell transport. *Proc Natl Acad Sci U S A* 107, 2491–96.

- Lewis, J.D., Lee, A.H., Hassan, J.A., Wan, J., Hurley, B., Jhingree, J.R., Wang, P.W., Lo, T., Youn, J.Y., Guttman, D.S., Desveaux, D., 2013. The Arabidopsis ZED1 pseudokinase is required for ZAR1-mediated immunity induced by the *Pseudomonas syringae* type III effector HopZ1a. *Proc Natl Acad Sci U S A* 110, 18722-18727.
- Lewsey, M., Surette, M., Robertson, F.C., Ziebell, H., Choi, S.H., Ryu, K.H., Canto, T., Palukaitis, P., Payne, T., Walsh, J.A., Carr, J.P., 2009. The role of the *Cucumber mosaic virus* 2b protein in viral movement and symptom induction. *Mol Plant Microbe Interact* 22, 642–54.
- Lewsey, M.G., Hardcastle, T.J., Melnyk, C.W., Molnar, A., Valli, A., Urich, M.A., Nery, J.R., Baulcombe, D.C., Ecker, J.R., 2016. Mobile small RNAs regulate genome-wide DNA methylation. *Proc Natl Acad Sci U S A* 113, E801–E810.
- Li, H., Durbin, R., 2009. Fast and accurate short read alignment with Burrows-Wheeler transform. *Bioinformatics* 25, 1754-1760.
- Li, H., Handsaker, B., Wysoker, A., Fennell, T., Ruan, J., Homer, N., Marth, G., Abecasis, G., Durbin, R.S., 2009. Genome project data processing the sequence alignment/map format and SAMtools. *Bioinformatics* 25, 2078-2079.
- Li, J., Yang, Z., Yu, B., Liu, J., Chen, X., 2005. Methylation protects miRNAs and siRNAs from a 3'-end uridylation activity in Arabidopsis. *Curr Biol* 15, 1501–1507.
- Li, X.H., Valdez, P., Olvera, R.E., Carrington, J.C., 1997. Functions of the *Tobacco etch virus* RNA polymerase (NIb): subcellular transport and protein-protein interaction with VPg/Proteinase (NIa). *J Virol* 71, 1598–1607.
- Licausi, F., Ohme-Takagi, M., Perata, P., 2013. APETALA2/Ethylene Responsive Factor (AP2/ERF) transcription factors: mediators of stress responses and developmental programs. *New Phytol* 199, 639-649.
- Lindbo, J.A., Silva-Rosales, L., Proebsting, W.M., Dougherty, W.G., 1993. Induction of a highly specific antiviral state in transgenic plants: implications for regulation of gene expression and virus resistance. *Plant Cell* 5, 1749–59.
- Liou, M.R., Hu, C.C., Chou, Y.L., Chang, B.Y., Lin, N.S., Hsu, Y.H., 2015. Viral elements and host cellular proteins in intercellular movement of *Bamboo mosaic virus*. *Curr Opin Virol* 12, 99–108.
- Llave, C., Franco-Zorrilla, J.M., Solano, R., Barajas, D., 2011. Target validation of plant microRNAs. *Methods Mol Biol* 732, 187-208.
- Llave, C., Xie, Z., Kasschau, K.D., Carrington, J.C., 2002. Cleavage of Scarecrow-like mRNA targets directed by a class of Arabidopsis miRNA. *Science* 297, 2053-2056.
- Love, M.I., Huber, W., Anders, S., 2014. Moderated estimation of fold change and dispersion for RNA-seq data with DESeq2. *Genome Biol* 15, 550.
- Lozano, R., Ponce, O., Ramirez, M., Mostajo, N., Orjeda, G., 2012. Genome-wide identification and mapping of nbs-encoding resistance genes in *Solanum tuberosum* group Phureja. *PLoS ONE* 7, e34775
- Lu, H., Chandrasekar, B., Oeljeklaus, J., Misas-Villamil, J.C., Wang, Z., Shindo, T., Bogyo, M., Kaiser, M., van der Hoorn, R.A., 2015. Subfamily-specific fluorescent probes for cysteine proteases display dynamic protease activities during seed germination. *Plant Physiol* 168, 1462-1475.

- Lucas, W.J., 2006. Plant viral movement proteins: agents for cell-to-cell trafficking of viral genomes. *Virology* 344, 169–84.
- Lucas, W.J., Wolf, S., 1993. Plasmodesmata: the intercellular organelles of green plants. *Cell Biol* 3, 308–15.
- Lukasik, A., Pietrykowska, H., Paczek, L., Szweykowska-Kulinska, Z., Zielenkiewicz, P., 2013. High-throughput sequencing identification of novel and conserved miRNAs in the *Brassica oleracea* leaves. *BMC Genomics* 14, 801.
- Makeyev, E.V., Bamford, D.H., 2002. Cellular RNA-dependent RNA polymerase involved in posttranscriptional gene silencing has two distinct activity modes. *Mol Cell* 10, 1417–1427.
- Mallory, A., Vaucheret, H., 2010. Form, function, and regulation of ARGONAUTE proteins. *Plant Cell* 22, 3879–3889.
- Mallory, A.C., Hinze, A., Tucker, M.R., Bouche, N., Gascioli, V., Elmayan, T., Laussergues, D., Jauvion, V., Vaucheret, H., Laux, T., 2009. Redundant and specific roles of the ARGONAUTE proteins AGO1 and ZLL in development and small RNA-directed gene silencing. *PLoS Genet* 5, e1000646.
- Malpica-López N., Rajeswaran R., Beknazariants D., Seguin J., Golyaev V., Farinelli L., Pooggin M.M., 2018. Revisiting the roles of tobamovirus replicase complex proteins in viral replication and silencing suppression. *Mol Plant Microbe Interact* 31, 125-144.
- Manabayeva, S.A., Shamekova, M., Park, J.W., Ding, X.S., Nelson, R.S., Hsieh, Y.C., Omarov, R.T., Scholthof, H.B., 2013. Differential requirements for Tombusvirus coat protein and P19 in plants following leaf versus root inoculation. *Virology* 439, 89–96.
- Manavella, P.A., Koenig, D., Weigel, D., 2012. Plant secondary siRNA production determined by microRNA-duplex structure. *Proc Natl Acad Sci U S A* 109, 2461–2466.
- Margis, R., Fusaro, A.F., Smith, N.A., Curtin, S.J., Watson, J.M., Finnegan, E.J., Waterhouse, P.M., 2006. The evolution and diversification of Dicers in plants. *FEBS Letters* 580, 2442–2450.
- Martin-Hernandez, A.M., Baulcombe, D.C., 2008. *Tobacco rattle virus* 16-kilodalton protein encodes a suppressor of RNA silencing that allows transient viral entry in meristems. *J Virol* 82, 4064–71.
- Martin, M.T., Cervera, M.T., Garcia, J.A., 1995. Properties of the active *Plum pox potyvirus* RNA polymerase complex in defined glycerol gradient fractions. *Virus Res* 37, 127–37.
- Matzke, M., Kanno, T., Daxinger, L., Huettel, B., Matzke, A.J., 2009. RNA-mediated chromatin-based silencing in plants. *Curr Opin Plant Biol* 21, 367–376.
- McCue, A.D., Panda, K., Nuthikattu, S., Choudury, S.G., Thomas, E.N., Slotkin, R.K., 2015. ARGONAUTE 6 bridges transposable element mRNA-derived siRNAs to the establishment of DNA methylation. *The EMBO* 34, 20–35.
- McKenna, A., Hanna, M., Banks, E., Sivachenko, A., Cibulskis, K., Kernytsky, A., Garimella, K., Altshuler, D., Gabriel, S., Daly, M., DePristo, M.A., 2010. The Genome Analysis Toolkit: a MapReduce framework for analyzing next-generation DNA sequencing data. *Genome Res* 20, 1297-1303.
- Melcher, U. 2003. *Turnip vein-clearing virus*, from pathogen to host expression profile. *Mol Plant Pathol* 4, 133–40.

- Melnyk, C.W., Molnar, A., Bassett, A., Baulcombe, D.C., 2011. Mobile 24 nt small RNAs direct transcriptional gene silencing in the root meristems of *Arabidopsis thaliana*. *Curr Biol* 21, 1678–1683.
- Mi, S., Cai, T., Hu, Y., Chen, Y., Hodges, E., Ni, F., Wu, L., Shan, L., Huanyu, Z., Chengzu, L., Chen, S., Hannon, G.J., Qi, Y., 2008. Sorting of small RNAs into Arabidopsis argonaute complexes is directed by the 5' terminal nucleotide. *Cell* 133, 116–127.
- Miozzi, L., Gambino, G., Burgyan, J., Pantaleo, V., 2013. Genome-wide identification of viral and host transcripts targeted by viral siRNAs in *Vitis vinifera*. *Mol Plant Pathol* 14, 30-43.
- Moissiard, G., Voinnet, O., 2004. Viral suppression of RNA silencing in plants. *Mol Plant Patho* 5, 71–82.
- Molnar, A., Melnyk, C.W., Bassett, A., Hardcastle, T.J., Dunn, R., Baulcombe, D.C., 2010. Small silencing RNAs in plants are mobile and direct epigenetic modification in recipient cells. *Science* 328, 872–875.
- Mondal, H.A., Louis, J., Archer, L., Patel, M., Nalam, V.J., Sarowar, S., Sivapalan, V., Root, D.D., Shah, J., 2018. Arabidopsis ACTIN-DEPOLYMERIZING FACTOR3 is required for controlling aphid feeding from the phloem. *Plant Physiol* 176, 879-890.
- Montgomery, T.A., Howell, M.D., Cuperus, J.T., Li, D., Hansen, J.E., Alexander, A.L., Chapman, E.J., Noah, F., Allen, E., Carrington, J.C., 2008. Specificity of ARGONAUTE7-miR390 interaction and dual functionality in TAS3 trans-acting siRNA formation. *Cell* 133, 128–141.
- Morel, J.B., Godon, C., Mourrain, P., Beclin, C., Boutet, S., Feuerbach, F., Proux, F., Vaucheret, H., 2002. Fertile hypomorphic ARGONAUTE (Ago1) mutants impaired in post-transcriptional gene silencing and virus resistance. *Plant Cell* 14, 629–39.
- Moreno, A., Fereres, A., 2012. Virus diseases in Lettuce in the mediterranean basin. *Ad Virus* 84, 247-288
- Moreno, I.M., Thompson, J.R., García-Arenal, F., 2004. Analysis of the systemic colonization of Cucumber plants by *Cucumber green mottle mosaic virus*. *J Gen Virol* 85, 749–59.
- Mourrain, P., Beclin, C., Elmayan, T., Feuerbach, F., Godon, C., Morel, J.B., Jouette, D., Lacombe, A.M., Nikic, S., Picault, N., Remoue, K., Sanial, M., Vo, T.A., Vaucheret, H., 2000. Arabidopsis SGS2 and SGS3 genes are required for posttranscriptional gene silencing and natural virus resistance. *Cell* 101, 533-542.
- Movahed, N., Patarroyo, C., Sun, J., Vali, H., Laliberte, J.F., Zheng, H., 2017. Cylindrical inclusion protein of *Turnip mosaic virus* serves as a docking point for the intercellular movement of TuMV replication vesicles. *Plant Physiol* 175, 1732-1744.
- Muangsan, N., Beclin, C., Vaucheret, H., Robertson, D., 2004. Geminivirus VIGS of endogenous genes requires SGS2/SDE1 and SGS3 and defines a new branch in the genetic pathway for silencing in plants. *Plant J* 38, 1004–14.
- Muller, M., Munne-Bosch, S., 2015. Ethylene response factors: a key regulatory hub in hormone and stress signaling. *Plant Physiol* 169, 32-41.
- Nawrath, C., Heck, S., Parinthawong, N., Mettraux, J.P., 2002. EDS5, an essential component of salicylic acid-dependent signaling for disease resistance in Arabidopsis, is a member of the MATE transporter family. *Plant Cell* 14, 275-286.

- Nguyen, H.D., Tomitaka, Y., Ho, S.Y., Duchêne, S., Vetten, H.J., Lesemann, D., Walsh, J.A., Gibbs, A.J., Ohshima, K., 2013. *Turnip mosaic potyvirus* probably first spread to eurasian Brassica crops from wild orchids about 1000 years ago. *PLoS One* 8, e55336.
- Nicaise, V., Candresse, T., 2017. *Plum pox virus* capsid protein suppresses plant pathogen-associated molecular pattern (PAMP)-triggered immunity. *Mol Plant Pathol* 18, 878–86.
- Nicolas, O., Laliberte, J.F., 1992. The complete nucleotide sequence of *Turnip mosaic potyvirus* RNA. *J Gen Virol* 73, 2785–93.
- Niehl, A., Amari, K., Gereige, D., Brandner, K., Mely, Y., Heinlein, M., 2012. Control of *Tobacco mosaic virus* movement protein fate by CELL-DIVISION-CYCLE protein 48. *Plant Physiol* 160, 2093–2108.
- Niehl, A., Amari, K., Heinlein, M., 2013a. CDC48 function during TMV infection: regulation of virus movement and replication by degradation? *Plant Signal Behav* 8, e22865.
- Niehl, A., Heinlein, M., 2011. Cellular pathways for viral transport through plasmodesmata. *Protoplasma* 248, 75–99.
- Niehl, A., Pasquier, A., Ferriol, I., Mely, Y., Heinlein M., 2014. Comparison of the *Oilseed rape mosaic virus* and *Tobacco mosaic virus* movement proteins (MP) reveals common and dissimilar MP functions for tobamovirus spread. *Virology* 456, 43–54.
- Niehl, A., Pena, E.J., Amari, K., Heinlein, M., 2013b. Microtubules in viral replication and transport. *Plant J* 75, 290–308.
- Niehl, A., Wyrsh, I., Boller, T., Heinlein, M., 2016. Double-stranded RNAs induce a pattern-triggered immune signaling pathway in plants. *New Phytol* 211, 1008–19.
- Niu, D., Wang, Z., Wang, S., Qiao, L., Zhao, H., 2015. Profiling of small RNAs involved in plant-pathogen interactions. *Methods Mol Biol* 1287, 61–79.
- Nobuta, K., Okrent, R.A., Stoutemyer, M., Rodibaugh, N., Kempema, L., Wildermuth, M.C., Innes, R.W., 2007. The GH3 acyl adenylase family member PBS3 regulates salicylic acid-dependent defense responses in Arabidopsis. *Plant Physiol* 144, 1144–1156.
- Olesen, P., Robards, A.W., 1990. The neck region of plasmodesmata: general architecture and some functional aspects. *Nato H46*, 146–70.
- Olmedo-Monfil, V., Durán-Figueroa, N., Arteaga-Vázquez, M., Demesa-Arévalo, E., Autran, D., Grimaneli, D., Slotkin, R.K., Martienssen, R.A., Vielle-Calzada, J.P., 2010. Control of female gamete formation by a small RNA pathway in Arabidopsis. *Nature* 464, 628–632.
- Olmedo, G., Guo, H., Gregory, B.D., Nourizadeh, S.D., Aguilar-Henonin, L., Li, H., An, F., Guzman, P., Ecker, J. R., 2006. ETHYLENE-INSENSITIVE5 encodes a 5'→3' exoribonuclease required for regulation of the EIN3-targeting F-Box proteins EBF1/2. *Proc Natl Acad Sci U S A* 103, 13286–93.
- Omarov, R. T., Ciomperlik, J. J., Scholthof, H. B., 2007. RNAi-associated ssRNA-specific ribonucleases in tobusvirus P19 mutant-infected plants and evidence for a discrete siRNA-containing effector complex. *Proc Natl Acad Sci U S A* 104, 1714–19.
- Omarov, R., Sparks, K., Smith, L., Zindovic, J., Scholthof, H.B., 2006. Biological relevance of a stable biochemical interaction between the tobusvirus-encoded P19 and short interfering RNAs. *J Virol* 80, 3000–3008.

- Opalka, N., Brugidou, C., Bonneau, C., Nicole, M., Beachy, R.N., Yeager, M., Fauquet, C., 1998. Movement of Rice yellow mottle virus between xylem cells through pit membranes. *Proc Natl Acad Sci U S A* 95, 3323–28.
- Oparka, K.J., Prior, D.A.M., Cruz, S.S., Padgett, H.S., Beachy, R.N., 1997. Gating of epidermal plasmodesmata is restricted to the leading edge of expanding infection sites of *Tobacco mosaic virus*. *Plant J.* 12, 781–89.
- Pantaleo, V., Burgyan, J., 2008. *Cymbidium ringspot virus* harnesses RNA silencing to control the accumulation of virus parasite satellite RNA. *J Virol* 82, 11851–11858.
- Pantaleo, V., Szittyá, G., Burgyan, J., 2007. Molecular bases of viral RNA targeting by viral small interfering RNA-programmed RISC. *J. Virol* 81, 3797–3806.
- Parent, J.S., Bouteiller, N., Elmayan, T., Vaucheret, H., 2015. Respective contributions of Arabidopsis DCL2 and DCL4 to RNA silencing. *Plant J* 81, 223–232.
- Park, M.Y., Wu, G., Gonzalez-Sulser, A., Vaucheret, H., Poethig, R.S., 2005. Nuclear processing and export of microRNAs in Arabidopsis. *Proc Natl Acad Sci U S A* 102, 3691–3696.
- Pauwels, L., Barbero, G.F., Geerinck, J., Tilleman, S., Grunewald, W., Perez, A.C., Chico, J.M., Bossche, R.V., Sewell, J., Gil, E., Garcia-Casado, G., Witters, E., Inze, D., Long, J.A., De Jaeger, G., Solano, R., Goossens, A., 2010. NINJA connects the co-repressor TOPLESS to jasmonate signalling. *Nature* 464, 788–791.
- Peiro, A., Izquierdo-Garcia, A.C., Sanchez-Navarro, J.A., Pallas, V., Mulet, J.M., Aparicio, F., 2014. Patellins 3 and 6, two members of the plant patellin family, interact with the movement protein of *Alfalfa mosaic virus* and interfere with viral movement. *Mol Plant Pathol* 15, 881–91.
- Peña, E.J., Heinlein, M., 2013. Cortical microtubule-associated ER sites: organization centers of cell polarity and communication. *Curr Opin Plant Biol* 16, 764–73.
- Peragine, A., Yoshikawa, M., Wu, G., Albrecht, H.L., Poethig, R.S., 2004. SGS3 and SGS2/SDE1/RDR6 are required for juvenile development and the production of trans-acting siRNAs in Arabidopsis. *Genes Dev* 3, 2368–2379.
- Peremyslov, V.V., Prokhnevsky, A.I., Avisar, D., Dolja, V.V., 2008. Two class XI myosins function in organelle trafficking and root hair development in Arabidopsis. *Plant Physiol* 146, 1109–16.
- Pitzalis, N., Heinlein, M., 2017. The roles of membranes and associated cytoskeleton in plant virus replication and cell-to-cell movement. *J Exp Bot* 69, 117–132.
- Pitzschke, A., Forzani, C., Hirt, H., 2006. Reactive oxygen species signaling in plants. *Antioxid Redox Signal* 8, 1757–64.
- Pontes, O., Li, C.F., Nunes, P.C., Haag, J., Ream, T., Vitins, A., Jacobsen, S.E., Pikaard, C.S., 2006. The Arabidopsis chromatin-modifying nuclear siRNA pathway involves a nucleolar RNA processing center. *Cell* 126, 79–92.
- Pooggin, M.M., 2013. How can plant DNA viruses evade siRNA-directed DNA methylation and silencing? *J Mol Sci* 14, 15233–59.
- Potuschak, T., Vansiri, A., Binder, B.M., Lechner, E., Vierstra, R. D., Genschik, P., 2006. The exoribonuclease XRN4 is a component of the ethylene response pathway in Arabidopsis. *Plant Cell* 18, 3047–57.

- Poulsen, C., Vaucheret, H., Brodersen, P., 2013. Lessons on RNA silencing mechanisms in plants from eukaryotic Argonaute structures. *Plant Cell* 25, 22–37.
- Prokhnevsky, A.I., Peremyslov, V.V., Dolja, V.V., 2008. Overlapping functions of the four class XI myosins in *Arabidopsis* growth, root hair elongation, and organelle motility. *Proc Natl Acad Sci U S A* 105, 19744–49.
- Pumplin, N., Voinnet, O., 2013. RNA silencing suppression by plant pathogens: defence, counter-defence and counter-counter-defence. *Nat Rev Microbiol* 11, 745–760.
- Qi, X., Bao, F.S., Xie, Z., 2009. Small RNA deep sequencing reveals role for *Arabidopsis thaliana* RNA-dependent RNA polymerases in viral siRNA biogenesis. *PLoS One* 4, e4971.
- Qi, Y., Denli, A.M., Hannon, G.J., 2005. Biochemical specialization within *Arabidopsis* RNA silencing pathways. *Mol Cell* 19, 421–428.
- Qin, H., Chen, F., Huan, X., Machida, S., Song, J., Yuan, Y.A., 2010. Structure of the *Arabidopsis thaliana* DCL4 DUF283 domain reveals a noncanonical double-stranded RNA-binding fold for protein - Protein interaction. *RNA* 16, 474–481.
- Radford, J.E., White, R.G., 2001. Effects of tissue-preparation-induced callose synthesis on estimates of plasmodesma size exclusion limits. *Protoplasma* 216, 47–55.
- Raja, P., Jackel, J.N., Li, S., Heard, I.M., Bisaro, D.M., 2014. *Arabidopsis* double-stranded RNA binding protein DRB3 participates in methylation-mediated defense against geminiviruses. *J Virol* 88, 2611–22.
- Raja, P., Sanville, B.C., Buchmann, R.C., Bisaro, D.M., 2008. Viral genome methylation as an epigenetic defense against geminiviruses. *J Virol* 82, 8997–9007.
- Randles, J., Ogle, H., 1997. Viruses and viroids as agents of plant disease. *Plant pathogens and plant diseases*. Rockvale Publication, Australia, pp. 104–126.
- Ratcliff, F., Harrison, B.D., Baulcombe, D.C., 1997. A similarity between viral defense and gene silencing in plants. *Science* 276, 1558–60.
- Ratcliff, F.G., MacFarlane, S.A., Baulcombe, D.C., 1999. Gene silencing without DNA: RNA-mediated cross-protection between viruses. *Plant Cell* 11, 1207–15.
- Reichel, C., Beachy, R.G., 1998. *Tobacco mosaic virus* infection induces severe morphological changes of the endoplasmic reticulum. *Proc Natl Acad Sci U S A* 95, 11169–74.
- Reichel, C., Beachy, R.G., 2000. Degradation of the *Tobacco mosaic virus* movement protein by the 26S proteasome. *J Virol* 74, 3330–37.
- Reichelt, S., Knight, A.E., Hodge, T.P., Baluska, F., Samaj, J., Volkmann, D., Kendrick-Jones, J., 1999. Characterization of the unconventional myosin VIII in plant cells and its localization at the post-cytokinetic cell wall. *Plant J* 19, 555–67.
- Reinhart, B.J., Weinstein, E.G., Rhoades, M.W., Bartel, B., Bartel, D.P., 2002. MicroRNAs in plants. *Gen and Dev* 16, 1616–1626.

- Roberts, I.M., Wang, D., Findlay, K., Maule, A.J., 1998. Ultrastructural and temporal observations of the potyvirus cylindrical inclusions (CIs) show that the CI protein acts transiently in aiding virus movement. *Virology* 245, 173–81.
- Rodriguez-Cerezo, E., Findlay, K., Shaw, J.G., Lomonosoff, G.P., Qiu, S.G., Linstead, P., Shanks, M., Risco, C., 1997. The coat and cylindrical inclusion proteins of a potyvirus are associated with connections between plant cells. *Virology* 236, 296–306.
- Rodriguez-Negrete, E. A., Carrillo-Tripp, J., Rivera-Bustamante, R. F., 2009. RNA silencing against geminivirus: complementary action of posttranscriptional gene silencing and transcriptional gene silencing in host recovery. *J Virol* 83, 1332–40.
- Rojas, M.R., Zerbini, M., Allison, R.F., Gilbertson, R.L., Lucas, W.J., 1997. Capsid protein and helper component-proteinase function as potyvirus cell-to-cell movement proteins. *Virology* 237, 283–95.
- Roossinck, M.J., Bazán, E.R., 2017. Symbiosis: viruses as intimate partners. *Annu Rev Virol* 4, 123–39.
- Rosas-Diaz, T., Zhang, D., Fan, P., Wang, L., Ding, X., Jiang, Y., Jimenez-Gongora, T., Medina-Puche, L., Zhao, X., Feng, Z., Zhang, G., Liu, X., Bejarano, E.R., Tan, L., Zhang, H., Zhu, J.K., Xing, W., Faulkner, C., Nagawa, S., Lozano-Duran, R., 2018. A virus-targeted plant receptor-like kinase promotes cell-to-cell spread of RNAi. *Proc Natl Acad Sci U S A* 115, 1388-1393.
- Ruiz-Ferrer, V., Voinnet, O., 2009. Roles of plant small RNAs in biotic stress responses. *Annu Rev Plant Biol* 60.
- Sager, R., Lee, J.Y., 2014. Plasmodesmata in integrated cell signalling: insights from development and environmental signals and stresses. *J Exp Bot* 65, 6337–58.
- Sager, R.E., Lee, J.Y., 2018. Plasmodesmata at a glance. *J Cell Sci* 131, jcs209346.
- Saito, T., Yamanaka, K., Okada, Y., 1990. Long-distance movement and viral assembly of *Tobacco mosaic virus* mutants. *Virology* 176, 329–36.
- Sambade, A., Brandner, K., Hofmann, C., Seemanpillai, M., Mutterer, J., Heinlein, M., 2008. Transport of TMV movement protein particles associated with the targeting of RNA to plasmodesmata. *Traffic* 9, 2073–88.
- Santovito, E., Mascia, T., Siddiqui, S.A., Minutillo, S.A., Valkonen, J.P.T., Gallitelli, D., 2014. Infection cycle of *Artichoke italian latent virus* in tobacco plants: meristem invasion and recovery from disease symptoms. *PLoS One* 9, e99446.
- Sastry, S.K., Zitter, T., 2014. Management of virus and viroid diseases of crops in the tropics, plant virus and viroid diseases in the tropics. Springer, Dordrecht, pp. 149-480.
- Schaad, M.C., Jensen, P.E., Carrington, J.C., 1997. Formation of plant RNA virus replication complexes on membranes: role of an endoplasmic reticulum-targeted viral protein. *EMBO* 16, 4049–59.
- Schauer, S.E., Jacobsen, S.E., Meinke, D.W., Ray, A., 2002. DICER-LIKE1: Blind men and elephants in Arabidopsis development. *Plant Sci* 7, 487–491.
- Schoelz, J.E., Angel, C.A., Nelson, R.S., Leisner, S.M., 2016. A model for intracellular movement of *Cauliflower mosaic virus*: the concept of the mobile virion factory. *J Exp Bot* 67, 2039–48.

- Scholthof, H. B., Alvarado, V. Y., Vega-Arreguin, J.C., Ciomperlik, J., Odokonyero, D., Brosseau, C., Jaubert, M., Zamora, A., Moffett, P., 2011. Identification of an ARGONAUTE for antiviral RNA silencing in *Nicotiana benthamiana*. *Plant Physiol* 156, 1548–55.
- Schwach, F., Vaistij, F.E., Jones, L., Baulcombe, D.C., 2005. An RNA-dependent RNA polymerase prevents meristem invasion by *Potato virus X* and is required for the activity but not the production of a systemic silencing signal. *Plant Physiology* 138, 1842–52.
- Seto, D., Koulana, N., Lo, T., Menna, A., Guttman, D.S., Desveaux, D., 2017. Expanded type III effector recognition by the ZAR1 NLR protein using ZED1-related kinases. *Nature Plants* 3, 17027.
- Shahid, S., Axtell, M.J., 2014. Identification and annotation of small RNA genes using ShortStack. *Methods* 67, 20-27.
- Shattuck, V.I., 1992. The biology, epidemiology and control of *Turnip mosaic virus*. *Plant Breed. Rev.* 14, 199-238.
- Shimura, H., Pantaleo, V., Ishihara, T., Myojo, N., Inaba, J., Sueda, K., Burgyan, J., Masuta, C., 2011. A viral satellite RNA induces yellow symptoms on tobacco by targeting a gene involved in chlorophyll biosynthesis using the RNA silencing machinery. *PLoS Pathog* 7, e1002021.
- Shivaprasad, P.V., Chen, H.M., Patel, K., Bond, D.M., Santos, B.A., Baulcombe, D.C., 2012. A microRNA superfamily regulates nucleotide binding site-leucine-rich repeats and other mRNAs. *Plant Cell* 24, 859–874.
- Siddiqui, S.A., Sarmiento, C., Kiisma, M., Koivumäki, S., Lemmetty, A., Truve, E., Lehto, K., 2008. Effects of viral silencing suppressors on *Tobacco ringspot virus* infection in two *Nicotiana* species. *J Gen Virol* 89, 1502–8.
- Simpson, C., Thomas, C., Findlay, K., Bayer, E., Maule, A. J., 2009. An Arabidopsis GPI-anchor plasmodesmal neck protein with callose binding activity and potential to regulate cell-to-cell trafficking. *Plant Cell* 21, 581–94.
- Smith, H. A., 1994. Transgenic plant virus resistance mediated by untranslatable sense RNAs: expression, regulation, and fate of nonessential RNAs. *Plant Cell* 6, 1441–53.
- Smith, L.M., Pontes, O., Searle, I., Yelina, N., Yousafzai, F.K., Herr, A.J., Pikaard, C.S., Baulcombe, D.C., 2007. An SNF2 protein associated with nuclear RNA silencing and the spread of a silencing signal between cells in Arabidopsis. *Plant Cell* 19, 1507–21.
- Smith, N.A., Eamens, A.L., Wang, M.B., 2011. Viral small interfering RNAs target host genes to mediate disease symptoms in plants. *PLoS Pathog* 7, e1002022.
- Song, J.J., Liu, J., Tolia, N.H., Schneiderman, J., Smith, S.K., Martienssen, R.A., Hannon, G.J., Joshua-Tor, L., 2003. The crystal structure of the Argonaute 2 PAZ domain reveals an RNA binding motif in RNAi effector complexes. *Nat Struc Biol* 10, 1026–1032.
- Song, J.J., Smith, S.K., Hannon, G.J., Joshua-Tor, L., 2004. Crystal structure of Argonaute and its implications for RISC slicer activity. *Science* 305, 1434–1437.
- Song, X., Li, P., Zhai, J., Zhou, M., Ma, L., Liu, B., Liu, Jeong, D.H., Nakano, M., Cao, S., Liu, C., Chu, C., Wang, X.J., Green, P.J., Meyers, B.C., Cao, X., 2012. Roles of DCL4 and DCL3b in rice phased small RNA biogenesis. *Plant J* 69, 462–474.

- Sparkes, I.A., Frigerio, L., Tolley, N., Hawes, C., 2009. The plant endoplasmic reticulum: A cell-wide web. *Biochem J* 423, 145–55.
- Sparkes, I.A., Teanby, N.A., Hawes, C., 2008. Truncated myosin XI tail fusions inhibit peroxisome, golgi, and mitochondrial movement in tobacco leaf epidermal cells: A genetic tool for the next generation. *J Exp Bot* 59, 2499–2512.
- Spoel, S.H., Dong, X., 2012. How do plants achieve immunity? Defence without specialized immune cells. *Nat Rev Immunol* 12, 89–100.
- Stocks, M.B., Mohorianu, I., Beckers, M., Paicu, C., Moxon, S., Thody, J., Dalmay, T., Moulton, V., 2018. The UEA sRNA Workbench (version 4.4): a comprehensive suite of tools for analyzing miRNAs and sRNAs. *Bioinformatics*, in press.
- Suffert, G., Malterer, G., Hausser, J., Viiliäinen, J., Fender, A., Contrant, M., Ivacevic, T., Benes, V., Gros, F., Voinnet, O., Zavolan, M., Ojala, P.M., Haas, J.G., Pfeffer, S., 2011. Kaposi's sarcoma herpesvirus microRNAs target caspase 3 and regulate apoptosis. *PLoS Pathog* 7, e1002405.
- Sun, T., Zhang, Y., Li, Y., Zhang, Q., Ding, Y., Zhang, Y., 2015. CHIP-seq reveals broad roles of SARD1 and CBP60g in regulating plant immunity. *Nat Commun* 6, 10159.
- Szittyá, G., Molnár, A., Silhavy, D., Hornyik, C., Burgyan, J., 2002. Short defective interfering RNAs of tombusviruses are not targeted but trigger post-transcriptional gene silencing against their helper virus. *Plant Cell* 14, 359–72.
- Tagami, Y., Inaba, N., Kutsuna, N., Kurihara, Y., Watanabe, Y., 2007. Specific enrichment of miRNAs in *Arabidopsis thaliana* infected with *Tobacco mosaic virus*. *DNA Res* 14, 227–233.
- Takeda, A., Iwasaki, S., Watanabe, T., Utsumi, M., Watanabe, Y., 2008. The mechanism selecting the guide strand from small RNA duplexes is different among Argonaute proteins. *Plant Cell Physiol* 49, 493–500.
- Tanner, N.K., Linder, P., 2001. DExD/H box RNA helicases: from generic motors to specific dissociation functions. *Mol Cell* 8, 251–262.
- Tantikanjana, T., Rizvi, N., Nasrallah, M.E., Nasrallah, J.B., 2009. A dual role for the s-locus receptor kinase in self-incompatibility and pistil development revealed by an *Arabidopsis* *rdr6* mutation. *Plant Cell* 21, 2642–2654.
- Thivierge, K., Cotton, S., Dufresne, P.J., Mathieu, I., Beauchemin, C., Ide, C., Fortin, M.G., Laliberte, J.F., 2008. Eukaryotic elongation factor 1A interacts with *Turnip mosaic virus* RNA-dependent RNA polymerase and VPg-Pro in virus-induced vesicles. *Virology* 377, 216–25.
- Thorvaldsdottir, H., Robinson, J.T., Mesirov, J.P., 2013. Integrative Genomics Viewer (IGV): high-performance genomics data visualization and exploration. *Brief Bioinform* 14, 178–192.
- Till, S., Lejeune, E., Thermann, R., Bortfeld, M., Hothorn, M., Enderle, D., Heinrich, C., Hentze, M.W., Ladurner, A.G., 2007. A conserved motif in Argonaute-interacting proteins mediates functional interactions through the Argonaute PIWI domain. *Nat Struct Mol Biol* 14, 897–903.
- Tilsner, J., Nicolas, W., Rosado, A., Bayer, E.M., 2016. Staying tight: plasmodesmal membrane contact sites and the control of cell-to-cell connectivity in plants. *Annu Rev Plant Biol* 67, 337–64.

- Tomlinson, J.A., 1987. Epidemiology and control of virus diseases of vegetables. *Ann appl Biol* 110, 661–81.
- Tomlinson, J.A., Carter, A.L., Dale, W.T., Simpson, C.J., 1970. Weed plants as sources of *Cucumber mosaic virus*. *Ann Appl Biol* 66, 11–16.
- Tomofumi, M., Ohki, S.T., 2004. Shoot meristem tissue of Tobacco inoculated with *Cucumber mosaic virus* is infected with the virus and subsequently recovers from infection by RNA silencing. *J Plant Pathol* 70, 363–66.
- Torres, M.A., 2010. ROS in biotic interactions. *Physiol Plant* 138, 414–29.
- Tsai, Y.C., Weissman, A.M., 2011. Ubiquitylation in ERAD: reversing to go Forward? *PLoS Biol* 9, e1001038.
- Tucker, E.B., 1990. Calcium-loaded 1,2-bis(2-aminophenoxy)ethane-N,N,N',N'-tetraacetic acid blocks cell-to-cell diffusion of carboxyfluorescein in staminal hairs of *Setcreasea purpurea*. *Planta* 182, 34–38.
- Tucker, E.B., Boss, W.F., 1996. Mastoparan induced intracellular Ca²⁺ fluxes may regulate cell-to-cell communication in plants. *Plant Physiol* 111, 459–67.
- Tucker, M.R., Okada, T., Hu, Y., Scholefield, A., Taylor, J.M., Koltunow, A.M.G., 2012. Somatic small RNA pathways promote the mitotic events of megagametogenesis during female reproductive development in Arabidopsis. *Dev* 139, 1399–1404.
- Uchiyama, A., Shimada-Beltran, H., Levy, A., Zheng, J.Y., Javia, P.A., Lazarowitz, S.G., 2014. The Arabidopsis synaptotagmin SYTA regulates the cell-to-cell movement of diverse plant viruses. *Front Plant Sci* 5, 1–17.
- Ueda, H., Yokota, E., Kutsuna, N., Shimada, T., Tamura, K., Shimmen, T., Hasezawa, S., Dolja, V.V., Hara-Nishimura, I., 2010. Myosin-dependent endoplasmic reticulum motility and F-actin organization in plant cells. *Proc Natl Acad Sci U S A* 107, 6894–99.
- Ueki, S., Spektor, R., Natale, D.M., Citovsky, V., 2010. ANK, a host cytoplasmic receptor for the *Tobacco mosaic virus* cell-to-cell movement protein, facilitates intercellular transport through plasmodesmata. *PLoS Patho* 6, e1001201.
- Vaistij, F.E., Jones, L., 2009. Compromised virus-induced gene silencing in RDR6-deficient plants. *Plant Physiol*, 149, 1399–1407.
- Valli, A.A., Gallo, A., Rodamilans, B., Lopez-Moya, J.J., Garcia, J.A., 2018. The HCPro from the Potyviridae family: an enviable multitasking Helper Component that every virus would like to have. *Molecular Plant Pathology* 19, 744-763.
- Varallyay, E., Valoczi, A., Agyi, A., Burgyan, J., Havelda, Z., 2010. Plant virus-mediated induction of miR168 is associated with repression of ARGONAUTE1 accumulation. *EMBO Journal* 29, 3507-3519.
- Vasudevan, D., Gopalan, G., Kumar, A., Garcia, V.J., Luan, S., Swaminathan, K., 2015. Plant immunophilins: a review of their structure-function relationship. *BBA*, 1850, 2145–2158.
- Vatén, A., Dettmer, J., Wu, S., Stierhof, Y.D., Miyashima, S., Yadav, S.R., Roberts, C.J., Campilho, A., Bulone, V., Lichtenberger, R., Lehesranta, S., Mahonen, A.P., Kim, J.Y., Jokitalo, E., Sauer, N., Scheres, B., Nakajima, K., Carlsbecker, A., Gallagher, K.L., Helariutta, Y., 2011. Callose biosynthesis regulates symplastic trafficking during root development. *Dev Cell* 21, 1144–1155.

- Vazquez, F., 2006. Arabidopsis endogenous small RNAs: highways and byways. *Plant Sci* 11, 460–68.
- Vazquez, F., Vaucheret, H., Rajagopalan, R., Lepers, C., Gascioli, V., Mallory, A.C., Hilbert, J.L., Bartel, D.P., Creté, P., 2004. Endogenous trans-acting siRNAs regulate the accumulation of Arabidopsis mRNAs. *Mol Cell* 16, 69-79.
- Verchot-Lubicz, J., Torrance, L., Solovyev, A.G., Morozov, S.Y., Jackson, A.O., Gilmer, D., 2010. Varied movement strategies employed by triple gene block-encoding viruses. *Mol Plant Microbe Interact* 23, 1231–47.
- Verchot, J., Driskel, B.A., Zhu, Y., Hunger, R.M., Littlefield, L.J., 2001. Evidence that *Soilborne wheat mosaic virus* moves long distance through the xylem in wheat. *Protoplasma* 218, 57–66.
- Verchot, J., Herndon, K.L., Carrington, J.C., 1992. Mutational analysis of the *Tobacco etch potyviral* 35-kDa proteinase: identification of essential residues and requirements for autoproteolysis. *Virology* 190, 298–306.
- Vijayapalani, P., Maeshima, M., Nagasaki-Takekuchi, N., Miller, W.A., 2012. Interaction of the trans-frame potyvirus protein P3N-PIPO with host protein PCaP1 facilitates potyvirus movement. *PLoS Pathog* 8, e1002639.
- Vogler, H., Akbergenov, R., Shivaprasad, P.V., Dang, V., Fasler, M., Kwon, M.O., Zhanybekova, S., Hohn, T., Heinlein, M., 2007. Modification of small RNAs associated with suppression of RNA silencing by tobamovirus replicase protein. *J Virol* 81, 10379-10388.
- Voinnet, O., 2005. Induction and suppression of RNA silencing: insights from viral infections. *Nat Rev Genet* 6, 206–20.
- Voinnet, O., Pinto, Y.M., Baulcombe, D.C., 1999. Suppression of gene silencing: a general strategy used by diverse DNA and RNA viruses of plants. *Proc Natl Acad Sci U S A* 96, 14147–52.
- Vrbsky, J., Akimcheva, S., Watson, J.M., Turner, T.L., Daxinger, L., Vyskot, B., Aufsatz, W., Riha, K., 2010. siRNA-mediated methylation of Arabidopsis telomeres. *PLoS Genetics* 6, e1000986.
- Walsh, J.A., Tomlinson, J. A., 1985. Viruses infecting winter Oilseed rape (*Brassica napus ssp. oleifera*). *Ann appl Biol* 107, 485–95.
- Wan, J., Cabanillas, D.G., Zheng, H., Laliberte, J.F., 2015. *Turnip mosaic virus* moves systemically through both phloem and xylem as membrane-associated complexes. *Plant Physiol* 167, 1374–88.
- Wang, H.W., Noland, C., Siridechadilok, B., Taylor, D.W., Ma, E., Felderer, K., Doudna, J.A., Nogales, E., 2009. Structural insights into RNA processing by the human RISC-loading complex. *Nat Struc Mol Biol* 16, 1148–1153.

- Wang, X., Wang, H., Wang, J., Sun, R., Wu, J., Liu, S., Bai, Y., Mun, J.H., Bancroft, I., Cheng, F., Huang, S., Li, X., Hua, W., Wang, J., Wang, X., Freeling, M., Pires, J.C., Paterson, A.H., Chalhoub, B., Wang, B., Hayward, A., Sharpe, A.G., Park, B.S., Weisshaar, B., Liu, B., Li, B., Liu, B., Tong, C., Song, C., Duran, C., Peng, C., Geng, C., Koh, C., Lin, C., Edwards, D., Mu, D., Shen, D., Soumpourou, E., Li, F., Fraser, F., Conant, G., Lassalle, G., King, G.J. Bonnema, G., Tang, H., Wang, H., Belcram, H., Zhou, H., Hirakawa, H., Abe, H., Guo, H., Wang, H., Jin, H., Parkin, I.A.P., Batley, J., Kim, J.S., Just, J., Li, J., Xu, J., Deng, J., Kim, J.A., Li, J., Yu, J., Meng, J., Wang, J., Min, J., Poulain, J., Hatakeyama, K., Wu, K., Wang, L., Fang, L., Trick, M., Links, M.G., Zhao, M., Jin, M., Ramchiary, N., Drou, N., Berkman, P.J., Cai, Q., Huang, Q., Li, R., Tabata, S., Cheng, S., Zhang, S., Zhang, S., Huang, S., Sato, S., Sun, S., Kwon, S.J., Choi, S.R., Lee, T.H., Fan, W., Zhao, X., Tan, X., Xu, X., Wang, Y., Qiu, Y., Yin, Y., Li, Y., Du, Y., Liao, Y., Lim, Y., Narusaka, Y., Wang, Y., Wang, Z., Li, Z., Wang, Z., Xiong, Z., Zhang, Z., 2011. The genome of the mesopolyploid crop species *Brassica rapa*. *Nat Gen* 43, 1035–1040.
- Wang, X.B., Wu, Q., Ito, T., Cillo, F., Li, W.X., Chen, X., Yu, J.L., Ding, S.W., 2010. RNAi-mediated viral immunity requires amplification of virus-derived siRNAs in *Arabidopsis thaliana*. *Proc Natl Acad Sci U S A* 107, 484–489.
- Wang, Y., Li, L., Tang, S., Liu, J., Zhang, H., Zhi, H., Jia, G., Diao, X., 2016. Combined small RNA and degradome sequencing to identify miRNAs and their targets in response to drought in foxtail millet. *BMC Genetics* 17, 1–16.
- Wang, Z., Chen, Y., Fang, H., Shi, H., Chen, K., Zhang, Z., Tan, X., 2014. Selection of reference genes for quantitative reverse-transcription polymerase chain reaction normalization in *Brassica napus* under various stress conditions. *Mol Genet Genomics* 289, 1023–1035.
- Wassenegger, M., Krczal, G., 2006. Nomenclature and functions of RNA-directed RNA polymerases. *Plant Sci* 11, 142–151.
- Wei, K.F., Wu, L.J., Chen, J., Chen, Y.F., Xie, D.X., 2012. Structural evolution and functional diversification analyses of Argonaute protein. *J Cell Biochem* 113, 2576–2585.
- Wei, T., Huang, T.S., McNeil, J., Laliberte, J.F., Hong, J., Nelson, R.S., Wang, A., 2010a. Sequential recruitment of the endoplasmic reticulum and chloroplasts for plant potyvirus replication. *J Virol* 84, 799–809.
- Wei, T., Wang, A., 2008. Biogenesis of cytoplasmic membranous vesicles for plant potyvirus replication occurs at endoplasmic reticulum exit sites in a COPI- and COPII-dependent manner. *J Virol* 82, 12252–64.
- Wei, T., Zhang, C., Hong, J., Xiong, R., Kasschau, K.D., Zhou, X., Carrington, J.C., Wang, A., 2010b. Formation of complexes at plasmodesmata for potyvirus intercellular movement is mediated by the viral protein P3N-PIPO. *PLoS Pathog* 6, e1000962.
- Wei, T., Zhang, C., Hou, X., Sanfaçon, H., Wang, A., 2013. The SNARE protein Syp71 is essential for *Turnip mosaic virus* infection by mediating fusion of virus-induced vesicles with chloroplasts. *PLoS Pathog* 9, e1003378.
- Weiberg, A., Bellinger, M., Jin, H., 2015. Conversations between kingdoms: small RNAs. *Curr Opin Biotech* 32, 207–215.
- Weiberg, A., Wang, M., Bellinger, M., Jin, H., 2014. Small RNAs: a new paradigm in plant-microbe interactions. *Annu Rev Phytopathol* 52, 495–516.
- Weiberg, A., Wang, M., Lin, F.M., Zhao, H., Zhang, Z., Kaloshian, I., Huang, H.D., Jin, H., 2013. Fungal small RNAs suppress plant immunity by hijacking host RNA interference pathways. *Science* 342, 118–123.

- Whitham, S.A., Yang, C., Goodin, M.M., 2006. Global impact: elucidating plant responses to viral infection. *Mol Plant Microbe Interact* 19, 1207-1215.
- Willmann, M.R., Endres, M.W., Cook, R.T., Gregory, B.D., 2011. The functions of RNA-dependent RNA polymerases in Arabidopsis. *The Arabidopsis Book*, 9, e0146.
- Wingard, S.A., 1928. Hosts and symptoms of ring spot, a virus disease of plants. *J Agri Res* 37, 127-53.
- Wolf, S., Deom, C.M., Beachy, R.N., Lucas, W.J., 1989. Movement protein of *Tobacco mosaic virus* modifies plasmodesmata size exclusion limit. *Science* 246, 377-79.
- Wright, K.M., Wood, N.T., Roberts, A.G., Chapman, S., Boevink, P., Mackenzie, K.M., Oparka, K.J., 2007. Targeting of TMV movement protein to plasmodesmata requires the actin/ER network: evidence from FRAP. *Traffic* 8, 21-31.
- Wu, H.W., Lin, S.S., Chen, K.C., Yeh, S.D., Chua, N.H., 2010. Discriminating mutations of Hc-Pro of Zucchini yellow mosaic virus with differential effects on small RNA pathways involved in viral pathogenicity and symptom development. *Mol Plant Microbe Interact* 23, 17-28.
- Xia, R., Zhu, H., An, Y., Beers, E.P., Liu, Z., 2012. Apple miRNAs and tasiRNAs with novel regulatory networks. *Genome Biology*, 13, R47.
- Xie, Z., Johansen, L.K., Gustafson, A.M., Kasschau, K.D., Lellis, A.D., Zilberman, D., Jacobsen, S.E., Carrington, J. C., 2004. Genetic and functional diversification of small RNA pathways in plants. *PLoS Biol* 2, 642-652.
- Xin, H.W., Ding, S.W., 2003. Identification and molecular characterization of a naturally occurring RNA virus mutant defective in the initiation of host recovery. *Virology* 317, 253-62.
- Xu, M.Y., Dong, Y., Zhang, Q.X., Zhang, L., Luo, Y.Z., Sun, J., Fan, Y.L., Wang, L., 2012. Identification of miRNAs and their targets from *Brassica napus* by high-throughput sequencing and degradome analysis. *BMC Genomics* 13, 421.
- Xu, S., Zhang, Z., Jing, B., Gannon, P., Ding, J., Xu, F., Li, X., Zhang, Y., 2011b. Transportin-SR is required for proper splicing of resistance genes and plant immunity. *PLoS Genet* 7, e1002159.
- Xu, X., and the Potato Genome Sequencing Consortium, 2011a. Genome sequence and analysis of the tuber crop Potato. *Nature*, 475, 189-195.
- Yang, H., Gou, X., He, K., Xi, D., Du, J., Lin, H., Li, J., 2010. BAK1 and BKK1 in *Arabidopsis thaliana* confer reduced susceptibility to Turnip crinkle virus." *J Plant Pathol* 127, 149-56.
- Yang, Z., Ebright, Y.W., Yu, B., Chen, X., 2006. HEN1 recognizes 21-24 nt small RNA duplexes and deposits a methyl group onto the 2' OH of the 3' terminal nucleotide. *Nucleic Acids Res*, 34, 667-675.
- Yasaka, R., Ohba, K., Schwingame, M.W., Fletcher, J., Ochoa-Corona, F.M., Thomas, J.E., Ho, S.Y., Gibbs, A.J., Ohshima, K., 2015. Phylodynamic evidence of the migration of *Turnip mosaic potyvirus* from Europe to Australia and New Zealand. *J Gen Virol* 96, 701-13.
- Ying H., Lijuan J., Qichen H., Dmitry G.V., Xuemei C., Jin-Biao, M., 2009. Structural insights into mechanisms of the small RNA methyltransferase HEN1. *Nature* 461, 823-827.

- Young, N.D., Debelle, F., Oldroyd, G.E.D., Geurts, R., Cannon, S.B., Udvardi, M.K., Benedito, V.A., Mayer, K.F.X., Gouzy, J., Schoof, H., Van De Peer, Y., Proost, S., Cook, D.R., Meyers, B.C., Spannagl, M., Cheung, F., De Mita, S., Krishnakumar, V., Gundlach, H., Zhou, S., Mudge, J., Bharti, A.K., Murray, J.D., Naoumkina, M.A., Rosen, B., Silverstein, K.A.T., Tang, H., Rombauts, S., Zhao, P.X., Zhou, P., Barbe, V., Bardou, P., Bechner, M., Bellec, A., Berger, A., Bergès, H., Bidwell, S., Bisseling, T., Choisine, N., Couloux, A., Denny, R., Deshpande, S., Dai, X., Doyle, J.J., Dudez, A.M., Farmer, A.D., Fouteau, S., Franken, C., Gibelin, C., Gish, J., Goldstein, S., González, A.J., Green, P.J., Hallab, A., Hartog, M., Hua, A., Humphray, S.J., Jeong, D.H., Jing, Y., Jöcker, A., Kenton, S.M., Kim, D.J., Klee, K., Lai, H., Lang, C., Lin, S., MacMil, S.L., Magdelenat, G., Matthews, L., McCarrison, J., Monaghan, E.L., Mun, J.H., Najjar, F.Z., Nicholson, C., Noirot, C., O'Bleness, M., Paule, C.R., Poulain, J., Prion, F., Qin, B., Qu, C., Retzel, E.F., Riddle, C., Sallet, E., Samain, S., Samson, N., Sanders, I., Saurat, O., Scarpelli, C., Schiex, T., Segurens, B., Severin, A.J., Sherrier, D.J., Shi, R., Sims, S., Singer, S.R., Sinharoy, S., Sterck, L., Viollet, A., Wang, B.B., Wang, K., Wang, M., Wang, X., Warfsmann, J., Weissenbach, J., White, D.D., White, J.D., Wiley, G.B., Wincker, P., Xing, Y., Yang, L., Yao, Z., Ying, F., Zhai, J., Zhou, L., Zuber, A., Dénarié, J., Dixon, R.A., May, G.D., Schwartz, D.C., Rogers, J., Qué-tier, F., Town, C.D., Roe, B.A., 2011. The Medicago genome provides insight into the evolution of rhizobial symbioses. *Nature* 480, 520–524.
- Yu, B., Yang, Z., Li, J., Minakhina, S., Yang, M., Padgett, R.W., Steward, R., Chen, X., 2005. Methylation as a crucial step in plant microRNA biogenesis. *Science* 307, 932–935.
- Zamore, P.D., Tuschl, T., Sharp, P.A., Bartel, D.P., 2000. RNAi: double-stranded RNA directs the ATP-dependent cleavage of mRNA at 21 to 23 nucleotide intervals. *Cell* 101, 25–33.
- Zavaliev, R., Levy, A., Gera, A., Epel, B.L., 2013. Subcellular dynamics and role of Arabidopsis β -1,3-Glucanases in cell-to-cell movement of tobamoviruses. *Mol Plant Microbe Interact* 26, 1016–30.
- Zhai, J., Jeong, D.H., De Paoli, E., Park, S., Rosen, B. D., Li, Y., González, A.J., Yan, Z., Kitto, S.L., Grusak, M.A., Jackson, S.A., Stacey, G., Cook, D.R., Green, P.J., Sherrier, D.J., Meyers, B.C., 2011. MicroRNAs as master regulators of the plant NB-LRR defense gene family via the production of phased, trans-acting siRNAs. *Genes Dev* 25, 2540–2553.
- Zhang, H., Liu, W.Z., Zhang, Y., Deng, M., Niu, F., Yang, B., Wang, X., Wang, B., Liang, W., Deyholos, M.K., Jiang, Y.Q., 2014. Identification, expression and interaction analyses of calcium-dependent protein kinase (CPK) genes in canola (*Brassica napus* L.). *BMC Genomics* 15, 211.
- Zhang, H., Xia, R., Meyers, B.C., Walbot, V., 2015. Evolution, functions, and mysteries of plant ARGONAUTE proteins. *Curr Opin Plant Biol*, 27 84–90.
- Zhang, W., Kollwig, G., Stecyk, E., Apelt, F., Dirks, R., Kragler, F., 2014. Graft-transmissible movement of inverted-repeat-induced siRNA signals into flowers. *Plant J* 80, 106–121.
- Zhang, X., Yuan, Y.R., Pei, Y., Lin, S.S., Tuschl, T., Patel, D.J., Chua, N.H., 2006. *Cucumber mosaic virus*-encoded 2b suppressor inhibits Arabidopsis Argonaute 1 cleavage activity to counter plant defense. *Genes Dev* 20, 3255–3268.
- Zhang, Z., Krainer, A.R., 2004. Involvement of SR proteins in mRNA surveillance. *Mol Cell* 16, 597–607.
- Zhang, Z., Zhang, X., 2012. Argonautes compete for miR165/166 to regulate shoot apical meristem development. *Curr Opin Plant Biol* 15, 652–658.
- Zheng, X., Zhu, J., Kapoor, A., Zhu, J.K., 2007. Role of Arabidopsis AGO6 in siRNA accumulation, DNA methylation and transcriptional gene silencing. *EMBO* 26, 1691–1701.

-
- Zheng, Y., Wang, Y., Wu, J., Ding, B., Fei, Z., 2015. A dynamic evolutionary and functional landscape of plant phased small interfering RNAs. *BMC Biol* 13, 32.
- Zhu, H., Hu, F., Wang, R., Zhou, X., Sze, S.H., Liou, L. W., Barefoot, A., Dickman, M., Zhang, X., 2011. *Arabidopsis* Argonaute 10 specifically sequesters miR166/165 to regulate shoot apical meristem development. *Cell* 145, 242–256.
- Zhu, H., Xia, R., Zhao, B., An, Y.Q., Dardick, C.D., Callahan, A.M., Liu, Z., 2012. Unique expression, processing regulation, and regulatory network of peach (*Prunus persica*) miRNAs. *BMC Plant Biol*, 12, 149.
- Zorzatto, C., MacHado, J.P.B., Lopes, K.V.G., Nascimento, K.J.T., Pereira, W.A., Brustolini, O.J.B., Reis, P.A.B., Calil, I.P., Deguchi, M., Sachetto-Martins, G., Gouveia, B.C., Loriato, V.A.P., Silva, M.A.C., Silva, F.F., Santos, A.A., Chory, J., Fontes, E.P.B., 2015. NIK1-mediated translation suppression functions as a plant antiviral immunity mechanism. *Nature* 520, 679–82.
- Zwicker, S., Mast, S., Stos, V., Pfitzner, A.J., Pfitzner, U.M., 2007. Tobacco NIMIN2 proteins control PR gene induction through transient repression early in systemic acquired resistance. *Mol Plant Pathol* 8, 385-400.

**APPENDIX 1: SUPPLEMENTARY FIGURES AND TABLES OF DRAFT MANUSCRIPT:
“VIRUS- AND HOST-DERIVED SMALL RNAS COORDINATE INFECTION IN OILSEED
RAPE” BY PITZALIS ET AL.**

Supplementary Figures:

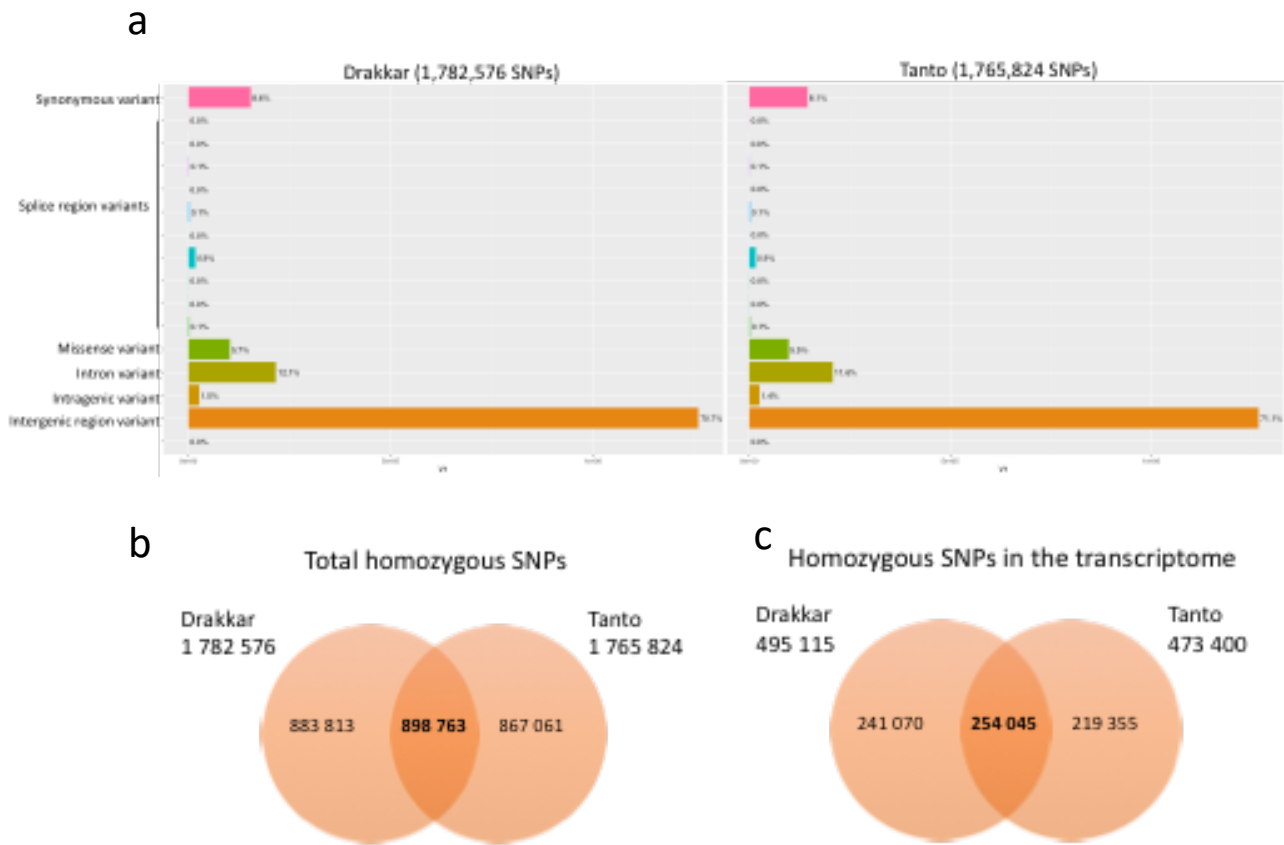


Fig. S1. Homozygous SNPs by which *B. napus* cvs. Drakkar and Tanto differ from the reference sequence of *B. napus* cv. Darmor-bzh. **a**, Distribution of SNP categories. Most SNPs are from intergenic regions. **b**, Total homozygous SNPs that are shared by or specific to the Drakkar and Tanto cultivars. **c**, Homozygous SNPs that map to transcribed genes and are either shared by or specific to the Drakkar and Tanto cultivars respectively.

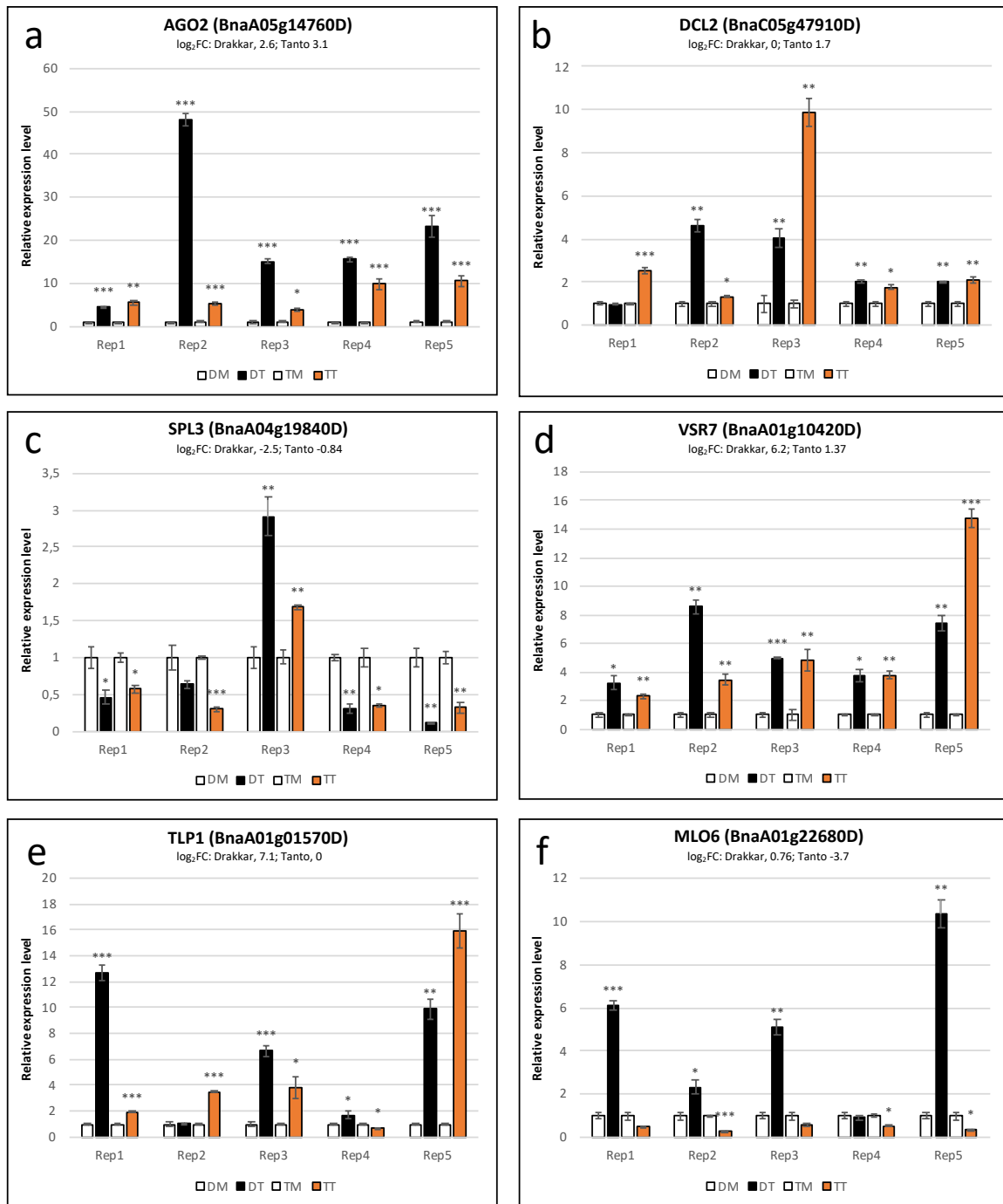


Fig. S2. Confirmation of RNAseq-based DEseq data by q-RT-PCR. Relative expression levels in local sites of virus-infected leaves in comparison to expression levels in mock-control tissues (set to 1) are shown. qRT-PCR assays were performed with original polyA RNA used for RNAseq (Rep1) as well as with polyA RNA isolated from new biological samples derived from four new independent experiments (Rep2-Rep5). **a**, RNAseq-based DEseq data indicated that a transcript for AGO2 (BnaA05g14760D) is induced by TuMV infection in both Drakkar (fold change [\log_2]: 2.6) and Tanto (fold change [\log_2]: 3.1). This upregulation in both cultivars is confirmed by qRT-PCR using independent RNA samples derived from the five independent experiments Rep1-Rep5. **b**, RNAseq-based DEseq data indicated that a transcript for DCL2 (BnaC05g47910D) is induced by TuMV

infection in Tanto (fold change [\log_2]: 1.7) but not in Drakkar RNAseq-based (fold change [\log_2]: 0.0). This upregulation Tanto is confirmed by qRT-PCR using independent RNA samples derived from the five independent experiments Rep1-Rep5. However, unlike the original sample (Rep1), samples Rep2-Rep5 indicate that DCL2 may also be virus-induced in Drakkar. **c**, RNAseq-based DEseq data indicated that a transcript for SPL3 (BnaA04g19840D) is downregulated by TuMV infection in both Drakkar (fold change [\log_2]: -2.5) and Tanto (fold change [\log_2]: -0.84). This downregulation in both cultivars is confirmed by qRT-PCR with samples from all replicative experiments except Rep3. **d**, RNAseq-based DEseq data indicated that a transcript for VSR7 (BnaA01g10420D) is induced by TuMV infection in both Drakkar (fold change [\log_2]: 6.2) and Tanto (fold change [\log_2]: 1.37). This induction in both cultivars is confirmed by qRT-PCR with samples from all replicative experiments. **e**, RNAseq-based DEseq data indicated that a transcript for TLP1 (BnaA01g01570D) is induced by TuMV infection in Drakkar (fold change [\log_2]: 7.1) but not in Tanto (fold change [\log_2]: 0.0). qRT-PCR analysis confirms the strong induction of this gene in Drakkar, although the induction is lower in the new repetitive samples. The RT-qPCR experiments also confirm a low or absent induction of this gene in Tanto, except in the Rep5 sample. **f**, RNAseq-based DEseq data indicated that a transcript for MLO6 (BnaA01g22680D) is induced by TuMV infection in Drakkar (fold change [\log_2]: 0.76) and suppressed in Tanto (fold change [\log_2]: -3.7). qRT-PCR analysis confirms the strong induction of this gene in Drakkar (except in Rep4), and the suppression of this gene in Tanto.

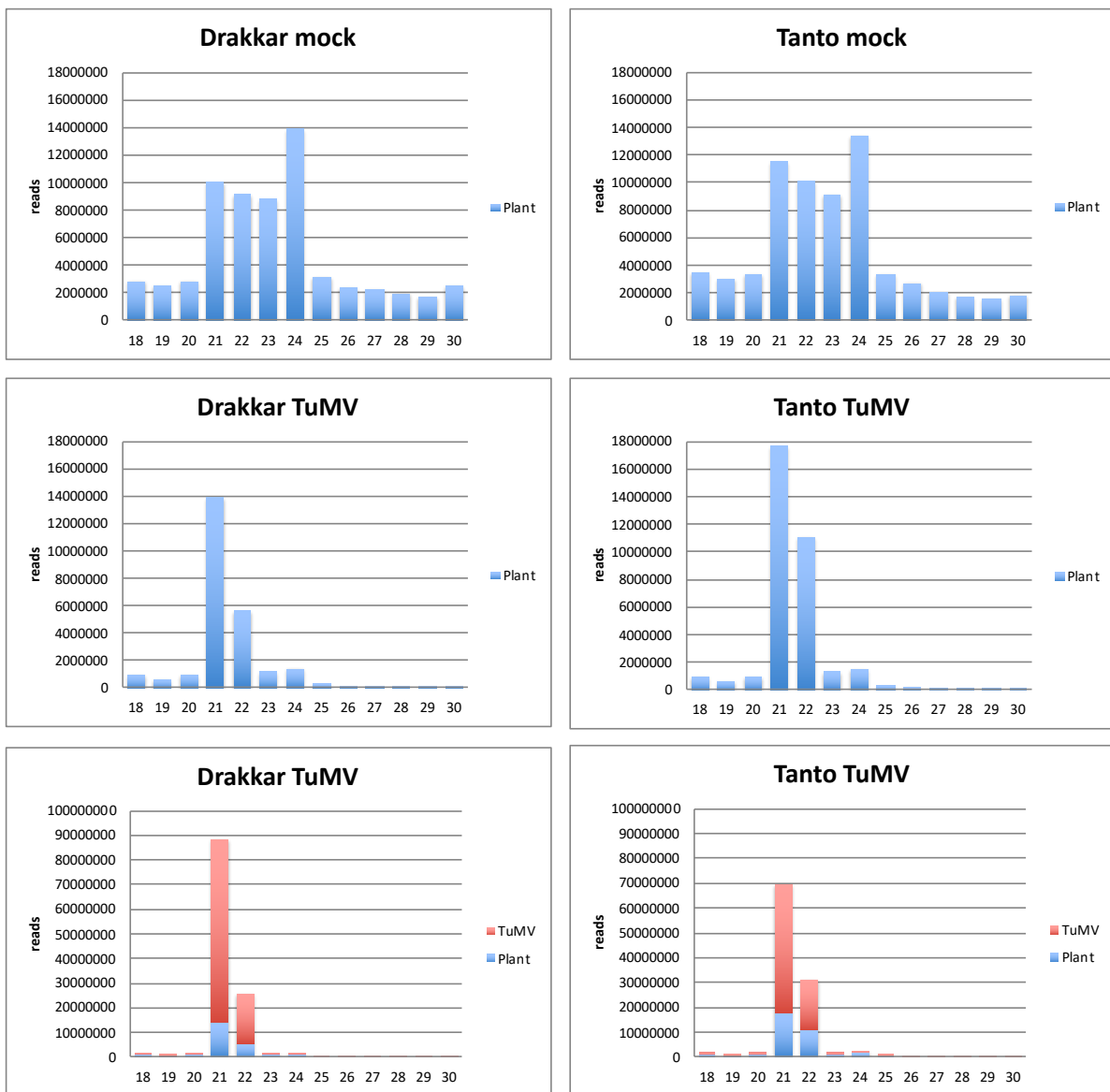


Fig. S3. Small RNA size distribution before and after TuMV infection in Drakkar and Tanto. Sizes of sRNAs within local infection sites in leaves and mock-treated control samples. The sRNA size distribution is very similar between Drakkar and Tanto. Panels at the top show the distribution of sRNAs in mock-treated control samples. The panels in the middle and at the bottom show the distribution of sRNAs within local infection sites. The panels in the middle show the sRNA size distribution only for host sRNAs, whereas the panels at the bottom show the size distribution for both host and viral sRNA. In comparison to the panels at the top, the panels in the middle illustrate the impact of virus infection on the host sRNA profile.

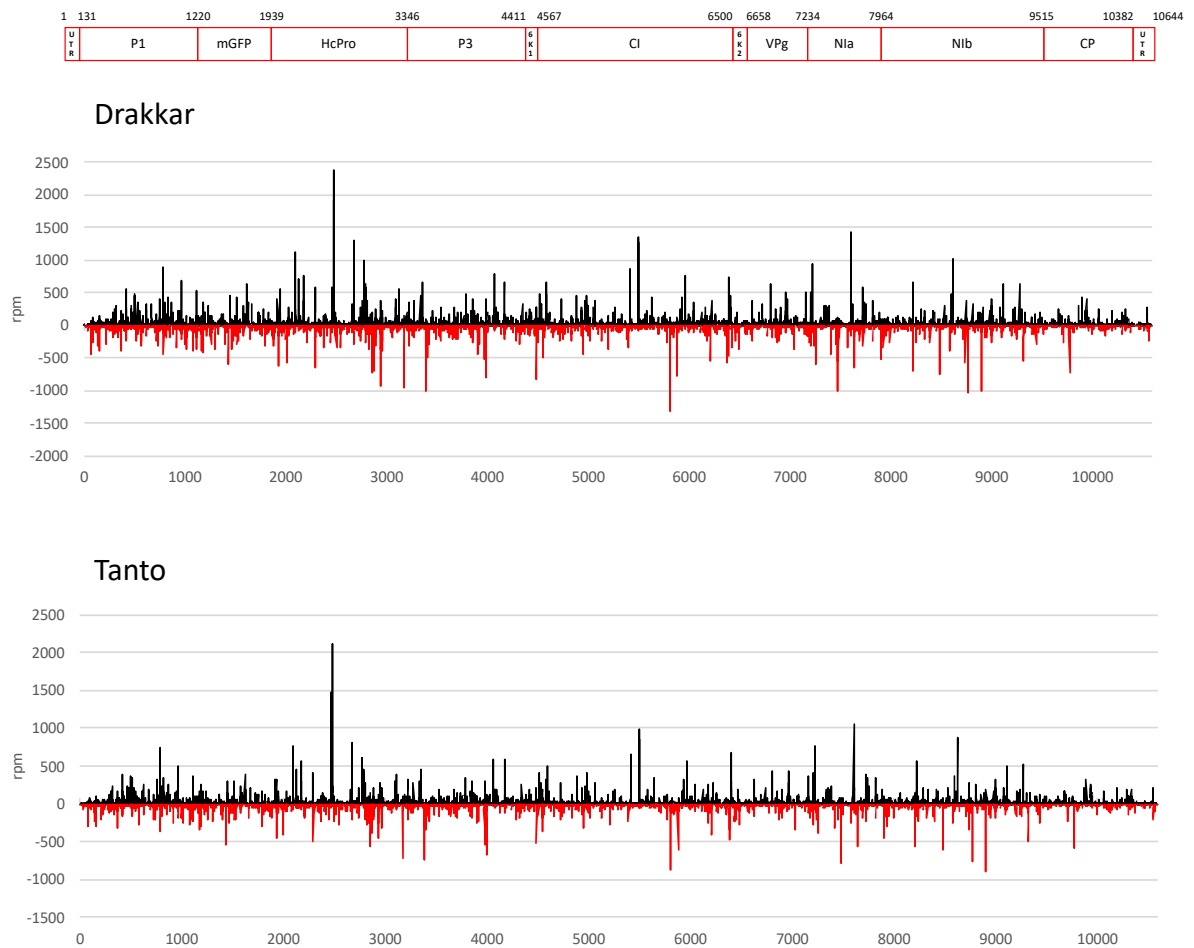


Fig. S4. Alignment of vsRNAs to the TuMV genome. The pattern of vsRNA shows the origin of vsRNAs derived from DCL cleavage of viral dsRNA. All reads were mapped without mismatch to the 10644 bases long viral RNA. vsRNA reads derived from the viral (+) strand are shown in black; vsRNA reads derived from the viral (-) strand are shown in red. The UTRs and protein-coding regions of the viral RNA are shown at the top of the figure.

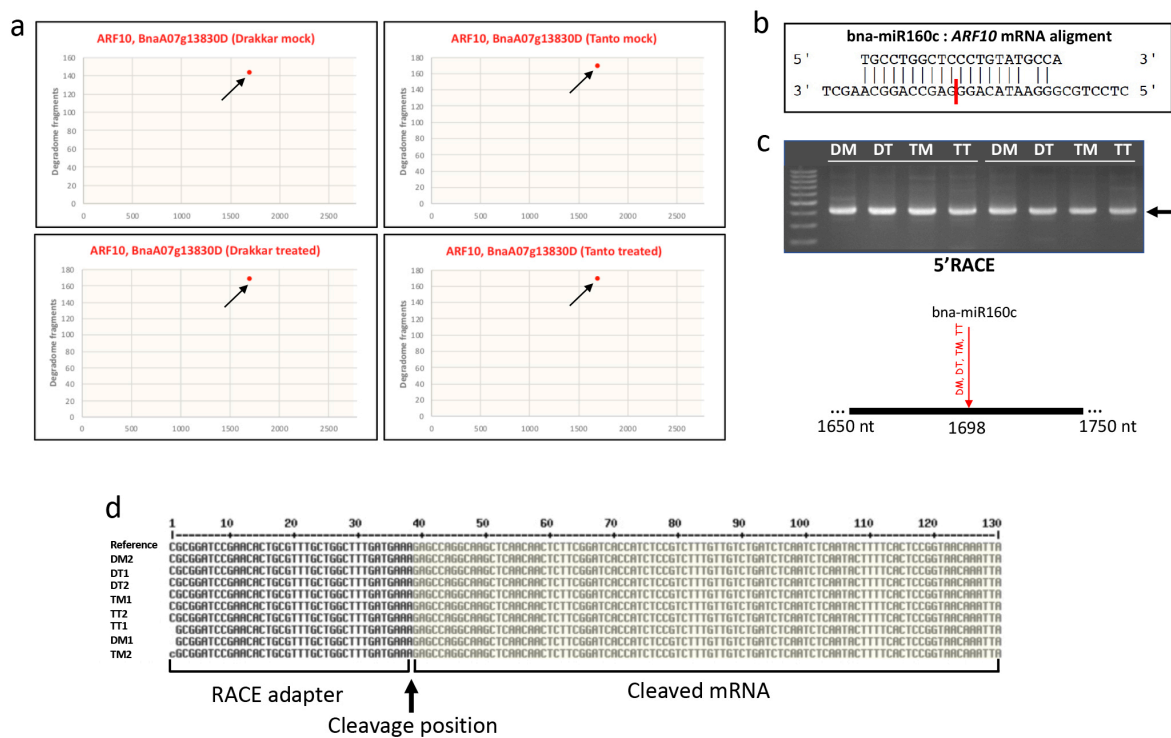


Fig. S5. Targeting of *ARF10* mRNA by *bna-miR160c*. **a**, Targeting of *ARF10* mRNA by *bna-miR160c* produced a highly defined PAREseq degradome signature (arrow) in mock (DM, TM) as well as infected Drakkar (DT) and Tanto (TT) samples. The T-plots generated by PAREsnip show the total number of degradome fragments (y axis) found for *ARF10* mRNA in the three replicate samples per condition analyzed by PAREseq and their mapping along the length of the *ARF10* mRNA (z-axis). **b**, Alignment of *bna-miR160c* to the *ARF10* mRNA by PAREsnip. The cleavage site within the miRNA:mRNA target pair behind nucleotide 1698 of the mRNA is indicated by a red line. **c**, 5' RACE analysis of independent biological samples confirmed the exact cleavage site at position 1698 of the transcript. The electrophoresis gel shows the RACE DNA fragment of corresponding size (arrow). **d**, Verification of the cleavage site by DNA sequencing of the RACE DNA fragment.

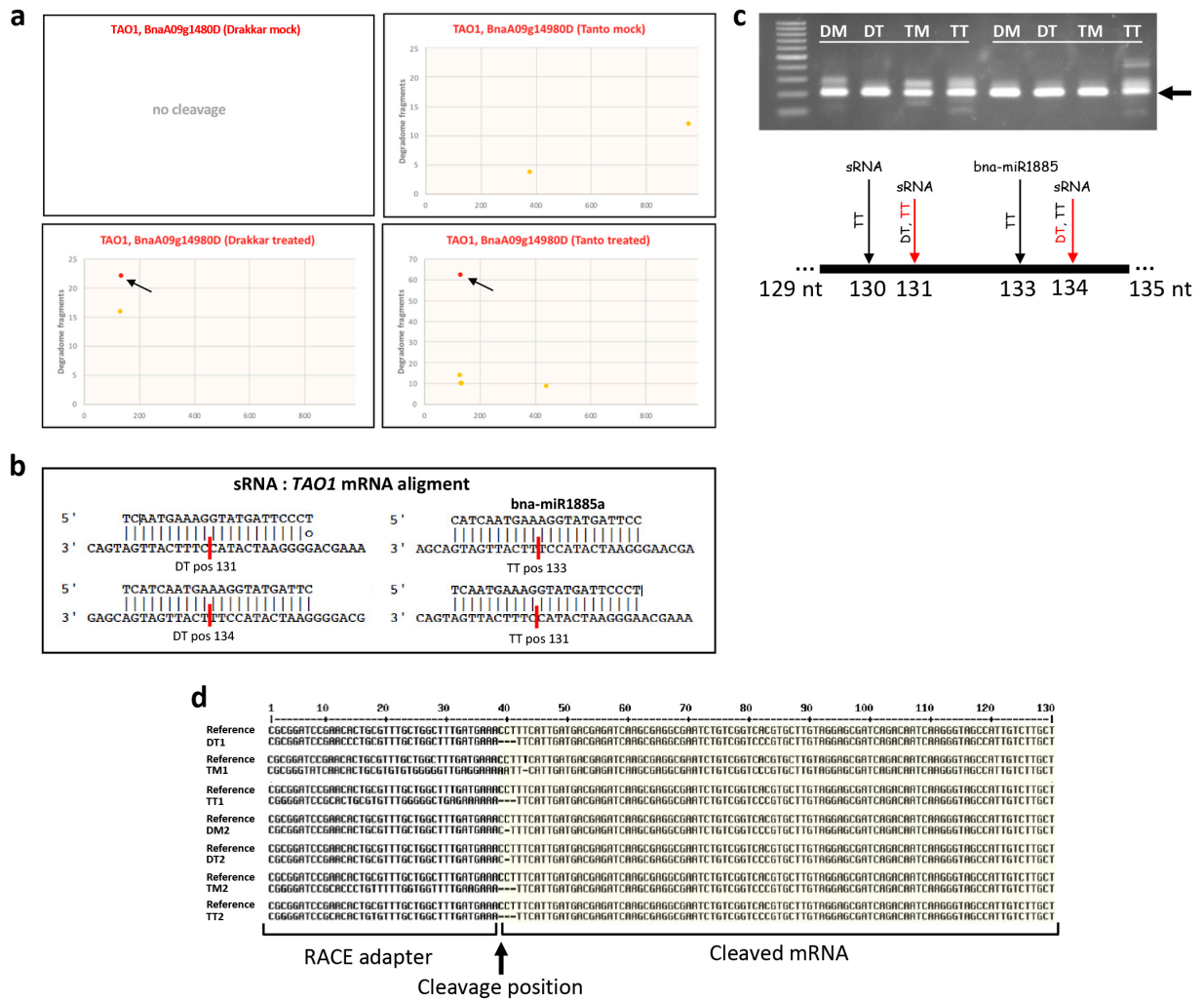


Fig. S6. Targeting of *Target of Avtb Operation 1 (TAO1)* mRNA by *bna-miR1885a* and related sRNAs. **a**, Targeting of *TAO1* mRNA by *bna-miR1885a* produced a highly defined PAREseq degradome signature (arrow) in TM as well as infected Drakkar (DT) and Tanto (TT) samples. The T-plots generated by PAREsnip show the total number of degradome fragments (y axis) found for *TAO1* mRNA in the three replicate samples per condition analyzed by PAREseq and their mapping along the length of the *TAO1* mRNA (z-axis). **b**, Alignment of *bna-miR1885a* and related siRNAs to the *TAO1* mRNA by PAREsnip. The specific cleavage sites within the miRNA:mRNA target pair behind nucleotide positions 131-134 of the mRNA are indicated by a red line. **c**, 5' RACE analysis of independent biological samples confirmed the exact cleavage sites at these positions of the transcript. Cleavage sites shown in red are the most dominant category 0 cleavage events indicated by the red dots and arrows in **(a)**. The electrophoresis gel shows the RACE DNA fragment of corresponding size (arrow). **d**, The specific cleavage sites were confirmed by DNA sequencing of the RACE DNA fragment.

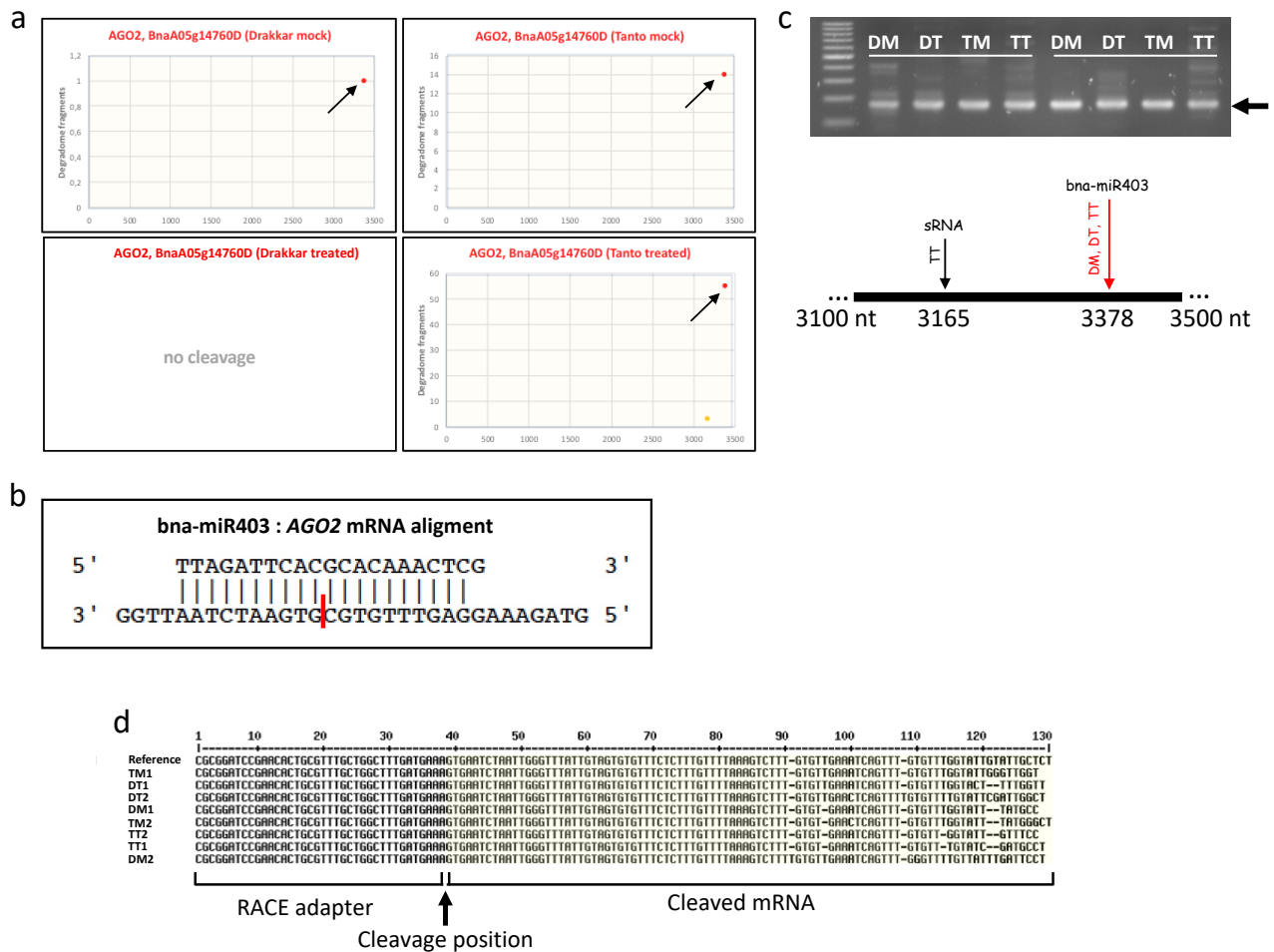


Fig. S7. Targeting of AGO2 mRNA by bna-miR403. **a**, Targeting of AGO2 mRNA by bna-miR403 produced a highly defined PAREseq degradome signature (arrow) in mock (DM, TM) as well as infected Tanto (TT) samples. The T-plots generated by PAREsnip show the total number of degradome fragments (y axis) found for AGO2 mRNA in the three replicate samples per condition analyzed by PAREseq and their mapping along the length of the AGO2 mRNA (z-axis). **b**, Alignment of bna-miR403 to the AGO2 mRNA by PAREsnip. The specific cleavage site within the miR403:AGO2mRNA pair behind nucleotide positions 3378 of the mRNA is indicated by a red line. **c**, 5' RACE analysis of independent biological samples confirmed the exact cleavage sites at this position of the transcript. The cleavage sites shown in red is the most dominant category 0 cleavage event indicated by the red dots and arrow in **(a)**. The electrophoresis gel shows the RACE DNA fragment of corresponding size (arrow). PAREsnip analysis indicates a second cleavage site at position 3165 of the *Ago2* mRNA. **d**, The specific cleavage site at position 3378 was confirmed by DNA sequencing of the RACE DNA fragment.

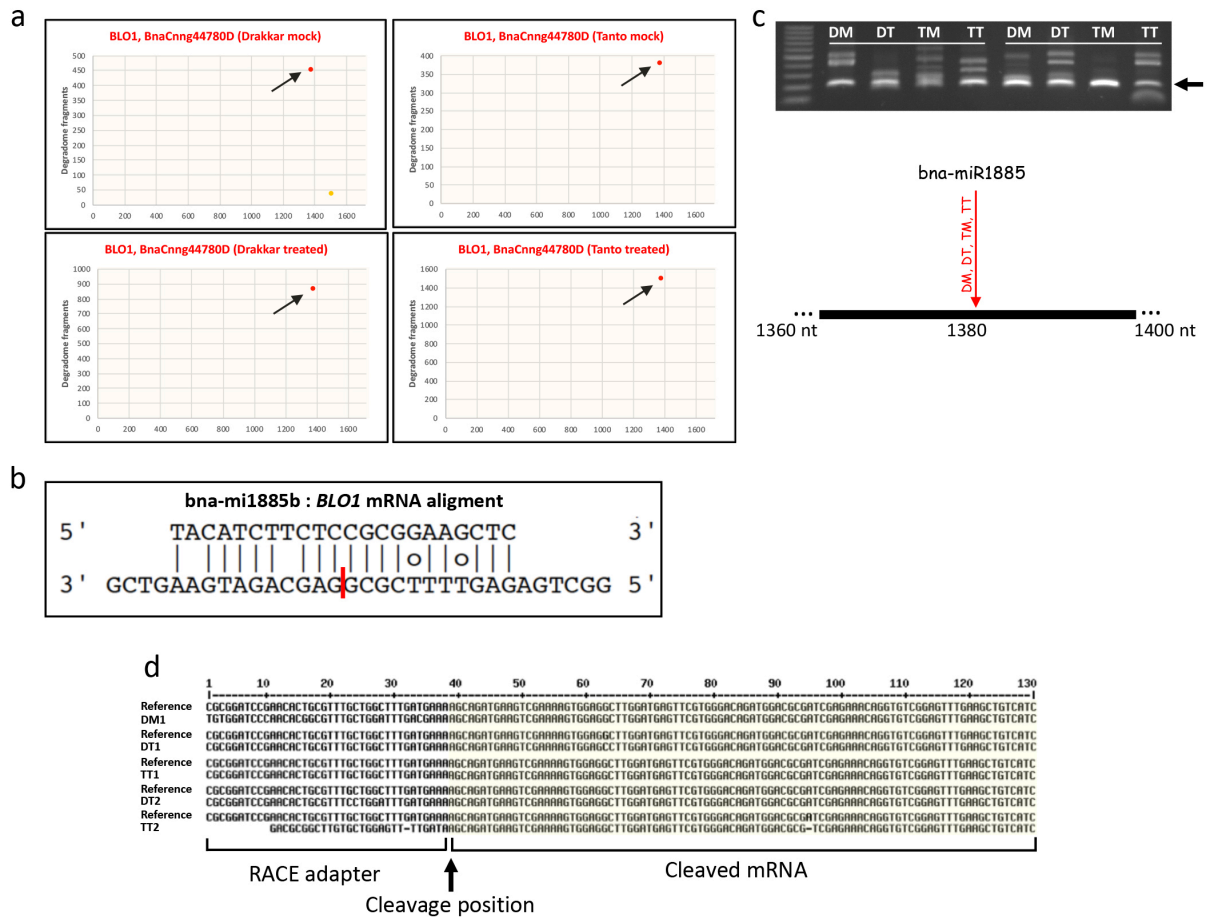


Fig. S8. Targeting of *Biogenesis of Lysosome-related organelles complex 1 subunit 2 (BLOS2)* mRNA by *bna-miR1885b*. **a**, Targeting of *BLOS2* mRNA by *bna-miR1885b* produced a highly defined PAREseq degradome signature (arrow) in mock (DM, TM) and infected (DT, TT) samples. The T-plots generated by PAREsnip show the total number of degradome fragments (y axis) found for *BLOS2* mRNA in the three replicate samples per condition analyzed by PAREseq and their mapping along the length of the *BLOS2* mRNA (z-axis). **b**, Alignment of *bna-miR1885b* to the *AGO2* mRNA by PAREsnip. The specific cleavage site within the miR1885b:*AGO2*mRNA pair behind nucleotide positions 1380 of the mRNA is indicated by a red line. **c**, 5' RACE analysis of independent biological samples confirmed the exact cleavage sites at this position of the transcript. The cleavage sites shown in red is the most dominant category 0 cleavage event indicated by the red dots and arrow in (**a**). The electrophoresis gel shows the RACE DNA fragment of corresponding size (arrow). **d**, The specific cleavage site at position 1380 of the mRNA was confirmed by DNA sequencing of the RACE DNA fragment.

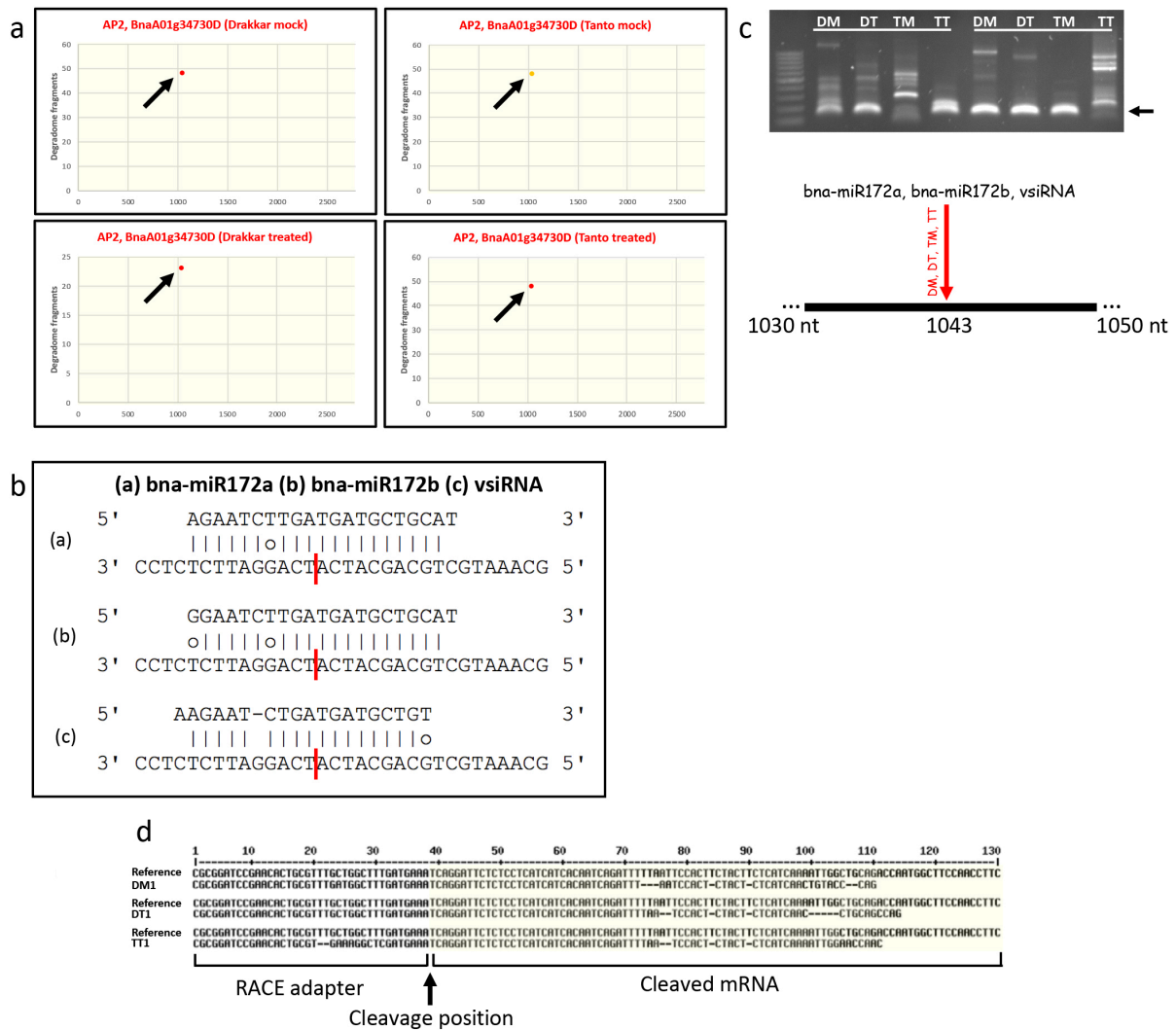


Fig. S9. Targeting of *AP2* mRNA by *bna-miR172a*, *bna-miR172b* and TuMV *vsiRNA*. **a**, Cleavage of *APETALA2* (*AP2*) mRNA produced a highly defined PAREseq degradome signature (arrow) in mock (DM, TM) and infected (DT, TT) samples. The T-plots generated by PAREsnip show the total number of degradome fragments (y axis) found for *AP2* mRNA in the three replicate samples per condition analyzed by PAREseq and their mapping along the length of the *AP2* mRNA (z-axis). **b**, *AP2* cleavage by *bna-miR172a*, *bna-miR172b* and a specific TuMV *vsiRNA*s. The alignment of *bna-miR172a*, *bna-miR172b* and *vsiRNA* to the *AP2* mRNA by PAREsnip is shown. The specific cleavage site associated with the three target pairs and its location behind nucleotide positions 1043 of the mRNA is indicated by a red line. **c**, 5' RACE analysis of independent biological samples confirmed the exact cleavage sites at this position of the transcript. The cleavage sites shown in red is the category 0 cleavage event indicated by the red dots and arrow in (a). The electrophoresis gel shows a RACE DNA fragment of corresponding size (arrow). **d**, The specific cleavage site at position 1043 of the mRNA was confirmed by DNA sequencing of the RACE DNA fragment.

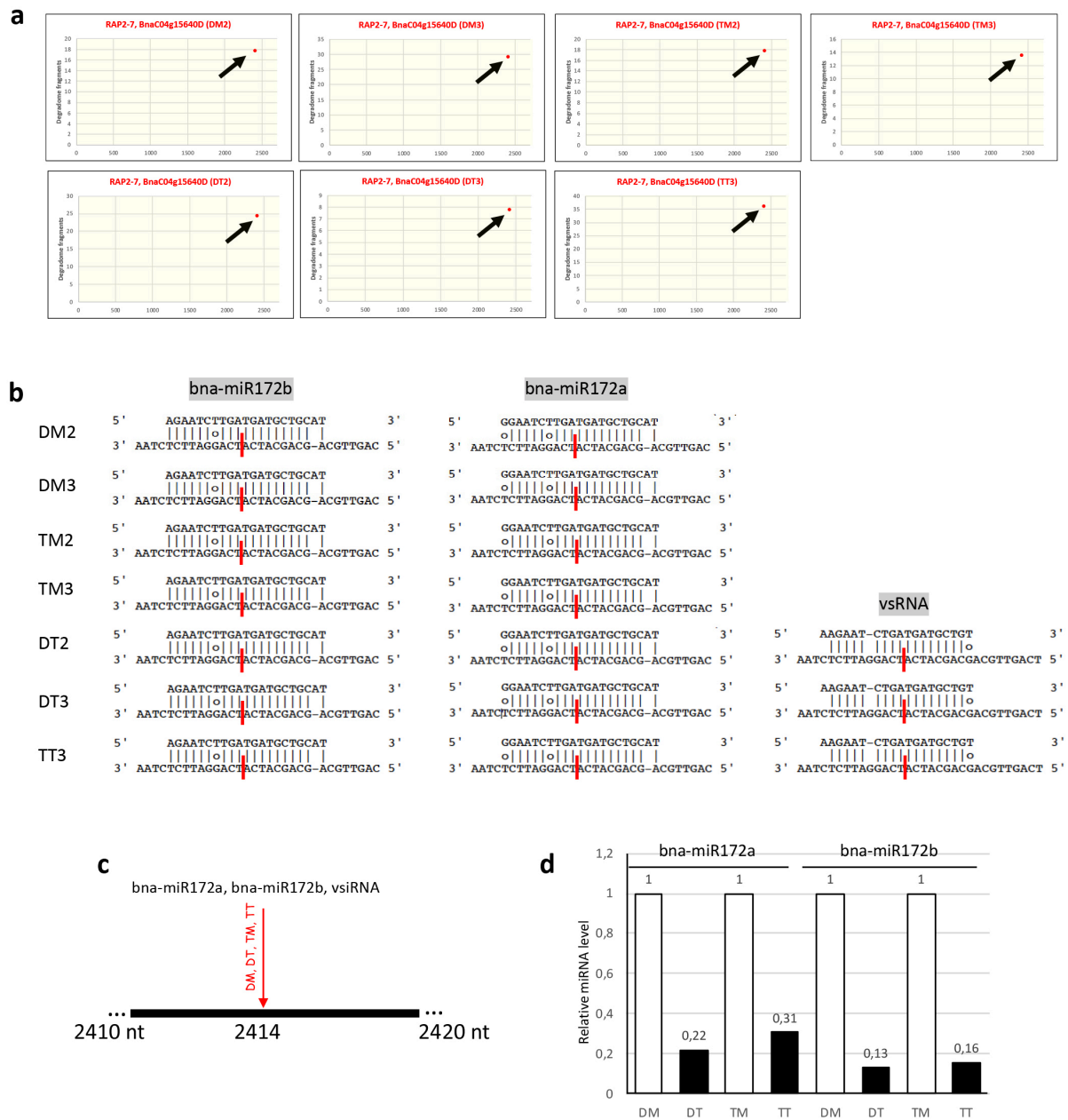


Fig. S10. Targeting of ERF *RAP2-7* mRNA by *bnamiR172a*, *bnamiR172b*, and TuMV vsRNA. Cleavage of *RAP2-7* mRNA produced a highly defined PAREseq degradome signature (arrow) in the seven PARE analysis replicates (DM2, DM3, DT2, DT3, TM2, TM3, TT3). The T-plots generated by PAREsnip show the total number of degradome fragments (y axis) found for *RAP2-7* mRNA in these samples in alignment along the length of the *RAP2-7* mRNA (z-axis). **b**, *RAP2-7* mRNA cleavage by *bnamiR172a*, *bnamiR172b* and a specific TuMV vsRNA. The alignment of *bnamiR172a*, *bnamiR172b* and the vsRNA to the *RAP2-7* mRNA as identified by PAREsnip analysis in the respective PARE analysis sample shown. As expected, the vsRNA:*RAP2-7* mRNA target pair occurred only in the infected samples (DT2, DT3, TT3). The specific cleavage site in the mRNA is indicated by a red line **c**, location of the specific cleavage site at nucleotide positions 2414. **d**, Levels of *bnamiR172a*

and *bnamiR172b* in the different samples, as determined by sRNAseq. Infection causes a strong reduction in the levels of these miRNAs. Cleavage of the same mRNA target by vsiRNA may complement this reduction in miR172 levels to maintain control over the expression of *RAP2-7*.

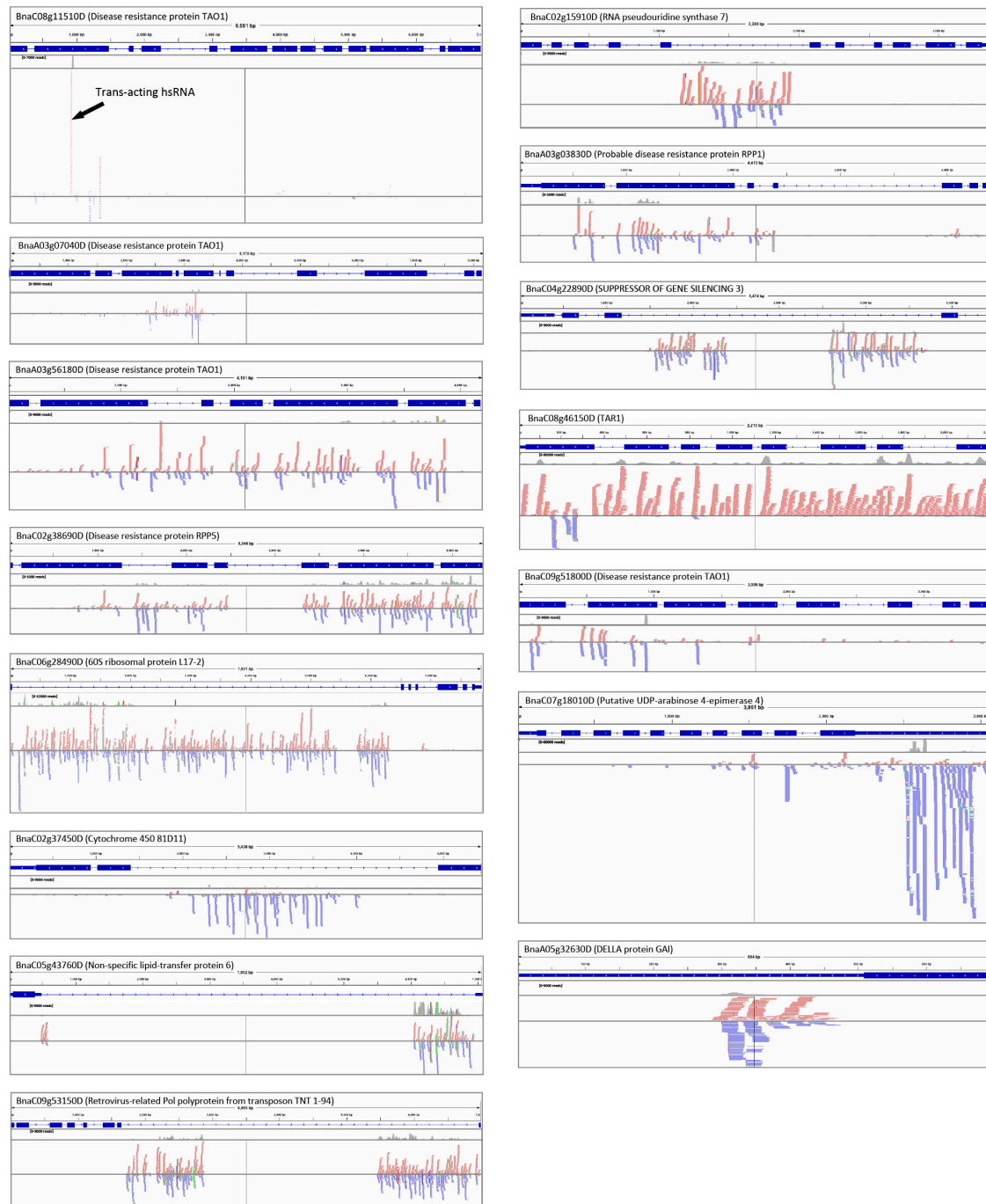


Fig. S11. Examples of host genes that produce trans-acting siRNAs associated with antiviral vRNA cleavage. The different panels show the identity of the host siRNA (hsRNA)-producing gene, the exon-intron structure of the mRNA and the alignment of hsRNAs to the mRNA. The panels show hsRNAs from mock-treated Drakkar samples. Thus, unlike va-phasiRNAs, the hsRNAs shown here

are expressed before infection. hsRNAs that target TuMV RNA for cleavage may constitute an antiviral defense layer that is already active before infection.

Supplementary Tables:

Table S1. RNAseq, sRNAseq, and PAREseq read and mapping statistics

RNAseq		Tophat 1mm			
sample	raw read pairs	read pairs after filtering	mapped to Drakkar transcriptome (%)	mapped to Tanto transcriptome (%)	mapped to virus (%)
DM1	43 912 453	41058168 (93.5%)	83.5%		
DM2	72 061 780	63849830 (88.6%)	84.9%		
DM3	77 108 467	69053540 (89.6%)	85.2%		
DT1	56 371 395	52684838 (93.5%)	82.7%		1.00%
DT2	79 992 678	71436541 (89.3%)	84.2%		0.90%
DT3	81 059 545	72219626 (89.1%)	83.4%		1.10%
TM1	52 507 664	49215556 (93.7%)		84.5%	
TM2	78 864 932	70708215 (89.7%)		85.1%	
TM3	80 875 384	72703910 (89.9%)		86.1%	
TT1	37 860 785	35427931 (93.6%)		83.3%	0.90%
TT2	74 880 253	66737776 (89.1%)		84.3%	0.80%
TT3	70 132 740	61864732 (88.2%)		84.3%	0.80%

sRNAseq		bowtie2 -t -N 0 --end-to-end --very-sensitive --score-min C,0,0			
sample	raw reads	reads after filtering	mapped to Drakkar transcriptome (%)	mapped to Tanto transcriptome (%)	mapped to virus (%)
DM1	56 025 255	27037795 (48.3%)	48.59%		0.01%
DM2	48 296 781	29994399 (62.1%)	41.92%		0.02%
DM3	66 801 262	49791620 (74.5%)	47.64%		0.06%
DT1	53 665 478	51503121 (96.0%)	13.38%		68.23%
DT2	50 094 688	42003172 (83.8%)	15.25%		64.56%
DT3	54 154 789	49288670 (91.0%)	14.30%		65.28%
TM1	56 422 412	40102411 (71.1%)		48.74%	0.01%
TM2	53 210 994	37955105 (71.3%)		44.33%	0.02%
TM3	56 518 524	36275037 (64.2%)		45.62%	0.06%
TT1	54 042 539	51476472 (95.3%)		21.27%	54.24%
TT2	40 112 100	34302205 (85.5%)		21.85%	52.24%
TT3	57 396 907	52282103 (91.1%)		21.99%	50.91%

PAREseq		bowtie2 -t -N 0 --end-to-end --very-sensitive --score-min C,0,0			
sample	raw reads	reads after filtering	mapped to Drakkar transcriptome (%)	mapped to Tanto transcriptome (%)	mapped to virus (%)
DM1	39 360 296	33032811 (83.9%)	15.76%		0.56%
DM2	10 330 179	7596192 (73.5%)	66.07%		0.00%
DM3	19 291 097	15995324 (82.9%)	72.80%		0.03%
DT1	31 138 488	26715785 (85.8%)	25.05%		2.36%
DT2	14 934 860	11254877 (75.4%)	57.97%		9.13%
DT3	27 356 001	22031176 (80.5%)	68.46%		8.23%
TM1	36 739 520	30524077 (83.1%)		66.68%	3.94%
TM2	8 138 303	6283685 (77.2%)		69.28%	0.00%
TM3	20 196 721	16981513 (84.1%)		74.20%	0.02%
TT1	37 590 376	33071083 (88.0%)		64.50%	0.89%
TT2	10 172 194	7663383 (75.3%)		61.07%	4.36%
TT3	25 146 645	21606965 (85.9%)		60.70%	6.62%

Table S2. DNA resequencing statistics

	Sequencing			Mapping to Darmor			Variant calling					
	read length (bases)	clean reads	mapped reads	% mapped	properly paired reads	% properly mapped	Raw SNPs	Good SNPs	Homozygous SNPs	heterozygous SNPs	Raw Indels	Good Indels
Drakkar	150	122 831 012	120 977 458	98.49	107 240 576	87.31	3 716 045	3 452 779	1 782 576 (1.5 np/kb)	1 670 203	767 119	714 714
Tanto	150	122 855 282	119 497 306	97.27	106 738 002	86.88	3 625 707	3 388 281	1 765 824 (1.5 snp/kb)	1 622 457	751 700	705 132

Table S3. Genes that are most strongly and significantly regulated within sites of local TuMV infection in both Drakkar and Tanto leaves.

	Foldchange (log ₂)		% identity			
	Drakkar	Tanto	UniProt	Drakkar	Tanto	Annotation
BnaA02g31430D	6.53	8.18	CB60G_ARATH	71.73	71.20	Calmodulin-binding protein 60 G
BnaA02g26270D	5.97	7.49	PP2B1_ARATH	56.73	56.74	F-box protein PP2-B1
BnaA02g12230D	5.89	7.41	unknown	-	-	-
BnaA02g04960D	5.52	7.28	GL33_ARATH	92.89	92.89	Germin-like protein subfamily 3 member 3
BnaA02g06790D	5.40	6.78	ZAT12_ARATH	84.76	85.37	Zinc finger protein ZAT12
BnaA01g35960D	4.90	6.42	DF206_ARATH	62.50	62.50	Defensin-like protein 206
BnaA01g35950D	4.86	6.16	DF207_ARATH	62.50	62.50	Defensin-like protein 207
BnaA01g34060D	4.81	6.00	BGL25_ARATH	91.76	91.77	Probable inactive beta-glucosidase 25
BnaA01g31270D	4.74	5.79	RLP12_ARATH	43.27	43.05	Receptor-like protein 12
BnaA01g34050D	4.61	5.57	BGL25_ARATH	67.34	67.34	Probable inactive beta-glucosidase 25
BnaA01g14050D	4.52	5.51	NBR1_ARATH	74.29	74.29	Protein NBR1 homolog
BnaA01g15320D	4.28	5.19	unknown	#N/A	#N/A	Unknown
BnaA01g05320D	4.14	4.82	RD19A_ARATH	93.75	93.75	Cysteine proteinase RD19a
BnaA01g26340D	4.03	4.64	MHCKB_DICDI	27.08	27.91	Myosin heavy chain kinase B
BnaA01g14380D	-5.45	-4.64	unknown	-	-	-
BnaA01g11840D	-5.39	-4.64	APR3_ARATH	92.60	92.60	5'-adenylsulfate reductase 3, chloroplastic
BnaA01g12340D	-5.34	-4.56	SAU36_ARATH	40.51	40.51	Auxin-responsive protein SAUR36
BnaA01g11780D	-5.06	-4.47	unknown	#N/A	#N/A	Unknown
BnaA01g13280D	-4.62	-4.41	COR13_ARATH	83.48	84.35	Cystine lyase COR13
BnaA01g10740D	-4.39	-4.35	CASL1_CANSA	43.27	43.28	Cannabidiolic acid synthase-like 1
BnaA01g06540D	-4.33	-4.32	GGP1_ARATH	84.55	84.55	Gamma-glutamyl peptidase 1
BnaA01g05120D	-4.33	-4.30	IGMT4_ARATH	50.96	50.96	Indole glucosinolate O-methyltransferase 4
BnaA01g05540D	-4.31	-4.23	SK2_ARATH	50.96	50.96	Shikimate kinase 2, chloroplastic
BnaA01g05060D	-4.18	-4.18	WRK18_ARATH	73.10	73.10	WRKY transcription factor 18

These genes respond significantly to TuMV infection in both Drakkar and Tanto. The fold-change values (log₂) represent significant differences between transcript levels within infection sites and transcript levels in mock-treated tissue samples (p-value: <0.05). These values are based on three independent infection experiments (biological replicates) for both Drakkar and Tanto. In each experiment, transcripts were detected with at least 150 mean reads. Only genes with strongest fold-changes ($|\log_2| \geq +4 / -4$) are shown.

Table S4: Genes that are most strongly and significantly regulated within sites of local TuMV infection in Tanto leaves but not in Drakkar leaves. These genes respond significantly to TuMV infection in Tanto but not in Drakkar. The fold-change values (\log_2) represent significant differences between transcript levels within infection sites and transcript levels in mock-treated tissue samples (p-value: <0.05). These values are based on three independent infection experiments (biological replicates) for both Drakkar and Tanto. In each experiment, transcripts were detected with at least 150 mean reads. Only genes with strongest fold-changes ($[\log_2] \geq +4 / -4$) are shown.

	Foldchange (\log_2)	UniProt	% identity	Annotation
BnaA01g00520D	8.30	C81F1_ARATH	83.63	Cytochrome P450 81F1
BnaA01g05280D	8.28	DTX47_ARATH	61.157	Protein DETOXIFICATION 47, chloroplastic
BnaA01g13360D	7.73	CHX17_ARATH	76.2	Cation/H(+) antiporter 17
BnaA01g15420D	7.40	PFKA3_ARATH	66.667	ATP-dependent 6-phosphofructokinase 3
BnaA01g33750D	6.52	TAO1_ARATH	58.311	Disease resistance protein TAO1
BnaA02g01560D	5.73	GH312_ARATH	87.547	4-substituted benzoates-glutamate ligase GH3.12
BnaA02g04040D	5.58	NC100_ARATH	83.696	NAC domain-containing protein 100
BnaA02g05170D	5.57	ALDO1_ARATH	78.508	Indole-3-acetaldehyde oxidase
BnaA02g05340D	5.52	CKX7_ARATH	89.024	Cytokinin dehydrogenase 7
BnaA02g09030D	5.50	unknown	-	-
BnaA02g10950D	5.38	ADF12_ARATH	94.253	Actin-depolymerizing factor 12
BnaA02g11760D	5.26	NRT31_ARATH	76.22	High-affinity nitrate transporter 3.1
BnaA02g13260D	5.11	YUID_BACSU	35	Uncharacterized membrane protein YuiD
BnaA02g15280D	5.09	DNJB6_XENTR	57.143	DnaJ homolog subfamily B member 6
BnaA02g17240D	5.08	C96AF_ARATH	54.237	Alkane hydroxylase MAH1
BnaA02g19960D	5.00	unknown	-	-
BnaA02g19970D	4.98	unknown	-	-
BnaA02g25150D	4.92	NIMI2_ARATH	76.147	Protein NIM1-INTERACTING 2
BnaA02g25550D	4.91	TDT_ARATH	89.46	Tonoplast dicarboxylate transporter
BnaA02g27620D	4.77	unknown	-	-
BnaA02g29990D	4.69	NSP5_ARATH	85.256	Nitrile-specifier protein 5
BnaA02g30040D	4.68	COL10_ARATH	68.584	Zinc finger protein CONSTANS-LIKE 10
BnaA02g31620D	4.51	PWD_ARATH	93.069	Phosphoglucan, water dikinase, chloroplastic
BnaA02g34380D	4.39	RGF9_ARATH	64.815	Root meristem growth factor 9
BnaA03g00550D	4.38	unknown	-	-
BnaA03g03700D	4.35	unknown	-	-
BnaA03g03710D	4.33	unknown	-	-
BnaA03g03740D	4.31	HS176_ARATH	89.677	17.6 kDa class II heat shock protein
BnaA03g05550D	4.30	FB244_ARATH	65.394	F-box protein At4g22390
BnaA03g12520D	4.23	unknown	-	-
BnaA03g13610D	4.16	PHF5B_ARATH	98.182	PHD finger-like domain-containing protein 5B
BnaA03g18980D	4.12	T5AT_TAXWC	31.735	Taxadien-5-alpha-ol O-acetyltransferase
BnaA03g19850D	4.10	SD16_ARATH	71.392	Receptor-like serine/threonine-protein kinase SD1-6
BnaA03g20310D	4.10	CHI4_BRANA	91.156	Basic endochitinase CHB4
BnaA01g00310D	-5.88	unknown	-	-
BnaA01g00740D	-5.11	YODA_ARATH	38.636	Mitogen-activated protein kinase kinase kinase YODA
BnaA01g10690D	-4.42	CML42_ARATH	81.579	Calcium-binding protein CML42
BnaA01g12860D	-4.25	PR1B1_ARATH	86.047	PRA1 family protein B1
BnaA01g12870D	-4.25	unknown	-	-
BnaA01g15080D	-4.12	AAPC_CENCI	38.415	Putative glucose-6-phosphate 1-epimerase
BnaA01g15130D	-4.04	AB10B_ARATH	65.835	ABC transporter B family member 10

Table S5: Genes that are most strongly and significantly regulated within sites of local TuMV infection in Drakkar leaves but not in Tanto leaves. These genes respond significantly to TuMV infection in Drakkar but not in Tanto. The fold-change values (\log_2) represent significant differences between transcript levels within infection sites and transcript levels in mock-treated tissue samples (p-value: <0.05). These values are based on three independent infection experiments (biological replicates) for both Drakkar and Tanto. In each experiment, transcripts were detected with at least 150 mean reads. Only genes with strongest fold-changes ($[\log_2] \geq +4 / -4$) are shown.

	Foldchange (\log_2)	UniProt	% identity	Annotation
BnaA01g01570D	7.17	TLP1_PRUPE	54.24	Thaumatin-like protein 1
BnaA01g01780D	6.85	DIN1_RAPSA	54.24	Senescence-associated protein DIN1
BnaA01g05610D	6.48	COPA2_ARATH	92.27	Coatomer subunit alpha-2
BnaA01g21570D	5.64	PATL1_DANRE	26.57	Protein PAT1 homolog 1
BnaA01g30530D	5.50	AGL97_ARATH	29.37	Agamous-like MADS-box protein AGL97
BnaA01g33090D	5.33	NAC60_ARATH	73.02	NAC domain-containing protein 60
BnaA01g33110D	5.30	NAC60_ARATH	70.15	NAC domain-containing protein 60
BnaA01g33140D	5.21	RPK2_ARATH	88.27	LRR receptor-like serine/threonine-protein kinase RPK2
BnaA01g35500D	4.84	GRXS4_ARATH	98.04	Monothiol glutaredoxin-S4
BnaA01g36060D	4.74	VIP5_ARATH	86.68	Protein RTF1 homolog
BnaA01g37020D	4.72	TPR2_ARATH	82.12	Topless-related protein 2
BnaA02g04780D	4.65	RFS6_ARATH	82.95	Probable galactinol--sucrose galactosyltransferase 6
BnaA02g06780D	4.61	ZAT12_ARATH	86.25	Zinc finger protein ZAT12
BnaA02g08420D	4.45	CKX3_ARATH	65.84	Cytokinin dehydrogenase 3
BnaA02g09670D	4.41	unknown	-	-
BnaA02g10970D	4.31	LTI65_ARATH	47.77	Low-temperature-induced 65 kDa protein
BnaA02g25380D	4.16	MY1R1_SOLTU	75.95	Transcription factor MYB1R1
BnaA02g29540D	4.08	AIG2_ARATH	55.29	Protein AIG2
BnaA01g02570D	-6.09	BZP53_ARATH	50	bZIP transcription factor 53
BnaA01g03580D	-5.89	DRL29_ARATH	85.17	Probable disease resistance protein At4g33300
BnaA01g04010D	-5.66	U587_DROPS	28.91	UPF0587 protein GA18326
BnaA01g08750D	-4.89	MYC4_ARATH	72.4	Transcription factor MYC4
BnaA01g09070D	-4.88	E1314_ARATH	50.58	Glucan endo-1,3-beta-glucosidase 14
BnaA01g09200D	-4.81	unknown	-	-
BnaA01g10260D	-4.72	P2A02_ARATH	62.44	Protein PHLOEM PROTEIN 2-LIKE A2
BnaA01g13950D	-4.28	PUMP4_ARATH	87.15	Mitochondrial uncoupling protein 4
BnaA01g14340D	-4.21	TPD1_ARATH	85.09	Protein TAPETUM DETERMINANT 1
BnaA01g16090D	-4.14	FAD4_ARATH	77.61	Fatty acid desaturase 4, chloroplastic }
BnaA01g16380D	-4.06	DYL2_RAT	50	Dynein light chain 2, cytoplasmic
BnaA01g18170D	-4.01	ERF39_ARATH	81.97	Ethylene-responsive transcription factor ERF039
BnaA01g18680D	-4.01	BBX32_ARATH	55.36	B-box zinc finger protein 32

Table S6: Genes that are more strongly and significantly regulated within sites of local TuMV infection in Tanto leaves than in Drakkar leaves. These genes respond to TuMV infection more strongly in Tanto than in Drakkar. The fold-change values (\log_2) represent significant differences between transcript levels within infection sites and transcript levels in mock-treated tissue samples (p-value: <0.05). These values are based on three independent infection experiments (biological replicates) for both Drakkar and Tanto. In each experiment, transcripts were detected with at least 150 mean reads. The table is based on genes with strongest fold-changes in Tanto ($[\log_2] \geq +4 / -3,8$).

	Foldchange (\log_2)		UniProt	% identity		Annotations
	Drakkar	Tanto		Drakkar	Tanto	
BnaA01g02270D	0.36	8.29	NFD4_ARATH	46.88	46.88	Protein NUCLEAR FUSION DEFECTIVE 4
BnaA01g05410D	0.76	8.04	GRP10_BRANA	95.92	95.92	Glycine-rich RNA-binding protein 10
BnaA01g08170D	1.13	7.98	YUC8_ARATH	92.2	92.20	Probable indole-3-pyruvate monooxygenase YUCCA8
BnaA01g08550D	-1.05	7.89	unknown	-	-	-
BnaA01g10250D	0.94	7.79	PATL6_ARATH	87.03	87.03	Patellin-6
BnaA01g13210D	-1.28	7.78	unknown	-	-	-
BnaA01g13700D	1.31	7.52	VEP1_ARATH	85.98	85.98	3-oxo-Delta(4,5)-steroid 5-beta-reductase
BnaA01g19210D	0.87	7.34	CIPK4_ARATH	78.66	78.90	CBL-interacting serine/threonine-protein kinase 4
BnaA01g20660D	0.78	7.32	PER34_ARATH	82.57	84.23	Peroxidase 34
BnaA01g27800D	0.52	7.28	DPYD_ARATH	73.23	73.23	Dihydropyrimidine dehydrogenase (NADP(+)), chloroplastic
BnaA01g27930D	1.08	7.15	CHX19_ARATH	65.52	71.68	Cation/H(+) antiporter 19
BnaA01g28680D	1.02	7.14	unknown	-	-	-
BnaA01g30490D	0.91	7.08	MD37C_ARATH	96.92	96.92	Probable mediator of RNA polymerase II transcription subunit 37c
BnaA01g31030D	0.90	7.05	RLP12_ARATH	42.26	42.15	Receptor-like protein 12
BnaA01g31190D	0.33	7.04	RLP12_ARATH	41.02	39.82	Receptor-like protein 12
BnaA01g31210D	0.90	6.91	RLP12_ARATH	40.09	40.20	Receptor-like protein 12
BnaA01g02860D	-0.39	-5.09	FUCO2_ARATH	85.42	86.11	Alpha-L-fucosidase 2
BnaA01g02460D	-0.43	-5.09	SPE2_ARATH	85.4	85.71	Arginine decarboxylase 2
BnaA01g03200D	-1.07	-4.77	RNHX1_ARATH	56.63	56.63	Putative ribonuclease H protein At1g65750
BnaA01g04750D	-0.77	-4.65	unknown	-	-	-
BnaA01g07460D	-0.80	-4.44	unknown	-	-	-
BnaA01g14730D	0.51	-4.12	TBL18_ARATH	83.63	83.63	Protein trichome birefringence-like 18
BnaA01g15810D	-0.68	-4.01	GPD3_ARATH	84.95	59.06	Glycerophosphodiester phosphodiesterase GDPDL3
BnaA01g17700D	-0.95	-3.96	GAT17_ARATH	56.91	56.91	GATA transcription factor 17
BnaA01g19120D	-0.79	-3.91	APS3_ARATH	70.54	70.12	ATP-sulfurylase 3, chloroplastic

Table S7: Genes that are more strongly and significantly regulated within sites of local TuMV infection in Drakkar leaves than in Tanto leaves. These genes respond to TuMV infection more strongly in Drakkar than in Tanto. The fold-change values (\log_2) represent significant differences between transcript levels within infection sites and transcript levels in mock-treated tissue samples (p-value: <0.05). These values are based on three independent infection experiments (biological replicates) for both Drakkar and Tanto. In each experiment, transcripts were detected with at least 150 mean reads. The table is based on genes with strongest fold-changes in Tanto ($[\log_2] \geq +4 / -4$).

	Foldchange (\log_2)		UniProt	% identity		Annotation DT
	Drakkar	Tanto		Drakkar	Tanto	
BnaA01g01000D	8.69	0.90	unknown	-	-	-
BnaA01g01300D	7.37	-0.41	UBC17_ARATH	94.59	91.89	Probable ubiquitin-conjugating enzyme E2 17
BnaA01g01690D	6.86	1.06	NIP1_ARATH	67.89	67.89	NEP1-interacting protein 1
BnaA01g10420D	6.22	1.38	VSR7_ARATH	92.67	92.67	Vacuolar-sorting receptor 7
BnaA01g13080D	6.20	1.08	unknown	-	-	-
BnaA01g13540D	6.01	0.52	UGE2_ARATH	67.11	67.11	UDP-glucose 4-epimerase 2
BnaA01g14240D	5.93	1.19	PPA24_ARATH	76.57	76.57	Probable inactive purple acid phosphatase 24
BnaA01g16400D	5.81	-0.60	NAC72_ARATH	72.7	72.70	NAC domain-containing protein 72
BnaA01g16910D	5.71	-0.54	ERF54_ARATH	69.77	69.44	Ethylene-responsive transcription factor ERF054
BnaA01g22310D	5.62	1.49	NRX1_ARATH	86.1	86.10	Probable nucleoredoxin 1
BnaA01g32540D	5.40	0.79	unknown	-	-	-
BnaA01g00140D	-7.25	-1.24	CADH7_ARATH	84.04	84.04	Cinnamyl alcohol dehydrogenase 7
BnaA01g01220D	-6.63	-1.01	unknown	-	-	-
BnaA01g02550D	-6.24	-0.86	unknown	-	-	-
BnaA01g02780D	-5.94	-1.48	ISPH_ARATH	50.63	50.63	4-hydroxy-3-methylbut-2-enyl diphosphate reductase, chloroplastic
BnaA01g03830D	-5.88	1.24	GRXC6_ARATH	91.67	91.67	Glutaredoxin-C6
BnaA01g04070D	-5.55	-0.89	LFS_ALLCE	36.15	36.15	Lachrymatory-factor synthase
BnaA01g05720D	-5.22	-0.80	PNSL4_ARATH	85.71	85.71	Photosynthetic NDH subunit of lumenal location 4, chloroplastic
BnaA01g06190D	-5.07	-1.25	FAD6C_BRANA	68.84	68.84	Omega-6 fatty acid desaturase, chloroplastic
BnaA01g06600D	-5.05	-0.72	unknown	-	-	-
BnaA01g08240D	-5.01	-0.91	TYDC2_ARATH	61.69	61.69	Probable tyrosine decarboxylase 2
BnaA01g08260D	-4.93	-1.39	PSB28_ARATH	88.75	85.71	Photosystem II reaction center PSB28 protein, chloroplastic
BnaA01g08510D	-4.90	0.81	CNBL1_ARATH	79.59	79.59	Calcineurin B-like protein 1
BnaA01g09270D	-4.74	-0.84	CHL11_ARATH	96.57	96.57	Magnesium-chelatase subunit Chl1-1, chloroplastic
BnaA01g09550D	-4.74	-0.71	unknown	-	-	-
BnaA01g10480D	-4.65	-0.64	C71AF_ARATH	67.57	67.57	Cytochrome P450 71A15
BnaA01g10670D	-4.63	-0.97	YCP9_SCHPO	32.56	32.56	Uncharacterized oxidoreductase C663.09c

Table S8: Known and newly identified *B. napus* miRNAs.

Known miRNAs		miRbase		size (nt)	
TTGGATTATAGTTGGATAAG	athmiR56323p	21	AGAACCAAAATGACGACTCGG	21	ACTGGACGACTTACAGGAAG
TTATGCTTTGATGCTCAAT	athmiR8635p	20	CGAACCATCCTTCCAAACC	21	TTGTGTTGGCTTCTGTTGATT
TTGATGCTGAGTGCCCA	athmiR775	21	GGCAGTCTCTTGGCTATC	19	TCA TCGTAAGAGACTCGCAT
TTTGTTATTTTCGATGCTCC	athmiR4239	21	GGCAGTCTCTTGGCTATC	19	GCTCACTGCTCTATCTGTGAGA
ACAGTGTGATCTGGTGGCT	athmiR5638b	21	TGACAGAGAGAGAGAGAGAG	20	TGAGAAAGCAGGGCAGCTGCAG
GATCTTTGAGAGTTTCCAG	athmiR2938	21	CCTCTCATCGATGGTCTAGA	21	TTAGATGACCTTCAACAACCT
TGAAATATAGATTGTTGACA	athmiR4243	21	TGACTAGCCCTTACCAATTC	21	TCTTGCTAAATGAGATTGCCA
TTGAAAGGACTGGAATCTCGAT	athmiR163	24	AGGTGGCAGCTAGCCAAATG	21	ATGTGCTTAAATGAGATTGCCA
GGACTGTGTGCTGCTCGAG	athmiR166b5p	21	GAAACAACATAGTTCACATCC	21	TGTTAAGAGAGTGTAAACGGTG
ACTGTATATGTAAGTGACA	athmiR5025	21	GGCTACAGAGTAGTCAAGCATG	22	TACCATATCTCCATCTCCAA
TAAGATCCGACTACACAAG	athmiR850	22	GCTACAGAGTAGTCAAGCATG	22	GAGGACTCTGAAAGACTCAC
TGGCTGGTGTATGTACACCG	athmiR778	21	TACGAGCCACTTGAACCTGAA	21	AGGGACTTTGTGAATTTAGGG
GGAGTCTCTTGGATATC	athmiR1693p	19	GGCAGTCTCTTGGCTATT	21	TGACAGAAAGTAGAGAGACAC
TGAAACCAAGTAGCTAAATAG	athmiR5957	17	TTGCGAGGAGAGATAGCGCCA	21	TGTTTGTGTACTCGTCTAGT
GGCAATCCATGTCCAA	athmiR8485p	21	GGCAAGTCACTCTGGCTATG	21	GTCCCTTAAAGCGTTTATGG
TAGACCAATTTGAGAAGGA	athmiR824	21	AAACTTCCACATACAAAATA	21	TTGGTGTATGTGTAGTCTTC
TGTTTTGGGTTTCTACCA	athmiR5711	21	CATCCAGGTGTTGTAGAAA	21	TTTTTCTCAAATTTATCCAA
GGAGCCAGGGAAGAGGAGT	athmiR4085p	21	AACAGAGCAGAAACAAGAACAT	21	TTGTACAATTTAAGTGTACG
TTCCCTGGTGCAGTTCGGGA	athmiR1688	21	TTATTTGTTACCCTATCTCC	21	TTGTACAATTTAAGTGTACG
AACTTTGTGATGACCAAG	athmiR399c	21	TTTCCCGTAAAGCTTAGAAC	21	GAGCTTCTCGTCCACT
AGATGGGAGATCGGGGATG	athmiR3932b3p	21	TGGGTGGTGCATATAAGAT	21	CGTGTCTCCCTCCCAAC
AGAGCTTCTGCTCCACT	athmiR8167a	22	GGGCTCTTCTATTGGCAGG	21	CGTGTCTCGTAAAGCGGAAA
CCCTCAATGATTTGTTGAGC	athmiR319b5p	21	CTGCTGCTGTTCCATGTTAA	22	TGATTTCTGTTGTAAGCGAAA
TTGAGATCTAACAATGGTGT	athmiR34413p	21	ATGGGACTCGAGCTTTAAT	22	CGAAATGCGATATCAATGT
AAACCCGGTGTGATATAGC	athmiR5724	21	TTGACAGAAATAGAGAGCAC	22	CCTGGTTTTGAGATTAATGAC
GCAGCATCATTAAGATTACA	athmiR172d5p	21	CATTGTTCTGTTTTTTTCA	21	GGAATGTTGCTGGATCGAGG
CACGTACTCCCTCTCCAAC	athmiR164a3p	21	TCGCTGTGATACCAAAATTGATG	22	AAATCCAAATTTCAATGCTAA
TTGTTAGGTCCTTAGTTCT	athmiR8403p	22	GCGTACAAGGACCAAGCATG	21	GGAAATGTTGCTGGATCGAGG
ATCTGAAGAAATAGCGGAT	athmiR56483p	21	ATTAAGCTGCGCGTTCGGCAGC	24	TCTCGCTGTGACGGCTTT
CACCTATCTCAACCCTAGTGA	athmiR8695p	21	TTGTTTTGGATCTTAGATACA	21	TTAGAGATTTGAGATCTTA
CACGTCTCCCTCTCCAAC	athmiR164e3p	21	GACTTATAA TGATCTCATGAA	21	TTTTTCTACTCTTGACCA
TTGCTTAAAGATTTTCTATGT	athmiR81703p	21	TAGCAAGGATGACTTGCCTG	21	TCAATAGATTGGACTATGTAT
CATCCATATTTTCACTCGAA	athmiR74b3p	21	CGTACAAGGATCAAGCATGA	21	TAATTCACCAATAAATCAACG
GGAGATCTTTCAGTCCAGTC	athmiR319c5p	21	TTTTCTCTTCTTGACCA	21	CGTACAACATAAATCAACG
AAATGCTGCAATATCTCTGC	athmiR8603p	21	CCTTGGAGAATATGCTCAA	21	GCTCTACTCTGCTCAC
GATGGATATATCTCAAGAC	athmiR5723	21	CTGAAGCTAGTGAAGAGAGA	21	GCAAGCAATCAAGATTCACA
TCGCTTGTGAGTGCAGAA	athmiR8613p	21	ACTTTGAAGCTTTGATTTGAA	21	ACCATGTTTAGACTTGAAT
AGAATCTTCAAGTGCAGAA	athmiR168b	21	TTTTCTCCAGCTTTGTTCT	21	TTGATAATTTGAAGATATAAA
TATGATCATCAGAAAACAGT	athmiR172d	21	AAATTAAGATGAATTTCTTAC	22	AGGCTTAAGAAGGATTTGTT
AAAGAGTTCGGAGGGTTTGAAGC	athmiR5631	24	TTTTCAATCTAGAGAAATGTTT	22	TGGAGCAGCGTTTCAATCGATC
AGATAGAAGCAATCTGGATA	athmiR34493p	21	TTTTCAATCTAGAGAAATGTTT	21	GATGAGGATAGGAGGAGGAG
CCGTATCTTGGCTGTCTAT	athmiR50243p	21	TTAGATACCATCAACAACG	21	GGAGCAGCGGTTCCATCGATC
AAACTATCTTGTGCTTAGA	athmiR95673p	21	ATCATGCTACTCTTTGGATT	21	AACATGAGGACTCAACAGTTA
TGAACCAAGTAGCTAAATAG	athmiR34375p	21	AAAAACAAGGATCCACGGAT	21	AAAAACAAGGATCCACGGAT
GGCAATCCATGTCCAA	athmiR5665	21	GATCCCGGCAACGGCGCCA	20	GATCCCGGCAACGGCGCCA
TAGACCAATTTGAGAAGGA	athmiR8175	20	AACTCATCAATCTCCCAATA	21	AACTCATCAATCTCCCAATA
TGTTTTGGGTTTCTACCA	athmiR3444a3p	21	ATATAGTCCAATCTATTTAAG	21	ATATAGTCCAATCTATTTAAG
GGAGCCAGGGAAGAGGAGT	athmiR8605p	21	AGGGTGTATATGAGAACACAC	21	AGGGTGTATATGAGAACACAC
TTCCCTGGTGCAGTTCGGGA	athmiR398c5p	21	TGTTCTGGTGTGTTTTTAAAC	21	TGTTCTGGTGTGTTTTTAAAC
AACTTTGTGATGACCAAG	athmiR5718p5	21	TGGCATAA TCTGTCAATTTCC	20	TGGCATAA TCTGTCAATTTCC
AGATGGGAGATCGGGGATG	athmiR447b	22	TTGGGACGAGATGTTTTTTGG	21	TTGGGACGAGATGTTTTTTGG
AGAGCTTCTGCTCCACT	athmiR34355p	21	AAAGACTGCTCAACTTTTAA	21	AAAGACTGCTCAACTTTTAA
CCCTCAATGATTTGTTGAGC	athmiR447b	22	GCTACTCTCTCTGCTCAC	21	GCTACTCTCTCTGCTCAC
TTGAGATCTAACAATGGTGT	athmiR172a5p	21	GTGGCATCAATCAAGATTCACA	21	GTGGCATCAATCAAGATTCACA
AAACCCGGTGTGATATAGC	athmiR5631	21	TGGCAGGAAAGACATAATTT	22	TGGCAGGAAAGACATAATTT
GCAGCATCATTAAGATTACA	athmiR159b5p	21	GAGCTCTTGAAGTTCATTTG	21	GAGCTCTTGAAGTTCATTTG
CACGTACTCCCTCTCCAAC	athmiR9552b5p	21	CTATCGTCTACTTGGTCCAGC	20	CTATCGTCTACTTGGTCCAGC
TTGTTAGGTCCTTAGTTCT	athmiR156f3p	23	TCGCTACTCTTTTCTGTCGA	21	TCGCTACTCTTTTCTGTCGA
ATCTGAAGAAATAGCGGAT	athmiR853p	22	TTGGGGTTTTCGAAATCAAGAG	21	TTGGGGTTTTCGAAATCAAGAG
CACCTATCTCAACCCTAGTGA	athmiR34395p	21	ACCGTGTGGAACTTGCCTTAA	21	ACCGTGTGGAACTTGCCTTAA
CACGTCTCCCTCTCCAAC	athmiR7715p	21	TGAGCCCTGTGGCAGCCCTC	21	TGAGCCCTGTGGCAGCCCTC
TTGCTTAAAGATTTTCTATGT	athmiR5655	21	AAGTAGACATAAAGAAAGGAG	21	AAGTAGACATAAAGAAAGGAG
CATCCATATTTTCACTCGAA	athmiR8293p	21	CAAATTAAGCTCAAGGTTAG	21	CAAATTAAGCTCAAGGTTAG
GGAGATCTTTCAGTCCAGTC	athmiR34473p	21	TTTTGAGTGTGTTTTTATGAA	21	TTTTGAGTGTGTTTTTATGAA
AAATGCTGCAATATCTCTGC	athmiR34363p	22	CAACAACGATTTTTGGTCTT	21	CAACAACGATTTTTGGTCTT
GATGGATATATCTCAAGAC	athmiR8895p	21	CACCACTCTCACTGTTCCC	21	CACCACTCTCACTGTTCCC
TCGCTTGTGAGTGCAGAA	athmiR8593p	21	TGATTTTACATAGATAGATA	21	TGATTTTACATAGATAGATA
AGAATCTTCAAGTGCAGAA	athmiR399e5p	22	GGCGAATCTCTATTTGGAGG	22	GGCGAATCTCTATTTGGAGG
TATGATCATCAGAAAACAGT	athmiR8683p	21	CTTCTAAGTGTGATAATGT	21	CTTCTAAGTGTGATAATGT
AAAGAGTTCGGAGGGTTTGAAGC	athmiR319c	21	TTGACCTGAAGGAGGCTCCTT	21	TTGACCTGAAGGAGGCTCCTT
AGATAGAAGCAATCTGGATA	athmiR164a	21	TGGAGAAGCAGGCGCTGCA	21	TGGAGAAGCAGGCGCTGCA
CCGTATCTTGGCTGTCTAT	athmiR156d3p	21	GCTCACTCTCTTCTGTGATA	21	GCTCACTCTCTTCTGTGATA

Known miRNAs (miRbase) & size (nt)

TGGAGAGGAGGCGCAGTGG	bnamiR164d	21	ATAGTACTAGTACTGCATGATCA	bnamiR6036	24	TTGTGATGATAAATGACCTC	bramiR5719	21	ATCATGCGATCTCTTTGGATT	athmiR393b3p	21
TCCGTTATCCCGCATGCTCC	alymirR4239	21	GTTTCGAGGCGAGTGGGAGG	athmiR5646	20	ATACAAAACCTCTCCACTTT	athmiR5638a	21	ATTTGAGTCATGCTGTTAAAG	athmiR5645a	20
CTTCTTAAGTGTGATAATGC	athmiR8683p	21	TCAAAATCAGAGAATCAACA	alymirR34343p	21	GGAATGTTGTGCGCCAGG	athmiR166e5p	21	AGAAAGGACTAGTAAGATGGCT	alymirR8445p	21
GTTTGGAGAAATATGCATCAT	alymirR8615p	21	TCAATGAGTGCATGTTGATG	athmiR397b	21	TGGTTCCCTGGCCAACTCCACT	alymirR34405p	22	ATGAATTTGGATCTAAATGGAG	athmiR8655p	21
TGCTGGCTCCCTCTTTGGCA	bnamiR160c	21	TAGAATGCTATTTGAATCCAG	athmiR406	21	CAATCTACTAGTCTCTCTT	alymirR8443p	22	AAACGAAACAAGAACTGATGA	alymirR8373p	21
AACGACTTCATCTCTTTGGC	alymirR34413p	21	TAATTTGGTGTCTTTCGATC	athmiR8703p	21	TTTGGAAATATTTGGCTGACT	athmiR56485p	22	TCACAGTCTCTGATTTCCAC	alymirR34333p	21
CCCCTTACAATGTCAGATAA	athmiR447c5p	21	AAATGGAGCAAGTGTGAAGGA	athmiR8165	21	TTTAAATCATATACTTTGGT	athmiR407	21	GCTGATTTCTGATTTTGAAC	alymirR34345p	21
TTTGGCTGATTTAGAAATGA	athmiR8184	21	TTTCTCGTGAATATCTGGCAT	athmiR780	21	TAAACTCGTACTCTCTCTTG	alymirR8313p	22	GACTATAATAATCTCATGAA	alymirR4003p	21
GGGCGCTCCATCTGGCAGG	bnamiR399b5p	21	GGGCAATATCACTTGGCAGA	alymirR39915p	22	TCTCCGTTGTAAATCAAA	alymirR8595p	21	AGATGCTCACTTTGCAAGCAA	alymirR8283p	22
TGGAGTAGAAAATGCAGTCTG	bnamiR6035	21	AACTATTTAAGCAGATGACT	athmiR5645c	21	CTGTAGTAGTGAAGAACCA	alymirR34453p	21	TTTGGAAAATTTGCTTACG	athmiR426	21
TCATATTAGTTCACTCTGCTG	bramiR9560b3p	24	AAAATTAAGTATGGCATCC	alymirR4242	21	TTCTCGAAGGTGCATGAAC	alymirR8253p	21	GTTCCCTTTAAAGCTTCAATG	alymirR395b5p	21
TTTTACTGCTACTGTGTCC	athmiR5012	21	TCTAGATTGCTTTCGCTGT	alymirR34495p	21	ACAAAACCTCTGGATGTTCT	athmiR782	21	GAATGATACTTGGATATAATC	bramiR95545p	21
TGGGTTGAGTTGAGTTGAGTTGGC	athmiR5653	24	TCTGTATGAGAGCAATGGAA	alymirR8475p	21	TAATCTGCAITCGGGTTTA	bnamiR2111c	21	TTTTCTCTGTTGAAATCTTTCG	athmiR4221	22
ACTCATAAGATCGTGACAGT	athmiR5026	21	CAACTGAGCTTCCATCTCT	alymirR4224	21	TGAGCTGCTACACGTTGATG	athmiR169b3p	22	GGCAATACTTGAGCAACA	athmiR73b5p	22
CAATAA TTTTCCCTCTA	athmiR4236	21	CGGCTCTATACAGTTGATG	alymirR8453p	21	ATAGTTTTCTTTGTTCTGCAC	athmiR413	21	AGCTGTATACAAAATGATGGAAT	athmiR8293p	21
TCTAGCAGCTTGAGCAGGT	athmiR780	21	TTTGGCTTCAACTCGGTCC	bramiR95575p	21	GGAATGTTGTTGGCTCGAAG	bnamiR166a*	21	GCAAGTTGACTTGGCTGTG	bnamiR169n	21
TCTTCTGCAAAAGCTTTGGA	bolmiR9410	22	TGACAGAAGAAAGAGAGCAC	athmiR156h	20	CAGCCAAGATGACTTGGCGG	bnamiR169n	21	TTGTTGATGACATCTATC	athmiR5019	21
TACTAA TATAAGTCTGCTGG	athmiR9410	22	TCAATCCAAGTATCACTCT	bramiR95543p	21	TTTGTGACATCTAGTGCTTT	bnamiR166a*	21	TTGTTGATGACATCTATC	alymirR8275p	21
TAGCAAAGATGACTTGGCTG	alymirR169n5p	21	GCAATCTCAAGATTCAGA	bramiR95543p	21	CAGCCAAGATGACTTGGCGG	bnamiR169n	21	GGAGTGTCAAGACACGGA	bolmiR398a5p	21
TTTTCTGGCCATCCACTTC	athmiR3440b5p	21	AGAAGAGGTACAAGGATGAGA	alymirR8315p	23	ATAGCAATGATAAGCAATG	athmiR81705p	21	GAATCGATGTTAAACAACAC	alymirR4225	21
ATGTAATAAATCAGTTGGCAAT	alymirR8225p	21	CTTGTCTACAATTTGGAAA	athmiR158a5p	22	CTATGGTCTACTCGTCAAG	bramiR9552a5p	21	TTGAGAGAAGAAATGATTTCA	athmiR5640	21
CAACTTAAATCAGTTGGCAAT	alymirR4234	21	AGACTAGCAGATCAAGAAC	bramiR5714	22	CGCTGCCATCTGAGTTTCA	bramiR9303p	21	TTGAAACATGTTTATAGGAA	athmiR867	21
GCTACTCTCTTCTGCTCC	alymirR156g3p	21	AAATAAGCTGTGGAAAGATC	bnamiR3916	21	GACTATAGCAACAAGATTTTC	alymirR1635p	21	ACAATGAAAGAAATCAAAATC	bramiR9593p	21
TGGCATGGAAGAGGTGAGAC	athmiR5020c	21	AATTAAGAATTCATCTTACT	athmiR1886.3	21	ACATATGATGCTCTTTGCG	athmiR5995b	21	TGCCAAAGGAGATTTGCCCG	athmiR399d	21
GCTAAGAGCGGTCTGATGGA	athmiR5630b	21	TTTGTCTACAATTTGGAAA	alymirR158b5p	20	TTCAAGCATCTTTGAAGAA	alymirR34415p	21	TGAAAGCTCCAGCAATGATCTGG	athmiR167d	22
TGAGATGAATCTTTGATGG	athmiR1886	21	TAACATTTTGGAGAAGATG	athmiR8303p	21	CAACGGAAAGGGAGCAGCA	alymirR8533p	21	AATGCGCAACTATATTTCC	athmiR5637	21
TTCTGATATGTTTATC	athmiR8355p	21	TTGATCCCAATCCAAAGCAAG	athmiR172c5p	21	GTCAATGGGTATGATCGAATG	athmiR5022	21	TCCAAAATGTAGACAAGC	alymirR158b3p	19
TTTAGTTGAGGAAATTTGGC	athmiR8183	21	GACCTCAGGATCGGATTACC	bramiR21113p	21	TGAAATGATGCTGCTCGAGA	alymirR166b5p	21	ACAAAATCCGCTTTGAAGA	athmiR8663p	20
TCTAAGTCTCTATTGATGT	athmiR776	21	TTGTAGTCTGAACCTCGTCTAGT	alymirR8335p	23	CGAGTCCAGCCTCTCAGA	alymirR1635p	20	CAAAATCAAACTTCAAGGTAC	alymirR8293p	21
TGTTTTGCTTGAATCTAAT	athmiR4035p	22	ACAAAACGATTACACAGCTCGTCT	bramiR95645p	24	TTCTAATCCCGCATGCACC	alymirR34435p	21	ATGTAGTCAATCTATTGAAG	bramiR8605p	21
TAGACCGATGTAACAAACAAG	athmiR833a3p	22	AGAACAAAGCGCTTATCTTAT	alymirR8525p	21	TGAAAGATGCTTTGGGATTTAT	athmiR56543p	23	CTTGAGAGAGAAACAACAGACG	athmiR2936	22
TGCTCACCTCTTCTGTCAGT	bramiR156e3p	23	GGAATCTTGATGATGCTGCAT	bnamiR172b	21	GGCAAGTTGCTCTGGCTACA	alymirR169a3p	21	TTGAGATTTGAAGTCTTGAAT	athmiR402	22
ACTTGGCTGATCTAAT	athmiR34345p	20	TGGTAAAGTTCCTTAAGCT	athmiR8445p	21	ACAGTTGTGTTTGTGTTTGT	athmiR5998a	21	TTGAAATGAAAGTCTTGAAT	athmiR8463p	21
TAAACAACATATAGTTGC	bramiR95675p	21	TGTAATCTAATATTAGACCC	alymirR4247	21	TAGGTCATGCTGGTAGTTCCACC	athmiR167c3p	23	TTTAGTCCGAGCTTCAATGGA	athmiR843	21
GGACATCTTCAAGATTGAG	alymirR172c5p	21	ATCATCGGATCTCTCGATT	bnamiR393*	21	TGACCAAGTAGACCCATAGTC	bramiR9552a3p	21	ATAGTGGGGCCAGTGGTAGGA	athmiR8171	21
TGAATTTGAGAAGTTGAGGTA	alymirR4249	21	GTCATTGATGATGATAGTTT	bramiR95565p	21	CTGAAGTGTGGGGGAACTC	alymirR399b5p	22	GGTCATTTGAGAACTGTGATG	alymirR34335p	21
GGAGCATCAAGATTACA	alymirR8685p	22	TTTTTTCAGCACAACTTTC	bnamiR403	22	ACACTAAAGGACCTAACTAAC	bnamiR395b	21	TTGTCGGGTTCAAATAGTAAAC	athmiR5651	22
CTTCTCGGCACTGAGGATGT	bramiR95563p	21	AAAGGATGCGCTGGAACACA	bolmiR9409	22	ATCTCGGATACAGTTTACC	alymirR8405p	22	TACAAGATGCTCGAGCAATA	alymirR4226	22
TCTACTTTCAACAATGGCT	athmiR1888a	21	ATTGTTCAATTTGGTGTG	athmiR869	21	TTCGTTGCTGCTGGACTTG	alymirR858b	21	CACGTTTCTACTACTCCAAC	bramiR164c3p	21
TAAGTTAAGATTGTAAGAA	alymirR4025p	22	TGGTCTTTGTTGGACCCATCG	alymirR8515p	24	TGCGGAAAGGATTTGCACATG	athmiR8180	19	AATTAATCCAACATCTCCA	alymirR34353p	21
TTGGCTATTGAACCTCTGTT	alymirR34455p	21	CACATCAACCACTCACTCC	alymirR4233	21	TGCGGAAAGGATTTGCACATG	athmiR8225p	21	TCTTCACTATTAGACGGACAA	athmiR5999	21
GGTCTTCTCCATCAAGG	alymirR397b3p	21	TGACAGAAAGAGAGAGCAC	athmiR156j	20	TTTTTGTATGTTGAAGTGTAT	athmiR857	21	AAGCTCAGGAGGATAGGCC	bnamiR390c	21
TCCCTCTTAGCTGGAGAAG	athmiR853	22	CTGAGTTGGAAAGCAGAAATC	alymirR395i	21	GCTGAGTTGGAAAGCAGAAATC	bramiR95573p	21	ATAGACAGAGTCACTCACAGA	athmiR8169	21
TGAAGCTGCCAGCATGATCT	bnamiR167d	20	TCTGATTTTTCGAAAGTCCCAAAA	alymirR34393p	22	GGCAAGTTGCTTGGCTAC	athmiR169a3p	20	AGGTGCTGAGTGTCTAGTGC	athmiR8168	21

Known miRNAs (miRbase) & size (nt)

CAGGTGGTTAGTGCAATGGAA	athmiR5660	21	TAGACCCACTGGAACTAAA	21	AAAGATAAGCGCTTAGTTCTTGA	21	CGAAATGGTGTGCAACCGACA	21	athmiR401	21	CGAAATGGTGTGCAACCGACA
ACAGCCTAAACCAATCGGAG	bnamiR1140	21	TGATGAGCGCGCAATATCT	22	AGAGCTCTCTGAGTCCATTC	21	TAGAGCCACTGGAAACTGAA	21	athmiR841b5p	21	TAGAGCCACTGGAAACTGAA
GGCGGAATCTCTATGGGAGA	alymiR3995d5p	22	ATGAGTTGGTCTAACCAATAACT	24	CGATGAAGTCTTTGGAAAGGTA	23	TGGATTTGGTCAAGAAACCGCA	22	alymiR34403p	22	TGGATTTGGTCAAGAAACCGCA
TGTGGGTGCAACAAGACGACA	alymiR8513p	24	TGATGAGCGCGCAATATC	21	AAAGTAAGCGCTTAGTTCTG	21	ACATGCTGGATCTACTTGAAG	21	alymiR8623p	21	ACATGCTGGATCTACTTGAAG
TCAATGCATTAAGAGTGACTA	athmiR1161	21	ACATTTATTTTGGCAATCA	21	AGATATGGTCTGACTAATACTT	21	TGACAGAAGAGAGTAGAGCACA	21	bnamiR156a	21	TGACAGAAGAGAGTAGAGCACA
GGGCTCCTTATAGTTCAACG	BnamiR159*	21	ACATTTATTTTGGCAATCA	21	AGATATGGTCTGACTAATACTT	21	TGACAGAAGAGAGTAGAGCACA	21	athmiR174b5p	21	TGACAGAAGAGAGTAGAGCACA
ATCTCGGATAGGATGATACC	bramiR111b3p	21	ATAAGAGCTGTTGAAAGGATC	21	TGAGTCTCACCACTCTTCCAC	23	TGAGATGAAGATTTGGATGATC	21	alymiR7485p	21	TGAGATGAAGATTTGGATGATC
GCAAGTGGACCTTGGCTCTGC	athmiR169f3p	21	ACAGTGGTGGAAACAATATGAGT	24	GGGCAAGATCACCATTGGCAGA	22	TCACCCATACCATACAGACCC	22	bnamiR6030	22	TCACCCATACCATACAGACCC
TAATCTAAACCTGGGTAGTA	alymiR165b5p	20	TGGGTGGCAACAAGACGAC	21	AAAGTATAATGGTTAGTGGTTTG	24	GTCTCCGAACTCACTTCAATG	22	alymiR395d5p	22	GTCTCCGAACTCACTTCAATG
GCAGTTGACCTTGGCTCTGT	athmiR849	21	ACCCGCTCTAAATTTTAAAC	21	GTGTGATGCTGATCAATTTA	22	TACATCTCTCCGCGAAGCTC	21	bramiR1885b	21	TACATCTCTCCGCGAAGCTC
TGACATCCAGATAGAAGCTTTG	athmiR169e3p	21	AGCTTTTAAGATCTGGTTGCG	21	TCATATAGTCTACCTCTGTG	24	AGAGCAAAAATCATTTGTGAT	22	alymiR34365p	22	AGAGCAAAAATCATTTGTGAT
TGATGGAAATTTCTGTGACT	athmiR5996	22	TAGACCTTTGTTGGCATCG	21	CCCGTCTGTATCAACTGAAT	21	TCATCTCTCTCTCATGATG	21	alymiR8473p	21	TCATCTCTCTCTCATGATG
TAGCCTAAGATTTGTGAAGA	athmiR179	21	TCAAGTGGTGCAGAGCCAGC	21	TTAGAAAATGGCAATTAATA	21	GCCTCTAGCCTTCTTGATCA	22	alymiR157a3p	22	GCCTCTAGCCTTCTTGATCA
TGACCGAGTAGACCGATAGTC	athmiR1888b	21	TCAAGCACCAGCTCGAAGAAGC	22	TTTGGATTGAAGGAGCTCT	21	TTGGATTGAAGGAGCTCT	22	athmiR159b3p	22	TTGGATTGAAGGAGCTCT
TGAGATGAAGATATGGGTGAT	bramiR9552b3p	21	TAATCTACCAATAACTTCAGC	22	TTTGGATTGAAGGAGCTCT	21	TTGGATTGAAGGAGCTCT	21	athmiR8473p	21	TTGGATTGAAGGAGCTCT
GTTCCCTTAAAGCTTCTATG	athmiR774b5p	21	TCTCTCCAAATAGTTAGGTT	21	TCTGAGGATTTTTTTTGGTGC	22	TCTGAGGATTTTTTTTGGTGC	21	athmiR5020b	21	TCTGAGGATTTTTTTTGGTGC
CTTTGCTATCGTTTGGAAAG	alymiR395h5p	22	TAATGTGATGATGAACCTGACC	21	TTGGCAGGAGGCTCTCCACAC	22	GATGGATATGCTCTCAAGGAC	20	athmiR8613p	20	GATGGATATGCTCTCAAGGAC
TGCTGGGATCGGAATCGAAA	bramiR1585p	22	GCCTATGAGGAGCCATGCATA	21	TTGGCAGGAGGCTCTCCACAC	22	CTTGATGATCACTAACCAT	21	alymiR8235p	21	CTTGATGATCACTAACCAT
GCCTATCCACTCGAGTTTCA	athmiR830a3p	21	GTTCACTTTAGAGAAATGTTGC	21	ATTTCTAGTGGGTCTGATTA	21	GAGCACCATTAAGATTTAC	20	alymiR156h3p	20	GAGCACCATTAAGATTTAC
CGTATGAGTGCAGCGTTGATG	athmiR5636	21	TTAAGTGGTGGTGAATGTTCAAT	23	TGCTGTTCCCTGCTCTCTC	21	TTCATCTCTCTCTGCCCACC	21	bnamiR159	21	TTCATCTCTCTCTGCCCACC
TTTGGAAAGTGATTTGTTGCT	alymiR34453p	21	TTTTTTGTCGTTGAATCAAT	22	TGTTGTTGACACTGGTGTAA	21	ATCTGCCACTCCACTCCA	21	athmiR4221	21	ATCTGCCACTCCACTCCA
TATGGAAATAATGTAGTATT	athmiR447a3p	21	ATTTGTACCTAGATCTGTA	22	AGAGAGTGTAGAAAGTTTCTCA	22	AGAGAAACAATAAATCACTT	24	bramiR95693p	24	AGAGAAACAATAAATCACTT
TGTAATTCGGGGTCTTCAAGC	bramiR9555b5p	21	ACGTGATAAGCCTCGAAGAA	21	TGGAAGAAGATGATAGAAATTA	21	TCACATTTATTAGGATGTGTC	22	alymiR4232	22	TCACATTTATTAGGATGTGTC
TGGATGCGAAGCGTGGTGT	athmiR42283p	21	TGAGCCTCTGTGTAGCCCTCA	22	ATGGATCACTAGATGGAGAT	21	AAAGATTTCAAAGTAGTGAAGA	22	alymiR4221	22	AAAGATTTCAAAGTAGTGAAGA
GGAGTGCATGAGAACACAGA	alymiR398a5p	21	GTTCTCTGAGCACTTCAATG	21	TTTAGCTCAGACCAGGTGGACT	24	TCCATAGCTCATCTGACC	21	alymiR34383p	21	TCCATAGCTCATCTGACC
TGCTCTGATACCAATGATG	bnamiR397a	22	GTTCTCTGAGCACTTCAATG	21	ATGATGATGATGATGATGAAA	21	TGGAAGAAGGTGAGACTTGCA	21	athmiR5020a	21	TGGAAGAAGGTGAGACTTGCA
GAGCCTAAGTATTTGTCAACAATG	alymiR845b3p	24	ACTATGCAATTTGTGAACAAA	21	AGGTCACTCTGCAGCTCAGT	19	AGCTAAGGATTTGCAATCTCA	21	athmiR56635p	21	AGCTAAGGATTTGCAATCTCA
GAAACGATGAGAGTTGGTGA	bramiR95663p	24	TTTGGCAATTTGCTCCTCAT	21	ACAAAGTTTTTACTGCAAT	21	TACAAGCTGAAGCTAATATTG	22	bramiR9535p	22	TACAAGCTGAAGCTAATATTG
TGAAGGACTTGGAACTCGATC	alymiR8393p	23	TTTGGCAATTTGCTCCTCAT	20	TCAAGGATTAAGCTATGAAGC	21	TCACTGTGTAATAGTAGTCA	22	athmiR8685p	22	TCACTGTGTAATAGTAGTCA
GCAAGTGCACCTTGGCTCTG	BnamiR161*	20	TGCAAAAGAGATTGGCTCG	21	TACCACTTCTCATCTGCC	21	ATTGTTAGTGGATAAGGGGGC	21	bramiR1140p5	21	ATTGTTAGTGGATAAGGGGGC
TGCAAGATGAGAGCAAAAGC	alymiR8385p	21	AATGAGAGAGAACTGCAAA	21	GGTCACTCTCAGCCCTCACT	23	CGCTATCCACTCTGAGCTTCC	22	athmiR5023	22	CGCTATCCACTCTGAGCTTCC
TAGCCAAGATGACTTGGCTCA	bnamiR169d	21	TGACATGGGACTGCCAAGCTA	21	TGAAATAGTCACTGTGGAAAG	22	TGACATGGGACTACAGACTAA	22	alymiR8483p	22	TGACATGGGACTACAGACTAA
TGATGTTATTTGGTGTAAA	alymiR8563p	21	TCAAGTTTGTAGCGATTTCCA	21	TTCTAAGCTTTACGGAAACC	21	TGTTCTGGAAATTTGCCACCT	21	alymiR4230	21	TGTTCTGGAAATTTGCCACCT
CATGTGCCCATCTCACCATC	athmiR164b3p	21	CATCAATGAAAGGATGATTTCC	22	AAATGGTATTATGCTAGATT	21	ATGGTCGAAAGTAGCCAAATC	21	athmiR4725p	21	ATGGTCGAAAGTAGCCAAATC
AAATCGTTGAGGCTGAAGTCGT	alymiR1633p	21	ATTTGGCAAACTGATCTGCG	21	GATCTCTGTGCAAGTGAAG	21	TCACTGGTACCAATCAATCCA	21	athmiR4725p	21	TCACTGGTACCAATCAATCCA
TGATGTTATTTGGTGTAAA	athmiR8563p	21	ATTTGGCAAACTGATCTGCG	21	TCAATGCAATTTGTACAACAT	21	ATAATCCCAAGCATCTCA	21	bramiR5654b	21	ATAATCCCAAGCATCTCA
TAGCCAAGATGACTTGGCTCA	athmiR5628	21	TCAATGCAATTTGTACAACAT	21	CAACAGTCTCAGATGGAAA	21	GGTGGAGCAGACACGAAGAT	21	alymiR8583p	21	GGTGGAGCAGACACGAAGAT
TTGAGAGCAACAAGACATAAT	alymiR167c3p	21	GCTCACTCTCTCTGCTCAC	21	TCAGAGTATCAGCCATGTGA	20	TTGGTTACCATATGGCCATC	21	athmiR774a	21	TTGGTTACCATATGGCCATC
GAATAGCGAAGATATGATTA	alymiR167c3p	21	GCTCACTCTCTCTGCTCAC	24	TTTGCAGCTCGATGATGCTC	21	CTCGAAGCTAGACGTTGGCAGG	24	alymiR34465p	24	CTCGAAGCTAGACGTTGGCAGG
AGGCTATGCTGGTGTTCAC	alymiR344415p	21	TTATACCAAAATTAATGCAAA	21	TGAGAATGCAAACTCTTAGCT	21	TATCTTGGAAACAACAGTTGA	21	alymiR73b5p	21	TATCTTGGAAACAACAGTTGA
CGAAGAAATGAAGTGGCTTTT	bramiR5717	21	ACTGAAGTAGAGATTTGGGTTT	21	ATAGTCAATTTTATCGGTCTG	21	TCCAAATGTAGACAAGAACA	20	alymiR158a3p	20	TCCAAATGTAGACAAGAACA
GTTTGGATTGTGCTTGGC	athmiR417	21	GTTGGTTGCGGATAACGGTA	21	TGCGACCAGGCTTCACTCCC	20	ATAGCTTGAAGCCGCTGTT	21	athmiR42285p	21	ATAGCTTGAAGCCGCTGTT
GAAGTAGTGAATTTGTTGGT	alymiR4228	21	GTTGGTTGCGGATAACGGTA	21	AAATGTTCAITTAAGGATATT	21	GCTCTCTAAAGCTTCTGTCATCA	21	athmiR8373p	21	AAACGAAACAAAATAAGTGGT
AAAGCTTGAAGCTGTGTT	bnamiR399b	21	AAATGTTCAITTAAGGATATT	21		21		21		21	

Published miRNAs (not present in miRbase) & size (nt)				
TGCGTGGTCCCTGTATACCA	BnamirC9	21	BnamirC25*	21
TGTGTGTGATGATAATCCGA	BnamirC51	21	BnamirC1	22
TCCTTGTGTGTGATGATAATC	BnamirC53*	21	BnamirC23a3	21
TTTCATCTAGAGAATGTGTGTC	BnamirC45	22	BnamirC56	21
TGATAATCCGACTCTATGAC	BnamirC54	21	BnamirC151	21
GGTCCGATATGAGAACACATG	BnamirC12	21	bramiRn73p	21
TTGGTTTGGATCTTGAAATC	BnamirC55	21	BnamirC47	21
ATGGTGTAGTACTGAGCAGA	BnamirC35	21	BnamirC33	22
TTGGATTATATAGTTGGATAAG	athmiR56323p	21	BnamirC53	21
NGCGGATATCTTAGATGAGGT	bramiRn215p	22	BnamirC13	21
GAATGATACTTGGATATGATC	bramiRn45p	21	BnamirC25	21
CGTCCGGGAAAGCAAAGTCG	BnamirC36	21	BnamirC28	21
TTGAAAACCTGCAAATTATA	bramiRn123p	21	BnamirC31	21
ATAGACTCTCTGATGAGCA	BnamirC6	21	BnamirC44	21
TTTCAAATGTAGACAAAGCT	bramiRn233p	21	BnamirC32	22
AAACTAAGAGATGAAATCTTAC	bramiRn203p	22	BnamirC23a2	22
TCAATGTTGGCTCAATTATGT	BnamirC10	21	BnamirC3	22
ATCCTCGGACACAGATACC	BnamirC34	21	BnamirC7	21
TAAGATGATGGAGCTTGGATC	BnamirC39	22	BnamirC42	21
ACTTGTCTCACTCATCAGTT	BnamirC46	20	BnamirC8	21
TTGGACGACTTTGTAGACGAC	BnamirC22a3	21	BnamirC14	21
TCACCAAATACACA TTGTGG	BnamirC52	21	BnamirC24	21
TTGAGTTTTTGGAGACTGGCC	BnamirC29	21	BnamirC20	21
TCAGAACCAACCAGAACAAAG	BnamirC23a1	22	BnamirC18	21
ATAAAACGATTACACAGCTCGTGC	bramiRn165p	24		
GTTTTGAGAGATTGGGAAGCT	BnamirC16	21		
TGTGAATGATGCGGAGATGT	BnamirC43	21		
CGAGTTGGTGGGAAAGACGG	BnamirC19	21		
TAAGATGATGGAACACTGGCC	BnamirC27	21		
TGAGCCAAAGATGACTTGTGCG	BnamirC26	21		
CAAGTAGACTACTTTCCAGACG	BnamirC38	22		
TGATTTATCCAAGGGTTCAGG	BnamirC37	21		
GCAAGTTGACTTTGGTCCGT	BnamirC32	21		
GGCGAGTCACGGGTGTCGGTC	BnamirC11	21		
CGAGCTGTGTAATCTGTTTTGTTA	bramiRn163p	23		
TTTCAGTCTCATAGTTAGT	BnamirC4	21		
TTTTTGGAGAAGGCTTAGGCA	BnamirC41	21		
AAATCGGATTATCATCACACA	BnamirC51*	21		
TCCTGGAGCACTTTCAAAGTAAG	BnamirC30	22		
CGCTCACAGCATCTGAAGTCT	BnamirC40	21		
GATGCATAACCACTAGATACG	BnamirC23a3*	21		
TAAACAACACATATACTTTGC	bramiRn195p	21		
TTATATCCAAGTATCATCTCT	bramiRn43p	21		
CGTGGTCCGTCGAAGTAGAGGA	BnamirC22a2	21		
CAAAGTAGACACTTTCCAGAC	BnamirC22a1	21		
AGAGTTTCTTAAGTCCATTC				
CCATAAAATCTGGATCA TTT				
TATCTACTGCTTATGCCACCA				
TGGGATTATCATCACAACT				
ACATTGGACTACATATATTAC				
GCTGAGTTGGAAACAAAAATC				
CAAAATGAGACAAAAGCAAAAC				
TTTTGCCTACTCTCCATACC				
TTATCATCACAACTAGATC				
ACCCTGTTGAGCTTGTCTTA				
TTGGACTGAAGGAACTCCCT				
ATGGATCCCGCGGATAAGGAT				
AGATCATCTCGGCTTCAIT				
TTAGCCACAACGGATTTAACA				
TTACAGAAACAGCAACAGCTGT				
TGGGATTGGCTTTGGCTTTTC				
CAAATCCTGTCA TCCCTACCA				
TTCCCGGACGACTTTAAATT				
CAGGAGAGATTGTGGATCCA				
CAGCTGGACGACTTAGTAGAC				
CTCTGTTGGAGCTTCGAGG				
TCGCGATCTAGATCTCTTAA				

Previously unknown miRNAs identified with Shortstack & size (nt)										
ATAGAGGATCTAGAAACTGGGTTT	TM_Cluster_25078	24	ATCATGGGATCTATTGGATT	TT_Cluster_60884	21	TCTGTGGCTTGTAGTACGCTC	DT_Cluster_9519	21	ACCAGTCTGAGATCATCGTTC	DT_Cluster_40687
ACGAGCTGTACTCGCTGCT	DM_Cluster_15438	21	TCTAAGATCTCTGCTCTATC	TM_Cluster_75018	21	GCTGTGCTCTCTCCCGGTA	DT_Cluster_100403	21	AATTTTGTAGAAACTATAAGA	TT_Cluster_22502
TTGTGATGAGAGCTCTGCT	TT_Cluster_140820	21	TATTGTTATATGTTTTGGTA	TT_Cluster_79458	21	AGACTCGTAGAAGACTTCT	TT_Cluster_129316	21	GAGAAAAATAGTATGGAT	TT_Cluster_2892
TCTATTAAAGTAACTCAGACT	DT_Cluster_86175	22	CTTGCGGAGTTTATGATCTC	TM_Cluster_45056	21	TCGTTCCGTGTGTTACACTC	DT_Cluster_85961	21	AGAGTTAAGTGGAGTCGAAGA	TM_Cluster_55184
AAAAGCTCTCTGATTGATC	TM_Cluster_54203	21	ATGAATACATAGTGTAGGAT	TT_Cluster_31975	24	ATCGAGAGAGATCGAAGAACC	DM_Cluster_36769	24	AAGAAAAAAGAACTCAAGCC	TT_Cluster_154549
AAAGCAACTCTCTGCTGATT	TM_Cluster_58223	21	TTTTGGATTTGTTTGAACA	TT_Cluster_115082	21	ATCCAATGTGTATTGCTACTT	DM_Cluster_43752	24	TATTTTTTTTTTATGTTATGT	TT_Cluster_162493
AGACTGATCTTATTAAGC	DM_Cluster_71480	21	AAGGATGAGACTGAGAGAG	TT_Cluster_149505	21	GAITTTTTCTCTTGAACCT	DT_Cluster_106347	21	GCAGATGATGAGCTGAGCA	TM_Cluster_32708
AAAGGGAAGGAGAAACGAGAA	TM_Cluster_23765	24	GTATTGGAGTTAATAGAACCC	DM_Cluster_72925	24	CGGAGAATATGATGAACAAG	TT_Cluster_12548	21	ATAAATGGATCTGGATGAAGA	TT_Cluster_8816
ATTGGAAGTGCCTTTAGAT	TM_Cluster_129	22	CGCATTTCTTTAGAGATC	TM_Cluster_53036	21	TTCCAGGCTCAACTCGGA	DT_Cluster_91815	20	TTGCTCAAAATATTAAAGAG	TT_Cluster_83274
AGAAGAGGAGAGAGAAAGG	TT_Cluster_123360	21	TGGCGACTCGAAGTAGAGA	DT_Cluster_65219	21	TTGGAGCGCTTTGAGACGACT	TM_Cluster_88781	22	TCAAGAAAGCTTACACAGGA	DM_Cluster_68457
TTTTCATCAGTTTATTTGGG	DM_Cluster_39202	21	AAAAGGATCGAGGATAAAA	DT_Cluster_48080	21	TTTTCTCAGAAACAGCGGTA	TM_Cluster_27816	21	TTGACAGAGAGATGAGCAC	TM_Cluster_40901
TTTTTCTTTCTTTCTTT	DT_Cluster_45893	21	TATTGATTTTGGTCTAGG	TM_Cluster_60327	21	TTTTTTTTAAATGTTATGTTG	TT_Cluster_48679	21	CCAGTGTCTGTTAGTTGAC	TM_Cluster_14381
CACGGAATGGTATATAGCT	DM_Cluster_56508	21	TATTAAAGTGTGACATGTT	TM_Cluster_51896	21	TACTGTAGACTAGACACT	TM_Cluster_33867	21	AATTTATCACTAAAAGGCACG	TM_Cluster_18970
TGAAGTTGTCATGAAGTCTC	DM_Cluster_54050	21	ATATGCAAGTTGTAATAAC	DT_Cluster_8963	21	TCCATAGTATGACAGACT	DM_Cluster_74956	21	AACGGAAATFAAGAACTCATCT	TT_Cluster_121736
TAATTCAGCTGTTGTAACCA	DT_Cluster_91375	22	CAATGAGAGTATGTAGGCTT	DM_Cluster_44186	23	CTTCTATAAATGCAAGCT	DM_Cluster_66235	21	ATGGAGTAGAAAATGCACTG	TT_Cluster_71899
TTGACAGAGAGAGCGAGCA	DM_Cluster_11733	21	TTTGGAGAGCTCTGAGTGA	DM_Cluster_52703	21	TTCCATTAATGTAAGACT	DM_Cluster_10076	21	AATTTGCTCAATGATGTCT	DT_Cluster_60726
AATCTGTTGAGATCTAGCT	DM_Cluster_70886	21	TGAAGATGAGATGACTGAT	DM_Cluster_59766	24	CCGAGTTAATGTACTGGTT	TM_Cluster_31961	21	TTCAGAATGAGATGTAAGG	TT_Cluster_87159
AGAGGTTGTAAGAAAGTTACC	DT_Cluster_90549	21	GGTAAAAGCTTCAGAAATG	TT_Cluster_75425	21	CTGGCTCTGATACCATGTGAAGT	DM_Cluster_58696	24	TACGGTAGACGAAATGGAAT	DT_Cluster_48536
ATTGGCAACTTATTTTTGGTC	TM_Cluster_31327	24	AGGCGGATTTGAAATGAGCC	TT_Cluster_125992	21	TCGCTTGGTGCAGGTCGGAAAC	DM_Cluster_69056	22	TTCCGCTTGAAGCTGCGCTC	TT_Cluster_99626
TTCCCTGTCGTTGAGACTC	TT_Cluster_61752	22	TGAAGATCTTAAATGAGCT	DT_Cluster_21302	21	TCAITTCATTTCTTGGCGAAG	TM_Cluster_33492	24	TTGATCTGAATCAAGAGGCTC	TT_Cluster_101146
CGGATCTCGCGGTAGCTAA	TT_Cluster_6709	22	ATTCATGATATGCTACTAC	TT_Cluster_155319	21	TAGTATCAAGTGCATATAT	TM_Cluster_24345	21	AAAAAGGAGGACTCTGGGCG	TM_Cluster_32824
TCAGGTTTTGGTTAGTATCC	DM_Cluster_3672	21	AAGATCTCTTTATGCTCCG	DT_Cluster_48947	21	ATTCATCAATCTCAGGATAG	DM_Cluster_4681	21	TTGGCAGACTCTCGATCAGT	TT_Cluster_149038
ATTTATGGCTCTCTTTTT	DM_Cluster_14659	21	TCATATGAGAAACGATCCGTA	TM_Cluster_648	23	TTGCTTGCATAGAAAACCTAG	TM_Cluster_86300	22	TCCAAAGCCTTCTATGTTCT	TM_Cluster_20495
AGACATCTGTAAGACTCTCT	DM_Cluster_73601	21	AAAAGCAATCTTGAAGCGGT	DM_Cluster_42401	21	AATGAGAGTTCTAGACTGTA	TT_Cluster_69922	22	TTTTTTTACTAATGACTGACCC	TM_Cluster_30020
ACCTTATCTCTCTATCCCTC	DM_Cluster_15748	24	TGAATATCTTATTTAGTAGA	TT_Cluster_4536	24	CTTTGCTTTAGGTTTCTGTT	TT_Cluster_98357	22	ACGAGACCGCTGTAGATTAGACA	TM_Cluster_30741
AAACTTACACAGATTTAGACC	TM_Cluster_65244	24	GAAACTTGGTGGTTGGTTTTCC	TT_Cluster_4536	21	TTATCGAGTGCAGGATTAGAATC	TM_Cluster_37650	22	CTTGTGCGAGTTTACGATCTC	DM_Cluster_29058
CTGGACACTTAGTAAAGGTCGT	TM_Cluster_86431	24	AATCTGTGTGAATAAAACTATAAC	DM_Cluster_264	24	GCAGACCCCTCTGACTCAGGCT	TM_Cluster_81182	22	AATGACCTCTTTTTCTCTT	DM_Cluster_28298
ATCTGATTAAGTTTTAAGTTGGA	DM_Cluster_39689	24	ACTATAGACCCTGAAACC	DT_Cluster_69998	21	TTTTTTTACTATTACAGCTC	TT_Cluster_57302	21	TAITTTTTTGTGCTTTCT	TM_Cluster_8390
AGCCTGCTCCTACCATGAAGT	TM_Cluster_16924	24	ACGGAAGCAATAAACAGATCT	TT_Cluster_71140	21	ATTCCAATGATTTCTTTGAC	TT_Cluster_50452	21	TTTTTTTGTATTGTTATATT	TT_Cluster_128447
AGGGAACAGACTCTGTAAAAGG	DM_Cluster_63218	24	TGACACATGACAGCCGCTGAC	TT_Cluster_160692	21	GTGGTCAAGTGCATGTCATC	DT_Cluster_16177	21	TGATTGAGAAATCTGGAGT	TT_Cluster_84234
TACAAAAATTTTTTTGT	TT_Cluster_117274	21	TAAAGTGAACCGCTGCCAG	DM_Cluster_21884	21	AAACCGGAGTAACTGAACCA	TM_Cluster_24871	24	AAGAAAAAACAACACCCAGGG	TM_Cluster_91189
ACATGATTCGATATGAATA	TT_Cluster_120913	22	TTGTTCTCGGAAATTCCTCG	DT_Cluster_51067	21	TATATGCACTGTAGCTAAA	DT_Cluster_31915	21	ATAGAATAGCTGTTACAAGA	TM_Cluster_37527
AGGACTATCCAGATATGAAGA	TT_Cluster_93529	22	AGAATCTGATGATGCTGCAAT	TM_Cluster_44652	22	AGAAGCACTGTTGAAGCCA	TT_Cluster_79242	21	GTTTTTTTTTTTTGTTGTTG	TT_Cluster_96434
TCTGAGTCTATTTTGTGAC	DT_Cluster_75500	21	TTCTCCACTCATGGCCTCT	TM_Cluster_4652	21	GGAGCAGAACCAAGTTAGTCT	TT_Cluster_45521	21	CGGAAGACATGTTCAAACTG	TM_Cluster_16626
TGGAGGAGACACAATACTG	TT_Cluster_160404	21	AGATCAAAACCTGAGAGAG	DM_Cluster_44652	22	CAAAACAAAACCAATCAGTT	TT_Cluster_87517	24	TTTTTTTTTTTATGTTGTTG	TT_Cluster_146472
TAGTGAAGCAGCAAGAGAA	TM_Cluster_11636	21	CATTGGTATGCTGTGCGCA	TT_Cluster_56504	21	TGTCAGATCGTTCACGTCGGTC	TT_Cluster_115914	21	TTCCAGTCCCAAGATGCGAAC	TT_Cluster_91710
TGATGAGCGGCTCAATATC	TM_Cluster_31773	21	AGTAGTTCTGTTAGTTTGGCC	TT_Cluster_110546	21	ATTGTTGATGATATATATA	TM_Cluster_15914	21	AGACTCATGTTTATGTTGCGC	TT_Cluster_153264
TTTTTGATTAAGAAATTAAGA	TT_Cluster_31043	21	CTTATATCTAGTAAGAACT	DM_Cluster_24381	21	GTAGCACTGTGTACATGTTGAG	TM_Cluster_62213	24	ACAGATCTGCTCCCTCTC	TM_Cluster_10927
TTGAAACCAAGATCTCACCT	TM_Cluster_18741	21	CTATAAATATTAATATTTAT	DT_Cluster_52593	21	AGCGGAATAAAGAACTTGTCTCT	TM_Cluster_44506	24	CAAAAGAAAGATTTGTCACACA	DT_Cluster_4696
AAACTAAGAGACATGTAATC	TT_Cluster_31175	21	TCTAAATAGAAATCATTTGGAAC	TM_Cluster_20159	24	GAAAGGCTAGAGAAGGCT	TM_Cluster_23018	21	TTTTTTTCTCTGTTAAACT	TM_Cluster_39415
CAAGTAGACTTTGGCTCTG	TT_Cluster_49493	21	TCTTGAGATCTGCTGGAGA	TT_Cluster_26154	21	TTGGATCTCAAGAGACTCT	TM_Cluster_392	21	AACTGGATCAATGTTGTTG	TT_Cluster_127969
ATCATGCTATCCCTTCGAT	TM_Cluster_14180	21	AAAAATGGTTTTGGCAGCC	TM_Cluster_51706	21	TCITTTATGTTGTTGTTAT	DM_Cluster_53371	21	TGTTGACTGTAGCTCAAGT	TT_Cluster_54797
CCGGTGAAGATCTCAAACT	TT_Cluster_49373	21	AAAGGAGATCGAATGTAAGA	DT_Cluster_90643	21	AAGGGAATCGCAATGCTCAGAGA	DM_Cluster_73944	24	TCTGGAAGATCAATGATAGT	DM_Cluster_23013
CTATACTTATGTTGGCCAG	DM_Cluster_65227	22	CTTTCAACTTATCAAAACTGT	TM_Cluster_34784	24	ATAGAGAGAGATAGACTGA	DM_Cluster_62902	21	CCGTAAACAAAAGTTAGTCAAC	TT_Cluster_7437
TAAATTAATGATTTGGGACT	TM_Cluster_35249	21	ACGCGAAATATAAAGAACTGTTCT	DM_Cluster_37382	24	AAAGCTGTAGATAAAAACTTAAAGC	TT_Cluster_81900	24	ACGCGAAATATAAAGAACTGTTCT	DM_Cluster_69658

Previously unknown miRNAs identified with Shortstack & size (nt)

GATGATGCTGGGATTTATT	DT_Cluster_99712	21	TCACACTCGTTCAATATGCGCA	DM_Cluster_32823	21	TATATGTAGACGGTAGGTACA	TT_Cluster_79511	21
TTGGTGATAATTGGATGGCA	DT_Cluster_24117	21	ATGGGATATGGAGATCTCTTC	DM_Cluster_21155	22	CTAGGCCGTAGCTATGGCCTT	TT_Cluster_7092	21
AGTATGATTTGGTATTGACA	DT_Cluster_29179	21	AATCAAGCTTCTCCGGCTCTC	DM_Cluster_54440	21	TCGAACCGCCTTCAAACAAGAG	DM_Cluster_65288	21
ATFACGAGGATCAAAAGCAATGT	DM_Cluster_64248	24	TTTTGAGATCTCTACATGGTA	TT_Cluster_31983	21	ACCTGCTTCTCTGTATAACC	TT_Cluster_6710	21
AAAATAACATTCATTAAGAGTTAA	DM_Cluster_35980	24	AATATAAAAACCCGCTTTTGA	TT_Cluster_122926	21	AGAGGTGTCAGAAAGAGTTACC	TT_Cluster_129180	21
FAGAAATCTTTTTATTTTTT	TT_Cluster_21225	21	GAAGACACAGAAAGCTGAAT	TT_Cluster_107573	21	TTTTAGTGTGAAAATATAGATG	TM_Cluster_90838	21
TTTTCTTGTCTGACGTTAGC	TM_Cluster_89694	21	TACTACCGTCTACATATA TG	TT_Cluster_79512	21	ACCGGATCTGAAAAGAAGACG	TT_Cluster_85098	21
TTATGCGCTGCTTAACCGAT	DM_Cluster_7814	21	TGCGGACACAGTTTGTGGCC	TT_Cluster_111347	21	TTATGTTATGTTATGTTGAGT	TT_Cluster_113382	21
TTTTTGTCATTTGCGTTTTGA	TM_Cluster_6643	22	GCAACTACTGTTGAAGTGTG	DT_Cluster_81732	21	AAAGATATATATATGTAGACACT	TM_Cluster_22037	24
ATTCGTTAAGCTCTGAGAGATTGC	DM_Cluster_39510	24	ATCAATGATTGGTGAAGAGT	DT_Cluster_17185	21			
TTAACTAAAAACTAAGAACC	TT_Cluster_90833	21	TTTTGACTTGCATCTCAAGTTG	DM_Cluster_65653	21			
ATCTGATCACAAAGTTAATCT	TM_Cluster_69182	21	TATCGGTAATCTTTAGTTTA	DT_Cluster_37598	21			
AACCCATCGTTGTGACAGA	TM_Cluster_41428	21	TCGAGTAAGCCAAAGCGCAC	DT_Cluster_23782	21			
AAGAGAGAAAGTGGACAGAAC	TT_Cluster_122750	21	ATCCATAGTATCAGAGATC	TT_Cluster_11273	21			
ATTTTCATGCGCTTTGTCGTAAG	DM_Cluster_23809	24	TCTCCTCGCAAACATCAGGT	TM_Cluster_17285	21			
TGAGATTGAGATTGTTCTTG	TT_Cluster_26085	21	AGGGATAAACATTCATGCTC	DT_Cluster_80569	21			
TTTTGATTGTTGGCGGTTGGA	TT_Cluster_28252	21	AACCTGACGATTTGAAGAAC	TT_Cluster_111866	21			
ACGAAGCATAGAACAGATCTTCT	TM_Cluster_77026	24	AATAGATAAGTCCACAGACT	TT_Cluster_11273	21			
AGGACTACTCCGGCACAGC	DT_Cluster_63465	22	CGATAAAGACTCAAAACATT	DM_Cluster_91467	21			
AAAAAAAAGAAACAATGATCTCT	DT_Cluster_108551	21	TTGGTGTGAAATAAAGTGACAGT	TM_Cluster_43468	24			
GCTATGAGATCAAAAGGTTGT	DT_Cluster_32516	21	CGATGAGTGGGGGCTTATCTT	TM_Cluster_73929	21			
GTGAGTCTAAAGTCTCAACTTT	TM_Cluster_74925	24	GAAGACTGTAGTTGTTGTTG	DM_Cluster_57845	21			
CTGCAGCTGCTCATGGCTG	TT_Cluster_159252	21	GGAGAGACATATTCGGGCTGA	TM_Cluster_21042	21			
AAAAACGGAAACCGAACCAAAACC	TM_Cluster_51842	24	ATTCGAGGACAGAGACGTACC	DT_Cluster_1457	22			
ATCCAAAAGTATTTCGTTGTTAT	DM_Cluster_59926	24	TAACATAAAAAAACTAAGAAC	TM_Cluster_30515	22			
ATCAAAATATAGTGGTTGTTATT	DM_Cluster_1748	24	ACTTGGTCAATTGTTGTTAG	TM_Cluster_29410	21			
TCAGAGACTTATATAAGT	DM_Cluster_76911	24	TCTGAATCCAAGTAAGTTAAT	DM_Cluster_58756	24			
AAATAAGTCTGGAAGGTTCTCC	DM_Cluster_49871	24	GCCGGTCTCGAGATTTGGGGAGG	TM_Cluster_58070	21			
ACTAGGAGATTTGACGCGACG	TT_Cluster_107634	21	TACTTTACTAATAATTAGGAT	TT_Cluster_103224	21			
TGCACTGCCCTTCCCTGGCT	DM_Cluster_72862	21	TTGTTGAAACCGAGCTAGTTGC	TM_Cluster_81969	21			
TGTAACCGGTTAATCTCTCT	DM_Cluster_58765	21	GAGAAITATTGGCAGCTGCATCGT	DM_Cluster_67885	21			
TATTACTAAAATCTCTCCC	TT_Cluster_39048	21	TCAGTGATTTACAGGCCAGC	TT_Cluster_24622	21			
TTGATGATGCTCTGTTGATG	DM_Cluster_33373	21	TAAGAACCACATAATCATG	TT_Cluster_107352	21			
ATGTTATATTTTAAATAGTTAGACT	DM_Cluster_75967	24	AGAGACGCGACTGACATTTGA	DT_Cluster_90935	20			
GTCAAGATCTCATCAAGTAGA	TT_Cluster_64750	21	AGTCTGAAACTTTTGACATTGC	DT_Cluster_95086	23			
TGTTCTGGGTTTTTACGGA	TM_Cluster_25944	21	TCACGGATTTATTTTTGGATC	TT_Cluster_157642	21			
AAACCTCTGATCTCATAGCTC	DM_Cluster_20384	21	CCGTGGGGGAAACCGTTGAGC	TT_Cluster_129472	22			
CATGAAGACTTCAAGAAGCT	DM_Cluster_54243	21	ACATGATCATCTGTTGATG	TT_Cluster_44854	21			
ATATTTCCGTTAAGAACTTCACC	DT_Cluster_120084	22	CGAGGCAATGAGACACAAGA	TT_Cluster_104489	21			
AACTATACTAAAACCTTGAAC	TT_Cluster_5829	21	TTCCCTTTCCGTTTATGTTT	TM_Cluster_70129	21			
ACGAAGCATAGAACAAGATCTT	TT_Cluster_139251	21	CCACGAGATCTCAAGCCTGA	DT_Cluster_10323	21			
ATTAAATAATACTGAGAGAA	TM_Cluster_87465	21						
TATAGTAAATAGTACTGCT	TM_Cluster_72019	21						
CATCGGTATAAATTAATTA	TT_Cluster_157177	21						
GCTACGTAAACCAAGCGGGA	TT_Cluster_23157	22						

Table S9: bna-miRNA:mRNA pairs in *B. napus*.

miRNA ^a	Target transcript ID	Predicted gene function	Cleavage position	miRNA:mRNA target pair (5'-3' : 3'-5')	Cleavage found in PAREseq replicates	DM	DT	TM	TT
bna-miR156	BnaA06g36780D	SPL 2 ¹	3011	TTA AACTG TCTCTCTCTCTCGTGGTAGTTCT	DT2 DT3 TT3	0.00	1.13	0.00	0.37
bna-miR156	BnaA06g36780D	SPL 2 ¹	3012	CTT AAACTG TCTCTCTCTCTCGTGGTAGTTCT	DT2 DT3 TT3	0.00	2.04	1.59	3.93
bna-miR156	BnaA04g19840D	SPL 3 ²	560	TGT GACTG TCTCTCTCGTGGTTCCGATTT	DM3 DT3 TT3	1.19	3.31	0.00	1.48
bna-miR156	BnaC04g44230D	SPL 3 ²	619	TGT GACTG TCTCTCTCGTGGTTCCGGAAT	DM3 DT3 TT3	1.19	3.31	0.00	1.48
bna-miR156	BnaC02g19100D	SPL 6 ³	1116	CTG ACTG TCTCTCTCTCGTGTTCATCTC	DM3 DT2 DT3 TM3 TT3	4.50	17.09	5.12	4.07
bna-miR156	BnaC02g14000D	SPL 6 ³	1095	CTG ACTG TCTCTCTCTCGTGTTCATCTC	DM3 DT2 DT3 TM3 TT3	4.50	17.09	5.12	4.07
bna-miR156	BnaC02g19100D	SPL 6 ³	1116	CTG ACTG TCTCTCTCTCGTGTTCATCTC	DM3 DT2 DT3 TM3 TT3	4.50	17.09	5.12	4.07
bna-miR156	BnaC02g14000D	SPL 6 ³	1095	CTG ACTG TCTCTCTCTCGTGTTCATCTC	DM3 DT2 DT3 TM3 TT3	4.50	17.09	5.12	4.07
bna-miR156	BnaA07g27730D	SPL 6 ³	639	CTG ACTG TCTCTCTCACTCGTGTTCATCT	DM3 DT2 DT3	4.50	17.09	0.00	0.00
bna-miR156	BnaA02g14580D	SPL 6 ³	1083	o ACT CGA CTG TCTCTCTCTCTCGTGTTCATCT	DM3 TM3 TT3	2.56	0.00	0.94	4.21
bna-miR156	BnaA07g27730D	SPL 6 ³	640	o ACT CGA CTG TCTCTCTCTCTCGTGTTCATCT	DM3 TM3 TT3	2.56	0.00	0.94	4.21
bna-miR156	BnaC02g19100D	SPL 6 ³	1117	o ACT CGA CTG TCTCTCTCTCTCGTGTTCATCT	DM3 TM3 TT3	2.56	0.00	0.94	4.21
bna-miR156	BnaC02g14000D	SPL 6 ³	771	o ACT CGA CTG TCTCTCTCTCTCGTGTTCATCT	DM3 TM3 TT3	1.75	0.00	1.06	1.43
bna-miR156	BnaC02g14000D	SPL 6 ³	1096	o ACT CGA CTG TCTCTCTCTCTCGTGTTCATCT	DM3 TM3 TT3	2.56	0.00	0.94	4.21
bna-miR156	BnaC07g11380D	SPL 10 ³	1568	CTT CAACTG TCTCTCTCTCTCTCGTGGCACCTT	DM2 DM3 DT2 DT3 TM2 TM3 TT3	18.84	0.86	14.61	34.85
bna-miR156	BnaA07g08830D	SPL 10 ³	1632	CTG CAACTG TCTCTCTCTCTCTCGTGGCACCTT	DM3 DT3 TM2 TM3 TT3	19.51	8.58	33.17	31.01
bna-miR156	BnaC07g11380D	SPL 10 ³	1567	TTC AACTG TCTCTCTCTCTCTCGTGGCACCTT	DM3 DT3 TM3 TT3	0.19	0.27	1.00	2.96
bna-miR156	BnaA07g08830D	SPL 10 ³	1631	TGC AACTG TCTCTCTCTCTCTCGTGGCACCTT	DM3 TM3 TT3	5.00	0.00	0.77	3.89
bna-miR156	BnaAnng25050D	SPL 11 ³	1341	CTG CAACTG TCTCTCTCTCTCTCGTGGCACCTT	DM3 DT3 TM2 TM3 TT3	19.51	8.58	33.17	31.01
bna-miR156	BnaC05g21270D	SPL 11 ³	1690	TTC AACTG TCTCTCTCTCTCTCGTGGCACCTT	DM3 DT3 TM3 TT3	0.19	0.27	1.00	3.01
bna-miR156	BnaAnng25050D	SPL 11 ³	1340	TGC AACTG TCTCTCTCTCTCTCGTGGCACCTT	DM3 TM3 TT3	5.00	0.00	0.77	3.89
bna-miR156	BnaC04g23930D	SPL 15 ³	952	CTC AAACTG TCTCTCTCTCTCTCGTGGCAACT	DM2 DM3 DT3 TM3 TT3	2.80	3.00	0.82	1.90
bna-miR160	BnaA07g13830D	ARF 10 ⁴	1698	TCG AACTG TCTCTCTCTCTCTCGTGGCAACT	DM3 DT2 DT3 TM2 TM3 TT2 TT3	8.94	12.50	18.38	20.22
bna-miR160	BnaA01g06910D	ARF 16 ⁴	2341	TAA TAGCGG ACCGAGGGACATTTGGTGGCCCTT	DM3 DT2 DT3 TM2 TM3 TT2 TT3	8.06	22.86	18.60	32.45
bna-miR160	BnaC01g08330D	ARF 16 ⁴	2324	TAA TAGCGG ACCGAGGGACATTTGGTGGCCCTT	DM3 DT2 DT3 TM2 TM3 TT2 TT3	8.06	22.86	18.60	32.45
bna-miR171	BnaAnng18550D	SCL 6 ⁵	840	o AACTA ACTCGG CGGGTTATAGGGACACGGT	DM3 DT2 DT3 TM3 TT3	4.13	4.22	5.30	0.97
bna-miR171	BnaAnng18540D	SCL 6 ⁵	851	o AACTA ACTCGG CGGGTTATAGGGACACGGT	DM3 DT2 DT3 TM3 TT3	4.13	4.22	5.30	0.97
bna-miR171	BnaC04g22080D	SCL 22 ⁶	816	o AACTA ACTCGG CGGGTTATAGGGACACGGT	DM3 DT2 TM3 TT3	14.50	4.53	1.06	0.60
bna-miR172	BnaC09g13430D	ERF RAP2-7	1039	o AAT CTCT AGG ACTACTACGACG-ACGTTGAC	DM2 DM3 DT2 DT3 TM2 TM3 TT3	16.60	10.03	14.48	6.66

brna-miR172	BnaA03g22100D	ERF RAP2-7 ⁷	2284	AGAACTTGTGATGCTGTCAT	o	AATCTCTAGGACTACTACGACG-ACGTTGAC	DM2 DM3 DT2 DT3 TM2 TM3 TT3	16.60	10.03	14.48	6.66
brna-miR172	BnaC03g26480D	ERF RAP2-7 ⁷	2328	AGAACTTGTGATGCTGTCAT	o	AATCTCTAGGACTACTACGACG-ACGTTGAC	DM2 DM3 DT2 DT3 TM2 TM3 TT3	16.60	10.03	14.48	6.66
brna-miR172	BnaC04g15640D	ERF RAP2-7 ⁷	2414	AGAACTTGTGATGCTGTCAT	o	AATCTCTAGGACTACTACGACG-ACGTTGAC	DM2 DM3 DT2 DT3 TM2 TM3 TT3	16.60	10.03	14.48	6.66
brna-miR172	BnaC03g26480D	ERF RAP2-7 ⁷	2328	GGAATCTGTGATGCTGTCAT	o o	AATCTCTAGGACTACTACGACG-ACGTTGAC	DM2 DM3 DT2 DT3 TM2 TM3 TT3	16.60	10.03	14.48	6.66
brna-miR172	BnaA03g22100D	ERF RAP2-7 ⁷	2284	GGAATCTGTGATGCTGTCAT	o o	AATCTCTAGGACTACTACGACG-ACGTTGAC	DM2 DM3 DT2 DT3 TM2 TM3 TT3	16.60	10.03	14.48	6.66
brna-miR172	BnaC04g15640D	ERF RAP2-7 ⁷	2414	GGAATCTGTGATGCTGTCAT	o o	AATCTCTAGGACTACTACGACG-ACGTTGAC	DM2 DM3 DT2 DT3 TM2 TM3 TT3	16.60	10.03	14.48	6.66
brna-miR172	BnaC09g13430D	ERF RAP2-7 ⁷	1039	GGAATCTGTGATGCTGTCAT	o o	AATCTCTAGGACTACTACGACG-ACGTTGAC	DM2 DM3 DT2 DT3 TM2 TM3 TT3	16.60	10.03	14.48	6.66
brna-miR172	BnaA10g12950D	AP2-like ERF TOE2 ⁸	2933	AGAACTTGTGATGCTGTCAT	o	ACACTCTAGGACTACTACGACGTAACACTCTC	DM3 DT2 DT3 TM2 TM3 TT3	0.75	5.00	11.14	9.95
brna-miR172	BnaC09g35430D	AP2-like ERF TOE2 ⁸	2671	AGAACTTGTGATGCTGTCAT	o	ACACTCTAGGACTACTACGACGTAACACTCTC	DM3 DT2 DT3 TM2 TM3 TT3	0.75	5.00	11.14	9.95
brna-miR172	BnaA10g12950D	AP2-like ERF TOE2 ⁸	2933	GGAATCTGTGATGCTGTCAT	o o	ACACTCTAGGACTACTACGACGTAACACTCTC	DM3 DT2 DT3 TM2 TM3 TT3	0.75	5.00	11.14	9.95
brna-miR172	BnaC09g35430D	AP2-like ERF TOE2 ⁸	2671	GGAATCTGTGATGCTGTCAT	o o	ACACTCTAGGACTACTACGACGTAACACTCTC	DM3 DT2 DT3 TM2 TM3 TT3	0.75	5.00	11.14	9.95
brna-miR172	BnaA07g12050D	AP2-like ERF TOE3 ⁹	2227	AGAACTTGTGATGCTGTCAT	o	CCTCTCTAGGACTACTACGCGGTAAGGGTG	DM3 TM2 TT3	1.56	0.00	8.75	0.46
brna-miR172	BnaC07g16190D	AP2-like ERF TOE3 ⁹	2185	AGAACTTGTGATGCTGTCAT	o	CCTCTCTAGGACTACTACGCGGTAAGGGTG	DM3 TM2 TT3	1.56	0.00	8.75	0.46
brna-miR172	BnaA07g12050D	AP2-like ERF TOE3 ⁹	2227	GGAATCTGTGATGCTGTCAT	o o	CCTCTCTAGGACTACTACGCGGTAAGGGTG	DM3 TM2 TT3	1.56	0.00	8.75	0.46
brna-miR172	BnaCmg39690D	ERF APETALA 2 ⁷	2233	GGAATCTGTGATGCTGTCAT	o o	CCTCTCTAGGACTACTACGCGGTAAGGGTG	DT2 DT3 TT3	0.00	0.53	0.71	1.25
brna-miR172	BnaCmg39690D	ERF APETALA 2 ⁷	2233	GGAATCTGTGATGCTGTCAT	o o	CCTCTCTAGGACTACTACGCGGTAAGGGTG	DT2 DT3 TT3	0.00	0.53	0.71	1.25
brna-miR172	BnaA01g34730D	ERF APETALA 2 ⁷	1043	AGAACTTGTGATGCTGTCAT	o	CCTCTCTAGGACTACTACGCGGTAAGGGTG	DM2 DM3 DT2 TM3 TT3	3.62	2.04	0.47	1.62
brna-miR172	BnaA01g34730D	ERF APETALA 2 ⁷	1043	AGAACTTGTGATGCTGTCAT	o o	CCTCTCTAGGACTACTACGCGGTAAGGGTG	DM2 DM3 DT2 TM3 TT3	3.62	2.04	0.47	1.62
brna-miR393	BnaC02g36370D	AUXIN SIGNALING F-BOX 2 ¹⁰	2591	TCCAAAGGATCCGATGATC	o	CTGTAGGTTCCCTAGCGTAAACAAGATGAA	DM2 DM3 DT2 DT3 TM3 TT3	7.08	2.00	5.77	8.70
brna-miR393	BnaA02g28290D	AUXIN SIGNALING F-BOX 2 ¹⁰	2531	TCCAAAGGATCCGATGATC	o	CTGTAGGTTCCCTAGCGTAAACAAGATGAA	DM2 DM3 DT2 DT3 TM3 TT3	7.08	2.00	5.77	8.70
brna-miR393	BnaC08g40890D	AUXIN SIGNALING F-BOX 3 ¹¹	2468	TCCAAAGGATCCGATGATC	o	CTGTAGGTTCCCTAGCGTAAACAAGATGAA	DM3 DT3 TM3 TT3	2.63	4.63	9.30	12.08
brna-miR393	BnaA08g24570D	AUXIN SIGNALING F-BOX 3 ¹¹	2640	TCCAAAGGATCCGATGATC	o	CTGTAGGTTCCCTAGCGTAAACAAGATGAA	DM3 DT3 TM3 TT3	2.63	4.63	9.30	12.08
brna-miR398	BnaA04g16310D	Supperoxide dismutase [Cu-Zn], chloroplast ²²	776	TGTTGTTCCAGGTCACCCCTG	o	TATTACA-AAGGGTCCAGTGGCGCTACTGCGCT	DM2 TM3 TT3	3.42	0.00	1.35	0.23
brna-miR403	BnaCmg68320D	ARGONAUTE 2 ²³	3030	TTAGATTCACGCACAAAATCG	o	GGTTAARTCTAAGTGGCTGTTTGAGGAACTCTA	DM1 DM3 DT1 DT2 DT3 TM2 TM3 TT3	62.32	9.04	9.78	5.46
brna-miR403	BnaA05g14760D	ARGONAUTE 2 ²³	3378	TTAGATTCACGCACAAAATCG	o	GGTTAARTCTAAGTGGCTGTTTGAGGAAAGATG	DM1 TM3 TT3	0.03	0.00	0.82	2.55

^a *Brassica napus* miRNA identified in sRNAseq and PAREseq data

SPL = SQUAMOSA PROTEIN-BINDING LIKE; ARF = auxin response factor; SCL = SCARECROW-LIKE; ERF = ethylene-responsive transcription factor;

Reference

- Rhoades, M. W. *et al.* Prediction of plant microRNA targets. *Cell* **110**, 513-520 (2002).
- Gandikota, M. *et al.* The miRNA156/157 recognition element in the 5' UTR of the Arabidopsis SBP box gene SPL3 prevents early flowering by translational inhibition in seedlings. *Plant J* **49**, 683-69 (2006).
- Xu, M. *et al.* Developmental functions of miR156-Regulated SQUAMOSA PROMOTER BINDING PROTEIN-LIKE (SPL) genes in Arabidopsis thaliana. *PLoS Genet* **12**, e1006263 (2016).
- Wang, J. W. *et al.* Control of root cap formation by MicroRNA-targeted AUXIN RESPONSE FACTOR (ARF) genes in Arabidopsis. *Plant Cell* **17**, 2204-2216 (2005).
- Llave, C., Xie, Z., Kasschau, K. D. & Carrington, J. C. Cleavage of SCARECROW-LIKE (SCL) mRNA targets directed by a class of Arabidopsis miRNA. *Science* **297**, 2053-2056 (2002).
- Ma, Z. *et al.* Arabidopsis miR171-targeted SCARECROW-LIKE (SCL) proteins bind to GT cis-elements and mediate gibberellin-regulated chlorophyll biosynthesis under light conditions. *PLoS Genet* **7**, e1002100 (2011).
- Kim, S., Soltis, P. S., Wall, K. & Soltis, D. E. Phylogeny and domain evolution in the APETALA2-like gene family. *Mol Biol Evol* **23** (2006).
- Yu, S. *et al.* Gibberellin regulates the Arabidopsis floral transition through miR156-targeted SQUAMOSA promoter binding-like transcription factors. *Plant Cell* **24**, 3320-3332 (2012).
- Jung, J. H., Lee, S., Yun, J., Lee, M., & Park, C. M. The miR172 target TOE3 represses AGAMOUS expression during Arabidopsis floral patterning. *Plant Sci* **215-216**, 29-38, (2014).
- Si-Ammour, A. *et al.* miR393 and secondary siRNAs regulate expression of the TIR1/AFB2 auxin receptor and auxin-related development of Arabidopsis leaves. *Plant Physiol* **157**, 683-691 (2011).
- Vidal, E. *et al.* Nitrate-responsive miR393/AFB3 regulatory module controls root system architecture in Arabidopsis thaliana. *Proc Natl Acad Sci U S A* **107**, 4477-4482, (2010).

stu-miR8005a	TTTAGAGTTAAAGGTTTAGAGTT	TTTAGGGTTAAGGTTTAGAGTT	TTTAGGGTTAAGGTTTAGAGTT	BnaC03g70840D	uncharacterized protein at4g26485	1266	TTTAGGGTTAGGGTTAGAGTT TCCAAATCCAAATCTCAAAATCCAAATCC	DM2 DM3 TM2	14.17	0.00	0.16	0.00
stu-miR8005a	TTTAGAGTTAAAGGTTTAGAGTT	TTTAGGGTTAAGGTTTAGAGTT	TTTAGGGTTAAGGTTTAGAGTT	BnaCmg53590D	FRUCTOSE-1,6-BISPHOSPHATASE, cytosolic	2962	TTTAGGGTTAGGGTTAGAGTT TCCAAATCCAAATCCCAAAATCTCAAAATCTC	DM2 DM3 TM2	17.23	0.00	0.16	0.00
stu-miR8005a	TTTAGAGTTAAAGGTTTAGAGTT	TTTAGGGTTAAGGTTTAGAGTT	TTTAGGGTTAAGGTTTAGAGTT	BnaC06g28920D	HISTONE-LYSINE N-METHYLTRANSFERASE, H3 lysine-9 specific SUVH7	427	TTTAGGGTTAGGGTTAGAGTT TCCAAATCCAAATCCCAAAATCCCAAAATCC	DM2 DM3 TM2	17.23	0.00	0.16	0.00
stu-miR8005a	TTTAGAGTTAAAGGTTTAGAGTT	TTTAGGGTTAAGGTTTAGAGTT	TTTAGGGTTAAGGTTTAGAGTT	BnaC05g1740D	UDP-GLYCOSYLTRANSFERASE 72B3	2528	TTTAGGGTTAGGGTTAGAGTT TCCAAATCCAAATCCCAAAATCTCAAAATCC	DM2 DM3 TM2	17.23	0.00	0.16	0.00
stu-miR8005a	TTTAGAGTTAAAGGTTTAGAGTT	TTTAGGGTTAAGGTTTAGAGTT	TTTAGGGTTAAGGTTTAGAGTT	BnaC07g33840D	unknown	534	TTTAGGGTTAGGGTTAGAGTT TCCAAATCCCAAAATCCCAAAATCCCAAAATCT	DM2 DM3 TM2	17.23	0.00	0.16	0.00
stu-miR8005a	TTTAGAGTTAAAGGTTTAGAGTT	TTTAGGGTTAAGGTTTAGAGTT	TTTAGGGTTAAGGTTTAGAGTT	BnaC09g4510D	SPlicing FACTOR UZAF large subunit B	2134	TTTAGGGTTAGGGTTAGAGTT TCCAAATCCCAAAATCCCAAAATCTCAAAATCC	DM2 DM3 TM2	17.23	0.00	0.16	0.00
stu-miR8005a	TTTAGAGTTAAAGGTTTAGAGTT	TTTAGGGTTAAGGTTTAGAGTT	TTTAGGGTTAAGGTTTAGAGTT	BnaC04g21710D	F-BOX/KELCH-repeat protein AT3G61590	3241	TTTAGGGTTAGGGTTAGAGTT TCCAAATCCCAAAATCGCAAATCTCAAAATCC	DM2 DM3 TM2	17.23	0.00	0.16	0.00
stu-miR8005a	TTTAGAGTTAAAGGTTTAGAGTT	TTTAGGGTTAAGGTTTAGAGTT	TTTAGGGTTAAGGTTTAGAGTT	BnaC09g16870D	Histone-lysine n-methyltransferase ATXR7	588	TTTAGGGTTAGGGTTAGAGTT TCCAAATCCCAAAATCCCAAAATCTCAAAATCTC	DM2 DM3 TM2	12.04	0.00	0.16	0.00
stu-miR8005a	TTTAGAGTTAAAGGTTTAGAGTT	TTTAGGGTTAAGGTTTAGAGTT	TTTAGGGTTAAGGTTTAGAGTT	BnaC08g20210D	Toll/interleukin-1 receptor-like protein	1829	TTTAGGGTTAGGGTTAGAGTT TCTCAAATCTCAAATCTCAAATCTCAAATTTTC	DM2 DM3 TM2	17.23	0.00	4.93	0.00
stu-miR8005a	TTTAGAGTTAAAGGTTTAGAGTT	TTTAGGGTTAAGGTTTAGAGTT	TTTAGGGTTAAGGTTTAGAGTT	BnaC08g03760D	P10-INTERACTING PROTEIN 1	337	TTTAGGGTTAGGGTTAGAGTT TCCAAATCCCAAAATCCCAAAATCCCAAAATCC	DM2 DM3 TM2	17.23	0.00	0.16	0.00
stu-miR8005a	TTTAGAGTTAAAGGTTTAGAGTT	TTTAGGGTTAAGGTTTAGAGTT	TTTAGGGTTAAGGTTTAGAGTT	BnaC05g16440D	unknown	528	TTTAGGGTTAGGGTTAGAGTT TCCAAATCCCAAAATCCCAAAATCTCAAAATCC	DM2 DM3 TM2	17.23	0.00	0.16	0.00
stu-miR8005a	TTTAGAGTTAAAGGTTTAGAGTT	TTTAGGGTTAAGGTTTAGAGTT	TTTAGGGTTAAGGTTTAGAGTT	BnaC08g43080D	EPSIN	1184	TTTAGGGTTAGGGTTAGAGTT TCCAAATCCCAAAATCTCAAAATCCCAAAATCC	DM2 DM3 TM2	17.23	0.00	0.16	0.00
stu-miR8005a	TTTAGAGTTAAAGGTTTAGAGTT	TTTAGGGTTAAGGTTTAGAGTT	TTTAGGGTTAAGGTTTAGAGTT	BnaC01g32070D	unknown	2296	TTTAGGGTTAGGGTTAGAGTT TCCAAATCCCAAAATCCCAAAATCTCAAAATCC	DM2 DM3 TM2	17.23	0.00	0.16	0.00
stu-miR8005a	TTTAGAGTTAAAGGTTTAGAGTT	TTTAGGGTTAAGGTTTAGAGTT	TTTAGGGTTAAGGTTTAGAGTT	BnaC07g21320D	PURPLE ACID PHOSPHATASE 7	5825	TTTAGGGTTAGGGTTAGAGTT TCCAAATCCCAAAATCTCAAAATCCCAAAATCC	DM2 DM3 TM2	17.23	0.00	0.16	0.00
stu-miR8005a	TTTAGAGTTAAAGGTTTAGAGTT	TTTAGGGTTAAGGTTTAGAGTT	TTTAGGGTTAAGGTTTAGAGTT	BnaC04g30340D	15.7 kDa heat shock protein, peroxisomal	357	TTTAGGGTTAGGGTTAGAGTT TCCAAATCCCAAAATCCCAAAATCTCAAAATCT	DM2 DM3 TM2	17.23	0.00	0.16	0.00
stu-miR8005a	TTTAGAGTTAAAGGTTTAGAGTT	TTTAGGGTTAAGGTTTAGAGTT	TTTAGGGTTAAGGTTTAGAGTT	BnaC02g08880D	unknown	708	TTTAGGGTTAGGGTTAGAGTT TCCAAATCCCAAAATCCCAAAATCTCAAAATCT	DM2 DM3 TM2	14.17	0.00	0.16	0.00
stu-miR8005a	TTTAGAGTTAAAGGTTTAGAGTT	TTTAGGGTTAAGGTTTAGAGTT	TTTAGGGTTAAGGTTTAGAGTT	BnaC06g18020D	unknown	517	TTTAGGGTTAGGGTTAGAGTT TCCAAATCCCAAAATCTCAAATCCCAAAATCC	DM2 DM3 TM2	17.23	0.00	0.16	0.00
stu-miR8005a	TTTAGAGTTAAAGGTTTAGAGTT	TTTAGGGTTAAGGTTTAGAGTT	TTTAGGGTTAAGGTTTAGAGTT	BnaC06g20530D	SYNAPTONEMLAL COMPLEX 2	5207	TTTAGGGTTAGGGTTAGAGTT TCCAAATCCCAAAATCTCAAATCCCAAAATCTCA	DM2 DM3 TM2	17.23	0.00	0.16	0.00
stu-miR8005a	TTTAGAGTTAAAGGTTTAGAGTT	TTTAGGGTTAAGGTTTAGAGTT	TTTAGGGTTAAGGTTTAGAGTT	BnaC05g30190D	LINOLEATE 9S-LIPOXYGENASE 5, chloroplastic	3792	TTTAGGGTTAGGGTTAGAGTT TCCAAATCCCAAAATCTCAAATCCCAAAATCC	DM2 DM3 TM2	17.23	0.00	0.16	0.00
stu-miR8005a	TTTAGAGTTAAAGGTTTAGAGTT	TTTAGGGTTAAGGTTTAGAGTT	TTTAGGGTTAAGGTTTAGAGTT	BnaC06g06260D	uncharacterized protein At1g24485	4115	TTTAGGGTTAGGGTTAGAGTT TCCAAATCCCAAAATCCCAAAATCTCAAAATCC	DM2 DM3 TM2	17.23	0.00	0.16	0.00
stu-miR8005a	TTTAGAGTTAAAGGTTTAGAGTT	TTTAGGGTTAAGGTTTAGAGTT	TTTAGGGTTAAGGTTTAGAGTT	BnaCmg10820D	unknown	5333	TTTAGGGTTAGGGTTAGAGTT TCCAAATCCCAAAATCCCAAAATCTCAAAATCT	DM2 DM3 TM2	17.23	0.00	0.16	0.00
stu-miR8005a	TTTAGAGTTAAAGGTTTAGAGTT	TTTAGGGTTAAGGTTTAGAGTT	TTTAGGGTTAAGGTTTAGAGTT	BnaA10g01220D	Histone-lysine n-methyltransferase MEDEA	2903	TTTAGGGTTAGGGTTAGAGTT TCCAAATCCCAAAATCCCAAAATCCCAAAATCC	DM2 DM3 TM2	17.23	0.00	0.16	0.00
stu-miR8005a	TTTAGAGTTAAAGGTTTAGAGTT	TTTAGGGTTAAGGTTTAGAGTT	TTTAGGGTTAAGGTTTAGAGTT	BnaC07g18670D	ALPHA-GLUCAN WATER DIKINASE 2	1317	TTTAGGGTTAGGGTTAGAGTT TCCAAATCCCAAAATCCCAAAATCTCAAAATCTC	DM2 DM3 TM2	12.04	0.00	0.16	0.00
stu-miR8005a	TTTAGAGTTAAAGGTTTAGAGTT	TTTAGGGTTAAGGTTTAGAGTT	TTTAGGGTTAAGGTTTAGAGTT	BnaC01g10210D	CALCINEURIN B-LIKE PROTEIN 1	1463	TTTAGGGTTAGGGTTAGAGTT TCCAAATCCCAAAATCCCAAAATCTCAAAATCTC	DM2 DM3 TM2	17.23	0.00	0.16	0.00
stu-miR8005a	TTTAGAGTTAAAGGTTTAGAGTT	TTTAGGGTTAAGGTTTAGAGTT	TTTAGGGTTAAGGTTTAGAGTT	BnaC06g0620D	Proteasome subunit alpha type-5-A	2881	TTTAGGGTTAGGGTTAGAGTT TCCAAATCCAAATCTCAAAATCTCAAAATCTCA	DM2 DM3 TM2	14.17	0.00	4.14	0.00

stu-miR8005a	TTTAGAGTTAAAGGTTTAGAGTT	TTTAGGGTTAAGGTTTAGAGTT	BnaC07g05560D	Probable disease resistance protein RPP1	1324	TTTAGGGTTAGGGTTTAGAGTT TCCAAATCCAAATCTCAAAATCCAAATCC	DM2 DM3 TM2	12.04	0.00	0.16	0.00
stu-miR8005a	TTTAGAGTTAAAGGTTTAGAGTT	TTTAGGGTTAAGGTTTAGAGTT	BnaC07g01030D	ALPHA-DIOXYGENASE 1	518	TTTAGGGTTAGGGTTTAGAGTT TCCAAATCCAAATCTCAAAATCCAAATCC	DM2 DM3 TM2	17.23	0.00	0.16	0.00
stu-miR8005a	TTTAGAGTTAAAGGTTTAGAGTT	TTTAGGGTTAAGGTTTAGAGTT	BnaC08g12110D	NDR1/HIN1-LIKE 3	1415	TTTAGGGTTAGGGTTTAGAGTT TCCAAATCCAAATCTCAAAATCCAAATCC	DM2 DM3 TM2	17.23	0.00	0.16	0.00
stu-miR8005a	TTTAGAGTTAAAGGTTTAGAGTT	TTTAGGGTTAAGGTTTAGAGTT	BnaC09g48090D	FORMIN-LIKE 20	1726	TTTAGGGTTAGGGTTTAGAGTT TCCAAATCCAAATCTCAAAATCTCAAAATCC	DM2 DM3 TM2	12.04	0.00	0.16	0.00
stu-miR8005a	TTTAGAGTTAAAGGTTTAGAGTT	TTTAGGGTTAAGGTTTAGAGTT	BnaC09g52700D	unknown	1488	TTTAGGGTTAGGGTTTAGAGTT TCCAAATCCAAATCTCAAAATCCAAATCC	DM2 DM3 TM2	17.23	0.00	0.16	0.00
stu-miR8005a	TTTAGAGTTAAAGGTTTAGAGTT	TTTAGGGTTAAGGTTTAGAGTT	BnaC09g27140D	PROTEASE DO-LIKE 4, mitochondrial	621	TTTAGGGTTAGGGTTTAGAGTT TCCAAATCCAAATCTCAAAATCCAAATCC	DM2 DM3 TM2	17.23	0.00	0.16	0.00
stu-miR8005a	TTTAGAGTTAAAGGTTTAGAGTT	TTTAGGGTTAAGGTTTAGAGTT	BnaC09g4320D	ATP SYNTHASE subunit O, mitochondrial	1382	TTTAGGGTTAGGGTTTAGAGTT TCCAAATCCAAATCTCAAAATCCAAATCC	DM2 DM3 TM2	17.23	0.00	0.16	0.00
stu-miR8005a	TTTAGAGTTAAAGGTTTAGAGTT	TTTAGGGTTAAGGTTTAGAGTT	BnaC08g0320D	unknown	1572	TTTAGGGTTAGGGTTTAGAGTT TCCAAATCCAAATCTCAAAATCTCAAAATCC	DM2 DM3 TM2	17.23	0.00	0.16	0.00
stu-miR8005a	TTTAGAGTTAAAGGTTTAGAGTT	TTTAGGGTTAAGGTTTAGAGTT	BnaC01g04980D	MYOSIN-15	563	TTTAGGGTTAGGGTTTAGAGTT TCCAAATCCAAATCTCAAAATCTCAAAATCC	DM2 DM3 TM2	14.17	0.00	0.16	0.00
stu-miR8005a	TTTAGAGTTAAAGGTTTAGAGTT	TTTAGGGTTAAGGTTTAGAGTT	BnaC04g05580D	DAL-RELATED 2	1014	TTTAGGGTTAGGGTTTAGAGTT TCCAAATCCAAATCTCAAAATCTCAAAATCC	DM2 DM3 TM2	17.23	0.00	0.16	0.00
stu-miR8005a	TTTAGAGTTAAAGGTTTAGAGTT	TTTAGGGTTAAGGTTTAGAGTT	BnaC02g23510D	GIBBERELLIN-REGULATED PROTEIN 1	413	TTTAGGGTTAGGGTTTAGAGTT TCCAAATCCAAATCTCAAAATCTCAAAATCC	DM2 DM3 TM2	17.23	0.00	0.16	0.00
stu-miR8005a	TTTAGAGTTAAAGGTTTAGAGTT	TTTAGGGTTAAGGTTTAGAGTT	BnaC03g03580D	Lipoyl synthase, chloroplastic	329	TTTAGGGTTAGGGTTTAGAGTT TCCAAATCCAAATCTCAAAATCTCAAAATCC	DM2 DM3 TM2	17.23	0.00	0.16	0.00
stu-miR8005a	TTTAGAGTTAAAGGTTTAGAGTT	TTTAGGGTTAAGGTTTAGAGTT	BnaC02g10540D	DEHYDRODOLICHL DIPHOSPHATE SYNTHASE 2	1113	TTTAGGGTTAGGGTTTAGAGTT TCCAAATCCAAATCTCAAAATCTCAAAATCC	DM2 DM3 TM2	17.23	0.00	0.16	0.00
stu-miR8005a	TTTAGAGTTAAAGGTTTAGAGTT	TTTAGGGTTAAGGTTTAGAGTT	BnaC06g2670D	LIPOXYGENASE 6, chloroplastic	1004	TTTAGGGTTAGGGTTTAGAGTT TCCAAATCCAAATCTCAAAATCTCAAAATCC	DM2 DM3 TM2	5.51	0.00	0.16	0.00
stu-miR8005a	TTTAGAGTTAAAGGTTTAGAGTT	TTTAGGGTTAAGGTTTAGAGTT	BnaC09g37860D	IMPORIN-5	1806	TTTAGGGTTAGGGTTTAGAGTT TCCAAATCCAAATCTCAAAATCTCAAAATCC	DM2 DM3 TM2	17.23	0.00	4.93	0.00
stu-miR8005a	TTTAGAGTTAAAGGTTTAGAGTT	TTTAGGGTTAAGGTTTAGAGTT	BnaC07g00720D	MONOTHOL GLUTAREDOXIN-5.2, chloroplastic	1162	TTTAGGGTTAGGGTTTAGAGTT TCCAAATCCAAATCTCAAAATCTCAAAATCC	DM2 DM3 TM2	17.23	0.00	0.16	0.00
stu-miR8005a	TTTAGAGTTAAAGGTTTAGAGTT	TTTAGGGTTAAGGTTTAGAGTT	BnaCmg23260D	SUCROSE SYNTHASE 3	1339	TTTAGGGTTAGGGTTTAGAGTT TCCAAATCCAAATCTCAAAATCTCAAAATCC	DM2 DM3 TM2	17.23	0.00	0.16	0.00
stu-miR8005a	TTTAGAGTTAAAGGTTTAGAGTT	TTTAGGGTTAAGGTTTAGAGTT	BnaC08g31090D	CYTOCHROME P450 76C3	607	TTTAGGGTTAGGGTTTAGAGTT TCCAAATCCAAATCTCAAAATCTCAAAATCC	DM2 DM3 TM2	17.23	0.00	0.16	0.00
stu-miR8005a	TTTAGAGTTAAAGGTTTAGAGTT	TTTAGGGTTAAGGTTTAGAGTT	BnaCmg17780D	unknown	1371	TTTAGGGTTAGGGTTTAGAGTT TCCAAATCCAAATCTCAAAATCTCAAAATCC	DM2 DM3 TM2	17.23	0.00	4.93	0.00
stu-miR8005a	TTTAGAGTTAAAGGTTTAGAGTT	TTTAGGGTTAAGGTTTAGAGTT	BnaC08g21260D	tRNA-DIHYDROURIDINE(20) SYNTHASE [NAD(P)+-like]	5585	TTTAGGGTTAGGGTTTAGAGTT TCCAAATCCAAATCTCAAAATCTCAAAATCC	DM2 DM3 TM2	17.23	0.00	0.16	0.00
ath-miR393a-5p	TCCAAGGGATCGGATTGATCC	TCCAAGGGATCGGATTGATTTT	BnaA02g28290D	AUXIN SIGNALING F-BOX 2	2531	TCCAAGGGATCGGATTGATTTT CTGTAGGTTCCCTAGGTTAACAAAGTATGAA	DM2 DM3 TM3	7.08	0.00	5.77	0.00
ath-miR393a-5p	TCCAAGGGATCGGATTGATCC	TCCAAGGGATCGGATTGATTTT	BnaC02g36370D	AUXIN SIGNALING F-BOX 2	2591	TCCAAGGGATCGGATTGATTTT CTGTAGGTTCCCTAGGTTAACAAAGTATGAA	DM2 DM3 TM3	7.08	0.00	5.77	0.00
ath-miR393a-5p	TCCAAGGGATCGGATTGATCC	TCCAAGGGATCGGATTGATTT	BnaA02g28290D	AUXIN SIGNALING F-BOX 2	2531	TCCAAGGGATCGGATTGATTTT TATTACA-AGGTTCCCTAGGTTAACAAAGTATGAA	DM2 DM3 TM3	7.08	0.00	5.77	0.00
ath-miR393a-5p	TCCAAGGGATCGGATTGATCC	TCCAAGGGATCGGATTGATTT	BnaC02g36370D	AUXIN SIGNALING F-BOX 2	2591	TCCAAGGGATCGGATTGATTTT CTGTAGGTTCCCTAGGTTAACAAAGTATGAA	DM2 DM3 TM3	7.08	0.00	5.77	0.00
bra-miR398-3p	TGTGTTCTCAGGTCACCCCG	TGTGTTCTCAGGTCACCCCG	BnaA04g16310D	SUPEROXIDE DISMUTASE [Cu-Zn], chloroplastic	776	TGTGTTCTCAGGTCACCCCG TATTACA-AGGTTCCCTAGGTTAACAAAGTATGAA	DM2 TM3 TT3	3.42	0.00	1.35	0.23
bra-miR1885b	TACATCTCTCCGGGAAGCTC	TACATCTCTCCGGGAAGCTCT	BnaA06g29450D	BLOCS2	319	TACATCTCTCCGGGAAGCTCT GTGGAAGTAGACGAGGCTTTTTCAGACTCGG	DM3 DT2 TT3	0.13	0.18	0.00	0.19
bra-miR160a,b,c,d	TGCTGGCTCCCTGTATGCCA	TGCTGGCTCCCTGTATGCCCT	BnaA07g13830D	AUXIN RESPONSE FACTOR 10	1698	TGCTGGCTCCCTGTATGCCCT TCGAAACGACGAGGACATAAAGGGCTCCT	DM3 TM2 TM3	8.94	0.00	18.38	0.00

bna-miR156d	681	-0.65	436	-0.95	BnaC04g44230D	SPL 3	619	TGACAGAAAGAGTGGAGCAC o TCTGACTCTCTCTGTTTCCGGAAT	DM3 DT3 TT3	1.19	3.31	0.00	1.48	153	-1.42	84	-0.83
bna-miR172b	359	-1.72	440	-1.73	BnaA07g12050D	AP2-like ERF TOE3	2227	GGAACTTGATGATCGC-AT o o CCTCTTAGGACTACTACGGCGTAAAGGTG	DM3 TM2 TT3	1.56	0.00	8.75	0.46	254	-0.25	513	0.08
bna-miR172a	591	-1.02	477	-0.70	BnaA07g12050D	AP2-like ERF TOE3	2227	AGAACTTGATGATCGC-AT o CCTCTTAGGACTACTACGGCGTAAAGGTG	DM3 TM2 TT3	1.56	0.00	8.75	0.46	254	-0.25	513	0.08
bna-miR172a	591	-1.02	477	-0.70	BnaC07g16190D	AP2-like ERF TOE3	2185	AGAACTTGATGATCGTGCAT o CCTCTTAGGACTACTACGTCGTAAGG	DM3 TM2 TT3	1.56	0.00	8.75	0.46	429	-0.24	932	-0.05
TM_Cluster_40901	2027	-1.23	2789	-1.44	BnaCmg61400D	SPL 6	771	TGACAGAAGAGTGGAGCAC o ACTGCACTCTCTCTCTCTGTTCAAT	DM3 TM3 TT3	1.75	0.00	1.06	1.43	509	-0.62	401	-0.05
bna-miR156g	8555	-1.13	11778	-1.65	BnaA02g14580D	SPL 6	1083	TGACAGAAGATAGAGAGCAC o ACTGCACTCTCTCTCTCTGTTCACT	DM3 TM3 TT3	2.56	0.00	0.94	4.21	197	-0.16	227	0.12
bna-miR156g	8555	-1.13	11778	-1.65	BnaA07g27730D	SPL 6	640	TGACAGAAGATAGAGAGCAC o ACTGCACTCTCTCTCTCTGTTCACT	DM3 TM3 TT3	2.56	0.00	0.94	4.21	149	-0.17	308	0.33
TM_Cluster_40901	2027	-1.23	2789	-1.44	BnaA02g14580D	SPL 6	1083	TGACAGAAGAGTGGAGCAC o ACTGCACTCTCTCTCTCTGTTCACT	DM3 TM3 TT3	2.56	0.00	0.94	4.21	197	-0.16	227	0.12
TM_Cluster_40901	2027	-1.23	2789	-1.44	BnaC02g19100D	SPL 6	1117	TGACAGAAGAGTGGAGCAC o ACTGCACTCTCTCTCTCTGTTCACT	DM3 TM3 TT3	2.56	0.00	0.94	4.21	329	-0.27	316	0.23
DM_Cluster_11733	907	-1.13	913	-1.70	BnaA07g27730D	SPL 6	640	TGACAGAAGAGTGGAGCAC o ACTGCACTCTCTCTCTCTGTTCACT	DM3 TM3 TT3	2.56	0.00	0.94	4.21	149	-0.17	308	0.33
DM_Cluster_11733	907	-1.13	913	-1.70	BnaC02g14000D	SPL 6	1096	TGACAGAAGAGTGGAGCAC o ACTGCACTCTCTCTCTCTGTTCACT	DM3 TM3 TT3	2.56	0.00	0.94	4.21	119	-0.15	150	0.01
DM_Cluster_11733	907	-1.13	913	-1.70	BnaC02g19100D	SPL 6	1117	TGACAGAAGAGTGGAGCAC o ACTGCACTCTCTCTCTCTGTTCACT	DM3 TM3 TT3	2.56	0.00	0.94	4.21	329	-0.27	316	0.23
bna-miR156d	681	-0.65	436	-0.95	BnaAnng25050D	SPL 11	1340	TGACAGAAGAGTGGAGCAC TGCAACTCTCTCTCTCTCTGTCATTT	DM3 TM3 TT3	5.00	0.00	0.77	3.89	68	0.70	73	0.71
DM_Cluster_11733	907	-1.13	913	-1.70	BnaCmg61400D	SPL 6	771	TGACAGAAGAGTGGAGCAC o ACTGCACTCTCTCTCTCTGTTCAAT	DM3 TM3 TT3	1.75	0.00	1.06	1.43	509	-0.62	401	-0.05
TM_Cluster_40901	2027	-1.23	2789	-1.44	BnaC02g14000D	SPL 6	1096	TGACAGAAGAGTGGAGCAC o ACTGCACTCTCTCTCTCTGTTCACT	DM3 TM3 TT3	2.56	0.00	0.94	4.21	119	-0.15	150	0.01
DM_Cluster_11733	907	-1.13	913	-1.70	BnaA02g14580D	SPL 6	1083	TGACAGAAGAGTGGAGCAC o ACTGCACTCTCTCTCTCTGTTCACT	DM3 TM3 TT3	2.56	0.00	0.94	4.21	197	-0.16	227	0.12
bna-miR156g	8555	-1.13	11778	-1.65	BnaC02g19100D	SPL 6	1117	TGACAGAAGAGTGGAGCAC o ACTGCACTCTCTCTCTCTGTTCACT	DM3 TM3 TT3	2.56	0.00	0.94	4.21	329	-0.27	316	0.23
TM_Cluster_40901	2027	-1.23	2789	-1.44	BnaA07g27730D	SPL 6	640	TGACAGAAGAGTGGAGCAC o ACTGCACTCTCTCTCTCTGTTCACT	DM3 TM3 TT3	2.56	0.00	0.94	4.21	149	-0.17	308	0.33
bna-miR156g	8555	-1.13	11778	-1.65	BnaC02g19100D	SPL 6	1117	TGACAGAAGAGTGGAGCAC o ACTGCACTCTCTCTCTCTGTTCACT	DM3 TM3 TT3	2.56	0.00	0.94	4.21	329	-0.27	316	0.23
TM_Cluster_40901	2027	-1.23	2789	-1.44	BnaA07g27730D	SPL 6	640	TGACAGAAGAGTGGAGCAC o ACTGCACTCTCTCTCTCTGTTCACT	DM3 TM3 TT3	2.56	0.00	0.94	4.21	149	-0.17	308	0.33
bna-miR156g	8555	-1.13	11778	-1.65	BnaCmg61400D	SPL 2	3011	TGACAGAAGATAGAGAGCAC TGAACCTCTCTCTCTCTGTTAGTCT	DT2 DT3 TT3	0.00	1.13	0.00	0.37	247	-0.41	234	0.38
bna-miR172a	591	-1.02	477	-0.70	BnaCmg39690D	Floral homeotic protein APETALA 2	2233	AGAACTTGATGATCGTGCAT o CCTCTTAGGACTACTACGAGTCGTAAGG	DT2 DT3 TT3	0.00	0.53	0.71	1.25	485	0.19	639	0.28
TM_Cluster_40901	2027	-1.23	2789	-1.44	BnaA06g36780D	SPL 2	3012	TGACAGAAGAGTGGAGCAC CTTAAACTCTCTCTCTCTGTTAGTTC	DT2 DT3 TT3	0.00	2.04	1.59	3.93	247	-0.41	234	0.38
bna-miR156g	8555	-1.13	11778	-1.65	BnaA06g36780D	SPL 2	3012	TGACAGAAGATAGAGAGCAC CTTAAACTCTCTCTCTCTGTTAGTTC	DT2 DT3 TT3	0.00	2.04	1.59	3.93	247	-0.41	234	0.38
DM_Cluster_11733	907	-1.13	913	-1.70	BnaA06g36780D	SPL 2	3012	TGACAGAAGAGTGGAGCAC CTTAAACTCTCTCTCTCTGTTAGTTC	DT2 DT3 TT3	0.00	2.04	1.59	3.93	247	-0.41	234	0.38
bna-miR172b	359	-1.72	440	-1.73	BnaCmg39690D	Floral homeotic protein APETALA 2	2233	GGAACTTGATGATCGTGCAT o o CCTCTTAGGACTACTACGAGTCGTAAGG	DT2 DT3 TT3	0.00	0.53	0.71	1.25	485	0.19	639	0.28
bna-miR166f	10405	-3.09	14049	-2.47	BnaC04g10480D	Homeobox-leucine zipper protein ATHB-8	1374	TGGAACCCGCTTCACTCCC o CTTAAAGCCTTCTGATGTTGTTATTTCT	DM1 TT1	49.71	0.00	0.00	0.06	108	-1.01	60	-0.04
TM_Cluster_20495	388	0.89	809	1.33	BnaA09g24940D	Formin-like protein 14	4123	TGGAAGG-TTCGTAAGAAACACAGTGGCCATAT	DM2 DM3	4.80	0.00	0.00	0.00	130	0.03	324	0.09

Table S16: Overview over levels of miRNAs and their corresponding mRNA targets

Virus-induced miRNA and target levels		miRNA sequence		Target transcript ID	Annotation	Cleavage found in PARseq replicates		miRNA fold change (log ₂)		mRNA target fold change (log ₂)	
miRNA	target miRNA	miRNA	miRNA	Target transcript ID	Annotation	Drakkar	Tanto	Drakkar	Tanto	Drakkar	Tanto
miR403	miR403	TTAGATTTCAGCCACCAACTCG	TTAGATTTCAGCCACCAACTCG	BnaCmg683200	AGO2	-1.72	-1.19	1.50	1.27	1.50	1.27
miR396	miR396	TCCAAGGATCGCATTTGATC	TCCAAGGATCGCATTTGATC	BnaA05g147600	AGO2	-1.72	-1.19	2.60	3.13	2.60	3.13
miR395	miR395	TCCAAGGATCGCATTTGATC	TCCAAGGATCGCATTTGATC	BnaA02g282900	AFB2	-2.00	-2.10	0.50	0.24	0.50	0.24
miR394	miR394	TCCAAGGATCGCATTTGATC	TCCAAGGATCGCATTTGATC	BnaC02g363700	AFB2	-2.00	-2.10	0.35	0.12	0.35	0.12
miR393	miR393	TCCAAGGATCGCATTTGATC	TCCAAGGATCGCATTTGATC	BnaA02g282900	AFB2	-0.14	-0.54	0.50	0.24	0.50	0.24
miR393	miR393	TCCAAGGATCGCATTTGATC	TCCAAGGATCGCATTTGATC	BnaC02g363700	AFB2	-0.14	-0.54	0.35	0.12	0.35	0.12
miR393	miR393	TCCAAGGATCGCATTTGATC	TCCAAGGATCGCATTTGATC	BnaC08g408900	AFB3	-0.14	-0.54	0.55	0.56	0.55	0.56
miR172	miR172	AGAACTCTTGATGATGCTGCAT	AGAACTCTTGATGATGCTGCAT	BnaC08g408900	AFB3	-2.00	-2.10	0.55	0.56	0.55	0.56
miR172	miR172	AGAACTCTTGATGATGCTGCAT	AGAACTCTTGATGATGCTGCAT	BnaA03g221000	ERF RAP2-7	-1.02	-0.70	0.53	1.04	0.53	1.04
miR172	miR172	AGAACTCTTGATGATGCTGCAT	AGAACTCTTGATGATGCTGCAT	BnaA03g221000	ERF RAP2-7	-1.72	-1.73	0.53	1.04	0.53	1.04
miR160	miR160	TGCTGCTCCCTGTATGCCA	TGCTGCTCCCTGTATGCCA	BnaCmg396900	APETALA 2	-1.02	-0.70	0.19	0.28	0.19	0.28
miR160	miR160	TGCTGCTCCCTGTATGCCA	TGCTGCTCCCTGTATGCCA	BnaCmg396900	APETALA 2	-1.72	-1.73	0.19	0.28	0.19	0.28
miR156	miR156	TGACAGAAGATGAGAGCAC	TGACAGAAGATGAGAGCAC	BnaA01g069100	ARF16	-1.03	-0.98	0.60	1.21	0.60	1.21
miR156	miR156	TGACAGAAGATGAGAGCAC	TGACAGAAGATGAGAGCAC	BnaC01g083300	ARF16	-1.03	-0.98	0.52	0.79	0.52	0.79
miR (Shortstack)	miR (Shortstack)	TTGACAGAAGATGAGAGCAC	TTGACAGAAGATGAGAGCAC	BnaA02g250500	SPL11	-1.13	-1.65	0.70	0.71	0.70	0.71
miR (Shortstack)	miR (Shortstack)	TTGACAGAAGATGAGAGCAC	TTGACAGAAGATGAGAGCAC	BnaA02g250500	SPL11	-0.65	-0.95	0.70	0.71	0.70	0.71
miR (Shortstack)	miR (Shortstack)	TTGACAGAAGATGAGAGCAC	TTGACAGAAGATGAGAGCAC	BnaA02g250500	SPL11	-1.23	-1.44	0.70	0.71	0.70	0.71
miR (Shortstack)	miR (Shortstack)	TTGACAGAAGATGAGAGCAC	TTGACAGAAGATGAGAGCAC	BnaA02g250500	SPL11	-1.13	-1.70	0.70	0.71	0.70	0.71
miR (Shortstack)	miR (Shortstack)	TTGACAGAAGATGAGAGCAC	TTGACAGAAGATGAGAGCAC	BnaA02g250500	SPL11	-1.13	-1.70	0.70	0.71	0.70	0.71
miR171	miR171	TTGACAGAAGATGAGAGCAC	TTGACAGAAGATGAGAGCAC	BnaA02g250500	SPL11	2.20	1.93	-0.60	-0.25	-0.60	-0.25
miR171	miR171	TTGACAGAAGATGAGAGCAC	TTGACAGAAGATGAGAGCAC	BnaA02g250500	SPL11	2.20	1.93	-0.61	-0.23	-0.61	-0.23
miR1885	miR1885	TACATCTTCCGGGAAAGCTC	TACATCTTCCGGGAAAGCTC	BnaA02g250500	SC16	2.29	2.85	0.44	0.64	0.44	0.64
miR1885	miR1885	TACATCTTCCGGGAAAGCTC	TACATCTTCCGGGAAAGCTC	BnaA04g163100	BLOC152	4.09	4.34	2.75	0.67	2.75	0.67
miR1885	miR1885	TACATCTTCCGGGAAAGCTC	TACATCTTCCGGGAAAGCTC	BnaA06g294500	BLOC152	2.29	2.85	0.10	0.63	0.10	0.63
miR (Shortstack)	miR (Shortstack)	TTGACAGAAGATGAGAGCAC	TTGACAGAAGATGAGAGCAC	BnaC07g113800	SPL10	-1.13	-1.70	-0.54	-0.34	-0.54	-0.34
miR (Shortstack)	miR (Shortstack)	TTGACAGAAGATGAGAGCAC	TTGACAGAAGATGAGAGCAC	BnaC07g113800	SPL10	-1.13	-1.65	-0.54	-0.34	-0.54	-0.34
miR (Shortstack)	miR (Shortstack)	TTGACAGAAGATGAGAGCAC	TTGACAGAAGATGAGAGCAC	BnaC07g113800	SPL10	-1.23	-1.44	-0.54	-0.34	-0.54	-0.34
miR (Shortstack)	miR (Shortstack)	TTGACAGAAGATGAGAGCAC	TTGACAGAAGATGAGAGCAC	BnaC04g239300	SPL15	-1.13	-1.70	-0.32	-0.83	-0.32	-0.83
miR (Shortstack)	miR (Shortstack)	TTGACAGAAGATGAGAGCAC	TTGACAGAAGATGAGAGCAC	BnaC04g239300	SPL15	-1.23	-1.44	-0.32	-0.83	-0.32	-0.83
miR156	miR156	TGACAGAAGATGAGAGCAC	TGACAGAAGATGAGAGCAC	BnaC04g239300	SPL15	-1.13	-1.65	-0.32	-0.83	-0.32	-0.83
miR156	miR156	TGACAGAAGATGAGAGCAC	TGACAGAAGATGAGAGCAC	BnaCmg614000	SPL6	-0.65	-0.95	-0.62	-0.05	-0.62	-0.05
miR6030	miR6030	TCCACCCATCCATACAGACC	TCCACCCATCCATACAGACC	BnaA02g169700	unknown	-0.09	-0.17	-0.78	-0.72	-0.78	-0.72
miR156	miR156	TGACAGAAGATGAGAGCAC	TGACAGAAGATGAGAGCAC	BnaC07g113800	SPL10	-0.65	-0.95	-0.54	-0.34	-0.54	-0.34
miR156	miR156	TGACAGAAGATGAGAGCAC	TGACAGAAGATGAGAGCAC	BnaA04g198400	SPL3	-0.65	-0.95	-2.52	-0.84	-2.52	-0.84
miR156	miR156	TGACAGAAGATGAGAGCAC	TGACAGAAGATGAGAGCAC	BnaC04g442300	SPL3	-0.65	-0.95	-1.42	-0.83	-1.42	-0.83
miR172	miR172	AGAACTCTTGATGATGCTGCAT	AGAACTCTTGATGATGCTGCAT	BnaC07g161900	AP2	-1.02	-0.70	-0.24	-0.05	-0.24	-0.05
miR (Shortstack)	miR (Shortstack)	TTGACAGAAGATGAGAGCAC	TTGACAGAAGATGAGAGCAC	BnaCmg614000	SPL6	-1.23	-1.44	-0.62	-0.05	-0.62	-0.05
miR (Shortstack)	miR (Shortstack)	TTGACAGAAGATGAGAGCAC	TTGACAGAAGATGAGAGCAC	BnaCmg614000	SPL6	-1.13	-1.70	-0.62	-0.05	-0.62	-0.05
miR156	miR156	TTGACAGAAGATGAGAGCAC	TTGACAGAAGATGAGAGCAC	BnaCmg614000	SPL6	-1.13	-1.65	-0.62	-0.05	-0.62	-0.05
miRCS-3	miRCS-3	TTATCAACAACACTAGATC	TTATCAACAACACTAGATC	BnaA10g271700	MT23	0.80	0.23	0.10	-0.15	0.10	-0.15
miRCS-1	miRCS-1	TGTTGTTGATGATTAATCCGA	TGTTGTTGATGATTAATCCGA	BnaC06g437900	PAT11	1.15	0.82	1.16	-0.44	1.16	-0.44
miR161	miR161	GTCATTTCAATGGCTTGATC	GTCATTTCAATGGCTTGATC	BnaA06g396500	RPP8-like2	5.83	5.89	0.13	-0.44	0.13	-0.44
miRCS-3	miRCS-3	TTATCAACAACACTAGATC	TTATCAACAACACTAGATC	BnaA10g271700	MT23	0.80	0.23	0.10	-0.15	0.10	-0.15
miRCS-1	miRCS-1	TGTTGTTGATGATTAATCCGA	TGTTGTTGATGATTAATCCGA	BnaC06g437900	PAT11	1.15	0.82	1.16	-0.44	1.16	-0.44
miR161	miR161	GTCATTTCAATGGCTTGATC	GTCATTTCAATGGCTTGATC	BnaA06g396500	RPP8-like2	5.83	5.89	0.13	-0.44	0.13	-0.44
miR171	miR171	TTGACAGAAGATGAGAGCAC	TTGACAGAAGATGAGAGCAC	BnaC04g220800	SC122	2.20	1.93	-0.97	0.05	-0.97	0.05
miR172	miR172	AGAACTCTTGATGATGCTGCAT	AGAACTCTTGATGATGCTGCAT	BnaC09g134300	ERF RAP2-7	-1.02	-0.70	0.30	-1.57	-1.02	-1.57
miR172	miR172	AGAACTCTTGATGATGCTGCAT	AGAACTCTTGATGATGCTGCAT	BnaC04g156400	ERF RAP2-7	-1.72	-1.73	0.78	-1.74	0.78	-1.74
miR172	miR172	AGAACTCTTGATGATGCTGCAT	AGAACTCTTGATGATGCTGCAT	BnaC04g156400	ERF RAP2-7	-1.02	-0.70	0.78	-1.74	0.78	-1.74
miR172	miR172	AGAACTCTTGATGATGCTGCAT	AGAACTCTTGATGATGCTGCAT	BnaC09g134300	ERF RAP2-7	-1.72	-1.73	0.30	-1.57	0.30	-1.57
miR172	miR172	AGAACTCTTGATGATGCTGCAT	AGAACTCTTGATGATGCTGCAT	BnaA10g129500	AP2	-1.72	-1.73	0.33	-0.04	0.33	-0.04
miR172	miR172	AGAACTCTTGATGATGCTGCAT	AGAACTCTTGATGATGCTGCAT	BnaA10g129500	AP2	-1.02	-0.70	0.33	-0.04	0.33	-0.04
miR172	miR172	AGAACTCTTGATGATGCTGCAT	AGAACTCTTGATGATGCTGCAT	BnaC09g354300	AP2	-1.02	-0.70	0.01	-0.22	0.01	-0.22
miR172	miR172	AGAACTCTTGATGATGCTGCAT	AGAACTCTTGATGATGCTGCAT	BnaC09g354300	AP2	-1.72	-1.73	0.01	-0.22	0.01	-0.22
miRCS3a-3	miRCS3a-3	TATCTACTGCTTATGCCACA	TATCTACTGCTTATGCCACA	BnaA07g282900	COX19	-0.13	0.60	-0.40	-0.35	-0.40	-0.35

Table S17: Targeting of host mRNA transcripts by vsiRNAs

vsiRNA										Host mRNA targets										DE target mRNA				
vsiRNA (strand)	Length	vsiRNA reads & FC(log2)			Target transcript ID	Predicted gene function	Cleavage position	vsiRNA:mRNA target pair (5'-3' : 3'-5')			Cleavage found in PAREseq replicates			Fragment signatures (rpm)			mRNA reads & FC(log2)							
		DM	DT	TT				DM	DT	TT	DM	DT	TT	DM	DT	TT	DM	DT	TT					
AAGAATCTGATGATGCTGT (-)	19	0.00	2.13	0.00	BnaC03g26480D	ERF RAP2-7	2328	AAGAATCTGATGATGCTGT				0.00	10.03	0.00	6.66	815	-0.39	1202	0.43					
AAGAATCTGATGATGCTGT (-)	19	0.00	2.13	0.00	BnaC04g15640D	ERF RAP2-7	2414	AAGAATCTGATGATGCTGT				0.00	10.03	0.00	6.66	1538	0.78	45574	-1.74					
AAGAATCTGATGATGCTGT (-)	19	0.00	2.13	0.00	BnaA10g12950D	AP2-like ERF TOE2	2933	AAGAATCTGATGATGCTGT				0.00	5.00	0.00	9.95	297	0.33	443	-0.04					
AAGAATCTGATGATGCTGT (-)	19	0.00	2.13	0.00	BnaC09g35430D	AP2-like ERF TOE2	2671	AAGAATCTGATGATGCTGT				0.00	5.00	0.00	9.95	232	0.01	342	-0.22					
AAGAATCTGATGATGCTGT (-)	19	0.00	2.13	0.00	BnaC09g13430D	ERF RAP2-7	1039	AAGAATCTGATGATGCTGT				0.00	10.03	0.00	6.66	652	0.30	3166	-1.57					
TCTTTGTCACCTCTGCTGT (-)	21	0.01	54.27	0.02	BnaC09g35230D	unknown	219	TCTTTGTCACCTCTGCTGT				0.00	13.49	0.00	0.00	3	-0.02	5	-0.27					
TCCTTCTCTCTCTGCTGT (-)	21	0.01	11.63	0.00	BnaC09g35690D	Non-functional pseudokinase ZED1	62	TCCTTCTCTCTCTGCTGT				0.00	4.17	0.00	0.00	197	-0.18	186	-0.35					
TCTTTGTCACCTCTGCTGT (-)	21	0.01	54.27	0.02	BnaC04g51540D	FBD-associated F-box protein At3g49020	114	TCTTTGTCACCTCTGCTGT				0.00	13.49	0.00	0.00	1	-0.54	0	-0.18					
TCTTTGTCACCTCTGCTGT (-)	21	0.01	54.27	0.02	BnaC04g04300D	unknown	213	TCTTTGTCACCTCTGCTGT				0.00	13.49	0.00	0.00	1	0.63	4	-0.04					
AAGAATCTGATGATGCTGT (-)	19	0.00	2.13	0.00	BnaA03g22100D	ERF RAP2-7	2284	AAGAATCTGATGATGCTGT				0.00	10.03	0.00	0.00	413	0.53	317	1.04					
AACTGCTCAGAGCTCATA (-)	21	0.01	32.88	0.04	BnaA10g13210D	Thiol protease aleurain	1221	AACTGCTCAGAGCTCATA				0.00	3.52	0.00	0.00	45621	-0.63	51819	0.27					
AAGAATCTGATGATGCTGT (-)	19	0.00	2.13	0.00	BnaA01g34730D	Floral homeotic protein APETALA 2	1043	AAGAATCTGATGATGCTGT				0.00	2.04	0.00	1.62	460	-0.44	487	0.12					
AAGAATCTGATGATGCTGT (-)	19	0.00	2.13	0.00	BnaC09g3960D	Floral homeotic protein APETALA 2	2233	AAGAATCTGATGATGCTGT				0.00	0.53	0.00	1.25	485	0.19	639	0.28					
TGTGTGTTGTTACTTCT (+)	21	0.01	8.67	0.00	BnaA03g1510D	Serine/arginine-rich splicing factor RS31A	356	TGTGTGTTGTTACTTCT				0.00	0.13	0.00	0.00	4	-0.19	4	0.19					
TACGAACTCTGAAAGC (+)	19	0.00	1.79	0.00	BnaC04g3330D	Nematode resistance protein-like HSPRO2	1241	TACGAACTCTGAAAGC				0.00	0.04	0.00	170.97	24819	-0.46	11586	0.49					
AGAACCGAGAACATTGAGAA (+)	20	0.01	4.14	0.00	BnaC02g37040D	Chlorophyll a-b binding protein 36, chloroplastic	863	AGAACCGAGAACATTGAGAA				0.00	10.41	0.00	0.00	535655	-0.48	315782	-0.03					
CAGAGAGGAGAGAAAGGAGA (+)	21	0.00	16.42	0.00	BnaC03g04180D	3-hydroxyacyl-facyl-carrier-protein] dehydratase FabZ	90	CAGAGAGGAGAGAAAGGAGA				0.00	0.18	0.00	0.65	603	-0.17	401	0.13					
CAGAGAGGAGAGAAAGGAGA (+)	21	0.00	16.42	0.00	BnaA01g09950D	unknown	203	CAGAGAGGAGAGAAAGGAGA				0.00	0.04	0.00	0.00	1	-0.04	3	0.51					
AGTGGACATAAGACAAAGA (+)	20	0.00	2.40	0.00	BnaC09g7120D	NAD (PH)-quinone oxidoreductase subunit 5, chloroplastic	63	AGTGGACATAAGACAAAGA				0.00	0.04	0.00	0.00	2632	-0.92	1831	0.34					
CAGAGAGGAGAGAAAGGAGA (+)	21	0.00	16.42	0.00	BnaC08g39950D	Phosphate transporter PHO1 homolog 3	3327	CAGAGAGGAGAGAAAGGAGA				0.00	0.22	0.00	0.00	436	-0.75	421	1.46					
TGTGTGTTGTTACTTCT (+)	21	0.01	8.67	0.00	BnaC01g7420D	unknown	66	TGTGTGTTGTTACTTCT				0.00	0.04	0.00	0.00	3855	-0.32	3867	0.18					
TCTTCTCTCTCTGCTGT (-)	21	0.00	14.53	0.00	BnaC04g03350D	60S ribosomal protein L7-3	1583	TCTTCTCTCTCTGCTGT				0.00	0.04	0.00	0.00	1877	-0.50	2166	-0.59					
TCCTTCTCTCTCTGCTGT (-)	21	0.01	11.63	0.00	BnaC02g09670D	Probable WRKY transcription factor 38	958	TCCTTCTCTCTCTGCTGT				0.00	0.04	0.00	0.00	181	0.25	178	-0.30					
AAAAAGAACGAGAGAGGAGAA (+)	21	0.00	8.38	0.01	BnaC06g38600D	Trehalose-phosphate phosphatase B	1252	AAAAAGAACGAGAGAGGAGAA				0.00	6.57	0.00	0.00	23	1.61	54	0.92					
AGAAATCTGAAACAAGTTG (+)	21	0.00	3.65	0.00	BnaC05g04690D	Oxygen-evolving enhancer protein 2, chloroplastic	1213	AGAAATCTGAAACAAGTTG				0.00	12.97	0.00	0.00	84174	-0.31	77609	-0.12					
AGAAAGAACTTTCACTGGAG (+)	20	0.00	3.11	0.00	BnaC03g07170D	F-box/kelch-repeat protein At5g15710	1324	AGAAAGAACTTTCACTGGAG				0.00	1.95	0.00	0.00	868	0.74	1116	0.05					
TCCTGAAGATTTCTGCA (+)	19	0.00	2.72	0.01	BnaUmg02970D	Ribulose biphosphate carboxylase/oxygenase activase, chloroplastic	58	TCCTGAAGATTTCTGCA				0.00	3.91	0.00	0.00	3584	0.02	5721	-0.81					

TCCTGAAGATTTCTGCA (+)	19	0.00	2.72	0.01	2.18	BnaC05g02020D	Probable serine/threonine-protein kinase At1g54610	3025	TT1	0.00	0.00	0.00	0.00	0.00	0.00	0.00	0.03	374	0.79	937	-0.24	
TACCAGAACTCATCGAAGC (+)	19	0.00	1.79	0.00	2.25	BnaA05g05590D	Nematode resistance protein-like HSPRO2	1238	TT1	0.00	0.00	0.00	0.00	0.00	0.00	0.00	170.97	20946	-0.27	12277	0.61	
TACCAGAACTCATCGAAGC (+)	19	0.00	1.79	0.00	2.25	BnaC05g16520D	Nematode resistance protein-like HSPRO2	227	TT1	0.00	0.00	0.00	0.00	0.00	0.00	0.00	0.12	0	NA	3	0.63	
TACCAGAACTCATCGAAGC (+)	19	0.00	1.79	0.00	2.25	BnaC04g05370D	Nematode resistance protein-like HSPRO2	572	TT1	0.00	0.00	0.00	0.00	0.00	0.00	0.00	170.97	0	NA	153	0.54	
TGAAGAACGACGACGAGAA (+)	19	0.00	2.77	0.00	2.00	BnaA05g06490D	Vacuolar cation/proton exchanger 1	3799	TT1	0.00	0.00	0.00	0.00	0.00	0.00	0.00	0.06	56218	0.06	37596	0.41	
TACCAGAACTCATCGAAGC (+)	19	0.00	1.79	0.00	2.25	BnaC01g08680D	Nematode resistance protein-like HSPRO2	227	TT1	0.00	0.00	0.00	0.00	0.00	0.00	0.00	0.12	0	NA	48	0.50	
TACCAGAACTCATCGAAGC (+)	19	0.00	1.79	0.00	2.25	BnaC08g27070D	Nematode resistance protein-like HSPRO2	227	TT1	0.00	0.00	0.00	0.00	0.00	0.00	0.00	0.12	0	NA	48	0.50	
TCCTGAAGATTTCTGCA (+)	19	0.00	2.72	0.01	2.18	BnaA10g02110D	Probable serine/threonine-protein kinase At1g54610	2920	TT1	0.00	0.00	0.00	0.00	0.00	0.00	0.00	0.03	168	1.22	896	-0.45	
TCCTTCTCTCTCTGCTGCT (-)	21	0.01	11.63	0.00	9.29	BnaC05g12820D	FAM32A	647	TT1	0.00	0.00	0.00	0.00	0.00	0.00	0.00	169.96	4196	-0.39	2181	0.07	
ATGTTGAGTTTTATATTT (-)	20	0.00	0.34	0.00	2.48	BnaC03g17480D	Pentatricopeptide repeat-containing protein At2g31400, chloroplastic	2750	TT1	0.00	0.00	0.00	0.00	0.00	0.00	0.00	0.09	549	-0.66	529	0.33	
TTTTCTTTAACTGTGTGCT (-)	21	0.00	31.87	0.01	19.91	BnaC07g43040D	CBL-interacting serine/threonine-protein kinase 6	1156	TT1	0.00	0.00	0.00	0.00	0.00	0.00	0.00	0.03	7528	-1.29	4024	-0.65	
TCCTTCTCTCTCTGCTGCT (-)	21	0.01	11.63	0.00	9.29	BnaA07g01940D	Nucleolar complex protein 2 homolog	3649	TT1	0.00	0.00	0.00	0.00	0.00	0.00	0.00	0.18	99	-0.23	182	-0.01	
TTTGAATCNCACAAATG (-)	21	0.04	106.27	0.04	74.96	BnaA06g04090D	Dihydropyridyl dehydrogenase 1, mitochondrial	1479	TT1	0.00	0.00	0.00	0.00	0.00	0.00	0.00	0.21	6339	-0.50	7445	-0.28	
CAGAGAAAGGAGAAAGGAGAG (+)	21	0.00	16.42	0.00	12.78	BnaC04g45550D	Phosphatidylinositol:ceramide inositolphosphotransferase 2	27	TT2	0.00	0.00	0.00	0.00	0.00	0.00	0.65	11056	-1.12	10110	-0.78		
CAAGCGAAGAGAAATCGAGC (+)	22	0.00	6.69	0.01	6.13	BnaC03g2010D	Aquaporin PIP-2	42	TT2	0.00	0.00	0.00	0.00	0.00	0.00	0.00	18.14	837	-1.76	1138	-1.75	
TTGATCTGAGATTTCTGCT (+)	21	0.01	8.69	0.00	5.64	BnaA03g39650D	Calcium sensing receptor, chloroplastic	152	TT2	0.00	0.00	0.00	0.00	0.00	0.00	0.00	20.62	34860	-0.90	25557	-1.10	
CAGAGAAAGGAGAAAGGAGAG (+)	21	0.00	16.42	0.00	12.78	BnaA06g32100D	Eukaryotic translation initiation factor 3 subunit 1	1675	TT2	0.00	0.00	0.00	0.00	0.00	0.00	0.65	676	-0.11	768	0.33		
TTGATCTGAGATTTCTGCT (+)	21	0.01	8.69	0.00	5.64	BnaCmg40790D	Calcium sensing receptor, chloroplastic	146	TT2	0.00	0.00	0.00	0.00	0.00	0.00	0.00	20.62	31417	-1.08	19182	-1.15	
GGCAGAGAAAGGAGAAAGGAGAG (+)	21	0.00	14.92	0.00	15.67	BnaC01g02600D	Chaperone protein dnaJ 11, chloroplastic	53	TT2	0.00	0.00	0.00	0.00	0.00	0.00	0.13	14229	0.09	11688	0.24		
GTTTGCCACATGCTCTTT (-)	21	0.01	6.52	0.01	4.24	BnaC02g18910D	ACT domain-containing protein ACR4	1806	TT2	0.00	0.00	0.00	0.00	0.00	0.00	0.00	13.70	123	1.28	183	-0.08	
TCTTCTCTCTCTGCTGCT (-)	21	0.00	14.53	0.00	10.41	BnaA06g03470D	Zinc finger CCH domain-containing protein 38	2657	TT2	0.00	0.00	0.00	0.00	0.00	0.00	0.13	214	0.34	388	0.11		
TCCTTCTCTCTCTCTGCT (-)	22	0.00	1.17	0.00	1.92	BnaA03g06780D	unknown	4415	TT2	0.00	0.00	0.00	0.00	0.00	0.00	0.00	13.18	181	0.98	357	0.45	
CCTTCTCTCTCTCTGCT (-)	21	0.00	11.17	0.00	8.13	BnaA05g29350D	unknown	559	TT2	0.00	0.00	0.00	0.00	0.00	0.00	0.00	14.48	2639	-0.04	5660	1.49	
TCCTTCTCTCTCTCTGCT (-)	21	0.01	11.63	0.00	9.29	BnaC06g00930D	DNA replication licensing factor MCM2	167	TT2	0.00	0.00	0.00	0.00	0.00	0.00	0.13	57	-0.33	29	0.12		
TCCTTCTCTCTCTCTGCT (-)	22	0.00	1.17	0.00	1.92	BnaA01g14170D	unknown	29	TT2	0.00	0.00	0.00	0.00	0.00	0.00	0.00	3.26	1837	-0.13	1248	-0.42	
TCTCCTCTCTCTCTCTGCT (-)	21	0.00	3.37	0.00	2.64	BnaA07g22880D	Anoctamin-like protein At1g73020	138	TT2	0.00	0.00	0.00	0.00	0.00	0.00	0.00	0.13	0	NA	0	NA	
TCTCCTCTCTCTCTCTGCT (-)	21	0.00	3.37	0.00	2.64	BnaCmg17860D	unknown	2377	TT2	0.00	0.00	0.00	0.00	0.00	0.00	0.00	22.57	2425	-0.38	3587	-0.59	
TCTCCTCTCTCTCTCTGCT (-)	21	0.00	3.37	0.00	2.64	BnaC07g15380D	Dehydrin ERD10	787	TT2	0.00	0.00	0.00	0.00	0.00	0.00	0.00	15.40	16379	-0.33	24732	-0.42	
TCCTTCTCTCTCTCTGCT (-)	22	0.00	1.17	0.00	1.92	BnaC06g00930D	DNA replication licensing factor MCM2	167	TT2	0.00	0.00	0.00	0.00	0.00	0.00	0.00	0.13	57	-0.33	29	0.12	
GAAGAGACACAGTTGAGG (-)	19	0.00	2.47	0.00	3.06	BnaC05g17050D	Proteasome subunit beta type-3-A	60	TT2	0.00	0.00	0.00	0.00	0.00	0.00	0.00	0.00	5.74	2360	0.23	2410	0.96
TCCTTCTCTCTCTCTGCT (-)	22	0.00	1.17	0.00	1.92	BnaA05g29030D	Dehydrin ERD14	527	TT2	0.00	0.00	0.00	0.00	0.00	0.00	0.00	13.18	92939	-0.04	94652	-1.37	
TCCTTCTCTCTCTCTGCT (-)	21	0.01	11.63	0.00	9.29	BnaA05g29030D	Dehydrin ERD14	527	TT2	0.00	0.00	0.00	0.00	0.00	0.00	0.00	13.18	92939	-0.04	94652	-1.37	

GAAGACACAGTTGGAGG (-)	19	0.00	2.47	0.00	3.06	BnaC08j05980D	Cytochrome c oxidase subunit 6b-1	191	TT2	0.00	0.00	0.00	1.17	740	-0.66	610	-0.40
TCCTTCTCTCTCTCTGCT (-)	22	0.00	1.17	0.00	1.92	BnaA02g36030D	Dehydrin ERD14	517	TT2	0.00	0.00	0.00	13.18	56906	0.21	128884	-1.36
TCCTTCTCTCTCTCTGCT (-)	21	0.01	11.63	0.00	9.29	BnaA02g36030D	Dehydrin ERD14	517	TT2	0.00	0.00	0.00	13.18	56906	0.21	128884	-1.36
AGAGAACTCTTGGTGGAT (+)	21	0.08	168.57	0.10	150.66	BnaC05g16520D	Nematode resistance protein-like HSPRO2	85	TT3	0.00	0.00	0.00	0.09	0	NA	3	0.63
AGAAATCTGAAACAAGTTG (+)	21	0.00	3.65	0.00	2.67	BnaC07g45570D	CMP- sialic acid transporter 4	520	TT3	0.00	0.00	0.00	0.23	61	-0.35	12	0.35
GGCAGAAAGGAGAAAGGA (+)	21	0.00	14.92	0.00	15.67	BnaC09g07830D	Protein indeterminate-domain 1	973	TT3	0.00	0.00	0.00	0.05	251	0.00	557	0.38
GGAAACGCTGAGGAAGCT (+)	21	0.04	25.98	0.02	20.14	BnaA09g07000D	NAC domain-containing protein 100	873	TT3	0.00	0.00	0.00	0.37	600	0.12	252	2.22
AGAGAACTCTTGGTGGAT (+)	21	0.08	168.57	0.10	150.66	BnaA01g06670D	Probable cyclic nucleotide-gated ion channel 17	2558	TT3	0.00	0.00	0.00	0.14	837	0.81	1946	0.81
CAACAANTGGGTAGAGAGT (+)	21	0.00	4.09	0.01	2.72	BnaC08g07130D	UDP-glycosyltransferase 71B2	1528	TT3	0.00	0.00	0.00	0.69	601	-0.97	519	0.69
AAAGTTGAAACATCGAGAT (+)	21	0.01	41.93	0.01	34.07	BnaC08g32250D	Serine/threonine-protein kinase EDR1	1551	TT3	0.00	0.00	0.00	0.05	0	NA	0	NA
TGAGCACGAGAGGTTGTAAT (+)	21	0.02	37.99	0.02	23.40	BnaA03g39650D	Calcium sensing receptor, chloroplastic	1917	TT3	0.00	0.00	0.00	0.05	34860	-0.90	25557	-1.10
AGCACGAGAGGTTGAAAGA (+)	21	0.01	1.11	0.00	1.39	BnaA07g33880D	unknwn	978	TT3	0.00	0.00	0.00	1.25	8919	-0.65	9072	0.04
AAATATGCTACTGATGAGAT (+)	21	0.01	6.59	0.01	2.41	BnaC02g28890D	unknwn	1569	TT3	0.00	0.00	0.00	0.74	1916	0.22	2503	0.01
AGAGAACTCTTGGTGGAT (+)	21	0.08	168.57	0.10	150.66	BnaC08g27070D	Nematode resistance protein-like HSPRO2	85	TT3	0.00	0.00	0.00	0.09	0	NA	48	0.50
AGAAATCTGAAACAAGTTG (+)	21	0.00	3.65	0.00	2.67	BnaA07g37360D	LOB domain-containing protein 37	438	TT3	0.00	0.00	0.00	0.79	14521	-0.27	6914	0.24
GGCAGAAAGGAGAAAGGA (+)	21	0.00	14.92	0.00	15.67	BnaA07g25910D	E3 ubiquitin-protein ligase SINA-like 2	274	TT3	0.00	0.00	0.00	0.14	1	-0.03	1	0.30
AGAAATCTGAAACAAGTTG (+)	21	0.00	3.65	0.00	2.67	BnaA03g40660D	LOB domain-containing protein 38	425	TT3	0.00	0.00	0.00	0.79	93	0.06	69	-0.56
AGAGAACTCTTGGTGGAT (+)	21	0.08	168.57	0.10	150.66	BnaC01g08680D	Nematode resistance protein-like HSPRO2	85	TT3	0.00	0.00	0.00	0.09	0	NA	48	0.50
CAAGCGAAGAGAAATCGAGC (+)	22	0.00	6.69	0.01	6.13	BnaC04g7810D	Putative fluoride ion transporter CrcB 2	1422	TT3	0.00	0.00	0.00	0.56	1057	-0.23	945	-0.13
AAAGAAGATGTTGGCAAAAC (+)	21	0.01	23.82	0.00	11.75	BnaA08g22410D	NAP1-related protein 2	1939	TT3	0.00	0.00	0.00	0.09	2302	-1.14	1840	-0.58
ATCTGAAGATTTCTGCGAG (+)	21	0.02	78.87	0.02	46.04	BnaA10g00130D	UDP-glucuronate 4-epimerase 3	3686	TT3	0.00	0.00	0.00	0.23	462	-0.09	1129	-0.03
AGAAATCTGAAACAAGTTG (+)	21	0.00	3.65	0.00	2.67	BnaC08g56620D	LOB domain-containing protein 37	442	TT3	0.00	0.00	0.00	0.79	8789	-0.17	7977	0.34
GAGAAATATCATGCTGTTGAA (+)	21	0.00	5.87	0.01	3.82	BnaC08g17310D	Tetraspanin-3	577	TT3	0.00	0.00	0.00	0.09	12239	-0.31	15096	0.58
ATACCTGAAGAACAGAACCGA (+)	21	0.02	107.91	0.06	79.43	BnaC01g13020D	unknwn	372	TT3	0.00	0.00	0.00	0.09	319	-1.17	112	-0.88
AAAGAACGAGAGGAGGCAAAA (+)	21	0.00	11.54	0.01	8.84	BnaA09g12090D	Putative pentatricopeptide repeat-containing protein A1g64310	1269	TT3	0.00	0.00	0.00	0.09	12	-0.51	8	-0.88
CGAGAAATATCATGCTGTTGAA (+)	22	0.00	5.81	0.00	7.81	BnaA05g34080D	Cystathionine gamma-synthase 1, chloroplastic	1101	TT3	0.00	0.00	0.00	0.05	16483	-0.89	7249	-0.88
CAGAAAGGAGAAAGAGGAGAG (+)	22	0.00	2.00	0.00	2.18	BnaC08g17310D	Thioredoxin H-type	788	TT3	0.00	0.00	0.00	0.14	72375	-0.95	58061	-0.35
GAAAGTTGAAACATCGAGAT (+)	21	0.00	5.75	0.00	2.41	BnaC02g27970D	unknwn	1650	TT3	0.00	0.00	0.00	0.37	3	-0.08	20	-0.25
AAAGTTGAAACATCGAGAT (+)	21	0.01	41.93	0.01	34.07	BnaC01g01120D	Protein RMD5 homolog A	2177	TT3	0.00	0.00	0.00	0.14	2018	1.10	2342	0.43
AGAAATGTTATCCACCATCC (-)	22	0.00	6.19	0.00	5.51	BnaA02g00880D	DEAD-box ATP-dependent RNA helicase 56	484	TT3	0.00	0.00	0.00	0.19	3026	0.46	5327	0.53
AGAAATGTTATCCACCATCC (-)	21	0.00	4.51	0.00	2.37	BnaC09g20450D	unknwn	2001	TT3	0.00	0.00	0.00	0.14	211	0.72	853	0.40

CATCTTCATAATCTCAAGA (-)	21	0.02	25.23	0.00	20.64	BnaA09g47450D	Aspartic proteinase A1	2386	CATCTTCATAATCTCAAGA o o	TT3	0.00	0.00	0.00	0.00	0.19	58685	0.94	92695	1.33
CAGATCCCTCTCTTTGTGC (-)	21	0.00	13.10	0.00	10.58	BnaC09g42190D	unknown	137	CAGATCCCTCTCTTTGTGC o o	TT3	0.00	0.00	0.00	0.00	0.28	0	NA	1	0.11
CTGCAGTATCCCTCAGGCAT (-)	21	0.00	5.97	0.00	3.05	BnaC08g41130D	unknown	2663	CTGCAGTATCCCTCAGGCAT o o	TT3	0.00	0.00	0.00	0.00	0.28	465	1.00	906	0.59
CATCTTCATAATCTCAAGA (-)	21	0.02	25.23	0.00	20.64	BnaC08g41720D	Aspartic proteinase	790	CATCTTCATAATCTCAAGA o o	TT3	0.00	0.00	0.00	0.00	0.19	37930	0.46	48931	0.66
CTTTAACTGTTTTGTATGT (-)	21	0.00	8.28	0.00	10.97	BnaA08g18480D	Purine permease 1	83	CTTTAACTGTTTTGTATGT o o	TT3	0.00	0.00	0.00	0.00	0.05	2275	-0.08	3497	0.37
AGAAATGTGTATCCACATCC (-)	21	0.00	4.51	0.00	2.37	BnaA09g18520D	unknown	2007	AGAAATGTGTATCCACATCC o o	TT3	0.00	0.00	0.00	0.00	0.14	565	-0.69	766	-0.38
TTATGTTGAGTTTATATT (-)	20	0.00	1.71	0.00	30.26	BnaA01g22950D	unknown	1566	TTATGTTGAGTTTATATT o o	TT3	0.00	0.00	0.00	0.00	0.14	280	1.15	233	0.36
AACTTTGTTTCAGTATTCTT (-)	21	0.00	4.54	0.00	2.19	BnaC05g10240D	unknown	45	AACTTTGTTTCAGTATTCTT o o	TT3	0.00	0.00	0.00	0.00	0.09	475	0.46	4591	1.14
TCAAGCACTGATATGTTCTG (-)	21	0.00	23.20	0.02	13.86	BnaA10g05040D	AP-2 complex subunit-sigma	976	TCAAGCACTGATATGTTCTG o o	TT3	0.00	0.00	0.00	0.00	0.05	1166	-0.47	959	0.13
TTTGCCTCTCTGTTCTTT (-)	21	0.02	12.25	0.00	9.24	BnaC04g1100D	Thylakoidal processing peptidase 1, chloroplastic	2000	TTTGCCTCTCTGTTCTTT o o	TT3	0.00	0.00	0.00	0.00	0.05	10971	-0.19	8170	-0.52
TTTCATCTGGATGTGTCCT (-)	21	0.02	14.11	0.00	11.95	BnaA03g13310D	Superoxide dismutase [Fe] 2, chloroplastic	1136	TTTCATCTGGATGTGTCCT o o	TT3	0.00	0.00	0.00	0.00	0.51	320	0.13	224	-0.40
TCAAGCACTGATATGTTCTG (-)	21	0.00	23.20	0.02	13.86	BnaC05g20230D	unknown	3275	TCAAGCACTGATATGTTCTG o o	TT3	0.00	0.00	0.00	0.00	0.23	347	1.06	619	0.13
TTTGCCTCTCTGTTCTTT (-)	21	0.02	12.25	0.00	9.24	BnaA04g17540D	Thylakoidal processing peptidase 1, chloroplastic	2341	TTTGCCTCTCTGTTCTTT o o	TT3	0.00	0.00	0.00	0.00	0.05	2020	-0.58	9542	-0.61
AGAAATGTGTATCCACATCC (-)	21	0.00	4.51	0.00	2.37	BnaA09g38720D	Transketolase-1, chloroplastic	2325	AGAAATGTGTATCCACATCC o o	TT3	0.00	0.00	0.00	0.00	0.09	14311	-0.83	13711	-0.77
TGACTTTGAAGTCTCTTCAA (-)	21	0.00	2.89	0.00	2.45	BnaA05g31990D	Sugar transporter ERD6-like 10	2442	TGACTTTGAAGTCTCTTCAA o o	TT3	0.00	0.00	0.00	0.00	0.14	5234	-0.52	6252	-0.37
TGCAAGTATCCCTCAGGCA (-)	19	0.00	2.30	0.00	1.82	BnaA03g21090D	Autophagy-related protein 8e	489	TGCAAGTATCCCTCAGGCA o o	TT3	0.00	0.00	0.00	0.00	0.05	24300	0.64	4689	0.13
TGCAGAGAATCTCAGGATC (-)	21	0.02	40.38	0.00	31.94	BnaA01g14050D	NBR1 homolog	708	TGCAGAGAATCTCAGGATC o o	TT3	0.00	0.00	0.00	0.00	0.05	2959	5.97	279	7.49
TTTTGCCTCTCTGTTCTTT (-)	21	0.01	15.07	0.01	11.06	BnaC04g29080D	U-box domain-containing protein 11	1379	TTTTGCCTCTCTGTTCTTT o o	TT3	0.00	0.00	0.00	0.00	0.14	0	NA	0	NA
CCTCTCTCTCTCTGCT (-)	21	0.00	11.17	0.00	8.13	BnaA02g05030D	Probable pollen receptor-like kinase 6	1004	CCTCTCTCTCTCTGCT o o	TT3	0.00	0.00	0.00	0.00	0.69	0	0.22	1	0.18
TCAAGCACTGATATGTTCTG (-)	21	0.00	23.20	0.02	13.86	BnaCmg48180D	Glucose-6-phosphate 1-dehydrogenase 1, chloroplastic	1159	TCAAGCACTGATATGTTCTG o o	TT3	0.00	0.00	0.00	0.00	0.14	2094	0.00	3135	-0.45

Table S19: PHAS loci that produce va-phasiRNAs in Drakkar

PHAS locus	Predicted gene function	transcript length	siRNA reads & rpm & ratio & PHAS Score					
			DM (reads, rpm)	DT (reads, rpm)	DT (reads, rpm)	DT rpm / DIM rpm	PHAS Score	
BnaA01g14050D	NBR1 homolog	2109	91	570	83110	250229	439	210.5
BnaC01g16550D	NBR1 homolog	2118	90	564	74021	222864	395	227.4
BnaA04g20150D	Chlorophyll a-b binding protein 1, chloroplastic	804	460	2882	18293	55077	19	178.9
BnaA04g12130D	Probable fructose-bisphosphate aldolase 1, chloroplastic	1173	79	495	10287	30972	63	42.1
BnaAnng22920D	Chlorophyll a-b binding protein 1, chloroplastic	804	277	1736	10046	30247	17	164.2
BnaC03g59520D	Chlorophyll a-b binding protein 1, chloroplastic	804	375	2350	9349	28148	12	98.7
BnaC04g33570D	Fructose-bisphosphate aldolase, chloroplastic	1173	79	495	8934	26899	54	47.6
BnaA02g05040D	unknown	753	206	1291	8803	26504	21	117
BnaA05g29390D	Chlorophyll a-b binding protein CP29.2, chloroplastic	867	161	1009	8490	25562	25	100
BnaA07g07560D	Chlorophyll a-b binding protein 1, chloroplastic	804	324	2030	8429	25378	13	86.5
BnaA07g19610D	ABC transporter G family member 35	4173	108	677	7975	24011	35	61.6
BnaA03g15830D	Chlorophyll a-b binding protein 1, chloroplastic	801	249	1560	7690	23153	15	75.4
BnaC03g18980D	Chlorophyll a-b binding protein 1, chloroplastic	801	253	1585	6797	20465	13	38.9
BnaC05g10980D	RNA-dependent RNA polymerase 1	3282	45	282	6467	19471	69	74.9
BnaA09g26570D	Chlorophyll a-b binding protein 1, chloroplastic	804	198	1241	6307	18989	15	61.1
BnaA08g17660D	Chlorophyll a-b binding protein 1, chloroplastic	804	248	1554	6017	18116	12	64.9
BnaC05g22880D	Chlorophyll a-b binding protein 1, chloroplastic	804	175	1097	5702	17168	16	52.1
BnaC06g14450D	Probable pectate lyase 22	1611	661	4142	5481	16502	4	443.6
BnaAnng23670D	ATPase 2, plasma membrane-type	2757	51	320	5457	16430	51	45.2
BnaA09g47880D	Zinc transporter 4, chloroplastic	1194	10	63	5290	15927	254	65.4
BnaC08g42250D	Zinc transporter 4, chloroplastic	1191	6	38	5248	15801	420	67.1
BnaC08g16670D	unknown	591	723	4530	4752	14307	3	934.2
BnaC07g09400D	Chlorophyll a-b binding protein 1, chloroplastic	804	234	1466	4742	14277	10	47.3
BnaA09g00390D	S-adenosylmethionine synthase	1098	29	182	4716	14199	78	120.1
BnaC07g39070D	NBR1 homolog	2076	12	75	4664	14042	187	42
BnaC04g08360D	S-adenosylmethionine synthase 3	1122	34	213	4646	13988	66	83.5
BnaC04g10770D	Chlorophyll a-b binding protein 1, chloroplastic	990	503	3152	4644	13982	4	105.3
BnaA02g22660D	Tubulin beta-4 chain	1341	30	188	4585	13805	73	97.4
BnaC05g27560D	Probable LRR receptor-like serine/threonine-protein kinase At4g08850	2241	50	313	4387	13208	42	51.9

BnaC04g10780D	Chlorophyll a-b binding protein 1, chloroplastic	801	238	1491	4242	12772	9	69.8
BnaC09g37170D	unknown	759	35	219	4176	12573	57	59.5
BnaC07g29410D	EIN3-binding F-box protein 2	1866	20	125	4169	12552	100	97.4
BnaC06g41790D	ARGONAUT 2	3108	71	445	4024	12116	27	76.1
BnaA06g37230D	Probable fructose-bisphosphate aldolase 2, chloroplastic	1182	109	683	3934	11845	17	30.2
BnaAnng14520D	Subtilisin-like protease SBT1.7	2283	32	201	3924	11814	59	67.2
BnaC05g17000D	Protein ToIB	2121	14	88	3918	11796	134	71.4
BnaC03g60280D	Probable fructose-bisphosphate aldolase 2, chloroplastic	1152	131	821	3810	11471	14	43.2
BnaA10g14810D	unknown	747	63	395	3708	11164	28	36.9
BnaA05g09400D	Chlorophyll a-b binding protein 1, chloroplastic	801	105	658	3640	10959	17	46.5
BnaA07g17260D	Putative calcium-transporting ATPase 11, plasma membrane-type	3078	15	94	3609	10866	116	75.4
BnaC04g42010D	Probable mediator of RNA polymerase II transcription subunit 37e	783	22	138	3579	10776	78	110.4
BnaC04g37750D	EIN3-binding F-box protein 1	1800	88	551	3555	10703	19	92.2
BnaC02g31030D	Tubulin beta-1 chain	1338	21	132	3523	10607	81	42
BnaA06g38620D	Pyrophosphate-energized vacuolar membrane proton pump	1821	778	4875	3370	10146	2	53.1
BnaA06g35940D	unknown	5187	14	88	3180	9574	109	62.7
BnaC03g05980D	Magnesium-chelataase subunit ChIH, chloroplastic	4155	126	790	3124	9406	12	31
BnaA06g04440D	Elongation factor 1-alpha 4	1383	16	100	3119	9391	94	79.6
BnaC04g50850D	Phosphatidylinositol 4-kinase gamma 4	1470	10	63	3083	9282	148	63.8
BnaCnng64010D	ABC transporter G family member 36	2145	25	157	3070	9243	59	43.4
BnaCnng07470D	Putative calcium-transporting ATPase 11, plasma membrane-type	3078	18	113	3065	9228	82	36.7
BnaC01g21920D	Cysteine proteinase RD19a	1107	28	175	3045	9168	52	60.9
BnaA06g15400D	Protein ToIB	2004	26	163	2988	8996	55	45.5
BnaC04g42020D	Probable mediator of RNA polymerase II transcription subunit 37e	723	12	75	2895	8716	116	79
BnaA05g28710D	Cell division control protein 48 homolog E	2427	15	94	2862	8617	92	30.4
BnaA03g10790D	Heat shock protein 90-4	1728	30	188	2762	8316	44	87.1
BnaC07g15280D	Catalase-3	1479	105	658	2710	8159	12	40.1
BnaCnng74930D	24-methylenesterol C-methyltransferase 2	1071	22	138	2654	7991	58	36.6
BnaA04g14890D	EIN3-binding F-box protein 1	1872	57	357	2597	7819	22	47.4
BnaCnng20770D	24-methylenesterol C-methyltransferase 2	1071	17	107	2592	7804	73	40.4

BnaA09g26890D	U-box domain-containing protein 17	2115	7	44	2588	7792	178	43.3
BnaAnng01730D	ABC transporter G family member 22	2157	20	125	2547	7669	61	30.8
BnaAnng35580D	Glycine-rich RNA-binding protein GRP2A	507	149	934	2377	7157	8	38.2
BnaC07g21430D	Protein NRT1/ PTR FAMILY 8.3	1758	11	69	2366	7124	103	45.6
BnaC07g19250D	unknown	5082	17	107	2347	7066	66	44.7
BnaC07g15930D	Subtilisin-like protease SBT1.7	2283	23	144	2329	7012	49	34.9
BnaA06g24650D	Leucine-rich repeat receptor-like serine/threonine-protein kinase BAM1	2916	42	263	2238	6738	26	61.8
BnaC08g38660D	Chlorophyll a-b binding protein CP24 10B, chloroplastic	780	61	382	2233	6723	18	54.9
BnaCngg03470D	Probable mediator of RNA polymerase II transcription subunit 37e	783	16	100	2198	6618	66	54.1
BnaC06g38300D	Nitrate reductase [NADH], clone PBNBR1405	2685	211	1322	2185	6579	5	32.8
BnaC05g40290D	ABC transporter C family member 7	5214	21	132	2070	6232	47	40
BnaC09g32520D	Transmembrane protein 245	1953	26	163	2053	6181	38	49.2
BnaC08g36330D	Transcription activator GLK1	3066	94	589	1950	5871	10	125.2
BnaAnng04540D	Probable LRR receptor-like serine/threonine-protein kinase At4g08850	1626	3	19	1899	5718	304	50.4
BnaC03g25510D	Aquaporin PIP1-2	861	32	201	1863	5609	28	32.7
BnaC01g38940D	Cell division control protein 48 homolog E	2433	8	50	1856	5588	111	33.1
BnaC02g40260D	Elongation factor 2	2517	21	132	1853	5579	42	48.8
BnaA03g26530D	S-adenosylmethionine synthase	1098	22	138	1773	5338	39	38.5
BnaA01g29630D	Subtilisin-like protease SBT1.4	2328	62	388	1766	5317	14	31.2
BnaC01g37240D	Subtilisin-like protease SBT1.4	2328	63	395	1766	5317	13	38.6
BnaA09g56570D	Chlorophyll a-b binding protein CP24 10B, chloroplastic	780	74	464	1694	5100	11	55.3
BnaC04g20690D	Calcium-transporting ATPase 12, plasma membrane-type	3102	23	144	1664	5010	35	37.8
BnaA03g00850D	Cell division control protein 48 homolog E	2397	5	31	1658	4992	159	31.1
BnaA01g22310D	Probable nucleoredoxin 1	1737	94	589	1639	4935	8	38.1
BnaA07g19580D	2-methyl-6-phytyl-1,4-hydroquinone methyltransferase, chloroplastic	1014	11	69	1632	4914	71	36
BnaC01g03600D	unknown	438	276	1729	1600	4817	3	30.3
BnaC01g33900D	Actin-2	1134	48	301	1593	4796	16	34.6
BnaA02g27980D	Thiamine thiazole synthase, chloroplastic	843	96	602	1593	4796	8	43
BnaC01g43180D	Probable nucleoredoxin 1	1737	45	282	1583	4766	17	37.6
BnaA09g04600D	EIN3-binding F-box protein 2	1851	16	100	1556	4685	47	34.8

BnaAnng33970D	Elongation factor 2	1530	15	94	1542	4643	49	56.3
BnaA07g07430D	unknown	744	174	1090	1522	4582	4	36.9
BnaCnng38780D	Elongation factor 1-alpha 4	1287	21	132	1521	4579	35	31.4
BnaA09g05850D	Probable mediator of RNA polymerase II transcription subunit 37e	795	21	132	1480	4456	34	34.1
BnaC09g14730D	unknown	264	215	1347	1480	4456	3	352.5
BnaA04g21850D	Vacuolar cation/proton exchanger 1	1398	32	201	1451	4369	22	30.2
BnaA03g49610D	Cytidine deaminase 1	873	72	451	1369	4122	9	31
BnaC03g13470D	Heat shock protein 90-2	1614	24	150	1351	4068	27	31.7
BnaC02g01960D	ABC transporter G family member 22	2259	13	81	1341	4038	50	169.7
BnaAnng09960D	Tubulin beta-4 chain	1338	12	75	1307	3935	52	30.3
BnaAnng07150D	unknown	699	11	69	1302	3920	57	41.9
BnaC04g06480D	Inorganic phosphate transporter 1-4	1524	53	332	1290	3884	12	34.4
BnaC03g76150D	Elongation factor 2	1200	21	132	1243	3742	28	30.3
BnaA10g29460D	Zinc finger CCH domain-containing protein 66	1560	17	107	1234	3715	35	33.4
BnaA07g33680D	Nitrate reductase [NADH], clone PBNBR1405	840	203	1272	1224	3685	3	32.7
BnaCnng23930D	Cytochrome P450 89A2	1488	1	6	1124	3384	540	32
BnaC07g23740D	Pentatricopeptide repeat-containing protein At3g26630, chloroplastic	1359	21	132	1089	3279	25	43.4
BnaCnng44170D	UDP-glucuronate 4-epimerase 6	1383	208	1303	879	2647	2	34.7
BnaC04g44100D	DEAD-box ATP-dependent RNA helicase 21	1773	12	75	858	2583	34	33.4
BnaA08g21730D	Catalase-3	1479	87	545	841	2532	5	32.4
BnaA01g26070D	unknown	1320	18	113	822	2475	22	33.9
BnaC08g37970D	Cationic amino acid transporter 8, vacuolar	1758	3	19	810	2439	130	31.5
BnaC07g36920D	GPN-loop GTPase 1	87	71	445	809	2436	5	310.5
BnaA07g00390D	Shikimate O-hydroxycinnamoyltransferase	1302	30	188	798	2403	13	49.1
BnaA05g24750D	Probable leucine-rich repeat receptor-like serine/threonine-protein kinase	627	70	439	703	2117	5	45.1
BnaC09g23240D	unknown	306	87	545	699	2105	4	43.8
BnaC06g37290D	3-hydroxy-3-methylglutaryl-coenzyme A reductase 1	1725	18	113	656	1975	18	62.5
BnaA07g32810D	3-hydroxy-3-methylglutaryl-coenzyme A reductase 1	1731	16	100	624	1879	19	64.7
BnaC09g15730D	unknown	417	45	282	529	1593	6	33.1
BnaC08g14130D	Pentatricopeptide repeat-containing protein At1g10270	2466	5	31	283	852	27	60.5
BnaC04g10550D	unknown	357	22	138	173	521	4	48.1

BnaC07g29950D	TRANSPARENT TESTA GLABRA 1	717	4	25	2241	6747	269	42.6
BnaC03g51090D	Probable inactive purple acid phosphatase 29	1272	5	31	945	2845	91	47.8
BnaA08g25040D	Aspartic proteinase A1	1581	15	94	872	2625	28	58.2
BnaC01g06430D	unknown	630	20	125	150	452	4	64.6
BnaC07g43630D	unknown	543	15	94	102	307	3	33
BnaC07g00300D	Transcription activator GLK1	1341	37	232	437	1316	6	40.1
BnaC04g46560D	Ribulose biphosphate carboxylase/oxygenase activase, chloroplastic	1320	265	1661	2830	8521	5	75.3
BnaC04g30870D	Ribulose biphosphate carboxylase small chain F1, chloroplastic	546	174	1090	940	2830	3	35.9

Table S20: PHAS loci that produce va-phasiRNAs in Tanto

PHAS locus	Predicted gene function	transcript length	siRNA reads & rpm & ratio & PHAS Score					
			TM (reads, rpm)	TT (reads, rpm)	TT (reads, rpm)	TT rpm / TM rpm	PHAS Score	
BnaA01g14050D	NBR1 homolog	2109	135	691	114844	232160	336	377
BnaC01g16550D	NBR1 homolog	2118	102	522	106357	215003	412	386.9
BnaC06g41790D	ARGONAUTE 2	3108	280	1433	19302	39019	27	273
BnaA07g19610D	ABC transporter G family member 36	4173	261	1336	16033	32411	24	139.3
BnaA04g20150D	Chlorophyll a-b binding protein 1, chloroplastic	804	966	4944	15481	31295	6	224.5
BnaC05g10980D	RNA-dependent RNA polymerase 1	3282	131	670	15172	30671	46	219
BnaA02g05040D	unknown	753	886	4534	13153	26589	6	155.9
BnaA10g27060D	Probable mediator of RNA polymerase II transcription subunit 37e	1365	113	578	11312	22867	40	38.1
BnaC05g48370D	Auxin transport protein BIG	15231	154	788	10170	20559	26	96.3
BnaC03g59520D	Chlorophyll a-b binding protein 1, chloroplastic	804	720	3685	9663	19534	5	93.3
BnaA08g17660D	Chlorophyll a-b binding protein 1, chloroplastic	804	628	3214	8176	16528	5	95.7
BnaAnng22920D	Chlorophyll a-b binding protein 1, chloroplastic	804	500	2559	7981	16134	6	207.7
BnaC07g39070D	NBR1 homolog	2076	18	92	7264	14684	159	93.6
BnaC03g18980D	Chlorophyll a-b binding protein 1, chloroplastic	801	498	2549	7218	14591	6	94.3
BnaCng68320D	ARGONAUTE 2	2664	100	512	7091	14335	28	596
BnaC07g19250D	unknown	5082	34	174	7067	14286	82	149.3
BnaA07g07560D	Chlorophyll a-b binding protein 1, chloroplastic	804	532	2723	7018	14187	5	105.1
BnaCng64010D	ABC transporter G family member 36	2145	110	563	6938	14025	25	72.8
BnaC04g42010D	Probable mediator of RNA polymerase II transcription subunit 37e	783	36	184	6884	13916	76	173.9
BnaC07g29410D	EIN3-binding F-box protein 2	1866	55	281	6858	13864	49	157
BnaC06g01910D	ABC transporter C family member 4	4497	28	143	6776	13698	96	63.5
BnaA09g25290D	ARGONAUTE 2	3072	86	440	6633	13409	30	374.5
BnaA04g12130D	Probable fructose-bisphosphate aldolase 1, chloroplastic	1173	222	1136	6384	12905	11	47.8
BnaC06g14450D	Probable pectate lyase 22	1611	1054	5394	6333	12802	2	475.3
BnaAnng23670D	ATPase 2, plasma membrane-type	2757	119	609	6257	12649	21	49
BnaC09g00800D	Callose synthase 12	5352	25	128	6234	12602	98	86.2
BnaA01g06820D	ATPase 2, plasma membrane-type	2847	105	537	6214	12562	23	32.6
BnaA09g26570D	Chlorophyll a-b binding protein 1, chloroplastic	804	483	2472	6184	12501	5	59.1
BnaA03g15830D	Chlorophyll a-b binding protein 1, chloroplastic	801	417	2134	6117	12366	6	119.6

BnaA06g09600D	RNA-dependent RNA polymerase 1	3330	47	241	5863	11852	49	42.3
BnaA03g32690D	ABC transporter C family member 3	3696	44	225	5849	11824	53	69.1
BnaA04g14890D	EIN3-binding F-box protein 1	1872	115	589	5744	11612	20	106.8
BnaC05g22880D	Chlorophyll a-b binding protein 1, chloroplastic	804	416	2129	5639	11399	5	53.6
BnaA02g05430D	Chaperone protein dnaJ 2	1272	42	215	5606	11333	53	85.1
BnaC05g43180D	Cell division control protein 48 homolog E	2427	16	82	5495	11108	136	59.8
BnaC04g46560D	Ribulose biphosphate carboxylase/oxygenase activase, chloroplastic	1320	641	3280	5436	10989	3	132.9
BnaA03g10790D	Heat shock protein 90-4	1728	36	184	5314	10742	58	117.1
BnaC08g16670D	unknown	591	994	5087	5301	10716	2	984.3
BnaA06g03880D	ABC transporter C family member 4	4557	34	174	5242	10597	61	47
BnaC04g33570D	Probable fructose-bisphosphate aldolase 1, chloroplastic	1173	201	1029	5199	10510	10	44.7
BnaA09g01630D	Callose synthase 12	5352	28	143	5197	10506	73	37.9
BnaC04g37750D	EIN3-binding F-box protein 1	1800	131	670	5101	10312	15	98.9
BnaC09g05190D	unknown	2046	5	26	4924	9954	389	36
BnaC03g05980D	Magnesium-chelatase subunit ChH, chloroplastic	4155	261	1336	4648	9396	7	37.7
BnaA09g35580D	Glycine-rich RNA-binding protein GRP2A	507	255	1305	4601	9301	7	79.7
BnaC04g01000D	BAG family molecular chaperone regulator 6	2733	5	26	4517	9131	357	88.8
BnaC04g42020D	Probable mediator of RNA polymerase II transcription subunit 37e	723	27	138	4488	9073	66	83.5
BnaA06g34380D	Protein NRT1/ PTR FAMILY 8.3	1974	9	46	4443	8982	195	47.8
BnaA10g27080D	Probable mediator of RNA polymerase II transcription subunit 37e	783	31	159	4349	8792	55	39.4
BnaA02g22660D	Tubulin beta-4 chain	1341	47	241	4295	8682	36	107
BnaA05g28710D	Cell division control protein 48 homolog E	2427	9	46	4276	8644	188	50.2
BnaA09g05630D	unknown	2169	4	20	4263	8618	421	50.9
BnaA03g39600D	Sacsin	13023	58	297	4144	8377	28	53.1
BnaC09g03470D	Probable mediator of RNA polymerase II transcription subunit 37e	783	28	143	4143	8375	58	89
BnaC02g12750D	Heat shock protein 90-4	1722	26	133	4084	8256	62	102.8
BnaA05g29390D	Chlorophyll a-b binding protein CP29.2, chloroplastic	867	304	1556	4033	8153	5	66.7
BnaC04g10780D	Chlorophyll a-b binding protein 1, chloroplastic	801	398	2037	3885	7854	4	78
BnaA10g27070D	Probable mediator of RNA polymerase II transcription subunit 37e	723	26	133	3884	7852	59	55.1
BnaC07g15280D	Catalase-3	1479	246	1259	3846	7775	6	40.6
BnaA03g49610D	Cytidine deaminase 1	873	155	793	3793	7668	10	84.1
BnaA07g17260D	Putative calcium-transporting ATPase 11, plasma membrane-type	3078	19	97	3758	7597	78	85.2
BnaA09g02450D	REF/SRPP-like protein At3g05500	711	12	61	3742	7565	123	113.4

BnaC01g40400D	unknown	768	132	676	3722	7524	11	87.1
BnaC04g10770D	Chlorophyll a-b binding protein 1, chloroplastic	990	610	3122	3682	7443	2	85.2
BnaA09g26890D	U-box domain-containing protein 17	2115	14	72	3653	7385	103	69.9
BnaA06g04440D	Elongation factor 1-alpha 4	1383	29	148	3617	7312	49	112.5
BnaA06g27640D	E1N3-binding F-box protein 2	1869	41	210	3584	7245	35	63
BnaAnng03650D	unknown	5613	39	200	3579	7235	36	56.9
BnaC04g50850D	Phosphatidylinositol 4-kinase gamma 4	1470	31	159	3530	7136	45	78
BnaC09g21440D	Beta-amylase 1, chloroplastic	1695	185	947	3423	6920	7	79
BnaC02g31030D	Tubulin beta-1 chain	1338	42	215	3393	6859	32	66.6
BnaCmgg71820D	ABC transporter C family member 3	1521	20	102	3382	6837	67	58.8
BnaC03g13930D	Heat shock protein 90-3	1731	15	77	3378	6829	89	73.5
BnaC03g37870D	Proteasome activator subunit 4	5355	11	56	3373	6819	121	38.3
BnaC03g37680D	Probable mediator of RNA polymerase II transcription subunit 37c	1953	18	92	3355	6782	74	60.5
BnaA06g37230D	Probable fructose-bisphosphate aldolase 2, chloroplastic	1182	251	1285	3276	6623	5	37.1
BnaA06g35940D	unknown	5187	15	77	3256	6582	86	69.8
BnaA10g14810D	unknown	747	119	609	3238	6546	11	49.7
BnaC07g21430D	NRT1/ PTR FAMILY 8.3	1758	14	72	3223	6515	91	39.5
BnaC01g38940D	Cell division control protein 48 homolog E	2433	11	56	3220	6509	116	71.3
BnaA03g32320D	Probable mediator of RNA polymerase II transcription subunit 37c	1959	14	72	3213	6495	91	52.2
BnaC05g05630D	Elongation factor 1-alpha 4	1464	42	215	3082	6230	29	45
BnaC03g13470D	Heat shock protein 90-2	1614	20	102	3069	6204	61	85.7
BnaC03g77220D	Polyadenylate-binding protein 2	1854	425	2175	3026	6117	3	60.3
BnaC09g37170D	unknown	759	118	604	3020	6105	10	55.8
BnaC08g36330D	Transcription activator GLK1	3066	336	1720	2982	6028	4	96.8
BnaC08g21780D	unknown	5628	41	210	2973	6010	29	42.3
BnaA09g05850D	Probable mediator of RNA polymerase II transcription subunit 37e	795	29	148	2941	5945	40	96.6
BnaCmgg24140D	Chlorophyll a-b binding protein CP29.2, chloroplastic	870	278	1423	2870	5802	4	33.1
BnaC03g13870D	Heat shock protein 90-2	1095	30	154	2859	5780	38	54
BnaA03g32640D	ABC transporter C family member 6	1509	18	92	2806	5672	62	37.8
BnaC02g40260D	Elongation factor 2	2517	50	256	2776	5612	22	76.5
BnaA09g26850D	Protein MEI2-like 5	2322	19	97	2701	5460	56	40
BnaC09g54000D	4-hydroxy-3-methylbut-2-en-1-yl diphosphate synthase (ferredoxin), chloroplastic	2211	41	210	2699	5456	26	30.5
BnaC07g50780D	Cytidine deaminase 1	942	119	609	2697	5452	9	58.6

BnaA03g00850D	Cell division control protein 48 homolog E	2397	10	51	2695	5448	106	60
BnaA03g14760D	SOBIR1	1938	25	128	2668	5393	42	72.2
BnaA08g15160D	U-box domain-containing protein 5	5406	28	143	2660	5377	38	48.6
BnaCnnng03460D	Probable mediator of RNA polymerase II transcription subunit 37e	723	13	67	2593	5242	79	30.5
BnaC03g73610D	ABC transporter C family member 3	2385	18	92	2586	5228	57	54.5
BnaA05g33630D	Auxin transport protein BIG	6681	33	169	2570	5195	31	37.4
BnaA07g05790D	Beta-amylase 1, chloroplastic	1713	138	706	2570	5195	7	31.5
BnaAnng07150D	unknown	699	12	61	2564	5183	84	48.8
BnaC05g17890D	QUIRKY	3024	39	200	2519	5092	26	48.7
BnaC08g14030D	NF-X1-type zinc finger protein NFXL1	2898	29	148	2518	5090	34	47.6
BnaC04g30810D	Ribulose biphosphate carboxylase small chain 1A, chloroplastic	546	252	1290	2501	5056	4	45.4
BnaA09g00390D	S-adenosylmethionine synthase	1098	51	261	2483	5019	19	71.1
BnaC05g11440D	ALG-2 interacting protein X	2571	22	113	2464	4981	44	37.4
BnaC04g30870D	Ribulose biphosphate carboxylase small chain F1, chloroplastic	546	309	1581	2452	4957	3	62.3
BnaA02g08820D	Heat shock protein 90-2	1656	18	92	2427	4906	53	75.1
BnaC03g17800D	SOBIR1	1935	31	159	2426	4904	31	37.1
BnaA01g15810D	GDPDL2	2274	30	154	2422	4896	32	35.9
BnaC07g29950D	TRANSPARENT TESTA GLABRA 1	717	9	46	2418	4888	106	40.7
BnaC06g06400D	Heat shock 70 kDa protein 14	2871	34	174	2384	4819	28	35.4
BnaC08g49360D	Glycine-rich RNA-binding protein 7	504	157	803	2383	4817	6	33.9
BnaC01g27600D	Probable mediator of RNA polymerase II transcription subunit 37e	1254	20	102	2369	4789	47	32.7
BnaA01g32030D	Cell division control protein 48 homolog A	2433	7	36	2312	4674	130	32.8
BnaCnnng26360D	unknown	438	122	624	2310	4670	7	42.8
BnaC06g38300D	Nitrate reductase [NADH], clone PBNBR1405	2685	421	2155	2293	4635	2	35.2
BnaC09g41970D	Probable endo-1,3(4)-beta-glucanase ARB_01444	2151	16	82	2262	4573	56	39.4
BnaC05g43540D	unknown	1104	1	5	2255	4559	891	41.3
BnaA06g00870D	Heat shock 70 kDa protein 14	2577	14	72	2156	4358	61	35.7
BnaCnnng38780D	Elongation factor 1-alpha 4	1287	31	159	2154	4354	27	77.8
BnaA08g25950D	NF-X1-type zinc finger protein NFXL1	2676	28	143	2150	4346	30	34
BnaC08g32100D	Probable protein phosphatase 2C 49	1128	10	51	2134	4314	84	49.1
BnaAnng01730D	ABC transporter G family member 22	2157	52	266	2122	4290	16	43.4
BnaC02g46810D	Chlorophyll a-b binding protein CP26, chloroplastic	846	245	1254	2119	4284	3	30.7
BnaA09g05860D	Probable mediator of RNA polymerase II transcription subunit 37e	717	21	107	2117	4280	40	52.9

BnaC09g34840D	E3 ubiquitin-protein ligase RING1-like	1068	21	107	2113	4271	40	36.9
BnaC01g01110D	Heat shock 70 kDa protein 9, mitochondrial	2043	7	36	2112	4269	119	45
BnaC01g31710D	Proteasome subunit alpha type-4-A	606	9	46	2102	4249	92	60.1
BnaA05g28110D	unknown	741	118	604	2097	4239	7	45.9
BnaC04g07660D	L-type lectin-domain containing receptor kinase IV.1	2022	23	118	2090	4225	36	40.3
BnaC03g11130D	ABC transporter F family member 1	2760	21	107	2033	4110	38	35.5
BnaC04g20690D	Calcium-transporting ATPase 12, plasma membrane-type	3102	36	184	2022	4088	22	40.9
BnaA10g00830D	NAC domain-containing protein 1	1428	17	87	2001	4045	46	48
BnaC09g32520D	Transmembrane protein 245	1953	43	220	1993	4029	18	51.9
BnaC05g40290D	ABC transporter C family member 7	5214	64	328	1964	3970	12	40.2
BnaAnng33970D	Elongation factor 2	1530	38	194	1946	3934	20	47.3
BnaC01g21920D	Cysteine proteinase RD19a	1107	61	312	1932	3906	13	46.4
BnaC03g51090D	Probable inactive purple acid phosphatase 29	1272	17	87	1919	3879	45	51.2
BnaCmg36540D	Tubulin beta-4 chain	1338	30	154	1916	3873	25	35.8
BnaC06g28800D	ATP-dependent zinc metalloprotease FTSH 1, chloroplastic	2109	121	619	1856	3752	6	33.9
BnaC05g17000D	To1B	2121	37	189	1837	3714	20	53.4
BnaA03g11140D	Heat shock protein 90-2	1092	14	72	1820	3679	51	37.2
BnaC02g44790D	Auxin-responsive protein SAUR32	387	7	36	1811	3661	102	45.1
BnaC03g01160D	Cell division control protein 48 homolog E	2430	9	46	1809	3657	79	43.5
BnaAnng12070D	Probable mediator of RNA polymerase II transcription subunit 37e	771	10	51	1805	3649	71	51.7
BnaA09g39770D	Probable protein phosphatase 2C 49	1125	12	61	1773	3584	58	88.9
BnaA10g14240D	Chaperone protein dnaJ 3	1269	7	36	1764	3566	100	36.6
BnaA09g22540D	Chlorophyll a-b binding protein CP26, chloroplastic	630	201	1029	1751	3540	3	31.3
BnaAnng04540D	Probable LRR receptor-like serine/threonine-protein kinase At4g08850	1626	4	20	1739	3515	172	62.9
BnaC05g30200D	TIME FOR COFFEE	4650	100	512	1734	3505	7	30.3
BnaA04g18310D	Pentatricopeptide repeat-containing protein At2g31400, chloroplastic	2190	23	118	1731	3499	30	36.2
BnaA01g30060D	ABC transporter C family member 3	3483	8	41	1725	3487	85	30.8
BnaA06g31350D	unknown	2055	22	113	1721	3479	31	36.9
BnaA03g32250D	ELC	1812	11	56	1680	3396	60	32
BnaA01g30490D	Probable mediator of RNA polymerase II transcription subunit 37c	1953	15	77	1652	3340	44	34.7
BnaC04g08360D	S-adenosylmethionine synthase 3	1122	60	307	1636	3307	11	42.1
BnaAnng09960D	Tubulin beta-4 chain	1338	33	169	1623	3281	19	43.5
BnaC05g09210D	Glyceraldehyde-3-phosphate dehydrogenase GAP2, chloroplastic	1200	313	1602	1598	3230	2	32.3

BnaA08g18750D	Calcium-transporting ATPase 1, chloroplasmic	3054	8	41	1596	3226	79	41.4
BnaA09g04600D	E1N3-binding F-box protein 2	1851	53	271	1593	3220	12	39.9
BnaC03g76150D	Elongation factor 2	1200	35	179	1562	3158	18	42.8
BnaC04g44100D	DEAD-box ATP-dependent RNA helicase 21	1773	17	87	1561	3156	36	49.6
BnaC09g06290D	Splicing factor 3B subunit 1	3627	19	97	1553	3139	32	34.4
BnaA07g15900D	Fructose-bisphosphate aldolase, cytoplasmic isozyme 2	1077	5	26	1545	3123	122	51
BnaA01g29630D	Subtilisin-like protease SBT1.4	2328	221	1131	1533	3099	3	37.2
BnaC06g14270D	Fructose-bisphosphate aldolase, cytoplasmic isozyme 2	1077	16	82	1517	3067	37	37.9
BnaC01g05230D	Glycine dehydrogenase (decarboxylating) 1, mitochondrial	3138	281	1438	1516	3065	2	30.6
BnaA07g07430D	unknown	744	278	1423	1502	3036	2	39.2
BnaC07g22660D	Phosphatidylinositol 4-kinase gamma 7	1848	60	307	1494	3020	10	32.3
BnaC03g37540D	Protein ELC	1779	9	46	1477	2986	65	33.9
BnaC08g42250D	Zinc transporter 4, chloroplasmic	1191	2	10	1464	2960	289	33.5
BnaA06g33610D	Phosphatidylinositol 4-kinase gamma 7	1851	45	230	1462	2955	13	31.8
BnaC04g47650D	Probable calcium-binding protein CML35	654	35	179	1455	2941	16	35.6
BnaA09g06770D	Splicing factor 3B subunit 1	3705	25	128	1455	2941	23	39.3
BnaC02g45020D	Ferredoxin--NADP reductase, leaf isozyme 1, chloroplasmic	3015	31	159	1441	2913	18	46.2
BnaA10g18410D	Probable endo-1,3(4)-beta-glucanase ARB_01444	2139	15	77	1432	2895	38	38.3
BnaA07g13530D	RuBisCO large subunit-binding protein subunit alpha, chloroplasmic	1791	16	82	1432	2895	35	45.8
BnaA10g25550D	Probable disease resistance protein At4g33300	1971	13	67	1425	2881	43	31.1
BnaA09g14520D	Subtilisin-like protease SBT1.7	2283	31	159	1422	2875	18	44.8
BnaA09g56570D	Chlorophyll a-b binding protein CP24 10B, chloroplasmic	780	175	896	1415	2860	3	44.6
BnaA08g25040D	Aspartic proteinase A1	1581	37	189	1412	2854	15	60.7
BnaA10g11620D	Chaperone protein ClpB	2826	52	266	1400	2830	11	31.6
BnaA01g24250D	CBL-interacting serine/threonine-protein kinase 7	1245	86	440	1376	2782	6	43.6
BnaA01g22310D	Probable nucleoredoxin 1	1737	46	235	1334	2697	11	48.1
BnaA08g18140D	26S proteasome non-ATPase regulatory subunit 11 homolog	1260	5	26	1319	2666	104	31.5
BnaC05g47720D	unknown	768	35	179	1315	2658	15	48.1
BnaA10g12520D	E3 ubiquitin-protein ligase RING1-like	1029	11	56	1302	2632	47	30.1
BnaA07g00390D	Shikimate O-hydroxycinnamoyltransferase	1302	117	599	1287	2602	4	54.5
BnaC09g15730D	unknown	417	52	266	1240	2507	9	71.8
BnaC09g73290D	NDR1/HIN1-Like protein 3	714	49	251	1215	2456	10	32
BnaC03g61170D	Heat shock 70 kDa protein 9, mitochondrial	2046	8	41	1210	2446	60	84

BnaA03g26530D	S-adenosylmethionine synthase	1098	35	179	1166	2357	13	30.1
BnaA01g26500D	Actin-8	1134	62	317	1104	2232	7	37.7
BnaC07g23740D	Pentatricopeptide repeat-containing protein At3g26630, chloroplastic	1359	44	225	1101	2226	10	34.2
BnaA07g06190D	UDP-glucuronate 4-epimerase 6	1362	130	665	1099	2222	3	32.5
BnaA09g13710D	Photosystem I chlorophyll a/b-binding protein 3-1, chloroplastic	816	86	440	1086	2195	5	35.2
BnaCnng39500D	SOBIR1	1926	18	92	1083	2189	24	33.5
BnaA02g10190D	Auxin-responsive protein SAUR32	387	8	41	1064	2151	53	39.3
BnaCnng19190D	L-type lectin-domain containing receptor kinase IV.4	1716	18	92	1063	2149	23	47.8
BnaCnng70090D	Phenolic glucoside malonyltransferase 1	1401	5	26	1052	2127	83	34.4
BnaA10g00410D	BPS1, chloroplastic	1053	95	486	1043	2108	4	31.3
BnaAnng33460D	Polyubiquitin	315	50	256	1040	2102	8	46
BnaA04g24870D	unknown	2367	65	333	1031	2084	6	34.9
BnaC03g32940D	S-adenosylmethionine decarboxylase proenzyme 3	1104	84	430	1022	2066	5	36.9
BnaC09g47020D	unknown	1428	36	184	1012	2046	11	31.9
BnaC03g26530D	unknown	1098	1	5	1005	2032	397	30.2
BnaA01g33660D	Glyceraldehyde-3-phosphate dehydrogenase, cytosolic	1026	1	5	999	2020	395	34.5
BnaA03g50170D	UDP-glucuronate 4-epimerase 1	1293	31	159	971	1963	12	36
BnaC05g12070D	Chlorophyll a-b binding protein CP24.10B, chloroplastic	777	117	599	966	1953	3	33.6
BnaC09g44830D	unknown	195	19	97	963	1947	20	46.5
BnaA09g51620D	NAC domain-containing protein 68	1278	4	20	958	1937	95	33.6
BnaAnng12060D	Probable mediator of RNA polymerase II transcription subunit 37e	432	2	10	946	1912	187	47.2
BnaA08g15870D	Heat shock 70 kDa protein 9, mitochondrial	2037	9	46	938	1896	41	55.5
BnaA05g37180D	unknown	777	26	133	936	1892	14	33
BnaC09g33600D	Temperature-induced lipocalin-1	558	4	20	921	1862	91	38.5
BnaC07g12870D	Probable galacturonosyltransferase-like 8	1149	33	169	888	1795	11	37.1
BnaA01g26070D	unknown	1320	39	200	817	1652	8	32.6
BnaA01g10750D	Reticuline oxidase-like protein	1707	36	184	812	1641	9	53.7
BnaC03g68420D	Tubulin alpha chain	1353	44	225	807	1631	7	34.9
BnaC06g37290D	3-hydroxy-3-methylglutaryl-coenzyme A reductase 1	1725	28	143	792	1601	11	43.1
BnaC03g13880D	Heat shock protein 90-3	438	11	56	773	1563	28	37.7
BnaA07g32810D	3-hydroxy-3-methylglutaryl-coenzyme A reductase 1	1731	24	123	742	1500	12	34.9
BnaA03g09920D	Temperature-induced lipocalin-1	564	2	10	728	1472	144	33.5
BnaA09g35490D	Putative serine/threonine-protein kinase-like protein CCR3	2376	8	41	728	1472	36	30.5

BnaC08g39050D	E3 ubiquitin-protein ligase RHAZA	504	72	368	721	1458	4	41.6
BnaA02g34980D	unknown	195	9	46	654	1322	29	41
BnaA06g40330D	Transcription factor MYC3	1350	21	107	650	1314	12	30.2
BnaA03g31400D	Transcription factor LUX	408	1	5	639	1292	252	40.8
BnaC08g08080D	Bifunctional purple acid phosphatase 26	1428	10	51	622	1257	25	119.1
BnaC08g14130D	Pentatricopeptide repeat-containing protein At1g10270	2466	6	31	599	1211	39	90.4
BnaA01g04620D	Probable sugar phosphate/phosphate translocator At4g32390	1056	15	77	596	1205	16	30.6
BnaA08g04620D	bZIP transcription factor 60	702	5	26	524	1059	41	47.6
BnaA09g29100D	Probable mediator of RNA polymerase II transcription subunit 37e	384	1	5	512	1035	202	30.1
BnaC01g06430D	unknown	630	37	189	455	920	5	123.4
BnaC07g43630D	unknown	543	17	87	375	758	9	79.2
BnaA02g01510D	GEM-like protein 5	819	7	36	349	706	20	30.7
BnaC08g22890D	Receptor-like protein kinase FERONIA	3531	12	61	349	706	11	166.8
BnaC05g11770D	Periodic tryptophan protein 2 homolog	2763	8	41	345	697	17	144.1
BnaA03g07990D	unknown	312	13	67	299	604	9	42.4
BnaC07g51300D	Tubulin-folding cofactor C	369	3	15	283	572	37	65.6
BnaA01g04890D	unknown	591	21	107	273	552	5	56.8
BnaA03g51870D	unknown	540	13	67	242	489	7	34.4
BnaA04g08510D	unknown	111	6	31	171	346	11	66.8
BnaA07g28470D	Glutathione S-transferase U11	705	1	5	158	319	62	38.8
BnaC06g26810D	unknown	369	19	97	138	279	3	33.8
BnaC03g60280D	Probable fructose-bisphosphate aldolase 2, chloroplastic	1152	321	1643	3705	7490	5	35.9
BnaC09g14730D	unknown	264	318	1627	2752	5563	3	706.3
BnaC02g01960D	ABC transporter G family member 22	2259	31	159	819	1656	10	64.8
BnaC07g36920D	GPN-loop GTPase 1	87	264	1351	1590	3214	2	427
BnaC07g00300D	Transcription activator GLK1	1341	94	481	945	1910	4	66.8

Table S21: PHAS loci that produce va-phasiRNAs in both Drakkar and Tanto

PHAS locus	Predicted gene function	transcript length	siRNA reads & rpm & ratio & PHAS Score										mRNA reads & FC(log2)					
			DM (reads, rpm)	DT (reads, rpm)	DT rpm / DM rpm	PHAS Score	TM (reads, rpm)	TT (reads, rpm)	TT rpm / TM rpm	PHAS Score	DT	TT						
BnaA01g14050D	NBR1 homolog	2109	91	570	83110	250229	439	210.5	135	691	114844	232160	336	377	2959	5.97	279	7.49
BnaC01g16550D	NBR1 homolog	2118	90	564	74021	222864	227.4	102	522	106357	215003	412	386.9	7201	7201	1.42	15409	0.96
BnaA04g20150D	Chlorophyll a-b binding protein 1, chloroplastic	804	460	2882	18293	55077	178.9	966	4944	15481	31295	6	224.5	1094135	1094135	-0.31	1114135	0.27
BnaA04g12130D	Probable fructose-bisphosphate aldolase 1, chloroplastic	1173	79	495	10287	30972	42.1	222	1136	6384	12905	11	47.8	94780	94780	-0.96	56836	-0.91
BnaAmng22920D	Chlorophyll a-b binding protein 1, chloroplastic	804	277	1736	10046	30247	164.2	500	2559	7981	16134	6	207.7	1104783	1104783	-0.36	569076	0.15
BnaC03g59520D	Chlorophyll a-b binding protein 1, chloroplastic	804	375	2350	9349	28148	98.7	720	3685	9663	19534	5	93.3	417531	417531	0.02	305188	0.73
BnaC04g33570D	Probable fructose-bisphosphate aldolase 1, chloroplastic	1173	79	495	8934	26899	47.6	201	1029	5199	10510	10	44.7	128831	128831	-0.68	56212	-0.96
BnaA02g05040D	unknown	753	206	1291	8803	26504	117	886	4534	13153	26589	6	155.9	9906	9906	-0.40	27852	1.49
BnaA05g29390D	Chlorophyll a-b binding protein CP29.2, chloroplastic	867	161	1009	8490	25562	100	304	1556	4033	8153	5	66.7	270995	270995	0.12	261389	-0.13
BnaA07g07560D	Chlorophyll a-b binding protein 1, chloroplastic	804	324	2030	8429	25378	86.5	532	2723	7018	14187	5	105.1	403662	403662	-0.74	229128	0.32
BnaA07g19610D	ABC transporter G family member 36	4173	108	677	7975	24011	61.6	261	1336	16033	32411	24	139.3	11558	11558	0.64	29843	-0.98
BnaA03g15830D	Chlorophyll a-b binding protein 1, chloroplastic	801	249	1560	7690	23153	75.4	417	2134	6117	12366	6	119.6	267044	267044	-0.34	199603	-0.18
BnaC03g18980D	Chlorophyll a-b binding protein 1, chloroplastic	801	253	1585	6797	20465	38.9	498	2549	7218	14591	6	94.3	384220	384220	-0.18	242674	0.08
BnaC05g10980D	RNA-dependent RNA polymerase 1	3282	45	282	6467	19471	74.9	131	670	15172	30671	46	219	192	192	1.68	2967	1.75
BnaA09g26570D	Chlorophyll a-b binding protein 1, chloroplastic	804	198	1241	6307	18989	61.1	483	2472	6184	12501	5	59.1	325731	325731	-0.25	212798	0.26
BnaA08g17660D	Chlorophyll a-b binding protein 1, chloroplastic	804	248	1554	6017	18116	64.9	628	3214	8176	16528	5	95.7	278219	278219	-0.23	317665	0.62
BnaC05g22880D	Chlorophyll a-b binding protein 1, chloroplastic	804	175	1097	5702	17168	52.1	416	2129	5639	11399	5	53.6	179754	179754	-0.12	117020	0.42
BnaC06g14450D	Probable pectate lyase 22	1611	661	4142	5481	16502	443.6	1054	5394	6333	12802	2	475.3	1	1	-0.21	0	-0.23
BnaAmng23670D	ATPase 2, plasma membrane-type	2757	51	320	5457	16430	45.2	119	609	6257	12649	21	49	8812	8812	0.86	15284	0.00
BnaC08g42250D	Zinc transporter 4, chloroplastic	1191	6	38	5248	15801	67.1	2	10	1464	2960	289	33.5	12455	12455	1.01	262	1.59
BnaC08g16670D	unknown	591	723	4530	4752	14307	934.2	994	5087	5301	10716	2	984.3	262	262	1.58	249	0.59
BnaA09g00390D	S-adenosylmethionine synthase	1098	29	182	4716	14199	120.1	51	261	2483	5019	19	71.1	10063	10063	1.39	9795	-0.35
BnaC07g39070D	NBR1 homolog	2076	12	75	4664	14042	42	18	92	7264	14684	159	93.6	2241	2241	1.36	5953	1.44
BnaC04g08360D	S-adenosylmethionine synthase 3	1122	34	213	4646	13988	83.5	60	307	1636	3307	11	42.1	20377	20377	0.26	14311	-0.36
BnaC04g10770D	Chlorophyll a-b binding protein 1, chloroplastic	990	503	3152	4644	13982	105.3	610	3122	3682	7443	2	85.2	425070	425070	-0.17	199007	0.94
BnaA02g22660D	Tubulin beta-4 chain	1341	30	188	4585	13805	97.4	47	241	4295	8682	36	107	15463	15463	0.76	15551	0.03
BnaC04g10780D	Chlorophyll a-b binding protein 1, chloroplastic	801	238	1491	4242	12772	69.8	398	2037	3885	7854	4	78	524035	524035	-0.12	299557	0.39
BnaC09g37170D	unknown	759	35	219	4176	12573	59.5	118	604	3020	6105	10	55.8	12900	12900	-0.53	12768	1.25
BnaC07g29410D	EIN3-binding F-box protein 2	1866	20	125	4169	12552	97.4	55	281	6858	13864	49	157	3690	3690	1.38	6255	-0.30
BnaC06g41790D	ARGONAUTE 2	3108	71	445	4024	12116	76.1	280	1433	49302	39019	27	273	515	515	1.62	275	1.68
BnaA06g37230D	Probable fructose-bisphosphate aldolase 2, chloroplastic	1182	109	683	3934	11845	30.2	251	1285	3276	6623	5	37.1	156206	156206	-0.63	136158	-0.82
BnaAmng14520D	Subtilisin-like protease SB.T1.7	2283	32	201	3924	11814	67.2	31	159	1422	2875	18	44.8	21663	21663	1.26	391	2.19

BnaC05g17000D	TolB		2121	14	88	3918	11796	134	71.4	37	189	1837	3714	20	53.4	4889	0.82	6470	0.96
BnaC03g60280D	Probable fructose-bisphosphate aldolase 2, chloroplastic		1152	131	821	3810	11471	14	43.2	321	1643	3705	7490	5	35.9	337891	-0.41	265827	-1.31
BnaA10g14810D	unknown		747	63	395	3708	11164	28	36.9	119	609	3238	6546	11	49.7	4259	-0.08	221	2.32
BnaA07g17260D	Putative calcium-transporting ATPase 11, plasma membrane-type		3078	15	94	3609	10866	116	75.4	19	97	3758	7597	78	85.2	1651	0.36	2516	-0.10
BnaC04g02010D	Probable mediator of RNA polymerase II transcription subunit 37e		783	22	138	3579	10776	78	110.4	36	184	6884	13916	76	173.9	7494	0.58	8197	0.02
BnaC04g37750D	EIN3-binding F-box protein 1		1800	88	551	3555	10703	19	92.2	131	670	5101	10312	15	98.9	5497	1.08	5577	0.50
BnaC02g31030D	Tubulin beta-1 chain		1338	21	132	3523	10607	81	42	42	215	3393	6859	32	66.6	11143	0.52	10691	-0.14
BnaA06g35940D	unknown		5187	14	88	3180	9574	109	62.7	15	77	3256	6582	86	69.8	85	0.27	135	0.96
BnaC03g05980D	Magnesium-chelatase subunit ChH, chloroplastic		4155	126	790	3124	9406	12	31	261	1336	4648	9396	7	37.7	6999	0.05	13921	-0.36
BnaA06g04440D	Elongation factor 4-alpha 4		1383	16	100	3119	9391	94	79.6	29	148	3617	7312	49	112.5	15039	0.36	20329	0.69
BnaC04g50850D	Phosphatidylinositol 4-kinase gamma 4		1470	10	63	3083	9282	148	63.8	31	159	3530	7136	45	78	1119	0.58	2158	0.05
BnaCmg64010D	ABC transporter G family member 36		2145	25	157	3070	9243	59	43.4	110	563	6938	14025	25	72.8	9022	0.35	19316	-1.24
BnaC01g21920D	Cysteine proteinase RD19a		1107	28	175	3045	9168	52	60.9	61	312	1932	3906	13	46.4	71963	0.57	107705	0.91
BnaC04g02020D	Probable mediator of RNA polymerase II transcription subunit 37e		723	12	75	2895	8716	116	79	27	138	4488	9073	66	83.5	2467	1.07	5877	-0.17
BnaA05g28710D	Cell division control protein 48 homolog E		2427	15	94	2862	8617	92	30.4	9	46	4276	8644	188	50.2	2722	1.41	4360	1.04
BnaC04g06560D	Ribulose biphosphate carboxylase/oxygenase activase, chloroplastic		1320	265	1661	2830	8521	5	75.3	641	3280	5436	10989	3	132.9	330879	0.04	528385	-0.83
BnaA03g10790D	Heat shock protein 90-4		1728	30	188	2762	8316	44	87.1	36	184	5314	10742	58	117.1	8390	0.61	9912	-0.36
BnaC07g15280D	Catalase-3		1479	105	658	2710	8159	12	40.1	246	1259	3846	7775	6	40.6	91411	0.90	169486	1.06
BnaA04g14890D	EIN3-binding F-box protein 1		1872	57	357	2597	7819	22	47.4	115	589	5744	11612	20	106.8	3940	0.48	6751	0.31
BnaA09g26890D	U-box domain-containing protein 17		2115	7	44	2588	7792	178	43.3	14	72	3653	7385	103	69.9	1984	-1.28	1588	-0.16
BnaAmg01730D	ABC transporter G family member 22		2157	20	125	2547	7669	61	30.8	52	266	2122	4290	16	43.4	224	1.96	15994	0.01
BnaAmg35580D	Glycine-rich RNA-binding protein GRP2A		507	149	934	2377	7157	8	38.2	255	1305	4601	9301	7	79.7	1087	1.91	313	2.15
BnaC07g21430D	NRT1/ PTR FAMILY 8.3		1758	11	69	2366	7124	103	45.6	14	72	3223	6515	91	39.5	293	1.61	6929	0.61
BnaC07g19250D	unknown		5082	17	107	2347	7066	66	44.7	34	174	7067	14286	82	149.3	77	0.91	156	1.66
BnaCmg29950D	TRANSPARENT TESTA GLABRA 1		717	4	25	2241	6747	269	42.6	9	46	2418	4888	106	40.7	1587	0.85	1823	1.48
BnaC03g03470D	Probable mediator of RNA polymerase II transcription subunit 37e		783	16	100	2198	6618	66	54.1	28	143	4143	8375	58	89	13013	0.10	7825	-0.55
BnaC06g38300D	Nitrate reductase [NADH], clone PBNBR1405		2685	211	1322	2185	6579	5	32.8	421	2155	2293	4635	2	35.2	24180	0.66	49284	-0.85
BnaC05g40290D	ABC transporter C family member 7		5214	21	132	2070	6232	47	40	64	328	1964	3970	12	40.2	10665	0.19	7900	-0.31
BnaC09g32520D	Transmembrane protein 245		1953	26	163	2053	6181	38	49.2	43	220	1993	4029	18	51.9	3386	0.29	3458	0.16
BnaC08g36330D	Transcription activator GLK1		3066	94	589	1950	5871	10	125.2	336	1720	2982	6028	4	96.8	12057	0.65	12947	0.47
BnaAmg04540D	Probable LRR receptor-like serine/threonine-protein kinase At4g08850		1626	3	19	1899	5718	304	50.4	4	20	1739	3515	172	62.9	1030	1.44	2189	0.49
BnaC01g38940D	Cell division control protein 48 homolog E		2433	8	50	1856	5588	111	33.1	11	56	3220	6509	116	71.3	192	1.85	3854	1.28
BnaC02g40260D	Elongation factor 2		2517	21	132	1853	5579	42	48.8	50	256	2776	5612	22	76.5	2593	1.15	5719	0.28
BnaA03g26530D	S-adenosylmethionine synthase		1098	22	138	1773	5338	39	38.5	35	179	1166	2357	13	30.1	2317	1.20	2959	-0.24
BnaA01g29630D	Subtilisin-like protease SBT1.4		2328	62	388	1766	5317	14	31.2	221	1131	1533	3099	3	37.2	7030	0.36	9424	0.33

BnaA09g56570D	Chlorophyll a-b binding protein CP24.108, chloroplastic	780	74	464	1694	5100	11	55.3	175	896	1415	2860	3	44.6	76392	-0.42	45146	0.80
BnaC04g20690D	Calcium-transporting ATPase 12, plasma membrane-type	3102	23	144	1664	5010	35	37.8	36	184	2022	4088	22	40.9	256	1.72	2154	1.84
BnaA03g00850D	Cell division control protein 48 homolog E	2397	5	31	1658	4992	159	31.1	10	51	2695	5448	106	60	648	3.73	1290	0.94
BnaA01g22310D	Probable nucleoredoxin 1	1737	94	589	1639	4935	8	38.1	46	235	1334	2697	11	48.1	1188	5.62	2130	1.49
BnaA09g04600D	EIN3-binding F-box protein 2	1851	16	100	1556	4685	47	34.8	53	271	1593	3220	12	39.9	224	2.07	7390	0.07
BnaAnng33970D	Elongation factor 2	1530	15	94	1542	4643	49	56.3	38	194	1946	3934	20	47.3	6638	0.65	8159	-0.02
BnaA07g07430D	unknown	744	174	1090	1522	4582	4	36.9	278	1423	1502	3036	2	39.2	35088	0.12	23165	0.00
BnaCmg38780D	Elongation factor 1- α 4	1287	21	132	1521	4579	35	31.4	31	159	2154	4354	27	77.8	8532	0.45	12216	0.02
BnaA09g05850D	Probable mediator of RNA polymerase II transcription subunit 37e	795	21	132	1480	4456	34	34.1	29	148	2941	5945	40	96.6	5815	0.34	7181	-0.29
BnaC09g14730D	unknown	264	215	1347	1480	4456	3	352.5	318	1627	2752	5563	3	706.3	116	0.44	71	0.58
BnaA03g49610D	Cytidine deaminase 1	873	72	451	1369	4122	9	31	155	793	3793	7668	10	84.1	1697	0.13	2609	0.38
BnaC03g13470D	Heat shock protein 90-2	1614	24	150	1351	4068	27	31.7	20	102	3069	6204	61	85.7	2550	0.61	5285	0.39
BnaC02g01960D	ABC transporter G family member 22	2259	13	81	1341	4038	50	169.7	31	159	819	1656	10	64.8	4529	0.29	8863	-0.66
BnaAnng09960D	Tubulin beta-4 chain	1338	12	75	1307	3935	52	30.3	33	169	1623	3281	19	43.5	5538	0.80	7420	-0.26
BnaA09g76150D	unknown	699	11	69	1302	3920	57	41.9	12	61	2564	5183	84	48.8	216	1.95	780	2.22
BnaC03g76150D	Elongation factor 2	1200	21	132	1243	3742	28	30.3	35	179	1562	3158	18	42.8	4213	1.22	6895	0.13
BnaC07g23740D	Pentatricopeptide repeat-containing protein At3g26630, chloroplastic	1359	21	132	1089	3279	25	43.4	44	225	1101	2226	10	34.2	3016	0.03	2363	0.03
BnaC03g51090D	Probable inactive purple acid phosphatase 29	1272	5	31	945	2845	91	47.8	17	87	1919	3879	45	51.2	12544	-0.18	18233	-1.17
BnaC04g30870D	Ribulose biphosphate carboxylase small chain F1, chloroplastic	546	174	1090	940	2830	3	35.9	309	1581	2452	4957	3	62.3	827514	-1.02	394604	-0.74
BnaA08g25040D	Aspartic proteinase A1	1581	15	94	872	2625	28	58.2	37	189	1412	2854	15	60.7	28771	0.81	39528	0.65
BnaC04g44100D	DEAD-box ATP-dependent RNA helicase 21	1773	12	75	858	2583	34	33.4	17	87	1561	3156	36	49.6	662	1.07	1189	0.59
BnaA01g26070D	unknown	1320	18	113	822	2475	22	33.9	39	200	817	1652	8	32.6	1459	0.85	1384	0.70
BnaC07g36920D	GPN-loop GTPase 1	87	71	445	809	2436	5	310.5	264	1351	1590	3214	2	427	117	0.46	49	0.23
BnaA07g00390D	Shikimate O-hydroxycinnamoyltransferase	1302	30	188	798	2403	13	49.1	117	599	1287	2602	4	54.5	2532	-0.07	2504	-1.07
BnaC06g37290D	3-hydroxy-3-methylglutaryl-coenzyme A reductase 1	1725	18	113	656	1975	18	62.5	28	143	792	1601	11	43.1	4082	0.69	4820	-0.37
BnaA07g22810D	3-hydroxy-3-methylglutaryl-coenzyme A reductase 1	1731	16	100	624	1879	19	64.7	24	123	742	1500	12	34.9	5438	0.30	6236	-0.64
BnaC09g15730D	unknown	417	45	282	529	1593	6	33.1	52	266	1240	2507	9	71.8	3367	1.05	2684	0.55
BnaC07g00300D	Transcription activator G1K1	1341	37	232	437	1316	6	40.1	94	481	945	1910	4	66.8	3752	-0.49	3161	1.05
BnaC08g14130D	Pentatricopeptide repeat-containing protein At1g10270	2466	5	31	283	852	27	60.5	6	31	599	1211	39	90.4	132	0.87	236	0.80
BnaC01g06430D	unknown	630	20	125	150	452	4	64.6	37	189	455	920	5	123.4	18010	-0.27	17667	0.15
BnaC07g43630D	unknown	543	15	94	102	307	3	33	17	87	375	758	9	79.2	30948	-0.95	16634	0.02

Table S23: va-phasiRNAs derived from Chlorophyll a-b binding protein 1 genes and associated with mRNA target cleavage

		Normalised reads					Normalised reads					Normalised reads					
va-phasiRNA	dsRNA strand	DM	DT	TM	TT	va-phasiRNA	dsRNA strand	DM	DT	TM	TT	va-phasiRNA	dsRNA strand	DM	DT	TM	TT
TGAAGATCTGTGAACGAGCT	+	20.96	133.72	46.38	88.70	TTCTGGGTGCGTAGCGAGGCC	+	9.09	79.41	19.57	51.47	ACAATGGCTTGAACAAAGAAT	-	7.91	20.02	9.43	14.35
TAAAGTCTCTGAGGTGGACC	+	11.46	136.08	26.68	108.25	GTGGACCAAGCTCGGGTTGCC	+	0.52	57.53	0.80	37.80	GTGGACCAAGCTCGGGTTGCC	-	1.71	27.01	1.23	18.63
CTGAAGATCTGTAACAGCC	+	1.15	72.60	5.34	49.11	AAATGGTGGGAGATTCTCC	+	1.77	42.17	0.00	36.11	TCTGGGAAACCGCCTTGAACC	-	6.20	18.94	23.54	29.15
AAATGGACCAAGTACTTGACT	+	18.37	72.33	46.63	46.52	TCTGGAAACCGCCTTGAACC	+	3.72	37.53	12.61	58.49	CCATGGGCTGCTGATGGGCC	-	0.90	22.99	1.42	17.98
AAAGTCTCTGAGCGTGGACC	+	3.08	178.85	16.77	127.30	TCTGTGAACAGCCTTGAACC	+	41.17	299.14	97.17	243.71	GAGCCGAGGACTTGCCTTACC	-	4.41	7.52	15.01	15.56
AAATGGACCTAAGTACTTGACT	+	1.68	67.65	9.91	28.85	TCCGAGAGATCAAGTACTTG	+	25.80	74.67	23.30	45.23	CGAACCGCCTTGAACCAACC	-	0.90	18.48	1.42	31.28
CTTCAAGGACTTCTGATGCT	+	81.76	197.98	223.18	147.39	CCATGGCTGCTGATGGGCC	+	0.89	46.54	0.81	36.31	ATGAGGATCACTGAGTAGCC	-	3.55	23.32	7.18	20.89
CGGCCTTGAACCAACCGCCT	+	24.72	45.46	58.66	45.77	CCGAGGACTTGCCTTACCAG	+	14.02	40.90	45.03	54.25	CGTGACCAAGCTCGGGTTGCC	-	0.00	16.65	0.00	25.11
TGAACCAAGCTTGAACCAAC	+	2.57	45.15	7.88	49.07	GAGCCGAGGACTTGCCTTACC	+	1.94	15.69	5.85	31.33	TCTCGGGATCGGCTGAGAGACC	-	3.55	16.27	0.00	24.58
ATGGACCAAGTACTTGACC	+	13.18	44.55	29.91	43.27	CGAACCGCCTTGAACCAACC	+	0.89	38.54	0.81	63.34	TGAACAAAGAATCCAAACATA	-	2.69	12.21	3.89	16.26
TTGGCTGAAGATCTGCGAACC	+	3.44	34.66	9.38	45.70	ATGAGGATCACTGAGTAGCC	+	1.68	47.44	3.91	42.09	AGAAGAAACGTTCTAATGGCT	-	4.36	12.13	27.25	16.82
TGAACCAAGCTTGAACCAAGG	+	0.00	48.61	1.61	32.52	CGTGGACCAAGCTCGGGTTGCC	+	0.00	35.21	0.00	50.90	AAGAAGAAACGTTCTAATGGCC	-	2.56	23.17	49.29	22.53
AAATGGCTAAGATGCTTGACC	+	1.68	34.77	0.00	35.24	TCTCGGGATCGGCTGAGAGACC	+	1.68	33.98	0.00	49.84	AGGCCGAGGACTTGCCTTACC	-	4.31	16.91	30.62	15.44
CCGGCTTGAACCAACCGCC	+	1.15	47.94	5.54	66.69	TGAACAAAGAATCCAAACATA	+	2.66	23.48	2.41	32.46						
TGAACCAAGCTTGAACCAACC	+	0.89	40.02	7.92	39.29	CTGAAGATCTGTGAACCAAGCT	+	1.67	25.03	0.00	50.89						
TTGGCTGAAGATCTGTAACC	+	17.41	302.45	36.62	219.25	AGCCGAGGACTTGCCTTACC	+	1.93	33.99	12.61	30.98						
GGAAGCGCAGCCTAGGGCTC	+	0.52	38.54	3.93	42.68	TAAGATCTCTGAGCGTGGACC	-	23.65	68.26	49.99	53.79						
ATCTGTAAACCAAGCCTTGAAC	+	0.00	63.13	7.15	43.34	AATGGACCAAGTACTTGACT	-	34.34	34.76	93.41	22.97						
ATCTGTAAACCAAGCCTTGAACC	+	8.28	38.44	30.33	53.02	AAGATGCTCTGAGCGTGGACC	-	6.07	91.12	29.83	63.38						
AAGGTAGCTCGGTGGCTCGCC	+	0.26	45.84	5.58	27.97	AATGGACCTAAGTACTTGACT	-	3.55	32.73	21.93	14.26						
CCTAGGGCTCGAGCATGGCC	+	3.09	50.71	4.46	37.55	AAGATGCTCTGAGCGTGAACC	-	0.85	24.10	2.66	16.12						
ACTCAGGTGATCCTCATGGGA	+	1.04	37.07	11.27	33.62	TTGGCTGAAGATCTGCGAACC	-	5.25	17.98	18.23	22.86						
TTCTGGGTGGTAGCGAGACC	+	19.16	75.82	64.40	84.07	AATGGCTAAGATGCTCTGAGC	-	3.55	17.93	0.00	17.51						
CCTCGCTGAAGATCTGTAA	+	0.00	59.00	0.00	31.14	CCGGCCTTGAACCAACCGCC	-	1.75	22.81	10.03	32.90						
TCTGTAGCCAGCCTTGAACC	+	7.93	33.66	9.69	25.51	GGAAGCGCAGCCTTAGGGCTC	-	1.71	19.33	7.37	21.16						
CTAGGGCTCGAGCATGGCCC	+	1.41	54.60	3.91	41.28	AAGGTAGCTCGGTGGCTCGCC	-	0.85	22.99	10.41	13.88						
GTCGGGAGATTCTCAACGG	+	1.77	31.41	3.99	26.54	CCTAGGGCTCGGAGCATGGCC	-	6.16	25.34	11.08	18.64						
ATGGTGGCGAGATTCTCAA	+	9.18	55.51	20.22	29.70	ACTCAGGTGATCCTCATGGGA	-	3.42	19.43	18.41	16.85						
ACAATGGCTTGAACAAAGAAT	+	4.24	40.76	4.64	29.02	CTAGGGCTCGGAGCATGGCCC	-	2.61	27.16	7.18	20.50						

Table S24: va-phasiRNAs derived from TAR1 genes and associated with mRNA target cleavage

va-phasiRNA		Normalised reads				Normalised reads				Normalised reads				
dsRNA strand	DM	DT	TM	TT	dsRNA strand	DM	DT	TM	TT	dsRNA strand	DM	DT	TM	TT
CGAGCTAAGGACGTCAGAGGAGCG	#N/A	#N/A	28.61	63.94	+	7.93	37.07	9.47	60.64	+	76.06	128.34	134.24	250.33
CCCCATCTCGAGGATATG	1.41	105.00	6.22	132.85	+	23.46	95.40	122.66	166.83	+	74.43	124.57	136.07	260.72
CATCTCTCGAGGATATGGGAC	1.41	65.82	6.96	261.61	+	11.88	45.74	20.56	90.87	+	96.30	160.73	598.68	538.61
GTTGGCCAAATCCGAGCTAA	1.93	90.11	3.24	33.75	+	53.33	197.69	146.20	378.64	+	16.81	27.95	50.20	52.33
TGTTTACCGCAGGGTGGG	9.35	297.89	32.46	563.56	+	19.59	70.58	23.71	101.14	+	63.63	102.89	115.62	225.72
TCCAGCTAAGAACGTCAGAA	5.64	174.13	0.00	0.67	+	17.03	60.41	40.25	103.44	+	38.38	61.22	44.84	145.48
TGGAGATATGGACGGAAGC	43.26	1122.33	111.30	928.51	+	12.69	45.00	122.06	75.33	+	114.78	180.52	373.41	479.41
CCAGCGGTTGGCCAAATC	8.11	194.14	5.31	102.73	+	99.10	341.97	277.03	668.17	+	9.95	15.47	44.67	30.00
TGGAGATATGGACGGAAGCT	28.59	542.56	44.06	384.72	+	15.20	50.45	20.51	28.58	+	23.01	34.98	59.69	41.18
GAACGTGAGGAGCTCTTGACA	3.09	54.08	0.00	0.25	+	365.18	1204.80	1283.32	2941.70	+	48.72	72.47	95.81	127.91
GTTCCACCTTGGCCGAGG	18.42	311.96	69.83	615.48	+	16.64	52.81	33.77	88.65	+	92.95	137.53	249.60	236.34
ATGGACGGAAGCTGATCTCC	44.51	721.86	77.21	419.08	+	38.29	112.07	61.04	195.35	+	17.40	25.67	27.59	60.16
GTCTCGACGTCGAGAAATC	177.74	2794.55	301.43	7106.17	+	109.87	319.01	216.40	447.47	+	50.71	74.37	134.66	178.54
TAAGAACTCAGGAGCGTCT	4.44	56.99	0.00	0.40	+	22.65	64.99	48.32	119.78	+	10.09	14.69	31.56	26.99
GTTGGCCAAATCCGAGCT	2.04	24.42	6.45	13.01	+	15.51	43.45	32.48	63.72	+	130.62	185.41	284.46	587.28
TGTTTACCGCAGCGGTTGGCC	10.78	120.29	7.65	112.79	+	21.08	57.98	96.27	105.81	+	38.73	54.85	109.75	77.18
GTCTCGACGTCGAGAAATC	101.30	1128.77	181.66	1889.19	+	955.47	2530.07	3144.52	3516.77	+	14.19	19.90	50.70	45.29
TGTTTCAAGAGTTCAACC	35.11	379.00	77.07	643.71	+	120.84	301.33	152.25	252.46	+	54.98	76.67	279.65	156.88
GTTTCCGTCGAGCGTCCG	29.87	302.31	74.39	413.97	+	25.95	64.56	48.99	55.05	+	59.62	79.40	155.58	204.14
TATGGGACGGAAGCTGATCTCC	37.80	377.74	93.06	415.63	+	830.30	1959.98	2077.74	3318.76	+	25.54	33.74	81.52	75.29
GAACGACCTGAGAACGATGAA	14.30	132.60	113.19	241.21	+	44.54	104.68	119.79	220.04	+	464.02	597.62	1711.42	900.63
AGGATATGGACGGAAGCTGA	59.45	517.07	105.38	247.38	+	17.62	39.44	49.46	74.32	+	40.25	51.83	163.42	151.43
CGCGGTTGGCCAAATCCGAG	10.50	90.11	27.48	56.01	+	21.24	47.42	36.61	108.15	+	38.14	45.73	93.98	83.38
AGCTGATCCCGTGTGTTAC	18.44	154.03	50.81	109.28	+	39.22	85.38	102.58	130.26	+	45.58	54.35	104.25	142.83
CGGAACTCGAAAGGGGATC	107.19	863.03	259.07	2036.74	+	12.79	27.32	18.88	67.41	+	253.07	296.40	613.72	498.18
AGGCCCTGATGATAGGAGGG	13.90	106.85	50.09	229.85	+	151.29	318.14	405.04	555.55	+	228.08	255.20	771.91	533.14
AGCTGATCCCGTGTGTTAC	31.33	238.62	49.87	126.22	+	40.26	81.04	92.73	101.54	+	29.79	32.74	75.04	64.03
CTAAGAACGTCAGGAGCGTCT	74.08	532.19	0.00	0.88	+	130.02	259.46	407.50	566.27	+	108.00	117.16	151.96	304.33
GCCGAAAGGGGAAAGGTTCC	11.17	79.65	38.65	149.09	+	65.80	129.54	125.25	169.79	+	1236.13	1339.37	2708.65	2249.48
GATCCCGTGTGTTACCGCA	28.71	186.86	44.09	119.75	+	19.86	38.79	41.58	129.90	+	29.10	31.37	77.89	128.69
AGGAGGCTTGTACATGCGGT	18.02	92.36	139.92	67.53	+	80.35	153.36	229.65	270.06	+	82.26	88.01	155.41	179.30
GCGGCTCGCTGCAAACTAGG	29.72	152.11	63.89	287.58	+	38.83	72.55	104.51	182.04	+	73.01	77.99	163.72	124.07
GTTGGCCAAATCCGAGCTAAG	6.37	31.77	4.02	35.32	+	67.80	122.62	163.65	221.13	+	85.30	90.44	175.86	215.73
TGGCCGTTTAGGCCAAGGAA	31.56	157.36	128.60	450.85	+	75.35	135.48	141.44	335.15	+	74.64	78.81	197.83	155.07
TATGGGACGGAAGCTGATCTC	119.99	563.81	182.12	368.24	+	289.94	497.11	1953.41	384.34	+	18.51	19.51	53.80	39.41

dsRNA strand		Normalised reads				dsRNA strand		Normalised reads				dsRNA strand		Normalised reads			
va-phasirRNA	+	DM	DT	TM	TT	va-phasirRNA	-	DM	DT	TM	TT	dsRNA strand	-	DM	DT	TM	TT
TGTTGAGCCATCCACGGGAATC	+	19.17	20.14	27.45	36.82	TAGTCGGATTTTGGCCAACC	-	13.93	255.39	76.00	163.78	ACCAAGATCGCACCGACGGC	-	17.58	123.69	38.09	209.00
ACTTCGAAAGGGGATCCGGTT	+	26.97	28.31	78.82	65.73	CCACCAAGATCTGACCCGACG	-	4.36	79.19	5.35	115.18	TTTGTAGAAATAGGTCGAGGACA	-	203.27	1363.51	538.52	2860.41
GCTGAAGCGCGGACCTATACC	+	42.50	44.19	147.43	141.61	AGATCTGCACCGAGCGCGCT	-	0.85	15.22	3.48	33.56	TACTCATCGAGCTGGCTCT	-	13.20	88.31	35.05	355.83
AAATGAAACTTTGAAGCCGGAAT	+	103.76	106.61	157.43	81.45	TATCCCTCTAAGAAGCCGCGCC	-	1.75	29.80	10.03	119.14	AGCAGCGAGATCCGAGGAC	-	0.00	6.51	4.08	14.09
TTAAGGTGGTGAAGAAAGCCG	+	13.32	13.45	31.21	35.31	AGAAAGCCGCGTGAAGGATG	-	1.80	30.06	27.28	53.97	GTCCCTCTAAGAAGCCGCGCG	-	6.20	40.25	13.09	105.07
TCCTAAGATCGGGGAAACC	+	297.22	291.49	406.86	528.42	AAGATCTGCACCGAGCGCGCT	-	0.90	14.86	1.23	44.97	TAATCGAACACACCCCTTTGT	-	1.80	11.34	6.14	17.68
AAAGATCGGGGAAACCCGTC	+	115.43	110.68	232.08	246.67	TGAGAAATAGTCTGAGGACATTTG	-	0.90	14.50	0.00	43.83	AAAGTTTGAAGATAGGTGCGAG	-	8.63	53.52	63.69	75.79
AAACCAAGGGGTGTTGGTC	+	813.37	739.76	1886.74	1963.55	TTGGCTTTACCCGATAGAATCT	-	4.31	66.36	9.24	217.09	AACCCGACTGTAGACAGCGC	-	14.23	78.93	102.12	105.59
CGGCCGTGGTGCAGACTTTGG	+	871.20	764.03	1259.97	1756.44	TCGACCAACCCCTTTGTGG	-	3.46	52.42	26.46	89.84	ACCCGACTGTAGACAGCGC	-	10.47	56.44	56.17	124.16
TAAAGCAATGATTAGAGCA	+	28.49	23.41	30.16	41.57	ACCACAAGATCTGCACCGACG	-	0.00	15.07	0.00	71.22	TAGGTTAGCGCGAGTTGGGCA	-	0.90	4.72	1.42	23.80
CAATGCTCCGACTTATTCTCA	+	39.41	28.06	84.22	88.50	AACTCTCTTGGCTAAAGCGCC	-	1.71	25.61	2.66	162.61	GAGACGGCGGAAACCCACG	-	9.53	47.34	4.08	80.94
GGTAAGCAGAACTGGCGATGC	+	39.95	27.14	61.99	68.14	GACTCTCGCAGCTGCAGAC	-	4.27	63.16	13.74	109.62	CAAAGATCTGCACCGACGGC	-	22.02	105.38	32.79	154.52
ATTAGGCGTCCGGAGCGCAA	+	29.99	19.33	36.02	59.45	ACACTCCGCTGTAGACAGCT	-	0.00	14.24	33.42	97.82	ATCCGTTGGATGGCTCAACAA	-	0.00	4.70	2.47	33.52
GCTAAGGACGTCAGGAGCGTTC	+	0.00	0.31	36.10	497.05	GTAACAAGGGGAGATAGCT	-	3.50	47.28	8.79	35.72	TGTCGGCAAGGTGTGAATCT	-	32.29	149.93	148.96	290.43
AGCTAAGGAGCTCAGGAGCGTC	+	0.00	0.13	39.44	662.83	CAACGGAGCTGATGACTCGA	-	0.90	12.10	12.72	26.69	ACTCATCGAGCTGGCTCTT	-	4.40	20.17	13.73	31.60
TGCTCCGTTCCGCAITTCGACC	-	#N/A	#N/A	44.07	58.66	ACTTCGGAGGAAACAGCTACT	-	0.90	11.26	6.18	24.51	TAGCTCGGATTTGGCCAACCG	-	4.41	19.97	33.01	20.37
CGTCTTAGCTGGGATTTGGC	-	#N/A	#N/A	121.64	188.13	TGAGAAATAGTCTGAGGACATT	-	5.30	64.62	14.18	90.52	TTTAAAAGTTTGAGAAATAGTCT	-	16.77	72.02	27.29	124.88
GAATAGTCTGAGGACATTGGG	-	0.85	55.66	3.48	105.77	GTCGGCTGTGCACCCGTGAGG	-	1.71	20.77	1.42	49.47	CTTAGGATCGACTAACCATG	-	8.71	37.09	34.06	52.79
CTCATGAGGCTGGCTCTTGG	-	1.71	83.91	4.90	143.58	ACCAAGATCTGCACCGACGGCC	-	1.75	21.24	2.66	71.73	GTCGAGAGCGGAAACCCCA	-	28.57	118.70	47.63	205.21
GACTTTAGGATCGACTAAC	-	0.85	38.20	16.17	67.47	TAAGGTTGCCCTCAACCGCA	-	0.00	11.46	12.09	26.52	TATTTAAAAGTTTGAGAAATAGG	-	8.80	36.47	17.84	24.79
AGAATAGTCTGAGGACATTGG	-	0.00	31.04	15.75	50.98	CACCAAGATCTGCACCGACGGC	-	2.61	29.45	15.19	131.87	AGATAAAGTTTTCGGGAATTC	-	1.80	7.27	16.76	16.88
GTCTGCTGTTTAATCGACC	-	0.00	30.35	16.42	87.19	CCTCTAATCAATGGCTTACC	-	1.80	20.05	1.23	36.26	GCCCTAGGTTTTGACGACCC	-	2.61	9.92	2.66	24.18
GTGTGAACCTGTTGAATAGTC	-	0.00	28.28	2.85	109.43	GAGAAATAGTTCGAGGACATTGC	-	6.20	68.62	11.04	358.72	TCAAGGTCGGTCCGCTGTGCA	-	3.46	13.07	12.09	28.36
CTCATGAGGCTGGCTCTTGG	-	4.27	120.42	77.86	237.77	CGACTCTAGGATCGACTAAC	-	9.70	106.91	27.24	232.10	GATCAGCTCCGTCACCATATC	-	6.07	21.39	8.16	13.25
ACTTCTTGGCCTAAAGGGC	-	0.00	27.11	1.42	106.78	TTAGCGCGAGTTGGGACCGC	-	5.35	58.26	11.87	135.48	TACTCATCGAGCTGGCTCTT	-	15.90	52.44	35.10	189.02
AGAATAGTCTGAGGACATTGG	-	0.00	849.78	61.44	2765.49	CATCGAGGCTGGCTTTGCC	-	10.51	110.09	31.36	144.62	ATAGAACTGTTCCGAGCTC	-	48.88	160.72	160.84	277.69
CGACGTCGACAGCGGCAACC	-	0.00	26.30	0.00	38.80	GAGCTCTGACGTTCTTAGC	-	1.75	18.31	#N/A	#N/A	TAGACAGCGCTCGTGGTGGCA	-	0.85	2.64	3.70	14.08
CTGTCTTAATCGAACCAACC	-	0.00	25.25	35.81	23.33	GAAGATCAAGGTCGGTGGCTG	-	0.00	9.38	0.00	28.61	TAAAGTTTGAGAAATAGTCTG	-	11.32	34.87	18.63	38.80
GCATCTCAAGACGCTCTGAGG	-	0.85	18.78	3.48	37.68	ACCCGATAGAAGCTGTTCCG	-	1.80	15.70	24.85	22.98	AAACAACCGGACTGTAGACA	-	3.50	10.58	30.53	25.16
GGTATAGGTCGGGCTTCCAGC	-	0.90	19.60	14.78	53.66	CGGTCCCGGAATTTAAACCGGA	-	0.85	7.22	0.00	25.46	TAAATCGAACCAACCCCTTTG	-	3.55	10.61	4.08	20.18
CCGTGGGATGGCTCAAAAGC	-	1.80	38.19	0.00	0.12	GAGCTCTGATTTCCGTTGGATG	-	0.00	8.18	2.06	28.99	TTGAGAAATAGTTCGAGGACATT	-	10.47	30.82	14.37	92.73
TCTTAGCTGGATTTTGGCCA	-	0.85	17.89	2.66	53.35	GTCCGCAAGGTTGAATCTG	-	6.92	52.47	4.08	91.32	AATAGTTCGAGGACATTGGT	-	5.34	15.67	24.55	40.98
ACTCATGAGCCCTGGCTCTTG	-	4.45	87.04	5.69	123.35	ATTGCCCAACTTCTTTGGCC	-	4.40	32.88	74.00	119.08	TCCGTCACATATCTCGAGAGG	-	13.16	37.29	20.43	36.11
GAGAATAGTTCGAGGACATTG	-	0.85	16.10	1.23	30.11	TAGGTTAGCGCGCAGTTGGCC	-	0.00	7.41	4.27	21.52	AGCTCGGATTTTGGCCAACCG	-	52.80	148.67	378.81	63.63

dsRNA strand		Normalised reads				dsRNA strand		Normalised reads			
va-phasiRNA	dsRNA strand	DM	DT	TM	TT	va-phasiRNA	dsRNA strand	DM	DT	TM	TT
ACTCTTAGGATCGACTAACCC	-	6.07	16.29	26.01	20.45	TCTCGGACGTCCGACAGCGGG	-	306.51	451.31	1402.23	1422.22
CCCCAATCGATCGGGGACC	-	25.40	67.54	47.53	195.45	AAAATGCCCACTGGAGCTCT	-	4.45	6.53	0.00	25.41
TGGCGCCTAGTTTTGCGAGG	-	0.90	2.35	1.23	15.53	TCTAATCAATGGCTTACCCGA	-	2.61	3.73	14.77	32.25
CTACCTATTAAGTTTGAGA	-	8.85	23.08	11.04	36.70	TTCTAGCTGGATTTGGCC	-	203.59	289.71	2.85	1.60
TTTTGGGTTCTAGATTAGCG	-	6.25	16.23	5.35	19.64	ATCGAGGCTGGCTTTGGCCC	-	57.01	79.21	214.29	161.12
GTTCTAGCTCGATTTTGGCC	-	20.19	49.70	0.00	0.06	ATTGCCCAAACCTCTTGGCC	-	62.22	86.00	382.64	140.59
GTCCGAGACATTGGTCCCCGA	-	0.00	2.46	1.42	21.25	TTGCCCTCAAACTCTCTGGCCT	-	14.87	20.28	75.69	83.48
CTTTGAAAGTTCCGCGATAAG	-	14.15	33.08	26.30	55.27	CAGGCCATCAATTTCCGGGGC	-	3.46	4.69	12.50	24.52
TGAACCTGTTGAATACATAG	-	77.13	171.22	229.34	411.16	GAGATCACTCCGTCACATA	-	23.90	32.30	32.58	22.82
CGCTCTGAGTTCTTAGCTC	-	48.70	101.28	0.00	0.48	TACCCGATAGAACTGTTTCC	-	46.92	62.92	49.09	102.58
TTTTCGAAGTTCCGCGATAAG	-	28.22	58.56	131.51	111.70	TTTGAAGATAGTCCGAGCAT	-	4.41	5.81	2.66	27.40
CACCAAGTCTGACCGACGG	-	126.72	262.92	283.96	459.48	TAGTCGGATTTGGCAAACCCG	-	20.42	26.86	83.91	39.74
TCCTACTCATAGGCGCTGGC	-	6.20	12.83	9.01	29.82	TGTCGGCAAGTGTGAATCG	-	30.41	37.07	133.79	108.00
ACAACCCGACTGTAAGACAG	-	29.34	60.34	151.21	135.51	TCAGGCCATCAATTTCCGGGG	-	4.45	5.39	8.20	41.24
CGCGACGTCCGACAGCGCG	-	47.38	95.44	350.64	151.98	CAACCCGACTGTAGACGCA	-	7.90	9.54	56.28	20.80
TTTTAGTGACTCTCGGACT	-	29.02	57.90	73.90	60.37	CCGTTCCGGAAATTTAACCG	-	19.50	23.29	53.55	45.95
TCAGGCCATCCATTTCCGGG	-	15.92	31.73	50.07	48.38	CTTAGCTCGGAATTTGGCCAAC	-	15.77	18.63	120.87	26.98
CGCCCCGAAATCGATCGCGGA	-	28.94	56.58	34.73	147.85	ATTTTCAAAGGGCCCGGGAA	-	16.68	19.48	47.60	24.65
CGATAGAACTGTTCCGAGC	-	71.55	136.47	44.75	238.06	TCGATCGGCGACCGATTGC	-	13.22	15.32	9.01	23.56
CGTCCCATATCTCGAGAGGA	-	172.94	326.00	311.97	170.30	TTAGCTCGGATTTGGCCAACC	-	175.30	202.64	366.78	173.10
CGCATGTCAAGAGGCTCCT	-	6.02	10.90	622.23	22.79	TCTAATCAATGGCTTTACCCG	-	8.80	9.99	6.36	23.51
GTCCCATATCTCGAGAGGATG	-	151.56	274.16	284.93	270.58	ATCGATCGGCGGACCGGATTG	-	14.16	15.28	43.14	32.82
CAACCCGACTCTAGACAGCGC	-	18.38	32.64	75.89	103.29	ATTCGTTGGGATGGCTCAACA	-	43.20	44.37	171.08	62.96
AGGCTCTGACGTTCTTAGCT	-	10.51	18.57	0.00	0.12	CCAAGGTGAACTCGTTGAA	-	81.80	82.59	215.93	175.72
ATCTGACCGACGGCGGCTCC	-	4.36	7.22	0.00	18.55	CCGAATCGATCGGCGGACCGGA	-	51.11	48.82	88.62	213.26
CCTACTACTCGAGGCTTGCTC	-	6.20	10.18	20.50	28.76	CCACCAAGATCTGACCCGACGG	-	34.10	23.72	82.59	103.97
CGGATAGAACTCGTTCCGAG	-	6.16	10.09	3.70	48.21	GCGGACCGGATGCTCCGTTTC	-	134.30	88.02	64.08	173.69
AACCCGACTCTAGACAGGGCC	-	3.50	5.68	11.53	370.66	AACAACCCGACTCTAGACAG	-	20.28	12.59	33.00	35.37
AGCTCGGATTTGGCCAACCGC	-	46.60	75.27	379.96	39.84	CGGTCCGTGGCTGAGGAGCT	-	36.12	17.95	45.24	48.94
CTCAAACTCTCTGGCCCTAA	-	18.42	29.66	26.60	49.83	ACCCGACTGTAGACAGCGCT	-	9.58	4.27	28.93	29.64
TTGGTCCGTTGTACAAGACA	-	3.42	5.42	13.06	30.96	CCCGGCTTAGGTCAACACT	-	58.29	25.16	43.78	49.41
CTGAGGAGGCTCTCCAGACT	-	19.40	29.77	49.58	45.93	CGTAGACAGCGCTCGTGGTGC	-	8.63	2.33	14.74	29.31
TGAACTGTTGAATACATCAGT	-	90.74	136.42	503.35	395.98	TCAAGAGCTCTGACGCTCT	-	0.00	0.15	20.88	23.56
CAGTTGGCACCGTAACCCGG	-	34.13	50.77	48.64	103.11						

Table S25: va-phasiRNAs produced from genes encoding Chlorophyll a-b binding protein 1' and targeting mRNAs within the gene family for cleavage

va-phasiRNA		va-phasiRNA ¹										Host mRNA targets ²										DE target mRNA ³			
va-phasiRNA	dsRNA (+) / (-) strand va-phasiRNA	Origin (gene family)	Normalized reads (positive / negative)					Fragment signatures (pm)					Cleavage found in PAR-seq replicates					mRNA reads & r ² (log2)							
			DM	DT	DT/DM reads	TM	TT	TT/TT reads	DM	DT	TM	TT	DM	DT	TM	TT	DM	DT	TM	TT					
TGAAGATCTGTGACCAAGCCCT	+	Chloro ⁶	20.96 / -	133.72 / -	6.38 / -	46.38 / -	88.70 / -	1.91 / -	BhaC03g595200	CABBP1	519	TGAAGATCTGTGACCAAGCCCT					0.00	25.42	0.00	44.55	417531	0.02	305188	0.73	
TAAGATCTCTGAGCGTGGACC	+ / -	Chloro	11.46 / 23.65	136.08 / 68.26	11.87 / 2.89	26.68 / 49.99	108.25 / 153.79	4.06 / 1.08	BhaC04g107800	CABBP1	465	TAAAGATCTGTGACCGTGGACC					0.00	16.13	0.00	32.99	524095	-0.12	299557	0.39	
TGAAGATCTGTGACCAAGCCCT	+	Chloro	20.96 / -	133.72 / -	6.38 / -	46.38 / -	88.70 / -	1.91 / -	BhaC04g107800	CABBP1	406	TGAAGATCTGTGACCAAGCCCT					0.00	34.96	0.00	43.95	524095	-0.12	299557	0.39	
TAAGATCTCTGAGCGTGGACC	+ / -	Chloro	11.46 / 23.65	136.08 / 68.26	11.87 / 2.89	26.68 / 49.99	108.25 / 153.79	4.06 / 1.08	BhaA09g265700	CABBP1	534	TAAAGATCTGTGACCGTGGACC					0.00	16.13	0.00	32.99	325731	-0.25	212798	0.26	
TAAGATCTCTGAGCGTGGACC	+ / -	Chloro	11.46 / 23.65	136.08 / 68.26	11.87 / 2.89	26.68 / 49.99	108.25 / 153.79	4.06 / 1.08	BhaA05g094100	CABBP1	465	TAAAGATCTGTGACCGTGGACC					0.00	16.13	0.00	32.99	185278	-0.12	131779	1.16	
TGAAGATCTGTGACCAAGCCCT	+	Chloro	20.96 / -	133.72 / -	6.38 / -	46.38 / -	88.70 / -	1.91 / -	BhaA05g094100	CABBP1	406	TGAAGATCTGTGACCAAGCCCT					0.00	34.96	0.00	43.95	185278	-0.12	131779	1.16	
CTGAAGATCTGTGACCAAGCCCT	+	Chloro	1.15 / -	72.60 / -	63.24 / -	5.34 / -	49.11 / -	9.19 / -	BhaC03g595200	CABBP1	520	CTGAAGATCTGTGACCAAGCCCT					0.00	3.52	0.00	5.04	417531	0.02	305188	0.73	
CTGAAGATCTGTGACCAAGCCCT	+	Chloro	1.15 / -	72.60 / -	63.24 / -	5.34 / -	49.11 / -	9.19 / -	BhaA05g094100	CABBP1	407	CTGAAGATCTGTGACCAAGCCCT					0.00	84.41	0.00	6.16	185278	-0.12	131779	1.16	
CTGAAGATCTGTGACCAAGCCCT	+	Chloro	1.15 / -	72.60 / -	63.24 / -	5.34 / -	49.11 / -	9.19 / -	BhaC04g107800	CABBP1	407	CTGAAGATCTGTGACCAAGCCCT					0.00	84.41	0.00	6.16	185278	-0.12	131779	1.16	
ANTGACCAAGTACTTGACT	+ / -	Chloro	18.37 / 34.34	72.33 / 34.76	3.94 / 1.01	46.63 / 93.41	46.52 / 22.97	1.00 / 0.25	BhaA05g094100	CABBP1	173	ANTGACCAAGTACTTGACT					0.00	2.73	0.00	0.32	185278	-0.12	131779	1.16	
AAGATGCTCTGAGCGTGGACC	+ / -	Chloro	3.08 / 6.07	17.885 / 91.12	58.09 / 15.02	16.77 / 29.83	127.30 / 63.38	7.59 / 2.12	BhaC04g107800	CABBP1	464	AAGATGCTCTGAGCGTGGACC					0.00	10.86	0.00	3.24	524095	-0.12	299557	0.39	
AATGGACCAAGTACTTGACT	+ / -	Chloro	18.37 / 34.34	72.33 / 34.76	3.94 / 1.01	46.63 / 93.41	46.52 / 22.97	1.00 / 0.25	BhaC04g107800	CABBP1	173	AATGGACCAAGTACTTGACT					0.00	2.73	0.00	0.32	524095	-0.12	299557	0.39	
AAGATGCTCTGAGCGTGGACC	+ / -	Chloro	3.08 / 6.07	17.885 / 91.12	58.09 / 15.02	16.77 / 29.83	127.30 / 63.38	7.59 / 2.12	BhaA05g094100	CABBP1	464	AAGATGCTCTGAGCGTGGACC					0.00	10.86	0.00	3.24	185278	-0.12	131779	1.16	
AAGATGCTCTGAGCGTGGACC	+ / -	Chloro	3.08 / 6.07	17.885 / 91.12	58.09 / 15.02	16.77 / 29.83	127.30 / 63.38	7.59 / 2.12	BhaA09g265700	CABBP1	533	AAGATGCTCTGAGCGTGGACC					0.00	10.86	0.00	3.24	325731	-0.25	212798	0.26	
ANTGACCAAGTACTTGACT	+ / -	Chloro	1.68 / 3.55	67.65 / 32.73	40.24 / 9.21	9.91 / 21.93	28.85 / 14.26	2.94 / 0.65	BhaC04g107800	CABBP1	173	ANTGACCAAGTACTTGACT					0.00	2.73	0.00	0.00	524095	-0.12	299557	0.39	
AAGATGCTCTGAGCGTGGACC	-	Chloro	- / -	24.10 / 24.10	- / 28.22	2.66 / 2.66	16.12 / 16.12	6.07 / 6.07	BhaC04g107800	CABBP1	464	AAGATGCTCTGAGCGTGGACC					0.00	10.86	0.00	0.00	524095	-0.12	299557	0.39	
AAGATGCTCTGAGCGTGGACC	-	Chloro	- / -	24.10 / 24.10	- / 28.22	2.66 / 2.66	16.12 / 16.12	6.07 / 6.07	BhaA05g094100	CABBP1	464	AAGATGCTCTGAGCGTGGACC					0.00	10.86	0.00	0.00	185278	-0.12	131779	1.16	
AATGGACCAAGTACTTGACT	+ / -	Chloro	1.68 / 3.55	67.65 / 32.73	40.24 / 9.21	9.91 / 21.93	28.85 / 14.26	2.94 / 0.65	BhaA05g094100	CABBP1	173	AATGGACCAAGTACTTGACT					0.00	2.73	0.00	0.00	185278	-0.12	131779	1.16	
AAGATGCTCTGAGCGTGGACC	-	Chloro	- / -	24.10 / 24.10	- / 28.22	2.66 / 2.66	16.12 / 16.12	6.07 / 6.07	BhaA09g265700	CABBP1	533	AAGATGCTCTGAGCGTGGACC					0.00	10.86	0.00	0.00	325731	-0.25	212798	0.26	
CTTCGAAGGACTTGATGCT	+	Chloro	81.76 / -	197.98 / -	2.42 / -	223.18 / -	147.39 / -	- / -	BhaA09g265700	CABBP1	146	CTTCGAAGGACTTGATGCT					0.00	3.82	0.00	0.42	325731	-0.25	212798	0.26	
CTTCGAAGGACTTGATGCT	+	Chloro	81.76 / -	197.98 / -	2.42 / -	223.18 / -	147.39 / -	- / -	BhaC03g595200	CABBP1	190	CTTCGAAGGACTTGATGCT					0.00	3.82	0.00	0.42	417531	0.02	305188	0.73	
TGAACCAAGCTTGAAACCAAC	+	Chloro	2.57 / -	45.15 / -	17.58 / -	7.88 / -	49.07 / -	6.23 / -	BhaC03g595200	CABBP1	509	TGAACCAAGCTTGAAACCAAC					0.00	3.50	0.00	0.28	417531	0.02	305188	0.73	
ATSGACCAAGTACTTGACC	+	Chloro	13.18 / -	44.55 / -	3.38 / -	29.91 / -	43.27 / -	1.45 / -	BhaC04g107800	CABBP1	172	ATSGACCAAGTACTTGACC					0.00	0.95	0.00	0.51	524095	-0.12	299557	0.39	
TTGCGTGAAGATCTGGAAAC	+ / -	Chloro	3.44 / 5.25	34.66 / 17.98	10.06 / 3.42	9.38 / 18.23	45.70 / 22.86	4.87 / 1.25	BhaC04g107800	CABBP1	411	TTGCGTGAAGATCTGGAAAC					0.00	5.40	0.00	2.08	524095	-0.12	299557	0.39	
GGCGCTTGAAACCAAGCCCT	+	Chloro	24.72 / -	45.46 / -	1.94 / -	58.66 / -	45.77 / -	0.78 / -	BhaA05g094100	CABBP1	391	GGCGCTTGAAACCAAGCCCT					0.00	4.99	0.00	3.38	185278	-0.12	131779	1.16	
TGAACCAAGCTTGAAACCAAC	+	Chloro	0.00 / -	48.61 / -	48.61 / -	1.61 / -	32.52 / -	20.17 / -	BhaA05g094100	CABBP1	396	TGAACCAAGCTTGAAACCAAC					0.00	3.50	0.00	0.28	185278	-0.12	131779	1.16	
AATGGACCAAGTACTTGACC	+ / -	Chloro	1.68 / 3.55	34.77 / 17.93	20.66 / 5.04	0.00 / 0.00	35.24 / 17.51	35.24 / 17.51	BhaA09g265700	CABBP1	540	AATGGACCAAGTACTTGACC					0.00	9.76	0.00	7.82	325731	-0.25	212798	0.26	

AATGGACCAAGTACTGACT	+ / -	Chloro	18.37 / 34.34	72.33 / 34.76	3.94 / 1.01	46.63 / 93.41	46.52 / 22.97	1.00 / 0.25	BnaC03g595200	CABBP1	286	AATGGACCAAGTACTGACT CCTCTACCGGTTCTGAAGTGAAGGACC	D13 TT3	0.00	0.86	0.00	0.60	41.7531	0.02	305188	0.73
TGAACCGCTTGAACCAAGG	+	Chloro	0.00 / -	48.61 / -	48.61 / -	1.61 / -	32.52 / -	20.17 / -	BnaC04g107800	CABBP1	396	TGAACCGCTTGAACCAAGG AGACGCTGGCAACTGGTTGTCGGAGA	D13 TT3	0.00	3.50	0.00	0.28	524095	-0.12	299557	0.39
AATGGCTAAGTACTGACTGAC	+ / -	Chloro	1.08 / 3.55	34.77 / 17.93	20.68 / 5.04	0.00 / 0.00	35.24 / 17.51	35.24 / 17.51	BnaC04g107800	CABBP1	471	AATGGCTAAGTACTGACTGAC GGTTTACGATTCAGAGACTGCGCACTGG	D13 TT3	0.00	1.72	0.00	5.60	524095	-0.12	299557	0.39
CCGGCTTGAACCAACCGCC	+ / -	Chloro	1.15 / 1.75	47.94 / 22.81	41.75 / 13.03	5.54 / 10.03	66.69 / 32.90	12.03 / 3.28	BnaA05g094100	CABBP1	392	CCGGCTTGAACCAACCGCC GCTGGCCGCAACTGGTTGTCGGAGA	D13 TT3	0.00	3.77	0.00	0.74	185278	-0.12	131779	1.16
TGAACCGCTTGAACCAAGG	+	Chloro	0.00 / -	48.61 / -	48.61 / -	1.61 / -	32.52 / -	20.17 / -	BnaC03g595200	CABBP1	509	TGAACCGCTTGAACCAAGG AGACGCTGGCAACTGGTTGTCGGAGA	D13 TT3	0.00	3.50	0.00	0.28	417531	0.02	305188	0.73
CCGGCTTGAACCAACCGCC	+ / -	Chloro	1.15 / 1.75	47.94 / 22.81	41.75 / 13.03	5.54 / 10.03	66.69 / 32.90	12.03 / 3.28	BnaC03g595200	CABBP1	505	CCGGCTTGAACCAACCGCC GCTGGCCGCAACTGGTTGTCGGAGA	D13 TT3	0.00	3.77	0.00	0.74	417531	0.02	305188	0.73
ATGGACCAAGTACTGACCC	+	Chloro	13.18 / -	44.55 / -	3.38 / -	2.91 / -	43.27 / -	1.45 / -	BnaC03g595200	CABBP1	285	ATGGACCAAGTACTGACCC CCTTACCGGTTCTGAAGTGAAGAGACT	D13 TT3	0.00	0.27	0.00	0.32	417531	0.02	305188	0.73
ATGGACCAAGTACTGACCC	+	Chloro	13.18 / -	44.55 / -	3.38 / -	2.91 / -	43.27 / -	1.45 / -	BnaA05g094100	CABBP1	172	ATGGACCAAGTACTGACCC CCTTACCGGTTCTGAAGTGAAGAGACT	D13 TT3	0.00	0.95	0.00	0.51	185278	-0.12	131779	1.16
TGAACCGCTTGAACCAAGG	+	Chloro	0.89 / -	40.02 / -	45.11 / -	7.92 / -	39.29 / -	4.96 / -	BnaC04g107800	CABBP1	396	TGAACCGCTTGAACCAAGG AGACGCTGGCAACTGGTTGTCGGAGA	D13 TT3	0.00	3.50	0.00	0.28	524095	-0.12	299557	0.39
CCGGCTTGAACCAACCGCC	+ / -	Chloro	1.15 / 1.75	47.94 / 22.81	41.75 / 13.03	5.54 / 10.03	66.69 / 32.90	12.03 / 3.28	BnaC04g107800	CABBP1	392	CCGGCTTGAACCAACCGCC GCTGGCCGCAACTGGTTGTCGGAGA	D13 TT3	0.00	3.77	0.00	0.74	524095	-0.12	299557	0.39
TTGGCTGAAGTACTGTAACC	+	Chloro	17.41 / -	30.245 / -	17.37 / -	36.62 / -	21.925 / -	5.99 / -	BnaC04g107800	CABBP1	411	TTGGCTGAAGTACTGTAACC GAGAGAGACTTGAAGACTGGTCGGAGAC	D13 TT3	0.00	5.40	0.00	2.08	524095	-0.12	299557	0.39
TGAACCGCTTGAACCAAGG	+	Chloro	0.89 / -	40.02 / -	45.11 / -	7.92 / -	39.29 / -	4.96 / -	BnaC03g595200	CABBP1	509	TGAACCGCTTGAACCAAGG AGACGCTGGCAACTGGTTGTCGGAGA	D13 TT3	0.00	3.50	0.00	0.28	417531	0.02	305188	0.73
TGAACCGCTTGAACCAAGG	+	Chloro	2.57 / -	45.15 / -	17.58 / -	7.88 / -	49.07 / -	6.23 / -	BnaC04g107800	CABBP1	396	TGAACCGCTTGAACCAAGG AGACGCTGGCAACTGGTTGTCGGAGA	D13 TT3	0.00	3.50	0.00	0.28	524095	-0.12	299557	0.39
TGAACCGCTTGAACCAAGG	+	Chloro	2.57 / -	45.15 / -	17.58 / -	7.88 / -	49.07 / -	6.23 / -	BnaA05g094100	CABBP1	396	TGAACCGCTTGAACCAAGG AGACGCTGGCAACTGGTTGTCGGAGA	D13 TT3	0.00	3.50	0.00	0.28	185278	-0.12	131779	1.16
GGAAAGCAGCAGCTGAGGCT	+ / -	Chloro	0.52 / 1.71	38.54 / 19.33	73.87 / 11.32	3.93 / 7.37	42.68 / 21.16	10.86 / 2.87	BnaA09g265700	CABBP1	403	GGAAAGCAGCAGCTGAGGCT AGGCTCTGTCGGACTGGAGGTTGTA	D13 TT3	0.00	0.36	0.00	0.14	325731	-0.25	212798	0.26
AAGTACTGAGCTGAGGCTGAC	+ / -	Chloro	3.08 / 6.07	17.885 / 9.112	58.09 / 15.02	16.77 / 29.83	127.30 / 63.38	7.59 / 2.12	BnaC03g595200	CABBP1	577	AAGTACTGAGCTGAGGCTGAC TGGTTCTGAGACTGCACTGGTTGTCGAC	D13 TT3	0.00	1.13	0.00	2.31	417531	0.02	305188	0.73
TGAACCGCTTGAACCAAGG	+	Chloro	0.89 / -	40.02 / -	45.11 / -	7.92 / -	39.29 / -	4.96 / -	BnaA05g094100	CABBP1	396	TGAACCGCTTGAACCAAGG AGACGCTGGCAACTGGTTGTCGGAGA	D13 TT3	0.00	3.50	0.00	0.28	185278	-0.12	131779	1.16
CGGCTTGAACCAACCGCT	+	Chloro	24.72 / -	45.46 / -	1.84 / -	58.66 / -	45.77 / -	0.78 / -	BnaC04g107800	CABBP1	391	CGGCTTGAACCAACCGCT CTGGCGAAGTGGTTGTCGGAGGCT	D13 TT3	0.00	4.99	0.00	3.38	524095	-0.12	299557	0.39
CGGCTTGAACCAACCGCT	+	Chloro	24.72 / -	45.46 / -	1.84 / -	58.66 / -	45.77 / -	0.78 / -	BnaC03g595200	CABBP1	504	CGGCTTGAACCAACCGCT CTGGCGAAGTGGTTGTCGGAGGCT	D13 TT3	0.00	4.99	0.00	3.38	417531	0.02	305188	0.73
ATCTGTGAACCAAGCTGAAAC	+	Chloro	0.00 / -	63.13 / -	63.13 / -	7.15 / -	43.34 / -	6.06 / -	BnaC03g595200	CABBP1	514	ATCTGTGAACCAAGCTGAAAC CTCTAGAAGCTGGCGAAGTGGTTGTC	TT1 TT3	0.00	0.00	0.00	0.59	417531	0.02	305188	0.73
ATCTGTGAACCAAGCTGAAAC	+	Chloro	8.28 / -	38.44 / -	4.64 / -	30.33 / -	53.02 / -	1.75 / -	BnaC04g107800	CABBP1	401	ATCTGTGAACCAAGCTGAAAC CTCTAGAAGCTGGCGAAGTGGTTGTC	TT1 TT3	0.00	0.00	0.00	0.59	524095	-0.12	299557	0.39
ATCTGTGAACCAAGCTGAAAC	+	Chloro	8.28 / -	38.44 / -	4.64 / -	30.33 / -	53.02 / -	1.75 / -	BnaA05g094100	CABBP1	401	ATCTGTGAACCAAGCTGAAAC CTCTAGAAGCTGGCGAAGTGGTTGTC	TT1 TT3	0.00	0.00	0.00	0.59	185278	-0.12	131779	1.16
ATCTGTGAACCAAGCTGAAAC	+	Chloro	8.28 / -	38.44 / -	4.64 / -	30.33 / -	53.02 / -	1.75 / -	BnaC03g595200	CABBP1	514	ATCTGTGAACCAAGCTGAAAC CTCTAGAAGCTGGCGAAGTGGTTGTC	TT1 TT3	0.00	0.00	0.00	0.59	417531	0.02	305188	0.73
ATCTGTGAACCAAGCTGAAAC	+	Chloro	0.00 / -	63.13 / -	63.13 / -	7.15 / -	43.34 / -	6.06 / -	BnaC04g107800	CABBP1	401	ATCTGTGAACCAAGCTGAAAC CTCTAGAAGCTGGCGAAGTGGTTGTC	TT1 TT3	0.00	0.00	0.00	0.59	524095	-0.12	299557	0.39
ATCTGTGAACCAAGCTGAAAC	+	Chloro	0.00 / -	63.13 / -	63.13 / -	7.15 / -	43.34 / -	6.06 / -	BnaA05g094100	CABBP1	401	ATCTGTGAACCAAGCTGAAAC CTCTAGAAGCTGGCGAAGTGGTTGTC	TT1 TT3	0.00	0.00	0.00	0.59	185278	-0.12	131779	1.16
AAGGTAGCTCGGTCGCTCGCC	+ / -	Chloro	0.36 / 0.85	45.84 / 22.99	175.72 / 26.93	5.58 / 10.41	27.97 / 13.88	5.02 / 1.33	BnaC03g595200	CABBP1	311	AAGGTAGCTCGGTCGCTCGCC SCATCTATGACCAAGCTGGCGCTCTA	D12	0.00	1.42	0.00	0.00	417531	0.02	305188	0.73
CCTAGGCTCGGTCGCTCGCC	+ / -	Chloro	3.09 / 6.16	50.71 / 25.34	16.43 / 4.11	4.46 / 11.08	37.55 / 18.64	8.43 / 1.68	BnaA05g094100	CABBP1	323	CCTAGGCTCGGTCGCTCGCC TGTGGATCCGGAGTTGTTGTCGGAGAGG	D12	0.00	3.47	0.00	0.00	185278	-0.12	131779	1.16
CCTGTGAGACTGTGTA	+	Chloro	0.00 / -	59.00 / -	59.00 / -	0.00 / -	31.14 / -	31.14 / -	BnaA05g094100	CABBP1	413	CCTGTGAGACTGTGTA CTCTGCTGAGACTGTGTA	D13	0.00	1.94	0.00	0.00	185278	-0.12	131779	1.16
ATGGTGGGAGACTGTGTA	+	Chloro	9.18 / -	55.51 / -	6.04 / -	20.22 / -	29.70 / -	1.47 / -	BnaC04g107800	CABBP1	729	ATGGTGGGAGACTGTGTA GTTTACAGCTGCTAGAGAGTTCAGGG	D13	0.00	23.60	0.00	0.00	524095	-0.12	299557	0.39
AAGTACTGAGCTGAGGCTGAAAC	-	Chloro	0.85 / 0.85	24.10 / 24.10	28.22 / 28.22	2.66 / 2.66	16.12 / 16.12	6.07 / 6.07	BnaC03g595200	CABBP1	577	AAGTACTGAGCTGAGGCTGAAAC TGGTTCTGAGACTGCACTGGTTGTCGAC	D13	0.00	1.13	0.00	0.00	417531	0.02	305188	0.73
TTCTGGCTGGTGAAGGAGCC	+	Chloro	9.09 / -	79.41 / -	8.73 / -	19.57 / -	51.47 / -	2.63 / -	BnaA07g075700	CABBP1	2055	TTCTGGCTGGTGAAGGAGCC TGGTTCTGAGACTGCACTGGTTGTCGAC	D13	0.00	0.18	0.00	0.00	213712	-0.76	117162	0.37
AAATGGCTGGGAGACTGCTC	+	Chloro	1.77 / -	42.17 / -	23.76 / -	0.00 / -	36.11 / -	36.11 / -	BnaA09g265700	CABBP1	800	AAATGGCTGGGAGACTGCTC TCACTGCTACCGGATATTTCTAGGTTT	D13	0.00	14.89	0.00	0.00	325731	-0.25	212798	0.26
ACANTGGCTTGAACCAAGAT	+ / -	Chloro	4.24 / 7.91	40.76 / 20.02	9.62 / 2.53	4.64 / 9.43	29.02 / 14.35	6.26 / 1.52	BnaA05g094100	CABBP1	682	ACANTGGCTTGAACCAAGAT GTGACCAAGCTGGGTCGCTGAC	D13	0.00	8.49	0.00	0.00	185278	-0.12	131779	1.16
GTGACCAAGCTGGGTCGCTGAC	+ / -	Chloro	0.52 / 1.71	57.53 / 27.01	110.27 / 15.82	0.80 / 1.23	37.80 / 18.63	47.40 / 15.10	BnaC04g107800	CABBP1	450	GTGACCAAGCTGGGTCGCTGAC CTGCACTGGTGGCAAGGAGGTTGTC	D13	0.00	3.31	0.00	0.00	524095	-0.12	299557	0.39
AATGGACCAAGTACTGACT	+ / -	Chloro	1.68 / 3.55	67.65 / 32.73	40.24 / 9.21	9.91 / 21.93	28.85 / 14.26	2.94 / 0.65	BnaC03g595200	CABBP1	286	AATGGACCAAGTACTGACT CCTCTACCGGTTCTGAAGTGAAGGACC	D13	0.00	0.86	0.00	0.00	417531	0.02	305188	0.73

AATGGACCTAAGTACTGACT	Chloro	+ / -	1.68 / 3.55	67.65 / 32.73	40.24 / 9.21	9.91 / 21.93	28.85 / 14.26	2.91 / 0.65	BnaC03g595200	CABBP1	286	AATGGACCTAAGTACTGACT CCTTTACCGGGTCTGAATCACTGAGAGCC	D13	0.00	0.86	0.00	0.00	417531	0.02	305188	0.73
TTGGTGAAGATCTGTGAAC	Chloro	+	17.41 / -	302.45 / -	17.37 / -	36.62 / -	219.25 / -	5.99 / -	BnaA09g265700	CABBP1	480	TTGGTGAAGATCTGTGAAC GAGGGAGGACTCTAAACACTCGCGCGAAC	D13	0.00	1.72	0.00	0.00	325731	-0.25	212798	0.26
AAATGTGGGGAGGATCTCC	Chloro	+	1.77 / -	42.17 / -	23.76 / -	0.00 / -	36.11 / -	36.11 / -	BnaA05g094100	CABBP1	731	AAATGTGGGGAGGATCTCC AAATGTGGGGAGGATCTCC	D13	0.00	14.89	0.00	0.00	185278	-0.12	131779	1.16
CCTTGCTGAAGATCTGTGAA	Chloro	+	0.00 / -	59.00 / -	59.00 / -	0.00 / -	31.14 / -	31.14 / -	BnaC04g107800	CABBP1	413	CCTTGCTGAAGATCTGTGAA GGGAGGAGGACTCTAAGACTTGGCGGGA	D13	0.00	5.08	0.00	0.00	524095	-0.12	299557	0.39
GTGGCGAGATCTCCCAACGG	Chloro	+	1.77 / -	31.41 / -	17.70 / -	3.99 / -	26.54 / -	6.66 / -	BnaC04g107800	CABBP1	726	GTGGCGAGATCTCCCAACGG TTACAGTGTCTAAGAGTGTCTCCAGGAAA	D13	0.00	1.82	0.00	0.00	524095	-0.12	299557	0.39
GTGGCAACGCTGGGTTGCC	Chloro	+ / -	0.52 / 1.71	57.53 / 27.01	110.27 / 15.82	0.80 / 1.23	37.80 / 18.63	47.40 / 15.10	BnaA09g265700	CABBP1	519	GTGGCAACGCTGGGTTGCC GTGGCAACGCTGGGTTGCC	D13	0.00	3.31	0.00	0.00	325731	-0.25	212798	0.26
AAATGTGGGGAGGATCTCC	Chloro	+	1.77 / -	42.17 / -	23.76 / -	0.00 / -	36.11 / -	36.11 / -	BnaC04g107800	CABBP1	731	AAATGTGGGGAGGATCTCC TTGGTGTACCACTGCTTAAGAGAGTCCAG	D13	0.00	14.89	0.00	0.00	524095	-0.12	299557	0.39
TTGGTGAAGATCTGTGAAC	Chloro	+ / -	3.44 / 5.25	34.66 / 17.98	10.06 / 3.42	9.38 / 18.23	45.70 / 22.86	4.87 / 1.25	BnaA09g265700	CABBP1	480	TTGGTGAAGATCTGTGAAC TTGGTGAAGATCTGTGAAC	D13	0.00	1.72	0.00	0.00	325731	-0.25	212798	0.26
GTGGCAACGCTGGGTTGCC	Chloro	+ / -	0.52 / 1.71	57.53 / 27.01	110.27 / 15.82	0.80 / 1.23	37.80 / 18.63	47.40 / 15.10	BnaA05g094100	CABBP1	450	GTGGCAACGCTGGGTTGCC TTGGTGTACCACTGCTTAAGAGAGTCCAG	D13	0.00	3.31	0.00	0.00	185278	-0.12	131779	1.16
AAATGTGGGGAGGATCTCC	Chloro	+	1.77 / -	42.17 / -	23.76 / -	0.00 / -	36.11 / -	36.11 / -	BnaC03g595200	CABBP1	844	AAATGTGGGGAGGATCTCC TTGGTGTACCACTGCTTAAGAGAGTCCAG	D13	0.00	14.89	0.00	0.00	417531	0.02	305188	0.73
ATGGACCAAGTACTGAAACC	Chloro	+	13.18 / -	44.55 / -	3.38 / -	2.991 / -	43.27 / -	1.45 / -	BnaA09g265700	CABBP1	241	ATGGACCAAGTACTGAAACC CTTACTGGGTCTAAGACTGAGAAAAGCT	D13	0.00	0.64	0.00	0.00	325731	-0.25	212798	0.26
TTCTGGGTGGGTAGCGAGACC	Chloro	+	19.16 / -	75.82 / -	3.96 / -	6.440 / -	84.07 / -	1.31 / -	BnaA07g075700	CABBP1	2055	TTCTGGGTGGGTAGCGAGACC TTGGGAGCCAGCTGCTCGGTTACC	D13	0.00	0.18	0.00	0.00	213712	-0.76	117162	0.37
ACATGGCTTGAACCAAGAT	Chloro	+ / -	4.24 / 7.91	40.76 / 20.02	9.62 / 2.53	4.64 / 9.43	29.02 / 14.35	6.26 / 1.52	BnaC03g595200	CABBP1	805	ACATGGCTTGAACCAAGAT TCACGTATCAACTGCTTACTAGTTGT	D13	0.00	1.63	0.00	0.00	417531	0.02	305188	0.73
CCATGGCTGGCTGCTATGGGCC	Chloro	+ / -	0.89 / 0.90	46.54 / 22.99	52.46 / 25.61	0.81 / 1.42	36.34 / 17.98	44.57 / 12.64	BnaA09g265700	CABBP1	207	CCATGGCTGGCTGCTATGGGCC GCATGTGTCCGAGCACTCCAGGAAACCG	D13	0.00	1.77	0.00	0.00	325731	-0.25	212798	0.26
CTTAGGCTCCGAGCATGGCC	Chloro	+ / -	3.09 / 6.16	50.71 / 25.34	16.41 / 4.11	4.46 / 11.08	37.55 / 18.64	8.43 / 1.68	BnaC03g595200	CABBP1	436	CTTAGGCTCCGAGCATGGCC CTGTGGATCCGGGCTCTCGGTTGAGCG	D13	0.00	0.54	0.00	0.00	417531	0.02	305188	0.73
GGAAAGCAGCAGCTAGGGCTC	Chloro	+ / -	0.52 / 1.71	38.54 / 19.33	73.87 / 11.32	3.93 / 7.37	42.68 / 21.16	10.86 / 2.87	BnaC04g107800	CABBP1	334	GGAAAGCAGCAGCTAGGGCTC AGTCTTTTGTGTAGTCCGAGGTGTGA	TT3	0.00	0.00	0.00	0.28	524095	-0.12	299557	0.39
AATGGCTAAGATGCTGTGACC	Chloro	+ / -	1.68 / 3.55	34.77 / 17.93	20.68 / 5.04	0.00 / 0.00	35.24 / 17.51	35.24 / 17.51	BnaA05g094100	CABBP1	471	AATGGCTAAGATGCTGTGACC GGTTACTGAGTCTGAGACTCGCACTGCG	TT3	0.00	0.00	0.00	5.23	185278	-0.12	131779	1.16
GGAAAGCAGCAGCTAGGGCTC	Chloro	+ / -	0.89 / 0.90	38.54 / 18.48	43.44 / 20.59	0.81 / 1.42	63.34 / 31.28	77.75 / 21.99	BnaC03g595200	CABBP1	509	GGAAAGCAGCAGCTAGGGCTC GMAACGGCTTGAACCAAAACC	TT3	0.00	0.00	0.00	0.28	417531	0.02	305188	0.73
ATGAGGATCACTGAGTAGGCC	Chloro	+ / -	1.68 / 3.55	47.44 / 23.32	28.22 / 6.56	3.91 / 7.18	42.09 / 20.89	10.76 / 2.91	BnaA05g094100	CABBP1	494	ATGAGGATCACTGAGTAGGCC AGGTTACTTGTAGTGGCAACGGTTACC	TT3	0.00	0.00	0.00	0.23	185278	-0.12	131779	1.16
TTGGTGAAGATCTGTGAAC	Chloro	+	17.41 / -	302.45 / -	17.37 / -	36.62 / -	219.25 / -	5.99 / -	BnaA05g094100	CABBP1	411	TTGGTGAAGATCTGTGAAC GAGGAGGACTCTAAGACTTGGCGGGAAC	TT3	0.00	0.00	0.00	0.83	185278	-0.12	131779	1.16
GTGGCAACGCTGGGTTGCC	Chloro	+ / -	0.00 / 0.00	35.21 / 16.65	35.21 / 16.65	0.00 / 0.00	50.90 / 25.11	50.90 / 25.11	BnaC04g107800	CABBP1	451	GTGGCAACGCTGGGTTGCC ATCTGACTGGTGGAGCCAGAGGGTCTAT	TT3	0.00	0.00	0.00	0.83	524095	-0.12	299557	0.39
CGAAACGCTTGAACCAAAACC	Chloro	+ / -	1.68 / 3.55	47.44 / 23.32	28.22 / 6.56	3.91 / 7.18	42.09 / 20.89	10.76 / 2.91	BnaC04g107800	CABBP1	396	CGAAACGCTTGAACCAAAACC AGACTTGGCGGACTTGGTTCGCGAGA	TT3	0.00	0.00	0.00	0.28	524095	-0.12	299557	0.39
ATGAGGATCACTGAGTAGGCC	Chloro	+ / -	0.00 / 0.00	35.21 / 16.65	35.21 / 16.65	0.00 / 0.00	50.90 / 25.11	50.90 / 25.11	BnaA09g265700	CABBP1	1943	ATGAGGATCACTGAGTAGGCC AGGTTACTTGTAGTGGCAACGGTTACC	TT3	0.00	0.00	0.00	0.51	213712	-0.76	117162	0.37
GTGGCAACGCTGGGTTGCC	Chloro	+ / -	0.00 / 0.00	35.21 / 16.65	35.21 / 16.65	0.00 / 0.00	50.90 / 25.11	50.90 / 25.11	BnaA09g265700	CABBP1	520	GTGGCAACGCTGGGTTGCC CTGGCAACAACTCGGTTGCC	TT3	0.00	0.00	0.00	0.83	325731	-0.25	212798	0.26
CCGGCTTGAACCAAAACC	Chloro	+ / -	1.15 / 1.75	47.94 / 22.81	41.75 / 13.03	5.54 / 10.03	66.69 / 32.90	12.03 / 3.28	BnaA09g265700	CABBP1	461	CCGGCTTGAACCAAAACC ACTGCGCGGACTGGTTCGCGAGGCT	TT3	0.00	0.00	0.00	0.05	325731	-0.25	212798	0.26
CTGAAGATCTGTGAACAGCT	Chloro	+	1.67 / -	25.03 / -	14.99 / -	0.00 / -	50.89 / -	50.89 / -	BnaA05g094100	CABBP1	407	CTGAAGATCTGTGAACAGCT TTACAGTGTCTAAGAGTGTCTCCAGGAAA	TT3	0.00	0.00	0.00	6.16	185278	-0.12	131779	1.16
CTGAAGATCTGTGAACAGCT	Chloro	+	1.67 / -	25.03 / -	14.99 / -	0.00 / -	50.89 / -	50.89 / -	BnaC03g595200	CABBP1	520	CTGAAGATCTGTGAACAGCT TTACAGTGTCTAAGAGTGTCTCCAGGAAA	TT3	0.00	0.00	0.00	5.04	417531	0.02	305188	0.73
GGAAACGCTTGAACCAAAACC	Chloro	+ / -	0.89 / 0.90	38.54 / 18.48	43.44 / 20.59	0.81 / 1.42	63.34 / 31.28	77.75 / 21.99	BnaA05g094100	CABBP1	396	GGAAACGCTTGAACCAAAACC AGACTTGGCGGACTTGGTTCGCGAGA	TT3	0.00	0.00	0.00	0.28	185278	-0.12	131779	1.16
ATGAGGATCACTGAGTAGGCC	Chloro	+ / -	1.68 / 3.55	47.44 / 23.32	28.22 / 6.56	3.91 / 7.18	42.09 / 20.89	10.76 / 2.91	BnaC04g107800	CABBP1	494	ATGAGGATCACTGAGTAGGCC AGGTTACTTGTAGTGGCAACGGTTACC	TT3	0.00	0.00	0.00	2.59	524095	-0.12	299557	0.39
TTGGTGAAGATCTGTGAAC	Chloro	+	17.41 / -	302.45 / -	17.37 / -	36.62 / -	219.25 / -	5.99 / -	BnaC03g595200	CABBP1	524	TTGGTGAAGATCTGTGAAC TTGGTGAAGATCTGTGAAC	TT3	0.00	0.00	0.00	0.37	417531	0.02	305188	0.73
TTGGTGAAGATCTGTGAAC	Chloro	+ / -	3.44 / 5.25	34.66 / 17.98	10.06 / 3.42	9.38 / 18.23	45.70 / 22.86	4.87 / 1.25	BnaA05g094100	CABBP1	411	TTGGTGAAGATCTGTGAAC GAGGAGGACTCTAAGACTTGGCGGGAAC	TT3	0.00	0.00	0.00	0.83	185278	-0.12	131779	1.16
TGAACAAGATCAAAACATA	Chloro	+ / -	2.66 / 2.69	23.48 / 12.21	8.82 / 4.53	2.41 / 3.89	32.46 / 16.26	13.47 / 4.18	BnaC04g107800	CABBP1	683	TGAACAAGATCAAAACATA AGGACTTCTTAAGTGTGTTACTGT	TT3	0.00	0.00	0.00	0.09	524095	-0.12	299557	0.39
CGGCTTGAACCAAAACC	Chloro	+	24.72 / -	45.46 / -	1.84 / -	5.866 / -	45.77 / -	0.78 / -	BnaA09g265700	CABBP1	460	CGGCTTGAACCAAAACC CTGCGCGGAACTGTGGCGGAGGAGCT	TT3	0.00	0.00	0.00	0.28	325731	-0.25	212798	0.26
TGAACAAGATCAAAACATA	Chloro	+ / -	2.66 / 2.69	23.48 / 12.21	8.82 / 4.53	2.41 / 3.89	32.46 / 16.26	13.47 / 4.18	BnaA07g075700	CABBP1	2132	TGAACAAGATCAAAACATA CGAACTTGTCTAAGTGTGTTACTGT	TT3	0.00	0.00	0.00	0.09	213712	-0.76	117162	0.37
TGAACAAGATCAAAACATA	Chloro	+ / -	2.66 / 2.69	23.48 / 12.21	8.82 / 4.53	2.41 / 3.89	32.46 / 16.26	13.47 / 4.18	BnaA09g265700	CABBP1	752	TGAACAAGATCAAAACATA TTAGTGTCTAAGTGTGTTACTGT	TT3	0.00	0.00	0.00	0.09	325731	-0.25	212798	0.26
TAAGATCTCTGCGGTGGACC	Chloro	+ / -	11.46 / 23.65	136.08 / 68.36	11.87 / 2.89	26.68 / 49.99	108.25 / 53.79	4.06 / 1.08	BnaC03g595200	CABBP1	578	TAAGATCTCTGCGGTGGACC ATCGTCTAAGAGTCTGAGTGTGCTGAT	TT3	0.00	0.00	0.00	0.79	417531	0.02	305188	0.73

GTAGATCCATCGTTCACGGAT	-	NBR1	0.00	38.86	38.86	0.00	94.43	94.43	BraA082g28040D	3-ketoseyl-CoA thiolase 1, peroxisomal	1613	GTAGATCCATCGTTCACGGAT ATCAGCTTAGGTAGCAGAGTCTTTCAGAA	TT3	0.00	0.00	0.05	482	0.12	654	0.38
TTGGCTTTGAAAGGACCTTGA	-	NBR1	2.61	19.48	7.48	10.66	37.65	3.53	BraCmg46650D	unknown	302	TTGGCTTTGAAAGGACCTTGA GCCAACCCGAAAGTTCACAGGGA-TCTTAT	TT3	0.00	0.00	0.14	3030	-0.52	7478	-0.52
CAGAAGAGCTCAACAGACTGCT	-	NBR1	0.00	17.54	17.54	0.00	24.02	24.02	BraC07g39070D	NBR1 homolog	3684	CAGAAGAGCTCAACAGACTGCT AGGTTCTTCGGAATGCTCAAGAGTTCA	TT3	0.00	0.00	0.05	2241	1.36	5953	1.44
ACGAGTGCAGTAGTAGAATCC	-	NBR1	2.61	45.10	17.31	4.12	73.73	17.91	BraC08g14680D	unknown	1152	ACGAGTGCAGTAGTAGAATCC TACGGCTACGTCATCATCTTCCTCCACCT	TT3	0.00	0.00	0.23	282	-0.32	311	0.34
CTGTCCATAGCTTTGAAAGGC	-	NBR1	0.00	4.85	4.85	0.00	22.20	22.20	BraA05g33370D	Probable protein phosphatase 2C 33	2361	CTGTCCATAGCTTTGAAAGGC GAGACACAGT-ALTGAAAATTCGGAATCT	TT3	0.00	0.00	0.05	5394	0.00	3387	0.21
TTCTGTTTCAMATCAGCACT	-	NBR1	0.00	18.07	18.07	0.00	19.29	19.29	BraC01g16550D	NBR1 homolog	2645	TTCTGTTTCAMATCAGCACT TGGTTCACATCAGCACT	TT3	0.00	0.00	0.19	7201	1.42	15409	0.96
CACCAAGCTTGCAGTGCACAGT	-	NBR1	0.00	13.61	13.61	0.00	39.88	39.88	BraC03g32940D	S-adenosylmethionine decarboxylase proenzyme 3	880	CACCAAGCTTGCAGTGCACAGT AAGCAGGTTTCGACATCATCTTCCTCCACCT	TT3	0.00	0.00	0.60	60577	-0.22	56260	-0.16
CAGAGAGCTCAACAGACTGC	-	NBR1	0.00	48.37	48.37	1.42	52.41	36.84	BraC07g39070D	NBR1 homolog	3684	CAGAGAGCTCAACAGACTGC AGTGTTCCTCGAAGTGTCTCAAGAGTTCA	TT3	0.00	0.00	0.05	2241	1.36	5953	1.44
TTAGAACACAGAGCTCAACT	-	NBR1	0.00	47.07	47.07	4.12	53.62	13.02	BraA03g46880D	NBR1 homolog	2454	TTAGAACACAGAGCTCAACT TAGAACAAACAGCTCAACT	TT3	0.00	0.00	0.05	2740	0.77	4843	0.45
TCCAATAAGATATGATCGGCC	-	NBR1	0.00	22.43	22.43	0.00	43.37	43.37	BraC07g39070D	NBR1 homolog	3028	TCCAATAAGATATGATCGGCC TAGTAAGATATGATCGGCC	TT3	0.00	0.00	0.09	2241	1.36	5953	1.44
AGGACAAAGCGACTGCTAGCT	-	NBR1	0.00	12.37	12.37	0.00	22.87	22.87	BraC08g11760D	NBR1 homolog	1744	AGGACAAAGCGACTGCTAGCT TAGTCGATCTCGAAGTGTCTCAAGAGTTCA	TT3	0.00	0.00	0.32	1275	1.12	1941	0.66
TTGANTGATCTCGAAGGCT	+	NBR1	0.00	24.58	24.58	0.00	39.09	39.09	BraA01g17500D	DOWNY MILDEW RESISTANCE 6	893	TTGANTGATCTCGAAGGCT TAGTCGATCTCGAAGTGTCTCAAGAGTTCA	TT3	0.00	0.00	0.19	883	0.90	1333	1.24
TCCAGAGAGCGTCAACAGAC	-	NBR1	0.00	26.80	26.80	0.00	44.02	44.02	BraA03g46880D	NBR1 homolog	2722	TCCAGAGAGCGTCAACAGAC CGTAACTA-STAGAACTTCGACTCTGG	TT3	0.00	0.00	0.09	2740	0.77	4843	0.45
TGCAGATGAGGACCGCCACC	-	NBR1	0.00	38.92	38.92	0.00	36.10	36.10	BraA01g04130D	unknown	9400	TGCAGATGAGGACCGCCACC GACCCTCACCCTCGGTGTCTCAAGAGTTCA	TT3	0.00	0.00	0.69	162	0.10	368	0.12
CTGCTCAAAGTGTACTGCTGT	-	NBR1	0.00	23.69	23.69	0.00	19.11	19.11	BraC07g36330D	Leucine-rich repeat receptor-like serine/threonine-protein kinase BAM3	2673	CTGCTCAAAGTGTACTGCTGT CTGTCC-AAGTGTACTGCT	TT3	0.00	0.00	0.37	131	-0.33	81	-0.34
CAGTAGTAGAATCCATCTGTA	-	NBR1	0.00	10.80	10.80	0.00	22.35	22.35	BraC04g3380D	WAT1-related protein Atg15540	1604	CAGTAGTAGAATCCATCTGTA TAGTGTAT-ATCTAGTTCGAGTATAGCT	TT3	0.00	0.00	0.37	3644	0.44	7641	1.19
TGCCCGCTGTATGTCCTC	+	NBR1	0.00	40.75	40.75	0.71	62.96	89.07	BraA01g04910D	Aspartate aminotransferase, chloroplastic	2379	TGCCCGCTGTATGTCCTC GTCCGCTGTATGTCCTC	TT3	0.00	0.00	0.28	672	0.41	1134	0.78
AGAGAGCGTCAACAGACTGCT	-	NBR1	0.00	29.47	29.47	0.00	25.53	25.53	BraA03g46880D	NBR1 homolog	2717	AGAGAGCGTCAACAGACTGCT GGTGTTCGGAAGTGTCTCAAGAGTTCA	TT3	0.00	0.00	0.14	2740	0.77	4843	0.45
GTAGAACTCGTTCACGGAT	-	NBR1	0.00	38.86	38.86	0.00	94.43	94.43	BraC08g00920D	3-ketoseyl-CoA thiolase 2, peroxisomal	1494	GTAGAACTCGTTCACGGAT ATCAGCTTAGGTAGCAGAGTCTTTCAGAA	TT3	0.00	0.00	0.05	406	0.20	674	0.66
TCCAGAGAGCGTCAACAGAC	-	NBR1	0.00	26.80	26.80	0.00	44.02	44.02	BraC07g39070D	NBR1 homolog	3688	TCCAGAGAGCGTCAACAGAC ATTGAGTGTTCGGAAGTGTCTCAAGAGTTCA	TT3	0.00	0.00	0.09	2241	1.36	5953	1.44
TCAAGTCAAGCTACTGTGTA	-	NBR1	0.00	42.37	42.37	0.00	55.12	55.12	BraA01g14050D	NBR1 homolog	2144	TCAAGTCAAGCTACTGTGTA TGAAGTCAAGTGTCTCAAGAGTTCA	TT3	0.00	0.00	0.14	2959	5.97	279	7.49
TTAGAACAAAGGCTCAACT	-	NBR1	0.00	47.07	47.07	4.12	53.62	13.02	BraA01g14050D	NBR1 homolog	2590	TTAGAACAAAGGCTCAACT TCAAACTCTGTCTCGAAGTGTCTCAAGAGTTCA	TT3	0.00	0.00	0.09	2959	5.97	279	7.49
TCCAGAGAGCGTCAACAGAC	-	NBR1	0.85	71.95	84.25	0.00	68.09	68.09	BraA03g46880D	NBR1 homolog	2722	TCCAGAGAGCGTCAACAGAC ATTGAGTGTTCGGAAGTGTCTCAAGAGTTCA	TT3	0.00	0.00	0.09	2740	0.77	4843	0.45
ACCACGATCCAAACGACTG	-	NBR1	0.90	24.93	27.77	4.08	40.98	10.05	BraA05g35060D	Beta-glucosidase 33	2311	ACCACGATCCAAACGACTG AGTCCG-GCTAGTGTCTCAAGAGTTCA	TT3	0.00	0.00	0.14	67	0.19	56	-0.12
CATCGGAATGTTGATCCCGA	-	NBR1	0.85	80.22	93.94	2.06	80.75	39.22	BraA01g14050D	NBR1 homolog	2546	CATCGGAATGTTGATCCCGA GAAAGTGTTCGGAAGTGTCTCAAGAGTTCA	TT3	0.00	0.00	0.14	2959	5.97	279	7.49
AGGACAAAGCGACTGCTAGCT	-	NBR1	0.00	12.37	12.37	0.00	22.87	22.87	BraC07g39070D	NBR1 homolog	2576	AGGACAAAGCGACTGCTAGCT TAGTCTGTTTCGGAAGTGTCTCAAGAGTTCA	TT3	0.00	0.00	0.32	2241	1.36	5953	1.44
CAGAGAGCGTCAACAGACTGCT	-	NBR1	0.00	17.54	17.54	0.00	24.02	24.02	BraA03g46880D	NBR1 homolog	2718	CAGAGAGCGTCAACAGACTGCT AGTGTTCGGAAGTGTCTCAAGAGTTCA	TT3	0.00	0.00	0.05	2740	0.77	4843	0.45
CATCGGAATGTTGATCCCGA	-	NBR1	0.85	80.22	93.94	2.06	80.75	39.22	BraC01g16550D	NBR1 homolog	2673	CATCGGAATGTTGATCCCGA GAAAGTGTTCGGAAGTGTCTCAAGAGTTCA	TT3	0.00	0.00	0.14	7201	1.42	15409	0.96
AGGACTGAGAGTCCCGAG	-	NBR1	0.00	34.60	34.60	2.06	61.12	29.69	BraC07g47570D	Auxin-responsive protein SAUR23	26	AGGACTGAGAGTCCCGAG AGGCTGTGAGTGTCTCAAGAGTTCA	TT3	0.00	0.00	0.93	1127	0.63	454	-0.16
TTAGAACAAAGGCTCAACT	-	NBR1	0.00	47.07	47.07	4.12	53.62	13.02	BraC01g16550D	NBR1 homolog	2717	TTAGAACAAAGGCTCAACT TAGAACAAAGGCTCAACT	TT3	0.00	0.00	0.05	7201	1.42	15409	0.96
TTAGAACAAAGGCTCAACT	-	NBR1	0.00	47.07	47.07	4.12	53.62	13.02	BraC03g43120D	Auxin-responsive protein IAA2	793	TTAGAACAAAGGCTCAACT TAGAACAAAGGCTCAACT	TT3	0.00	0.00	0.05	2515	0.12	10032	-1.77
TAACACTGTTGCTTAACACT	+	NBR1	0.52	26.45	50.70	0.00	40.38	40.38	BraC01g03280D	NLP2	3196	TAACACTGTTGCTTAACACT TAGGATGTCAACAACAGTGTCTCCCT	TT3	0.00	0.00	0.14	372	-0.32	302	0.20
TTGAGATCTGTTGATTGGA	-	NBR1	0.00	15.30	15.30	0.00	21.64	21.64	BraA01g14050D	NBR1 homolog	1200	TTGAGATCTGTTGATTGGA GGCAACTTCAACAACAGTGTCTCCCT	TT3	0.00	0.00	0.09	2959	5.97	279	7.49
TCCAATAGATATGATCGGCC	-	NBR1	0.00	22.43	22.43	0.00	43.37	43.37	BraA01g14050D	NBR1 homolog	2195	TCCAATAGATATGATCGGCC TAGGAGTATTCTACATAGCCGCTCACT	TT3	0.00	0.00	0.37	2959	5.97	279	7.49
CTGCTCAAAGTGTACTGCT	-	NBR1	0.00	23.69	23.69	0.00	19.11	19.11	BraA01g14050D	NBR1 homolog	2849	CTGCTCAAAGTGTACTGCT GTCTCAAGTGTACTGCT	TT3	0.00	0.00	0.05	2959	5.97	279	7.49

Table S27: va-phasiRNAs produced from genes for 'TAR1' and targeting mRNAs within the gene family and other genes

va-phasiRNA ¹										Host mRNA targets ²										DE target mRNA ³			
va-phasiRNA	dsRNA (+/-) strand va-phasiRNA	Origin (gene family)	DM	DT	DT/DM reads	Normalized reads (positive / negative)	TT	TT/TTM reads	Target transcript ID	Predicted gene function	Cleavage position	vsRNA:mRNA Target pair (5' : 3')	Cleavage found in PAREseq replicates	DM	DT	TM	TT	DM	DT	TM	TT		
CCGAGAGGGGAAGGTTCCA	+	TAR1 ⁴	17.03	60.41	3.55	40.25	103.44	2.57	BnaA09g0570D	Ribulose biphosphate carboxylase small chain 1A, chloroplastic	907	CCGAAGAGGGGAAGGTTCCA o	D72 D73 TT1 TT2 TT3	0.00	548.73	0.00	135.27	329765	-1.19	100342	-0.88		
CCGAAGAGGGGAAGGTTCCA	+	TAR1	17.03	60.41	3.55	40.25	103.44	2.57	BnaA09g0570D	Ribulose biphosphate carboxylase small chain F4, chloroplastic	756	CCGAAGAGGGGAAGGTTCCA o	D72 D73 TT1 TT2	0.00	548.73	0.00	40.77	439500	-1.05	269908	-0.85		
CAACCAGCTGTAGACAGGCC	-	TAR1	18.38	32.64	1.78	75.89	103.29	1.36	BnaA09g04420D	TAR1	614	CAACCAGCTGTAGACAGGCC	D72 D73 TT3	0.00	5.72	0.00	1.20	239430	-1.00	101442	-0.78		
CAACCAGCTGTAGACAGGCC	-	TAR1	18.38	32.64	1.78	75.89	103.29	1.36	BnaA09g04420D	TAR1	610	CAACCAGCTGTAGACAGGCC	D72 D73 TT3	0.00	5.72	0.00	1.20	143979	-1.14	60510	-0.80		
ACCAGCTGTAGACAGGCC	-	TAR1	10.47	56.44	5.39	56.17	124.16	2.21	BnaA09g04420D	TAR1	612	ACCAGCTGTAGACAGGCC	D72 D73 TT3	0.00	7.99	0.00	12.59	239430	-1.00	101442	-0.78		
CAACCAGCTGTAGACAGGCC	-	TAR1	18.38	32.64	1.78	75.89	103.29	1.36	BnaA09g0730D	Puative uncharacterized protein ART3	614	CAACCAGCTGTAGACAGGCC	D72 D73 TT3	0.00	5.72	0.00	1.20	32584	-0.17	17996	-0.74		
GGTAACACACGGGAGATCAGCT	-	TAR1	8.80	36.47	4.14	17.84	24.79	1.39	BnaA09g04420D	TAR1	213	GGTAACACACGGGAGATCAGCT	D72 D73 TT3	0.00	6.91	0.00	0.79	239430	-1.00	101442	-0.78		
ACCAGCTGTAGACAGGCC	-	TAR1	10.47	56.44	5.39	56.17	124.16	2.21	BnaA09g04420D	TAR1	608	ACCAGCTGTAGACAGGCC	D72 D73 TT3	0.00	7.99	0.00	12.59	143979	-1.14	60510	-0.80		
GGTAACACACGGGAGATCAGCT	-	TAR1	8.80	36.47	4.14	17.84	24.79	1.39	BnaA09g0730D	Puative uncharacterized protein ART3	213	GGTAACACACGGGAGATCAGCT	D72 D73 TT3	0.00	6.91	0.00	0.79	32584	-0.17	17996	-0.74		
GGTAACACACGGGAGATCAGCT	-	TAR1	8.80	36.47	4.14	17.84	24.79	1.39	BnaA09g22160D	TAR1	1213	GGTAACACACGGGAGATCAGCT	D72 D73 TT3	0.00	6.91	0.00	0.79	257765	-1.01	114234	-0.85		
CAACCAGCTGTAGACAGGCC	-	TAR1	18.38	32.64	1.78	75.89	103.29	1.36	BnaA09g22160D	TAR1	1614	CAACCAGCTGTAGACAGGCC	D72 D73 TT3	0.00	5.72	0.00	1.20	257765	-1.01	114234	-0.85		
GGTAACACACGGGAGATCAGCT	-	TAR1	8.80	36.47	4.14	17.84	24.79	1.39	BnaA09g04420D	TAR1	209	GGTAACACACGGGAGATCAGCT	D72 D73 TT3	0.00	6.91	0.00	0.79	143979	-1.14	60510	-0.80		
ACCAGCTGTAGACAGGCC	-	TAR1	10.47	56.44	5.39	56.17	124.16	2.21	BnaA09g0730D	Puative uncharacterized protein ART3	612	ACCAGCTGTAGACAGGCC	D72 D73 TT3	0.00	7.99	0.00	12.59	32584	-0.17	17996	-0.74		
GGGAGCTGTAGACAGGCC	-	TAR1	47.38	95.44	2.01	390.64	151.98	0.43	BnaA09g22160D	TAR1	650	GGGAGCTGTAGACAGGCC	D72 D73 TT3	0.00	14.03	0.00	2.68	257765	-1.01	114234	-0.85		
ACCAGCTGTAGACAGGCC	-	TAR1	10.47	56.44	5.39	56.17	124.16	2.21	BnaA09g22160D	TAR1	1612	ACCAGCTGTAGACAGGCC	D72 D73 TT3	0.00	7.99	0.00	12.59	257765	-1.01	114234	-0.85		
CCAGGAAGTTTGGGCAATA	+	TAR1	99.10	341.97	3.45	277.03	668.17	2.41	BnaA03g61150D	Serine hydroxymethyltransferase 1, mitochondrial	3042	CCAGGAAGTTTGGGCAATA	D72 D73 TT3	0.00	5.15	2.64	0.00	43289	-0.26	69289	-0.79		
CTCATGAGGCTGTGCTTGG	-	TAR1	0.00	28.28	28.28	2.85	109.43	38.45	BnaA06g42820D	Casein kinase II subunit beta	1443	CTCATGAGGCTGTGCTTGG	D73 TT2 TT3	0.00	9.53	0.00	78.23	1090	-0.24	960	-0.08		
CTTTCGAGTTCGGGCATAAG	-	TAR1	14.15	33.08	2.34	26.30	55.27	2.10	BnaA03g3180D	Actin-depolymerizing factor 5	146	CTTTCGAGTTCGGGCATAAG	D72 D73	0.00	6.99	0.00	0.00	91	0.95	58	-0.13		
CATCGAGGCTGTGCTTGG	-	TAR1	10.51	110.09	10.47	31.36	144.62	4.61	BnaA06g42820D	Casein kinase II subunit beta	1441	CATCGAGGCTGTGCTTGG	D72 D73	0.00	4.34	0.00	0.00	1090	-0.24	960	-0.08		
CTTTCGAGTTCGGGCATAAG	-	TAR1	14.15	33.08	2.34	26.30	55.27	2.10	BnaA03g61510D	Actin-depolymerizing factor 5	1066	CTTTCGAGTTCGGGCATAAG	D72 D73	0.00	6.99	0.00	0.00	1669	0.97	1200	-0.06		
CCACCAAGATCTGCACAGG	-	TAR1	4.36	79.19	18.17	5.35	115.18	21.52	BnaA03g20170D	unknown	130	CCACCAAGATCTGCACAGG	D72 D73	0.00	3.55	0.00	0.00	0	NA	0	NA	0	
TACTCATGAGGCTGTGCTT	-	TAR1	13.20	88.31	6.69	35.05	355.83	10.15	BnaA09g22160D	TAR1	3274	TACTCATGAGGCTGTGCTT	D72 D73	0.00	3.59	0.00	0.00	257765	-1.01	114234	-0.85		
GGGTTGCGCAAAATCGAGCT	+	TAR1	15.20	50.45	3.32	20.51	28.58	1.39	BnaA08g29260D	Nuclear pore complex protein NUP214	7841	GGGTTGCGCAAAATCGAGCT	D72 D73	0.00	4.01	0.00	0.00	126	0.74	285	0.12		
AGGCTCGATGAGTAGAGGG	+	TAR1	13.90	106.85	7.69	50.09	229.85	4.59	BnaA03g07490D	Stem-specific protein TSJ11	1821	AGGCTCGATGAGTAGAGGG	D72 D73	0.00	5.44	0.00	0.00	44213	-0.31	27325	0.63		
TACTCATGAGGCTGTGCTT	-	TAR1	15.90	52.44	3.30	35.10	189.02	5.39	BnaA09g04420D	TAR1	1720	TACTCATGAGGCTGTGCTT	D72 D73	0.00	3.59	0.00	0.00	239430	-1.00	101442	-0.78		
TACTCATGAGGCTGTGCTT	-	TAR1	13.20	88.31	6.69	35.05	355.83	10.15	BnaA09g04420D	TAR1	1720	TACTCATGAGGCTGTGCTT	D72 D73	0.00	3.59	0.00	0.00	239430	-1.00	101442	-0.78		
TACTCATGAGGCTGTGCTT	-	TAR1	15.90	52.44	3.30	35.10	189.02	5.39	BnaA09g22160D	TAR1	3274	TACTCATGAGGCTGTGCTT	D72 D73	0.00	3.59	0.00	0.00	257765	-1.01	114234	-0.85		
TTGAGAATGATGAGGAGCAT	-	TAR1	10.47	30.82	2.95	14.37	92.73	6.46	BnaA06g04090D	Dihydroxylyl dehydrogenase 1, mitochondrial	1447	TTGAGAATGATGAGGAGCAT	D72 D73	0.00	7.75	0.00	0.00	6339	-0.50	7445	-0.28		
CCACCAAGATCTGCACAGG	-	TAR1	4.36	79.19	18.17	5.35	115.18	21.52	BnaA03g56370D	unknown	130	CCACCAAGATCTGCACAGG	D72 D73	0.00	3.55	0.00	0.00	0	NA	0	NA	0	
CCGCGCTTAGTCCACCACT	-	TAR1	58.29	25.16	0.43	43.78	49.41	1.13	BnaA03g72010D	Aquaporin PIP2	15	CCGCGCTTAGTCCACCACT	D72 D73	0.00	0.27	0.00	0.09	837	-1.76	1138	-1.75		
CCACCAAGATCTGCACAGG	-	TAR1	4.36	79.19	18.17	5.35	115.18	21.52	BnaA09g04420D	TAR1	1790	CCACCAAGATCTGCACAGG	D72 D73	0.00	2.75	0.00	0.09	143979	-1.14	60510	-0.80		
CTCAAACTCTTGCTTAA	-	TAR1	18.42	29.66	1.61	26.60	49.83	1.87	BnaA02g04300D	Aspartate aminotransferase, cytoplasmic isozyme 1	3462	CTCAAACTCTTGCTTAA	D72 D73	0.00	1.42	0.00	0.28	1641	-0.15	1805	-0.03		

CCCCGAATCGATCGGGGACC	-	TAR1	25.40	67.54	2.66	47.53	195.45	4.11	Bra08h46150D	TAR1	828	CCCCGAATCGATCGGGGACC	DT3 TT3	0.00	2.36	0.00	0.32	143979	-1.14	60510	-0.80
AGATCTGCACCGAGCGCGCT	-	TAR1	0.85	15.22	17.82	3.48	33.56	9.64	Bra02g61110D	unknown	383	AGATCTGCACCGAGCGCGCT	DT3 TT3	0.00	1.41	0.00	0.69	25737	-1.12	12547	-0.80
CCGAATCGATCGGGGACCGGA	-	TAR1	51.11	48.82	0.96	88.62	213.26	2.41	BraAnn22160D	TAR1	1880	CCGAATCGATCGGGGACCGGA	DT3 TT3	0.00	2.27	0.00	1.34	257765	-1.01	114234	-0.85
AAACAACCGACTCGTAGACAG	-	TAR1	20.28	12.59	0.62	33.00	35.37	1.07	Bra08h46150D	TAR1	612	AAACAACCGACTCGTAGACAG	TT2 TT3	0.00	0.00	0.00	22.33	143979	-1.14	60510	-0.80
AACAACCCGACTCGTAGACAG	-	TAR1	20.28	12.59	0.62	33.00	35.37	1.07	BraAnn22160D	Putative uncharacterized protein ART3	616	AACAACCCGACTCGTAGACAG	TT2 TT3	0.00	0.00	0.00	22.33	32584	-0.17	17996	-0.74
AACAACCCGACTCGTAGACAG	-	TAR1	20.28	12.59	0.62	33.00	35.37	1.07	BraAnn22160D	TAR1	1616	AACAACCCGACTCGTAGACAG	TT2 TT3	0.00	0.00	0.00	22.33	257765	-1.01	114234	-0.85
AACAACCCGACTCGTAGACAG	-	TAR1	20.28	12.59	0.62	33.00	35.37	1.07	BraA09g04420D	TAR1	616	AACAACCCGACTCGTAGACAG	TT2 TT3	0.00	0.00	0.00	22.33	299490	-1.00	101442	-0.78
CTGAGGAGCGCTCTCCAGACT	-	TAR1	19.40	29.77	1.53	49.58	45.99	0.93	BraAnn00930D	unknown	1389	CTGAGGAGCGCTCTCCAGACT	DZ	0.00	1.87	0.00	0.00	2942	-0.20	2085	0.00
GTAAATAATCCGAGCGGGAAC	+	TAR1	63.63	102.89	1.62	115.62	225.72	1.95	BraA06g39060D	Pyruvate-sensitive aminopeptidase	2000	GTAAATAATCCGAGCGGGAAC	DZ	0.00	2.31	0.00	0.00	4126	1.02	7452	0.36
GGTTAGTGTGATCTTAAGAGTGG	+	TAR1	108.00	117.16	1.08	151.96	304.33	2.00	BraA08g11840D	Probable disease resistance protein Atg33300	3113	GGTTAGTGTGATCTTAAGAGTGG	DZ	0.00	0.09	0.00	0.00	5912	0.01	8859	0.28
AGAGAGCTTGTGACATGCGGT	+	TAR1	18.02	92.36	5.13	139.92	67.53	0.48	BraA09g24660D	RNA polymerase II transcriptional coactivator KLP	210	AGAGAGCTTGTGACATGCGGT	DZ	0.00	0.89	0.00	0.00	1223	0.03	1319	0.13
GMACGACTGAGAGAGATGAA	+	TAR1	14.30	132.60	9.27	113.19	241.21	2.13	BraAnn51140D	Transcription repressor OFP15	714	GMACGACTGAGAGAGATGAA	DZ	0.00	3.20	0.00	0.00	125	-1.01	21	-1.01
CGAGCTCGAGAGCGGGAAC	-	TAR1	32.30	849.78	26.31	61.44	2765.49	45.01	BraAnn22160D	TAR1	648	CGAGCTCGAGAGCGGGAAC	DZ	0.00	1.33	0.00	0.00	257765	-1.01	114234	-0.85
ATTGCCCAAACCTCTTGCC	-	TAR1	4.40	32.88	7.47	74.00	119.08	1.61	BraA10g17340D	2-hydroxyacyl-CoA lyase	1403	ATTGCCCAAACCTCTTGCC	DZ	0.00	1.69	0.00	0.00	3693	0.29	3325	0.34
GMCGCTCTGAGTCTTAGC	-	TAR1	1.75	18.31	10.46	#N/A	#N/A	#N/A	BraA04g1350D	Histone H1.2	846	GMCGCTCTGAGTCTTAGC	DZ	0.00	4.80	0.00	0.00	5973	0.67	4998	1.03
GGCCGAGAGGGGMAAGTTCC	+	TAR1	11.17	79.65	7.13	38.65	149.09	3.86	BraAnn21760D	TAR1	832	GGCCGAGAGGGGMAAGTTCC	DZ	0.00	0.18	0.00	0.00	47012	-1.01	20912	-0.79
CGAGCTCGAGAGCGGGAAC	-	TAR1	32.30	849.78	26.31	61.44	2765.49	45.01	Bra05g18830D	ADP-ribosylation factor 1	906	CGAGCTCGAGAGCGGGAAC	DZ	0.00	3.29	0.00	0.00	2747	-0.95	1994	-0.57
GTCGCTGCAAACTAGGGCC	+	TAR1	7.93	37.07	4.67	9.47	60.64	6.40	Bra02g04560D	GEM-like protein 5	1177	GTCGCTGCAAACTAGGGCC	DZ	0.00	1.78	0.00	0.00	9378	-1.30	10291	-0.23
GTCGCTGCAAACTAGGGCC	+	TAR1	7.93	37.07	4.67	9.47	60.64	6.40	BraA02g01510D	GEM-like protein 5	1141	GTCGCTGCAAACTAGGGCC	DZ	0.00	1.78	0.00	0.00	8779	-0.33	12866	0.21
GMACGACTGAGAGATGAA	+	TAR1	14.30	132.60	9.27	113.19	241.21	2.13	BraA05g08210D	Transcription repressor OFP15	761	GMACGACTGAGAGATGAA	DZ	0.00	3.20	0.00	0.00	349	-0.10	310	-1.37
AGAAATGCTGAGGACATGTC	-	TAR1	0.85	38.20	44.74	16.17	67.47	4.17	BraAnn03470D	Probable mediator of RNA polymerase II transcription subunit 37e	369	AGAAATGCTGAGGACATGTC	DZ	0.00	2.22	0.00	0.00	13013	0.10	7825	-0.55
TTCTTAGCTGGATTTTGCC	-	TAR1	203.59	289.71	1.42	2.85	1.60	0.56	Bra09g49110D	unknown	3724	TTCTTAGCTGGATTTTGCC	DZ	0.00	3.73	0.00	0.00	2447	0.25	3898	0.21
TATGGGAGGAAAGCTGATCC	+	TAR1	37.80	377.74	9.99	93.06	415.63	4.47	BraA04g38650D	Abscisic-aldehyde oxidase	4210	TATGGGAGGAAAGCTGATCC	DZ	0.00	2.04	0.00	0.00	242	0.69	592	0.85
AGGAGCTGATGGCTGGATC	+	TAR1	74.43	124.57	1.67	136.07	260.72	1.92	BraA04g27920D	Ribulose biphosphate carboxylase small chain F1, chloroplastic	800	AGGAGCTGATGGCTGGATC	DZ	0.00	2.58	0.00	0.00	153	-2.47	68959	-1.12
TAAGTTTGAGAAATAGTGA	-	TAR1	11.32	34.87	3.08	18.63	38.80	2.08	Bra01g42660D	Casein kinase II subunit alpha-2	2276	TAAGTTTGAGAAATAGTGA	DZ	0.00	4.26	0.00	0.00	3956	0.18	4929	0.14
ATTGCCCAAACCTCTTGCC	-	TAR1	62.22	86.00	1.38	382.64	140.59	0.37	Bra09g40570D	2-hydroxyacyl-CoA lyase	1394	ATTGCCCAAACCTCTTGCC	DZ	0.00	1.69	0.00	0.00	5556	0.31	6178	0.27
TGTGGCCGAGGTGTGAATCG	-	TAR1	30.41	37.07	1.22	133.79	108.00	0.81	BraA04g08110D	Apartic proteinase PCS1	934	TGTGGCCGAGGTGTGAATCG	DZ	0.00	0.09	0.00	0.00	2688	-1.34	8138	-0.73
ATGGGCGAGAGCTGATCTCC	+	TAR1	44.51	721.86	16.22	77.21	419.08	5.43	BraA07g13340D	60S acidic ribosomal protein P2-2	540	ATGGGCGAGAGCTGATCTCC	DZ	0.00	0.98	0.00	0.00	3567	-0.78	2075	-0.44
GATCTTAAGAGTGGGGGAAA	+	TAR1	16.64	52.81	3.17	33.77	88.65	2.63	BraAnn09000D	Guanylylaminyl diphosphate reductase, chloroplastic	1119	GATCTTAAGAGTGGGGGAAA	DZ	0.00	3.38	0.00	0.00	51471	-0.43	43448	-0.08
GAGCTCTGAGTCTTAGC	-	TAR1	1.75	18.31	10.46	#N/A	#N/A	#N/A	BraA09g04420D	TAR1	257	GAGCTCTGAGTCTTAGC	DZ	0.00	5.42	0.00	0.00	239430	-1.00	101442	-0.78
GTTGGCCAAATCCGAGCT	+	TAR1	2.04	24.42	12.00	6.45	13.01	2.02	Bra02g6840D	Protein TIC 55, chloroplastic	1985	GTTGGCCAAATCCGAGCT	DZ	0.00	2.31	0.00	0.00	12179	-0.22	13798	-0.01
GTTCCACCTGGCCGAGAG	+	TAR1	18.42	311.96	16.94	69.83	615.48	8.81	Bra02g09010D	Tubulin alpha-5 chain	1247	GTTCCACCTGGCCGAGAG	DZ	0.00	1.07	0.00	0.00	1652	-0.03	2624	-0.55
TCCGAGCTAAGAAAGCTCAGGA	+	TAR1	5.64	174.13	30.90	0.00	0.67	0.67	Bra09g419270D	La-related protein 6A	1022	TCCGAGCTAAGAAAGCTCAGGA	DZ	0.00	0.98	0.00	0.00	4571	0.64	4208	0.68
TATTAAGTTTGAGAAATAGG	-	TAR1	8.72	35.65	4.09	12.94	55.73	4.31	BraA06g01690D	CURVATURE THYLAKOID 1C, chloroplastic	1122	TATTAAGTTTGAGAAATAGG	DZ	0.00	4.09	0.00	0.00	58754	-0.47	33630	0.00
CGCGGTTGGCCAAATCCGAG	+	TAR1	10.50	90.11	8.58	27.48	56.01	2.04	BraA06g13930D	Probable purine permease 14	717	CGCGGTTGGCCAAATCCGAG	DZ	0.00	0.18	0.00	0.00	15550	-1.02	12616	-0.47

AGTCTATCGGTAAAGCAA	+	TAR1	9.95	15.47	1.55	44.67	30.00	0.67	BnaO2g22400D	VAN3-binding protein	1931	AGTCTATCGGTAAAGCAA GTCTTAAGATGGATATTCGGTAGGAAAT	TT3	0.00	0.00	0.00	0.19	2536	-1.03	1553	-1.35
TGTCGGCCAGAGTGTACTCG	-	TAR1	30.41	37.07	1.22	133.79	108.00	0.81	BnaO4g5960D	Aspartic proteinase PCS1	934	TGTCGGCCAGAGTGTACTCG CGTCAGCGGTGTACACATTAAGCCTGG	TT3	0.00	0.00	0.00	0.46	7524	-0.72	8197	-0.94
GATGCGCTGAAGCCGCGCAC	+	TAR1	17.62	39.44	2.24	49.46	74.32	1.50	BnaO9g33120D	unknown	555	GATGCGCTGAAGCCGCGCAC ACTTTCAGCGACTCAAGCGCTTTTGGCC	TT3	0.00	0.00	0.00	0.19	300	1.04	586	-0.15
CGCGAATTCGAAGGGGATCC	+	TAR1	130.62	185.41	1.42	284.46	587.28	2.06	BnaO2g40260D	Elongation factor 2	2663	CGCGAATTCGAAGGGGATCC TGCAGGTTTGGAGTTCTCTAGAGAGAT	TT3	0.00	0.00	0.00	0.14	2593	1.15	5719	0.28
TGGCGCTTAAAGCAAGAA	+	TAR1	31.56	157.36	4.99	128.60	450.85	3.51	BnaO3g04540D	Transmembrane 9 superfamily member 8	2084	TGGCGCTTAAAGCAAGAA TACTCTGCAAACTCTTCTTCACTCC	TT3	0.00	0.00	0.00	0.05	1131	0.47	1631	0.04
AGCTCGGATTTGGCCACCG	-	TAR1	52.80	148.67	2.82	378.81	63.63	0.17	BnaHng36730D	Putative uncharacterized protein ART3	239	AGCTCGGATTTGGCCACCG GGAAATCGAGCTAAACAGGTTGGCGACGCC	TT3	0.00	0.00	0.00	0.05	32384	-0.17	17996	-0.74
ACCGATAGAACTGTTCCG	-	TAR1	1.80	15.70	8.75	24.85	22.98	0.92	BnaO2g28770D	Dihydroflavonol-4-reductase	1212	ACCGATAGAACTGTTCCG GGCTGCGCTATTTTGGCGTGGCAGGCGCT	TT3	0.00	0.00	0.00	0.14	42	-0.32	17	-0.45
TTGTCGGTGTACAAGACA	-	TAR1	3.42	5.42	1.59	13.06	30.96	2.37	BnaO8g46150D	TAR1	1005	TTGTCGGTGTACAAGACA GAGGAACACCGCAAAAGTCTCTCAAGCTA	TT3	0.00	0.00	0.00	0.79	143979	-1.14	60510	-0.80
GACTCTAGAGTCACTAAC	-	TAR1	0.85	30.23	35.40	6.14	42.37	6.90	BnaO8g46150D	TAR1	1886	GACTCTAGAGTCACTAAC GGAGGATGATCTCAGGTAATGGGTACAG	TT3	0.00	0.00	0.00	0.23	143979	-1.14	60510	-0.80
CCTACTATCAGGCGCTGGCT	-	TAR1	6.20	10.18	1.64	20.50	28.76	1.40	BnaO9g04420D	Pentatricopeptide repeat-containing protein A1:lg60770	1722	CCTACTATCAGGCGCTGGCT GGGAGGATGATCTCAGGTAATGGGTACAG	TT3	0.00	0.00	0.00	0.74	239430	-1.00	101442	-0.78
TGTTGAGCATCCAGGAAATC	+	TAR1	19.17	20.14	1.05	27.45	36.82	1.34	BnaO1g22570D	unknown	721	TGTTGAGCATCCAGGAAATC GAAATGCTAGCTCTCACTACTACTACTAGG	TT3	0.00	0.00	0.00	0.19	14	-0.14	16	-0.16
TAGGTTAGCGCGAGTTGGCCA	-	TAR1	0.90	4.72	5.26	1.42	23.80	16.73	BnaO8g46150D	TAR1	1540	TAGGTTAGCGCGAGTTGGCCA CAAGATCAATGGCGTCAACCGTGCAT	TT3	0.00	0.00	0.00	0.28	143979	-1.14	60510	-0.80
CGAGTCCGACAGCGGCAACC	-	TAR1	32.30	848.78	26.31	61.44	2765.49	45.01	BnaO3g45530D	Probable plastid-lipid-associated protein 11	2170	CGAGTCCGACAGCGGCAACC CAGAGTCCGACGCTCTGCTTACAGGACAC	TT3	0.00	0.00	0.00	0.14	277	0.27	300	-0.06
ATCGATGCGCGACCGATTG	-	TAR1	14.16	15.28	1.08	43.14	32.82	0.76	BnaO7g50850D	Cytokinin dehydrogenase 4	2548	ATCGATGCGCGACCGATTG ATCGATGCGCGACCGATTG	TT3	0.00	0.00	0.00	0.14	0	NA	1	0.02
TAGAGAGCGCTCGTGTGCGA	-	TAR1	0.85	2.64	3.09	3.70	14.08	3.80	BnaO8g46150D	TAR1	598	TAGAGAGCGCTCGTGTGCGA TAGAAGCGCTCTGCTGCGA	TT3	0.00	0.00	0.00	2.55	143979	-1.14	60510	-0.80
CCTACTATGAGCGCTGGCT	-	TAR1	6.20	10.18	1.64	20.50	28.76	1.40	BnaHng22160D	TAR1	3276	CCTACTATGAGCGCTGGCT GGGAGGATGATCTCAGGTAATGGGTACAG	TT3	0.00	0.00	0.00	0.74	257765	-1.01	114234	-0.85
AAACAACCCAGCTGTAGACA	-	TAR1	3.50	10.58	3.02	30.53	25.16	0.82	BnaHng36730D	Putative uncharacterized protein ART3	617	AAACAACCCAGCTGTAGACA AGGGTTTGGCGTGTAGACTCTCTCGGAA	TT3	0.00	0.00	0.00	2.45	32384	-0.17	17996	-0.74
TAGGTTAGCGCGAGTTGGCC	-	TAR1	0.00	7.41	7.41	4.27	21.52	5.04	BnaHng22160D	TAR1	3098	TAGGTTAGCGCGAGTTGGCC CAGATCAATGGCGTCAACCGTGCAT	TT3	0.00	0.00	0.00	0.51	143979	-1.14	60510	-0.80
ACCACCAAGCTGACCCAGCG	-	TAR1	0.00	15.07	15.07	0.00	71.22	71.22	BnaO8g46150D	TAR1	1791	ACCACCAAGCTGACCCAGCG ATGATGCTGCTTCACTACTACTACTACTAGG	TT3	0.00	0.00	0.00	0.19	70	-0.07	89	-0.71
ATTCCTGGGATGGCTGCAACA	-	TAR1	0.00	4.70	4.70	2.47	33.52	13.59	BnaO9g05890D	ROOT PRIMORDIUM DEFECTIVE 1	665	ATTCCTGGGATGGCTGCAACA ACGAAGGATCTACAGAGGCTGCAAGCT	TT3	0.00	0.00	0.00	0.09	1351	0.57	1550	0.23
GTGAGGACANTGCGTCCCGA	-	TAR1	0.00	2.46	2.46	1.42	21.25	14.94	BnaO2g16050D	NUCLEAR FUSION DEFECTIVE 4	116	GTGAGGACANTGCGTCCCGA CTGAGACGCTCTGCTGCTC	TT3	0.00	0.00	0.00	0.14	47012	-1.01	20912	-0.79
CCCATCTCTGAGGATATG	+	TAR1	1.41	105.00	74.53	6.22	132.85	21.37	BnaHng21760D	TAR1	2493	CCCATCTCTGAGGATATG CAGGGGGTAGGAGGCTCTTACCCTGCT	TT3	0.00	0.00	0.00	0.09	355	0.46	518	-0.10
GAAGATCAAGTCTGGTGGCTG	-	TAR1	0.00	9.38	9.38	0.00	28.61	28.61	BnaOng62280D	Rab3 GTPase-activating protein catalytic subunit	3713	GAAGATCAAGTCTGGTGGCTG GGCTCTACTGCTGCTGCTGCTGCTGCTG	TT3	0.00	0.00	0.00	0.19	257765	-1.01	114234	-0.85
TTTGTGGGTTTAGGTTAGCG	-	TAR1	6.25	16.23	2.60	5.35	19.64	3.67	BnaHng22160D	TAR1	3109	TTTGTGGGTTTAGGTTAGCG TGGGAACACCAAGATCAATCGCGCTCAA	TT3	0.00	0.00	0.00	0.23	143979	-1.14	60510	-0.80
CGTAGACGCGCTGCTGCTG	-	TAR1	8.63	2.33	0.27	14.74	29.31	1.99	BnaO8g46150D	TAR1	600	CGTAGACGCGCTGCTGCTG CTGAGCATCTGCGGAGACACCTGCTCC	TT3	0.00	0.00	0.00	0.19	143979	-1.14	60510	-0.80
TTTGTGGGTTTAGGTTAGCG	-	TAR1	6.25	16.23	2.60	5.35	19.64	3.67	BnaO8g46150D	TAR1	1551	TTTGTGGGTTTAGGTTAGCG TGGGAACACCAAGATCAATCGCGCTCAA	TT3	0.00	0.00	0.00	0.19	143979	-1.14	60510	-0.80
AACTCTTGGCTTAACGGCC	-	TAR1	1.71	25.61	15.00	2.66	162.61	61.21	BnaHng22160D	TAR1	344	AACTCTTGGCTTAACGGCC GAGTGAAGGAAAGGATTCGGATACAG	TT3	0.00	0.00	0.00	0.09	257765	-1.01	114234	-0.85
TCAAGAGCTCTGAGCTCT	-	TAR1	0.00	0.15	0.15	20.88	23.56	1.13	BnaO4g03780D	Beta-glucosidase 26, peroxisomal	2001	TCAAGAGCTCTGAGCTCT ATGAAGTTGCAAGACTCAGAGCAACCTA	TT3	0.00	0.00	0.00	0.05	5922	0.21	2492	-0.85
TAAAGCAATGATAGAGGCA	+	TAR1	28.49	23.41	0.82	30.16	41.57	1.38	BnaOng67370D	unknown	363	TAAAGCAATGATAGAGGCA GCCATTGCTTACTACTCTGCTGCTGCTG	TT3	0.00	0.00	0.00	0.05	3342	-1.03	1416	-1.00
ACTTGAAGGGATCGGTT	+	TAR1	26.97	28.31	1.05	78.82	65.73	0.83	BnaOng33930D	unknown	246	ACTTGAAGGGATCGGTT TAGTAAAGGAGGATGAGGCA	TT3	0.00	0.00	0.00	0.09	936	-0.10	801	0.20
TAGTAAAGGAGGATGAGGCA	-	TAR1	0.00	7.41	7.41	4.27	21.52	5.04	BnaOng04420D	TAR1	1544	TAGTAAAGGAGGATGAGGCA CAGATCACTGCGCTCAACCGTGCAT	TT3	0.00	0.00	0.00	0.28	239430	-1.00	101442	-0.78
ACTCTTAGACTCACTAAC	-	TAR1	6.07	16.29	2.69	25.01	20.45	0.79	BnaO9g04420D	TAR1	1889	ACTCTTAGACTCACTAAC ACTTAGATGATCTACTGATGATGATACAGT	TT3	0.00	0.00	0.00	0.32	239430	-1.00	101442	-0.78
CGAGCTAAGAGACTCAGAGCG	+	TAR1	#N/A	#N/A	#N/A	28.61	63.94	2.24	BnaO9g52700D	Receptor-like protein kinase 2	89	CGAGCTAAGAGACTCAGAGCG CTGCTGATCACTGAGGAGGCG	TT3	0.00	0.00	0.00	0.42	542	-0.14	431	-0.36
CAAGATGCAAGGAGCGCG	-	TAR1	0.85	16.10	18.85	1.23	30.11	24.40	BnaO2g36110D	unknown	385	CAAGATGCAAGGAGCGCG GAGTCTGAGCTGAGAGGCG	TT3	0.00	0.00	0.00	0.32	25737	-1.12	12547	-0.80
AAACCCGACTGACAGCGCC	-	TAR1	3.50	5.68	1.62	11.53	41.18	3.57	BnaO8g46150D	TAR1	609	AAACCCGACTGACAGCGCC TTGTTGGGCTGAGCATCTCTGCGAGCAC	TT3	0.00	0.00	0.00	0.93	143979	-1.14	60510	-0.80

TAGTGTAGCGCGAGTGTGGC	-	TAR1	0.00	7.41	7.41	4.27	21.52	5.04	BnaO08g46150D	TAR1	1540	TAGTGTAGCGCGAGTGTGGC CAAGATCAATCGGGGTCAACCCGTGGCAT	TT3	0.00	0.00	0.28	143979	-1.14	60510	-0.80
GGCGACCGGATTCCTCGTTC	-	TAR1	134.30	88.02	0.66	64.08	173.69	2.71	BnaO08g46150D	TAR1	814	GGCGACCGGATTCCTCGTTC TCCGCGCTGGCTTAACGACAAAGCGGTAGA	TT3	0.00	0.00	0.23	143979	-1.14	60510	-0.80
CGACTCTTAGAGTGAAGTAAACC	-	TAR1	9.70	106.91	11.02	27.24	232.10	8.52	BnaO04g05970D	Ribose-phosphate pyrophosphokinase 1, chloroplastic	2640	CGACTCTTAGAGTGAAGTAAACC TGCTGTGAATCTGCTGAATTTTCTGT	TT3	0.00	0.00	0.32	1146	-0.07	1096	-0.33
ACCAAGATCTCACCGAAGCGC	-	TAR1	17.58	123.69	7.04	38.09	209.00	5.49	BnaO02g36110D	unknown	387	ACCAAGATCTCACCGAAGCGC ATGTTGTTCTAGAGTGGCTTGGGAGGG	TT3	0.00	0.00	0.14	25737	-1.12	12547	-0.80
TIAGCGCGAGTGTGGCACCG	-	TAR1	5.35	58.26	10.89	11.87	135.48	11.42	BnaO02g36110D	unknown	137	TIAGCGCGAGTGTGGCACCG ATCAATTTGGCTTACACCCGCGGATTTGGC	TT3	0.00	0.00	0.28	25737	-1.12	12547	-0.80
TCTAATATTGGCTTTACCGA	-	TAR1	2.61	3.78	1.43	14.77	32.25	2.18	BnaO09g04420D	unknown	1382	TCTAATATTGGCTTTACCGA ACCGAGATTAAGTAAACCGAATGGGCTACTTG	TT3	0.00	0.00	0.28	239430	-1.00	101442	-0.78
GACTCTAGGATGCACTAAC	-	TAR1	0.85	30.23	35.40	6.14	42.37	6.90	BnaO02g36110D	unknown	485	GACTCTAGGATGCACTAAC GGGCTGGAATCTCTAGTGTGGTACAG	TT3	0.00	0.00	0.23	25737	-1.12	12547	-0.80
GATCTCCGTTGTTACCGA	+	TAR1	28.71	186.86	6.51	44.09	119.75	2.72	BnaO03g22460D	Zinc finger CCH domain-containing protein 29	1554	GATCTCCGTTGTTACCGA ACTCTTAGGCGCAAGTATGSGGCTCCAGGT	TT3	0.00	0.00	0.23	1862	-0.79	1591	-0.23
TTCAATGTGAACGCACTTGC	+	TAR1	78.01	77.99	1.07	163.72	124.07	0.76	BnaO03g11200D	Probable IHR receptor-like serine/threonine-protein kinase ALG63430	2637	TTCAATGTGAACGCACTTGC TTCATGTGAACGCACTTGC	TT3	0.00	0.00	0.05	419	0.11	479	-0.07
AGATCTGACCGGCGGCGCT	-	TAR1	0.85	15.22	17.82	3.48	33.56	9.64	BnaO09g03360D	Calmodulin-4	270	AGATCTGACCGGCGGCGCT AGATCTCACCGAAGCGGCT	TT3	0.00	0.00	0.14	1215	-1.27	641	-0.30
TGCGGAAGGATGATTTGTA	+	TAR1	289.94	497.11	1.71	1953.41	384.34	0.20	BnaO05g01900D	unknown	2982	TGCGGAAGGATGATTTGTA TGGGGAAGATCATGTCGTGA	TT3	0.00	0.00	0.14	0	0.26	0	-0.25
ACCGATAGAACTGTTCCG	-	TAR1	1.80	15.70	8.75	24.85	22.98	0.92	BnaO02g07420D	Subtilisin-like protease SBT4.9	3700	ACCGATAGAACTGTTCCG GCTTGGCTTACTTGGCTTGGCAAGCGCT	TT3	0.00	0.00	0.14	2	-0.54	1	0.09
AAACAACCCGACTGTAGACA	-	TAR1	3.50	10.58	3.02	30.53	25.16	0.82	BnaO02g16080D	F-box protein ALG50450	823	AAACAACCCGACTGTAGACA CGTGTGTGGCTGGGCTTAGTGGTGA	TT3	0.00	0.00	0.19	7727	0.91	8707	0.46
CCACCAGATGTCACGACG	-	TAR1	4.36	79.19	18.17	5.35	115.18	21.52	BnaO06g03610D	Mellicase-like transcription factor CHR27	4217	CCACCAGATGTCACGACG CGATTCACCTTGGCGAAG	TT3	0.00	0.00	0.37	293	0.43	545	0.14
AAANTGCCCCTGAGACTCT	-	TAR1	4.45	6.53	1.47	0.00	25.41	25.41	BnaO08g46150D	TAR1	1470	AAANTGCCCCTGAGACTCT TGGTTTTACCGGTAACCTCGAGACTAAG	TT3	0.00	0.00	0.14	143979	-1.14	60510	-0.80
AACTCTTGGCTTAACGGCC	-	TAR1	1.71	25.61	15.00	2.66	162.61	61.21	BnaO06g40090D	Homeobox-leucine zipper protein HAT1	835	AACTCTTGGCTTAACGGCC CAAGTGAAG-GAAGCGTGGCTGGAAGACA	TT3	0.00	0.00	0.09	2137	0.10	3490	-0.76
GTCCGCAAGTGTGAACTCG	-	TAR1	6.92	52.47	7.58	4.08	91.32	22.39	BnaA0ng2160D	TAR1	435	GTCCGCAAGTGTGAACTCG GGAACCGGCTTCACTGAGGAACTAT	TT3	0.00	0.00	0.23	257765	-1.01	114234	-0.85
AGTCAACCTTGGCGAAG	+	TAR1	12.69	45.00	3.55	122.06	75.33	0.62	BnaA10g30630D	Ankyrin repeat-containing protein ALG02620	651	AGTCAACCTTGGCGAAG AGTCAACCTTGGCGAAG	TT3	0.00	0.00	0.09	577	1.97	2083	0.61
TTGGCTTACCGATGAACTC	-	TAR1	4.31	66.36	15.39	9.24	217.09	23.49	BnaO09g04420D	TAR1	1354	TTGGCTTACCGATGAACTC TAGTACGAAATGGGCTTCTGASCAAAAG	TT3	0.00	0.00	0.09	239430	-1.00	101442	-0.78
ATCGAGCGCTGGCTTGGCC	-	TAR1	57.01	79.21	1.39	214.29	161.12	0.75	BnaA0ng2160D	TAR1	3369	ATCGAGCGCTGGCTTGGCC TGAATGCTCGGACGAAAGCAAGCGGCGCC	TT3	0.00	0.00	0.14	257765	-1.01	114234	-0.85
ACGCCGATGATCGATGGCGGA	-	TAR1	6.16	10.09	1.64	3.70	48.21	13.03	BnaO08g31010D	unknown	1134	ACGCCGATGATCGATGGCGGA GAGCTCGGCTTACTTGGCTGATGAGA	TT3	0.00	0.00	0.05	430	0.80	710	0.16
GAGCTCTGATTCGTTGGATG	-	TAR1	0.00	8.18	8.18	2.06	28.99	14.08	BnaA0ng2160D	TAR1	3013	GAGCTCTGATTCGTTGGATG GAACTCGAGGCTAAGGCACTCTACCGAGTT	TT3	0.00	0.00	0.05	257765	-1.01	114234	-0.85
CGTCTGCGACGTGGGAGAA	+	TAR1	464.02	597.62	1.29	1711.42	900.63	0.53	BnaO02g16080D	F-box protein ALG50450	650	CGTCTGCGACGTGGGAGAA TGTGGAAGCGCTGCAAGCTCTGCGGCA	TT3	0.00	0.00	0.23	7727	0.91	8707	0.46
AAACCGACTGTAGACAGCC	-	TAR1	14.23	78.93	5.55	102.12	105.59	1.03	BnaA0ng2160D	TAR1	1613	AAACCGACTGTAGACAGCC TTGTTGGGCTGAGCATCTGCGGAGCAC	TT3	0.00	0.00	0.33	257765	-1.01	114234	-0.85
TCTAAGAGTCGGGGAAACC	+	TAR1	297.22	291.49	0.98	406.86	528.42	1.30	BnaO04g38970D	Transcription factor LHW	3803	TCTAAGAGTCGGGGAAACC TCAAGGCTTACGCTTTTCTTTGTTA	TT3	0.00	0.00	0.05	869	-0.64	775	-0.30
AGTCTATCGGGTAAAGCCAA	+	TAR1	9.95	15.47	1.55	44.67	30.00	0.67	BnaO0ng6730D	unknown	375	AGTCTATCGGGTAAAGCCAA AGCTTCTGGCTTACGCTTTTCTTTGTTA	TT3	0.00	0.00	0.09	3342	-1.03	1416	-1.00
ACGGAACTGAGACTCGAAGT	+	TAR1	1236.13	1339.37	1.08	2708.65	2249.48	0.83	BnaO03g64120D	Vacuolar protein sorting-associated protein 28 homolog 1	899	ACGGAACTGAGACTCGAAGT TGTGGAAGCGCTGCAAGCTCTGCGGCA	TT3	0.00	0.00	0.05	2249	-0.12	2417	0.72
TATGGACGAACTGATCTC	+	TAR1	37.80	377.74	9.99	93.06	415.63	4.47	BnaO04g12310D	Membrane metalloprotease ARASP, chloroplastic	287	TATGGACGAACTGATCTC AAACCGACTGTAGACA	TT3	0.00	0.00	0.09	6283	-0.85	4246	-0.12
AAAGAACCAGCTGTAGACA	-	TAR1	3.50	10.58	3.02	30.53	25.16	0.82	BnaO08g46150D	TAR1	613	AAAGAACCAGCTGTAGACA AGGTTGTTGGCTGAGATCTGCGGAG	TT3	0.00	0.00	0.245	143979	-1.14	60510	-0.80
TTGCTCAACTCTTGGCT	-	TAR1	14.87	20.28	1.36	75.69	83.48	1.10	BnaA0ng2160D	TAR1	352	TTGCTCAACTCTTGGCT CAATAGAGTGGGAGCAAGGATGGC	TT3	0.00	0.00	0.32	257765	-1.01	114234	-0.85
TTAATGACCAACACCTTG	-	TAR1	3.55	10.61	2.98	4.08	20.18	4.95	BnaA0ng36730D	Puative uncharacterized protein ART3	1572	TTAATGACCAACACCTTG GTCCGACGACAGAAATATGCTGTGGG	TT3	0.00	0.00	0.14	32584	-0.17	17956	-0.74
GTCTGCTTAAATGACC	-	TAR1	0.00	31.04	31.04	15.75	50.98	3.24	BnaA0ng36730D	Puative uncharacterized protein ART3	1583	GTCTGCTTAAATGACC GTCCGACGACAGAAATATGCTGTGGG	TT3	0.00	0.00	0.19	32584	-0.17	17956	-0.74
CAANTGAAACTGTAAAGCCA	+	TAR1	23.01	34.98	1.52	59.69	41.18	0.69	BnaO08g47040D	unknown	389	CAANTGAAACTGTAAAGCCA CAACAAGATCTGACGACG	TT3	0.00	0.00	0.14	127	-1.10	34	-1.09
CCACCAGATCTGACGACG	-	TAR1	34.10	23.72	0.70	82.59	103.97	1.26	BnaO02g36110D	unknown	389	CCACCAGATCTGACGACG TGAATGGCTTACGCTGCTGGAG	TT3	0.00	0.00	0.09	25737	-1.12	12547	-0.80
TGTGGCCAAAGTGTGAAC	-	TAR1	32.29	149.93	4.64	148.96	290.43	1.95	BnaO09g17830D	Glutathione gamma-glutamylcysteinyltransferase 1	1136	TGTGGCCAAAGTGTGAAC GCAACA-CCGTTCCGATGGGCGCCACCG	TT3	0.00	0.00	0.05	1	-0.47	1	0.32

Table S28: TuMV vsrRNAs associated with vRNA cleavage in Drakkar

vsrRNA	(-) strand	vsrRNA mean reads	vsrRNA mean reads (rpm)	Cleavage Position	vsrRNA:vRNA target pair (5' - 3' - 3' - 5')	Fragment signatures	Fragment signatures (rpm)
TTTCATCTGGATGTGTGCTC	Y	1994	186	10231		12238	203.96
ATCAGCCAATACACCTTCAA	Y	1620	151	9868		3508	58.46
CTGAGCTGGTCTCTATCAA	Y	439	41	9431		861	14.35
TTTTGGCTCTCGTTCCTTT	Y	2108	197	9606		573	9.55
TTTTGGCTCTCGTTCCTTT	Y	166	16	9606		573	9.55
TTTTGGCTCTCGTTCCTTT	Y	1716	160	9605		541	9.02
TTTTGGCTCTCGTTCCTTT	Y	324	30	9605		541	9.02
CATCTCAATCTCAAAGA	Y	3525	329	9479		494	8.23
TGGTCTCTCTCTCAGGTAT	Y	689	64	2475		240	4.00
TCCTCTCTCTCTCTGCG	Y	1626	152	9570		225	3.75
TCCTCTCTCTCTCTGCG	Y	165	15	9570		225	3.75
TCCTCTCTCTCTCTGCG	Y	466	44	9572		206	3.43
CTCTCTCTCTCTCTGCG	Y	544	51	9562		180	3.00
TTCTCTCTCTCTCTGCG	Y	2016	188	9596		113	1.88
AGCTTCTCAGGCTGTTCC	Y	419	39	9405		102	1.70
TTTTGGCTCTCGTTCCTTT	Y	2108	197	9585		60	1.00
TTTTGGCTCTCGTTCCTTT	Y	166	16	9585		60	1.00
AGTAATCTCTCTCTCTCT	Y	398	37	8372		54	0.90
CAGATCCCTCTCTCTGTC	Y	1880	176	9171		47	0.78
TTTTGGCTCTCGTTCCTTT	Y	1716	160	9584		46	0.77
TTTTGGCTCTCGTTCCTTT	Y	324	30	9584		46	0.77
CAACTTTGTTTCAAGTATTT	Y	349	33	8421		41	0.68
CAACTTTGTTTCAAGTATTT	Y	271	25	8421		41	0.68
CAITGGAAATTTAGTTTTCT	Y	181	17	6692		37	0.62
CATTCGATCAGTTTGGCA	Y	211	20	425		35	0.58
TCCTCTCTCTCTGCGTCT	Y	2016	188	9566		32	0.53
CACCTCTACCCATTTTGT	Y	415	39	6721		29	0.48
CACCTCTACCCATTTTGT	Y	102	10	6721		29	0.48
ATTCATCAGTGACATAATT	Y	168	16	8302		23	0.38
TGACTTTGAAGTCTTTCAA	Y	418	39	5387		22	0.37
CTCTCTCTCTCTCTGGG	Y	104	10	10073		19	0.32
CCTCTCTCTCTCTGCT	Y	1573	147	9569		18	0.30
TGACTTTGAAGTCTTTCAA	Y	418	39	5913		16	0.27
AACTTTGTTTCAAGTATTT	Y	654	61	8420		13	0.22
TGCAGAAAATCTCAGGATC	Y	5840	546	6865		13	0.22
CTTTAATCGTTTTGTATGT	Y	805	75	35		1	0.02

Drakkar-specific

Table S29: TuMV vsRNAs associated with vRNA cleavage in Tanto

vsRNA	(-) strand	vsRNA mean reads	vsRNA mean reads (rpm)	Cleavage Position	vsRNA-vRNA target pair (5'-3', 3'-5')	Fragment signatures	Fragment signatures (rpm)
TTTTCACTGGATGTGGCTTC	Y	1619	150	10231	TTTTCACTGGATGTGGCTTC	7682	123.22
CTCTTCTCGCCCTGCTTTC	Y	476	44	9562	CTCTTCTCGCCCTGCTTTC	6006	96.34
ATACGCAATACAGCTTCAAA	Y	1396	130	9868	ATACGCAATACAGCTTCAAA	4111	65.94
CAGTGTGCTGCTTTCATCTG	Y	413	38	10243	CAGTGTGCTGCTTTCATCTG	1494	23.96
TTTGGCTCTCGTTCCTTTC	Y	1240	115	9605	TTTGGCTCTCGTTCCTTTC	1144	18.35
CATCTTCAATAATCTCAAGA	Y	2767	257	9479	CATCTTCAATAATCTCAAGA	889	14.26
CTTAGCTGCTGCTTCTTCAA	Y	248	23	9431	CTTAGCTGCTGCTTCTTCAA	435	6.98
TTTGGCTCTCGTTCCTTTC	Y	1471	137	9606	TTTGGCTCTCGTTCCTTTC	426	6.83
TTTTGCTCTCGTTCCTTTC	Y	195	18	9606	TTTTGCTCTCGTTCCTTTC	426	6.83
TCCTCTCTCGTTCCTTTC	Y	350	33	9572	TCCTCTCTCGTTCCTTTC	176	2.82
TCCTCTCTCGTTCCTTTC	Y	113	10	9572	TCCTCTCTCGTTCCTTTC	176	2.82
TCCTCTCTCGTTCCTTTC	Y	1208	112	9570	TCCTCTCTCGTTCCTTTC	144	2.31
TCCTCTCTCGTTCCTTTC	Y	246	23	9570	TCCTCTCTCGTTCCTTTC	144	2.31
TCGATCTGCTGCTTCAAGTAT	Y	411	38	2475	TCGATCTGCTGCTTCAAGTAT	144	2.31
GTCTCTGATCTTGAATCT	Y	673	63	1182	GTCTCTGATCTTGAATCT	125	2.01
TCCTCTCTCGTTCCTTTC	Y	1377	128	9566	TCCTCTCTCGTTCCTTTC	100	1.60
CTCTCTCTCGTTCCTTTC	Y	1072	100	9569	CTCTCTCTCGTTCCTTTC	89	1.43
TGTTGAGTTTTATATTTT	Y	460	43	12	TGTTGAGTTTTATATTTT	89	1.43
TGTTGAGTTTTATATTTT	Y	431	40	12	TGTTGAGTTTTATATTTT	89	1.43
TGTTGAGTTTTATATTTT	Y	209	19	15	TGTTGAGTTTTATATTTT	79	1.27
TTATGTTGAGTTTTATAT	Y	4284	398	15	TTATGTTGAGTTTTATAT	79	1.27
CAACTTGTTCAGTATTTCT	Y	190	18	8421	CAACTTGTTCAGTATTTCT	52	0.83
CAACTTGTTCAGTATTTCT	Y	186	17	8421	CAACTTGTTCAGTATTTCT	52	0.83
AACCTTGTTCAGTATTTCT	Y	308	29	8420	AACCTTGTTCAGTATTTCT	48	0.77
AGCTTCTCAGCGGCTTCTCC	Y	273	25	9405	AGCTTCTCAGCGGCTTCTCC	44	0.71
TTTGGCTCTCGTTCCTTTC	Y	1240	115	9584	TTTGGCTCTCGTTCCTTTC	22	0.35
CAGATTCCTCTCTTGTGTC	Y	1483	138	9171	CAGATTCCTCTCTTGTGTC	20	0.32
AGTAATCTCTCTTCTTCTT	Y	288	27	8372	AGTAATCTCTCTTCTTCTT	18	0.29
TTTTGCTCTCGTTCCTTTC	Y	1471	137	9585	TTTTGCTCTCGTTCCTTTC	17	0.27
TTTTGCTCTCGTTCCTTTC	Y	195	18	9585	TTTTGCTCTCGTTCCTTTC	17	0.27
TATGTGAGTTTTATAT	Y	172	16	14	TATGTGAGTTTTATAT	16	0.26
AGGAGCTTCCCTCTGTGTC	Y	431	40	9376	AGGAGCTTCCCTCTGTGTC	12	0.19
ATGTTGAGTTTTATATTTT	Y	346	32	13	ATGTTGAGTTTTATATTTT	12	0.19
ATTCATCAGTGAATTAAT	Y	129	12	8302	ATTCATCAGTGAATTAAT	9	0.14
TTTTCTTTAACGTGTGCTTC	Y	2742	255	8056	TTTTCTTTAACGTGTGCTTC	8	0.13
CAITCGATAGGTTTTGCGA	Y	148	14	425	CAITCGATAGGTTTTGCGA	8	0.13
AAGAATCTGATGATGCTGT	Y	205	19	8997	AAGAATCTGATGATGCTGT	7	0.11
TTTGAATCAATCAAAATG	Y	10697	993	8229	TTTGAATCAATCAAAATG	6	0.10
AGAATTTGTATCCCAATCC	Y	326	30	3798	AGAATTTGTATCCCAATCC	6	0.10
AGAATTTGTATCCCAATCCG	Y	744	69	3798	AGAATTTGTATCCCAATCCG	6	0.10
CACCTCTACCCATTTTGT	Y	251	23	6721	CACCTCTACCCATTTTGT	5	0.08
GGGATCTTCGAAGGGCA	Y	160	15	1849	GGGATCTTCGAAGGGCA	5	0.08
CTTATGCTGGATTTCTGGG	Y	1966	183	2331	CTTATGCTGGATTTCTGGG	4	0.06
CTTATGCTGGATTTCTGGGA	Y	188	17	2331	CTTATGCTGGATTTCTGGGA	4	0.06
TGAGGAATCTGATGATG	Y	161	15	9002	TGAGGAATCTGATGATG	3	0.05
TTTTCTTTAACGTGTGCTTC	Y	2742	255	8055	TTTTCTTTAACGTGTGCTTC	3	0.05
CGACTTTGAAGTCTTTCAA	Y	330	31	5912	CGACTTTGAAGTCTTTCAA	3	0.05
CGAGATCTCTCTTTTGTG	Y	117	11	9172	CGAGATCTCTCTTTTGTG	2	0.03
TGTTCTCGAGTGTGATCT	Y	1070	99	6350	TGTTCTCGAGTGTGATCT	2	0.03
TTTGAATCAATCAAAATG	Y	10697	993	5301	TTTGAATCAATCAAAATG	2	0.03
AGAGATTTCAAAAGCCAAC	Y	312	312	3597	AGAGATTTCAAAAGCCAAC	2	0.03
GTTCCTCAGTGTGAATAA	Y	133	12	1373	GTTCCTCAGTGTGAATAA	2	0.03
CTTAACTGTTTTGTATGT	Y	1154	107	35	CTTAACTGTTTTGTATGT	2	0.03
TGACTTTGAAGTCTTTCAA	Y	330	30	5913	TGACTTTGAAGTCTTTCAA	1	0.02
TGAGAACTTTGTGACACAG	Y	175	16	4508	TGAGAACTTTGTGACACAG	1	0.02
TGCTCGGAATGTCTCTGCT	Y	4206	391	4422	TGCTCGGAATGTCTCTGCT	1	0.02
TGCTCGGAATGTCTCTGCT	Y	295	27	4422	TGCTCGGAATGTCTCTGCT	1	0.02

Table S33: Oligonucleotide adapters and primers used for 5'RACE analysis

	Name	Nucleic acid sequences (5' - 3')	Gene annotations
5' RACE adapter	5'RACE Adapter	GCUGAUGGCGAUGAAUGAACACACUGUUUUGCUGGCUUUUGAUGAAA	-
5' RACE adapter primers	5'RACE outer primer	GCTGATGGCGATGAATGAACACTG	-
	5'RACE inner primer	CGCGGATCCGAACACTGCGTTTGCTGGCTTTGATG	-
	Gene-specific primers	TTTCTCCTCTTCTCCGC	ARF10
	BnaA07g13830D-1	CITTTCTCCTCTTCTCCGCCTC	
	BnaA07g13830D-2	GGGAGAAAGCGAAGACAGT	SCL6
	BnaAnng18540D-1	GTCGGGAGAAAGCGAAGACAGTG	AGO2
	BnaAnng18540D-2	CACCATAAGTAGTCTCCGCTC	AGO2
	BnaCnng68320D-1	CCATTACATAATGCAGTCTCTGCTCC	TAO1
	BnaA05g14760D-1	GACCAACCTTCCCTG	
	BnaA09g14980D-1	CACACAGGTTTCATCAAAGG	
	BnaA09g14980D-2	GTTTGGTTCAGACACAATGAAACG	BLOS2
	BnaCnng44780D-1	CGATGTTGATGATGACGACACTCAG	
	BnaCnng44780D-2	CATGAGAGAAAGGTTGGAAGC	APETALA 2

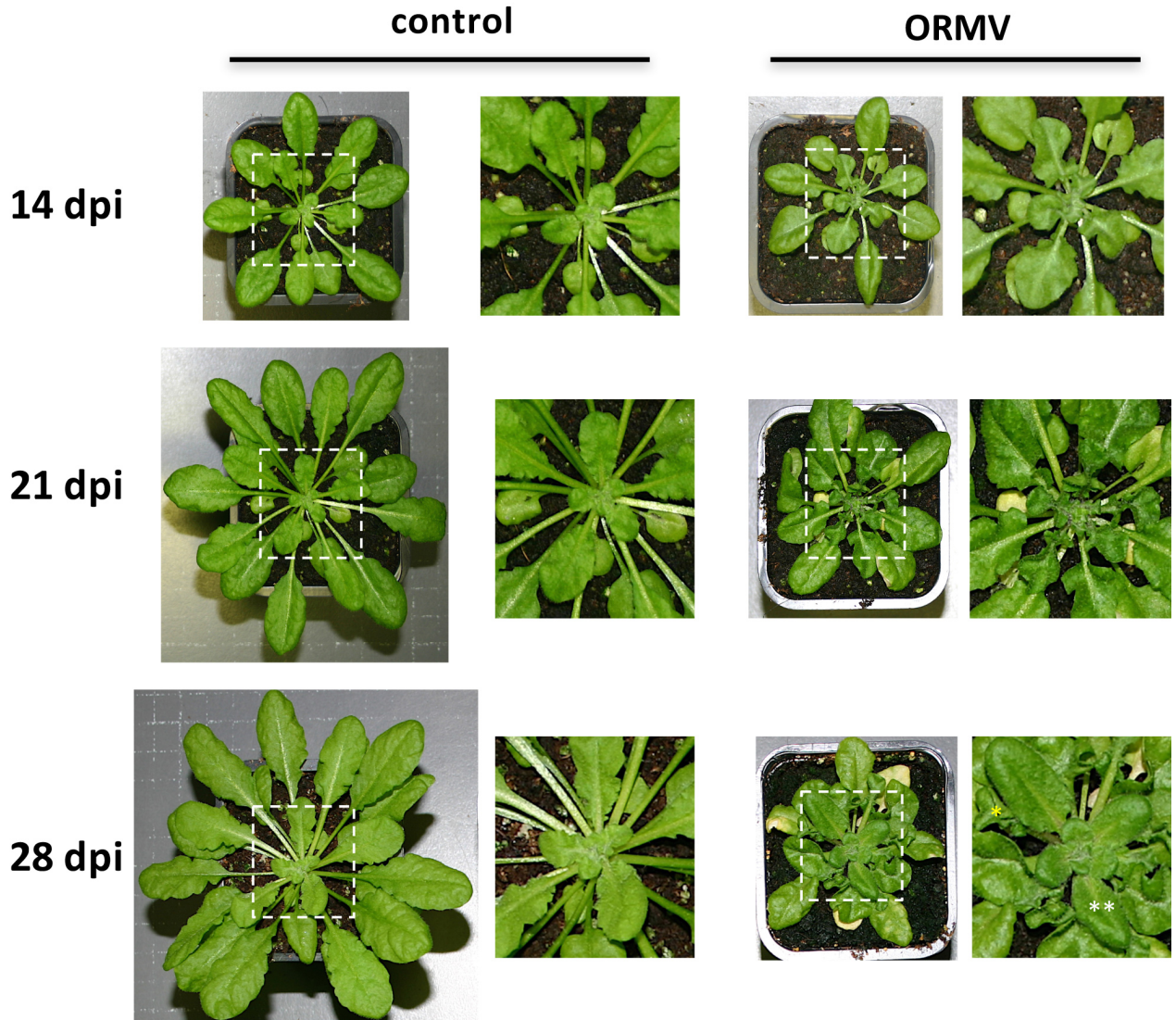
**APPENDIX 2: SUPPLEMENTARY FIGURES AND TABLES OF PUBLICATION:
“CROSSTALK BETWEEN PTGS AND TGS PATHWAYS IN NATURAL ANTIVIRAL
IMMUNITY AND DISEASE RECOVERY” KØRNER ET AL. 2018**

In the format provided by the authors and unedited.

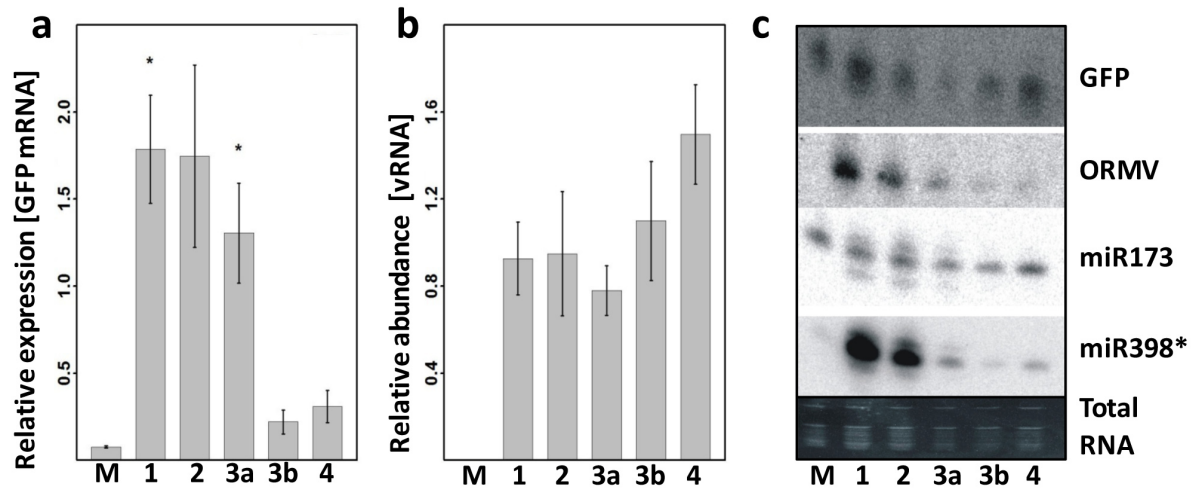
Crosstalk between PTGS and TGS pathways in natural antiviral immunity and disease recovery

Camilla Julie Kørner¹, Nicolas Pitzalis², Eduardo José Peña^{2,3}, Mathieu Erhardt², Franck Vazquez^{1,4} and Manfred Heinlein ^{1,2*}

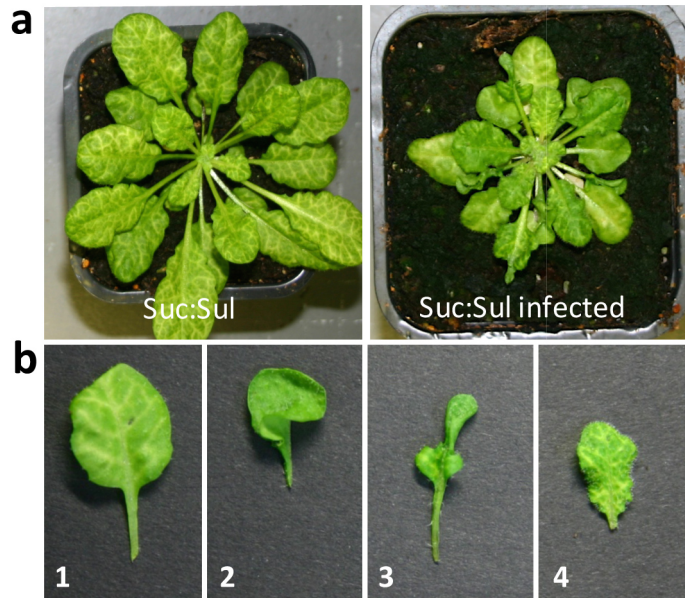
¹Zurich-Basel Plant Science Center, Department of Environmental Sciences, University of Basel, Basel, Switzerland. ²Université de Strasbourg, CNRS, IBMP UPR 2357, Strasbourg, France. Present address: ³Instituto de Biotecnología y Biología Molecular, Facultad de Ciencias Exactas, UNLP-CONICET, La Plata, Buenos Aires, Argentina. ⁴MDPI, Basel, Switzerland. *e-mail: manfred.heinlein@ibmp-cnrs.unistra.fr



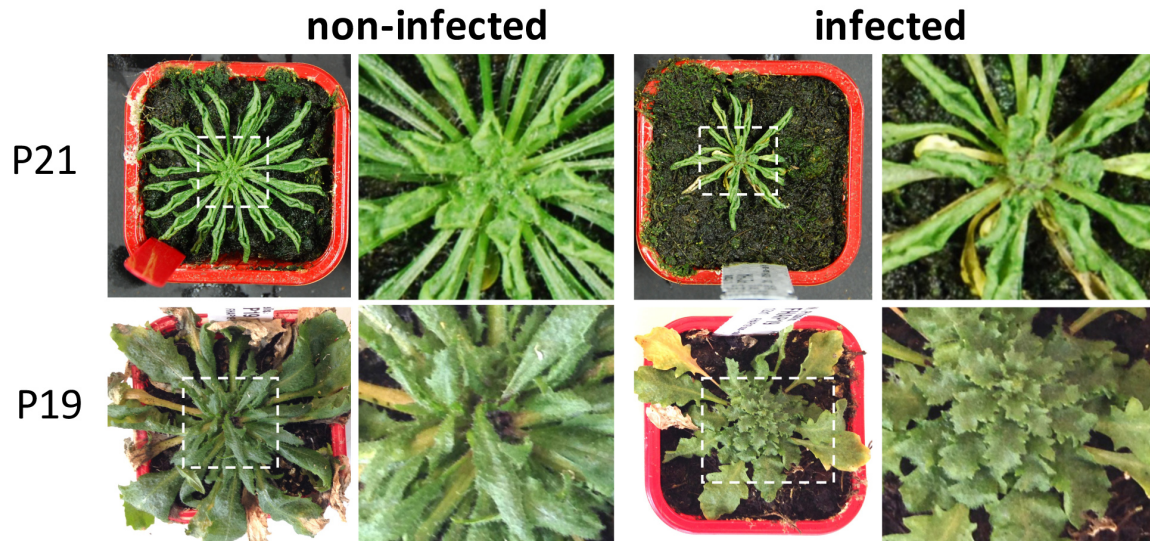
Supplementary Figure S1. Symptoms and symptom recovery during ORMV infection in Arabidopsis. Non-infected control plants and ORMV-infected plants at 14, 21, and 28 dpi. Whole plants and enlarged central parts (within the area delimited by white rectangle) are shown. As has been reproduced in several recovery experiments, leaves emerging of infected plants at 21 dpi show strong symptoms, whereas leaves emerging at 28 dpi and onwards are recovered and are free of symptoms. Examples of symptomatic and recovered leaves are labeled with one yellow and two white asterisks, respectively.



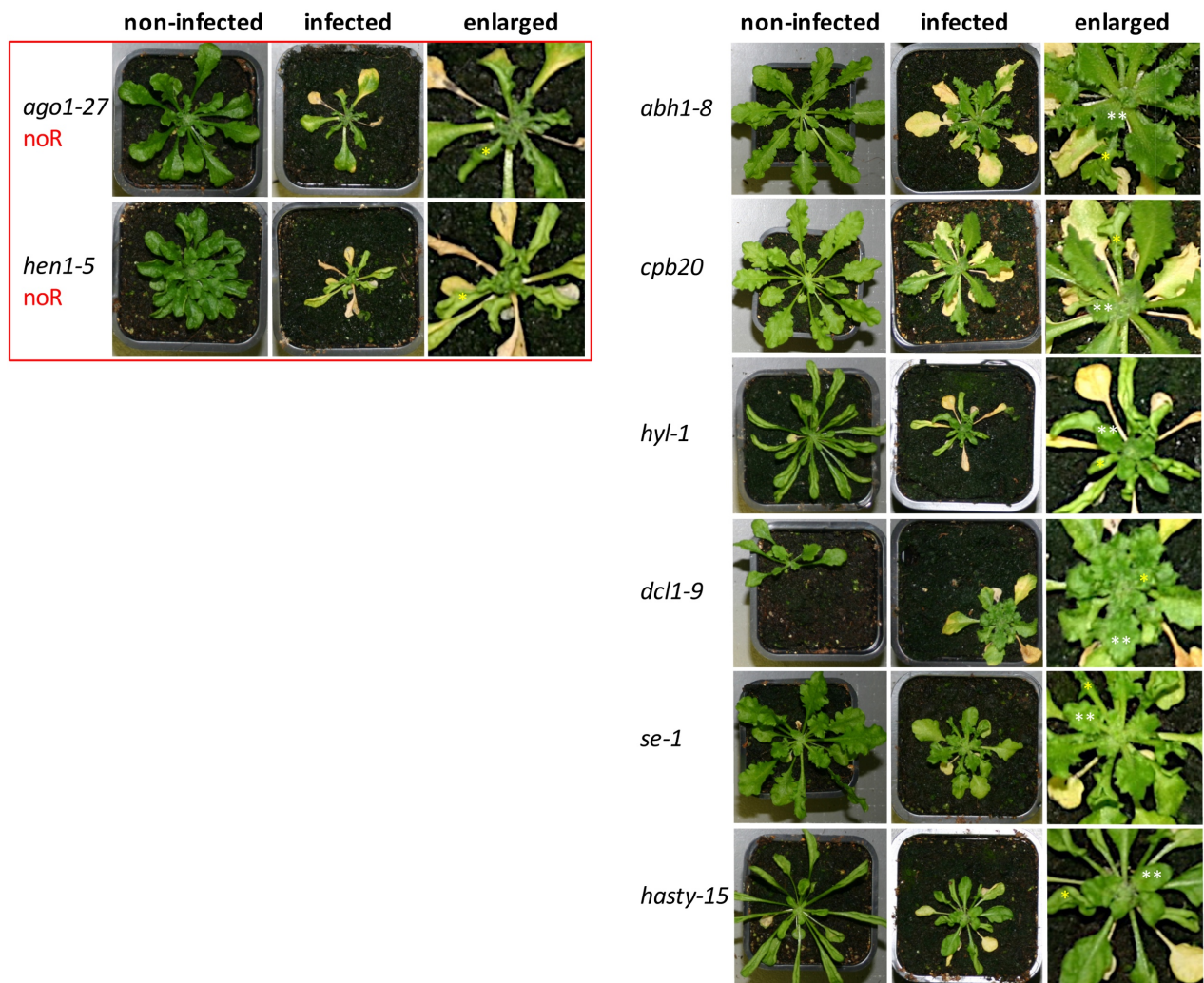
Supplementary Figure S2. Analysis of STs in L8z2 plants. Accumulation of GFP mRNA (a) and viral RNA (b) in leaves of the different STs, measured by RT-qPCR; $n = 3 \pm SE$, Student's t-test * $p < 0.05$. The level of GFP mRNA (a) in ST3a tissue was similar as in the other fluorescent symptom types (ST1 and ST2) and clearly higher than in mock-inoculated tissues. In contrast, GFP mRNA levels were similar to mock in the recovered, non-fluorescent tissues of ST3b and ST4. The amount of viral RNA (b) was similar in all infected tissues. (c), Northern blot showing the levels of GFP-derived siRNAs (GFP) and vsiRNAs (ORMV) as well as of miR173 and miR398*, in leaves of the different STs. Similar vsiRNA levels occur also in the different STs of infected wild type Col-0 plants (not shown). Stained total RNA is shown as loading control. M, mock.



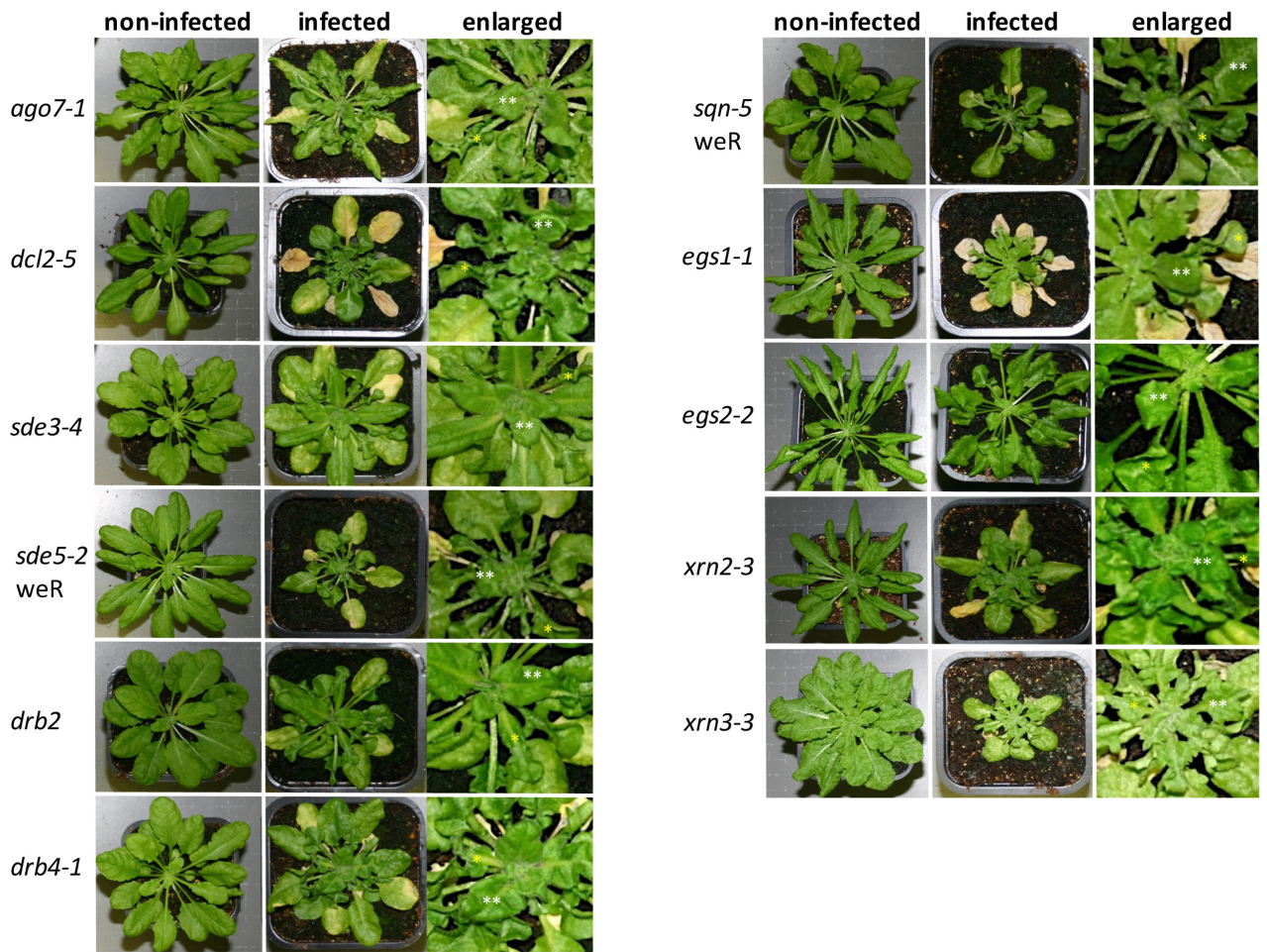
Supplementary Figure S3. Symptoms, recovery, and correlation with viral silencing suppression in ORMV-infected *Arabidopsis* Suc:Sul plants. (a), Non-infected and ORMV-infected Suc:Sul plants. **(b)** Examples of individual leaf STs of an infected Suc:Sul plant at 28 dpi. The virus suppresses vein bleaching (silencing of the *SULFUR* gene) in ST2 leaves, and partly also in ST3 leaves, whereas there is no suppression of *SULFUR* silencing in recovered ST4 leaves. These observations have been reproduced in several recovery experiments.



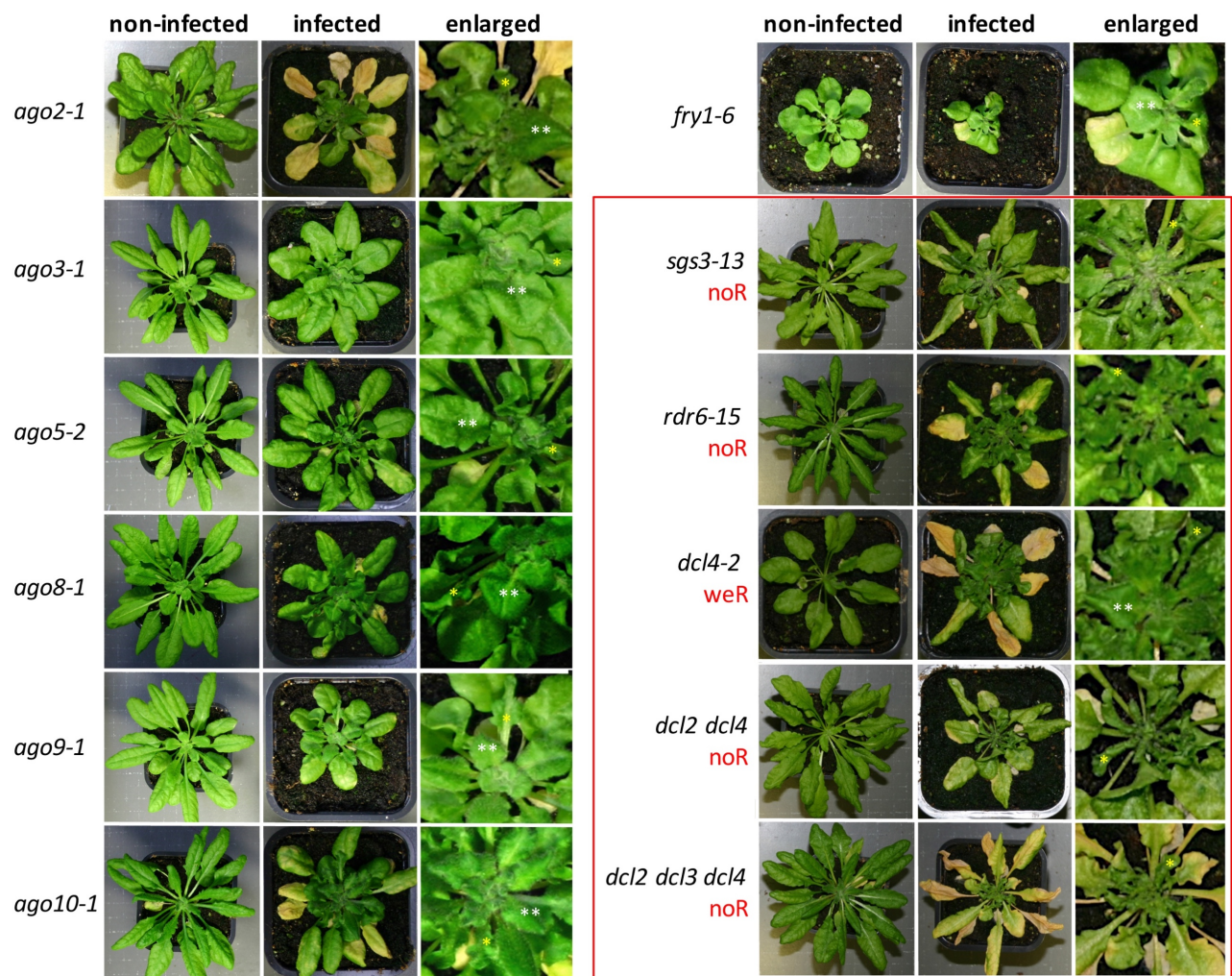
Supplementary Figure S4. Suppression of recovery in VSR-expressing transgenic plants. Examples of non- infected and ORMV-infected plants expressing either closterovirus P21-VSR or the tombusvirus P19-VSR. Plant areas within the dashed rectangles are shown enlarged. Neither P21 nor P19 plants allow disease recovery.



Supplementary Figure S5. Recovery phenotypes of Arabidopsis mutants. Non-infected and ORMV-infected plants at 28 dpi. The central parts of the infected plants are shown enlarged. Infected plants are usually stunted and are thus smaller than non-infected plants of the same age. For size comparison between infected and non-infected plants the pot size can serve as a reference. In the enlarged images, examples of symptomatic and recovered leaves are labelled with one (*) and two (**) asterisks, respectively. *ago1-27* and *hen1-5* mutants (left) impaired in components shared by several endogenous sRNA pathways do not show recovery. Mutants impaired in the biogenesis of miRNAs (right) recover normally. noR, no recovery.

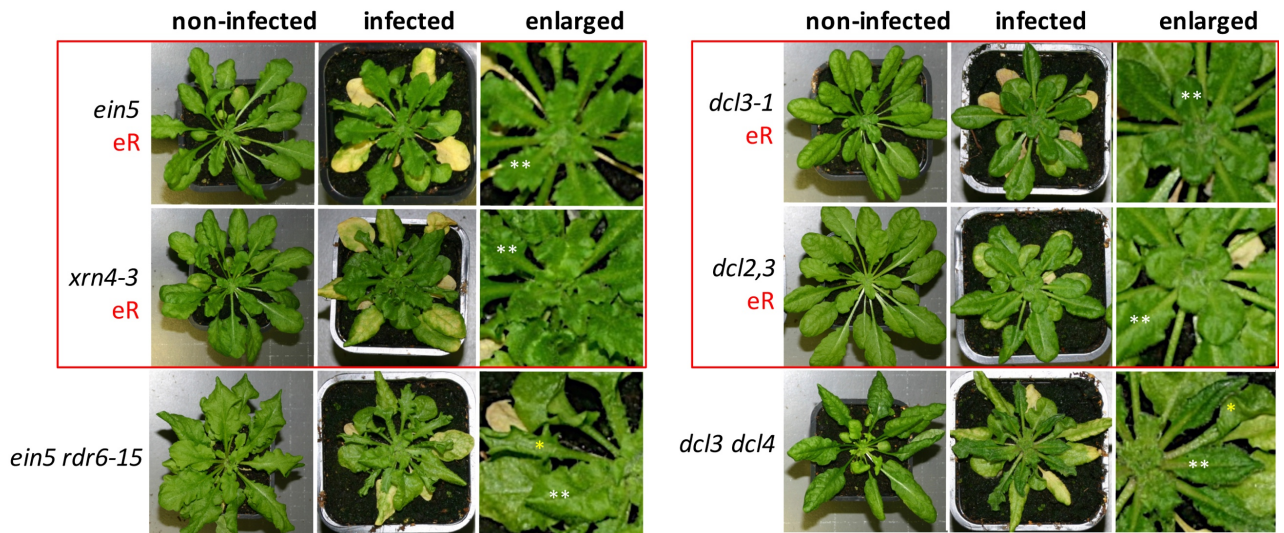


Supplementary Figure S6. Recovery phenotypes of *Arabidopsis* mutants impaired in the biogenesis of various classes of siRNAs. Non-infected and ORMV-infected plants at 28 dpi. The central parts of the infected plants are shown enlarged. Infected plants are usually stunted and are thus smaller than non-infected plants of the same age. For size comparison between infected and non-infected plants the pot size can serve as a reference. In the enlarged images, examples of symptomatic and recovered leaves are labelled with one (*) and two (**) asterisks, respectively.



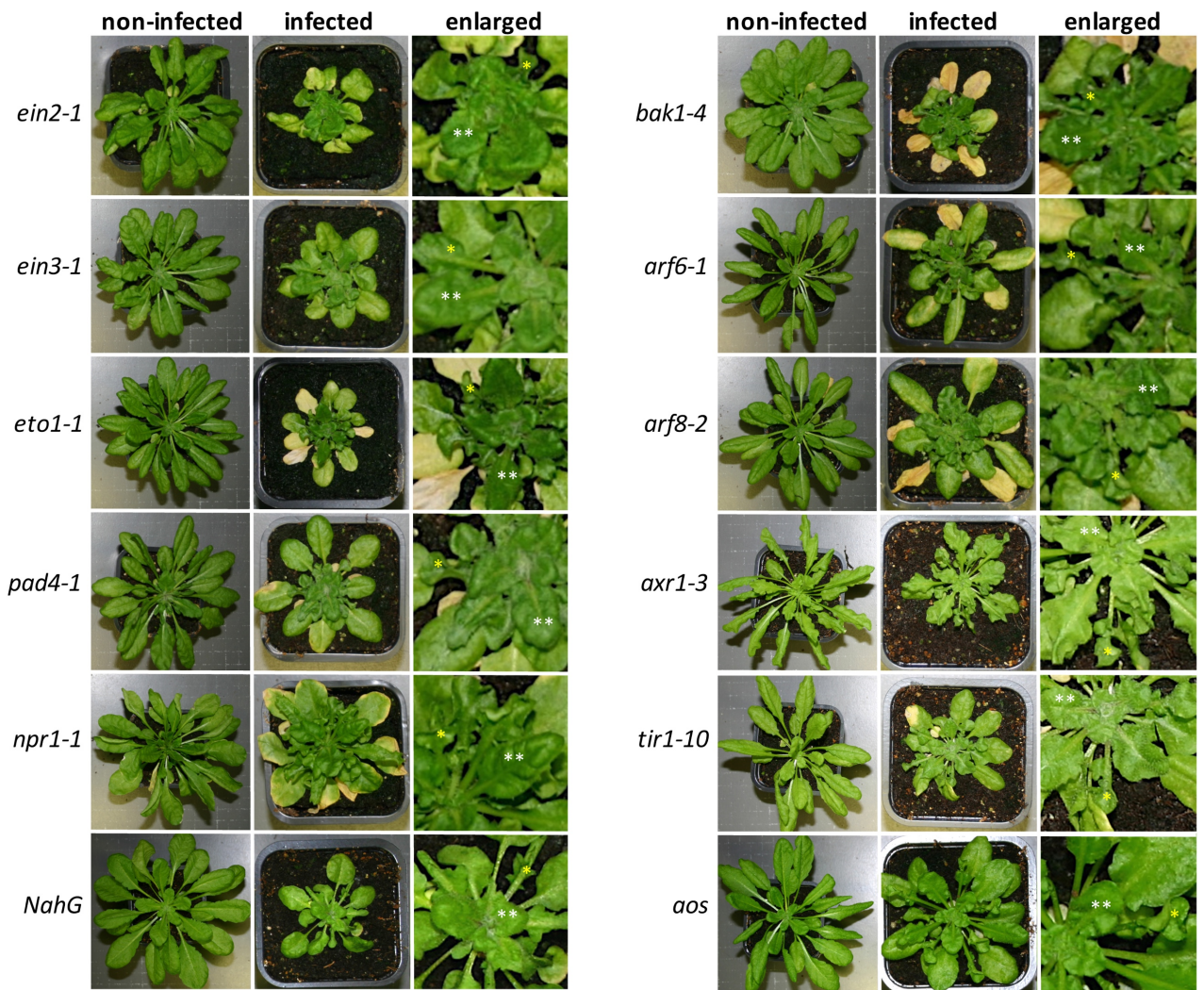
Supplementary Figure S7. Recovery phenotypes of Arabidopsis mutants impaired in the biogenesis of various classes of siRNAs. Non-infected and ORMV-infected plants at 28 dpi. The central parts of the infected plants are shown enlarged. Infected plants are usually stunted and are thus smaller than non-infected plants of the same age. For size comparison between infected and non-infected plants the pot size can serve as a reference. In the enlarged images, examples of symptomatic and recovered leaves are labelled with one (*) and two (**) asterisks, respectively.

Mutants affected in general factors needed for the production and amplification of various classes of siRNAs do not recover (*rdr6-15* and *sgs3-13*) or recover weakly (*dcl4-2*). noR; no recovery; weR, weak (delayed) recovery.



Supplementary Figure S8. Recovery phenotypes of Arabidopsis mutants affecting the steady state level of siRNAs. Non-infected and ORMV-infected plants at 28 dpi. The central parts of the infected plants are shown enlarged. Infected plants are usually stunted and are thus smaller than non-infected plants of the same age. For size comparison between infected and non-infected plants the pot size can serve as a reference. In the enlarged images, examples of symptomatic and recovered leaves are labelled with one (*) and two (**) asterisks, respectively.

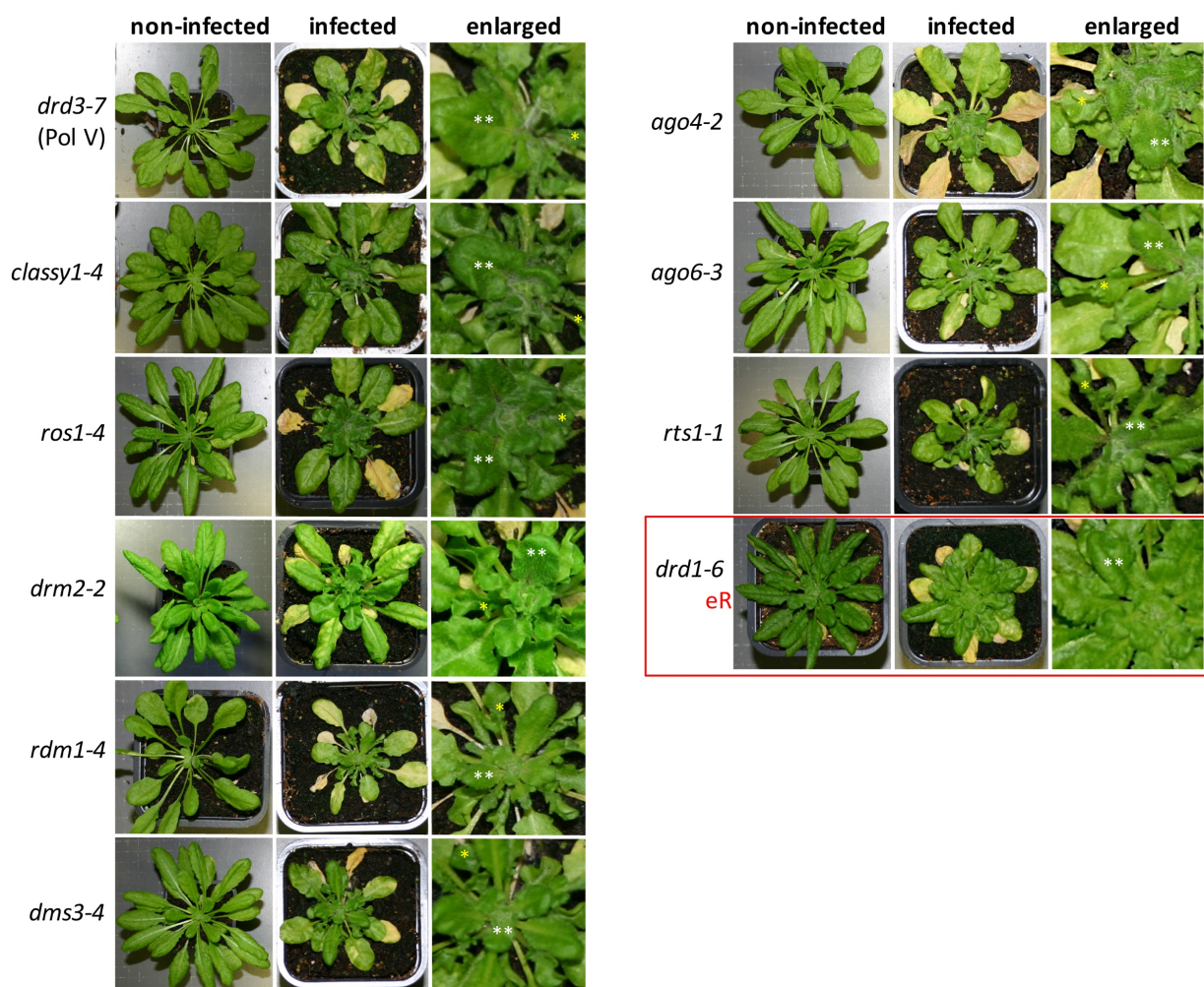
ein5 and *xrn4-3* mutants show enhanced (early) recovery (eR). This effect is RDR6-dependent as shown by normal recovery of the *ein5 rdr6-15* double mutant. *dcl3-1* single and *dcl2 dcl3* double mutants also show enhanced (early) recovery. This effect is DCL4-dependent, since the *dcl3 dcl4* double mutant recovers normally.



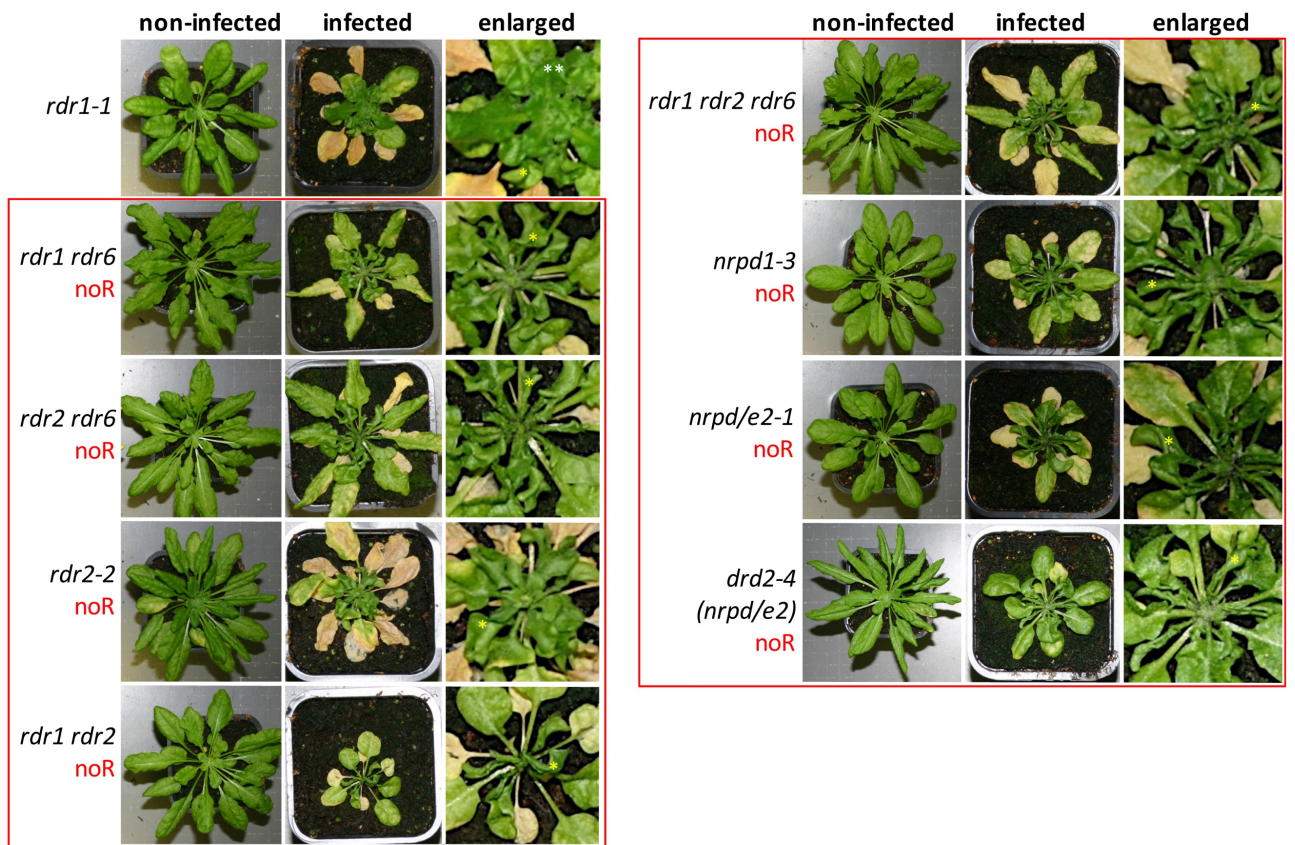
Supplementary Figure S9. Recovery phenotypes of *Arabidopsis* mutants affected in ethylene, salicylic acid (SA), jasmonic acid (JA) and auxin synthesis and signaling recover normally. Non-infected and ORMV-infected plants at 28 dpi. The central parts of the infected plants are shown enlarged. Infected plants are usually stunted and are thus smaller than non-infected plants of the same age. For size comparison between infected and non-infected plants the pot size can serve as a reference. In the enlarged images, examples of symptomatic and recovered leaves are labelled with one (*) and two (**) asterisks, respectively.

Supplementary Figures S10 and S11. Recovery phenotypes of Arabidopsis TGS mutants acting up- or downstream of DCL3. Non-infected and ORMV-infected plants at 28 dpi. The central parts of the infected plants are shown enlarged. Infected plants are usually stunted and are thus smaller than non-infected plants of the same age. For size comparison between infected and non-infected plants the pot size can serve as a reference. In the enlarged images, examples of symptomatic and recovered leaves are labelled with one (*) and two (**) asterisks, respectively.

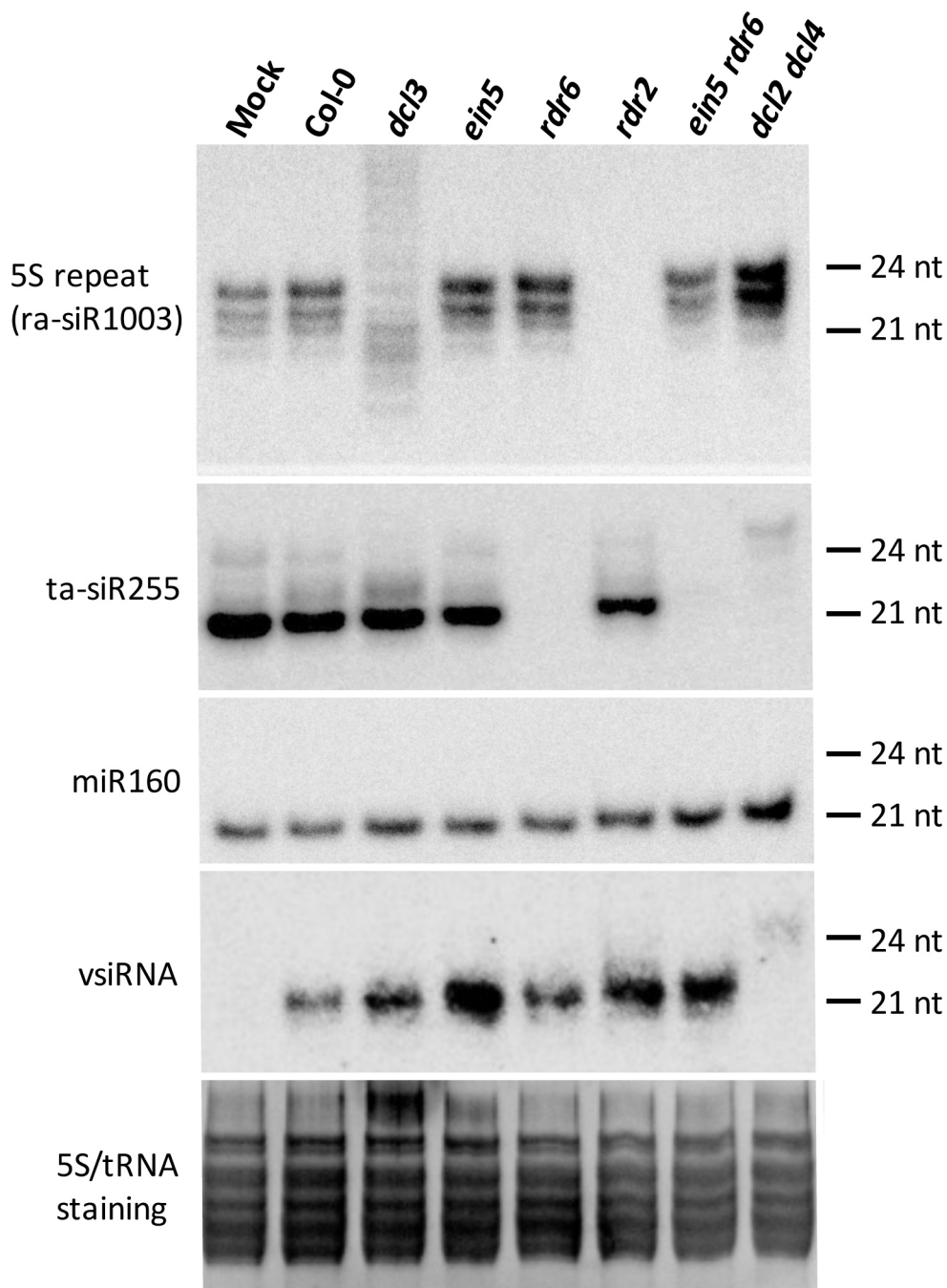
Mutants more directly involved in chromatin remodeling and DNA methylation (e.g. *rdm1*, *drd3*, *classy1*, *drm2*, *dms3*, *rts1*, *ago4*, *ago6*, *ros1*) recover normally. However, *rdr2-2* and several Pol IV-subunit mutants (*nrpd1-3*, *nrpd/e2-1*, *drd2-4*) do not recover. *drd1* shows enhanced (early) recovery. The DRD1 gene encodes a subunit of the chromatin-remodeling complex that mediates the recruitment of Pol IV and Pol V to chromatin. Enhanced recovery in the *drd1* mutant may indicate that the recruitment of Pol IV to chromatin competes with the role of Pol IV in recovery. eR, enhanced (early) recovery; noR, no recovery.



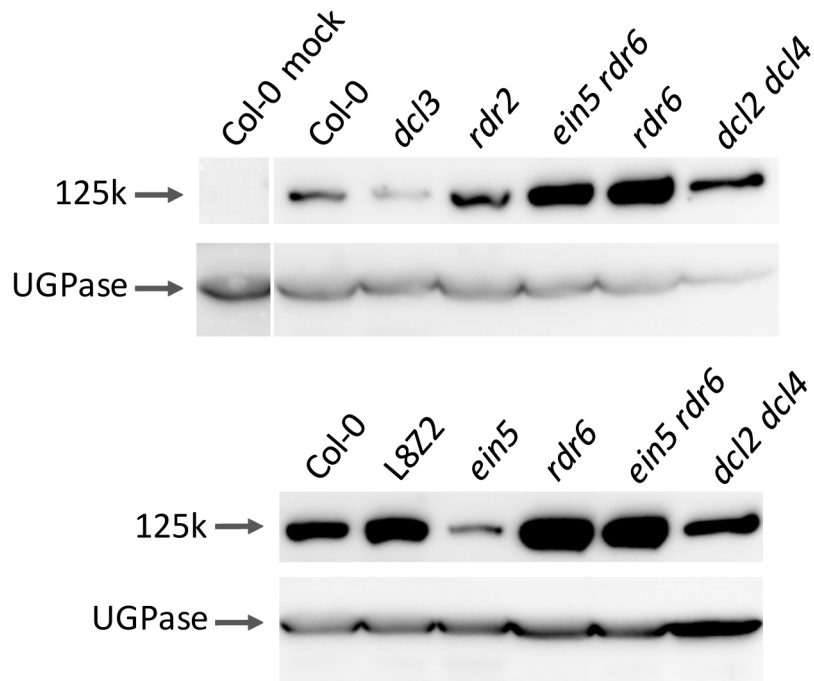
Supplementary Figure S10 (legend above)



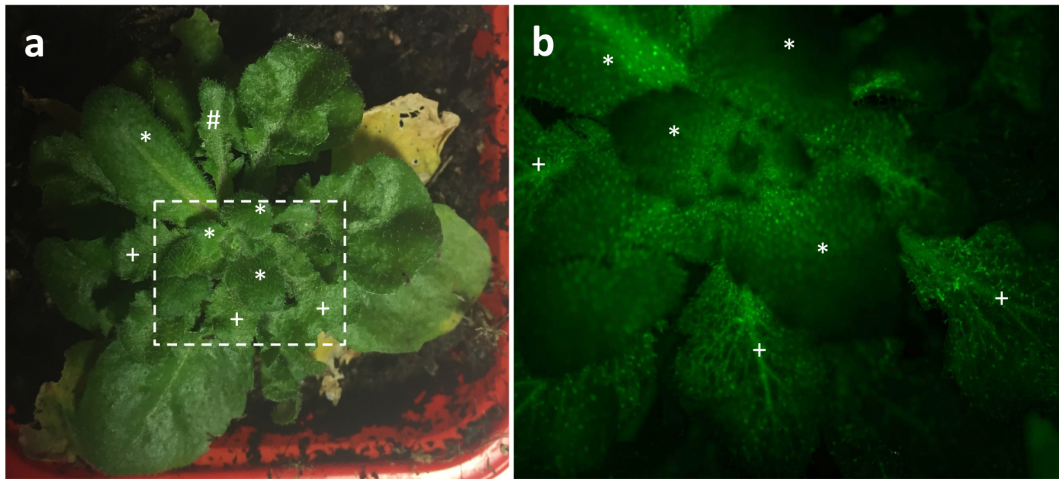
Supplementary Figure S11 (legend above)



Supplementary Figure S12. sRNA analysis of ORMV-infected Col-0 wild type plants and silencing pathway mutants. sRNA species in recovered ST4 (Col-0, *dcl3*, *ein5*, *ein5 rdr6*) and corresponding non-recovered leaves of mutants (*rdr6*, *rdr2*, *dcl2 dcl4*), in which recovery is absent, were analyzed. The analysis was performed with the same RNA samples also used for viral RNA analysis (Fig. 1d). The mutants affected the accumulation of specific sRNA species as expected and shown previously⁹. None of the mutants affected the accumulation of miR160. The accumulation of 5S rDNA repeat-derived ra-siR1003 was affected in *dcl3* and *rdr2* mutants but not in *rdr6* mutants, whereas the production of tasiR255 was affected in *rdr6*, *ein5 rdr6*, and *dcl2 dcl4* mutants but not in *rdr2* or *dcl3* mutants. As is also expected, production of vsRNAs was abolished in *dcl2 dcl4*, as is consistent with the lack of recovery in this double mutant. Relative to Col-0 wild type, the vsRNA levels were higher in mutants showing enhanced recovery (*ein5*, *dcl3*) and reduced in *rdr6*, which interferes with the formation of secondary siRNAs and does not support recovery.



Supplementary Figure S13. VSR expression in recovered leaves of ORMV-infected Col-0 wild type plants and silencing pathway mutants. The 125k-VSR is expressed in infected tissues irrespective of recovery. The amount of the VSR in recovered leaves is lower in mutants undergoing early recovery (*ein5*, *dcl3*) and higher in the upper leaves of *rdr6* mutants in which recovery is inhibited. L8z2 plants, which contain a continuously active silencing system, produce relatively high levels of the VSR whereas *dcl2 dcl4* plants, in which siRNA synthesis is inhibited, contain relatively low levels of the VSR. The Western blot analysis was replicated two times. UGPase, UDP-glucose pyrophosphorylase.



Supplementary Figure S14. Recovery in sink tissues. (a), AtSUC:GFP plant infected with ORMV (28 dpi). The part of the plant within the rectangle is shown in (b). *, recovered ST4 leaves; +, partially symptomatic ST3/ST4 transition leaves; #, strongly symptomatic ST3 leaf. (b), GFP fluorescence of the plant parts highlighted by the rectangle in (a). Recovered leaves are sinks as shown by the diffusion of GFP throughout the leaf tissue; in ST3/ST4 transition leaves, GFP starts to remain within the phloem, thus indicating that these leaves undergo the sink-source transition. *, recovered ST4 leaves; +, partially symptomatic ST3/ST4 transition leaves. (c), Recovered leaf showing diffused GFP. (d) ST3/ST4 transition leaf showing diffused GFP in the leaf base (sink) and GFP remaining in the veins (source), thus indicating the sink-to-source transition. (e), Flattened ST2 leaf showing the typical source pattern with GFP retained in the veins.

Supplementary Table S1: Occurrence and timing of recovery in hormone pathway mutants

Timing	ATG number	Mutant	# plants ¹	Gene function
Early	AT1G54490	<i>ein5-1</i>	14/14	Ethylene signalling / RNA decay
		<i>xrn4-3</i>	21/22	
Normal	AT5G03280	<i>ein2-1</i>	4/4	Ethylene signaling
	AT3G20770	<i>ein3-1</i>	4/4	
	AT3G51770	<i>eto1-1</i>	4/4	
	AT3G52430	<i>pad4-1</i>	4/4	SA-defense signaling
	AT1G64280	<i>npr1-1</i>	5/7	
	-	<i>NahG</i>	3/8	Innate immunity / brassinosteroid signaling
	AT4G33430	<i>bak1-4</i>	4/4	
	AT1G30330	<i>arf6-1</i>	4/4	Auxin signaling
	AT5G37020	<i>arf8-2</i>	4/4	
	AT1G05180	<i>axr1-3</i>	4/4	
AT3G62980	<i>tir1-10</i>	4/4		

¹ number of plants showing specific recovery phenotype / number of plants infected.

Supplementary Table S2: Table of nucleic acid qPCR primers and Northern blot hybridization probes

	Name	ATG number	Forward primer or probe	Reverse primer
qPCR	GAPDH	At1g13440	TTGGTGACAACAGGTC AAGCA	AAACTTGTGCTCAATGCAATC
	EXP	At4g26410	GAGCTGAAGTG GCTTCCATGAC	GGTCCGACATACCCATGATCC
	18S	At3g41768	CGTCCTGCC TTTGTACAC	CGAACACTTCACCGGATCATT
	ORMV CP	-	CAAGCGGCAAGAGATACTGTTAGAC	GCTGGTTCGGTGT CACAATCG
	GFP 5	-	GCCCGACAACC ACTACCTGAG	GCGGGCGGT CACGAACTC
Probe Fig S2c	ORMV_siRNA	-	AATTGGTGCTCGTTGATGGTGTTTC	TCTACCGTCTCACATTGTCCTTG
	GFP_siRNA	-	CACATGAAGCAGCAGCACTT	TGCTCAGGTAGTGGTTGTGCG
	miRNA398*	-	TGTTACATGCCACTCCTTTG	
	miRNA173	-	GTGATTTCTCTCTGCAAGCGAA	
Probe Fig 1d	ORMV_subgen_as_1	-	TCTCCGGTCTATATCTATACTTATTACTATTTACATCCCT	
	ORMV_subgen_as_2	-	TTTTCTTTTATATTGTAACGAATCAGGACCGGGCGTATC	
	ORMV_subgen_as_3	-	AAATACTGGTACTGATTCGAGCTCGTGATGTTGTAAACCA	
	ORMV_subgen_as_4	-	CTGGTTAAGCATCGCTGTGGGCTCTGCCACATCGCTGCG	
	ORMV_subgen_as_5	-	CCGCTTGAGTTTGGTACGACTGCGACAACGCAGACACGCA	
	ORMV_subgen_as_6	-	CTCAGAAGGTTAGAGA ACTGCTGTCTAACAGTATCTCTTG	
Probe Fig S12	siR1003	-	ATGCCAAGTTTGGCCTCACGGTCT	
	ta-siR255	-	TACGCTATGTTGGACTTAGAA	
	miR160	-	TGGCATA CAGGGAGCCAGGCA	
	ORMV_1 s	-	GCACGCTCGAGACGCCCTAAGGTCCAT	
	ORMV_2 s	-	AGGCCGTACTCCCTAGCGGGTGGTC	
	ORMV_3 s	-	CGCTGCGACCTTTTCAAGGGACGCGA	

UNIVERSITE DE STRASBOURG
RESUME DE LA THESE DE DOCTORAT EN FRANCAIS

Discipline : Science du Vivant

Présentée par : Pitzalis Nicolas

Titre : Interactions plantes-virus : rôle des petits ARN non-codants dérivés du virus et de l'hôte au cours d'une infection et d'une maladie

**Unité de recherche : UPR 2357, CNRS
Institut de Biologie Moléculaire des Plantes (IBMP)**

Directeur de thèse : Dr. Manfred Heinlein, Directeur de recherche, IBMP-CNRS

L'objectif principal de cette thèse était d'acquérir de nouvelles connaissances sur les interactions plantes-virus en étudiant le rôle des petits ARN dérivés de virus et de l'hôte dans la régulation de l'expression génique lors de la propagation locale de l'infection virale dans les feuilles malades et guéries. Dans le cadre de ma thèse, j'ai également contribué à un article de synthèse sur les modèles actuels du mouvement des virus à travers les plasmodesmes (PD) (Pitzalis and Heinlein 2017).

Le rôle des petits ARN dérivés du virus et de l'hôte dans les interactions plantes-virus

Les événements cellulaires impliqués dans la réplication virale locale et le mouvement de cellule à cellule ont été intensément étudiés ces dernières années. Cependant, nous en savons encore très peu sur les interactions entre les plantes et les virus, qui jouent un rôle dans l'orchestration de ces processus au niveau de l'expression des gènes. Ainsi, comme décrit dans le chapitre II de cette thèse, différentes approches de séquençage profond (RNAseq, sRNAseq, PAREseq) ont été utilisées pour étudier les modifications induites par le virus dans le transcriptome de l'hôte, la régulation des gènes et du virus par de petits ARN (sRNA) codés par le virus et l'hôte. En utilisant une analyse bioinformatique des données de séquençage, l'accent a été mis sur l'identification des sRNA dérivés de l'hôte ou du virus qui ciblent les transcrits de l'ARN messager (mRNA) hôte ou l'ARN viral par clivage du complexe RISC (RNA-Induced Silencing Complex). Les travaux ont été appliqués chez le colza (*B. napus*) infecté par le TuMV, qui représente un pathosystème économique important. Pour obtenir des informations sur le processus de réplication et de propagation du virus en cours, nous avons utilisé une version du virus étiquetée GFP, ce qui nous a permis d'isoler des échantillons d'ARN des sites de propagation de l'infection dans les feuilles inoculées. Des données fiables et des conclusions ont été obtenues grâce à l'analyse d'échantillons provenant de trois expériences biologiques indépendantes. De plus, l'utilisation d'échantillons de deux cultivars différents

nous a permis d'interpréter les résultats en fonction de la sensibilité spécifique du cultivar face au virus. Fait important, les différentes approches NGS (RNAseq, sRNAseq, PAREseq) ont toujours été appliquées aux mêmes échantillons d'ARN individuels, de sorte que les différents niveaux d'analyse et les résultats respectifs pour un échantillon donné pouvaient être combinés, mutuellement corrélés et interprétés.

L'analyse du RNAseq à l'échelle du génome a révélé de nombreux gènes montrant des différences dans l'accumulation de leurs transcrits entre les échantillons contrôles traités par simulation et ceux traités par le virus. Parmi ceux-ci, de nombreux gènes induits par le virus étaient significativement positivement ou négativement régulés, soit chez les deux cultivars, soit de manière spécifique à un cultivar. Certains des transcrits différentiellement exprimés ont été prédit pour coder des protéines connues pour jouer des rôles importants dans la défense des agents pathogènes. Un exemple est la CALMODULIN-BINDING PROTEIN 60G (CB60G), induite chez les deux cultivars et connue pour agir en tant que régulateur immunitaire favorisant l'expression des gènes clés impliqués dans la biosynthèse de l'acide salicylique et régulant les mécanismes de "pathogen-associated molecular pattern (PAMP)-triggered immunity (PTI)", "effector-triggered immunity (ETI) et la "résistance systémique acquise" (SAR) (Sun et al. 2015). La susceptibilité virale chez le cultivar Drakkar a été corrélée, entre autres, à une forte induction de l'expression de la sous-unité alpha-2 du complexe coatomer COP I (Ahn et al. 2015), qui pourrait jouer un rôle dans la formation de vésicules de réplication et dans leur mouvement (Wei and Wang 2008) (voir chapitre I). Par ailleurs, le phénotype plus résistant du cultivar Tanto pourrait être corrélé, à l'induction spécifique de transcrits codant pour TARGET OF AVR-B OPERATIONAL1 (TAO1), une protéine similaire au récepteur TIR-NB-LRR (Eitas et al. 2008), cible activée lors d'une attaque pathogène. La validité générale de nos données mRNAseq a été confirmée en testant l'expression de plusieurs gènes par analyse RT-qPCR. L'ARN original analysé par NGS-mRNAseq a été comparé avec ceux de nouveaux échantillons provenant de quatre autres expériences d'infection indépendantes. Cette partie du travail a fourni des listes de gènes classés selon le degré d'induction ou de répression de la transcription dans les sites d'infection locale de TuMV-GFP. Deux cultivars différents présentant des susceptibilités virales différentes ont été analysés.

Pour révéler les mRNA qui pourraient être ciblés par les sRNAs dérivé de l'hôte ou du virus et induit par le virus, de petits fragments d'ARN (appelés "reads") ont d'abord été comptés et alignés sur le transcriptome du génome viral et celui de Tanto et Drakkar avant de réaliser les annotations. Comme découvert par des études antérieures (par exemple Tagami et al. 2007; Vogler et al. 2007, Hu et al. 2011), l'infection virale a provoqué des changements radicaux dans le profil de taille des sRNAs. Alors que les sRNAs des échantillons de Tanto et de Drakkar présentaient des profils identiques et typiques de sRNAs de 21 nt à 24 nt de long, les profils étaient fortement dominés par les ARN interférent (siRNA) de 21 nt et 22 nt dérivés du virus lors de l'infection (vsiRNA). Ces profils, ainsi que les profils de vsiRNAs alignés sur le génome du TuMV, étaient presque identiques entre les deux cultivars de *B. napus*, ce qui indique que

les différences de sensibilité au virus ne peuvent être expliquées par des différences évidentes dans le traitement (processing) des sRNAs. En mappant les sRNA dérivés de l'hôte sur les micro ARN (miRNA) des *Brassicaceae* dans la base de données miRbase (Kozomara and Griffiths-Jones 2014), plusieurs petits fragments de sRNAs correspondaient à des miRNAs connus. De plus, en utilisant le logiciel Shortstack (Axtell, 2013), de nombreux miRNAs inconnus auparavant ont été identifiés.

Les données sur les sRNAs et les mRNAs ont finalement été combinées aux résultats de l'analyse PAREseq pour révéler les sRNAs alignés sur les extrémités 5' clivées des mRNAs et sont compatibles avec les conditions de jumelage RISC d'après le logiciel PAREsnip (Folkes et al. 2012). L'analyse a révélé des paires miRNAs:mRNA cibles déjà connues, telles que les miRNAs ciblant les mRNAs codant pour des protéines spécifiques de liaison au promoteur Squamosa (SPL), des facteurs de réponse aux auxines (ARF), des protéines Scarecrow-like (SCL), des facteurs de transcription sensibles à l'éthylène (ERF-RAP2-7, AP2), les protéines F-box de signalisation auxines (AFB2, AFB3) et les protéines Superoxyde dismutases (Llave et al. 2002; Rhoades et al. 2002; Allen et al. 2005; Wang et al. 2005a; Wang et al. 2005b, Kim et al. 2006; Gandikota et al. 2007; Vidal et al. 2010; Si Ammour et al. 2011; Yu et al. 2012; Lu et al. 2013; Ma et al. 2014; Jung et al. 2014; Xu et al. 2016), confirmant ainsi l'analyse PARE. De plus, ce travail a permis d'identifier de nouveaux candidats pour les paires de miRNA:mRNA, tels que miR1885b:BLOS2 ou miRC23a:COX19. L'activité de clivage de certaines paires miRNA:mRNA cibles, connues et prédites, a été confirmée par des tests 5'RACE (Rapid Amplification of cDNA Ends) spécifiques. Basé sur les résultats obtenus par le logiciel PAREsnip, ces expériences ont permis, en utilisant des échantillons biologiques indépendants, de confirmer certains sites de clivages, au sein de cibles mRNAs prédits.

L'un des objectifs importants était de déterminer si le virus infectieux pouvait utiliser, les siRNAs produits à partir de son génome, en tant qu'effecteurs d'ARN pour le ciblage par le complexe RISC des gènes de l'hôte. L'analyse a en effet révélé la présence de vsiRNAs dans les paires cibles vsiRNA:mRNA qui n'apparaissaient qu'après infection. Un vsiRNA prédominant a été trouvé dans les paires cibles vsiRNA:mRNA et implique des transcrits de gènes ERF également ciblés par miR172. Ce vsiRNA a été trouvé similaire à la séquence miR172 et de plus, est prédit être responsable du clivage exactement sur le même locus dans le transcrit cible. Cela suggère que les virus peuvent coder pour des vsiRNAs évolués pour imiter l'activité des miRNAs hôtes et, par conséquent, pour contrôler les gènes cibles spécifiques des miRNAs pendant l'infection.

La cartographie des sRNAs sur deux transcriptomes de cultivars différents et l'analyse de l'alignement avec le programme ShortStack (Axtell, 2013) ont conduit à l'identification de nombreux loci phasés (PHAS) qui produisent de petits ARN interférents secondaires (phasiRNA) en phase. Les phasiRNAs sont produits par la conversion d'un transcrit en ARN double brin (ARNdb) par des ARN polymérases dépendant de l'ARN (RDR6 ou RDR1). Ils sont traités ensuite de l'ARNdb en siRNAs phasés par DCL4 (Fei et al. 2013). Ceci est en faveur de l'hypothèse où la production de phasiRNAs représente un mécanisme permettant de réguler à la baisse le transcrit spécifique dont ces siRNAs sont issus et de produire des siRNAs capables

de cibler des séquences homologues en trans (Fei et al. 2013). Ainsi, à la différence des gènes TAS non-codants d'*Arabidopsis*, connus parmi les premiers loci permettant la production de siRNAs agissant en trans (tasiRNAs) (Vazquez et al. 2004), les loci PHAS se réfèrent à des gènes codants, dont font parties les gènes de la famille des LRR impliqués dans la défense contre des agents pathogènes, ainsi que les gènes des familles PPR et MYB, comme illustré chez *Arabidopsis thaliana*, *Medicago truncatula* et *Prunus persica* (Fei et al. 2013; Zhai et al. 2011). L'analyse des loci PHAS chez des plants de *B. napus* contrôles ou infectés par TuMV, a révélé que certains loci PHAS produisent des siRNAs phasiques seulement après l'infection. La production de siRNAs secondaires associés au virus (vasiRNA) à partir de gènes codants lors d'une infection virale, a été découverte chez *Arabidopsis* et nécessite RDR1 pour leurs synthèse et Argonaute (AGO) 2 pour le clivage de transcrits cibles (Cao et al. 2014). Ainsi, les loci induisant la production de siRNAs phasiques identifiés dans notre analyse, peuvent représenter des loci produisant des vasiRNAs. Cependant, comme la voie de synthèse des phasiRNAs dans *B. napus* n'est pas connu, il est préférable de les distinguer en tant que va-phasiRNAs et non vasiRNAs. Notre étude indique que l'infection virale chez le colza stimule la production de phasiRNAs sur de nombreux gènes codants qui sont liés à la défense (par exemple, homologue TAO1, AGO2, NBR1). Parmi ces gènes, nous avons trouvé des membres de trois petites familles de gènes (codant pour la protéine Chlorophyll a-b binding protein 1, NBR1 homolog, et TAR1) qui produisent des va-phasiRNAs associés au clivage de leurs propres transcrits ou de transcrits de gènes homologues. Cela suggère que le processus de production de va-phasiRNA pourrait représenter un mécanisme pour atténuer les effets de l'infection sur l'homéostasie transcriptionnelle. Il est intéressant de noter que les membres de la famille NBR1 et TAR1 produisent également des va-phasiRNAs avec le potentiel de cibler les transcrits d'autres gènes. Les données suggèrent que particulièrement NBR1 peut organiser des centres inductibles ("hub") par le virus pour la synthèse de siRNAs et le ciblage induit du virus par tout un réseau d'autres gènes.

Les résultats de l'analyse PAREsnip indiquent que le génome viral peut également être clivé par des siRNAs dérivés du virus et de l'hôte (vsiRNA, hsRNA). La grande majorité des événements de clivage était associée à des hsRNAs uniques, dérivés de gènes annotés comme étant des gènes de résistance aux maladies (TAO1 et RPP5), tous deux codant pour des protéines de type récepteur TIR-NB-LRR. Le clivage de l'ARN viral (vRNA) par le biais des vsiRNAs ou hsRNAs peut contribuer à la sensibilité spécifique du cultivar pour le virus, car certains sites de clivage sont prédits de manière spécifique à un cultivar. Il est intéressant de noter que certaines des paires cibles d'hsRNA:vRNA incluent des va-phasiRNAs actifs en trans et sont dérivés des gènes NBR1 et TAR1. Ce résultat pourrait corroborer l'hypothèse de l'évolution des gènes NBR1 en tant qu'hub induit par le virus induisant la production de siRNAs secondaires. Celui-ci pourrait avoir évolué, à condition, que les va-phasiRNAs dérivés du même hub soient capables de contrôler à leur tour le virus. Il est également intéressant de noter que les gènes NBR1 de *B. napus* sont hautement homologues du gène codant pour la protéine AT4G24690/NBR1 de l'autophagie chez *Arabidopsis* (identité de 81 à 84%), impliquée

dans les défenses antivirales impliquant la dégradation des protéines et des particules virales par autophagie (Hafren et al. 2017; Hafren and Hofius 2017). Il a été montré que cette protéine supprime l'infection du TuMV chez *Arabidopsis* en ciblant le VSR du virus (HcPro) (Hafren et al. 2018). Ainsi, en induisant la conversion de transcrite NBR1 en siRNAs secondaires, le virus peut avoir eu la possibilité d'obtenir un contrôle généralisé de l'expression du gène hôte, en supprimant les taux de transcrite NBR1 et en contrôlant les fonctions antivirales de la protéine NBR1.

En conclusion, cette étude a impliqué une analyse NGS et des expériences *in vivo* réalisées sur *B. napus*, la culture d'oléagineux la plus largement produite dans l'Union Européenne. Les résultats mettent en évidence des gènes exprimés différemment et des sRNAs dérivés du virus ou de l'hôte en corrélation avec les extrémités 5' des mRNAs clivés, indiquant leur rôle dans le clivage par RISC. Collectivement, les données suggèrent que *B. napus* utilise des siRNAs endogènes dérivés de gènes de résistance, pour cibler le virus, alors que le virus, à son tour, utilise ses propres siRNAs pour cibler l'hôte. De plus, en induisant la production de siRNAs secondaires à partir de gènes codants, le virus semble avoir la possibilité de cibler d'autres gènes. Les gènes sensibles au virus, et en particulier les gènes prédits comme cibles des siRNAs ou des va-phasiRNAs, peuvent avoir un rôle important dans l'infection virale chez *B. napus* et pourraient représenter d'importants nouveaux loci, candidats pour l'amélioration des cultures. Cependant, il est important de noter que les paires cibles de sRNA:RNA identifiées sont prédites et que des expériences supplémentaires sont nécessaires pour démontrer si ces paires de cibles sont effectivement fonctionnelles dans le clivage de l'ARN par RISC. Une approche pour obtenir des preuves à l'appui de cette hypothèse pourrait être d'utiliser l'immunoprécipitation de la protéine AGO pour déterminer si des sRNAs candidats, sont effectivement présents dans les complexes AGO-RISC. Le clivage par RISC d'une cible de mRNA est généralement éprouvé par l'utilisation d'une construction test et d'une construction témoin d'une séquence cible mutée dans laquelle la séquence mRNA cible de siRNA, est fusionnée à un rapporteur, par exemple le transcrite GFP. La fluorescence, réduite s'il y a clivage de l'ARN rapporteur, sera comparée entre les tissus infectés et les tissus témoins. Cependant, cette approche peut nécessiter la production de plantes transgéniques, étant donné que *B. napus* ne convient pas aux tests d'expression transitoire basés sur l'agroinfiltration. Comme les génomes d'ADN de Drakkar et Tanto ont été séquencés dans le cadre de ce projet, il pourrait être possible d'identifier des polymorphismes nucléotidiques (Single Nucleotide Polymorphisms, SNPs) spécifiques à des cultivars, qui correspondent aux paires cibles sRNA:mRNA, eux même présent dans un seul cultivar, et utiliser ces SNPs dans des croisements génétiques afin de corréler les SNPs spécifiques au clivage de transcrite par des expériences 5'RACE d'un gène. Le rôle des gènes au cours de l'infection virale doit être testé à l'aide de mutants spécifiques de ces gènes. Cependant, étant donné que *B. napus* est une espèce allotétraploïde avec un génome fortement amplifié (Chalhoub et al. 2014), il est presque impossible de créer des mutants récessifs dans lesquels une fonction donnée est abolie. L'analyse fonctionnelle des gènes dépend plutôt d'approches dominantes telles que

l'ARN interférence (RNAi) ou le CRISPR/CAS9, qui peuvent affecter l'expression de tous les membres d'une famille de gènes donnée.

Néanmoins, les résultats obtenus dans cette étude ont révélé un réseau complexe d'interactions potentielles médiées par les sRNAs entre *B. napus* et le virus et ont permis d'identifier de nouvelles cibles génétiques importantes pour l'amélioration des cultures.

Processus conduisant à la guérison des symptômes viraux et favorisant la santé des plantes

Les virus sont des parasites intracellulaires obligatoires et la plupart des études sur les virus se sont concentrés sur la symptomatologie des maladies virales. Cependant, l'infection virale ne déclenche pas toujours des maladies. Bien que des études sur la diversité virale aient démontré la présence de virus dans des milliers de plantes, souvent aucun symptôme de maladie pouvant être corrélé à la présence du virus n'a été observé, même si les plantes contenaient des virus liés à d'importants agents pathogènes (Roossinck 2012; Roossinck and Bazán 2017). Roossinck and García-Arenal 2015). Ainsi, la plupart des plantes à l'état sauvage, semblent tolérer les virus et la pathologie de l'infection virale peut être considérée comme une exception plutôt que comme une règle. Étant donné que les virus produisent des maladies et des pertes de rendement importantes dans les cultures, il est nécessaire de comprendre les processus par lesquels les plantes peuvent promouvoir leur santé en présence de virus. Pour obtenir une telle information, le phénomène d'“auto-guérison des symptômes”, donc la capacité des plantes à se remettre de la maladie, a été étudié. En utilisant l'infection par ORMV chez *Arabidopsis* comme modèle, il a été constaté que la guérison se produisait en présence de virus répliquant, indiquant ainsi que les feuilles guéries avaient acquis un état de tolérance. Par une analyse plus poussée, nous avons montré que les symptômes de la maladie étaient corrélés à l'activité du suppresseur de silencing (VSR) et que la plante était capable de maîtriser cette activité. En examinant les mutants d'*Arabidopsis* affectés dans diverses voies liées à la défense et aux hormones, nous avons constaté que le mécanisme sous-jacent impliquait des gènes de voie de RNA silencing post-transcriptionnel (PTGS) nécessaires à la synthèse de siRNAs primaires et secondaires ainsi que des gènes de signalisation du RNA silencing. De plus, les mutants de gènes requis pour la production de siRNAs primaires et secondaires ont également montré une guérison plus rapide. Avec la découverte supplémentaire que la guérison était limitée aux tissus de destination (tissus “puits”, les parties des feuilles importatrices de sucres), cela nous a conduit au modèle selon lequel la guérison se produit lors du transport des siRNAs dérivés du virus (vsiRNA) depuis leur source de production jusqu'à leurs tissus puits, et que les vsiRNAs qui s'accumulent dans ces tissus sont responsables de la saturation et de l'inactivation du VSR responsable de la maladie.

Globalement, cette étude démontre que les plantes peuvent utiliser le RNA silencing couplé à une communication intercellulaire et à la régulation systémique pour prendre le contrôle de l'activité VSR dans les jeunes tissus éloignés du site d'infection pour contrôler (surmonter) la maladie établie. Cette conclusion implique que la santé des plantes peut être favorisée par la force d'importation des tissus puits et par le contrôle de l'activité des gènes qui agissent contre la production efficace de vsiRNAs (par exemple EIN5/XRN4). Les résultats sont

cohérents avec les rapports précédents indiquant l'importance du RNA silencing et d'un VSR "faible" dans la guérison des symptômes. Cependant, contrairement à ces rapports antérieurs, nos résultats plaident contre une exigence d'inhibition ou de suppression virale comme condition préalable à la guérison ; nous montrons plutôt que le virus lui-même n'est pas affecté pendant ce processus. Ainsi, l'auto-guérison des symptômes ne dépend pas de la "destruction" de l'agent pathogène mais plutôt de la capacité des plantes infectées à "gérer" correctement le virus. Cette capacité des plantes à rester en bonne santé malgré l'omniprésence du virus dans l'environnement, devrait en effet être attendue de par une coévolution virus-hôtes. Pour soutenir la propagation, un virus ne devrait pas tuer son hôte mais plutôt promouvoir son développement (sa santé). L'apparition de maladies virales graves chez les plantes cultivées peut être le résultat d'une surexploitation des croisements qui peut avoir entraîné la perte d'importants mécanismes mis en place au cours de la coévolution.

Publications:

Pitzalis, N., Heinlein, M., 2017. The roles of membranes and associated cytoskeleton in plant virus replication and cell-to-cell movement. *J Exp Bot* 69, 117–132.

Kørner, C.J., Pitzalis, N., Peña, E.J., Erhardt, M., Vazquez, F., Heinlein, M., 2018. Crosstalk between PTGS and TGS pathways in natural antiviral immunity and disease recovery. *Nature Plants* 4, 157-164.

Plant-virus interactions: role of virus- and host-derived small non-coding RNAs during infection and disease

Abstract: Virus infection in plants depends on the ability of viruses to replicate and spread their genomes between cells through plasmodesmata, and to overcome host antiviral defense responses, such as RNA silencing. RNA silencing relies on 21-24 nt long small RNAs (sRNAs) that are processed from double-stranded RNA (dsRNA) precursor molecules by Dicer-like (DCL) enzymes and guide Argonaute (AGO)-containing RNA-induced Silencing complexes (RISC) to homologous RNA targets (viral RNA or host RNA) for sequence-specific cleavage or translational repression. Antiviral RNA silencing is triggered by viral dsRNA produced during replication of the viral genome. The viral dsRNA is processed by DCL4 and DCL2 into virus-derived siRNAs (vsiRNAs). However, the functions of vsiRNAs and of the Virus-encoded Suppressor of RNA silencing (VSR) in plant-virus interactions is not well understood. In this thesis, I investigated the role of host- and virus-derived sRNAs during infection of Rapeseed (*Brassica napus*, Canola) by the UK1 strain of *Turnip mosaic virus* (TuMV-UK1). By using a TuMV derivative tagged with a gene encoding green fluorescent protein (TuMV-GFP), two rapeseed cultivars ('Drakkar' and 'Tanto') that differ in susceptibility to this virus were identified. Transcriptional profiling of local infection foci in Drakkar and Tanto leaves by next generation sequencing (NGS) revealed numerous differentially expressed genes. The same RNA samples from mock- and virus- treated Drakkar and Tanto leaves were also used for the global NGS profiling of sRNAs (sRNAseq) and their potential RNA targets (PAREseq). The bioinformatic analysis and their *in vivo* validation led to the identification of transcript cleavage events involving known and yet unknown miRNAs. Importantly, the results indicate that TuMV hijacks the host RNA silencing pathway with siRNAs derived from its own genome (vsiRNAs) to target host genes. The virus also triggers the widespread targeting of host messenger RNAs (mRNAs) through activation of phased, secondary siRNA production from PHAS loci. In turn, both vsiRNAs and host-derived siRNAs (hsRNAs) target and cleave the viral RNA by the RISC-mediated pathway. These observations illuminate the role of host and virus-derived sRNAs in the coordination of virus infection. Another chapter of this thesis is dedicated to the analysis of virus-induced diseases by using Arabidopsis plants infected with the *Oilseed rape mosaic tobamovirus* (ORMV) as a model. Initially, the infected plants develop leaves with strong disease symptoms. However, at a later stage, disease-free, "recovered" leaves start to appear. Analysis of symptoms recovery led to the identification of a mechanism in which the VSR and virus derived-siRNAs play a central role. I used Arabidopsis mutants impaired in transcriptional and post-transcriptional silencing pathways (TGS and PTGS respectively) and a plant line carrying a promoter-driven GFP transgene silenced by PTGS (Arabidopsis line 8z2). Using various techniques able to monitor virus infection, small and long viral RNA molecules, VSR activity, as well as phloem-mediated transport within these lines, this study led to the identification of genes required for disease symptoms and disease symptom recovery. Moreover, the observations allowed to propose a model in which symptoms recovery occurs upon robust delivery of antiviral secondary vsiRNAs from source to sink tissues, and establishment of a vsiRNA dosage able to block the VSR activity involved in the formation of disease symptoms.

Résumé : L'infection virale chez les plantes dépend de la capacité des virus à se répliquer, à diffuser leur génome à travers les cellules par le biais de plasmodesmes et à surmonter les réponses de défense antivirale de l'hôte, telles que le RNA silencing. Le RNA silencing repose sur des petits ARN (sRNA) de 21-24 nt créés à partir de molécules précurseurs d'ARN double brin (ARNdb) par des enzymes de type Dicer (DCL). En s'associant aux protéines Argonautes (AGO), faisant partie des complexes induisant le RNA silencing (RISC), ils sont guidés vers des cibles à ARN homologues (ARN viral ou hôte) pour induire soit leur clivage de manière séquence-spécifique, soit leur répression traductionnelle. Le RNA silencing antiviral est déclenché par les ARNdb viraux produits lors de la réplication du génome viral. L'ARNdb viral est traité par DCL4 et DCL2 en sRNA interférent (siRNA) dérivés du virus (vsiRNA). Cependant, les fonctions des vsiRNAs et du suppresseur de RNA silencing (VSR) codé par le virus, dans un contexte d'interactions plantes-virus, ne sont pas bien comprises. Dans cette thèse, j'ai étudié le rôle des sRNAs dérivés de l'hôte et du virus lors de l'infection du colza (*Brassica napus*, Canola) par la souche UK1 du virus de la mosaïque du navet (TuMV-UK1). En utilisant un dérivé de TuMV fusionné avec un gène codant pour la protéine fluorescente verte (TuMV-GFP), deux cultivars de colza ('Drakkar' et 'Tanto') qui diffèrent par leur susceptibilité à ce virus ont été identifiés. Le profil transcriptionnel des foyers d'infection locale, dans les feuilles de Drakkar et de Tanto, par séquençage nouvelle génération (NGS) a révélé de nombreux gènes exprimés de manière différentielle. Les mêmes échantillons d'ARN provenant de feuilles de Drakkar et de Tanto, traitées par des virus ou utilisées en contrôle, ont également servi à établir le profil NGS des sRNAs (sRNAseq) et de leurs cibles potentielles d'ARN (PAREseq). Les analyses bioinformatiques et leur validation *in vivo*, ont permis d'identifier les événements de clivage de transcrits impliquant des micro ARN (miRNA) connus et encore inconnus. Fait important, les résultats indiquent que TuMV détourne la voie du RNA silencing de l'hôte avec des siRNAs issus de son propre génome (vsiRNA) pour cibler les gènes de l'hôte. Le virus déclenche également le ciblage à grande échelle des ARN messagers (ARNm) de l'hôte par l'activation de la production de siRNAs secondaires en phase, à partir de locus PHAS. À leur tour, les vsiRNAs et les siRNAs dérivés de l'hôte (hsRNAs) ciblent et clivent l'ARN viral par le complexe RISC. Ces observations éclairent le rôle des siRNAs dérivés de l'hôte et du virus dans la coordination de l'infection virale.

Un autre chapitre de cette thèse est consacré à l'analyse des maladies induites par des virus en utilisant comme modèle de plante Arabidopsis, infectée par un *tobamovirus*, le virus de la mosaïque du colza (ORMV). Initialement, les plantes infectées développent des feuilles présentant de forts symptômes de maladie. Cependant, à un stade ultérieur, des feuilles "guéries" et saines, commencent à apparaître. L'analyse de cette guérison des symptômes a permis d'identifier un mécanisme dans lequel, le VSR et les vsiRNAs, jouent un rôle central. J'ai utilisé des mutants d'Arabidopsis altérés dans les voies de silencing transcriptionnelle (TGS) et post-transcriptionnelle (PTGS) et une lignée végétale exprimant un transgène GFP sous contrôle d'un promoteur affaibli par PTGS (lignée Arabidopsis 8z2). Par diverses techniques d'analyse de l'infection virale, des petites et longues molécules d'ARN viral, de l'activité VSR, ainsi que du transport phloémien dans ces lignées, j'ai pu identifier des gènes nécessaires à l'apparition des symptômes de la maladie et du phénotype de guérison des symptômes. De plus, ces observations ont permis de proposer un modèle dans lequel cette guérison dépend d'un adressage important de vsiRNAs secondaires antiviraux depuis leur source de production jusqu'à leurs tissus de destination, et l'établissement d'un apport en vsiRNAs capable de bloquer l'activité VSR impliquée dans la formation des feuilles symptomatiques.